

ANNUAL REPORT

1994



**Institut Max von Laue
Paul Langevin
Grenoble - France**

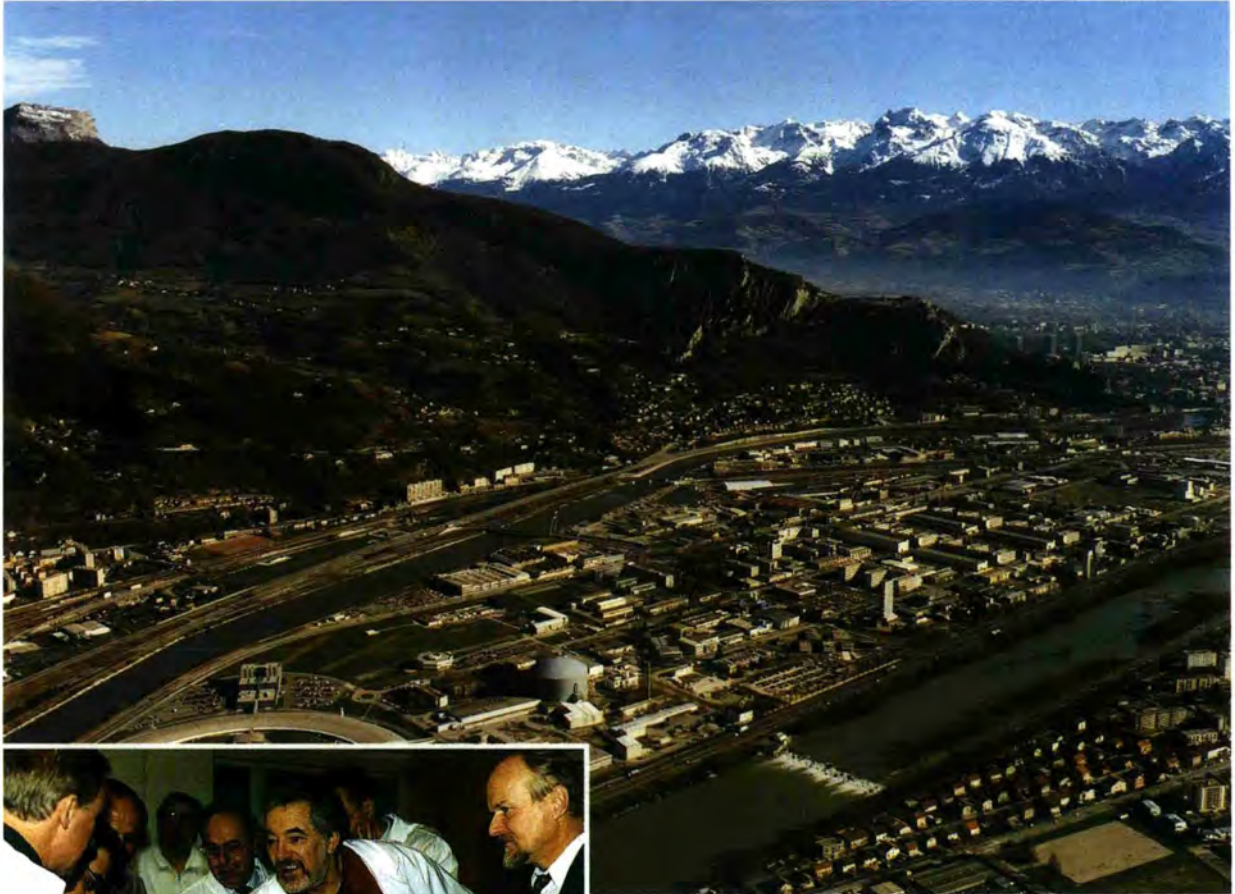
ANNUAL REPORT

1994

Institut
Max von Laue
Paul Langevin



Grenoble - France



The ILL with its High Flux Reactor between the rivers Isère and Drac (in the foreground). Behind the City of Grenoble the mountains of the "Chaîne de Belledonne".

Reinhard Scherm, Director, on 6 January 1995 in the reactor control room asking for detailed information on the start-up.

Front cover

The Cherenkov light of the new reactor at full power. This blue light inside the swimming-pool is created by particles (electrons) which move in water faster than light.

CONTENTS



– ORGANIZATION OF THE ILL	P. 5
– EXPERIMENTAL FACILITIES	P. 7
– VISITS AND EVENTS	P. 8
– DIRECTOR'S REPORT	P. 14
– ILL-ESRF-EMBL-COOPERATION	P. 20
– COLLEGES	P. 21
COLL. 2 - THEORY	P. 22
COLL. 3 - NUCLEAR AND FUNDAMENTAL PHYSICS	P. 25
COLL. 4 - STRUCTURAL AND MAGNETIC EXCITATIONS	P. 37
COLL. 5 - CRYSTAL AND MAGNETIC STRUCTURES	P. 49
COLL. 6 - LIQUIDS, DISORDERED MATERIALS AND METAL PHYSICS	P. 60
COLL. 8 - BIOLOGICAL STRUCTURES AND DYNAMICS	P. 77
COLL. 9a - MOLECULAR SPECTROSCOPY, SURFACES AND MESOPHASES	P. 81
COLL. 9b - STRUCTURE AND DYNAMICS OF LARGE MOLECULES, COLLOIDS AND POLYMERS	P. 89
– DIRECTORATE SERVICE	P. 95
– SCIENCE DIVISION (DS)	P. 97
SCIENTIFIC SUPPORT	P. 98
NUCLEAR AND FUNDAMENTAL PHYSICS (NFP) GROUP	P. 103
DIFFRACTION (DIF) GROUP	P. 106
THREE-AXIS SPECTROMETER (TAS) GROUP	P. 113
TIME-OF-FLIGHT AND HIGH RESOLUTION (TOF/HR) GROUP	P. 120
SMALL PROJECTS	P. 125

C O N T E N T S



– PROJECTS AND TECHNIQUES DIVISION (DPT)	P. 127
INSTRUMENTATION BRANCH	P. 129
DEVELOPMENT BRANCH (BD)	P. 134
– RESULTS – INSTRUMENTS – TECHNIQUES	P. 140
– REACTOR DIVISION (DR)	P. 151
– ADMINISTRATION DIVISION (DA)	P. 157
FINANCE AND MANAGEMENT INFORMATION SYSTEMS	P. 158
PURCHASING	P. 160
PERSONNEL AND HUMAN RESOURCES	P. 161
BUILDING AND SITE MAINTENANCE SERVICE	P. 163
– COMMUNICATIONS	P. 165
WORKSHOPS, BOOKS, PROCEEDINGS	P. 165
THESES	P. 166
SEMINARS	P. 167
CONFERENCE CONTRIBUTIONS	P. 171
PUBLICATIONS – ILL-REPORTS 1994	P. 176
AUTHOR INDEX	P. 193
PAPERS ACCEPTED FOR PUBLICATION	P. 200

Associates of the ILL

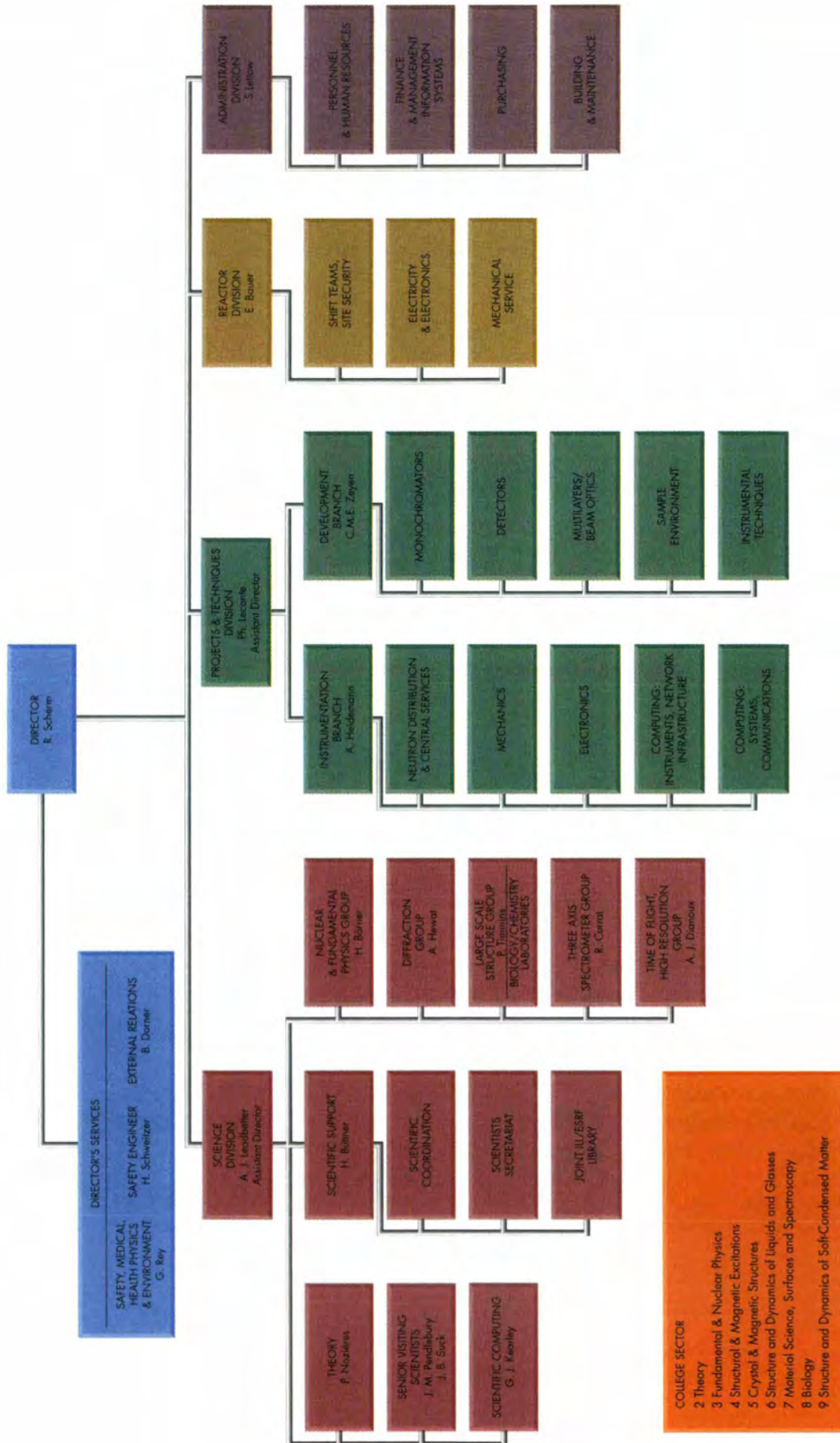


Countries with scientific membership

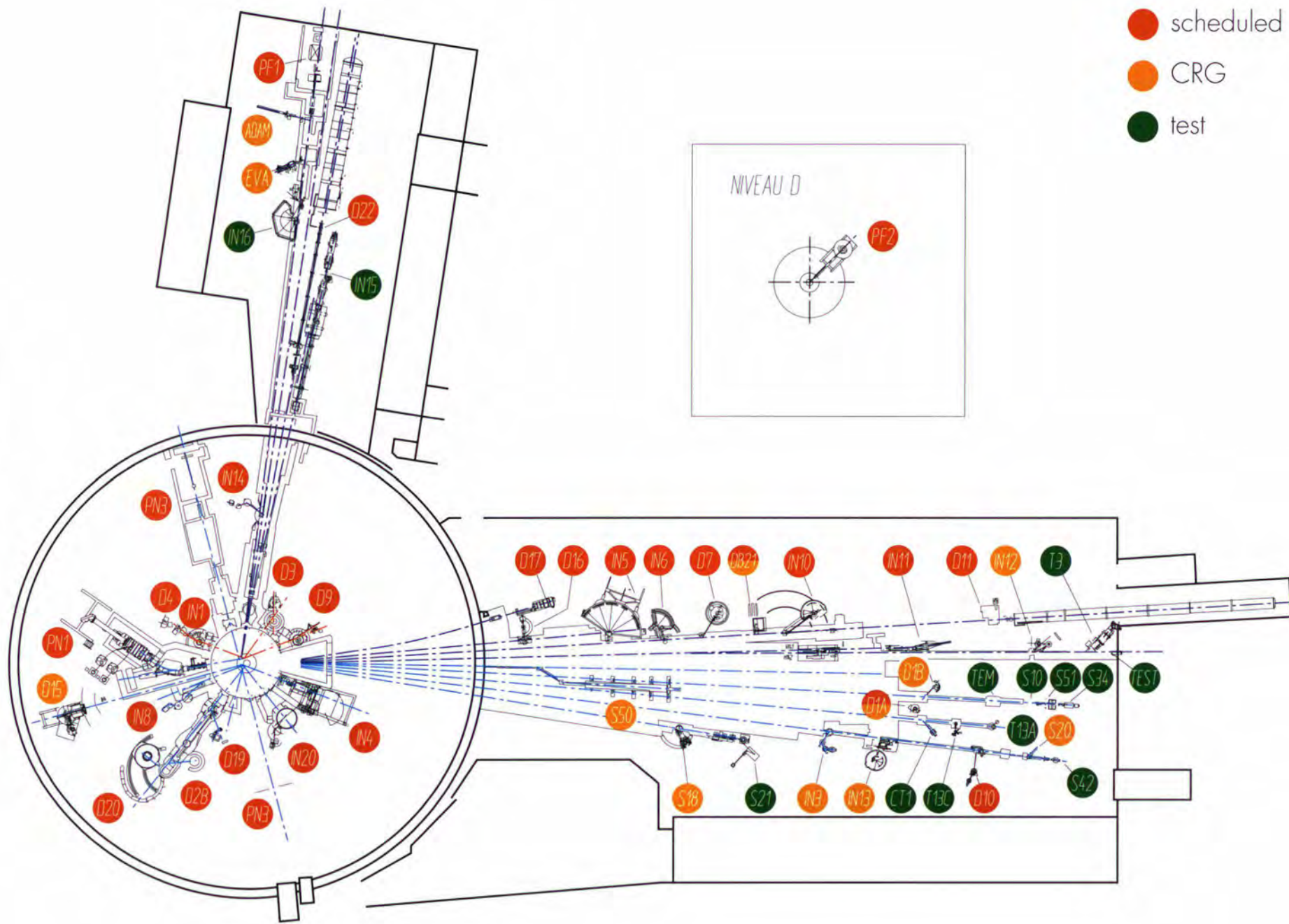
Steering Committee (at its last meeting)		
<ul style="list-style-type: none"> ○ Hennies (KFK) ○ Schmidt-Küntzel (BMBF) ○ Schunck (BMBF) ○ Steiner (HMI, Berlin) 	<ul style="list-style-type: none"> ○ Cesarsky (CEA) ○ Bouchard (CEA) ○ Comès (CNRS) ○ Sevin (CNRS) 	<ul style="list-style-type: none"> ○ Taylor (RAL) ○ Ward (EPSRC) ○ Wilkins (EPSRC)

Scientific Council	
Plenary Session 30 participants	Subcommittees 66 members

GENERAL ORGANIGRAM



- COLLEGE SECTOR**
- 2 Theory
 - 3 Fundamental & Nuclear Physics
 - 4 Structural & Magnetic Excitations
 - 5 Crystal & Magnetic Structures
 - 6 Structure and Dynamics of Liquids and Glasses
 - 7 Material Science, Surfaces and Spectroscopy
 - 8 Biology
 - 9 Structure and Dynamics of Soft-Condensed Matter



"VISITS AND EVENTS" IN 1994



Workshop "Journée des Polymères et Colloïdes" organised by B. Berge (UJF), E. Geissler (UJF) and P. Lindner (ILL) on 2-3 February at the ILL.



J. Charvolin, Director, and E. Bauer, Head of the Reactor Division, the driving forces behind the reactor refurbishment, on 24 February in front of the new reactor vessel just after its arrival.



R. Dautray, Haut Commissaire du CEA, France, came to the ILL on 2 March to witness the new reactor vessel being lowered into its final position inside the swimming pool: (from left to right) J. Charvolin, J.P. Schwarz, Chef de Cabinet, B. Farnoux, CEA, E. Bauer, R. Dautray, J.P. Martin, Head of the Project Group.

"VISITS AND EVENTS" IN 1994



J.P. Martin, explaining details of the refurbishment to J. Charvolin and R. Dautray.



R. Dautray paid particular attention to the new turned-down grid, pictured here with E. Bauer, J.P. Schwarz, J.P. Martin and J. Charvolin.



E. Bauer gives details about the new turned-down grid to R. Dautray.



J. Gadbin, Préfet du Département Isère, visited the ILL on 13 April, and was welcomed by J. Charvolin.



J. Charvolin, E. Bauer, J. Gadbin and J.F. Veyrat observe the activity around the new reactor vessel inside the swimming pool (still dry).

"VISITS AND EVENTS" IN 1994



Ceremony for the signing of the Swiss scientific membership agreement at the ILL on 20 April: (from left to right) P. Schofield, British Associate Director of ILL, G.M. Schuwey, Director of the Swiss Federal Office for Education and Science, P. Zinsli, Vice-Director of this Federal Office, H.-H. Hennies, Chairman of the ILL Steering Committee, D. Lauga, Secrétaire Général de la Préfecture, Mme. F. Rambaud, Conseillère Déléguée chargée des technologies nouvelles et de la recherche de l'Université.

G.M. Schuwey and J. Charvolin signing the agreement, with Ch. Blomeyer (ILL) in close attendance.



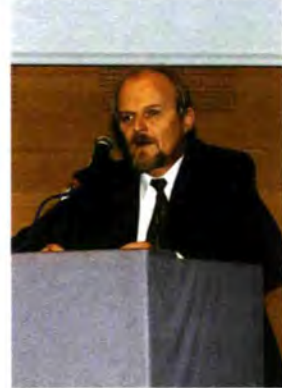
G.M. Schuwey expresses his satisfaction about the new agreement.



On 28 October a ceremony to honour the changes in the Directorate was held at the ILL: (left to right) Philippe Leconte, new French Associate Director, Alan Leadbetter, British Associate Director, Jean Charvolin, outgoing Director, Ekkehardt Bauer, Head of the Reactor Division and Reinhard Scherm, new Director.

"VISITS AND EVENTS" IN 1994

At the celebration on 29 November for the completion of the refurbishment of the Reactor several speakers addressed the guests:
H.-H. Hennies, Chairman of the ILL Steering Committee
J. Charvolin, former Director
E. Bauer, Head of the Reactor Division
J.P. Martin, Head of the Project Group
R. Scherm, Director, explaining "Focussing Techniques"
A.J. Leadbetter, British Associate Director, Master of Ceremony.



The Apéritif after the ceremony on 29 November was followed by a buffet dinner and dance.

"VISITS AND EVENTS" IN 1994



The beam tubes H13 with part of the IN20 monochromator protection and H12 at the right (partly covered) in March 1994.



The instrument IN20 on H13 after the reinstatement at the end of 1994. On the right hand side the monochromator protection for the new IN4 on H12 under construction.



The beam tubes H6, H8 (partly covered) and IH2 (inclined) in March 1994.



The instruments PN3 (GAMS) on H6 and IN1 + D4 on H8 after the reinstatement end of 1994.

"VISITS AND EVENTS" IN 1994



On 6 January 1995, Jean Claude Deyres, assisted by Robert Pratt, pushed the handle to move the control rod out of the reactor core. The reactor went critical at 10.29 hrs.



On 6 January 1995, Philippe Leconte, Alan Leadbetter, Ekkehardt Bauer, Jean-Paul Martin and Jean Tribolet observing the start-up of the reactor from the reactor control room.

Der erste Sonnabend im neuen Jahr 1995 - wir können aufatmen. Das vergangene Jahr war das letzte Jahr einer langen Pause, der Übergang zur zweiten Lebensperiode des Instituts.

1994 erlebten wir die Endphase der Reaktorerneuerung. Ende Februar wurde der neue Schwerwassertank geliefert. Dann brach scheinbar hektische, in Wirklichkeit dagegen wohlorganisierte Betriebsamkeit aus. Der Tank wurde vorbereitet und eingebaut, alle Anschlüsse gelegt. In der Experimentierhalle (Niveau C) baute eine Mannschaft nacheinander alle Strahlrohre ein und testete sie. Hand in Hand damit begann dann ein zweites Team mit dem Wiederaufbau der jeweiligen Instrumente.

Ende Juli war der Reaktor technisch fertiggestellt. Ebenso waren alle Instrumente mechanisch wieder aufgebaut, die meisten schon betriebsbereit. Eine solch beeindruckende Leistung läßt sich nicht anordnen. Alle Beteiligten, organisiert in mehreren selbständigen Teams, haben ihr Bestes gegeben. Hierbei haben alle über die Grenzen der Divisionen oder Services hinweg eng zusammengearbeitet. Unvergessen bleiben die vielen Mitarbeiter und Kollegen, die während der vergangenen Jahre das Institut verließen und doch bis zuletzt mit vollem Einsatz geholfen haben, den Reaktor und die Instrumente wieder in Gang zu bringen. Stellvertretend für alle möchte ich hier zwei Namen nennen: Jean-Paul Martin und David Wheeler, die beide in einem fulminanten Einsatz ihre Karriere mit einem Ausrufezeichen beendeten.

In den verbleibenden Monaten bis zum Jahresende wurden an vielen Instrumenten neue Computer, neue Elektronik und verbesserte

Software implementiert. Diese Zeit wurde auch genutzt, um die Instrumente mit neuen systematischen Sicherheitseinrichtungen auszustatten.

Man könnte das vergangene Jahr als Übergang ansehen mit neuer Organisationsstruktur, verringertem Personalstand und reduziertem Budget. Die neue Struktur, 4 Divisionen untergliedert in Instrumentengruppen, 'branches' bzw. 'services', zur Jahresmitte 93 eingeführt, hat 1994 mit den geschilderten Erneuerungsarbeiten ihre erste Probe bestanden.

Die Bewährungsprobe im normalen Betrieb mit mehr als 1000 ideenreichen und anspruchsvollen Nutzern steht noch bevor. Die Personalreduktion hat vor allem die technischen Dienste betroffen, die oft "unsichtbaren Helfer" hinter den Kulissen, die so wichtig für das Gelingen mancher Experimente sind. Deshalb bitte ich hier nochmals unsere CRG-Gäste um Verständnis, daß sie selbständig operieren müssen und nicht mehr selbstverständlich Zugang zu allen Werkstätten des Hauses haben können.

Große Veränderungen gab es im Management des Instituts: Im Mai verließ uns Peter Schofield zum Ende seiner Amtszeit. Er hatte die Abteilung "Projets et Techniques" neu geordnet und zuletzt den Wiederaufbau der Instrumente besorgt. Ihm folgte Alan Leadbetter als 'British Director'. Alan ist ein alter Freund des Hauses, war er doch schon zu den Gründerjahren einer der ersten Nutzer. Bis vor kurzem Direktor von Daresbury übernahm er die Science Division am ILL. Zur Jahresmitte verließ uns Hans-Martin Spilker, um im Bundesministerium für Bildung, Wissenschaft, Forschung und Technologie (BMBF) die Leitung eines Referats zu übernehmen. Seinen Assistenten Christian Blomeyer finden wir jetzt in der

Forschungsanlage Jülich wieder. Die Leitung der Verwaltungsabteilung übernahm Sigurd Lettow, vorher Personalchef des KfK.

Wir hatten alle gehofft, daß Jean Charvolin sein Direktorat noch mit dem Wiederanfahren des Reaktors abschließen würde. Seine neue Aufgabe in der Direction Générale des CNRS wurde so dringend, daß er uns zum 31. Oktober verließ. Seine Nachfolge als 'directeur français' trat Philippe Leconte an. Vom CEA Saclay bringt er große Erfahrung im Management großer Projekte im Bereich der Kernphysik mit. Mit Jean Charvolin hat die "ancienne équipe" das ILL durch stürmische Zeiten zu neuen Ufern geführt. Unser Dank hierfür verpflichtet das Institut sowie die "nouvelle équipe" für die kommenden Jahre wissenschaftlicher Aktivität.

Mit den wissenschaftlichen Mitgliedsländern wurden im Berichtsjahr neue Verträge abgeschlossen. Spanien unterzeichnete am 10. Februar, die Schweiz am 20. April, und Österreich am 14. Dezember. Unsere Schweizer Freunde nahmen auch gleich die Gelegenheit wahr und übernehmen für einige Jahre IN3 und DIA (1/2). Sie unterzeichneten die ersten CRG-Verträge.

Das wissenschaftliche Leben des Instituts war - wenn auch auf Sparflamme - nie zum Erliegen gekommen; dafür sorgten schon die primären Tugenden der Wissenschaftler Neugierde, Spieltrieb und Ehrgeiz. Die ILL-Wissenschaftler fanden sich - ein letztes Mal - in der umgekehrten Rolle als Gäste und Nutzer an anderen Neutronenquellen. Als ein Beispiel für Aktivitäten während des langen Winters sei Jean Pannetier genannt, dem am 28. November der Prix Paul Pascal von der Académie des Sciences überreicht wurde. Unsere herzlichen Glückwünsche!

Im Oktober erlebte das Institut endlich wieder einen "echten" Wissenschaftlichen Rat. Unter 600 proposals, an Qualität so gut wie vor 4 Jahren, mußten die Subcommittees auswählen: schwierige Diskussionen, Hoffnungen, Enttäuschungen und Erfüllungen.

Das wissenschaftliche Leben des ILL umfaßt nicht nur, was am Institut sichtbar ist. 52 Experimentatoren am ILL stehen mehr als 1000 Kollegen an vielen Universitäten und Forschungslabors gegenüber. In Zukunft werden diese Aktivitäten um eine Facette reicher sein: Den Kern der 25 'scheduled instruments' werden etwa 10 CRG-Instrumente, - auch sie teilweise öffentlich zugänglich - ergänzen: Ein "zentrales Kaufhaus mit bunten Boutiquen" unter einem Dach. Ich erwarte mir davon lebendige Bereicherung.

Heute, am 7. Januar 1995 können wir mit Optimismus in die Zukunft sehen. Am 3. Januar war die Betriebsgenehmigung des DSIN (ohne technische oder zeitliche Begrenzung) eingetroffen. Am Morgen des 6. Januar wurde der "neue" Reaktor zum ersten Mal angefahren und erreichte am 7. Januar um 21.15 Uhr seine volle Leistung.

Reinhard Scherm

On the first Saturday in 1995 we all breathed a sigh of relief. The past year had been a long hiatus, the last transition to the Institut's new lease of life.

1994 saw the last phase of reactor refurbishment. At the end of February, the new heavy water vessel was delivered, sparking off what seemed like frenzied, but was in fact highly-organised activity. The vessel was prepared and installed, and its connections fitted. In the Level C experiment hall, one crew installed and tested all the beam tubes, while another crew began rebuilding the corresponding instruments.

By the end of July, the reactor was technically ready. Similarly, all the instruments had been mechanically rebuilt and most were already operational. Such an impressive performance could not simply have been ordained - everyone involved, organised into several autonomous teams, gave their very best, cooperating closely and transcending the barriers of Divisions and Services. But let us not forget the many staff and colleagues who have left the Institut in recent years and who, right up to the end, showed total commitment to bringing the reactor and the instruments back on stream. From all those who deserve a mention, I would like to name two names - Jean-Paul Martin and David Wheeler - each of whom showed commitment beyond the cause of duty, and thus ended their careers on a resounding note.

In the second half of the year, many instruments were fitted with new computers and electronics, and improved software. This period was also used to implement new safety systems around the instruments.

The past year might be viewed as a transition due to the new organisational structure, smaller workforce and reduced budget. The new structure introduced in mid-1993 - 4 Divisions broken down into Instrument Groups, Branches and Services - passed its first test in 1994 with the refurbishment work described above.

The real test - normal operation and the arrival of more than thousand inventive and exacting users - still lies ahead. The staff cuts have above all taken their toll on the technical services, those often "unseen helpers" behind the scenes, who are so important to the success of many experiments. For this reason I must apologise to our CRG guests, who will need to operate autonomously and no longer have automatic access to all our workshops.

There has been a major reshuffle within the ILL Management: in May, Peter Schofield left the Institut at the end of his term of office, having reorganised the Projects and Techniques Division and, more recently, supervised the reconstruction of the instruments. He is succeeded as "British Director" by Alan Leadbetter. Alan is an old friend of the Institut, having been one of its first users back in the early days. Until recently Director of Daresbury, he has taken charge of ILL's Science Division. Mid-way through the year, Hans-Martin Spilker left to take up a managerial position in the German Ministry for Education, Science, Research and Technology (BMBF). His assistant Christian Blomeyer is now at the Forschungsanlage Jülich. Sigurd Lettow, former head of personnel at KFK, has taken over as head of the Administration Division.

We had all hoped that Jean Charvolin would end his directorship by presiding over the reactor restart. So pressing were his new duties for the CNRS General Management that he was obliged

to take leave of the Institut on 31 October. His successor as "Directeur Français" is Philippe Leconte, who brings with him from CEA Saclay a wealth of experience in the management of large-scale nuclear physics projects. Jean Charvolin and the "ancienne équipe" steered the ILL through stormy seas towards new shores. In full acknowledgement of this achievement, the "nouvelle équipe" must now clear the decks and get down to scientific activity.

In the year of this report, new contracts were concluded with the Scientific Member countries: Switzerland signed on 20 April, Spain on 10 February and Austria on 14 December. What is more, our Swiss friends have recently opted to take over instruments IN3 and D1A (50% of beam time) for a number of years and have thus been the first to sign CRG agreements.

Although the flame of scientific life at the Institut burned low, it was never actually quenched; curiosity, the instinct to gamble and a sense of ambition, the basic virtues of all scientists, saw to that. ILL's scientists found themselves - for the last time - in the reversed role of being guests and users at other neutron sources. As an example of activity over the long winter we should mention Jean Pannetier, who was awarded the Prix Paul Pascal by the "Académie des Sciences" on 28 November. We extend to him our warmest congratulations.

In October, the Institut was at last able to convene a "genuine" Scientific Council once more. The subcommittees had to choose from 600 proposals, equal in quality to those of four years ago. This meant hard discussions, hopes, disappointments and fulfilment.

But there is more to ILL's scientific life than meets the eye. Our 52 experimentalists are in touch with more than 1,000 fellow scientists in numerous universities and research laboratories. In the future their work will be enriched by an important new facet: ILL's nucleus of 25 scheduled instruments is now complemented by some 10 CRG instruments, also partly open to the public. Henceforth, ILL may be compared to a large department store flanked by a variety of independent boutiques, all under one roof. I have high expectations for a lively new departure.

Today, on 7 January 1995, we can look forward to the future with optimism. On 3 January the authorisation to restart was received from the DSIN (with neither technical nor time limit). On the morning of 6 January, the "new" reactor came on stream for the first time and, on 7 January at 9.15 pm, it reached full power.

Reinhard Scherm

Le premier samedi de l'année 1995, nous pouissions un soupir de soulagement. L'année écoulée était bien la dernière d'une longue période d'arrêt, la transition vers une deuxième période de vie de l'Institut.

L'année 1994 a vu la phase finale de la remise en état du réacteur. Fin février, le nouveau bidon réflecteur était livré. Une période d'activité intense commençait alors, dans ce qui, à première vue, aurait pu sembler un climat d'extrême agitation, mais qui, en réalité, était très bien organisée. Le bidon était préparé et monté, puis tous les raccords effectués. Dans le hall d'expérimentation, au niveau C, une équipe effectuait le montage des canaux et procédait aux tests tandis qu'une autre équipe commençait le remontage des instruments correspondants.

Fin juillet, le réacteur était techniquement prêt pour le redémarrage. Le remontage des instruments était terminé et la plupart d'entre eux étaient déjà opérationnels. Il aurait été difficile d'imposer une performance aussi exceptionnelle. L'ensemble du personnel concerné, organisé en plusieurs équipes autonomes, donnait le maximum. Tous, sans distinction de Divisions ou de Services, travaillaient en collaboration étroite. N'oublions pas de mentionner les nombreux collaborateurs et collègues, qui ont quitté l'Institut au cours des dernières années, et qui ont cependant, jusqu'à la fin, participé activement à la remise en service du réacteur et des instruments. Parmi tous ceux qui mériteraient d'être mentionnés, je voudrais citer deux noms, ceux de Jean-Paul Martin et de David Wheeler, qui, de par leur engagement exceptionnel, ont terminé leur carrière en apothéose.

Au cours des mois suivants et jusqu'à la fin de l'année, de nombreux instruments étaient équipés de nouveaux ordinateurs, de nouveaux systèmes électroniques et de logiciels améliorés. Cette période

était également mise à profit pour mettre en place de nouveaux dispositifs de sécurité autour des instruments.

L'année écoulée pourrait être considérée comme une période de transition avec de nouvelles structures, un personnel restreint et un budget réduit. La nouvelle structure organisationnelle de l'ILL, introduite à la mi-93, avec 4 Divisions divisées en groupes d'instruments, en branches et en services, a subi avec succès son premier test avec le travail de remise en état du réacteur.

Le véritable test, c'est-à-dire le fonctionnement normal du réacteur et l'arrivée d'un millier d'utilisateurs imaginatifs et souvent exigeants, est encore devant nous. La réduction du personnel a, avant tout, affecté le personnel des services techniques, ces "aides souvent invisibles" qui travaillent en coulisses, mais qui sont tellement importantes pour la réussite de nombreuses expériences. C'est la raison pour laquelle je demande, une fois encore, à nos invités CRG de se montrer compréhensifs s'ils doivent travailler de manière autonome et n'ont plus automatiquement accès à tous les ateliers de l'ILL.

De nombreux changements sont intervenus au niveau de la Direction de l'Institut : Peter Schofield nous a quitté en mai, à la fin de son mandat. Il avait réorganisé la Division "Projets et Techniques", et plus récemment, veillé au remontage des instruments. Alan Leadbetter lui a succédé en tant que "British Director". Alan est un vieil ami de l'Institut, il avait été l'un des premiers utilisateurs de l'Institut lors des années pionnières de l'ILL. Avant de prendre en charge la Division Science de l'ILL, il était Directeur de Daresbury. Hans-Martin Spilker nous a quitté à la mi-94 pour occuper un poste de direction au Ministère Fédéral de la Recherche et de la Technologie (BMFT). Son assistant, Christian Blomeyer, se trouve maintenant

au KFA Jülich. C'est actuellement Sigurd Lettow, auparavant Chef du Personnel au KFK, qui dirige la Division Administration.

Nous avons tous espéré que le mandat de Jean Charvolin ne s'achèverait pas avant le redémarrage du réacteur. Cependant, ses nouvelles tâches à la Direction Générale du CNRS ne pouvaient attendre, il a quitté l'Institut le 31 octobre. Philippe Leconte lui a succédé en tant que "Directeur français". Il apporte du CEA Saclay une grande expérience dans la gestion de grands projets dans le domaine de la Physique Nucléaire. Jean Charvolin et "l'ancienne équipe" ont su mener l'ILL à travers les tempêtes vers de nouveaux rivages. Nous leur sommes reconnaissants de ce qu'ils ont accompli, il est maintenant temps pour l'Institut et la "nouvelle équipe" de se tourner vers l'avenir qui sera consacré aux activités scientifiques.

Au cours de l'année, de nouveaux contrats ont été signés avec les Membres Scientifiques. L'Espagne a signé le 10 février, la Suisse le 20 avril et l'Autriche le 14 décembre. Nos amis suisses en ont profité pour se porter acquéreurs pour quelques années des instruments IN3 et DIA (50% du temps de faisceau). Ils ont été les premiers à signer des contrats CRG.

La vie scientifique à l'ILL, même si elle était en veilleuse, ne s'était jamais éteinte; les vertus essentielles des scientifiques, la curiosité, l'instinct du jeu et l'ambition, y sont pour beaucoup. Les scientifiques de l'ILL se sont retrouvés - pour la dernière fois cette année - dans le rôle d'invités et d'utilisateurs auprès d'autres sources neutroniques. En tant qu'exemple de la continuité des activités des scientifiques de l'ILL au cours de ce long hiver, je voudrais mentionner Jean Pannetier, qui s'est vu attribué

le 28 novembre le Prix Paul Pascal de l'Académie des Sciences. Nous lui adressons toutes nos félicitations.

En octobre, l'ILL était à nouveau en mesure de tenir un "véritable" Conseil Scientifique. Les Sous-Comités ont dû faire leur choix parmi les 600 propositions d'expérience, qui, en qualité, n'avaient rien à envier à celles d'il y a 4 ans : ce fut le théâtre de discussions difficiles, d'espoirs, de déceptions et de satisfactions.

Cependant, la vie scientifique de l'ILL ne se limite pas à la partie visible. Les 52 expérimentateurs de l'ILL sont en contact avec plus de 1000 collègues dans de nombreuses universités et laboratoires de recherche. A l'avenir, une nouvelle facette viendra enrichir les activités de l'ILL. Aux 25 instruments programmés de l'ILL, qui sont au centre des activités scientifiques, viennent désormais s'ajouter 10 instruments CRG, qui seront également partiellement accessibles au public : nous pouvons comparer l'ILL à un "grand magasin entouré de boutiques indépendantes" placés sous un même toit. Je pense que cela sera un enrichissement pour l'activité scientifique de l'Institut.

En ce jour du 7 janvier 1995, nous pouvons regarder vers l'avenir avec optimisme. Le 3 janvier, nous recevions l'autorisation de redémarrage du réacteur de la DSIN (sans limitation technique ou de durée). Le 6 janvier au matin, le "nouveau" réacteur entrain en service pour la première fois, il atteindra sa puissance nominale le 7 janvier à 21h29.

R. Scherm

Relations with ESRF and EMBL

The relations with ESRF have continued to develop at the management level through direct contacts between the Director of ILL and the Director-General of ESRF, and in regular meetings between the two Heads of Administration.

ILL and ESRF together went on pressing for much-needed improvements in the provision of international schooling for the children of their non-French staff in local schools. Thanks to their active participation in the "Association pour le Développement de l'Enseignement International dans la Région Grenobloise" (ADEIRG) they achieved convincing results. In 1994, after years of inertia, the "Conseil Régional", "Conseil Général" and "Municipalité de Grenoble" (regional, departmental and municipal authorities), as well as the "Rectorat" and "Académie" (education ministry and local education authority) all joined the project to improve the material conditions of Grenoble's international schooling facilities.

Since the three research centres are evolving together on a common site and within the same administrative framework, there is an increasing need for rapidly available data on matters of equal concern to each organisation (such as visitors and guests, etc.). For this reason, a DP system developed by ILL was put into operation at the

end of 1992 for the administration of the joint site. Over the following years, the management of the joint Works Medical Service and the telephone directory as well as the management of instrument users, handled by the Users' Office (ESRF) and the Scientific Coordination Office (ILL) respectively, were integrated into the joint applications. This allowed the sharing of data on users from the different institutes and at the same time the automatic preparation of site access formalities on the basis of the experiment schedules. Redundant information is thus kept to a minimum and data are no longer entered more than once. Investment costs have been shared. Operation, training, user support and software maintenance are handled by a single team and each institute's financial contribution is much lower than would have been the case, had there been separate applications and teams.

As reported in the last Annual Report, EMBL had planned an extension to the ILL/EMBL building (ILL20) to provide additional office and laboratory space, with the possibility of access to ILL staff. The construction work has progressed rapidly and will be successfully completed in early 1995. Due to the great synergies offered by the joint use of the new facilities, the ILL has been vigorous in its support of the extension right from the outset.

COLLEGES



The scientific life of the ILL is organised through the Colleges. The Colleges are the forum for scientific contacts and exchanges. The College Secretaries organize seminars and meetings.

The scientists have their hierarchical positions defined in the Science Division. In this respect, they are instrument responsables and have the duty of dealing with more technical topics. As regards their scientific activities on the other hand, they are left with the utmost freedom, to choose individually their main fields of interest.

The College Secretaries are elected in June each year for a term of one year, which can be renewed for a second year.

College Secretaries in 1994

		Spring	Autumn
College 2:	Theory	M. Fabrizio	P. Bares
College 3:	Nuclear and Fundamental Physics	J. Last	G. Fioni
College 4:	Structural and Magnetic Excitations	J. Kulda	J. Kulda
College 5:	Crystal and Magnetic Structures	G.J. McIntyre (5a) B. Ouladdiaf (5b)	G.J. McIntyre (5a) C. Ritter (5b)
College 6:	Liquids, Disordered Materials and Metal Physics	I. Anderson	I. Anderson
College 8:	Biological Structures and Dynamics	L. Vuillard	L. Vuillard
College 9a:	Molecular Spectroscopy, Surfaces and Mesophases	G. Kearley	H.J. Lauter
9b:	Large Molecules	P. Lindner	C. Lartigue

The Colleges (except Theory) correspond one-to-one to the Subcommittee of the Scientific Council. The College Secretaries (with help from the Scientific Coordination Office, H. Büttner) prepare the meetings of the Subcommittees. They classify the proposals by subjects and collect advice on their technical feasibility from the College members. In the meetings of the Subcommittees they act as secretary to the Chairperson. One experienced ILL scientist (if possible a Visiting Senior Scientist) per Subcommittee also attends the meetings.

By the end of the year, Colleges 6, 9a and 9b were re-configured into

College 6: Structure and Dynamics of Liquids and Glasses	College 7: Material Science, Surfaces and Spectroscopy
6-01 Monoatomic liquids and gases	7-01 Metallurgy and metal physics
6-02 Molecular liquids and gases	7-02 Dynamics of H in metals
6-03 Liquid alloys	7-03 Dynamics of solid solutions
6-04 Molten salts and ionic solutions	7-04 Dynamics and disorder in quasicrystals
6-05 Glasses and amorphous (including polymeric glasses)	7-05 Chemi- and physisorbed species
	7-06 Dynamics of intercalation compounds
	7-07 Dynamics and disorder in molecular systems
	7-08 Magnetic excitations in inorganic complexes
College 9: Structure and Dynamics of Soft-Condensed Matter	
9-10 Colloidal systems – micelles, microemulsions, amphiphilic aggregates, surfactant systems, latex dispersion	
9-11 Polymeric systems – solutions, melts, polyelectrolytes, blends, co-polymers, elastomers, gels, networks, liquid crystals	

Theory

Members of the College

Internal Members

P.-A. Bares	E. Krotscheck
S. Barnes	T. Martin
A. Dyugaev	V. Mineev
I. Dzyaloshinski	P. Nozières
B. Clements	P. Quemerais
M. Fabrizio	S. Scheidl
B. Fourcade	P. Stamp
F. Gebhard	A. Szprynger
F. Glück	B. Toperverg
A. Gogolin	M. Walker
E. Kats	

External Members

M. Altarelli (ESRF)	M. Papoular (ESRF)
P. Carra (ESRF)	G. Santoro (ESRF)
P. Johansson (ESRF)	B. Thole (ESRF)
H. König (ESRF)	M. Van Veenendaal (ESRF)
D. Núñez-Regueiro (ESRF)	

Scientific activity in 1994

The scientific activity of the Theory College in 1994 has concentrated on condensed matter: strongly correlated systems with or without impurities (mainly in low dimensions), heavy-fermions, metal-to-insulator transitions, disordered systems, crystal growth and membranes. The composition of the theory group has varied considerably during the year: A. Dyugaev, E. Kats and V. Mineev moved back to their home institutions in Russia. B. Clements, F. Gebhard and S. Scheidl left for the USA, Marburg and Köln, respectively, while M. Fabrizio is leaving soon for Trieste. T. Martin joined the College Theory last October. A number of active physicists visited the ILL for shorter periods: E. Abrahams, P. Anderson, N. Prokof'ev, C. Varma and A. Zawadowski.

P.-A. Bares and F. Gebhard (6 months), have studied the structure of eigenstates of a one-dimensional $1/r$ -Hubbard Hamiltonian. The hope was to better understand the metal-to-insulator transition in low dimensions. This model exhibits a Mott-transition at zero U as the Fermi surface is nested (despite an asymmetry in the band dispersion). An "exact asymptotic solution" of the model that generalizes the conventional Bethe-Ansatz has been obtained. The ground-state as well as excited states have been studied and the critical exponents of correlation functions have been calculated by a generalization of the finite size scaling in conformal field theory. These results were presented by F. Gebhard at the "International Euroconference on Magnetic Correlations, Metal-Insulator transitions, and Superconductivity in Novel Materials" in Würzburg, Germany, in September 1994.

P.-A. Bares has proposed a simple and novel strategy to construct a whole class of one-dimensional exactly solvable models with defects in the presence of strong correlations. Short-range interactions between few impurities can also be incorporated. The results are promising because until very recently the only models that could be solved exactly in the presence of an (few) impurity(ies) are non-interacting in the bulk. He has illustrated the idea by performing detailed calculations in a t - J -model with impurity, i.e., evaluated the finite size-spectrum and the low- and high-temperature thermodynamics of the model. The bulk-impurity coupling is infrared finite, though. Due to the infinite one-site repulsion, the results are beyond the reach of conventional perturbation theory and bosonization techniques. Moreover, the thermodynamic Bethe Ansatz allowed to go beyond conformal field theory methods. More recently, P.-A. Bares has guessed the formal solution of a Hubbard model with impurity. This work is still in its preliminary stage. In a related investigation, he has been trying to generate by Quantum Inverse Scattering Methods the eigenstates of the Hubbard model in a form (Quantum determinant) that is suited to the exact (at all distances) evaluation of correlation functions.

B. Clements has continued investigating the structure, excitations and thermodynamics of thin films of liquid ^4He on weakly attractive substrates. Work related to the structure, growth and stability properties of the films has been done in collaboration with E. Krotscheck (USA), H. Lauter (ILL) and M. Saarela (Finland). These authors have argued that superfluid He films adsorbed on a graphite substrate, exist in both uniform and non-uniform surface-covering phases. The transition between the two phases is first order and should provide an explanation for the anomalous behaviour of the superfluid density recently observed in torsional oscillator experiments performed on ^4He films adsorbed to graphite. Another work on the dynamical excitations in films has been performed in collaboration with E. Krotscheck, H. Lauter, M. Saarela and C. Tymczak (USA). These authors used a generalized Feynman theory of excitations to incorporate three-phonon scattering effects in the dispersion curves and dynamic form factor. Besides these collaborations and together with E. Krotscheck, B. Clements has been developing a variational density matrix theory to study the finite-temperature properties of Bose films in the liquid-gas regime. Presently, as a function of the film's coverage, the theory gives satisfactory results for the heat capacity, superfluid density chemical potential and sound velocity, and determines accurately the liquid-gas critical point.

M. Fabrizio and A. Gogolin studied, in collaboration with S. Scheidl, the effects of the long-range Coulomb interaction in the transport properties of low-dimensional semiconductor devices (quantum wires). The Coulomb interaction shows up in a non-trivial low-temperature dependence of the conductance. M. Fabrizio and A. Gogolin

generalized bosonization techniques to deal with one-dimensional interacting electron systems with open boundaries. There are various applications of this method. An interesting one is related to the prediction of the static electron density distortions ($2k_F$ -oscillations) in doped quasi-one-dimensional materials, which should show up in the neutron scattering experiments. Another application concerns the two-terminal conductance experiments in quantum wires. In another direction of research, they applied the abelian bosonization technique to the four channel Kondo model. Together with P. Nozières, they have generalized the Anderson-Yuval approach to the multichannel Kondo-problem. An analytical description of the cross-over from non-Fermi-liquid to Fermi-liquid behaviour in the two channel Kondo model (with channel anisotropy) follows. These results might be relevant to point-contact spectroscopy experiments.

M. Fabrizio continued his collaboration with P. Carra and B. T. Thole on the properties of magnetic elements analysed by X-ray measurements. They also developed a theory of inelastic resonant X-ray scattering. M. Fabrizio, in collaboration with B.T. Thole, has studied how much information can be extracted from the analysis of moments of X-ray absorption spectra.

B. Fourcade shares his time between the University Joseph Fourier of Grenoble, where he is Maître de Conférences, and the ILL where he is a scientific collaborator. His research activity focuses on the physics of vesicles. In particular he has been interested in the thermal fluctuations of membranes, that play an important role in these systems and whose topology is very complex. He has developed various approaches (numerical as well as analytical) to deal with the description of sponge-phases. Recent results allow to establish a relationship with biological systems.

F. Glück (two months) has been involved in theoretical work related to neutron decay measurements. He worked out a general method to describe neutron decay distributions in the infinite nuclear mass approximation. Exploiting simple analytical results, he investigated the dependence of various decay distributions on the electron-neutrino angular (a), electron-asymmetry (A) and neutrino-asymmetry (B) correlation coefficients. In the case B two types of experiments have been realized: i) measurements of asymmetry of those decay events for which the electron and proton have the same sign of momentum projection onto the quantization axis of the neutron spin; ii) proton asymmetry measurements without electron detection. He has been studying the deviations from the standard model. He calculated the dependence of the a , A , B correlation coefficients on the neutron lifetime and on several other nuclear observables. Using recent experimental data, he performed a fit analysis considering the coupling-constant ratios as free theoretical parameters.

A. Gogolin studied, in collaboration with N. Prokof'ev, the persistent current in one-dimensional rings of interacting electrons with impurities. They established the relationship of this problem to that of a quantum dissipative particle. The latter is believed to describe different physical situations, e.g. the tunneling of heavy ions in metals. The novel relationship between the two problems might be important for the further investigations. He also wrote a review article that discusses, in simple terms, recent theoretical achievements in the field of quantum wires.

E. Kats (three months) calculated fluctuational contributions into the dynamic properties of nematic liquid crystals constructed from lines, e.g. worm-like micelles, and discussed structural properties. He also investigated fluctuations of surfaces (membranes) by applying chiral field theory and derived Einstein type relations for these fluctuations.

T. Martin has been pursuing projects that he was involved in before his arrival at ILL. These include a research on Rabi oscillations in semiconductor nanostructures, which are exploited to conceive a switching device. He has been interested in the formalism used to describe edge states in the fractional Quantum Hall Effect. He is working on the effects of carrier statistics in noise correlation measurements. He is also actively recruiting speakers for the "ILL Thursday Colloquium".

V. Mineev (3 months) developed a theory to describe the basal plane anisotropy of the upper critical field in the hexagonal heavy-fermion superconductor UPt_3 . He showed that a recent experimental discovery of the sign change of the anisotropy above the tetracritical point in the (H,T) -plane strongly supports a model of unconventional superconductivity where the order parameters (transforming according to different one-dimensional irreducible representations of the hexagonal group) mix. In the light of the above observation, he critically reviewed the current models of the superconducting phase transition in UPt_3 .

P. Nozières has invested a considerable amount of time and energy in the preparation of a series of lectures for the Collège de France on "State variables, fluctuations, irreversibility: thoughts on the thermodynamics close and far from equilibrium". Besides this heavy duty, he has proposed in collaboration with C. Dupont and J. Villain a new mechanism to describe the instability of vicinal surfaces grown by Molecular Beam Epitaxy. Recent experiments by S. Balibar, C. Guthmann and E. Rolley on the propagation of (longitudinal and transverse) capillary surface waves have shown the importance of the adsorption of the ^3He Isotope on the surface. P. Nozières has carefully analyzed the thermodynamics of this adsorption by the crystalline surface-steps. He has also been interested in strongly correlated Fermi systems and has been able to provide a simple physical picture for the Mott transition. In 3D, the Mott-Hubbard gap is due to a spin-density wave that induces Bragg reflection on the boundary of the Brillouin zone.

How can the gap survive in 1D (despite the fact that there is no long-range order)? This question is being investigated in simplified models. Another work was inspired by Deutscher's experiments on spectroscopy with a superconducting point-contact. The current-voltage characteristic depends critically on the mass-ratio of the two materials in contact. In the heavy-fermion materials, there is a discrepancy between the mass-ratio obtained from the above point-contact spectroscopy and that inferred from specific heat measurements. The experimental data for an abrupt interface can be accounted for in terms of the non-locality of the self-energy. Finally, another direction of research he is being involved in concerns the analysis of the multi-channel Kondo problem by a perturbation method "à la Anderson-Yuval". This work is being performed in collaboration with M. Fabrizio and A. Gogolin.

P. Quemerais continued work on the electron-phonon systems. He has been considering the possibility of ordering of polarons in doped ionic crystals as observed in $\text{La}_{2-x}\text{Sr}_x\text{NiO}_{4+y}$. Ionic crystals are essentially characterized (Frohlich 1950) by three parameters: the frequency of the infra-red vibrations of the ions, the static and the high frequency dielectric constants. It has been demonstrated (Viinetski and Giterman 1958) that provided some conditions on the dielectric constants are fulfilled, the polarons have repulsive interactions at all distances, and so the formation of bipolaron is prohibited. This situation is mostly fulfilled by real materials. Doping consists of injecting into the crystal a finite density of point charges (electrons or holes) plus a uniform charge (with opposite sign) of identical density. When the condition that prohibits the formation of bipolarons is fulfilled by the crystal parameters, and the density is low enough, the crystallization of polarons is possible (as in the Wigner crystallization). When the density reaches some critical value - roughly the size of a single polaron - a metal-to-insulator transition should occur.

S. Scheidl (one year) worked on transport properties of disordered systems. He investigated the mobility of a single particle under the influence of a driving force in one dimension, when a random potential and thermal fluctuations are present. An explicit and general expression for the mobility in terms of stochastic properties of the random potential was derived. Specific applications of this result lead, in some cases, to the existence of a localization transition and non-Arrhenius-like thermal activation. In collaboration with D. Feinberg (CNRS), he started an investigation of the current-voltage characteristic of strongly inhomogeneous high-temperature superconductors. This characteristic is described by the thermal mobility of interacting vortices in the two-dimensional CuO_2 planes subject to the static pinning potential arising from impurities. In a mean-field approach, they identified different regimes depending on the density of vortices, i.e., the strength of the magnetic field and the strength of the pinning centers.

B. Toperverg (three months) has been working on a variety of topics including: i) quantum paramagnetic fluctuations of spin-one systems with strong uniaxial anisotropy in a transverse magnetic field. He derived equations for the dynamic magnetic-susceptibility-tensor within the framework of the Vaks-Larkin-Pikin perturbation theory. He studied how the local spectrum of independent spin-one moments evolves into a band-spectrum and evaluated fluctuation corrections to the mean-field results. Special attention has been paid to the soft mode responsible for the transition to a frustrated 120° spin chiral-phase. These theoretical results were used to fit recent experimental data on RbFeCl_3 (Dorner, Petitgrand); ii) conformal roughness in periodic multilayered structures. He derived equations for the neutron specular reflections and scattering in non-specular directions from periodic multilayers with imperfect interfaces. He formulated the Distorted Wave Born Approximation for the case of multilayers in terms of a spin-1/2 problem. He calculated the cross section for the scattering from correlated inhomogeneities on different interfaces using an exact solution for a finite number of ideal multilayers. The results are employed (in collaboration with Schärpf and Anderson) to elaborate an algorithm for data treatment; iii) magnetic flux density correlations with superconducting substrate imperfections in random Josephson media. The magnetic flux distribution in Josephson media, e.g. Josephson vortices in high- T_c ceramics, is strongly correlated with the fluctuations of the superconducting substrate. These correlations reveal themselves in the pattern arising from the interference of the polarized neutron scattering off the magnetic field gradients and off the scattering-length density fluctuations. Experiments at Geesthacht and at Saclay confirm the theoretical predictions.

Secretary: Pere-Anton Bares.

Nuclear and Fundamental Physics

Members of the College

P. Ageron	M. Jentschel
H.G. Börner	A. Jungclaus
W. Drexel	J. Last
K. Eder	D. May
H.R. Faust	U. Mayerhofer
G. Fioni	J.M. Pendlebury
P. Geltenbort	A. Williams

External Members

Z. Bao (CIAE, Beijing)	F. Glück (CERN, Geneva)
Yu. Borisov (PNPI-Gatchina)	M. Hesse (Univ. Tübingen)
T. Friedrichs (TU Braunschweig)	A. Oed (ILL)
	R. Oliver (ILL)

Guests

M. Ashgar (Univ. Alger)	U. Köster (TU München)
S. Baessler (Univ. Heidelberg)	P. Liaud (LAPP Annecy)
Y. Chibane (Univ. Sussex)	C. Metz (Univ. Heidelberg)
H. Fujimoto (NRLM, Tsukuba)	M. Piboule (UJF, Grenoble)
R. Georgii (TU München)	A. Pichlmaier (TU München)
K. Green (RAL, Oxford)	N. Ramsey (Univ. Harvard)
M. Gross (ISN, Grenoble)	C. Raven (Univ. Heidelberg)
P. Harris (RAL, Oxford)	K. Smith (Univ. Sussex)
P. Iaydjiev (INRNE, Sofia)	N. Vatin-Perignon (UJF, Grenoble)
F. Keller (UJF, Grenoble)	

Summary

Another year has passed without neutrons at ILL and the scientific life of the College was strongly limited by the reinstallation of the instruments which absorbed most the scientists' activities. At the present moment, all Nuclear and Fundamental Physics instruments are ready to come into operation and this gives a strong motivation to all college members in view of the imminent reactor restart.

Subcommittee 3 of the Scientific Council examined in October forty-four research proposals, for a total of 2219 days of beam time. The long reactor shut-down seems not to have influenced the interest of users, and the number of proposals received did not change with respect to the previous years. All available beam time was allocated for experiments (721 days). Even so, many proposals had to be postponed.

During 1994 three members of the College were awarded PhDs: Andrea Jungclaus at the University of Göttingen with a thesis on "Nuclear Spectroscopic Investigation in $^{148-154}\text{Sm}$ and ^{168}Er using neutron induced reactions", Robert Georgii at the Technical University of München with a thesis on "Nuclear structure of ^{124}Te - Two frequencies interferometer for crystal spectrometers" and Richard Oliver

at the Joseph Fourier University of Grenoble with a thesis on "The geology and geochemistry of the intrusive rocks on the Valsenestre region, and their context within the magmatic province of the haut Dauphiné".

As a concrete sign of the restart of all scientific activities at ILL, two new thesis students have joined the College: Michael Jentschel from FZ-Rosendorf is working on solid state applications of the GRID (Gamma Ray Induced Doppler broadening) method and Daniel May from the University of Sussex is involved in the neutron electric dipole moment experiment.

A workshop on "Nuclear Fission and Fission-Product Spectroscopy" was held at the Château de la Baume in the Grenoble area from the 2nd to the 4th of May 1994. Including this meeting, all three main research areas of the College, Fundamental Physics, Gamma Ray Spectroscopy and Nuclear Fission, have been covered during the reactor shut down. This has helped significantly to keep the contact with the user community and stimulated fruitful scientific discussions on the future use of ILL instruments.

Scientific Highlights in 1994

At the PN1 "Lohengrin" Mass Spectrometer

Far asymmetric fission yield from Lohengrin data

It has been well known for 50 years that a simple description of the fission yield $Y(A,Z)$ based on the Q-value is not successful, the two main reasons being firstly that, the strong neutron evaporation spoils any correlation between secondary yield and Q-value and secondly, that discrete fission modes govern the maximum yield regions. These reasons impose structures strongly altering the Q-value description, making such a correlation erratic. Two prerequisites for a Boltzmann description of nuclear fission containing only the Q-value, are therefore the absence of fission modes, whose locations for a given compound system are *a priori* not known, and the absence of neutron evaporation for the fragment considered. The only known fission region which fulfills these requirements, is supposed to be situated in far asymmetric fission for isotopes in the light wing. Here, around the magic shells $Z = 28$ and $N = 50$ we know that n-evaporation is strongly suppressed and we can assume that we are far from strong fission channels. Being cautious on the points mentioned, we tried to identify a systematic behaviour for far asymmetric fission by using exclusively data up to a given value of nuclear charge where we are confident not to be located outside the area where the simplified Boltzmann prescription applies.

This has been shown for the thermal neutron induced fission of ^{235}U and ^{249}Cf for which reasonably large data sets exist for the far asymmetric yield in the light wing. The yields integrated over the kinetic energy follow a simple correlation with the reaction Q-value:

$$Y(A,Z) = e^{\alpha Q + \beta} \quad (1)$$

where α and β are free parameters to be determined by a fit to the data set.

The results for other fissioning systems from $^{230}\text{Th}^*$ to $^{250}\text{Cf}^*$ which have been also investigated on the Lohengrin spectrometer, are shown in Fig. 1. The logarithm of the yield has been plotted against the reaction Q-value, and it confirms the validity of the prescription [1]. In some cases only a few data exist, as the primary aim of these measurements was the determination of abundances in "standard" fission, which includes the region of highest yield between masses of about $A=90$ to symmetric splits. In the near future measurements will be carried out to get more complete data sets for several fissioning nuclei. This will enable a realistic estimate of the production rate of n-rich isotopes in the region from $A=65$ to $A=90$, as for instance for the double-magic nucleus ^{78}Ni , which is now expected to have a yield of $4.55 \cdot 10^{-7}$ /fission when a ^{235}U target is used.

Investigations of a Boltzmann description of the nuclear fission process have also shown that by including few additional terms in eq. 1, a surprisingly good description of fission yield throughout the whole fission product region is achieved. These terms include the Coulomb interaction, the pairing attenuation and the introduction of a fission channel. It is this last term which need to be changed for different compound systems and it is therefore responsible for the rapid change of the yield over the whole actinide region. There is evidence that a simple gaussian distribution centered on a given nucleon number, may account for a discrete fission mode [2].

The PIAFE-phase 1 project

A significant part of the R&D program on the PIAFE (Production Ionisation et Accélération de Faisceaux Exotiques) phase 1 project [3] which concerns the ILL side of the facility has been carried out. It is proposed to implant a high-intensity ion source for fission products in the H9 tube and to extract neutron rich isotopes. The estimated intensities are much higher than any other planned or existing facility and would allow accurate spectroscopic investigations of very n-rich nuclei.

A feature of the fission source will be the fast burn-up of the target material in the ILL reactor high neutron flux. Accurate Montecarlo simulations have shown that the burn-up can be stabilized by surrounding the target with a 2 mm thick rhenium antireactivity shield. The use of this high refractory metal will help to confine the fission products inside the source container and will also assure the mechanical stability.

Beam optics calculations on the transport of the 1^+ ion beam over 15 meters, from the fission source to the ILL reactor experiment hall, have been completed [4]. A periodic system of 10 electrostatic Einzel lenses will be used, providing a matched beam within an envelope of about 1.5 cm. Additional calculations have been carried out to investigate a possible use of a part of the BILL spectrometer as high-resolution mass separator. A mass resolution of about 12 MeV, which is comparable to the Q-value of neighbouring isotopes in a given mass chain, is expected [5].

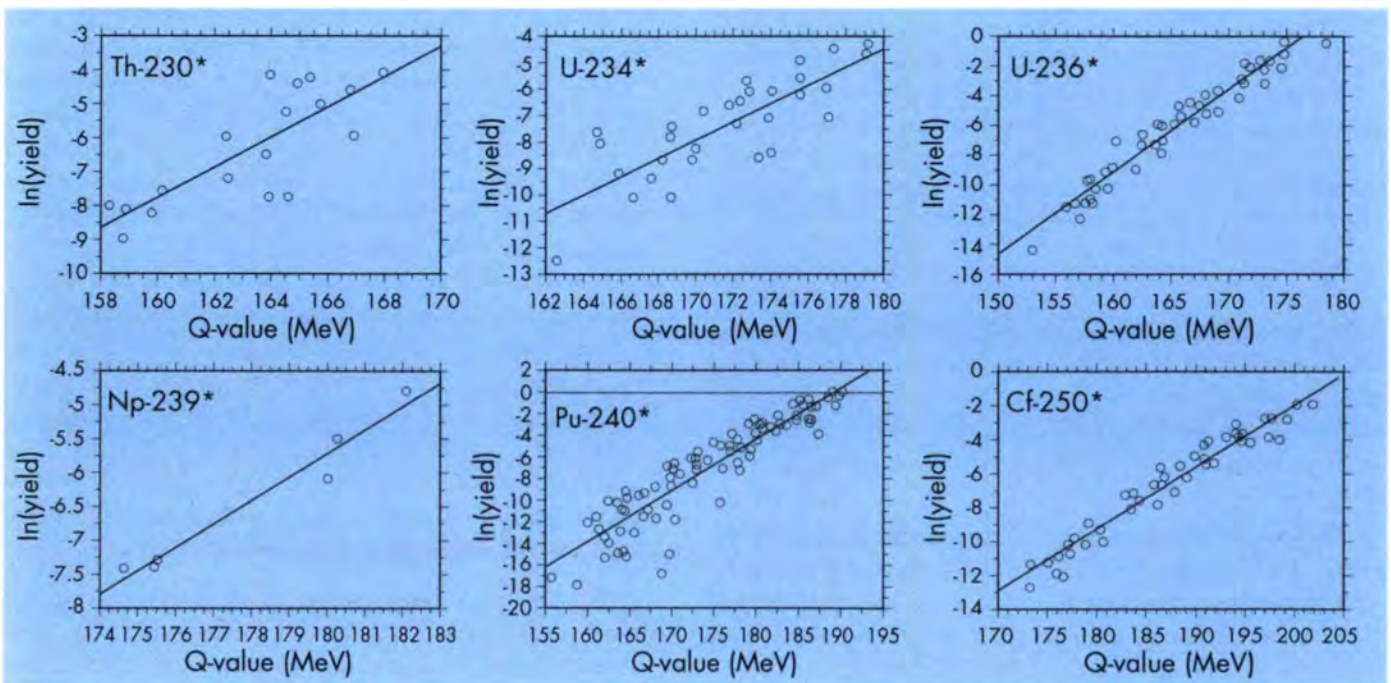


Fig. 1: Correlation plots between the logarithm of the yield and the reaction Q-value for asymmetric fission from Lohengrin data.

**At the PN3 “GAMS” gamma-spectrometer
GRID - Lifetime measurements**

The work on the interpretation of results obtained with the GRID-method has been continued with the evaluation of lifetimes obtained for specific negative parity states in ^{144}Nd (Cookeville - ILL collaboration): In vibrational nuclei a quintuplet of negative parity states (1^- to 5^-) can be produced by the coupling of the single phonon quadrupole and octupole excitations (QOC). Up to now, the identification of such QOC states has relied primarily on level energy systematics and the observation of enhanced $B(E1; 1_1^- \rightarrow 0_1^+)$ values.

To gain further insight into the structure of such states, detailed studies of levels and transitions in ^{144}Nd have been carried out, using the thermal neutron capture reaction. One important result is the assignment of negative parity to a state at 2205 keV (4^-). Additionally, to obtain absolute transition strengths, the lifetimes (or limits thereon) of 11 excited states in ^{144}Nd including the 3_1^- , 5_1^- , and 1_1^- states, were measured using the GRID-technique. The results show that the absolute E2 and E3 transition rates from the 5_1^- and 1_1^- states are consistent with their structure being formed by the coupling of the lowest quadrupole (2_1^+) and octupole (3_1^-) excitations [6]. The level at 2205 keV may be another member of this quadrupole-octupole coupled quintuplet but its lifetime has still to be determined in a future experiment.

**Molecular Dynamics Simulations
of Crystal-GRID experiments**

The GRID method is based on the fact that in a neutron capture reaction a recoiling excited nucleus is produced by the emission of primary γ -quanta (γ_1) after thermal neutron capture. The Doppler broadening of subsequently emitted secondary γ -quanta (γ_2) is measured with very high resolution γ -spectrometers. Up to now all these experiments have been carried out using polycrystalline targets and the spectrometer GAMS4. Smooth γ -line profiles were measured, which allow to extract lifetimes, assuming that the slowing down process was known [7].

However, if one uses monocrystalline targets, angle dependent information on the stopping process inside the target is not completely smeared out. This results in a fine structure depending on the spectrometer alignment, which should allow one to extract the complete information about both, the slowing down process and the lifetime, respectively. The expected intensity distribution of the measured γ_2 -rays can be taken from [8]

$$I(E) = \sum_i \int_0^\infty dt \exp(-t/\tau) \delta\left[E - E_{\gamma_2} \left(1 + \frac{(\vec{v}(t), \vec{n})}{c}\right)\right]$$

The quantity τ is the lifetime of the intermediate nuclear state, E_{γ_2} is the transition energy of the secondary gamma quanta, $\vec{v}(t)$ the velocity of the recoiling atom after time t and \vec{n} the unit vector corresponding to the spectrometer axis. The summation is taken over the number of recoiling atoms.

To investigate the effect of lifetime, the interatomic potentials and the details of the decay process on the measured line shapes, we have performed simulations using Molecular Dynamics (MD) techniques (FZ-Rosendorf - ILL collaboration).

The lifetimes for the nuclear states of ^{49}Ti have been measured at ILL in 1988 using the GRID method with polycrystalline targets [7]. Therefore the lifetime $\tau=16.2$ fs of the 3261 keV state is known with high precision. In a first approximation this value can be taken to study interatomic forces and decay processes. But the lifetime can also be extracted from the Crystal-GRID experiment explicitly. We have chosen crystals of SrTiO_3 (Perovskite structure) and TiO_2 (rutile structure), because in both cases O-atoms are the nearest neighbors of the Ti-atoms. This guarantees a high number of collisions between the recoiling ^{49}Ti and the

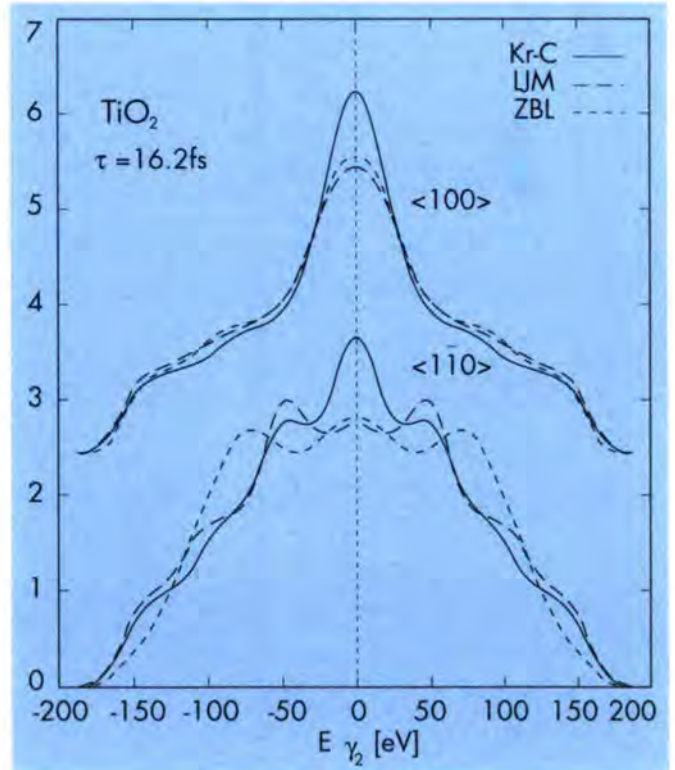


Fig. 2: Doppler broadened lineshapes calculated for GRID-measurements of monocrystalline TiO_2 targets. The MD simulations refer to the secondary-transition 3261- \rightarrow 1752 keV following the nuclear reaction $^{48}\text{Ti}(n, \gamma)^{49}\text{Ti}$. Depending on the spectrometer alignment one can extract details of interatomic forces and/or the lifetime of the 3260.7 keV- state from these lineshapes. This is demonstrated using different potentials. Here the lifetime is fixed ($\tau = 16.2\text{fs}$)

lighter ^{16}O -atoms, leading to strong channeling with only a small loss of kinetic energy at each collision. As single crystals are used, one expects anisotropic distributions of the channeling and blocking directions.

For the simulations we have assumed, that 7200 atoms start with a kinetic energy of 261eV (corresponding to the γ_1 transition $8142 \rightarrow 3261$ keV) in arbitrary chosen directions. The slowing down of each atom was followed by the simulation for a time of 80 fs. To study the effect of the interatomic interactions we have used three different potentials: the Ziegler-Biersack-Littmarck (ZBL), the Lenz-Jensen-Moliere (LJM) and the Kr-C potentials [9]. The corresponding γ_2 line shapes, resulting from different spectrometer alignments for the TiO_2 , are shown in Fig.2. There the instrumental response function is already taken into consideration.

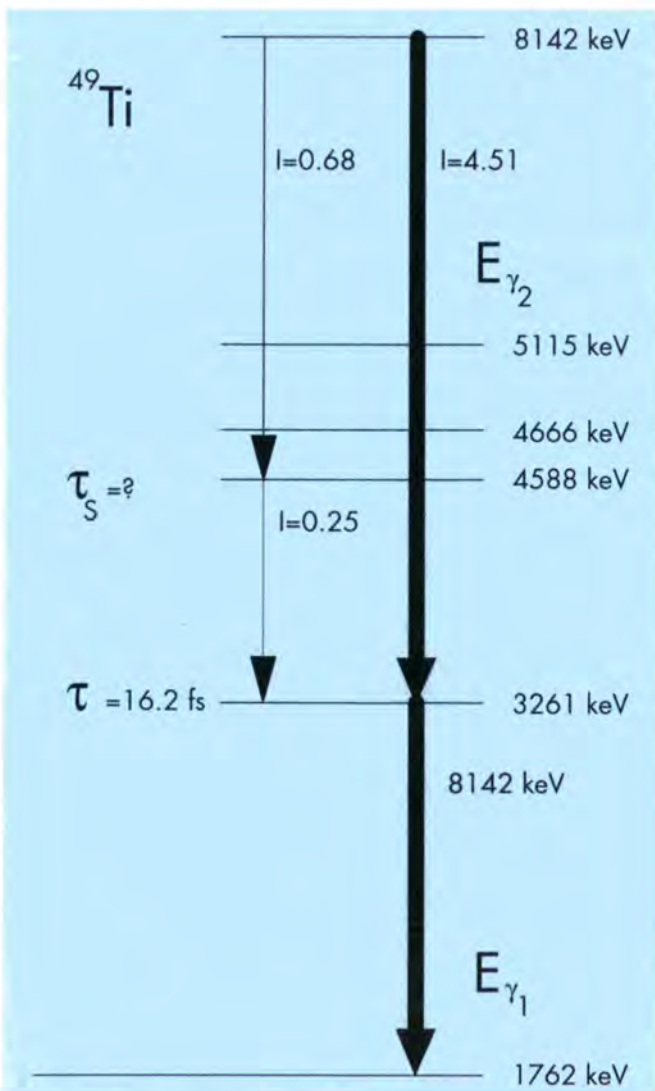


Fig. 3a: The γ -cascade following the nuclear reaction $^{48}\text{Ti}(n, \gamma)^{49}\text{Ti}$ and feeding the 3261 keV level. The intensity ratio between the direct and the side feeding transition is $\approx 21:1$.

From a comparison of the line shapes of the $\langle 100 \rangle$ and the $\langle 1\bar{1}0 \rangle$ spectrometer-target alignment it is evident, that the $\langle 100 \rangle$ direction is less sensitive to small variations of the interatomic potential. This property can be used to extract the lifetime of the nuclear state under consideration without exact knowledge of the interatomic potential. The line shapes for the $\langle 1\bar{1}0 \rangle$ alignment depend more strongly on potential changes: maxima are shifted or disappear. Assuming that the lifetime is known, one can use these profiles to fit the interatomic potential.

The level scheme of ^{49}Ti (Fig.3a) shows in addition to the direct feeding (df) transition $8142 \rightarrow 3261$ keV a side feeding (sf) transition $8142 \rightarrow 4588 \rightarrow 3261$ keV. The influence of this sf-transition depends on the lifetime of the 4588 keV state and was studied assuming that $\tau_S = 5$ fs or $\tau_S \gg 10$ fs (In the latter case the $8142 \rightarrow 4588$ keV transition can be neglected). The resulting simulated line shapes for the LJM-potential are shown in Fig.3b for the $\langle 1\bar{1}0 \rangle$ alignment.

At the cold polarised neutron beam facility PF1 Neutron decay properties

Scientific activities at the new facility PF1 have been focused on preparations for experiments which have been approved for running after the reactor restart.

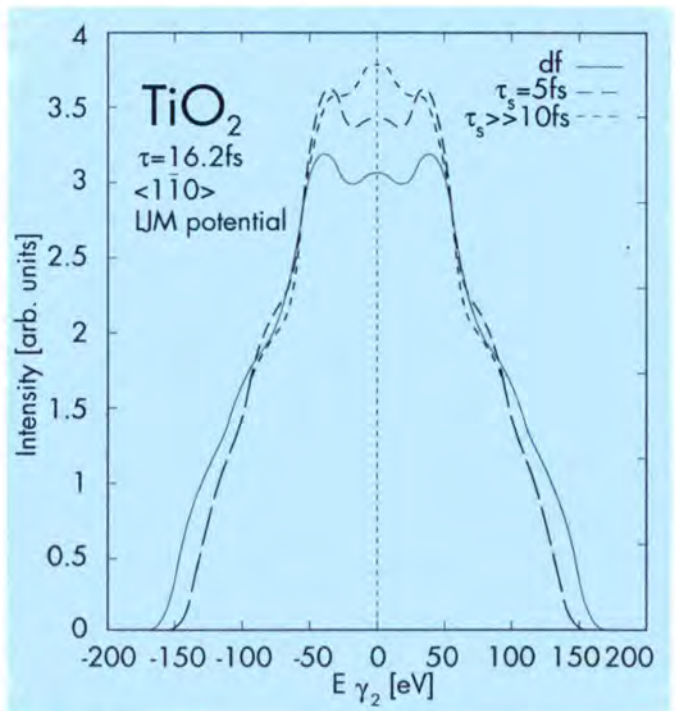


Fig. 3b: The influence of side feeding details on the lineshapes of GRID-measurements is demonstrated. In this calculation the lifetime of the 3261 keV state was assumed to be known with $\tau = 16.2$ fs and the lifetime of the 4588 keV state was varied. Direct feeding (df) from 8142 to 3261 keV is also designated.

The first of these will be the PERKEO II neutron decay spectrometer. In June this was moved to the ILL where it was set up with its magnetic shielding adjacent to PF1. This Heidelberg-ILL collaborative experiment will measure correlation coefficients in polarised neutron decay via electron and perhaps proton detection. First tests of the scintillation detectors for the electrons revealed promising characteristics: small position dependence and high photoelectron numbers. The gain drift of the associated phototubes in the strong magnetic field was larger than expected and this prompted a small modification to be made to the light guides. Following the installation phase, detailed studies of the magnetic mirror effects in the magnet and other sources of systematic errors are in progress.

Later in 1995 running time has been allocated to a Sussex-RAL-ILL-Glasgow collaboration experiment on the measurement of neutron decay correlations using a decay proton trap and decay proton detection.

Also for PF1, an ILL experiment has been approved to calibrate a γ -ray polarimeter which may be used later in an experiment at PN3 to provide a new measurement of the sign of electron antineutrino helicity. A short initial run before the reactor stop showed rather beautiful results from the polarimeter which are shown in Fig. 4.

Neutron decay is a fundamental process stimulated by the electro-weak interaction. Like nuclear β -decay, an electron and antineutrino are emitted. Indeed, nuclear decay can be regarded as the decay of one of the neutrons bound in the nucleus. Neutron decay furnishes a large number of measurable parameters. Some of the more important are (i) the mean lifetime τ_n (ii) the angular correlation coefficient A between and electron emission direction and the neutron spin vector, (iii) the angular correlation coefficient B between the antineutrino emission direction and the neutron spin vector, (iv) the angular correlation coefficient "a" between the electron emission direction and the antineutrino emission direction. Additionally, there are correlations with energy. For example, there is a slight dependence of the A coefficient on electron emission energy which carries information about the "weak magnetism" form factor. Corresponding parameters can be measured from nuclear β -decays. Each type of decay, including that of the free neutron, has its own mixture of Fermi type transitions ($\Delta I=0$) where the electron and the antineutrino are produced with antiparallel spins, and Gamow-Teller ($\Delta I=1$) transitions where they are produced with parallel spins. The overall collection of data provides tests of the theory of the weak interaction at low energies. For this purpose it is vital to add the neutron decay data to the nuclear β -decay data since experimental results of sufficient accuracy on angular correlations which can be related to the Fermi transitions are only obtained from the neutron case.

For some years now there has been an on-going program of experiments at the ILL for improved measurements in the neutron case. A new experimental result $A_0 = -0.1160(15)$

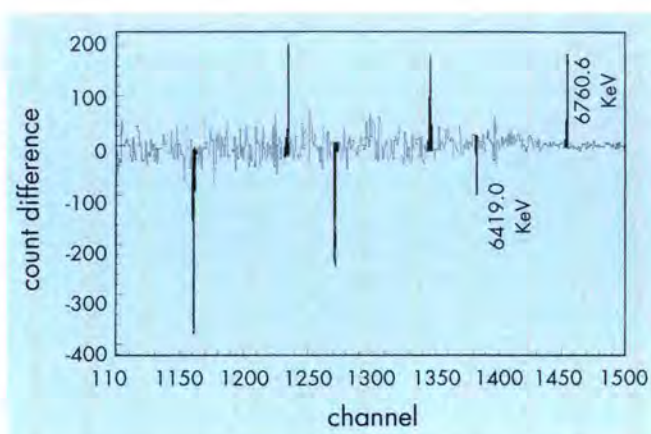


Fig. 4: Results from a γ -ray polarimeter test. Polarised neutrons were captured in a titanium target giving rise to circularly polarised gamma rays via several different transition processes. Shown here are the changes of the γ -ray detection rate following the polarimeter when the neutron spin polarisation is reversed causing the γ -ray helicity to be reversed. Some of the transitions give positive helicity γ -rays and others give negative helicity depending on the spin value of the final nuclear state. Whether the peaks in the figure are positive or negative, distinguishes the sign of the helicity. The magnitudes of the peaks provide information about the efficiency of the polarimeter which has, as its active elements, magnetised soft iron.

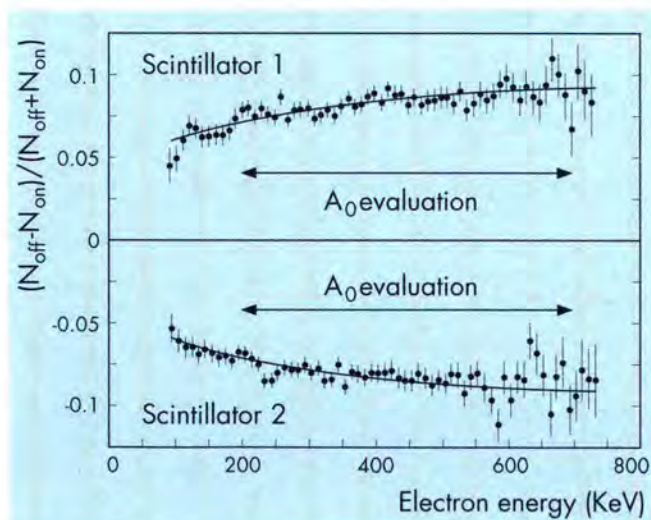


Fig. 5: Results on neutron decay obtained with a time projection chamber in coincidence with plastic scintillators. Shown here are the asymmetries in the rates of emission of decay electrons through the northern and southern hemispheres defined with respect to the neutron spin vector. There are values for each of the two scintillators placed at opposite ends of the chamber. The asymmetries are made evident by periodically reversing the spin direction of the neutrons of the beam which is passing through the chamber. The asymmetries are plotted as a function of the energy of the emitted electron. N_{on} , N_{off} mean intensities with neutron spin flipper on and off.

has just been announced and submitted to Physics Letters by the TU Munich-LAPP Annecy-ILL collaboration [10]. This was derived from an experiment carried out at ILL in 1990 in which decays were observed as a beam of cold polarised neutrons was passed through a multiwire proportional time projection chamber. The measured asymmetries are shown in Fig. 5. For comparison with this experiment, we give the other most recent measurements of the $A_0 = -0.1146(19)$ from the Heidelberg-ILL-ANL collaboration in 1986 using the PERKEO spectrometer and $A_0 = -0.1116(14)$ from an experiment in PNPI, Gatchina in 1990. Assuming the standard (V-A) model of the electroweak interaction the A_0 coefficient can be combined with the value of τ_n to obtain values for the weak interaction coupling constants g_V and g_A . Fig. 6 shows how they are constrained by the experimental results for the parameters τ_n and A_0 . The calculated g_V from PNPI A_0 value had shown some discrepancy with the g_V result from nuclear β -decays and from the muon decay. The discrepancy prompted speculation about it being evidence for heavy right handed W bosons. The new ILL experiment shows no discrepancy.

A. Pichlmaier from TU Munich was invited to the ILL for two months and made a study of different ways of making measurements of neutron polarisation.

F. Glück from the Institute for Particle and Nuclear Research in Budapest was invited to ILL for three months to pursue his theoretical studies on neutron and nuclear decay theory as introduced above. In the first part of his work, he looked at which kinds of measurements would be most helpful for improving the theory. He concluded that it would be useful to concentrate on the case where the electron and the proton emerge from the same hemisphere defined in relation to the direction of the neutron spin and on the case of the correlation between the proton recoil direction and the neutron spin vector. For his second study at ILL he reformulated the relevant weak interaction theory in terms of the new operators L_j and R_j where, most generally, j can stand for each of the Scalar, Vector, Axial vector and Tensor components. The new feature was to use L and R components associated to the emission of purely right and purely left handed antineutrinos respectively. In making a best fit to available nuclear and free neutron decay data he finds no disagreement with the Standard Model [11] within 95% confidence

$$-1.272 < \frac{L_A}{L_V} < -1.263, \quad \left| \frac{L_S}{L_V} \right| < 0.005,$$

$$\left| \frac{R_T}{L_V} \right| < 0.008, \quad \left| \frac{R_V}{L_V} \right| < 0.08, \quad \left| \frac{R_A}{L_V} \right| < 0.11, \quad \left| \frac{R_S}{L_V} \right| < 0.08, \quad \left| \frac{R_T}{L_V} \right| < 0.09.$$

Concluding results for the measurement on neutron-antineutron oscillations

The final outcome for this experiment on the H53 cold neutron beam at ILL, that $\tau_{n\bar{n}} \geq 0.86 \cdot 10^8$ s with 90% confidence, was published in mid year [12]. This result from the Heidelberg-ILL-Padova-Pavia collaboration sets

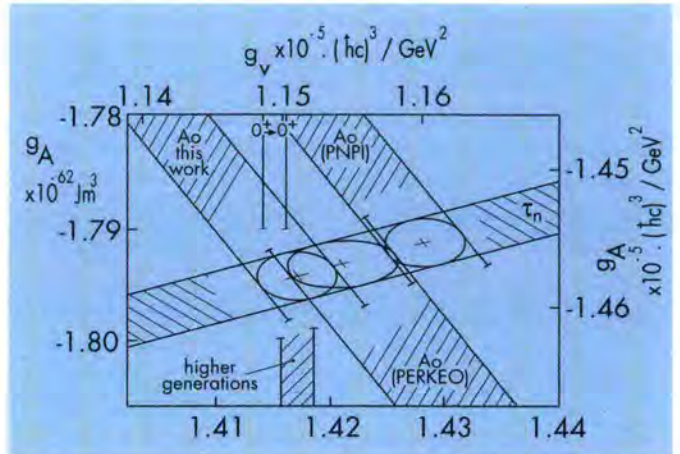


Fig. 6: The 'weak force' coupling constants as determined from the measured neutron decay electron emission asymmetry coefficient A_0 and the neutron lifetime. The predicted values are likely to be within the ellipses which from left to right respectively are obtained from i) the time projection chamber A_0 result just reported, ii) the earlier PERKEO spectrometer result and iii) the earlier PNPI result. The g_V ranges obtained from the $0^+ \rightarrow 0^+$ decays and from muon decay (higher generations) are also shown.

valuable limits to the strength of some possible baryon number changing interactions. Results from proton decay experiments have reached the same level of sensitivity, although in that case the conclusions are hedged about with model dependent assumptions concerning the behaviour of nucleons bound in nuclei. Baryon number changing processes are a feature of theories attempting a grand unification of "strong" forces and "electroweak" forces.

Concluding results from the 17 keV neutrino searches using the BILL magnet

In 1989 Simpson and Hime observed an anomaly in the β -spectrum of ^{35}S . They explained it by postulating the admixture of 1% branch, involving a heavy neutrino with a mass of 17 keV/c². Coming at a time of great interest in neutrino masses, this stimulated many other experiments looking for such an effect. In particular, a sequence of experiments has been carried out exploiting the high resolution of the BILL magnetic spectrometer at the ILL. A fuller account appears in the blue box. The first ILL experiment in 1990 used the level D facility PN2 with an in-pile target of ^{176}Lu . Subsequently, the PN2 facility was dismantled and during the stop of the reactor the BILL magnetic spectrometer from PN2 was housed at the ILL cold neutron facility for fundamental physics. In that position, further β -spectrum searches for a 17 keV neutrino have been carried out using targets containing ^{177}Lu prepared in the SILOE reactor at the CENG. The last of these experiments, run by an ILL-TU Munich collaboration, was completed in early 1994. It was characterised by the use, after the magnetic deflection, of a double detector in the focal plane.

After passing through the gas of a multiwire position sensitive detector the β -particles were incident on a silicon detector. The demand for consistency between the energy determined by the magnetic deflection and that determined from the pulse amplitude of the silicon detector proved to be a very effective way of discriminating against background electrons. The final conclusion, about to be published is that any 17 keV neutrino branch in the beta decay of ^{177}Lu is less than 0.2% at 95% confidence level [13].

At the PF2 Very Cold Ultra Cold Neutron Facility

Following refurbishment and reinstallation, with the help of H. Nagel of TU Munich, of the vertical and curved guides from the vertical cold source to the turbine house, all is ready for testing the VCN und UCN outputs with the first arrival of neutrons. Several quite long experiments for PF2 have been accepted at the October meeting of the Scientific Council. These include (i) a new measurement of the neutron electric dipole moment by Sussex-RAL-Washington-Harvard-PNPI collaboration (ii) a new neutron lifetime experiment using a variable geometry Fomblin coated trap by a Kurchatov-TU Munich-ILL-Sussex collaboration (iii) two experiments investigating loss mechanisms suffered by UCN, one a Kurchatov-ILL group and one from a Rhode Island-ILL group and (iv) the continued development and application of the 100 Å VCN grating interferometer.

The setting up at ILL of the ^{199}Hg magnetometer for use in the neutron EDM measurement has been completed. Its mode of operation was presented in a poster at the 14th International Atomic Physics Conference at Boulder in August. Also in connection with the EDM project Yu. Borisov from Petersburg Nuclear Physics Institute was invited to ILL for 5 months. From his experience in PNPI he was able to provide expert assistance with the system for creating the high electric field in the 22 and 33 litre UCN storage traps where the leakage currents have to be kept below 10^{-8} amps.

Following the non-reinstallation of the IH3 VCN/UCN source in the level C hall an effort is being made to create a wide velocity range VCN beam at PF2 to operate alongside the existing 20% resolution fixed wavelength 100 Å beam. K. Eder has returned to the ILL for three months to work on this project.

At the S51-INAA facility for Geological Studies

Due to the long shut down of the SILOE reactor no further irradiations were made during 1994. However, this did allow the backlog of measurements to be cleared. These included geochemical studies of calc-alkaline volcanism, within the Permian rocks to the East of the Pennic Front, allowing the establishment of an hitherto unknown 1000 km long subduction zone which existed some 240 Ma ago.

Other studies were finished on pyroclastic volcanic rocks from southern Peru and the Bolivian Altiplano which in conjunction with other methods (fission track and K/Ar dating) has allowed precise age determinations for these rocks at 2.42 ± 0.11 Ma [14].

Secretary: Gabriele Fioni

References

- [1] H. Faust and G. Fioni, Proc. Workshop on Nucl. Fission and Fission-Product Spectroscopy, ILL report 94FA05T (1994)91-96
- [2] H. Faust, Proc. Workshop on Nucl. Fission and Fission-Product Spectroscopy, ILL report 94FA05T (1994)107-117
- [3] Overview of the PIAFE project, PIAFE Collaboration Report, ISN Grenoble (1994)
- [4] G. Fioni, J.L. Belmont, J.M. De Conto, H. Faust, An electrostatic beam line for low energy ions, PIAFE Collaboration Report, ISN Grenoble (1994)
- [5] U. Köster, ILL report 94KO13T (1994)
- [6] S.J. Robinson, J. Jolie, H.G. Börner, P. Schillebeeckx, S. Ulbig and K.P. Lieb, PRL73 (1994) 412
- [7] H.G. Börner, J. Jolie, F. Hoyler, S. Robinson, M.S. Dewey, G. Greene, E. Kessler, and R.D. Deslattes, Phys. Lett. 215B(1988)45
- [8] K.-H. Heinig, D. Janssen, ILL report 92HGB16T (1992)
- [9] Eckstein, Computer simulation of ion-solid interaction, Springer-Series in material science 10 (1991)
- [10] K. Schreckenbach, P. Liaud, R. Kossakowski, H. Nastoll, A. Bussiere and J.P. Guillaud, submitted to Phys. Lett. B
- [11] F. Glück and J. Last, ILL report to be published
- [12] M. Baldo-Ceolin, P. Benetti, T. Bitter, F. Bobisut, E. Calligarich, R. Dolfini, D. Dubbers, P. El-Muzeini, M. Genoni, D. Gibin, A. Gigli Berzolari, K. Gobrecht, A. Guglielmi, J. Last, M. Laveder, W. Lippert, F. Mattioli, F. Mauri, M. Mezzetto, C. Montanari, A. Piazzoli, G. Puglierin, A. Rappoldi, G.L. Raselli, D. Scanicchio, A. Sconza, M. Vascon and L. Visentin, Z. Phys. C63, 409-416 (1994)
- [13] K. Schreckenbach et al., to be published
- [14] L. Bellot-Gurlet, F. Keller, E. Labrin, R.A. Oliver, G. Poupeau and N. Vatin-Perignon, Journal of South American Earth Science, in press.

Workshop on Nuclear Fission and Fission-Product Spectroscopy

On the occasion of the twentieth anniversary of the Lohengrin spectrometer and to make the point of the present scientific knowledge in view of the imminent reactor restart, a workshop on Nuclear Fission and Fission-Product Spectroscopy was organised by ILL. From the 2nd to the 4th of May, 1994 about 60 scientists from all over the world participated in this meeting held at the Château de la Baume in the Grenoble area.

Many interesting lectures on binary fission, tripartition, fission models, nuclear spectroscopy and experimental techniques were given. Progress in the understanding of the fission process appeared to be seen in different approaches which are used to describe the distribution of nuclear charge and mass for various fission product regions. Attempts for modelling concentrated mainly on the yield of light particles from different compound systems and on far asymmetric abundances. During the shut down of the ILL facility, experimental activities on fission went on in different laboratories concentrating on charged particle induced fission using accelerated beams, where mainly global mass and energy distributions are obtained. With respect to the spectroscopy of fission products, reports were given from experiments carried out on accelerator based facilities like ISOLDE/CERN and Jyväskylä in Finland. These activities are mainly concentrated on questions of astrophysical relevance concerning r-process nuclei which are produced in nuclear fission at a very high yield. A more powerful facility like PIAFE is strongly needed to progress in the investigations of more neutron rich regions.

It was outlined in a number of contributions that the Lohengrin spectrometer is an essential facility in the systematic investigation of the nuclear fission process. In particular, it is expected that measurements on ternary fission, far asymmetric fission and the possibility to study the fission process from exotic targets can lead to an understanding of the changing features of fission characteristics throughout the actinide region.

The participation of scientists from Western, Central and Eastern Europe and from North America has demonstrated a growing interest to address the remaining problems in nuclear fission by increased collaborative research. Notably the opening of the Russian centres makes it possible to have access to rare transuranium targets only existing in microgram amounts. The investigation of these materials on the Lohengrin spectrometer at the ILL will considerably increase the data base for nuclear fission and will allow us to establish the systematics of yield and energy distribution extending towards regions where strong changes in the fission characteristics are likely to occur.

The workshop helped to have an overview of the future users program on the Lohengrin facility and the specific needs of the different groups and enabled us to organise the

most meaningful cooperative activities. As a side issue of the workshop, discussions took place with Russian colleagues on purchase policies for rare transuranic elements needed to perform future experiments.

The scientific contributions to the workshop are available in a bound version published as an ILL report, number 94FA05T.

Herbert Faust
Gabriele Fioni

Recently completed experiments in particle physics with neutrons

**Conclusion of the n - \bar{n} experiment:
Grand Unification must wait**

Dirk Dubbers and Mike Pendlebury

This year has seen the publication of the final result for the neutron-antineutron oscillation period derived from data collected between August 1989 to April 1991 [1]. This experiment, with its magnetically shielded 70 m long neutron free flight path and its huge antineutron detector in a special building far beyond the guide hall, became the largest instrument ever used at the ILL.

Oscillations, between emitted neutrons and subsequently the antineutron state, would be caused by baryon number changing forces linking baryons to antibaryons. The period of the oscillations provides a measure of the strength of such forces; the weaker the forces, the longer the period of the oscillation. If such forces do not exist then baryon number is conserved. If they are very feeble then baryon number is very nearly conserved. There is nothing particularly exotic about antimatter; antiparticles are produced in large numbers in accelerators. Nevertheless, they have always been observed to be produced in pairs. For example, the production of an antineutron with baryon number -1 has always been seen to be accompanied by the production of a neutron with baryon number $+1$. Unlike the process of oscillation, this production in pairs leaves the total baryon number unchanged.

True conservation laws in physics are the consequence of symmetries. Conservation of charge, for instance, is a consequence of the local gauge symmetry of the electrodynamic interaction. One aim of modern particle physics is to derive nature's laws from a simple set of such symmetry principles. In the last few decades this program has seen considerable progress. Extension of the local gauge principle to the "weak interaction" made it possible to find the common underlying symmetry of the thus unified electroweak interaction. New predictions from this electroweak unification, such as that of the existence of weak neutral current interactions, were beautifully verified by experiments in the 1980s. This success prompted ideas which lead to the so-called Grand Unified Theories (GUTS) in which the strong forces are combined in a rational way with the electroweak forces to make an even grander scheme. GUTS make their own predictions of new phenomena, including the existence of very weak forces capable of changing total baryon number which could cause protons to decay, albeit very slowly, and in some cases, neutrons to transform into antineutrons. It was already known that

the weak forces cause neutral K mesons to oscillate, but in that case there is no change of baryon number because mesons are not baryons and have baryon number zero.

Baryon and lepton conservation laws are the modern form of the mass conservation laws postulated early in the history of science. They do not belong to the genuine conservation laws mentioned above, which are backed by an underlying symmetry principle. Quite to the contrary: GUTS require that all leptons and quarks, the "fundamental Fermions", are at some level closely enough related that they should be able to transform into each other, in contradiction to the conventional hypothesis of separate baryon and lepton conservation. It is a feature of the weak interaction, for instance, that it is the main agent by which d or s quarks can change into u quarks; these processes are rather slow and the interaction is weak, because they go via the W boson which is rather heavy. In an analogous way, according to GUTS, a proton which comprises three quarks should decay even more slowly, transforming itself eventually into leptons, in the form of positrons, electrons, neutrinos and antineutrinos. The even greater slowness in the case of proton decay derives from its going via the postulated, very much heavier still, X boson.

In spite of the recent program of experiments stimulated by the GUTS, proton decay and neutron oscillations have, so far, proved to proceed at rates too slow to be detected. Nevertheless, the constraints which the experimental results impose on the theories are a useful contribution to progress. For example, the simplest GUT made a rather precise prediction for the proton decay rate. The new experiments have caused this GUT to be discarded. There is a class of GUTS which is less simple but more symmetric: the "left-right symmetric" GUTS which have parity non-conservation that has arisen subsequently from spontaneous symmetry breaking between left and right. These GUTS predict a longer lived proton, as required by the experiments. They also predict spontaneous matter to antimatter transitions as required for neutron-antineutron oscillations.

At ILL in the 1980s an experiment to search for spontaneous transitions of free neutrons to antineutrons was built up, first on a smaller scale by a CERN-ILL-Padova-Rutherford-Sussex collaboration [2] and later, on a larger scale by a Heidelberg-ILL-Padova-Pavia collaboration [1].

The principle of the experiment was rather simple: a cold beam of neutrons was flying freely over some distance (3 m in the first, 70 m in the second experiment) to a point where a detector could reveal antineutrons (see Fig. 1). At the detector a carbon foil spanned the beam. If an antineutron, made of antimatter, had hit the

foil then it would have annihilated into a number of pions, which would have been detected in a large particle track detector surrounding the beam (see Fig. 2).

The real experiment, however, posed a number of challenging technical problems that had to be solved in order to reach the sensitivity required. First of all, the detector was hit by cosmic rays at a rate of 10^5 per second, which had to be suppressed electronically before any pion vertex emanating from an antineutron annihilation event could be detected. Then, only 10^{-5} of the cold neutrons which passed the detector at a rate of 10^{11} s^{-1} could be allowed to contribute to the background radiation noise seen in this very sensitive detector. The neutron beam (in the second experiment) had to be tailored with the help of a 34 m long neutron-optical horn system before the free flight in order to be fully contained, without a halo, on the distant target foil of 1 m diameter. And, finally, in the 100 m^3 free flight beam volume, the earth's magnetic field had to be reliably reduced from 50 microtesla to 5 nanotesla in order to assure degeneracy between neutrons and antineutrons.

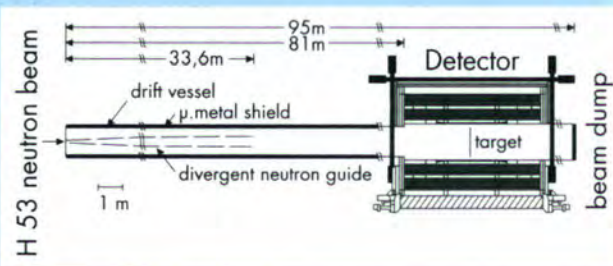


Fig. 1: The $n\bar{n}$ experimental set-up.

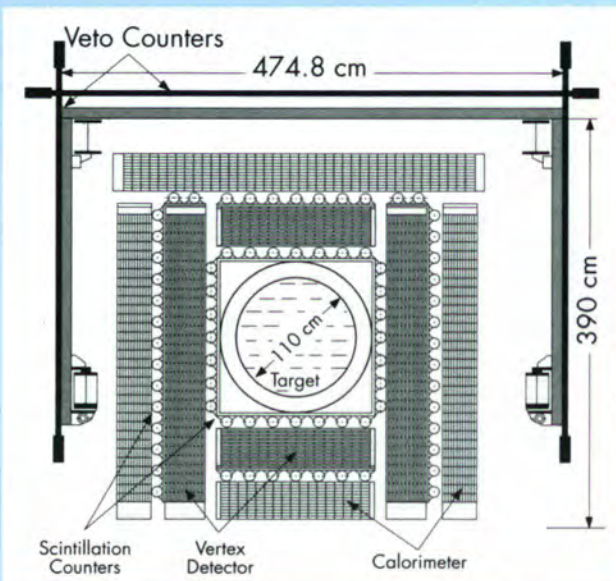


Fig. 2: The $n\bar{n}$ annihilation detector (cross sectional view).

During two years of data taking with 52% antineutron detection efficiency, not a single antineutron candidate event appeared in the detector. From this a lower limit was obtained on the average time a neutron would have to wait before it transforms into an antineutron. This limit is $0.86 \cdot 10^8 \text{ s}$, or roughly three years, see [1] and references therein.

What can be done with this number? The case is not as clear cut as with the proton decay search where the non-observation of proton decay was sufficient to discard the favourite theory of the time (which was based on the mathematical group $SU(5)$). The now favourite left-right symmetric model (based on the group $SO(10)$) has several alternative spontaneous symmetry breaking paths that it can follow. Some of these paths have become less likely due to this new limit on the neutron oscillation time. This is small step forward, but not the decisive step to decide the question of grand unification, which is still waiting to be solved.

Heavy Neutrinos

Klaus Schreckenbach

The possible existence of heavy neutrinos has profound implications for both the standard model of electroweak interaction and for cosmology. Therefore a wide discussion was started when in 1985 Simpson claimed the observation of a neutrino like particle with $17 \text{ keV}/c^2$ mass in the nuclear beta decay of ^3H . The existence of this heavy neutrino was later on confirmed in experiments on nuclear beta decays of ^{35}S , ^{63}Ni , ^{14}C and, observing internal brems-strahlung in ^{71}Ge . The heavy neutrino seemed to occur with a probability, i.e. an admixture $\sin^2\theta$, of about 1% beside the normal (almost) massless electron antineutrino. Soon, the debate became more controversial when several groups did not observe this effect in nuclear beta decay although their experiments were thought to be sensitive enough: possible systematic uncertainties in low energy beta spectroscopy were discussed but no definite conclusion emerged. It is evident, that a neutrino-like particle with a mass of 17 keV is very difficult to accommodate within the standard models of cosmology and particle physics. From the CERN experiments on the decay width of the Z^0 boson it was deduced that there are only three neutrino families. Furthermore, if we believe in the standard big-bang scenario of the Universe, the light element production rates also put stringent limits on the number of relativistic particles due to the thermodynamics of the expansion of the early Universe. Taking into account the recent value of the neutron lifetime - it enters in the balance between protons and neutrons during the light element production - a fourth neutrino family is excluded and even an extra singlet

state particle seems to be unlikely. A possible candidate would be the known tau neutrino. Again from the big bang scenario the density of these tau neutrinos in the Universe should be of the order of the photon number density, i.e. the density of the microwave background. A neutrino mass of a few tenths of an eV would already close the Universe (i.e., eventually stop the expansion). Stable 17 keV neutrinos of that density would make the Universe far too massive. The decay of these heavy neutrinos into lighter ones is not fast enough in standard particle theories even at a cosmological time scale. A new singlet state particle which decays sufficiently fast, was left as one of the few possibilities. The nuclear beta decay is a three body decay (daughter nucleus, electron and antineutrino), where the kinetic energy is essentially shared between the lighter partners the electron and the antineutrino. The neutrino interacts only via the weak force and is thus extremely difficult to detect directly. An indirect signature of a neutrino mass can be looked for in the beta spectrum through its influence on the phase space and energy balance in the decay. Simpson investigated firstly the beta decay of ^3H where the available kinetic energy is just 18.7 keV minus the neutrino mass. A cut-off like deviation ("kink") from the normal spectral shape near 1.7 keV electron energy was interpreted as the emission of a heavy particle occurring with a small probability in concurrence with the normal (almost) massless electron antineutrino. The ^3H activity was implanted in a solid state detector. In the nuclei ^{35}S , ^{63}Ni and ^{14}C used later for heavy neutrino searches, the available energy excess was 167 keV, 67 keV and 156 keV, respectively. The kinks were observed again 17 keV below that beta end point energy in experiments by Simpson, Hime, Jelly [3] and for ^{14}C by a group in Berkeley. For all these experiments solid state detectors were used.

Several other experiments on ^{35}S and ^{63}Ni did not confirm those findings, in particular, those carried out with magnetic electron spectrometers. But they were criticised, because corrections with not well understood spectral shapes in these experiments could just have hidden the small kink and some suspected that the authors were prejudiced against the 17 keV neutrino hypothesis.

In our approach at the ILL we investigated the nuclear beta decay of ^{177}Lu using the magnetic spectrometer BILL in various configurations. The end point energy in the ^{177}Lu beta decay is 500 keV which is relatively high compared to the other beta decays studied. This has the advantage that a number of distorting effects in high precision electron spectroscopy (detector response, target thickness effects, electron scattering cross sections etc.) are smaller and change less with energy compared to the low energy cases. The feasibility relied on the high resolution of the BILL magnets which is better than 1 keV at 500 keV.

In our most recent experiment on ^{177}Lu [4] we combined two spectroscopic methods. We used the second magnet of the BILL spectrometer together with an electron detector, which was composed of a multiwire proportional counter (MWPC) in coincidence with rear mounted solid state Si(Li) detectors. The experiment was carried out at the site of the former PN7 beam position during the ILL reactor shut down. The target activity (about 60 mCi ^{177}Lu) was produced by neutron activation of ^{176}Lu at the SILOE reactor. The target layer of $35 \mu\text{g}/\text{cm}^2$ in the form of oxide was evaporated onto a carbon backing.

The aim of this recent experiment was to measure the beta spectrum in the last 100 keV below the end point and to compare it with the predicted shape including higher order theoretical shape corrections as well as experimentally measured detector response functions. For a convincing result the agreement must be such that no further free shape parameter apart from a possible massive neutrino branch enters.

The thin MWPC has, at 500 keV electron energy an energy independent efficiency. Nevertheless, in earlier experiments [5] we always found a deviation from the theoretical shape of ^{177}Lu a few keV below the end point, when we measured the spectrum with the magnetic fields and the MWPC alone. Similar effects were observed by other groups. The most probable cause is electron scattering in the beam tube of the spectrometer. We had introduced diaphragms to limit this effect. With the Si(Li) detector behind the MWPC we were now able to detect the remaining scattering events as shown in Fig. 3. For this purpose monoenergetic electron lines

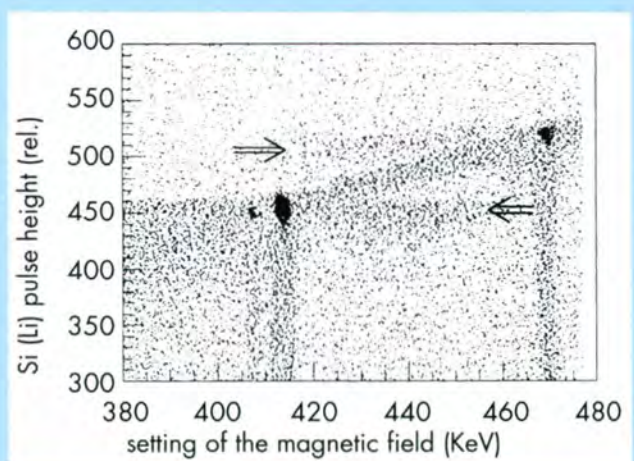


Fig. 3: The pulse height of the electron events in the Si(Li) are displayed versus the energy settings of the magnetic spectrometer taken with a ^{181}Hf source. Events are concentrated at the energies of internal conversion electrons. The horizontal shadow stripes (marked by arrows) correspond to Mott scattering of those monoenergetic electrons in the spectrometer.

(internal conversion electrons) in ^{181}Hf beta decay were investigated. We observed with the Si(Li) detector electrons which did not correspond to the actual setting of the magnetic field. These electrons stem most probably from Mott scattering, i.e. scattering at the atomic nucleus without energy loss, at the diaphragms or beam tube walls. We have evaluated this effect quantitatively and convoluted it into the theoretical shape. We then obtained a perfect description of the measured spectrum. The best fit to the spectrum yielded, for a 17 keV neutrino branch, a probability close to zero with an upper limit of 0.3% at a confidence level of 90% (Fig. 4 and 5). We believe that this experiment is free of systematic uncertainties at the level of the statistical precision. A further outcome of the experiment are limits for neutrino masses up to 100 keV (Fig. 5). This bridges the gap to an early BILL experiment on the β^+ and β^- decay of ^{64}Cu which covered the range of 100 to 450 keV.

Recently Bowler and Jelly reinvestigated the experimental conditions of their positive findings of 17 keV neutrinos. They found a possible explanation for the kink in terms of target inhomogenities. All measurements taken together, including our ILL result, now indicate strongly that the 17 keV neutrino like particle does not really exist. The standard model of cosmology and particle physics is no longer confronted with that type of heavy neutrino problem.

The recent measurements on ^{177}Lu were part of the diploma of K. Dannewitz and thesis of S. Schönert (TU München, Jan. 1995).

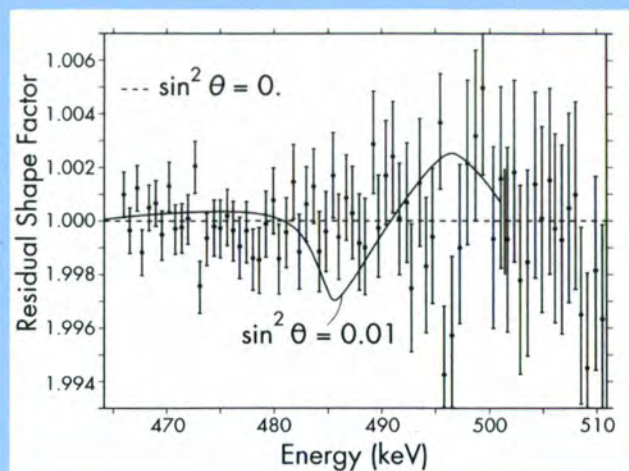


Fig. 4: Ratio of the experimental electron spectrum to the theoretical shape with zero neutrino mass convoluted with the detection response and corrected for an energy independent background. A hypothetical 1% branch with a 17 keV neutrino is indicated for illustration (solid line).

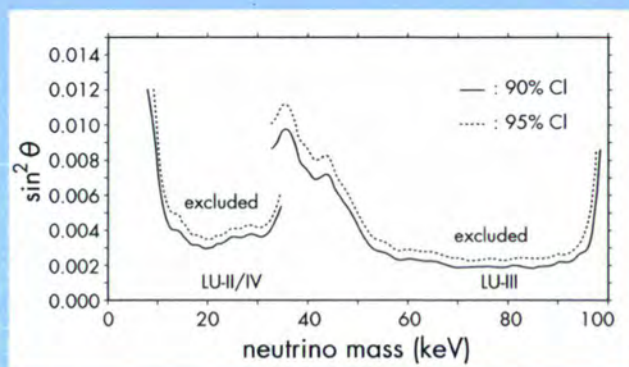


Fig. 5: Search for massive neutrino branches in the beta decay of ^{177}Lu . The regions above the curves are excluded with the given confidence levels. Lu-III was a measurement over a wider energy region.

References

- [1] M. Baldo-Ceolin, P. Benetti, T. Bitter, F. Bobisut, E. Calligarich, R. Dolfini, D. Dubbers, P. El-Muzeini, M. Genoni, D. Gibin, A. Gigli Berzolari, K. Gobrecht, A. Guglielmi, J. Last, M. Laveder, W. Lippert, F. Mattioli, F. Mauri, M. Mezzetto, C. Montanari, A. Piazzoli, G. Puglierin, A. Rappoldi, G.L. Raselli, D. Scanicchio, A. Sconza, M. Vascon and L. Visentin, *Z. Phys.* **C63**, 409-416 (1994)
- [2] M. Baldo-Ceolin, C.J. Batty, K. Green, G. Fidecaro, M. Fidecaro, L. Lanceri, W. Mampe, A. Marchioro, F. Mattioli, J.M. Pendlebury, H.B. Prosper, G. Puglierin, P. Sharman, K.F. Smith, *Phys. Lett.*, **156 B**, 122 (1985)
- [3] A. Hime, *Mod. Phys. Lett.* **A7** (1992) 1301 (Review)
- [4] S. Schönert, K. Schreckenbach, S. Neumaier, F. von Feilitzsch and L. Oberauer, *Nucl. Phys.* **A28** (1992) 176
- [5] K. Schreckenbach, G. Colvin and F. von Feilitzsch, *Phys. Lett.* **129B** (1983) 265

Structural and Magnetic Excitations

Members of the College

Internal members

T. Baumbach	A. Magerl
J. Bossy	P. Mikulik
A. Bouvet	A.P. Murani
S. Bramwell	H. Mutka
T. Chattopadhyay	S. Pouget
R. Currat	N. Pyka
Ch. Doll	O. Randl
B. Dorner	B. Roessli
B. Farago	O. Schaeerpf
J. Kulda	H. Schober
H.J. Lauter	C.M.E. Zeyen

External members

M. Alba (CENG)	P. Monceau (CNRS)
G. Dolino (UJF)	L.P. Regnault (CENG)
C. Filippini (CNRS)	M. Vallade (UJF)
B. Fåk (CENG)	Ch. Vettier (ERSF)

Introduction

The past year has been marked by a number of issues both inside and outside the ILL. The most important one for the majority of the college members was the approaching reactor startup. As a consequence, the reinstallation of the instruments and their preparation for the user oriented operation became a clear priority before experiments at other neutron sources. The impact of this time consuming task was particularly sensed in the College 4 as all of the three axis instruments operated by ILL are placed in the reactor hall and hence directly affected by the reactor reconstruction.

Despite the increased workload the college members continued their scientific activities whose scope ranges, similarly to preceding years, from phonon physics to magnetic excitations and phase transitions in a variety of types of compounds. Some of the results are reported on the following pages.

The movements on the college member list involved E. Garcia Matres who finished her thesis early in 1994 and Steve Bramwell who left ILL for a post in England by the end of summer. After years marked by the departures of numerous colleagues it is a particular pleasure to announce the return of Jacques Bossy (CNRS Grenoble) and the new arrivals of Bertrand Roessli (PSI Würenlingen), Niels Pyka (LLB Saclay) and Helmut Schober (KFA Karlsruhe) having started their five year contracts at ILL in April, July and October, respectively.

Scientific Trends and Highlights in 1994

Anomalies in the lattice dynamics of Pr_2CuO_4

Within the scope of the investigation of the lattice dynamics of superconducting cuprates and their parent non-sc compounds, the phonon dispersion curves along the main symmetry directions in a single crystal of Pr_2CuO_4 [1] were studied at the Orphée reactor at LLB, Saclay. Pr_2CuO_4 is the first member of the series of rare-earth cuprates which crystallizes in the T' -phase (R_2CuO_4 , $\text{R} = \text{Pr, Nd, Sm, Gd}$) having a tetragonal structure without a structural phase transition. Generally the observed phonons are well defined and can be described by a shell model with only nearest-neighbour forces of the Pr-O, Cu-O, O-O and Pr-Cu pairs. Rigid ion models lead to a relatively large number of parameters and a larger overall error than in the case of shell models due to the fact that a strong polarisability of the oxygen atoms has to be taken into account. In addition to the short range Born-von-Kármán forces long range Coulomb forces are indispensable which is expressed by the large Lyddane-Sachs-Teller splittings observed in this compound and characterising a strong ionic isolator.

The system was examined for the instability of the rotational mode of the Cu-O(1) square lattice, observed earlier in Nd_2CuO_4 , and a frequency some 20% above the value of Nd_2CuO_4 was found with harmonic phonon line shapes but being close to a strong crystal electric field excitation which complicated the measurement considerably. These observations are consistent with the assumption that the lanthanide contraction plays the essential role for this latent structural instability of the T' -phase.

An anomalous softening of the B_{1g} -mode ($\nu = 8.95$ THz) of Pr_2CuO_4 has been observed at low temperatures by inelastic neutron scattering, corroborating the Raman spectroscopy results [2] at the Brillouin zone center. This softening is extended over a wide q-range in the a-b plane and along the c-axis (Fig. 1). According to our analysis, the corresponding displacement pattern is an out-of-phase vibration of facing O(2) atoms, leading to washboard-like distortions of the O(2) planes. The energy of this warping mode is some 10% below the corresponding value of Nd_2CuO_4 and the thermal parameter U_{33} of the O(2) atom is some 15% larger. From a neutron diffraction analysis and from the comparison of typical interatomic distances one furthermore learns that the Pr-O(2) bond is under compression. These results strongly suggest that Pr_2CuO_4 is on the border of a lattice instability where the O(2) atoms tend to occupy the apical position of the Cu-O octahedra of the T-phase rather than the planar arrangement of the T' -phase.

The B_u -mode at $\nu = 7.75$ THz has an analogous displacement pattern to B_{1g} , but in this case the O(1) atoms are out-of-phase elongated along c. In a restricted q-range in the basal plane this mode has an anomalous temperature dependence ($d\nu/dT < 0$) too. The corresponding thermal

parameter U_{33} of the O(1) atom is significantly larger than in Nd_2CuO_4 which means that also the basal-plane oxygens have the tendency to disorder along c . In contrast, the dispersion curves linked to the E_{1u} and E_{2u} modes (in-plane O(1), O(2) elongations, respectively) become more stiff at low temperatures, i.e. they are not affected and behave quite normally.

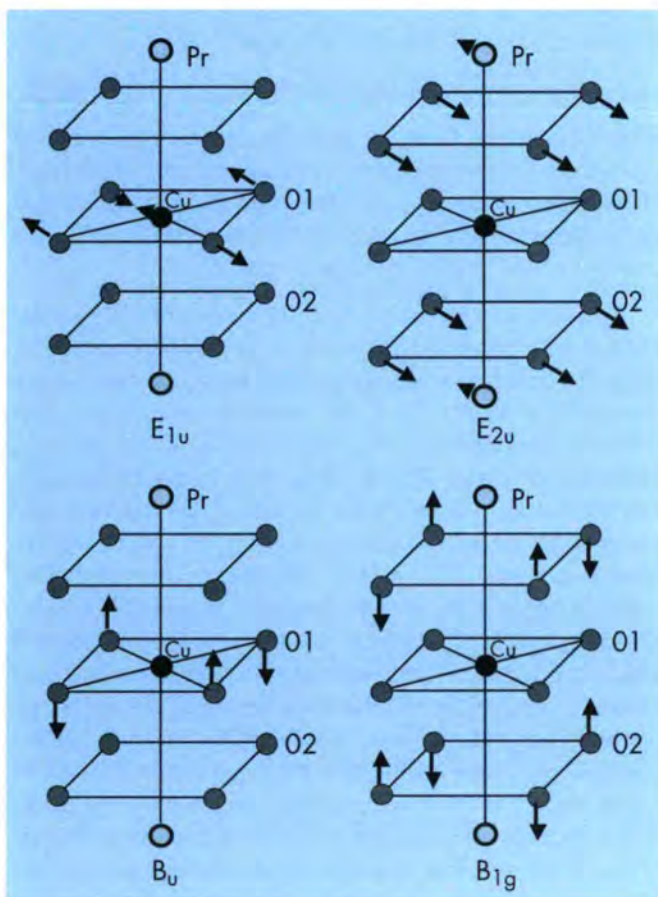
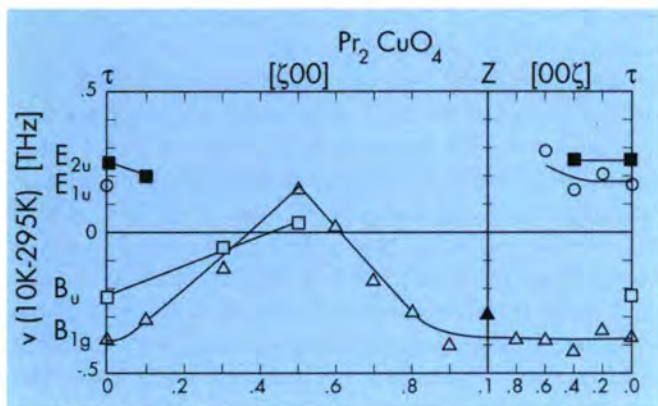


Fig. 1: (a) The Q -dependence of the frequency shift of selected modes along the $[100]$ and $[001]$ directions in Pr_2CuO_4 ; the lines are guides to eye only.

(b) The displacement patterns of the four Γ -point modes from Fig. 1a. The relative lengths of the vectors correspond to each other, displacements of minor importance are suppressed.

Quantum paramagnetic fluctuations in RbFeCl_3 in an applied magnetic field

RbFeCl_3 belongs to the family of AFeX_3 compounds where the Fe^{2+} -ion has an effective spin $S = 1$ and is described by the Hamiltonian:

$$H = \sum_{ij} \left\{ [D(S_i^z)^2 - g\mu\mathbf{H}\mathbf{S}_i] \delta_{ij} - J_{ij}\mathbf{S}_i\mathbf{S}_j \right\},$$

where the sum is running over the spin sites arranged in a triangular lattice within the basal plane and forming chains along the c -axis. The single site part of the Hamiltonian contains two terms. The first one describes the strong uniaxial anisotropy characterised by the constant D , and the second corresponds to the Zeeman splitting in an applied magnetic field H . For $H = 0$ the single site level scheme consists of a singlet ground state ($m = 0$) and a degenerate excited doublet state ($m = \pm 1$). This degeneration is lifted in an applied field. If the applied field H_{\perp} is perpendicular to the c -direction the eigenfunctions of the triplet states become linear combinations of the $m = 0, \pm 1$ functions. Therefore none of the local spin projections is a conserved quantity anymore and on-site magnetisation fluctuations persist even in the limit $T \rightarrow 0$.

Exchange interactions are positive in the direction along the c -axis, $J_{ij} = J_1 > 0$, and negative in the basal plane, $J_{ij} = J' < 0$. They couple the neighbouring spins and lead from a discrete spectrum to three branches of collective excitations. At low temperatures, however, only two of them can be excited. For one of the excited modes the magnetisation fluctuations are polarised parallel to the field direction, while these fluctuations for the other one are polarised in the plane perpendicular to the field. These two modes have different dispersion curves and depend on the direction of the mode propagation. Thus, the collective excitations propagating along the chains are of the ferromagnon type. On the contrary, in the basal plane the Fourier transform of the exchange integral $J'(q)$ shows quite pronounced minima at the wave vectors $q = (1/3, 1/3, 2\ell)$, $\ell = \text{integer}$, which correspond to the antiferromagnetic frustrated type of correlations of the staggered magnetisation fluctuations at the neighbouring sites. Below 2.50 K the system exhibits long range order which is driven by the mode softening at the points $(1/3, 1/3, 2\ell)$ corresponding to the frustrated 120° magnetic structure.

The main goal of the present experiment was to study the paramagnetic quantum fluctuations in the simplest case, i.e. far away from this phase transition. It should lead to a better understanding of the general structure of these fluctuations and of the role of the fluctuational corrections renormalising their spectrum and their amplitudes. The experiment at 5.5 K up to 5.5 Tesla was performed at LLB Saclay in December 1993. Fig. 2a presents a part of the measured and calculated dispersion curves (for the direction perpendicular to the c -direction) [3]. In the theoretical approach the values of the parameters D , J_1 and J' as determined from a fit to the experimental data at $H_{\perp} = 0$ were kept fixed. The renormalisation of these parameters due to the quantum fluctuations was introduced by additional field dependent

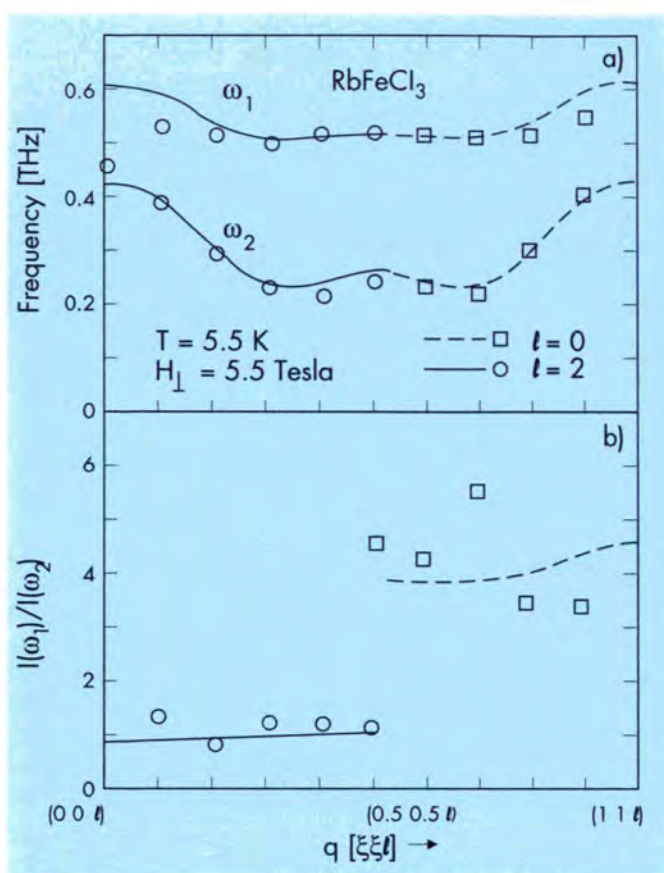


Fig. 2: Magnetic excitations in RbFeCl_3 ; a) dispersion curves of the two modes and b) the ratio of their intensities. The lines are calculated from the theory by Toperverg [3]. Data and calculations for $\xi \leq 0.5$ correspond to $l = 2$ and the ones for $\xi \geq 0.5$ to $l = 0$.

parameters and fitted to the data. A satisfactory quantitative description of the spectrum was reached. The validity of the theoretical approach was tested further by calculating intensities without introducing any additional parameters. Fig. 2b shows the ratios of the intensities which were plotted instead of absolute intensities to eliminate the influence of sample volume and size, absorption, magnetic form factor etc. The agreement between experiment and calculation is satisfactory, if one takes into account that intensities are much more difficult to determine than frequencies. On the other hand the reproduction of intensities is a very sensitive probe to a theory.

Cu spin excitations in Pr_2CuO_4

The magnetism of two-dimensional Cu-O layers in the high temperature superconducting cuprates has attracted considerable interest ever since the antiferromagnetic ordering was reported in the parent compound La_2CuO_4 [4]. All these materials are characterised by a strong, nearly isotropic, nearest-neighbour exchange coupling within the layer and a much weaker interlayer coupling. The Cu spins provide one of the best physical realisations of a two-dimensional quantum Heisenberg antiferromagnet - a system of central importance itself in the study of the quantum magnets.

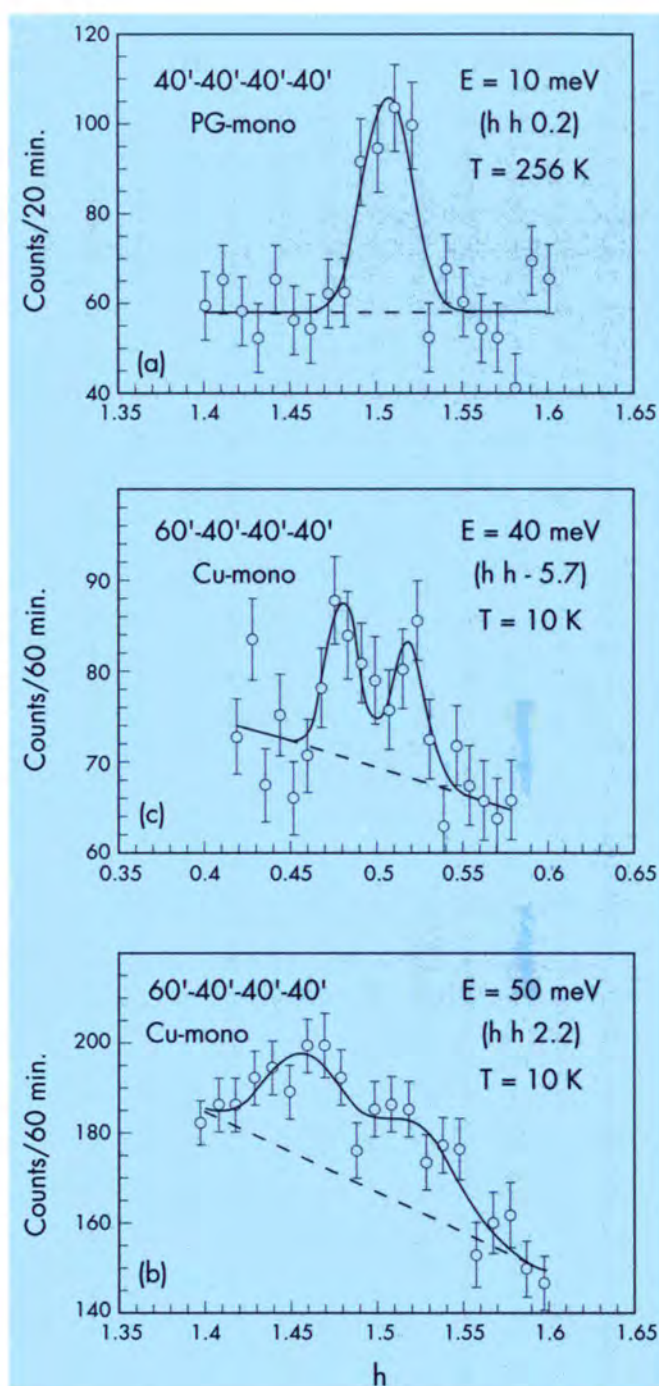


Fig. 3: Typical constant-energy scans for 10, 40, and 50 meV. Solid lines are results from Gaussian fits and dashed lines are the fitted background. The two clearly-resolved peaks shown in (b) and (c) correspond to the $+q$ and $-q$ magnon branches, which are not resolved in (a) because of the closer spacing of the spin waves and coarser instrumental resolution employed.

The Cu spin dynamics was investigated in the parent insulating compound Pr_2CuO_4 of the electron-doped superconductor on a rather large single crystal of weight of about 7 g by inelastic neutron scattering at the NIST reactor [5]. The non-collinear spin structure of the tetragonal R_2CuO_4 compounds consists of four sublattices and therefore the spin waves consist in general of four branches.

All of the four branches propagating in the a-b plane are degenerate and highly dispersive, with a spin wave velocity which is expected to be very large as found in other cuprate materials. Due to the very steep nature of the dispersion propagating in the a-b plane, it was necessary to make measurements of the spin wave velocity with the constant-energy technique, in order to resolve the +q and -q spin wave branches. Fig. 3 shows typical constant energy scans for $\Delta E = 10, 40$ and 50 meV. The two clearly resolved peaks at 40 and 50 meV correspond to the +q and -q magnon branches. The Cu spin wave velocity has been determined from these data to be 0.85 ± 0.08 meV \AA , which corresponds to an in-plane nearest-neighbour exchange constant $J = 130 \pm 13$ meV. This value agrees well with that determined from the temperature variation of the inverse correlation length above the ordering temperature.

Finite size effects in antiferromagnetic chains

Quite particular finite-size effects have been predicted and observed in the spin $S = 1$ Heisenberg antiferromagnetic chain. While it is known that the bulk excitations can only occur above a collective (Haldane) gap, the chain ends possess low lying excited states that merge into the ground state at the thermodynamic limit. In a first approach such excited states are revealed as "free" spins located at the chain ends. At low temperatures interactions between these chain end states become visible as it has been demonstrated by the deviation of susceptibility and magnetisation from usual H/T scaling (Brillouin behaviour) [6,7]. The observed properties are partly explained by random exchange models, for example the susceptibility follows a power law $\chi \sim T^{-a}$, where a ≈ 0.6 was observed in the spin $S=1$ quasi-1D

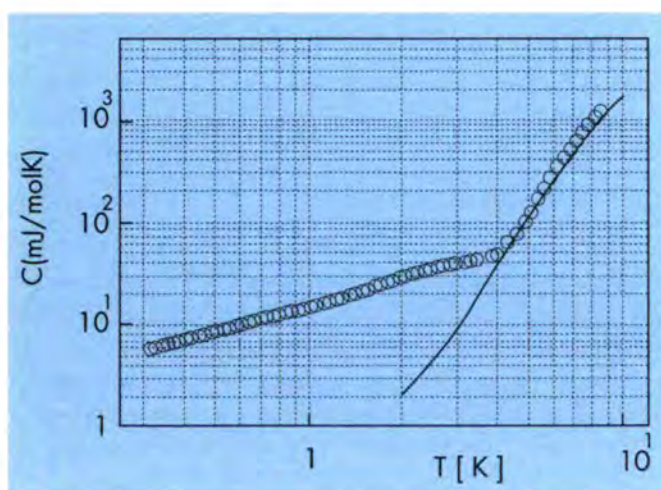


Fig. 4: The specific heat of the quasi-1D antiferromagnet AgVP_2S_6 (open circles) with the rather small Debye contribution subtracted (measured by C. Marcenat, R. Calemczuk, CEA-DRF/MC-Laboratoire de Cryophysique). The excess magnetic contribution dominates at low temperatures but merges in the lattice contribution due to a low-lying optical mode at around $T = 5\text{K}$. The latter can be estimated using the generalized phonon density-of-states from neutron data (solid line).

Heisenberg antiferromagnet AgVP_2S_6 . A related behaviour should appear in the low-T specific heat: $C \sim T^c$, with $c = 1-a$. In the case of AgVP_2S_6 , displayed in Fig. 4, the excess magnetic contribution is dominating at low temperatures but the observation range is limited from above due to a strong increase originating from low lying optical-type lattice modes. The corresponding peak is clearly visible in the generalised phonon density-of-states obtained from neutron data, and the form of the lattice contribution to the specific heat is well reproduced by the curve calculated using the experimental density-of-states. In the low-T range the magnetic specific heat follows a power law T^c , with $c = 0.88$. The relation connecting the specific heat and susceptibility exponents, predicted by random exchange models: $c = 1-a$, is not observed.

Critical dynamics in CdCr_2S_4

An investigation of critical dynamics in the CdCr_2S_4 insulating ferromagnet was undertaken by means of both triple-axis and spin echo measurements. Recently, new theoretical developments on magnetic critical dynamics led to a revival of interest in this field, which was one of the hot topics in the seventies. For ferromagnets, the predicted value $5/2$ of the critical exponent z was experimentally verified at that time; measurements as a function of temperature were also performed in order to check the Resibois-Piette scaling function. The spin echo technique appeared to be a very powerful tool, as it allowed to extend the accessible momentum transfer range towards low q values, thanks to its high energy resolution. It is just at low q 's, where dipolar effects become relevant; a measure of their strength is the dipolar wave number q_d , which delimits the exchange and dipolar regimes. When decreasing the momentum transfer and entering the dipolar regime, a crossover was therefore expected, from $z = 5/2$ to the $z = 2$ value associated with a nonconserved order parameter. Experimentally, this crossover has not been observed yet. On the other hand, theories based on short range magnetic interaction only, predict a non exponential spectral function $F(q,t)$; again, this was not observed when probing EuO dynamics using spin echo technique. This point is now understood as mode coupling calculations including dipolar interaction showed that the crossover from exchange to dipolar behaviour also concerns the $F(q,t)$ line shape, which should be exponential below q_d . They also predicted the change in z to occur only close to $q_d/10$. Triple axis measurements performed at high q values on EuO and EuS ($q_d \approx 0.27 \text{\AA}^{-1}$) evidenced non Lorentzian quasielastic line shapes. But, due to its small dipolar wave number ($\approx 0.05 \text{\AA}^{-1}$), the ideal system for testing, over a large q range, the theoretical predictions concerning critical dynamics in the exchange regime, appears to be the insulating ferromagnet CdCr_2S_4 . Three axis experiments were performed both at the ILL and Risø National Lab. The data were successively fitted assuming first a Lorentzian spectral function $F(q,\omega)$, and then the model calculated by Iro [8] in the frame of the renormalisation group (RG) theory. Fig. 5 presents the results of these two adjustments, for a spectrum recorded at

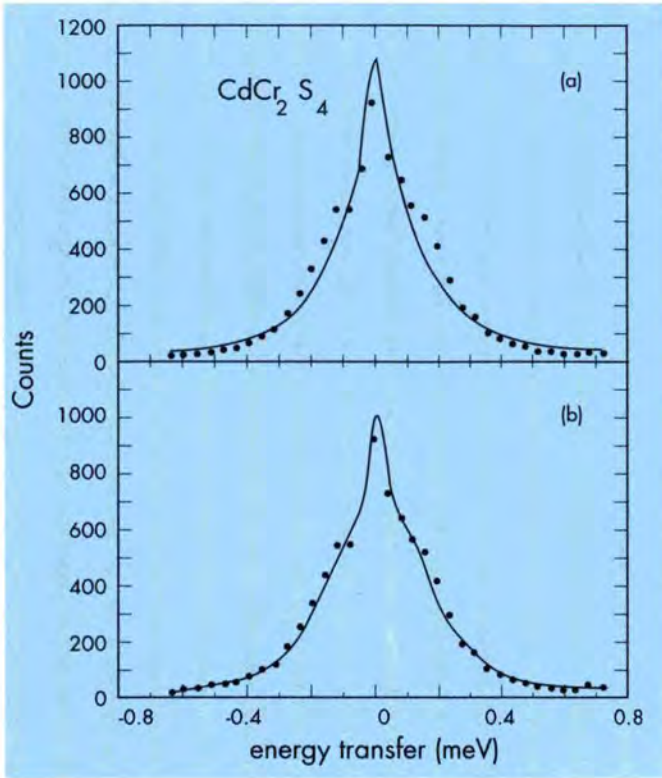


Fig. 5: Quasielastic critical scattering recorded at $T_C=84.3K$ and $q=0.14 \text{ \AA}^{-1}$. The solid lines result from three contributions: the convolution of the adjusted model with the instrumental resolution, the Gaussian profile of elastic incoherent scattering and the measured inelastic background; (a) Lorentzian model and (b) exchange regime renormalization group model.

$T_C = 84.3 \text{ K}$ and $q = 0.14 \text{ \AA}^{-1}$, on the cold neutron spectrometer IN14, at the ILL. Departure from a Lorentzian behaviour is obvious, as well as the excellent agreement obtained with the RG model. This last point was verified in the whole probed q -range ($0.06 - 0.20 \text{ \AA}^{-1}$). From these measurements, the value of the z exponent was deduced (2.52 ± 0.05), and the RG scaling function verified up to $1/q\xi \approx 0.6$ [9]. A preliminary spin echo experiment was also performed at LLB. The data were analyzed considering the $F(q,t)$ function calculated by Folk [10], in the frame of the mode coupling theory. The promising results which were obtained should be confirmed by more precise forthcoming measurements.

Heavy fermions and/or valence fluctuation systems

The two characteristic properties of heavy fermion and valence fluctuation compounds viz. the constant low temperature bulk susceptibility $\chi(o)$ and the linearly temperature dependent specific heat ($=\gamma T$) at low T 's are closely comparable in magnitude for the two cubic Yb-based compounds YbInAu_2 and YbAl_3 ($\chi(o) = 4.85 \times 10^{-3}$ and $4.62 \times 10^{-3} \text{ emu mole}^{-1}$; and $g = 40$ and $39 \text{ mJ mole}^{-1} \text{ K}^{-2}$ respectively). Paramagnetic scattering from YbInAu_2 was investigated on IN4 (Fig. 6a) with the aim to compare it with that from YbAl_3 (Fig. 6b) which showed a peculiar 'gap-

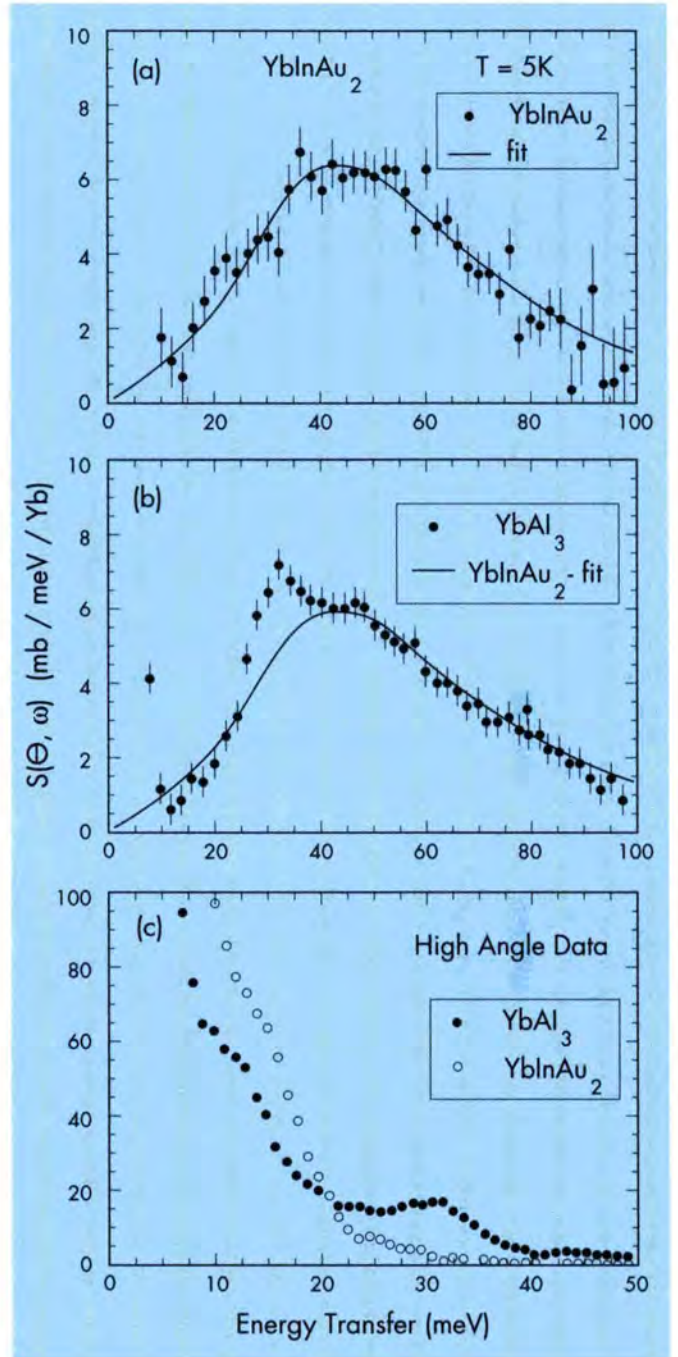


Fig. 6: Magnetic spectral response of YbInAu_2 at $5K$ (a). The solid curve represents a least-squares fit to the KMH single-ion spectral function for an Anderson impurity. Low temperature paramagnetic spectral response of YbAl_3 at $5K$ (b). The solid curve represents a "superposition" of the fit to the YbInAu_2 data by a slight adjustment of the vertical amplitude. High angle data representing scattering by phonons, plotted on an expanded energy scale (c). The marked hump due to optic phonons in YbAl_3 around $\sim 30 \text{ meV}$ contrasts with the weaker structures at lower energies observed in YbInAu_2 .

like' spectral response, with an energy "gap" of ~ 32 meV, in measurements performed almost a decade ago as well as more recently [11]. In contrast to YbAl_3 the magnetic response of YbInAu_2 shows the commonly observed inelastic Lorentzian, also well described by the single ion Kuramoto Müller-Hartmann spectral distribution calculated within the Anderson impurity model [12]. The solid curve in Fig. 6a represents a least-squares fit to the KMH function which yields a characteristic Kondo energy of 35 ± 1 meV. Also, the same curve (with the same spectral parameters) can describe fairly closely the YbAl_3 data above 40 meV. The 'fit' is shown in Fig. 6b where only a slight adjustment of the vertical amplitude is required to superpose the least-squares fit obtained for YbInAu_2 on to the YbAl_3 data.

Fig. 6c shows the high angle data representing mainly phononic contribution for both samples, since the magnetic contribution is relatively weak at high Q 's due to the magnetic form-factor. Presence of high energy optic phonon modes in YbAl_3 represented by the marked hump situated ($\omega \geq 30$ meV) close to the Kondo energy of the system, and their apparent absence at similar energies in YbInAu_2 where they are presumably lower lying, consistent with the higher masses of In and Au atoms relatively to the Al, suggests that some form of electron-phonon (magneto-vibrational) coupling may be responsible for "distorting" the spectral shape in YbAl_3 to its peculiar "gap-like" form. These observations are rather interesting and await theoretical input.

First results from Japanese three-axis spectrometer PONTA with spin-echo (TASSE)

This ILL-Japan collaboration led to the construction of a very successful Spin-Echo option for the Polarised Neutron Three-Axis spectrometer PONTA [13] of the Institute for Solid State Physics (ISSP), of the University of Tokyo located at the JAERI JRR-3M reactor. This thermal neutron TASSE delivers a relative energy resolution of nearly 10^{-5} .

The first real experiment performed in December 1994 was concerned with the investigation of the dynamics of an order-disorder phase transformation in KDCO_3 . Diffuse X-ray and neutron scattering experiments had evidenced the existence of diffuse streaks in the high temperature phase ($T_c = 80^\circ\text{C}$) condensing into sharp superlattice peaks. These diffuse streaks join normal Bragg peaks to superlattice reflections. Fig. 7 shows the critical dynamics behaviour of the relaxation time Γ of the shear motion of $(\text{CO}_3\text{-D-CO}_3)$ dimers in this material close to the order disorder transition.

A further critical effect was discovered in this experiment. Close to the normal Bragg peaks Huang-like diffuse scattering was observed. In contrast to normal Huang scattering which is elastic, the present observations show that this diffuse scattering is quasi-elastic in nature and hence arises from dynamical defects. The energy width of this diffuse scattering also decreases from $\Gamma = 15 \mu\text{eV}$ at $T_c + 20\text{K}$ to zero as the transition temperature is approached from above.

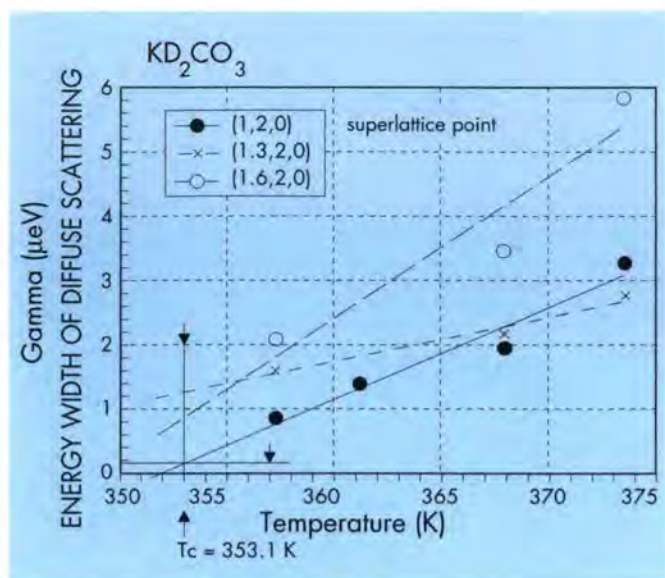


Fig. 7: The critical dynamics at different positions in reciprocal space on a line from the superlattice point (1 2 0) towards the Bragg peak (2 2 0). The full line corresponds to the scattering at the superlattice position and corresponds to the critical slowing down of the $(\text{CO}_3\text{-D-CO}_3)$ dimers. Towards the Bragg peak the diffuse scattering is Huang-like and shows different dynamics.

References

- [1] N.M. Pyka, A.S. Ivanov, M. Braden, W.Reichardt, A.Yu. Rumiantsev, N.L. Mitrofanov, to be published.
- [2] E.T. Heyen, R. Liu, M. Cardona et al., Phys. Rev. B43, 2857 (1991).
- [3] B. Toperverg, B. Dorner, A. Sonntag and D. Petitgrand, to be published.
- [4] R.J. Birgeneau and G. Shirane, in Physical Properties of High Temperature Superconductors I, edited by D.M. Ginsberg (World-Scientific, Singapore 1989).
- [5] I.W. Summerlin, J.W. Lynn, T. Chattopadhyay, S.N. Barilo, D.I. Zhigunov and J.L. Peng, Phys. Rev. B51, 5824 (1995) and references therein.
- [6] H. Mutka, C. Payen and P. Molinié, Sol. St. Commun. 85, 597 (1992).
- [7] H. Mutka, C. Payen and P. Molinié, J. Mag. Mag. Mat. (1994) to be published.
- [8] H. Iro, J. Mag. Mag. Mat. 73, 175 (1988).
- [9] S. Pouget and M. Alba, to be published.
- [10] C. Aberger and R. Folk, Phys. Rev. B38, 6693 (1988).
- [11] A.P. Murani Phys. Rev. Lett. 54, 1444 (1985); Phys. Rev. B50, 9882 (1994).
- [12] A.P. Murani and J. Pierre, Physica B, to be published.
- [13] C.M.E. Zeyen, M. Nishi, K. Nakajima, Y. Kawamura, S. Watanabe, K. Sasaki, T. Sakaguchi, K. Kakurai and Y. Endoh, Proceedings ICNS'94 to be published in Physica B.

Secretary: Jiri Kulda

Low-energy excitations of bucky-balls in solid compounds

H. Schober

Graphite and diamond are the two natural forms of carbon encountered on earth. While in graphite the carbon atoms are arranged in two-dimensional sheets they form a highly connected three-dimensional network in diamond. The recently discovered synthetic forms of pure carbon [1] differ from the natural species in that the atoms are grouped together in large molecular units. Out of this class of pure carbon molecules called *Buckminsterfullerenes* the one featuring sixty atoms (C_{60}) is outstanding in several respects. With the atoms placed at the vertices of a truncated icosahedron (see figure 1) it is not only the most symmetric but also the most readily available member. Due to its similarity with a soccer ball the C_{60} molecule is also referred to as bucky-ball. As can be seen upon inspection of figure 1 the surface of the bucky-balls consists of pentagons and hexagons. While the pentagons are regular, i.e. possess five-fold symmetry, the hexagons are not. This is due to the fact that the edges hexagons share among themselves are somewhat shorter than the ones they share with neighboring pentagons. At low enough temperatures the bucky-balls aggregate to form systems of well-defined translational symmetry (crystals), i.e. the center-of-mass positions of the bucky-balls form a regular three-dimensional network as the carbon atoms do in the case of diamond (see figure 2).

As the bucky-balls are not really spherical the crystal structure of these so-called *fullerites* is not completely solved unless we have determined the orientations of the molecules with respect to each other. "Are pentagons facing hexagons?" etc. is the kind of question we are led to ask. The situation is rendered even more complicated by the fact that these molecular orientations necessarily change with time due to thermal excitation. For sufficiently low temperatures this time dependence can be described by small-amplitude wobbling about well-defined mean orientations, in analogy to the motion of a disk suspended on a steel wire. The mean orientations correspond to equilibrium positions of the molecules with respect to the forces acting upon them. These equilibrium orientations are constant in time. However, they are not required to be identical for all, or for even a subset of molecules (long-range orientational order) but, to the contrary, may be distributed randomly among a more or less extended set of allowed values. In which case we are dealing with a statically disordered system.

At higher temperatures, orientational disorder may be created dynamically. In this scenario the molecules do no longer possess well-defined equilibrium orientations.

After sufficiently long time periods the bucky-balls have completely lost any memory of previous orientations. The angles the molecules tumble through may or may not be restricted to sub-sets of allowed values. Thus the molecular motion may resemble more or less that of a freely spinning sphere (no preferred orientations) or, to the contrary, better be viewed as a jump process (between preferred orientations). Depending on external

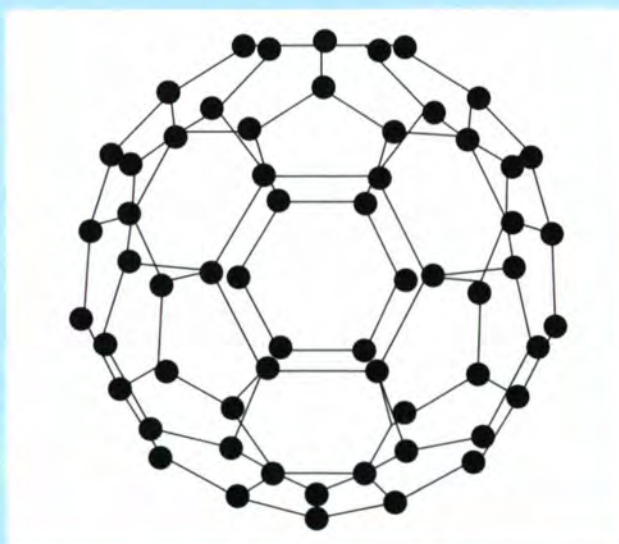


Figure 1: Schematic view of a C_{60} molecule. The carbon atoms occupy the vertices of a truncated icosahedron.

conditions like temperature and doping with guest atoms all of these possibilities are realized in fullerites [2]. This is part of the reason why they constitute one of the most fascinating topics of investigation in present-day solid-state physics.

In this article, we want to show how detailed information about the motion of the bucky-balls (intermolecular excitations) can be obtained using inelastic neutron scattering (INS). We will not be concerned with motions of the carbon ions involving a deformation of the bucky-balls. The deformation of the molecules requires such high energies (> 30 meV) that they do not appreciably perturb the molecular motions (< 10 meV). To put it into different words, in all that follows the bucky-balls can be considered stiff entities with no internal degrees of freedom.

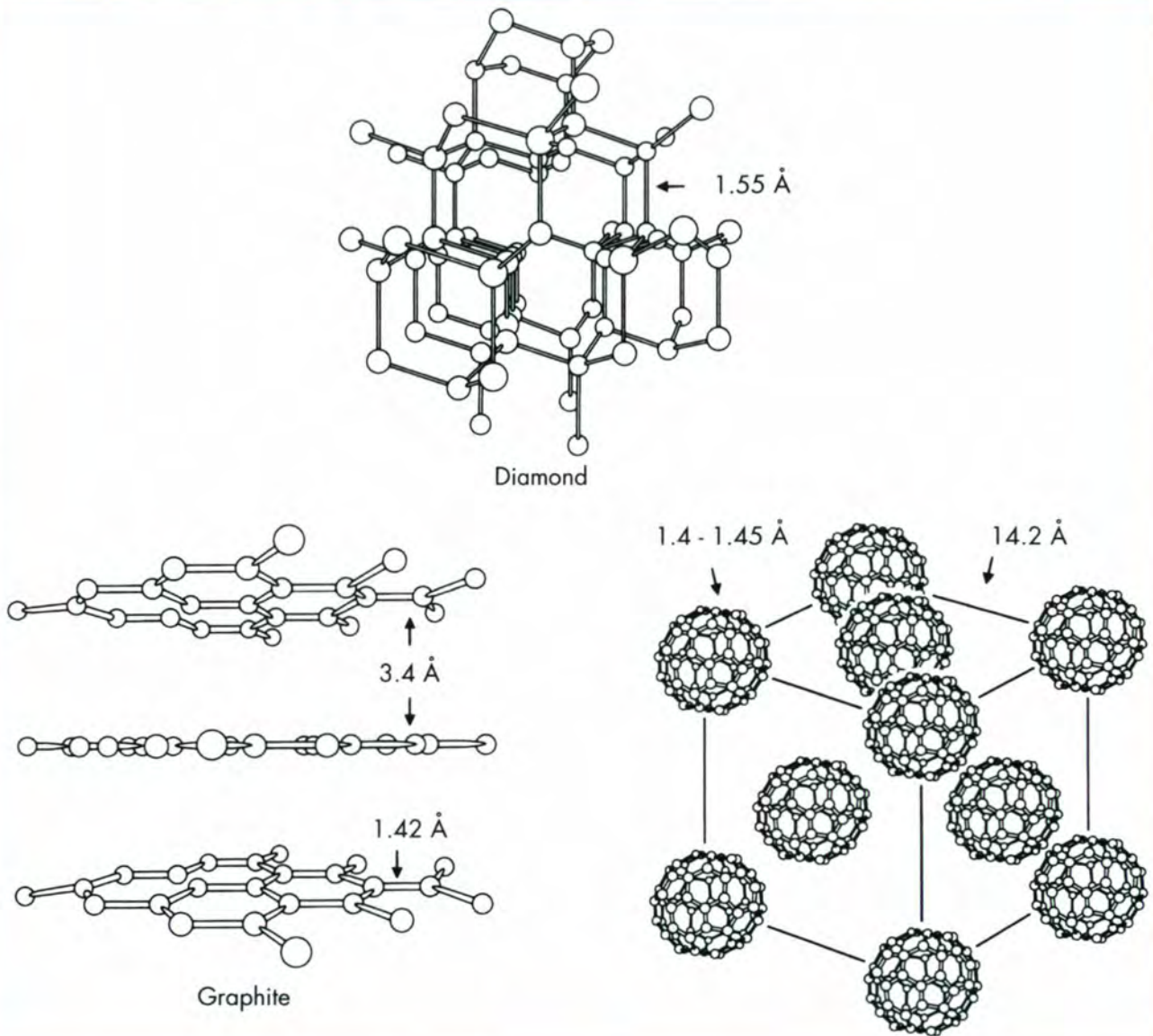


Figure 2: Representation of solid carbon forms: diamond, graphite and C_{60} in the fcc plastic phase (taken from [11]).

We want to point out that similar experiments as the ones described here have been carried out in parallel at the National Institute of Standards and Technology (NIST) [3] [4]. Both studies come up with essentially the same conclusions. The differences reside in the experimental techniques employed. While the NIST group used three-axis spectrometers for their investigations our measurements were done on a thermal time-of-flight machine.

Before discussing the dynamics we would like to make a remark concerning the five-fold symmetry of the molecules (evident in the pentagons of figure 1). It is, by

principle, impossible to construct a space-filling regular arrangement (crystals) of units possessing five-fold symmetries. Therefore, bucky-balls can, a priori, not form regular crystals unless they undergo deformation due to the fields arising from the crystalline environment. However, these deformation are extremely small due to the strong bonds acting between the atoms of a molecule. Even in the doped fullerides, where the effect should be enhanced by the additional (non-five-fold) crystalline field created by the guest atoms, the bucky-balls are found to be confined to the surface of a sphere. Noticeable deformation is only encountered within this surface [5].

In the room temperature face-centered cubic (fcc) phase (see figure 2) the deformation problem, mentioned above, is circumvented by a random distribution of

molecular orientations. This orientational disorder is achieved dynamically, i.e. by a perpetual reorientation of the molecules. INS measurements are particularly suited to gain insight into the details of this rotational motion. In figure 3 we present time-of-flight spectra of C_{60} powder collected with the Karlsruhe spectrometer at the Siloé reactor of the CENG in Grenoble [6]. For completeness we mention that the data have been summed over all scattering angles and were consecutively symmetrized using the detailed balance law. Above 260 K broad structureless contributions dominate the inelastic part of the spectra within the energy window $-6 \text{ meV} < \hbar\omega < 6 \text{ meV}$. This *quasi-elastic* scattering is a clear signature of uncorrelated molecular motion. This interpretation is confirmed by a detailed data analysis. A rotational diffusion model is capable of predicting both the shape (exemplified by a pseudo-line-width) and strength of the experimental signals (intensities) as a function of the moment $\hbar Q$ transferred from the scattered neutron to the C_{60} powder (see figure 4). In such a model the rotational movements of the molecules are assumed to be uncorrelated, each molecule undergoing a random-walk rotational diffusion. This is in perfect analogy to the random-walk translational diffusion of gas molecules (Brownian motion), with the main difference that the motion of a chosen carbon atom is confined to the surface of a sphere fixed in space while in the gas phase they may attain any point in three-dimensional space. The only parameter entering the above described model is the rotational diffusion constant D_r which comes out to be $1.8 \cdot 10^{10} \text{ s}^{-1}$, in very good agreement with nuclear magnetic resonance results. This value of D_r is quite remarkable. It is inferior by just a factor of three to what is expected for unhindered gas phase rotation (the hypothetical case of an isolated bucky-ball allowed

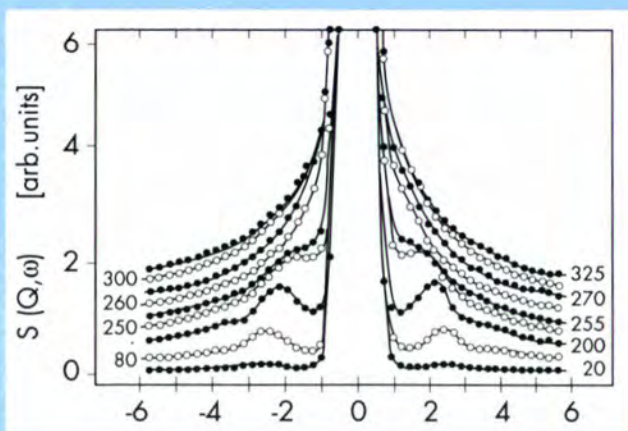


Figure 3: Symmetrized time-of-flight data for C_{60} powder at various temperatures integrated over the full range of scattering angles.

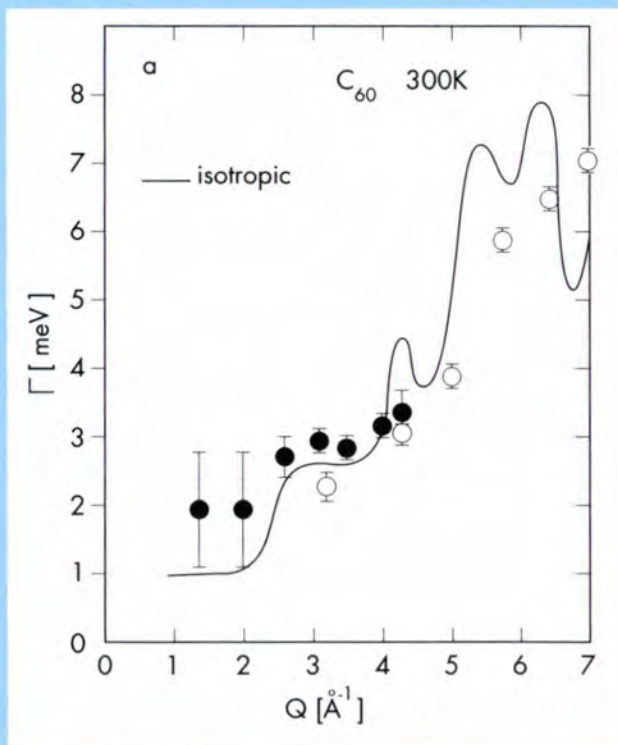
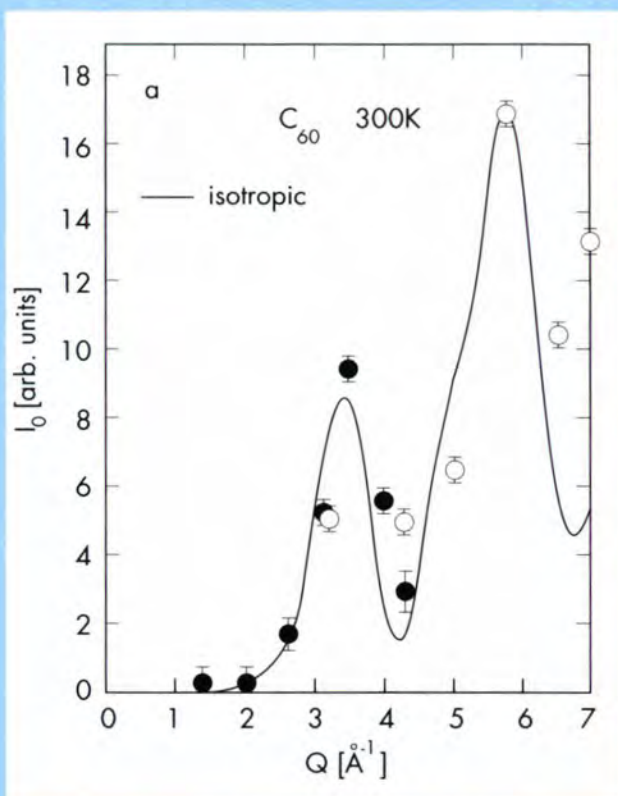


Figure 4: Intensity I_0 and pseudo-linewidth Γ of the quasi-elastic signal in the plastic phase of C_{60} as a function of wavevector transfer. The theoretical results obtained with a rotational diffusion model are given as full lines.

to spin freely in space) and larger than what is found for bucky-balls in organic solution [2]. The bucky-balls of a C_{60} crystal at room-temperature are, therefore, rotating practically unhindered by the energy barriers of the crystalline potential. For such a combination of translational order and rotational diffusion one has coined the expression *plastic crystal* [7].

Coming back to figure 3 we observe that below temperatures of about 260 K inelastic peaks emerge from the quasi-elastic intensities. These peaks become better defined and shift to higher energies as the sample is cooled down further. We are dealing with a transition from a plastic phase to a phase with preferred orientations. Details about this phase will be given later. The first-order nature of the transition is well exemplified by the fact that the inelastic peaks do not go continuously to zero but abruptly disappear at the transition temperature. Corresponding discontinuities can be observed in many other physical properties like e.g. the lattice constants. From the dependence of the intensities on momentum transfer and temperature it can be concluded that the inelastic peaks arise from small-amplitude rotational movements of the bucky-balls about well-defined equilibrium orientations. Due to the interactions between bucky-balls the motions of neighboring molecules are coupled, i.e. we are dealing with collective movements involving the ensemble of the crystal (librons). The center-of-mass vibrations of the bucky-balls (translational phonons) contribute also to the inelastic intensities, however, do not lead to peaks in the time-of-flight spectra. Details, concerning the phonons, will be given later in the discussion.

The low-temperature phase of C_{60} is no longer fcc but simple cubic (sc) with four molecules in the unit cell. The molecular orientation in the sc phase is not dictated by symmetry but depends on the potentials acting between the molecules. Actually besides the global minima there exist local side-minima in this inter-molecular potential (about 11 meV higher in energy). At elevated temperatures the molecules possess sufficiently high energies to overcome the separating barriers (≈ 200 meV) and populate these side minima. As we do not observe any signature of these jumps in the neutron data these must happen on time-scales not accessible to our instrument, i.e. long compared to 10^{-11} s. As the sample is cooled past 80 K about 15% of the molecules get trapped in the energetically unfavorable orientations. We are dealing with an orientational glass.

Due to the high connectivity of the three-dimensional bucky-ball network long-range orientational order (as given by the width of the Bragg peaks) is maintained in the sc phase despite the high concentration of

orientational impurities (molecules populating the side-minima). It is in this sense that we apply the expression *ordered phase*. As already mentioned above, the bucky-balls interact with each other and the low-energy rotational excitations in the ordered phase are, therefore, collective and their frequencies show dispersion, i.e. they depend on the wavevector. Given 4 molecules in the primitive cell of the ordered phase, each possessing six degrees of freedom, we get 24 elementary low-energy excitations for a given wavevector. Contrary to what was said about the separation into inter- and intra-molecular excitations a clear distinction between purely translational and rotational modes is not possible. Many inter-molecular modes constitute hybrids involving both types of motion. This can be easily understood on the basis of the close-packing of the bucky-balls. Due to the ruggedness of the molecules, which after all are not really spherical, their rotational movements may be appreciably facilitated - lowered in energy - if accompanied by a center-of-mass motion of neighboring molecules. This is what has to be understood under the expression of translational-rotational coupling.

As our measurements are performed on powder samples we integrate over whole regions in Q-space. This renders an interpretation of the signal width rather difficult. The width may arise from dispersion of the branches as well as from anharmonicities in the inter-molecular potential. Experiments carried out on single crystals [8] indicate that the anharmonic broadening is small compared to our energy resolution. This leads to some interesting questions concerning the origin of the libron mode softening as a function of temperature (≈ 1.7 meV at 250 K and ≈ 2.6 meV at 20 K see figure 3). In purely harmonic crystals the frequencies are independent of temperature. Anharmonicities lead to mode softening and such everyday phenomena as thermal expansion. The absence of anharmonic signatures in the single crystal data of C_{60} forces us to look for a different explanation of the libron softening. Part of the answer certainly has to be found in the coupling of rotational and translational excitations mentioned above. The center-of-mass movements of the bucky-balls modify the effective rotational potential seen by the molecules, making it softer as temperature increases. At low temperatures this potential is characterized, as discussed above, by appreciable energy barriers. These barriers are incompatible with the nearly free rotation of the bucky-balls observed in the plastic phase at room temperature. Further experiments, in particular, on single crystals will be necessary to come up with a detailed explanation of the order-disorder transition in fullerenes.

So far we did not analyse the details of the time-of-flight data but concentrate on its main features like the quasi-elastic scattering above 260 K and the emerging peaks at lower temperatures. This can be done by using the concept of the density-of-states. The density-of-states is the number of elementary excitations (phonons, librions) present in the system as a function of energy. It enters several important physical quantities like the specific heat or the electron-phonon coupling constant. While, due to the strong quasi-elastic contributions, it is impossible to determine a meaningful density-of-states in the plastic phase this poses no problem in the orientationally ordered phase. The density-of-states of C_{60} is shown in figure 5 for a sample temperature of 200 K.

Using the single crystal results [8] we are able to separate the phononic from the librionic contributions to the density-of-states (within the limitations imposed by the rotational-translational coupling). As can be seen the libron frequencies are not confined to the main band around 2 meV - prominent in the time-of-flight data of figure 3 - but there are side-bands at 3.5 meV and 5 meV. This result puts rather stringent conditions on the inter-molecular potentials governing the rotational motion of the bucky-balls.

As mentioned in the beginning, C_{60} crystals can be doped with a large variety of guest atoms. The dopants occupy the voids between the molecules. Putting atoms inside the bucky-balls is by far more complicated as, due to the high stability of the molecular cages, this can only be achieved during the formation process of the bucky-balls themselves. The best-known examples of intra-molecular doped fullerenes are alkali-metal compounds. We only consider crystals of stoichiometries A_3C_{60} and A_6C_{60} where A stands for rubidium (Rb) or potassium (K). A_3C_{60} crystals are metals with rather high superconducting transition temperatures (e.g. $T_c \approx 29$ K for Rb_3C_{60}), while A_6C_{60} crystals are insulators. The coupling between the charge carriers of the A_3C_{60} compounds (electrons located on the bucky-balls), responsible for superconductivity, is considered to be phonon mediated and of the BCS-type. Although the high transition temperatures favor a coupling by high-energy intra-molecular vibrations there exist several theories predicting contributions from the low-energy inter-molecular excitations. We have, therefore, undertaken a detailed study of these excitations [9]. The densities-of-states of both Rb_3C_{60} and K_3C_{60} are dominated by a strong peak arising from the small-amplitude rotations (librons) of the bucky-balls (see figure 5). Due to the additional interactions of the bucky-balls with the alkali-metal ions the rotational potentials are stiffer than in pure C_{60} shifting the librionic excitations to higher frequencies. Figure 5 shows also the

alkali-ion contributions to the low-frequency spectrum of the fullerides. As the alkali-ions occupy two symmetrically inequivalent sites in A_3C_{60} these contributions are denoted by A(1) (tetrahedral sites) and A(2) (octahedral sites), respectively. The single contributions to the over-all spectrum are the result of simple lattice-dynamical calculations. They should therefore be considered tentative, the over-all spectrum constituting the experimental result. While the libron peak of the A_3C_{60} samples softens appreciable between

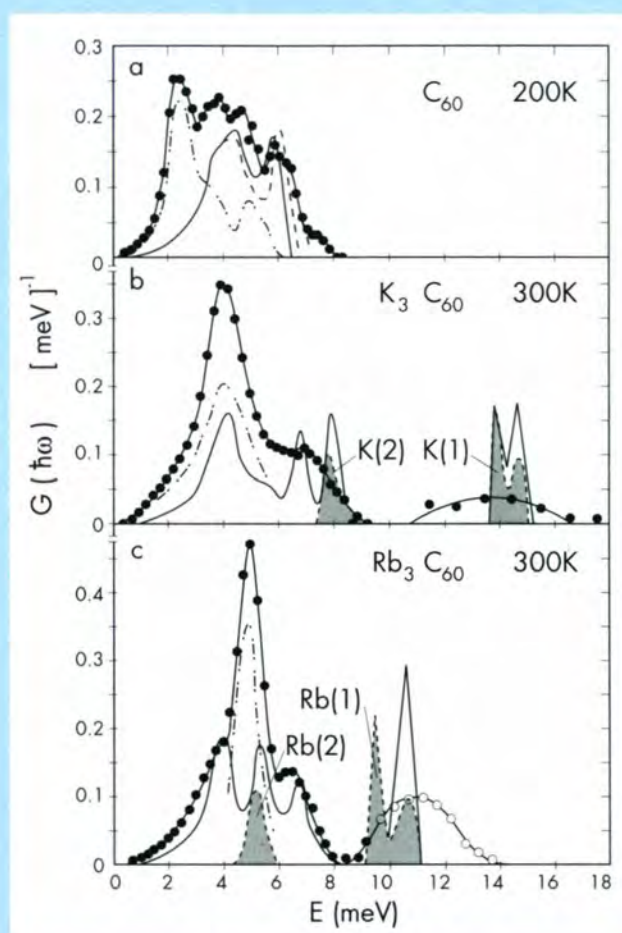


Figure 5: Intermolecular vibration spectrum for **a** C_{60} at 200 K **b** K_3C_{60} at 300 K and **c** Rb_3C_{60} at 300 K. The points constitute the experimental results (full dots from down-scattering, open dots from up-scattering experiments performed with an incident energy of 17.4 meV). Full lines indicate the translational contribution to the density-of-states as obtained from lattice-dynamical model calculations [9]. The extra broken line in 4a reproduces the translational contribution as extrapolated from the single crystal data [8]. The dash-dotted curves give an estimate of the distribution of librionic modes as obtained by subtracting the translational part from the experimental density-of-states. Hatched areas correspond to contributions involving alkali-ion modes (K(1), K(2) and Rb(1), Rb(2) distinguish the two inequivalent alkali-ion sites, see text).

70 K and room temperature no such softening can be observed in the A_6C_{60} systems. Thus the superconducting samples show a tendency to develop a plastic phase in analogy to pure C_{60} . However, crude extrapolations indicate that the systems will break-up before this phase transition can actually happen. No trend towards a plastic crystal is observed in the insulating alkali-metal fullerides at temperatures below 300 K. So far a comprehensive theoretical description of the low-frequency excitation spectrum in fullerides is missing. Due to the close-to-spherical symmetry of the bucky-balls the rotational spectrum is very sensitive to the details of the inter-molecular potentials rendering many theoretical approaches inappropriate. The problem is enhanced by the strong temperature effects. Rotational disorder phenomena - already mentioned in connection with pure C_{60} - add further difficulty to carrying-out lattice-dynamical calculations. Just as an example we want to mention merohedral disorder in doped fullerides. In A_3C_{60} compounds the bucky-balls arranged in a face-centered lattice randomly assume one out of two inequivalent orientations, while they are orientationally ordered in the body-centered A_6C_{60} compounds.

We hope to have shown that the dynamics of fullerenes constitutes a rich and extremely fascinating domain of scientific investigation. Although an appreciable amount of physical insight has been gained over the last years, there is still ample space for both experimental and theoretical progress. One should not forget that the chemistry of bucky-balls is still in its early days and that new compounds are discovered on a regular basis. The latest in this series are quasi one- and two-dimensional crystals made up of C_{60} polymers [10] and further surprises surely lay ahead. The biological and pharmaceutical exploitation of the C_{60} properties has even just started.

References

- [1] Krätschmer, W., Lamb, L.D., Fostiropoulos, Huffman, D.R., *Nature* **347**, 354 (1990).
- [2] Heiney, P.A., *J. Phys. Chem. Solids*, **53**, 1333 (1992).
- [3] Copley, J.R.D., David, W.I.F., Neumann, D.A., *Neutron News*, **4**, 20 (1993).
- [4] Neumann, D.A., Copley, J.R.D., Reznik, D., Kamitakahara, W.A., Rush, J.J., Paul, R.L., Lindstrom, R.M., *J. Phys. Chem. Solids*, **54**, 1699 (1993).
- [5] Rosseinsky, M., David, B., *ISIS Annual Report 1994*, RAL, Chilton, Didcot (1994)
- [6] Renker, B., Gompf, F., Heid, R., Adelman, P., Heiming, A., Reichardt, W., Roth, G., Schober, H., Rietschel, H., *Z Phys. B* **90**, 325 (1993).
- [7] Prassides, K., Kroto, H.W., Taylor, R., Walton, D.R.M., David, W.I.F., Tomkinson, J., Haddon, R.C., Rosseinsky, M.J., Murphy, D.W., *Carbon*, **30**, 1277 (1992).
- [8] Pintschovius, L., Renker, B., Gompf, F., Heid, R., Chaplot, S.L., *Phys. Rev. Lett.* **69**, 2662 (1992).
- [9] Renker, B., Gompf, F., Schober, H., Adelman, P., Heid, W., Bornemann, H.J., *Z. Phys. B* **92**, 451 (1993).
- [10] Oszlanyi, G., Forro, L., *Solid State Communications*, **93**, 265 (1995).
- [11] Ramirez, A.P., *Condensed Matter News*, **3**, 9 (1994).

Crystal and Magnetic Structures

Members of the College at ILL

T. Baumbach	A. Magerl
S. Bramwell	S.A. Mason
P.J. Brown	G.J. McIntyre
J. Buckley	A.P. Murani
T. Chattopadhyay (ETH Zurich)	M. Nutley
P. Convert	B. Ouladdiaf
F. Fauth (PSI)	J. Pannetier
M.-T. Fernández-Díaz	S. Pouget
A. Filhol	P. Radaelli
H.E. Fischer	M. Reehuis
E. García-Matres y Cortes	E. Ressouche (CENG)
B. Hamelin	C. Ritter
A.W. Hewat	O. Schärpf
O. Isnard (UJF)	E. Suard
J. Kulda	F. Tasset
P. Langan	P. Timmins
M.S. Lehmann	C. Wilson
E. LeLièvre-Berna	C. Zeyen

External Members

M. Alba (CENG)	Å. Kvik (ESRF)
M. Anne (CNRS)	M. Marezio (CNRS)
R. Arons (CENG)	J.C. Marmeggi (CNRS)
M. Bacmann (CNRS)	E. Pebay-Peyroula (IBS)
J. Baruchel (ESRF)	C. Riekell (ESRF)
E.F. Bertaut (CNRS)	M. Schlenker (CNRS)
M. Bonnet (CENG)	J. Schweizer (CENG)
J.X. Boucherle (CENG)	J.L. Soubeyroux (CNRS)
A. Fitch (ESRF)	C. Vettier (ESRF)
D. Fruchart (CNRS)	T. Vogt (detached to BNL)
D. Givord (CNRS)	C. Wilkinson (EMBL)
C. Janot (UJF)	G. Zaccari (IBS)

Introduction

For most members of College 5, pure scientific activity was put on the back burner in 1994 as attention was focused on re-installing and testing the instruments in anticipation of the reactor restart. Careful scrutiny was made of safety aspects in implementation of the new security interlocks and procedures. Considerable time was also spent migrating to the new world of Unix and exploring its exciting graphics possibilities.

One happy aspect of 1994 has been a rejuvenation of the College with the arrival of several new scientists; Paul Langan, Henry Fischer, Paolo Radaelli, Eddy LeLièvre-Berna, François Fauth, Maria-Teresa Fernández-Díaz and Emmanuelle Suard. François, who is associated with PSI Würenlingen, is the first, we hope, of many CRG scientists. Autumn saw the rebirth of one College member, with Jane Brown now a long-term visitor in her role as Visiting

Professor at the Loughborough University of Technology. After three years of decline the student numbers are also now increasing. Claire Wilson, who is in the final stages of her thesis, has been joined by Jason Buckley and, at a distance, by Jacqueline Cole. We heartily welcome all these new members, and look forward to their active and stimulating participation in College life.

Alas, some of the College members on detachment during the shut-down did indeed succumb to the temptation of distant delights. We wish Juan Rodríguez-Carvajal and Manfred Reehuis many years of fruitful research in their new positions at LLB and HMI respectively.

It is a pleasure to congratulate Jean Pannetier on his receiving the Paul Pascal prize from the Académie Française for his work in solid-state chemistry. He describes one aspect of this work in this year's blue box for College 5.

The October subcommittee marked the return to a 'normal' scientific life within the College. The demand for beam-time was just as high as before the shut-down, with superconductors, hydrates and hydrides, and large structures, like zeolites, clathrates and fullerenes, being very popular in College 5a; metals and intermetallic compounds, high-Tc-like materials and molecular magnets the most popular in College 5b. ICNS '94 in Sendai, Japan, gave many members the opportunity to appraise the recent advances made at other sources, and to attract new proposers for future scientific subcommittees.

We were thrilled that Clifford Shull, the first pioneer of magnetic neutron diffraction, shared the 1994 Nobel prize in physics. In his honour we devote the scientific highlights in this year's College report to magnetic crystallography.

Scientific Highlights in 1994 Crystallography and Magnetism

The magnetic structure of the AF2 phase of Mn_5Si_3

The intermetallic compound Mn_5Si_3 , which at ambient temperature has the hexagonal $D8_8$ structure, undergoes a transformation to orthorhombic symmetry on cooling below 100 K. The orthorhombic cell is related to the hexagonal one by the transformation:

$$\mathbf{a}_{\text{orth}} = \mathbf{a}_{\text{hex}}; \quad \mathbf{b}_{\text{orth}} = \mathbf{a}_{\text{hex}} + 2\mathbf{b}_{\text{hex}}; \quad \mathbf{c}_{\text{orth}} = \mathbf{c}_{\text{hex}}.$$

In the absence of orthorhombic distortion $b_{\text{orth}} = \sqrt{3}a_{\text{orth}}$. The dependence of the lattice parameters on temperature in the range 4 to 300 K is shown in Fig. 1. Below the transition at 100 K $b_{\text{orth}} < \sqrt{3}a_{\text{orth}}$ but in a further transition at 66 K the distortion changes dramatically so that $b_{\text{orth}} > \sqrt{3}a_{\text{orth}}$.

It is known that the two distortive transitions are associated with magnetic ordering; at 100 K the paramagnetic phase orders to an antiferromagnetic phase (AF2) and at 66 K the AF2 phase transforms to a second antiferromagnetic phase AF1. The structure of the low-temperature AF1 phase has recently been redetermined using

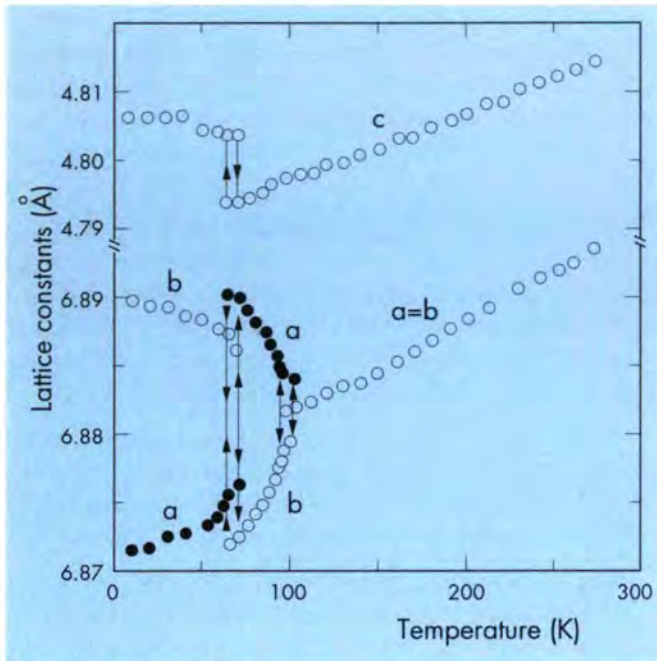


Fig. 1: Temperature dependence of the lattice constants of Mn_5Si_3 referred to the hexagonal cell.

neutron polarimetry and two different models have been proposed for the AF2 phase based on powder-diffraction studies in which the magnetic peaks were not well resolved. In these two models one site (Mn1), of the two nonequivalent Mn sites in the $D8_8$ structure carries the largest moment, although in the AF1 structure and in the isomorphous Mn_5Ge_3 compound the Mn1 atoms have lower moments than do Mn2.

Because of this apparent contradiction and because of the current interest in the stability of Mn moments the AF2 structure has been redetermined using a combination of high-resolution powder diffraction (IRIS at ISIS), single-crystal measurements (SXD at ISIS) and neutron polarimetry (CRYOPAD at ILL) [1]. The polarimetric measurements show unequivocally that the moment directions are confined to the a - b plane. The absence of any intensity in $h0l$ reflections with $h+l$ odd shows that, as in the AF1 phase, the vector sum of the moments projected down b_{orth} is zero. Combination of all the observations leads to the structure illustrated in Fig. 2. In this structure there is no moment on the Mn1 sites and only four out of the six Mn2 atoms carry moments. The coupling of the Mn2 moments of atoms at the same height in the cell is the same in the AF1 phase as in the AF2 phase but neighbouring Mn2 atoms which differ in height by $c/2$ are antiferromagnetically coupled in the AF2 phase whereas they are nearly perpendicular to one another in the AF1 structure.

With this arrangement Mn1-Mn2 coupling is completely frustrated, and accordingly at the AF1 to AF2 transition the Mn1 atoms lose their ordered moments. One may conjecture that the abrupt expansion of the c -axis observed on

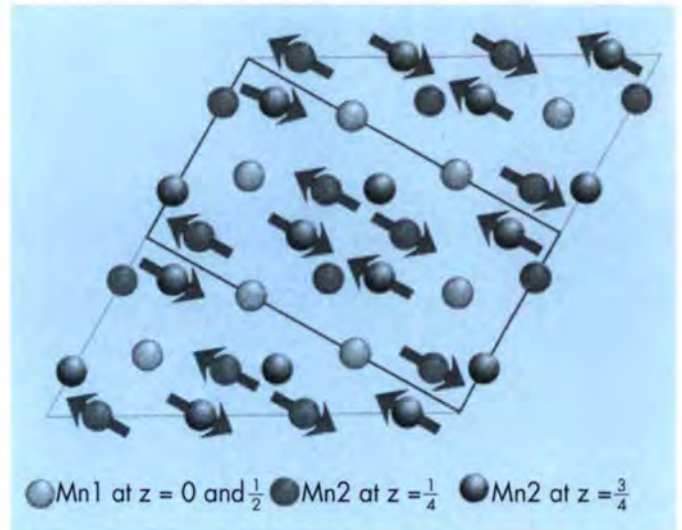


Fig. 2: Projection on the a - b plane of the magnetic structure of the AF2 phase of Mn_5Si_3 . Only the Mn atoms are shown.

transforming from AF2 to AF1 is due to the appearance of moments on the Mn1 atoms since the shortest Mn-Mn distance in the structure is that between the Mn1 atoms separated by $c/2 = 2.397 \text{ \AA}$ at 70 K. This separation is probably just below the limit required for stability of a Mn moment and has to increase to somewhat above 2.4 \AA when the Mn1 atoms acquire moments in the AF1 phase. The distortion $b_{\text{orth}} < \sqrt{3}a_{\text{orth}}$ must be characteristic of the antiferromagnetic Mn2-Mn2 coupling scheme, and the change to $b_{\text{orth}} > \sqrt{3}a_{\text{orth}}$ due to the establishment of Mn1-Mn2 magnetic coupling, but a detailed analysis must await determination of the changes in the structural parameters in the two transitions.

Diffuse magnetic neutron scattering in the frustrated antiferromagnet MnS_2

Valuable information about the magnetic interaction parameters and the mechanism of magnetic phase transitions can be obtained from diffuse magnetic neutron scattering investigations above the ordering temperature. This is because the diffuse magnetic neutron-scattering cross-section is directly proportional to the generalised wave-vector-dependent susceptibility tensor and thus measures the Fourier components of the microscopic magnetisation fluctuations.

A good example is the frustrated Heisenberg antiferromagnet MnS_2 which is based on a fcc lattice. The semiconductor MnS_2 orders at $T_N = 48 \text{ K}$ in a first-order phase transition to a type-III antiferromagnet with the wave vector $\kappa = [1 \ 1/2 \ 0]$. The magnetic moments are parallel to the cubic edge along which the chemical cell is doubled. To understand the first-order antiferromagnetic phase transition and to obtain information about the magnetic interaction parameters a study was made of the diffuse magnetic

neutron scattering in MnS_2 above T_N . The diffuse magnetic scattering was found to be centred at incommensurate positions corresponding to the wave vector $\kappa = [1 k_y 0]$ where k_y is temperature dependent. The component k_y increases continuously from 0.40 at $T = 115$ K to 0.44 at a temperature just above $T_N = 48$ K. At T_N , k_y locks into the commensurate value of $1/2$. Thus the first-order phase transition in MnS_2 can be understood as a lock-in transition from incommensurate magnetic short-range order to a commensurate long-range ordered phase.

The initial diffuse magnetic neutron-scattering investigations were performed at the ILL with a single detector and were necessarily confined to a small portion of the reciprocal space. After the unfortunate shutdown of the ILL reactor this investigation was continued on the flat-cone diffractometer E2 at BENSC [2]. This instrument is equipped with a multidetector which allowed very efficient scanning of larger parts of reciprocal space.

Fig. 3 (page 140) shows the scans on the $hk0$ reciprocal layer of MnS_2 at $T = 8.3$ and 51.9 K. At $T = 8.3$ K nuclear and magnetic Bragg peaks are observed along with some weak diffuse scattering. At $T = 51.9$ K, which is above the magnetic ordering temperature, strong diffuse scattering is observed. A careful examination reveals that the magnetic diffuse scattering is centered at incommensurate positions whereas the magnetic Bragg peaks are situated at commensurate positions corresponding to the wave vector $\kappa = [1 1/2 0]$. The diffuse magnetic scattering persists even at $T = 200$ K which is about four times the ordering temperature.

A second interesting aspect is the presence of diffuse scattering at $T = 8.3$ K well below T_N . This diffuse scattering is supposed to be due to magnetic excitations in the ordered magnetic phase. It would be interesting to investigate the temperature dependence of this scattering up to T_N .

Magnetic coupling in $R_6\text{Mn}_{23}$ compounds

$R_6\text{Mn}_{23}$ compounds, where R = rare earth, crystallise in the $\text{Th}_6\text{Mn}_{23}$ -type structure which is fcc with space group $\text{Fm}\bar{3}\text{m}$. The R atoms are located on the 24e site while the Mn atoms occupy four non-equivalent sites, namely 4b, 24d, $32f_1$ and $32f_2$. The $R_6\text{Mn}_{23}$ compounds, with $R = \text{Er, Dy, Tb}$ or Ho , order ferrimagnetically around 420 K. Powder diffraction experiments were carried out using D1A installed at LLB Saclay (for $R = \text{Er}$ and Dy) and DN5 at Siloé (for $R = \text{Tb}$ and Ho).

In all patterns the observed diffraction peaks could be indexed in the space group $\text{Fm}\bar{3}\text{m}$, i.e. only reflections with hkl all even or all odd are observed. The magnetic contribution to the diffraction pattern is superimposed on the nuclear peaks ($\kappa = [000]$). At room temperature excellent agreement is obtained between calculation and observation when using a collinear ferrimagnetic arrangement along the $[111]$ direction. The R moments are ferromagnetically

coupled to the Mn moments at the $32f_1$ and $32f_2$ sites which are in turn coupled antiferromagnetically to the remaining Mn moments (24d and 4b sites). The low-temperature patterns show the same Bragg peaks. However, the intensity of some peaks increases strongly in a way that cannot be explained by a collinear configuration.

The low-temperature magnetic structure is in fact umbrella-type around the $[111]$ direction for the R moments and collinear ferrimagnetic for the Mn moments also along $[111]$. It can be described by the basis functions of the three-dimensional irreducible representation Γ_{5g} of space group $\text{Fm}\bar{3}\text{m}$ associated with the wave vector $\kappa = [000]$ [3].

Polarised-neutron diffraction on Y_6Mn_{23} had given evidence of ferrimagnetic coupling in this compound [4]. The moments on the $32f_1$ and $32f_2$ sites are ferromagnetically coupled and are antiparallel to the moments at the 24d and 4b sites. Magnetisation and torque measurements indicated a very weak magnetocrystalline anisotropy, the easy axis being $[111]$. For $R_6\text{Mn}_{23}$ ($R = \text{Er, Dy, Tb}$ and Ho) the values of the Mn magnetic moments are still close to those obtained for Y_6Mn_{23} . The differences in moment values can be associated with the dependence of the exchange interaction on the Mn-Mn interatomic distance. The Curie temperatures of all the $R_6\text{Mn}_{23}$ compounds are very similar, therefore the Mn-Mn interactions are predominant in comparison with the Mn-R and the R-R ones.

At room temperature, the collinear order of the R moments arises from the exchange field of the surrounding Mn moments. If the R-Mn(24d) interactions are predominant, the R-Mn coupling is then identical to that encountered in other 3d-4f compounds where the 3d-3d interactions are positive. With decreasing temperature the R moments become non collinear, while the Mn moments remain along the $[111]$ direction. The local symmetry of the R environment is axial (4mm) and corresponds to the cell axis on which the R atom in question is located. The crystal-field Hamiltonian can be written as:

$$H_{cf} = \alpha V_2^0 O_2^0 + \beta (V_4^0 O_4^0 + V_4^4 O_4^4) + \gamma (V_6^0 O_6^0 + V_6^4 O_6^4)$$

where α, β, γ are the Stevens coefficients; $O_2^0 \dots$ are equivalent operators, which represent complicated expressions of the total momentum J and its projections J_x, J_y, J_z ; $V_2^0 \dots$ characterize the environment of the rare earth. For both O_4^0 and V_4^0 the lower index indicates the order in the expansion. Depending on the value of α , the easy direction is along or perpendicular to the local symmetry axis. For Er α is positive, while it is negative for Dy, Ho and Tb . In the case of $\text{Er}_6\text{Mn}_{23}$, the Er moments tend to be along the local four-fold axis. This tendency competes with the Er-Mn interactions which tend to maintain the Er moments along the Mn magnetisation direction. In the case of $R = \text{Dy, Ho}$ and Tb the R moments tend to be perpendicular to the local four-fold axis.

Manganese magnetism in RMn₂ compounds

The magnetic ground state of manganese in RMn₂ compounds is known to depend sensitively on the Mn-Mn near neighbour distance $d_{\text{Mn-Mn}}$. A critical distance of about $d_c = 2.67 \text{ \AA}$ divides the series into two regions. Compounds where $d_{\text{Mn-Mn}} > d_c$ see the manganese site develop at low temperatures an intrinsic moment of $\mu_{\text{Mn}} = 2.5 - 3.3 \mu_B$. The sudden appearance of this localised moment coincides with the onset of antiferromagnetic order and is accompanied by a marked increase in the volume of the unit cell. In the case of YMn₂ the volume anomaly, $\Delta V/V$, is as large as 5%. In contrast, for those compounds where $d_{\text{Mn-Mn}} < d_c$ only some of the Mn sites develop a moment which is induced by the strongly polarising magnetic environment arising from the magnetically ordered sublattice of 4f electrons. This is the case for e.g. DyMn₂ and HoMn₂ where one in four of the chemically equivalent Mn sites possesses an induced moment. The differences in character of intrinsic and induced moments are underlined by the absence of a volume anomaly associated with the appearance of the latter.

Neutron-diffraction studies on the pseudo-binary system Dy_{1-x}Y_xMn₂ explored the transition between intrinsic and induced Mn moments [5]. A complicated magnetic phase diagram revealed the existence of DyMn₂-like behaviour for $x \leq 0.25$ and YMn₂-like behaviour for $x \geq 0.8$. A broad region extending from $x = 0.35$ to $x = 0.75$ showed neither the long-range order (LRO) of the rare earth sublattice typical for DyMn₂, nor the YMn₂-type LRO of the Mn sublattice. Broad short-range-order peaks, reminiscent of the antiferromagnetic correlations of the rare-earth sublattice, were found for concentrations in this part of the phase diagram. Although there is no sign of LRO in the Mn sublattice, the thermal expansion behaviour of compounds with $0.3 \leq x < 0.75$ shows a distinct anomaly of $\Delta V/V \approx 1\%$ at about 20 K. It was suggested that this anomaly has to be related to the development of an intrinsic Mn moment no greater than $1 \mu_B$. Due to the fact that this intrinsic moment is not long-range ordered and also due to its magnitude it can be considered as a new magnetic ground state of Mn in RMn₂ compounds.

Information on this new magnetic ground state of manganese was gained by performing magnetostriction measurements in collaboration with the University of Zaragoza [6]. The parallel (λ_{\parallel}) and perpendicular (λ_{\perp}) magnetostrictions were measured using polycrystalline samples of DyMn₂, Dy_{0.7}Y_{0.3}Mn₂, Dy_{0.3}Y_{0.7}Mn₂ and Dy_{0.2}Y_{0.8}Mn₂ in pulsed and steady magnetic fields up to 15 T. The anisotropic magnetostriction λ_t and the volume magnetostriction ω can be evaluated from $\lambda_t = \lambda_{\parallel} - \lambda_{\perp}$ and $\omega = \lambda_{\parallel} + 2\lambda_{\perp}$.

As expected the magnetostriction of DyMn₂ is determined by the large anisotropy originating from the local 4f quadrupolar moment of the Dy atoms. The volume

magnetostriction of $\omega = -5 \times 10^{-4}$ can be related to a small lattice contraction of $\Delta V/V = 0.05\%$ arising from the spin reorientation of the Dy spins at low temperatures.

The temperature dependence of the volume magnetostriction measured at different field values for Dy_{0.7}Y_{0.3}Mn₂ and Dy_{0.3}Y_{0.7}Mn₂ is shown in Fig. 4. Fig. 4a shows how the magnetostriction in Dy_{0.7}Y_{0.3}Mn₂ is influenced by the application of an external field. Coming from high temperatures the curve for $H = 0 \text{ T}$ shows a sudden increase of ω at 20 K. This change in ω corresponds to the volume anomaly measured by neutron diffraction. For $H = 1 \text{ T}$ the transition has already strongly decreased and for $H = 4 \text{ T}$ the volume anomaly is no longer visible. It can be concluded that the intrinsic manganese moment becomes unstable in applied fields. Fig. 4b shows similar behaviour for Dy_{0.3}Y_{0.7}Mn₂: The thermal variation of ω below T_N is dependent on the applied field strength. For values of $H > 8 \text{ T}$ no anomaly can be found. However, the situation gets complicated in Dy_{0.3}Y_{0.7}Mn₂ as the thermal expansion above T_N is also influenced by the external field.

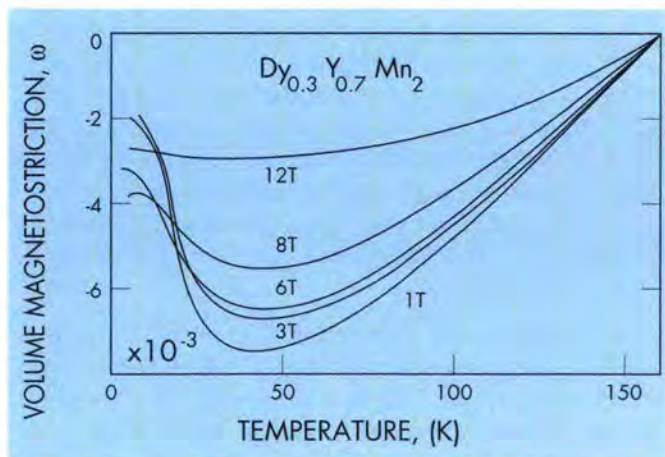
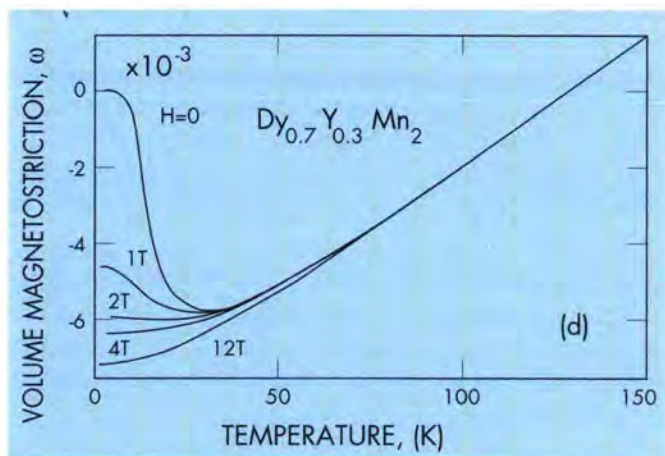


Fig. 4: Temperature dependence of the volume magnetostriction ω measured at several values of the applied magnetic field a) Dy_{0.7}Y_{0.3}Mn₂ b) Dy_{0.3}Y_{0.7}Mn₂

This additional effect of the external field will not be discussed here: Important with respect to the stability of the intrinsic Mn moment is the fact that the critical field needed to suppress the rise of the moment increases with increasing Y concentration.

The dependence of the critical field on the Y concentration can have two origins: the increasing Mn-Mn distance and/or the decreasing Dy-Dy interactions. Going to $\text{Dy}_{0.2}\text{Y}_{0.8}\text{Mn}_2$ there are only small changes in $d_{\text{Mn-Mn}}$ while at the same time the Dy-Dy interactions decrease strongly. Magnetostriction data showed that even the application of a field of 12 T does not influence the volume magnetostrictive behaviour of $\text{Dy}_{0.2}\text{Y}_{0.8}\text{Mn}_2$: the intrinsic manganese moment has thus become stable. This confirms the different nature of the magnetic ground state for $1-x < 0.3$ and supports the idea that the Dy-Dy interactions starting for $1-x \geq 0.3$ are responsible for the destabilisation of the YMn_2 -type long-range order of the Mn sublattice.

Knowing these results it was interesting to study the similar pseudo-binary system $\text{Ho}_{1-x}\text{Y}_x\text{Mn}_2$. Neutron diffraction resulted in the magnetic phase diagram shown in Fig. 5 [7]. In contrast to $\text{Dy}_{1-x}\text{Y}_x\text{Mn}_2$ the transition from the intrinsic manganese moment (for $1-x < 0.15$) to the induced manganese moment (for $1-x > 0.3$) takes place via an intermediate nonmagnetic region. This allows, in the absence of any perturbing R-Mn interactions, precise determination of the critical Mn-Mn distance necessary to sustain an intrinsic Mn moment, namely $d_c = 2.663 \text{ \AA}$.

The neutron studies on the $\text{Ho}_{1-x}\text{Y}_x\text{Mn}_2$ system revealed a further interesting aspect. In pure YMn_2 the magnetic frustration resulting from the superposition of antiferromagnetic order upon a tetrahedral Mn site stacking gives rise to both a tetragonal distortion of the unit cell and an incommensurate magnetic structure with propagation

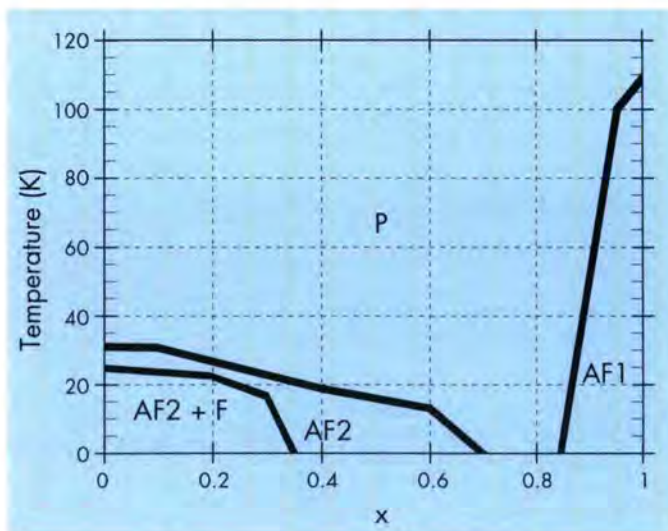


Fig. 5: The magnetic phase diagram of $\text{Ho}_{1-x}\text{Y}_x\text{Mn}_2$. P stands for paramagnetic, AF1 and AF2 for antiferromagnetic order of first and second type for a fcc lattice and F stands for ferromagnetism.

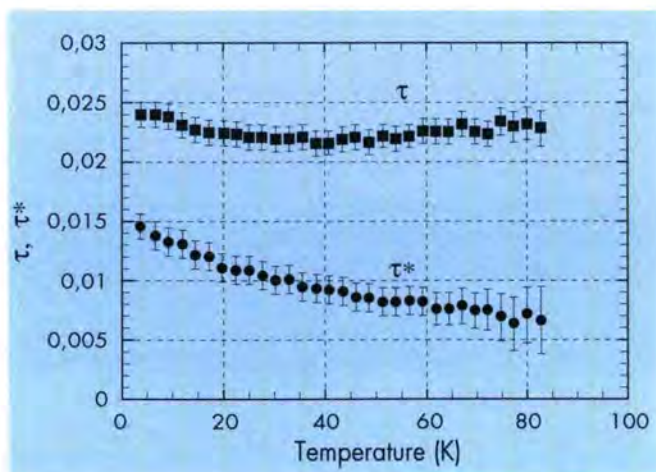


Fig. 6: Temperature dependence of the components τ and τ^* of the incommensurate propagation vector $\kappa = [\tau \tau^* 1]$ of $\text{Ho}_{0.05}\text{Y}_{0.95}\text{Mn}_2$.

vector $\kappa = [0.018 \ 0.003 \ 1]$. Upon doping YMn_2 with small amounts of Tb or Dy, the propagation vector becomes commensurate, $\kappa = [001]$, but a significant tetragonal distortion was found for e.g. $\text{Dy}_{0.1}\text{Y}_{0.9}\text{Mn}_2$. However, upon doping, with 5% Ho, the incommensurability of the magnetic structure becomes even larger. Fig. 6 displays the T-dependence of $\kappa = [\tau \tau^* 1]$ below T_N .

One might speculate that in the case of Ho substitution the tetragonal distortion of the lattice below T_N is suppressed, leaving incommensurability as the only route by which the magnetic frustration can be relieved.

Hyperfine-induced nuclear polarisation in Nd_2CuO_4

Magnetic properties of the parent materials R_2CuO_4 ($\text{R} = \text{Nd, Pr, Sm, Eu}$) of the electron-doped superconductors $\text{R}_{2-x}\text{M}_x\text{CuO}_4$ ($\text{M} = \text{Ce, Th}$) have been investigated quite intensively. The three-dimensional ordering temperature T_N (Cu) of Nd_2CuO_4 lies in the temperature range from 245 to 276 K. Below T_N (Cu) the magnetic moments of the Cu ions order with a propagation or wave vector $\kappa = [1/2 \ 1/2 \ 0]$. Nd_2CuO_4 undergoes two spin-reorientation phase transitions at 75 and 30 K. The Nd magnetic moments are polarised at all temperatures below the Néel temperature, but the amount of polarisation increases as the temperature decreases. At T_N (Nd) = 1.5 K the Nd magnetic moments order with the same wave vector as that of the Cu sublattice. In addition to these four magnetic phase transitions the temperature variation of the magnetic reflections at very low temperatures suggests a further phase transition at about 400 mK. All magnetic peaks increase in intensity below this temperature, but the effect is particularly significant for the peak at $(1/2 \ 1/2 \ 0)$. This reflection, which is absent at higher temperatures, increases dramatically below 400 mK and does not show any sign of saturation down to the lowest temperature of the measurements, which was about 70 mK. A neutron diffraction investigation of Nd_2CuO_4 in the temperature range from 33 to 500 mK was performed on the

two-axis diffractometer at BENS [8]. The data strongly suggest that induced magnetic ordering of the ^{143}Nd and ^{145}Nd nuclei takes place below about 400 mK.

Seven magnetic superstructure reflections were measured along with three nuclear reflections for calibration and to determine the absolute scale. Fig. 7 shows the temperature variation of the magnetic reflections. It is seen that below about 400 mK all reflections increase in intensity. Since the electronic sublattice magnetisation is already saturated at this low temperature, no electronic spin-reorientation model can explain the increase in observed intensity at lower temperature. If the electronic moments were tilted from the (001) plane the $1/2\ 1/2\ l$ reflections with higher values of l would decrease in intensity at the same time. Since the hyperfine interaction constant of Nd is relatively large the observed increase in intensity is attributed to the polarisation of ^{143}Nd and ^{145}Nd nuclei which possess non-zero nuclear moments.

The $1/2\ 1/2\ 0$ reflection is a pure nuclear polarisation peak and its intensity has a simple relationship to the polarisation of the nuclear moments. A simple analysis of the temperature variation of this reflection can also be made. Natural Nd has two isotopes ^{143}Nd and ^{145}Nd with nuclear spin $I = 7/2$ with abundances 12.3% and 8.3%, respectively.

The hyperfine parameter $a_0 = \frac{\mu H_{\text{eff}}}{kl}$ ($\mu =$ nuclear magnetic moment, $H_{\text{eff}} =$ effective hyperfine field at the nucleus, $k =$ Boltzmann constant) have been derived from NMR experiments on a dilute (10%) alloy in Gd metal to be 834(3) and 519(3) MHz or 40.03(14) and 24.91(14) mK for ^{143}Nd and ^{145}Nd , respectively.

The intensity of the scattered neutrons is proportional to the square of nuclear polarisation given by the Brillouin function by

$$F^2 = \text{const.} \left[B_{I=7/2} \left(\frac{a_0 I}{T} \right) \right]^2$$

A least-squares fit of experimental intensities to the above equation gave a hyperfine parameter $a_0 = 720(16)$ MHz or 34.6(8) mK. This value agrees with the value obtained from literature within the experimental error. Fig. 8 shows the temperature variation of the observed intensity of the $1/2\ 1/2\ 0$ reflection along with the calculated temperature variation of the intensity for which the scale factor and the hyperfine parameter have been fitted. The agreement is quite good and shows that the nuclear polarisation alone can explain the temperature variation quite successfully.

The anomalous non-superconductivity of $\text{PrBa}_2\text{Cu}_3\text{O}_{7-\delta}$

The superconducting transition temperature for $\text{Pr}_x\text{Y}_{1-x}\text{Ba}_2\text{Cu}_3\text{O}_{7-\delta}$ falls with increasing x , until superconductivity is entirely suppressed at compositions, $x > 0.5$. In contrast, doping of $\text{YBa}_2\text{Cu}_3\text{O}_7$ with other rare-earth ions has little effect on the superconducting properties.

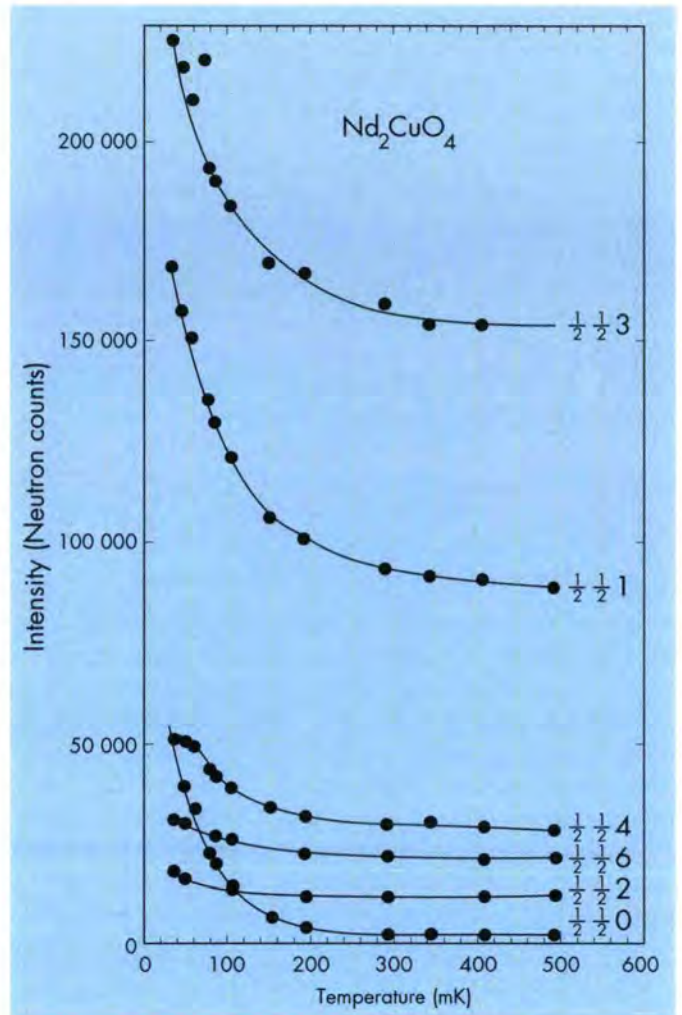


Fig. 7: Temperature variation of the superstructure reflections of Nd_2CuO_4 at low temperature.

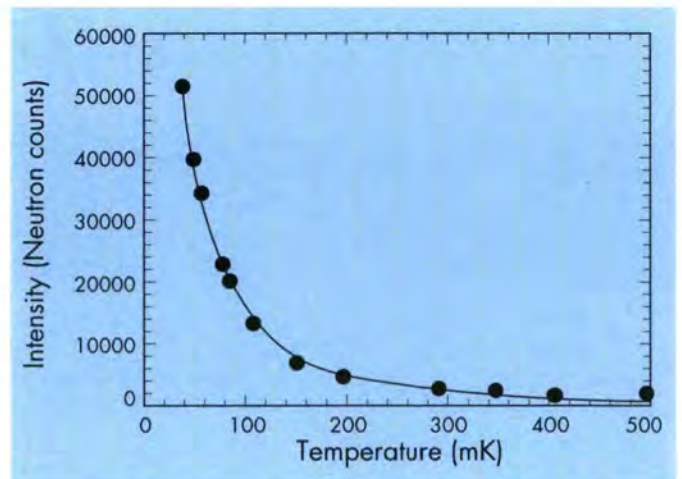


Fig. 8: Least squares fit of the temperature variation of the intensity of the $(1/2, 1/2, 0)$ reflection to the square of the Brillouin function

Furthermore, the Pr member of the $\text{RBa}_2\text{Cu}_3\text{O}_{7-\delta}$ family ($R = \text{rare-earth}$) shows anomalous magnetic behaviour. The R spins for the superconducting members all order antiferromagnetically below 2.5 K, but the Pr spins in $\text{PrBa}_2\text{Cu}_3\text{O}_{7-\delta}$ order at the surprisingly high temperature of 17 K. The mechanism for this anomalous behaviour is still much debated, and its explanation could aid the general understanding of high-temperature superconductivity.

Two different mechanisms have been proposed for this anomalous behaviour. The first proposes that the Pr valence state is greater than 3+ which results in filling and localisation of the current-carrying holes in the conduction band of the CuO_2 plane thought to play a central role in the observed superconductivity, while the second argues that Pr remains 3+, and so no hole-filling occurs, but that there is hybridisation between the Pr 4f electrons and the CuO_2 conduction electrons which nevertheless localises the holes. A combination of these two ideas is probable, with the hybridisation between the Pr 4f electrons and the conduction electrons producing a fluctuating valence state. This could also provide an indirect exchange mechanism for the high-temperature antiferromagnetic ordering of the Pr ions.

Hybridisation would cause a distortion of the Pr 4f electron shells, which could be observed in the induced magnetisation density of $\text{PrBa}_2\text{Cu}_3\text{O}_{7-\delta}$. Indeed, evidence of this was hinted at in a preliminary experiment on D3 in 1990 on a very small crystal of $\text{PrBa}_2\text{Cu}_3\text{O}_{7-\delta}$ [9]. Much bigger crystals are now available and have allowed detailed (unpolarised) neutron-diffraction studies at Risø of the

Cu(1), Cu(2) and Pr magnetic ordering in various oxygenation states, as described in the 1992 Annual Report. One of these crystals (oxygen concentration of 6.73(2) oxygen atoms per unit cell) has now been used for a polarised-neutron experiment at LLB.

The structure was assumed to be orthorhombic and therefore twinned, so that only the projection of the magnetic structure down $[1 -1 0]$ could be determined. The limited data also necessitated model fitting, but clearly indicated that the spin density localised around the Pr site was not spherically symmetric.

Analysis of the induced magnetisation density distribution revealed a sizeable moment on the Ba site. This may be explained by the presence of a small percentage (7.8%) of Pr^{3+} ions upon this site, quite feasible in view of the similar radii of Pr^{3+} and Ba^{2+} ions. (The subsequent positive charge due to this substitution is however not thought to play a significant role in the absence of superconductivity in $\text{PrBa}_2\text{Cu}_3\text{O}_{7.0}$.) Additionally small magnetic moments were found to be present on the two Cu

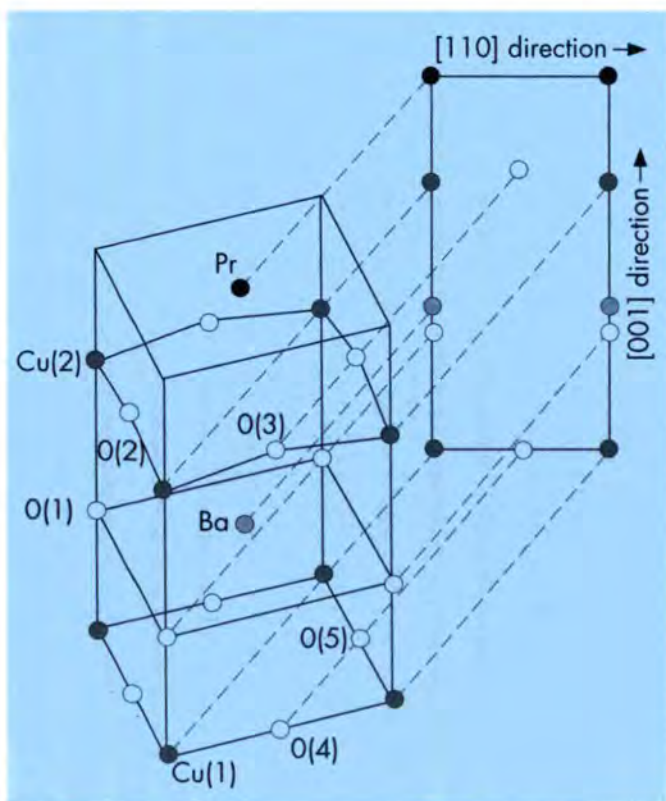


Fig. 9: The atomic structure of orthorhombic $\text{PrBa}_2\text{Cu}_3\text{O}_{7.8}$

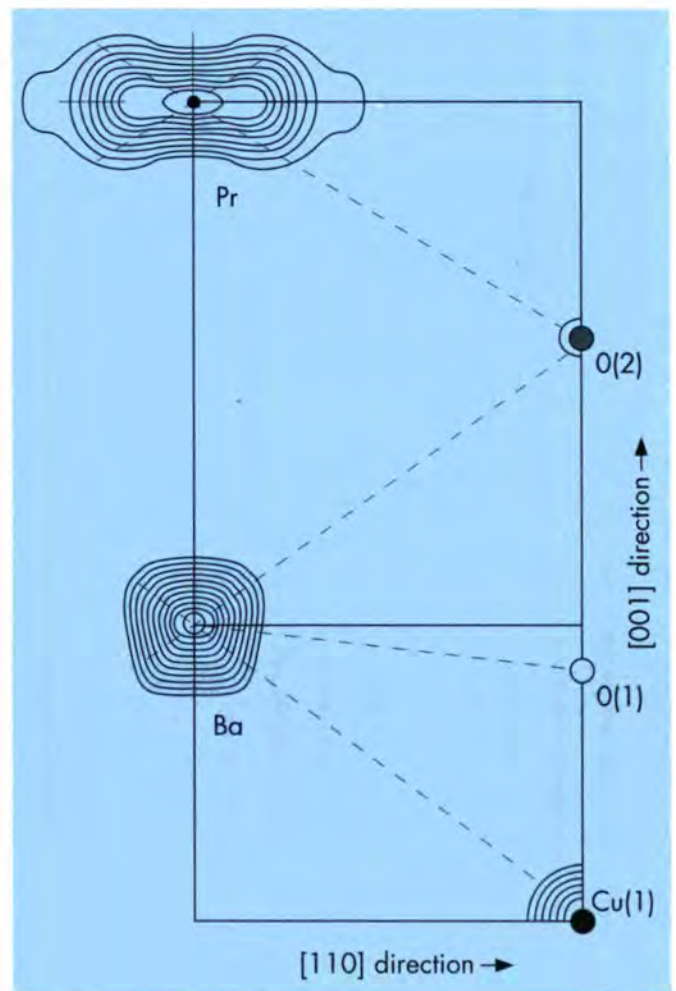


Fig. 10: The modelled magnetic-density distribution of $\text{PrBa}_2\text{Cu}_3\text{O}_{6.73}$ in the 110 plane through Pr. The contours surrounding the Cu(1), Cu(2) and Ba sites are at $0.02 \mu_B \text{ \AA}^{-3}$ intervals, those surrounding the Pr site are at $0.2 \mu_B \text{ \AA}^{-3}$ intervals.

sites, as also observed in $\text{YBa}_2\text{Cu}_3\text{O}_7$ [10]. The total induced moments on the Pr, Cu(1) and Cu(2) sites were found to be $0.34(1) \mu_B$, $0.024(3) \mu_B$ and $0.006(4) \mu_B$ respectively. The final model included a multipolar description of the spin at the Pr and Ba sites, and some magnetic moment on the two Cu sites, and is shown in Fig.9 and 10.

The modelled magnetisation density around the Pr site in $\text{PrBa}_2\text{Cu}_3\text{O}_{6.73}$ is strongly non-spherical and extends towards the Cu sites in the CuO_2 planes. One cause of this deviation from a spherical free-ion distribution may be the hybridisation of the Pr 4f electrons with the conduction electrons of the CuO_2 plane. It is significant that the modelled density around the (partially substituted) Ba site also extends towards the Cu sites in the CuO_2 planes.

While plausible and very encouraging, the results of this experiment should not be overly interpreted until a similar experiment has been performed on a superconducting member of the $\text{RBa}_2\text{Cu}_3\text{O}_7$ family.

Giant magnetoresistance and interfacial structure in Fe/Cr superlattices

A correlation between interfacial structure and giant magnetoresistance (GMR) has been established for Fe/Cr superlattices (Ref. [11] and references therein), a superlattice being a single-crystal multilayered structure. However, most previous studies were qualitative in that the interfacial structural disorder was expressed in terms of growth temperature, sputtering pressure or annealing temperature. In order to understand more quantitatively the effects of interfacial structure on GMR, parallel measurements of x-ray diffraction and magnetoresistance were made for five Fe/Cr samples subjected to one-hour anneals at various temperatures up to 460 C. Annealing is known to increase the thickness of the Fe/Cr interface through atomic diffusion, a structural change which can be characterised quantitatively by x-ray diffraction, and which is known to have a strong effect on GMR.

Since the GMR is also sensitive to other structural parameters such as the thickness of the non-magnetic Cr layers, great care was taken to produce five quasi-identical samples using simultaneous molecular beam epitaxy growth. The x-ray data were taken at the D23 anomalous dispersion beamline at the DCI synchrotron at LURE, where an x-ray wavelength of 2.075 \AA was chosen to enhance the Fe/Cr contrast and thereby significantly increase the measured intensity. Fig. 11 shows an example of the high-quality x-ray reflectivity curves obtained for these samples, attesting to the homogeneity of the superlattice.

A preliminary Fe/Cr annealing study suggested that the GMR was also affected by the nature of the roughness at the Fe/Cr interfaces, and not simply by its magnitude. Specifically, the lateral correlation length ξ_x of the interfacial roughness is believed to play a role. This parameter is very approximately equal to the average distance between roughness "bumps" along an interface, allowing therefore a distinction between interdiffusion (small ξ_x) and "coarser" roughness (large ξ_x). By performing small-angle off-specular x-ray diffraction

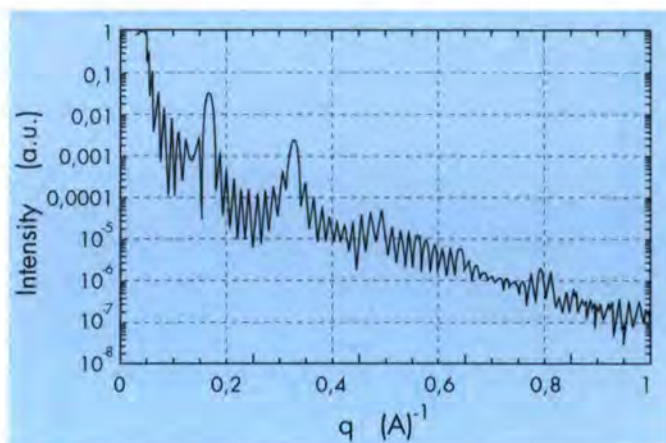


Fig. 11: Reflectivity curve for a 10-bilayer Fe/Cr superlattice having a period of 39 \AA , taken with an x-ray wavelength of 2.075 \AA . Note the presence of superlattice peaks and Kiessig fringes up to relatively large q values, due to the high quality of the sample.

measurements in addition to specular curves, such as that shown in Fig. 11, ξ_x can be accessed (See also the College 6 section of this Annual Report).

Presently magnetoresistance measurements at low temperature are underway for these five samples, which will then be analysed and correlated with the x-ray results.

Secretaries: Garry J. McIntyre (5a)
Clemens Ritter (5b)

References

- [1] J.B. Forsyth and P.J. Brown, *J. Phys. Condensed Matter*, (in preparation).
- [2] T. Chattopadhyay, T. Brückel, D. Hohlwein and R. Sonntag, *J. Magn. Magn. Mater.* 140-144 (1995) 1795.
- [3] B. Ouladdiaf, J. Déportes and J. Rodriguez-Carvajal, *Physica B*, (in press, Proceedings of ICNS'94).
- [4] A. Delapalme, J. Déportes, R. Lemaire, K. Hardman and W.J. James, *J. Appl. Phys.* **50** (1979) 1987.
- [5] C. Ritter, R. Cywinski, S.H. Kilcoyne, S. Mondal and B.D. Rainford, *Phys. Rev.* **B50** (1994) 9894.
- [6] C. Ritter, C. Marquina and M.R. Ibarra, *J. Mag. Mag. Mat.* (submitted).
- [7] C. Ritter, R. Cywinski and S.H. Kilcoyne, *Zeitschrift f. Naturforschung* (in press).
- [8] T. Chattopadhyay and K. Siemensmeyer, *Europhys. Lett.* **29**. (1995) 579.
- [9] M.P. Nutley, A.T. Boothroyd and G.J. McIntyre, *J. Mag. Mag. Mat.* **104-107** (1992) 623.
- [10] J.X. Boucherle, J.Y. Henry, R.J. Papoular, J. Rossat-Mignod, J. Schweizer, F. Tasset and G. Uimin, *Physica B*, **192** (1993) 25.
- [11] H.E. Fischer, F. Petroff, P. Beliën, S. Lequien, G. Verbanck, Y. Bruynseraede, S. Lefebvre and M. Bessière, *J. de Physique*, **IV** (1994) C9-121.

***In situ* neutron powder-diffraction studies of battery electrodes**

J. Pannetier, ILL and Y. Chabre, Laboratoire de Spectrométrie Physique, UJF Grenoble et CNRS.

Several electrochemical reactions of relevance for battery applications simultaneously involve electron transfer and the insertion of protons within the lattice of crystalline solids. For instance the widely used alkaline batteries operate by reduction of manganese dioxide MnO_2 into MnOOH while the rechargeable metal hydride batteries recently commercialized are based on two such systems, $\text{Ni}(\text{OH})_2/\text{NiOOH}$ as positive electrode and $\text{LaNi}_5/\text{LaNi}_5\text{H}_x$ as negative one. The reduction/oxidation of these systems usually lead to complex structural modifications of the host lattice. Many experimental techniques, including standard crystallographic methods, have been used to investigate these transformations and their influence on the behavior of batteries. Neutron powder diffraction is particularly well suited for this purpose. First the scattering lengths of ^1H and $^2\text{H}(\text{D})$ are comparable with those of oxygen and of many metals which leads to more accurate structure determination (proton sites, site occupancies) than X-rays. Then the penetration depth of neutron beams through most materials makes it possible to investigate the structural mechanisms of proton intercalation/deintercalation by *in situ* measurements performed in conditions close to usual battery operation. An additional advantage (or complementarity) of neutrons over X-ray powder techniques is the fact that neutron diffraction provides true bulk information on the sample whereas X-ray beams probe only a few tens to a few hundred microns below the sample surface. Comparison of X-ray and neutron results is then an effective way to discriminate between surface-only and bulk reactions. The use of high flux diffractometers such as D1B or D20 also enables fast data collection rates (typically of the order of a few minutes) thus allowing to measure the kinetics of the processes.

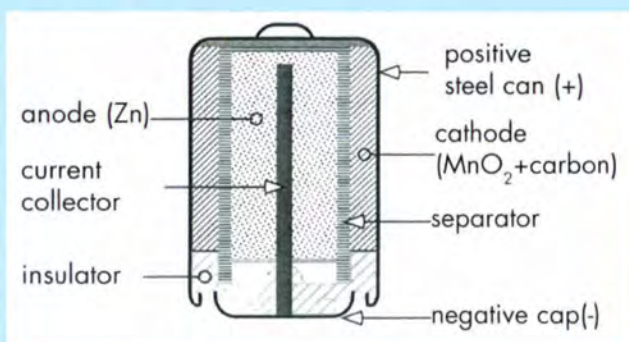
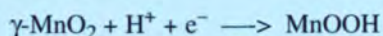


Fig. 1: Schematic diagram of an alkaline zinc/manganese dioxide battery. Electrode materials and separator are impregnated with 9M KOH.

Alkaline Zn-MnO_2 primary batteries (one-shot sources of power) account for a large fraction of the portable power source market. Their general design is shown in fig. 1.

The positive electrode material MnO_2 is a semiconductor and has to be mixed with some graphite which provides electronic conductivity. These batteries, as well as the older Leclanché ones with chloride electrolyte, operate by the reduction of a synthetic manganese dioxide, named $\gamma\text{-MnO}_2$, by the overall chemical reaction:



This simple reaction actually hides a series of phenomena that include manganese reduction from Mn^{4+} to Mn^{3+} with proton insertion into the tunnels of the host structure, and a structural transition induced by the Jahn-

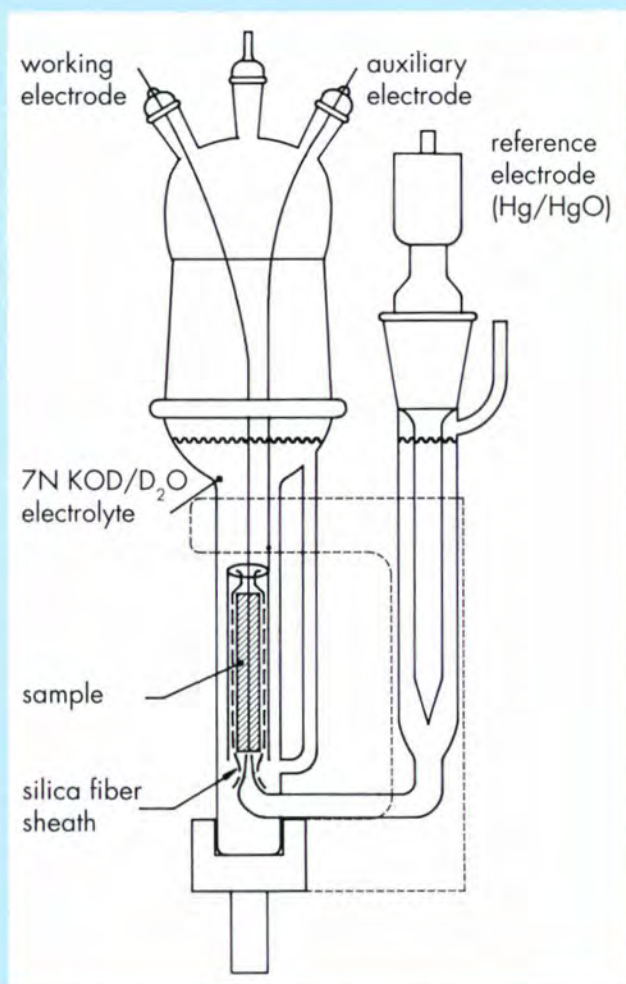


*Fig. 2: Schematic of the electrochemical cell used for *in situ* neutron powder diffraction experiments [3]. It has been designed to minimize the amount of extraneous material in its in-beam part and to get as homogeneous intercalation as possible.*

Teller distortion of manganese coordination octahedra $[\text{MnO}_6]$. Most known details about these transformations have been derived for long by conventional *ex situ* techniques and, in particular, X-ray powder diffraction [1]. The last approach is largely hampered by two problems: partly reduced manganese oxides easily get oxidized which may modify samples during their preparation before X-ray examination, and the penetration depth of $\text{CuK}\alpha$ X-ray beams into manganese oxides limits investigation to the surface of the particles only. Nevertheless, these results led to the conclusion that reduction of MnO_2 into MnOOH occurs in two steps with the probable formation of an intermediate oxyhydroxide with composition $\text{Mn}_2\text{O}_4\text{H}$ [2]. This result is however at variance from the electrochemical studies which give smooth voltage/composition curves, thus suggesting a continuous reduction process.

In situ neutron powder diffraction experiments could be performed rather easily by using a specific electrochemical cell in silica (fig. 2), a deuterated electrolyte (7N KOD in D_2O) and a high flux

diffractometer such as D1B or D20. In such a design the reduction of MnO_2 can be performed in conditions close to the usual discharge of a AA battery.

An unexpected result was that the evolution of lattice parameters with the degree of reduction is completely different when measured *in situ* as opposed to *ex situ* (see fig. 3). This simple qualitative result shows that the reduction of $\gamma\text{-MnO}_2$ (i.e., the discharge of the battery) proceeds along different paths depending on how this reduction (discharge) is performed. The difference in the two paths could be elucidated by a comparison of the *in situ* and *ex situ* experiments, using a structural model recently developed for $\gamma\text{-MnO}_2$ [4]. In short, $\gamma\text{-MnO}_2$ are poorly crystalline materials whose structure can be described as a ramsdellite affected by two kinds of extended structural defects, an intergrowth of rutile like units, called De Wolff disorder, and microtwinning. Although these two defects strongly influence the final stages of reduction and the reversibility of the reduction [4], they appear to have little influence on the different reaction paths followed during *in situ* and *ex situ* investigations and, for the sake of simplicity, we shall

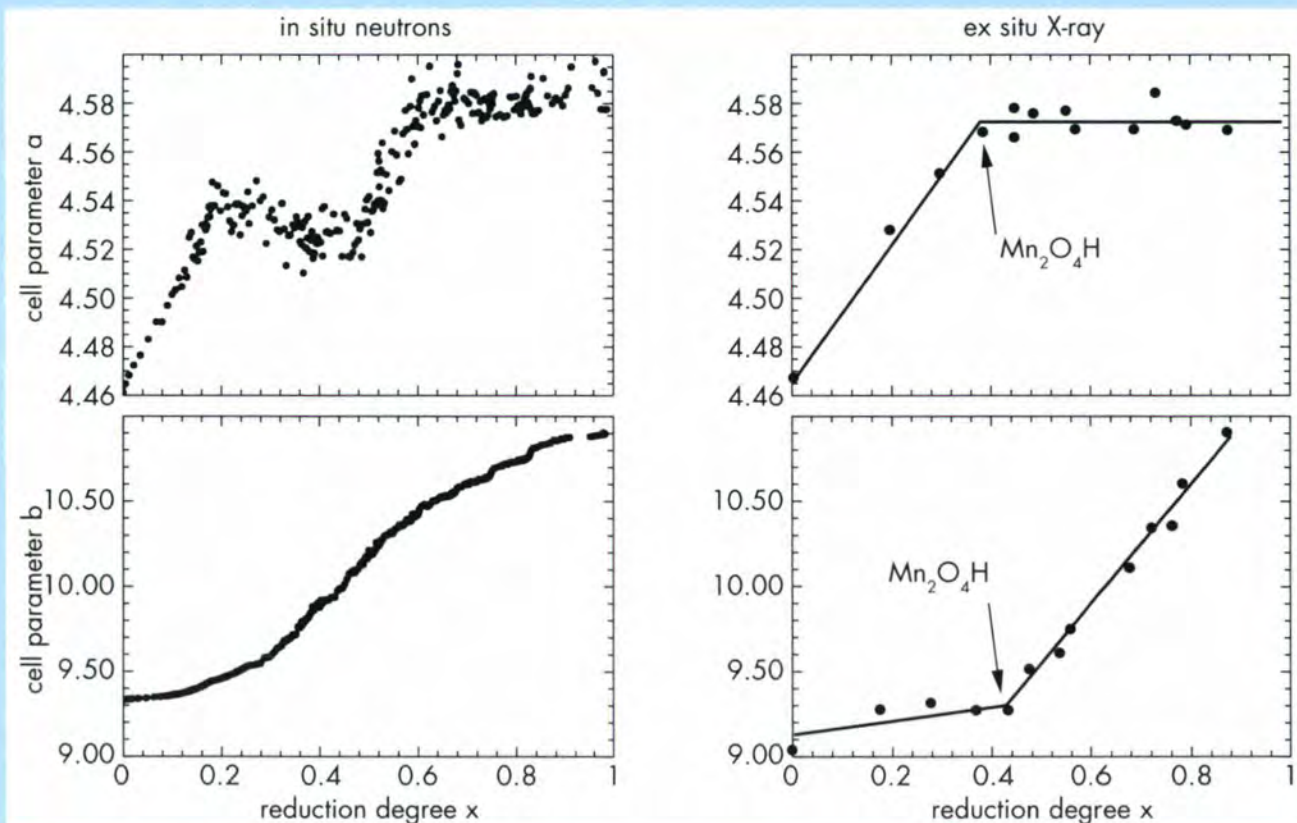


Fig. 3: Evolution of the lattice parameters a and b of γ -manganese dioxide upon reduction from MnO_2 ($x=0$) to MnOOH ($x=1$) in alkaline electrolyte: left: *in situ* NPD data; right: *ex situ* XRD data (adapted from [1]).

Owing to the crystallographic structure of the host lattice, cell parameter c is almost not modified by the reduction.

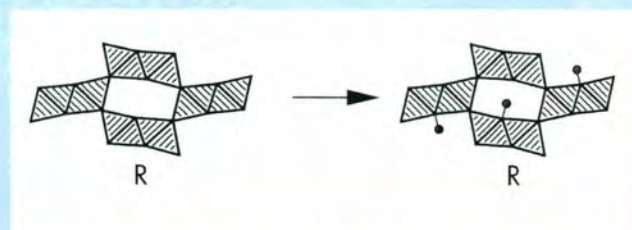


Fig. 4: Ideal representation of the first stage of proton insertion into the tunnels **R** of the ramsdellite structure. Protons are represented as small circles.

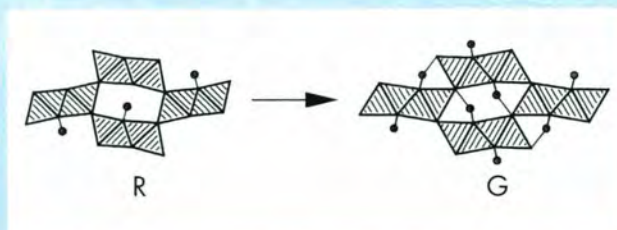


Fig. 5: Ideal representation of the second stage of proton insertion. Note the change in cross section of the tunnels (from **R** to **G**) upon the influence of a Jahn-Teller distortion of Mn^{3+} coordination octahedra.

ignore them hereafter; further details can be found in reference [4]. The basic building unit of the ramsdellite structure is a double chain **R** of edge-sharing $[\text{MnO}_6]$ octahedra running along the *c* axis. These chains are linked together by the corners of the octahedra, thus forming a 3D network that encloses wide tunnels (fig. 4, left) into which protons can intercalate (fig. 4, right). When reduction is performed very slowly, that is by keeping the sample close to equilibrium, it proceeds essentially in two steps:

– discharge starts with the reduction to Mn^{3+} of Mn^{4+} atoms located in chains **R** and concomitant intercalation of protons into the large tunnels of ramsdellite blocks, as shown in fig. 4. The cross section of the tunnel is however such that no hydrogen bonding can be formed ($\text{O-H}\cdots\text{O} = 3.33 \text{ \AA}$) which, for steric reasons, limits insertion to half a proton per Mn and eventually leads to the half-reduced compound $\text{Mn}_2\text{O}_4\text{H}$.

– then, when the ramsdellite tunnels are half-filled and the potential drops below some critical value V_c , a structural transition takes place. This transition, which is related to the onset of a cooperative Jahn-Teller distortion of $[\text{Mn}^{3+}\text{O}_6]$ octahedra, modifies the shape of the tunnels from close to orthogonal in cross-section (conformation **R**) to skewed (conformation **G**) as found in the fully reduced compound known as groutite or α - MnOOH (fig. 5, right).

Although this change in cross-section of the tunnels might seem a very minor modification, it enables the formation of hydrogen bonding ($\text{O-H}\cdots\text{O} = 2.63 \text{ \AA}$) across the tunnels and the accommodation of additional protons, eventually leading to the composition MnOOH .

This simple two-step model accounts for slow reductions, either when the voltage of the cell is decreased very slowly or when the sample is allowed to re-equilibrate in open circuit after constant current discharge at low rate: this case corresponds to the *ex situ* data shown in fig. 3, right. In contrast, if reduction (battery discharge) is performed at high rate and the

potential drops below a critical value V_c (estimated $\approx 1.3 \text{ V}$ vs the Zn negative electrode) which triggers the transition **R** \rightarrow **G**, then the two steps pictured in figures 4 and 5 take place simultaneously within every particle. This mechanism, which corresponds to the usual conditions of battery discharge, brings complex structural arrangements where all different tunnel conformations (**R** and **G** layers) can coexist within every crystallite at every average reduction degree. From simple crystal chemistry arguments, one can calculate that this second mechanism leads to a smooth variation of cell parameter **b** (along which layers **R** and **G** are stacked), a change in the evolution of **a** at the critical potential V_c , and a selective broadening of diffraction lines. All three features are indeed observed in *in situ* data (fig. 3, left).

These results, as recent ones on partly substituted LaNi_5 [5,6], clearly show that *in situ* neutron diffraction experiments enable us to observe kinetics or out-of-equilibrium effects that are relevant to understanding battery operation but might otherwise escape the usual *ex situ* experiments.

References

- [1] J.P. Gabano, B. Morignat, E. Fialdes, B. Emery and J.F. Laurent, *Z. Physik. Chem. neue Folge* **46**, 359 (1965).
- [2] W.C. Maskell, J.E.A. Shaw and F.L. Tye, *J. Applied Electrochem.*, **12**, 101 (1982).
- [3] M. Ripert, Thèse INPG Grenoble (1990).
- [4] Y. Chabre and J. Pannetier, *Progress in Solid State Chemistry*, **23**, 1-130 (1995).
- [5] M. Latroche, A. Percheron-Guégan, Y. Chabre, C. Poinsignon and J. Pannetier, *J. Alloys Compounds*, **189**, 59 (1992).
- [6] M. Latroche, A. Percheron-Guégan, Y. Chabre, J. Bouet and J. Pannetier, *Progress in Batteries and Battery Materials*, **13**, 225 (1994).

Liquids, Disordered Materials and Metal Physics

Members of the College at ILL

I. Anderson	A. Kollmar
T. Baumbach	C. Lartigue
M. Bée	H.J. Lauter
M. Boudard	P. Lindner
P. Chieux	A. Magerl
J.C. Cook	H. Mutka
A.J. Dianoux	V. Passiouk
C. Doll	R. Oeser
O. Dubos	S. Pouget
B. Farago	O. Randl
H. Fischer	C. Ritter
B. Frick	O. Schärpf
A. Heidemann	J.-B. Suck
C. Janot	C. Zeyen
G.J. Kearley	

External members

M. Anne (CNRS)	A.-M. Hecht (UJF)
J.-P. Beaufils (UJF)	J.F. Jal (Univ. Lyon)
P. Becker (CNRS)	J.-F. Legrand (UJF)
M. Benmouna (UJF)	F. Livet (INPG)
F. Bley (INPG)	Y. Maréchal (CENG)
A. Bourret (CENG)	I. Morfin (UJF)
F.R. Boutin (Pechiney)	J.P. Morlevat (CENG)
J. Bouvaist (Pechiney)	M. Pineri (CENG)
Y. Bréché (INPG)	C. Poinignon (INPG)
A. Chamberod (CENG)	D. Quenard (CSTB)
B. Chenal (Pechiney)	G.M. Raynaud (Pechiney)
A. Cohen-Addad (UJF)	F. Rieutord (CENG)
F. Cyrot (CNRS)	M. Rinaudo (CNRS)
P. Desre (INPG)	G. Robert (CENG)
J. Dupuy (Univ. Lyon)	P. Sainfort (Pechiney)
B. Fåk (CENG)	F. Volino (CENG)
P. Guyot (INPG)	A. Yavari (INPG)

Introduction

“The olde order changeth, yielding place to new” (Morte d’Arthur)

This report will be the last for College 6 in its present form. After the October sub-committee meeting in which over 100 proposals were discussed within College 6, it was decided to attempt a re-organisation between College 6, 9a and 9b. The result of numerous discussions was the formation of three Colleges:

College 6: Structure & dynamics of liquids and glasses

College 7: Material science, surfaces and spectroscopy

College 9: Structure and dynamics of soft condensed matter

The past year has been largely devoted to preparation of the instruments for the long-awaited reactor start-up. However, it is clear from the scientific highlights outlined below that scientific activity still flourishes in the College.

Scientific Highlights

Neutron Brillouin Scattering in an amorphous solid

The study of the dispersion relation of collective excitations in amorphous solids, investigated previously on IN4 and IN6 at the HFR and on HET at ISIS [1], has been continued by an experiment performed using the small angle, two-dimensional position sensitive detector on the time-of-flight spectrometer PHAROS at the neutron spallation source of LANSCE in the Los Alamos National Laboratory [2]. As extensive computer simulations had been done for the metallic glass $Mg_{70}Zn_{30}$, this glass was chosen. Experiments were performed at 100 K and 297 K, with the aim to find the best experimental conditions for Neutron Brillouin Scattering (NBS) experiments on amorphous solids and at the same time extending the measured dispersion relation to lower Q-values. In order to cover the dispersion curve of longitudinal excitations ($v_1 \approx 4300$ m/s) (the only accessible modes in the first pseudo-Brillouin-zone (PBZ) in neutron inelastic scattering experiments), in the dynamical region of the experiment, an incident energy of 187 meV was chosen, which at the same time had the advantage of giving maximum absorption of the neutrons in the Cd-grid (7x7x20 mm) in which the melt spun ribbons had been pressed to reduce the multiple scattering in the sample material.

Even though the statistical accuracy of the data was somewhat low using a constrained two-channel maximum entropy method to separate the structure assigned to the excitations from the broader “background” due to multiple scattering, it was possible to extend the dispersion relation, obtained previously just across the boundary of the first PBZ, far into the middle of the PBZ. Possibly even modes involving only Mg atoms and modes only involving Zn atoms could be separated, assuming a width corresponding to a lifetime > 0.1 ps of these excitations. Supposing the validity of this separation, which would be the first achieved so far, and using the information obtained from the computer simulations it was possible to continue the previously measured dispersion relations to lower Q-values. The results show that the energy of Mg-Mg vibrations strongly depends on the momentum transfer while the Zn-Zn vibrations follow a nearly dispersionless branch.

Interestingly, the maxima in the inelastic part of the dynamic structure factor taken at room temperature are at least as pronounced as in the data taken at 100 K in spite of the higher possibility to excite multiphonon processes in multiple scattering at room temperature. Taking into account the higher probability and the additional information from

the neutron energy gain side of the dynamic structure factor, NBS experiments on amorphous solids seem to profit from the higher temperature, as long as these multiphonon contributions do not dominate the spectra.

Structure and dynamics of quasicrystals

C. Janot, M. de Boissieu and M. Boudard have continued their investigations on both structure and dynamical properties of quasicrystals, in particular AlPdMn.

- High resolution diffraction experiments using in addition anomalous dispersion have been carried out on the new ESRF beam lines. From the analysis of the Bragg peak profiles and intensities, as functions of temperature, the occurrence of a structural phase transition between 700 to 800°C has been demonstrated. The transition seems to leave unaltered the geometrical quasiperiodic order and might be of the chemical order-disorder type. Relation to the fragile-ductile transition also observed is under consideration.

- Triple axis experiments at the Léon Brillouin Laboratory have been pursued. The very good crystallographic quality of the single grains now available has allowed the investigation of vibrational modes beyond the previously observed long wavelength propagating acoustic mode. Flat branches (Fig. 1) of broad excitations (1 THz) have been observed. These optical-like branches are hierarchically distributed at 1.8, 3.4, and 5.8 THz. Their features are consistent with the idea of hierarchical mode localisation into self similar clusters of the structure.

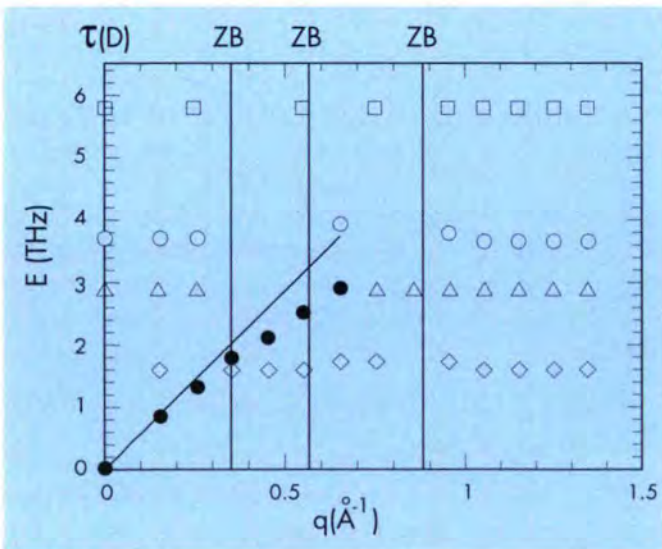


Fig. 1: Typical dispersion relation measured in an AlPdMn quasicrystal for the transverse geometry : (●) acoustic modes, (◊, Δ, ○, □) optical-like flat branches; the full line shows the sound velocity measured with ultrasonic waves.

- The ultrasonic wave velocity has been measured on surfaces of quasicrystal single grains, using acoustic microscopy equipment of the Physics Department of the Ecole Polytechnique Fédérale de Lausanne. Unexpected anisotropy effects have been observed. They have been explained by the presence of oriented decagonal cavities within the crystal and emerging at the surfaces. Acoustic images (Figs. 2 and 3) show indeed the formation of standing waves around and into the cavities.

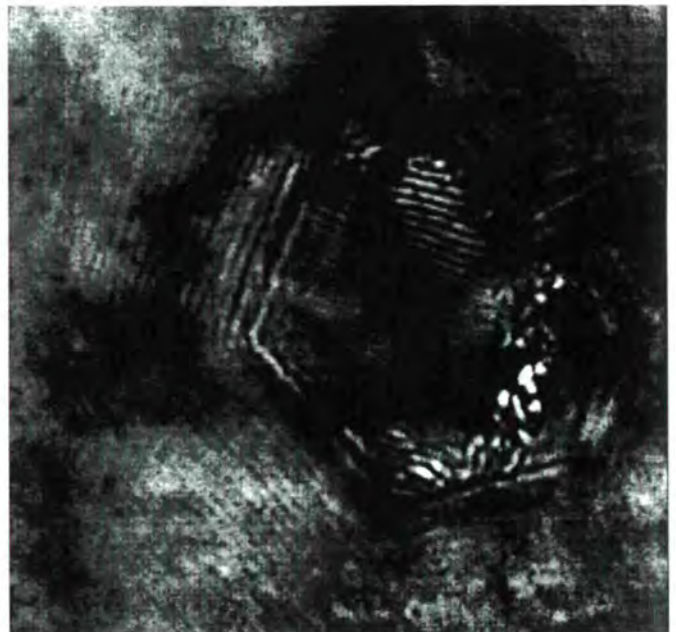


Fig. 2: Acoustic image around a decagonal cavity on a two-fold surface of an AlPdMn single grain. Fringes due to Rayleigh standing waves are visible.

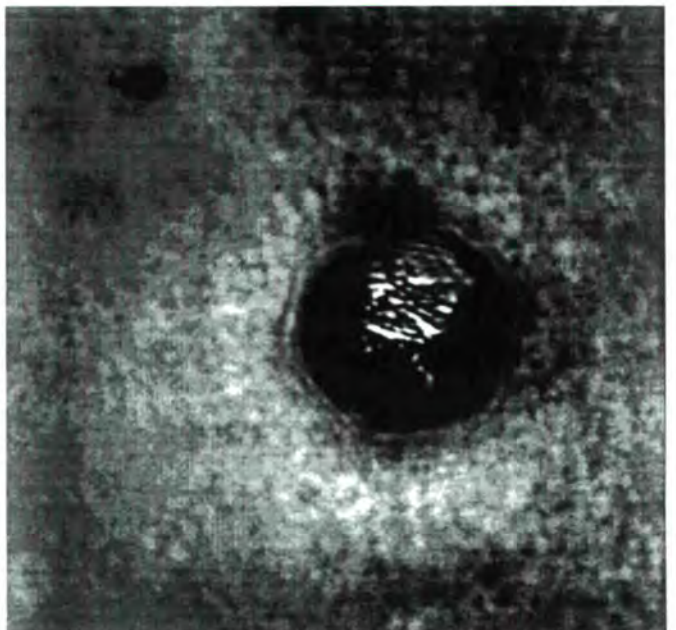


Fig. 3: Acoustic image showing interference effects in a cavity.

– A model for quasicrystal structure has also been developed in which physical properties are explained along the line of a hierarchical molecular solid.

Scattering from periodic nano-structured solids

Artificial super-structured solids such as multilayers, superlattices, surface gratings, quantum well wires and quantum dots and their structural and physical properties are a recent field of interest in solid state physics.

One common feature of periodic nano-structured solids is that their super-structure generates a fine structure of the reciprocal lattice points resolvable by X-ray and neutron scattering techniques. X-ray scattering methods successfully applied for the structure investigation are symmetrical and asymmetrical X-ray diffraction (XRD and AXRD), specular and non-specular x-ray reflection (SXR, NSXR) and grazing incidence diffraction (GID). Investigating different parts of reciprocal space they provide partly complementary information.

Planar superlattices create truncation rods through each reciprocal lattice point (RPL) containing equidistant longitudinal satellites. Applying grazing incidence - or exit diffraction techniques such as GID and AXRD, multiple scattering takes place since the Ewald-sphere crosses both the HKL and the 000-truncation rod, that means diffraction and specular reflection occur simultaneously. The reduction of the penetration depth due to simultaneous specular reflection makes these methods sensitive to the surface and near surface interfaces. Particularly the non-coplanar scattering (e.g. GID) allows us to measure the diffracted intensity of a chosen scattering vector Q under different angles of incidence (see Fig. 4 page 140), making the method depth selective.

A real superlattice gets a two-dimensional RPL fine structure in the case of defects correlated in the growth direction (correlated interface roughness or lattice strain relaxation), giving rise to resonant diffuse scattering (RDS) (Fig. 5 page 140).

Lateral surface gratings generate a two dimensional fine structure consisting of equidistant longitudinal grating truncation rods (Fig. 6 page 141).

Since the Ewald-sphere crosses a two-dimensional fine structure in several points apart from the origin it gives rise to Umweganregung between the upper grating and the lower planar multilayer.

Based on the dynamical diffraction theory, a theoretical description of scattering from epitaxial nano-structured solids including Umweganregung has been developed and confirmed by X-ray experiments [3-4]. The figures show maps of the scattered intensities first of a planar superlattice in the GID mode (Fig. 4) for the Bragg-diffraction from the (220) lattice planes perpendicular to the surface for different incident angles, and in the NSXR-mode, measuring the diffuse scattering due to perpendicular correlated interface

roughness (Fig. 5). The transversal (Q_z -) sheets are caused by a super-periodicity of the lattice modulation (GID) and of the interface defects (NSXR). In both methods they became slightly bent due to refraction. The grid of Bragg-like resonances is generated by simultaneous specular reflection when the superlattice Bragg-condition is fulfilled.

Fig. 6 is a reciprocal space map of an epitaxial multilayered surface grating. It contains several equidistant grating truncation rods. The intensity profile along the truncation rods depends on the grating shape, the strain and the composition of the grating period. The planar multilayer influences also the non-zero order truncation rods due to Umweganregung.

Specular and Off-Specular Small-Angle X-ray Scattering in Multilayers

Specular small-angle x-ray diffraction (i.e. reflectivity curves) only probes the q_z direction in reciprocal space, meaning that only structural parameters along the growth direction (e.g. perpendicular to a multilayer's interfaces) are accessible, such as layer thicknesses and interfacial thicknesses. In order to access structural parameters in the horizontal or lateral direction (parallel to the interfaces), one must perform off-specular x-ray diffraction (also called diffuse scattering), since only these measurements have a non-zero q_x component in momentum transfer (where q_x lies in the scattering plane and is parallel to the sample's surface).

Two types of small-angle off-specular scans are commonly performed: i) ω -rocks (or rocking curves) having fixed detector angles 2θ , and ii) 2θ -rocks (or detector scans), having fixed incident angles ω . An ω -rock has a reciprocal space trajectory which is very nearly along q_x , whereas a detector scan has both q_x and q_z components.

For a multilayer, there are 3 additional structural parameters that can be extracted from these off-specular scans which are not accessible from specular measurements: 1) the horizontal correlation length ξ_x of the interfacial roughnesses (very approximately the distance between roughness "bumps" along an interface), 2) the fractal dimension h of the interface profiles (also a lateral structural parameter), and 3) the vertical correlation length ξ_z of the interfacial roughnesses (the distance in the growth direction over which the profiles of interfaces continue to track each other).

The two correlation lengths ξ_x and ξ_z have different effects on the diffuse intensity in the $q_x q_z$ plane caused by interfacial disorder. The parameter ξ_x causes an amassing of diffuse intensity in the q_x direction around the specular ridge, while ξ_z causes an amassing of diffuse intensity in the q_z direction around all specular peaks (including Kiessig fringes). Note that a determination of ξ_x allows a distinction between interfacial diffusion (small ξ_x) and interfacial roughness (large ξ_x).

To simulate small-angle off-specular diffraction measurements [5], we first employed the matrix-method technique to calculate the specular electric fields at each interface of the sample (i.e. a full dynamical reflectivity theory), and then applied a formalism equivalent to the Distorted-Wave-Born-Approximation (DWBA) for calculating the diffusely scattered intensity from these E-fields. Since the diffraction angles of superlattice peaks are in general sufficiently larger than the critical angle, a kinematic treatment of diffuse scattering suffices for simulating the widths of the diffuse scattering intensity in q_z .

Figure 7 shows a detector scan for a very high quality 45-bilayer Fe/Ir superlattice given by $(\text{Ir}_{26\text{\AA}}/\text{Fe}_{9\text{\AA}})_{45}/\text{Ir}_{140\text{\AA}}/\text{MgO}(001)$, using an x-ray wavelength of $\lambda = 1.1065 \text{ \AA}$. The x-ray data were obtained using the D23 anomalous scattering beamline at the DCI synchrotron at LURE, Orsay, and the sample was produced at l'Université de Nancy. The specular peak has been subtracted from the data and is not simulated. Visible are three resonant diffuse scattering peaks (at exit angles of $1.25, 3.0$ and 4.75°) and the Yoneda peak at the far left. In addition, two sharp, s-shaped peaks appear in the simulation (at 1.0 and 1.8°) which are due to a dynamic effect involving both specular and diffuse scattering. However, these dynamic specular + diffuse peaks are absent in the data, likely washed out due to an additional structural disorder which is not included in our model. From this detector scan and a complementary ω -rock, we extracted values of $\xi_x = 30 \text{ \AA}$ and $\xi_z = 200 \text{ \AA}$ for the interfaces of this superlattice.

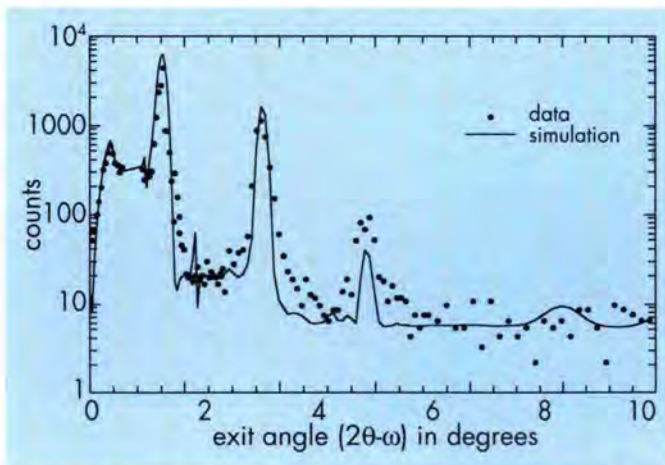


Fig. 7: Off-specular x-ray data (circles) and simulation (solid line) for a 2θ -rock (i.e. detector scan) about $\omega = 0.7^\circ$ for an Fe/Ir superlattice, as a function of the exit angle $\theta_{det} = 2\theta - \omega$. The q -space trajectory of such a scan includes q_z as well as q_x components, and the simulation was performed for $\xi_x = 30 \text{ \AA}$ and $\xi_z = 200 \text{ \AA}$.

Hopping on complex crystal lattices

Diffusion on crystal lattices is studied by methods such as QNS (quasi-elastic neutron scattering) or QMS (quasi-elastic Mössbauer spectroscopy). The experimentally found scattering law $S(\mathbf{Q}, \omega)$ is compared to the Fourier transform of the model self-correlation function $G_s(\mathbf{r}, t)$. The first formulations of the latter were restricted to diffusion on Bravais lattices, but the growing complexity of the systems examined made necessary an extension to non-Bravais lattices with equally or even differently occupied sublattices. Recently, a rigorous derivation for this most general case has been given [6]: The corresponding scattering law is shown to consist of m Lorentzians, where m is the number of non-equivalent sublattices:

$$S(\mathbf{Q}, \omega) = \sum_{p=1}^m w_p(\mathbf{Q}) \cdot \frac{|M_p(\mathbf{Q})|}{|M_p(\mathbf{Q})|^2 + \omega^2}$$

Both the weighting factor $w_p(\mathbf{Q})$ and the halfwidths (hwhm) of the m Lorentzians, $M_p(\mathbf{Q})$, are calculated from the non-hermitian "jump matrix" $\tilde{\mathbf{A}}$, which contains all the information on the jump mechanism:

$$\tilde{A}_{ij} = \frac{1}{n_{ji} \cdot \tau_{ji}} \cdot \sum_k \exp(-i \mathbf{Q} \cdot \mathbf{l}_{ij}^k) - \delta_{ij} \cdot \sum_j \frac{1}{\tau_{ij}}$$

Here n_{ij} is the number of sites of the j^{th} sublattice surrounding a site of the i^{th} sublattice, τ_{ij} is the average residence time of the jumping atom on a site of type i before jumping to a site of type j , and \mathbf{l}_{ij}^k is defined to be the vector connecting a site of local symmetry i to the k^{th} site of its neighbours with local symmetry j . The halfwidths $M_p(\mathbf{Q})$ are the eigenvalues of $\tilde{\mathbf{A}}$ and the weights $w_p(\mathbf{Q})$ can be calculated from the eigenvectors of the hermitized form of $\tilde{\mathbf{A}}$,

$$w_p = \left| \sum_j \sqrt{c_j} \cdot b_j^p \right|^2$$

where c_j stands for the probability that the jumping atom is found on sublattice j , and b_j^p denotes the j^{th} component of the eigenvector \mathbf{b}^p .

Details and applications to systems of very different complexity can be found in [6], see also Blue Box.

Dynamics of hydrogen in α -LaNi₅

The hexagonal LaNi₅/H system is one of the most intensively studied materials suitable for the chemical storage of gaseous hydrogen. Its broad applicability for many processes involving hydrogen has been reported in a great number of publications.

In spite of the extensive knowledge of the macroscopic properties of LaNi₅H_x and many other ternary hydrides, very little information about the microscopic structure and dynamics could be obtained so far. This is mainly due to the lack of single-crystalline samples for this class of compounds. The problem arising with the preparation

of single crystals is that many intermetallic phases cannot be prepared directly from the melt. For this reason standard methods such as zone melting fail. But even when it is possible to prepare single crystals of the intermetallic compound it is not easy to charge them with hydrogen without causing severe crystal damage. The lattice expansion and the embrittlement accompanying hydrogenation breaks up bulk samples into hydride powders. For this reason, scattering studies were restricted to more or less qualitative investigations.

Furthermore, since natural Ni causes a great deal of isotope-incoherent scattering in thermal neutron-scattering experiments [$\sigma_{\text{inc}} = 5.2$ b] it has not been possible to work at low hydrogen concentrations. The incoherent neutron scattering of the diffusing particle bears information on single-particle properties and provides access to the self-diffusion coefficient D_S . In typical low-concentration LaNi_5 hydrides, e.g., $\text{LaNi}_5\text{H}_{0.1}$, there are 50 times more Ni atoms than H atoms. Consequently, in spite of the particularly high hydrogen incoherent scattering cross section of 79.9 b there is little chance of “seeing” H beside Ni.

However, working at low hydrogen concentrations provides two advantages for the investigation of the fundamentals of hydrogen diffusion. First, it should be possible to observe simple uncorrelated hopping processes at moderate temperatures. At a composition of $\text{LaNi}_5\text{H}_{0.1}$ there is only one H atom in every tenth unit cell, so that H-H interactions are virtually nonexistent. Second, it is possible to prepare low-concentration single-crystalline samples of LaNi_5 hydride and thus make full use of the power of neutron scattering.

In order to avoid the above-mentioned scattering contrast problem a large high-quality $\text{La}^{60}\text{Ni}_5$ single crystal has been prepared ($\sigma_{\text{inc}}^{60\text{Ni}} = 0$ b). Several experiments have been performed [7] with this sample: (i) quasielastic neutron scattering (QENS) studies in the μeV regime probing hydrogen diffusion at hopping frequencies of 0.03-0.3 GHz (Fig. 8); (ii) quasielastic neutron-scattering studies in the meV regime probing fast hydrogen jump processes of 50 GHz, which can be interpreted by a localised motion over adjacent sites on the corners of regular hexagons (Fig. 9 and 10); and (iii) inelastic neutron-scattering studies of local vibrations in the range of 25 THz of the isolated H oscillators in their metal surrounding. Thus, this represents a series of neutron-scattering experiments covering six

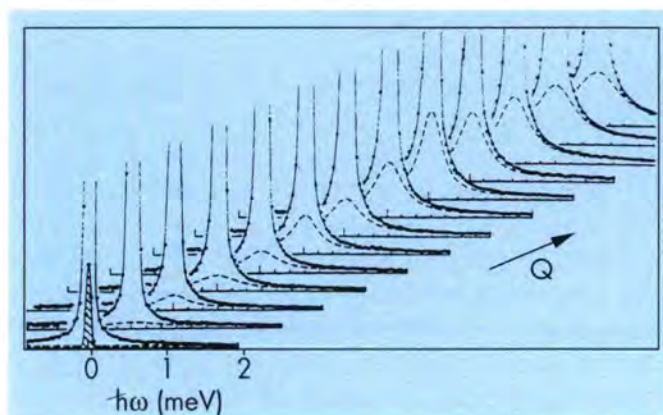


Fig. 9: QENS spectra of $\text{La}^{60}\text{Ni}_5\text{H}_{0.12}$ as obtained on the time-of-flight spectrometer IN6 ($T = 440$ K, $0.29 \text{ \AA}^{-1} \leq Q \leq 2.02 \text{ \AA}^{-1}$). The dashed line represents the quasielastic portion. The shaded spectrum is reduced in size by a factor of 50.

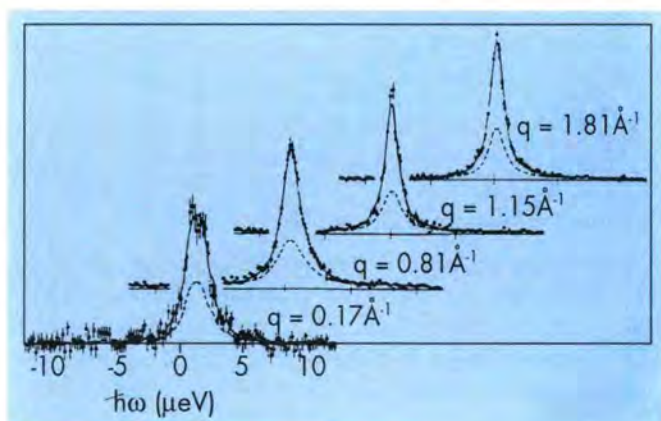


Fig. 8: QENS spectra of $\text{La}^{60}\text{Ni}_5\text{H}_{0.08}$ at 423 K obtained with the IN10 spectrometer in the c direction. The ordinates are intensities in arbitrary units. The quasielastic portion is indicated by the dashed line. The slight shift of the zero-energy line at small Q is an instrumental effect and is corrected for in the data treatment.

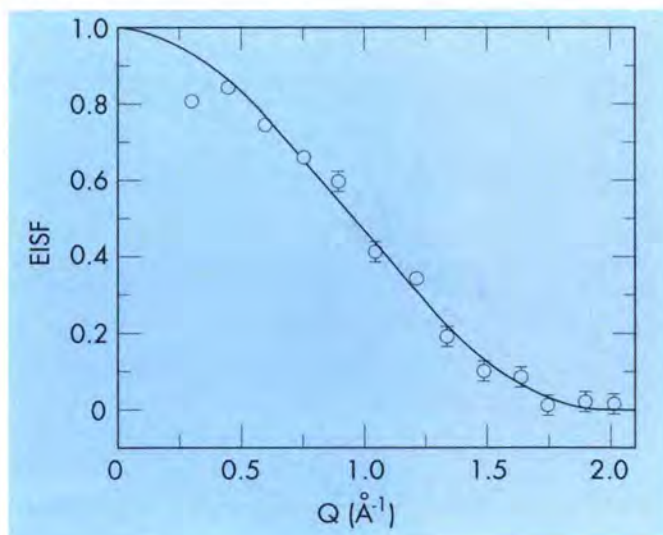


Fig. 10: Elastic-incoherent structure factor of the localised hydrogen diffusion in $\text{La}^{60}\text{Ni}_5\text{H}_{1.2}$. The open circles represent the weighted average from four measurements between 380 and 440 K. The solid line is the theoretical EISF with a jump distance of 1.18 Å.

decades in the dynamic range of hydrogen nuclei in LaNi_5 . For this reason different neutron-scattering techniques represented by four different spectrometer types were used: a beryllium-filter spectrometer (BT4 at NIST) and a time-of-flight spectrometer (MARI at ISIS) both operated with thermal neutrons to detect the THz processes; cold neutron time-of-flight spectrometers for the fast (IN6 at ILL and MIBEMOL at LLB), and a high-resolution backscattering spectrometer for the slow diffusion processes in the GHz regime (IN10 at ILL). By aligning the scattering vector in these experiments with selected crystal directions the single crystal nature of the sample has permitted to separate several types of motions from each other.

The interpretation of these experiments is based on a two-site model. This model suggests the population of a low-energy octahedral 3f site located in the basal plane, and an energetically higher tetrahedral 6m site in the (002) lattice plane. The former is characterised by equal distances to each neighbouring site of the same type in the basal plane, thus forming infinite layers perpendicular to the *c* axis. The latter exhibits two distances, a very short one which always connects six of the sites to a regular hexagon, and a long one that represents the shortest distance between two hexagons in this layer. 3f and 6m sites are interconnected by jump vectors such that the diffusing H atom can reach eight 6m sites from every 3f site, and four 3f sites from every 6m site. With these interlayer jumps a translation parallel to the hexagonal *c* axis is achieved. Based on these considerations a jump model to describe the microscopic steps in the diffusional process has been developed.

The diffusive process can be described in terms of an extended Chudley-Elliott model involving three different jump processes on two time scales.

(i) Jumps take place within the basal plane with a rate of 3.1×10^7 Hz. This process leads to macroscopic hydrogen transport perpendicular to the hexagonal axis.

(ii) Parallel to the *c* axis jumps between alternating octahedral and tetrahedral sites are observed. Jumps leaving the basal plane occur with a rate of 1.5×10^7 Hz and returning into the basal plane with a rate 3.4×10^8 Hz. This corresponds to a difference in site energies of 109 meV (10.5 kJ/mol) or an occupancy of the 6m sites of less than 0.1% for $\text{LaNi}_5\text{H}_{0.1}$.

(iii) Within the hexagons of 6m sites the H atoms perform fast jumps with a rate of 5.3×10^{10} Hz. This jump rate is much larger than the rate between the planes. So this process can be regarded as confined to the 6m hexagons. The corresponding elastic-incoherent structure factor of this process agrees perfectly with the theoretical prediction made on the basis of the crystal structure and is consistent with the low occupation of these sites in $\alpha\text{-LaNi}_5\text{H}_{0.1}$.

From the quasielastic linewidths of $\alpha\text{-LaNi}_5$ (at $Q \rightarrow 0$) the macroscopic diffusion coefficients are obtained. The anisotropy of hydrogen diffusion with respect to the main crystallographic directions is negligible at 423 K in spite of the anisotropy of the complex jump mechanism. The self-diffusion coefficient at that temperature is $D_s = 3 \times 10^{-11} \text{ m}^2 \text{ s}^{-1}$.

Huang diffuse scattering

It is well known that measurements of the diffuse scattering close to reciprocal lattice points (Huang scattering) can be used to determine the long ranging part of the displacement field and strength of the force dipole tensor caused by defects in crystals. In addition to the symmetric Huang scattering an asymmetric scattering is observed due to the interference of the scattering from displaced atoms far from the defect with the scattering from the defect itself. Although the theory has been applied with success to cubic lattices it has only recently been evaluated for defects in hexagonal lattices [8, 9] and the results compared with diffuse scattering measurements from deuterium defects in solid solution with yttrium.

For both the tetrahedral and the octahedral sites the force dipole tensor is cubic if only first neighbour atoms are taken into account but is of the form

$$P_{ij} = \begin{bmatrix} A & 0 & 0 \\ 0 & A & 0 \\ 0 & 0 & B \end{bmatrix}$$

if further neighbours are included. The shape of the Huang scattering around a particular reciprocal lattice point depends on the ratio A/B and thus on the relative values of the Kanzaki forces, f_i , for the i^{th} shell of atoms surrounding the defect.

Fig. 11 page 141, shows some Huang iso-intensity curves calculated for D in the tetrahedral site of yttrium assuming first and second neighbour Kanzaki forces.

The symmetric Huang scattering alone is not sufficient to describe the diffuse scattering in $\text{YD}_{0.5}$ where significant asymmetries are observed [10]. Inclusion of the asymmetric terms in the calculation of the diffuse scattering allows verification that the tetrahedral sites are occupied in preference to the octahedral sites and imposes some limits on the values of the first and second neighbour Kanzaki forces. The calculations have also pointed to further measurements which must be made to determine more accurately the displacement field surrounding the deuterium.

Secretary: Ian Anderson

References

- [1] J.-B. Suck, P.A. Egelstaff, R.A. Robinson, S.D. Sivia, A.D. Taylor, *Europhysics Letters* **19**, 207 (1992).
- [2] C.J. Benmore, B.J. Olivier, J.-B. Suck, R.A. Robinson, P.A. Egelstaff, submitted for publication.
- [3] V. Holy, T. Baumbach; *Phys. Rev. B* Vol. **49** No.15, 10668-10676 (1994).
- [4] T. Baumbach, V. Holy, U. Pietsch, M. Gailhanou; *Physica B* **198**, 249-252 (1994).
- [5] H.E. Fischer, H. Fischer, O. Durand, O. Pellegrino, S. Andrieu, M. Piecuch, S. Lefèbvre, M. Bessièrre, *Nuclear Instruments and Methods B*, in press.
- [6] O.G. Randl, B Sepid, G. Vogl, R. Feldwisch and K. Schroeder, *Phys. Rev. B* **49** (1994) 8768.
- [7] C. Schönfeld, R. Hempelmann, D. Richter, T. Springer, A.J. Dianoux, J.J. Rush, T.J. Udovic and S.M. Bennington, *Phys. Rev. B* **50**, 853 (1994).
- [8] M. Kuijper, "Theory of Huang diffuse scattering for hcp lattices", ILL University of Twente, Report de Stage (1994).
- [9] R. Van Buuren, "Huang diffuse scattering from YD_x ", ILL-University of Twente, Report de Stage (1994).
- [10] This data was taken on the TASI spectrometer at the JRR-3M reactor in Tokai-Mura by C.M.E. Zeyen in collaboration with Dr. Aizawa (see ILL Annual Report 1993).

Workshop on "Random Tiling and Quasicrystals",

held at the Institut Laue-Langevin, 7-8 December 1994, organised by Christian Janot and Marc de Boissieu.

About 50 people attended this workshop, whose subject matter was related to the very nature of quasicrystals. Since the early days of quasicrystals a long lived controversy has been continued about what is really mastering their structure stability and growth process. One description takes for granted that the ground state at 0° K is the perfect quasiperiodic tiling as deduced from convenient slicings of an hyperspace periodic image. The alternative approach suggests that quasicrystals are random tiling structure, entropically stabilised at high temperature. The interesting point is that a transition can be considered which transforms easily perfect tiling to random tiling and vice versa. This transition involves special atomic jumps, called dynamical phasons or tile-flips, which are typical of quasicrystals. High resolution diffraction experiments, diffuse scattering measurements and inelastic scattering data demonstrate that most of the structure can be understood in the frame of perfect quasiperiodicity. But a certain amount of phason defects must also be considered. Molecular dynamics and Monte Carlo simulation favour the random tiling models at non-zero temperature and demonstrate the role of phason jumps into diffusion mechanisms.

Vivid discussions have confirmed that the workshop subject had been appropriately selected.

C. Janot

Fast diffusion in ordered alloys

G. Vogl¹, O.G. Randl and B. Sepiol²

We have shown in recent years that the remarkable softening of the lattice in some bcc metals is not only, in an interesting way, connected to the tendency of these metals to undergo martensitic phase transitions, but at the same time is the reason for the unusually high diffusivities [1].

In a naive way one might expect that ordered structures are particularly stable and disfavour the diffusion of their constituents. The message of the present report, however, will be that ordered alloys may behave in just the opposite way.

The aim of the project described here is to reveal the atomistic mechanisms of diffusion processes in ordered alloys, **intermetallic phases** or **intermetallics** in metallurgic terms, and at the same time to determine the connections between diffusion, phonons and defect concentration.

Various experimental methods have been applied: elastic, quasielastic and inelastic neutron scattering, quasielastic Mössbauer spectroscopy and measurements of tracer diffusion. Nearly all studies need single crystals, which we grow ourselves. Most of the investigations are joint ventures with other groups.

In this report we concentrate on the diffusion of the transition metal partner in DO₃ alloys (Fe₃Si structure, see Fig. 1). Fig. 2 shows a comparison of diffusivities in various metallic systems, elementary metals and alloys, from where it is evident that Fe atoms in Fe₃Si and Ni atoms in Ni₃Sb, (both of DO₃ structure) diffuse orders of magnitude faster than metal atoms in their own lattices (self-diffusion).

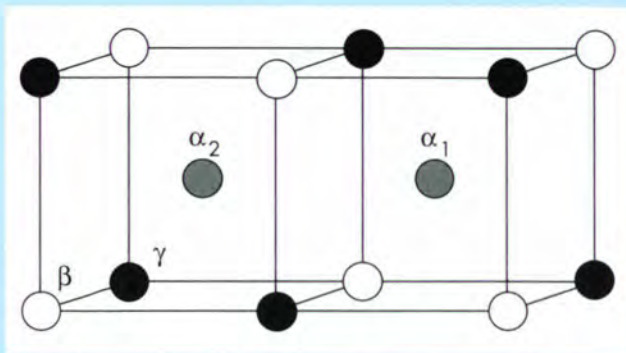


Fig. 1: Unit cell of the DO₃ structure, also named Fe₃Si structure. α_1 , α_2 and γ : Fe; β : Si.

This study started with quasielastic spectroscopy, and that method is still at the centre of our investigations, using the unique facilities in Grenoble (neutrons) and in Vienna (Mössbauer). For readers not familiar with quasielastic Mössbauer spectroscopy (QMS), a "sister" of quasielastic neutron scattering (QNS), a few comments are due: both methods, QMS and QNS, examine energy broadening of the incoherent atomic motion, e.g. diffusion. But, whereas for QNS the elastic line comes from **scattering** of neutrons, for QMS the elastic line is the **resonance line due to nuclear emission or resonant absorption** of a gamma quantum. The underlying theory is analogous: The incoherent scattering function $S(\mathbf{Q}, \omega)$ of QNS corresponds to the emission or absorption function of QMS. $S(\mathbf{Q}, \omega)$ is the double Fourier transform of the self-correlation function $G_s(\mathbf{r}, t)$ and reads in both cases

$$S(\mathbf{Q}, \omega) = (1/2\pi) \cdot \iint G_s(\mathbf{r}, t) \cdot \exp[i(\mathbf{Q}\mathbf{r} - \omega t)] d\mathbf{r} dt.$$

There are, however, a few differences between QMS and QNS which are of practical nature:

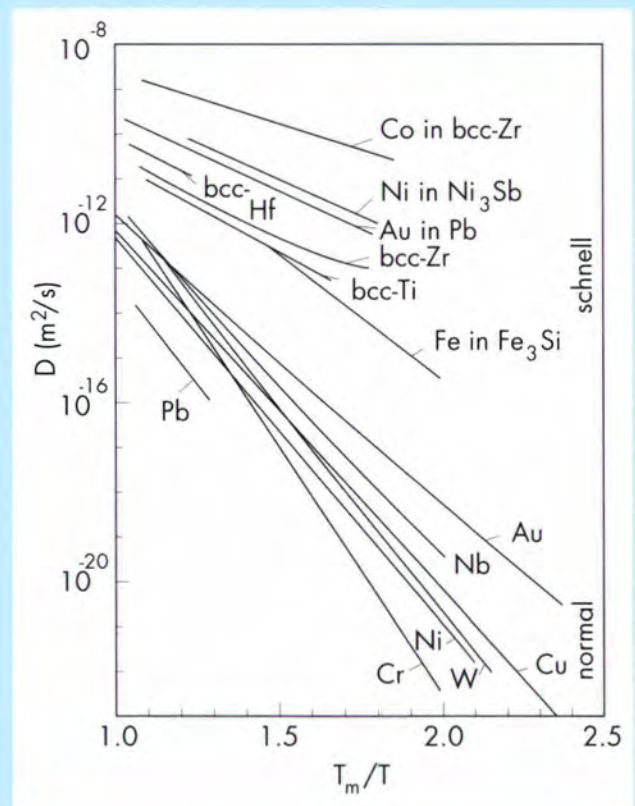


Fig. 2: Arrhenius plot of a few typical diffusivities normalized to the melting temperature T_m . Several orders of magnitude separate the diffusivities of metals with "normal" behaviour from those with "fast" diffusion. The values for Fe₃Si are from [5].

– Whereas in QNS **both the direction and the length** of the neutron scattering vector \mathbf{Q} are variables, for QMS only **the direction** of the photon wave vector \mathbf{Q} can be varied. This might sometimes be a limitation in the endeavour to obtain maximum information on the diffusion jump vector. But since (for ^{57}Fe) the length of \mathbf{Q} is 7.3 \AA^{-1} , the sensitivity of QMS for details of the jump process may sometimes be higher than at the present version of the neutron backscattering spectrometer IN10 where the maximum length of \mathbf{Q} is 2 \AA^{-1} . (This situation will hopefully improve markedly in the near future with the (311) Si monochromator and analysers permitting to scan to higher \mathbf{Q} values).

– The energy resolution for ^{57}Fe QMS is one to two orders of magnitude better than for QNS.

– The two methods are complementary in that the best suited elements are different: for QNS a high incoherent scattering cross-section of the nuclei of the diffusing atoms is needed, whereas QMS needs “Mössbauer nuclei”, as e.g. ^{57}Fe or ^{119}Sn , and thus has a rather limited range of application.

Lattices with atomic order are of non-Bravais type, i.e. the elementary cell contains more than one atom. As described in more detail in the general part of the present College 6 Report, the quasielastic spectrum is composed of m broadened Lorentzians (weights $w_p(\mathbf{Q})$, hwhm $M_p(\mathbf{Q})$), if there are m atoms in the unit cell:

$$S(\mathbf{Q}, \omega) = \sum_{p=1}^m w_p(\mathbf{Q}) \frac{|M_p(\mathbf{Q})|}{|M_p(\mathbf{Q})|^2 + \omega^2}$$

For a comparison of the detailed theories of QMS and QNS for non-Bravais lattices see Randl et al. [2].

We shall now demonstrate the joint venture of different methods on the example of the Fe-Si system.

Fe-Si System

1) Quasielastic Mössbauer spectroscopy

As explained above, the Mössbauer spectrum is composed of several broadened lines, their deconvolution usually leading to ambiguous results. It is therefore worthwhile to take care to reduce the complexity of the spectra. Fig. 3 shows a spectrum taken with the [113] direction of an Fe_3Si single crystal, oriented parallel to the gamma wave vector. This case is particularly simple: for stoichiometric Fe_3Si the spectrum consists of **only two** differently broadened Lorentzians [3].

A small increase of the Fe concentration leads to a much more complicated spectrum [4]. From the \mathbf{Q} dependence of the widths and the weights of the Lorentzians the jump vectors of the Fe atom can be deduced: In the stoichiometric alloy it is a jump between the α and γ sublattices (compare Fig. 1), whereas for non-stoichiometry, jumps to and from antisites on the β sublattice contribute significantly. From the absolute value of the line broadening the diffusivity can be deduced. The diffusivity values are surprisingly high for the stoichiometric Fe_3Si alloy, but decrease rapidly when the Fe concentration is increased. Recent tracer measurements [5] have confirmed the results, proving that Fe atoms in $\text{Fe}_{80}\text{Si}_{20}$ diffuse an order of magnitude more slowly than in Fe_3Si . The surprising message is: **The more order, the faster diffusion.**

In trying to elucidate the reasons for this unexpected result we have performed various investigations: we have searched for lattice softening, we have hunted for extraordinarily high defect concentrations and we have started studies on Ni_3Sb where we were able to apply quasielastic neutron scattering instead of Mössbauer spectroscopy.

2) Inelastic Neutron Spectroscopy

In the ILL Annual Report 1993 we briefly reported on measurements of the dispersion relations in Fe-Si alloys. We searched for lattice softening as one possible explanation for the fast Fe diffusion (compare our extensive work on group 4 metals [1]) and its strong concentration dependence. The result was: The transverse

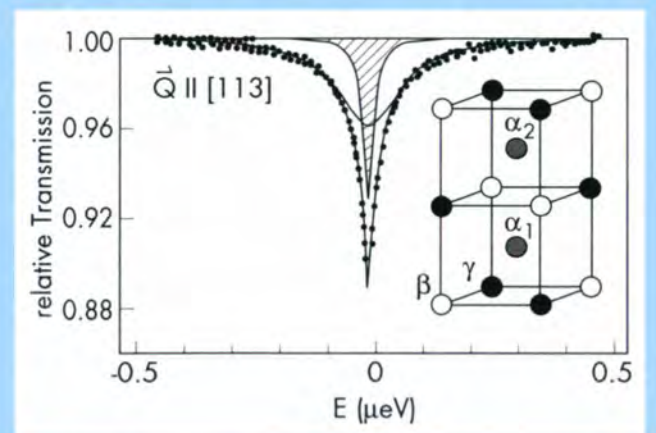


Fig. 3: Mössbauer spectrum of Fe_3Si single crystal in [113] direction at 720°C . The Mössbauer spectrum is composed of two Lorentzians, one which is nearly unbroadened (hatched) and a second line which is much broader. The line through the data points is the sum of the two Lorentzians and a best fit of the data.

acoustic phonon branches are rather low in frequency (see Fig. 4), an effect evidently common to all bcc metals (DO_3 resembles bcc), but there is hardly any concentration dependence. Therefore, the order of magnitude difference in the diffusivities of Fe in Fe_3Si and $\text{Fe}_{80}\text{Si}_{20}$ remains unexplained.

Systematic investigations of the lattice structure of $\text{Fe}_{75}\text{Si}_{25}$, $\text{Fe}_{80}\text{Si}_{20}$ and $\text{Fe}_{84}\text{Si}_{16}$ were performed at the Saphir reactor in Villigen. No unusual effects in the diffraction spectra were observed which might give a hint to the reason for the extremely high vacancy concentrations.

Comparison to the Ni-Sb System and Conclusions

1) Quasielastic Neutron Spectroscopy

The last QNS measurements before the shut down of the HFR were made on a Ni-Sb alloy with DO_3 structure. A figure showing an extremely broad quasielastic line, never before seen for diffusion of metal atoms in a metallic system, may be found in the ILL Annual Report 1993 [6]. A definitive interpretation of the mechanism of the extremely fast diffusion, however, has to wait for measurements after the restart of the reactor. The new version IN10B, looks particularly promising, hopefully permitting to scan the shoulders of very broad lines and at the same time to measure a rather broadened central line. These measurements are already scheduled after the HFR restart.

2) Inelastic Neutron Spectroscopy

The DO_3 structure of Ni_3Sb is restricted to temperatures above 530°C . By analogy to the softening observed in the group 4 metals (Ti, Zr, Hf) when lowering the temperature to the transition temperature between the high-temperature bcc phase and the low-temperature hexagonal phase, we might expect a similar softening of the transverse acoustic phonon branches in Ni_3Sb . Indeed, we found that the frequencies of this branch are rather low, but there is no indication of a particular softening when approaching the phase transition at 530°C . The phonons were strongly damped, indicating a high degree of disorder.

3) Lattice structure

An intriguing phenomenon was found in systematic studies of the DO_3 structure of Ni_3Sb : The (200) and the (222) superstructure lines are missing [7]. A possible explanation for the absence of the reflections is a high vacancy concentration on the α sublattices. This would imply that the stabilisation of the DO_3 type structure in the Ni-Sb system, i.e. the structure which melts congruently (in fact $\text{Ni}_{72.5}\text{Sb}_{27.5}$ and **not**

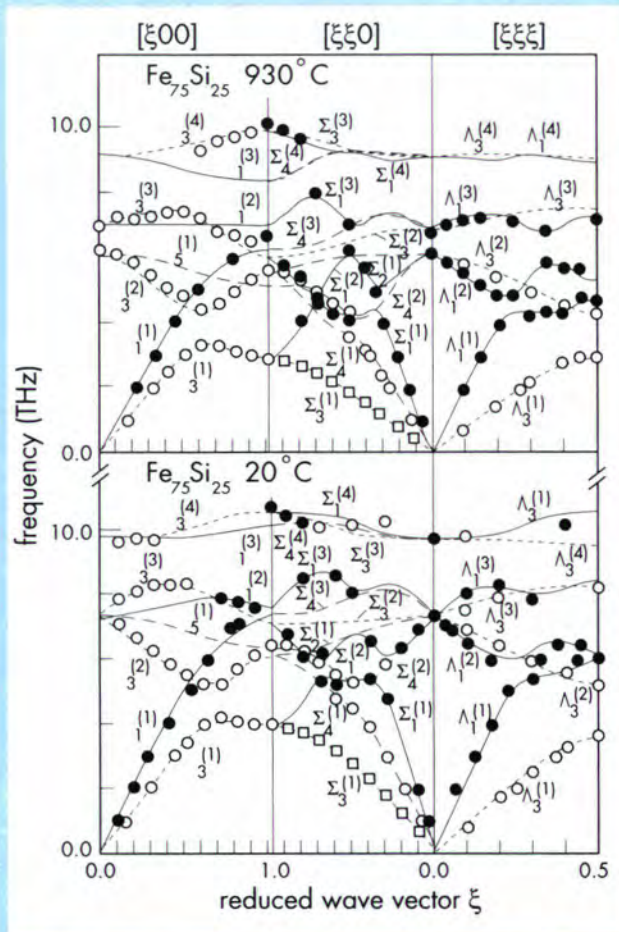


Fig. 4: Phonon dispersion curves in $\text{Fe}_{75}\text{Si}_{25}$ at two different temperatures. The dispersion curves for $\text{Fe}_{80}\text{Si}_{20}$ (the latter are not shown) are practically the same - there is no significant dependence on alloy composition.

$\text{Ni}_{75}\text{Sb}_{25} = \text{Ni}_3\text{Sb}$), is due to the participation of several percent of vacancies. We expect that these extremely high vacancy concentrations will pave the way to solving the puzzle of the very fast diffusion. But two questions remain open:

- What are the vacancy concentrations on the other Ni sublattice (γ sublattice) which are necessary to allow Ni jumps between α and γ sublattices?
- Why have no vacancies been detected in Fe_3Si , the other DO_3 alloy, where again Fe atoms diffuse fast, although not as fast as Ni atoms in Ni_3Sb ?

Measurements of the superstructure reflections in a series of compositions around Ni_3Sb and at various temperatures are scheduled after the HFR restart. A complementary method appears to be available in Grenoble in the near future, i.e. studying the development of the superstructure reflections directly in

the synchrotron beam during heating or cooling of the specimen. This might tell us how the vacancy concentration changes as a function of temperature.

The dispersion relations were measured at Orphée in Saclay, the structure factors at Saphir in Villigen, the tracer diffusivities in Münster. Thanks are due to F. Altorfer, W. Bührer and M. Zolliker (Villigen), B. Hennion (Saclay), W. Petry (now Garching), H. Mehrer and A. Gude (Münster).

References

- [1] W. Petry, ILL Annual Report 1992; for original literature: A. Heiming, W. Petry, J. Trampenau, M. Alba, C. Herzig, H.R. Schober and G. Vogl, Phys. Rev. B **43**, 10948 (1991) and following papers, cited in W. Petry, Phase Trans. **31**, 119 (1991).
- [2] O.G. Randl, B. Sepiol, G. Vogl, R. Feldwisch and K. Schroeder, Phys.Rev. B **49**, 8768 (1994).
- [3] B. Sepiol and G. Vogl, Phys.Rev. Lett. **71**, 731 (1993).
- [4] B. Sepiol and G. Vogl, Hyperfine Interactions, in print.
- [5] A. Gude, H. Mehrer and B. Sepiol, to be published.
- [6] ILL Annual Report 1993, p. 70; B. Sepiol, O.G. Randl, C. Karner, A. Heiming and G. Vogl, J.Phys.: Condens. Matter **6**, L42 (1994).
- [7] O.G. Randl, Dissertation, Universität Wien (1994).

¹ ILL visitor from September 1, 1994. Permanent address: Inst. für Festkörperphysik der Universität Wien, Strudlhofgasse 4, A-1090 Wien, Austria.

² Inst. für Festkörperphysik der Universität Wien, Strudlhofgasse 4, A-1090 Wien, Austria.

A slowing down of the interest in the glass transition?

B.Frick

When a glass forming sample is cooled down close to T_g its shear viscosity increases dramatically and the structural relaxation times get incredibly long - several minutes at T_g , a slowing down phenomenon. So what is the interest to investigate the glass transition on the timescale of nano- to picoseconds with neutrons?

The interest comes from the fact that the atomic or molecular units in the glass, which occupy definitely non-equilibrium positions, start to move locally very fast, i.e. on the picosecond time scale, even below or close to the glass transition temperature T_g . This is measured by neutron scattering as a Debye-Waller factor anomaly and a quasielastic-like scattering and can be interpreted as a precursor towards the glass transition: the so called "fast process" or "fast β -relaxation". Increasing the temperature further above the glass transition temperature we might observe structural relaxation, the α -relaxation. These experimental observations were found to be similar to theoretical predictions for very different types of materials.

About a decade ago it was realised that mode-coupling theories (MC) [1,2,3] might account for the universal behaviour of glasses and some time later an exciting activity in inelastic neutron scattering started at the ILL. Initially followed up by a few groups [4,5,6], the interest into the glass transition grew rapidly as can be judged from the two ILL workshops on "Dynamics of Disordered Materials" in 1988 [7] and 1993 [8]. The proceedings of these workshops show the important role which neutron scattering has played in this area and that, without doubt, neutron scattering did enter here a field which had been reserved until then for experimental techniques which explore the dynamics on a much longer time scale. Furthermore, a large part of the inelastic neutron scattering experiments employed the unique high energy resolution instruments at the ILL. Now, with the prospect of the ILL reactor restart a new wave of proposals concerning the glass transition has been received, demonstrating that the interest in this field has not diminished. Certainly we should ask the question, do we just go on at the point where we stopped 4 years ago, do we expect to learn more than what we already know from our previous experiments and what are the new aspects? Can neutron scattering compete with the light scattering technique which profits from a vast dynamic range and which was successfully applied to test mode-coupling theory [9]? In the following I hope to show that all these questions can be answered positively.

Let me first review the status of the comparison between the **mode-coupling theory (MC)** (see info-box 1) and experiments. The MC-theory merits the new interest into the glass transition. It describes the dynamics of simple liquids on the picosecond time scale by equations of motion for the density correlation and predicts on cooling, or with increasing density, a divergence of the viscosity η at a critical temperature T_c , which is located above the glass transition temperature T_g (see eq. (1), infobox 1). The same critical exponents which enter into the power law for the viscosity (eq. (1)) are governing the spectral behaviour of the dynamic scattering law (eqs. (3), (4)). As a consequence the microscopic density correlations scale above T_c , according to the MC-theory, with the same temperature dependence as the macroscopic shear viscosity.

Thus the experimental effort has mainly concentrated on the determination of the critical temperature T_c and the critical exponents a and b . Many neutron scattering experiments have located T_c at about 20-40 K above T_g . Employing the neutron spin echo technique [4,10] it was shown that the α -process, related to flow processes above T_c , does, on the microscopic scale, follow the same stretched exponential time dependence as on a macroscopic scale. For the critical exponents above T_c qualitative agreement was found in many neutron scattering experiments. Quantitative agreement with eq. (2) was found in fewer experiments: Fig. 1 gives an example for a thorough investigation on ortho-terphenyl [11] (for other examples see [7,8] and references therein). In the meantime results from light scattering experiments gave good agreement with the MC predictions (e.g. [9]). Light scattering has the advantage of a superior statistical accuracy and a wider dynamical range. However, a weakness in the data interpretation presents the unknown frequency dependence of the light-vibration coupling coefficient $C(\omega)$ (see below).

Nevertheless, deviations from the MC predictions for the ratio of the critical exponents a and b in eq. (1) are reported, e.g. for polybutadiene [12,13]. More serious deviations are found for less "fragile glass formers" [14], i.e. for glass forming samples which show above T_g a weaker Vogel-Fulcher temperature dependence for the α -relaxation. For polyisobutylene it was shown that the anomalous intensity increase close to the glass transition, which is usually ascribed to the fast process, does not arise from quasielastic contributions only. Rather, the low frequency vibrational spectrum of the glass changes above T_g and fills up gradually the minimum between the elastic line and the low frequency vibrational excitations. Therefore a straightforward removal of a harmonic vibrational background is not possible. There are furthermore some examples where the fast process is observed already far below T_g [15, 16]. These

observations add to the suspicion that the fast process might be of vibrational origin and that a description by MC theory might be inappropriate below T_c .

This point of view is taken by the soft potential model (SP) (17). This model or modifications of it might be able to explain both, low temperature anomalies of amorphous samples and the Boson peak. The Boson peak consists of additional low frequency excitations which are observed for glasses but not for the crystalline

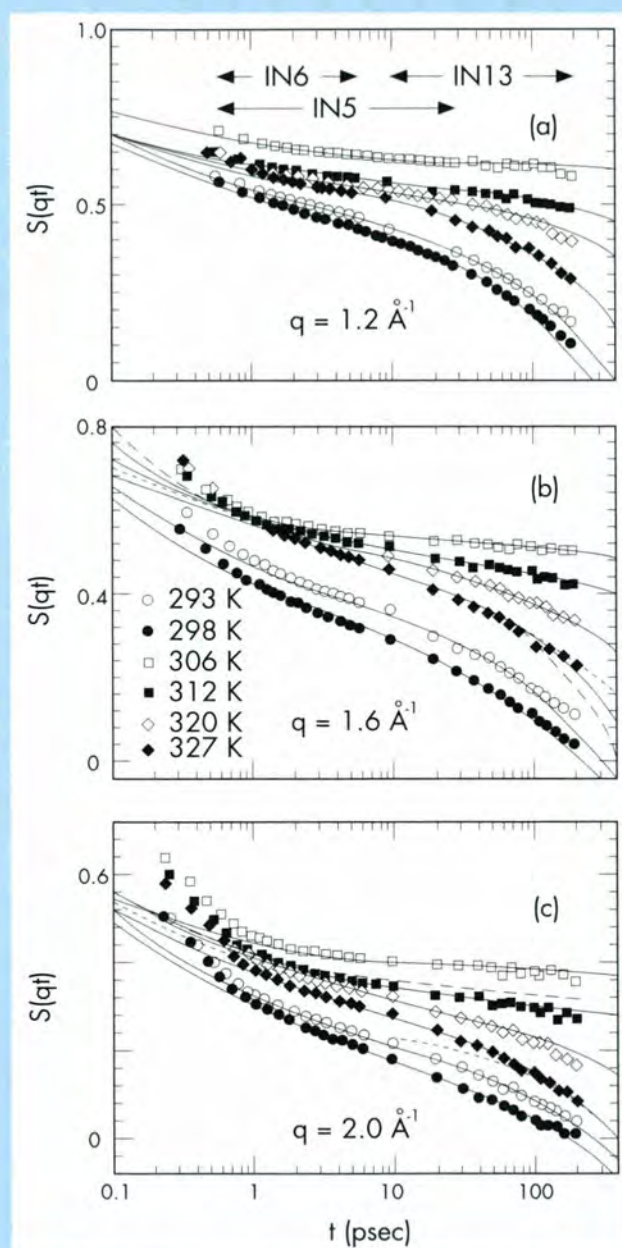


Fig. 1: Intermediate scattering function of ortho-terphenyl for three different Q -values and different temperatures. The solid line fit-curves for the MC-theory with a fixed $\lambda = 0.77$ show a relatively good agreement with the experiment above the initial decay from vibrational contributions [11].

counterpart of the same sample. On the basis of the SP-model, recent neutron scattering experiments on polycarbonate were interpreted by a **vibration-relaxation (VR)** crossover (15). The idea of the VR-model (see info-box 2) is, that due to the nonequilibrium glassy state and the complex energy landscape, atoms are not necessarily located in the energy minimum but might, in the extreme case, even be located on top of a local potential barrier. The low frequency excitations of the glass are thus described via a random dynamic matrix which allows the assumption of a constant eigenvalue density around zero (18). Both situations are present in the glass, harmonic potentials (having positive eigenvalues) and unstable locations in a double well potential (having negative eigenvalues). Thus relaxation and vibrational contributions are closely related.

The VR-model was tested on polycarbonate [15] and on polybutadiene data [19]. For the latter we show first results in Fig. 2. The polybutadiene data were taken on IN6 and are Fourier transformed to time space applying multiple scattering corrections. The solid lines in Fig. 2a correspond to the VR-model. In Fig. 2b we find the parameters which result from the fits with this model. As for polycarbonate the VR-model ascribes a large part of the fast process in polybutadiene to a softening of the Boson peak. This can be clearly seen from Fig. 2b (open symbols), where it is shown that the peak frequency moves clearly towards lower frequency with increasing temperature.

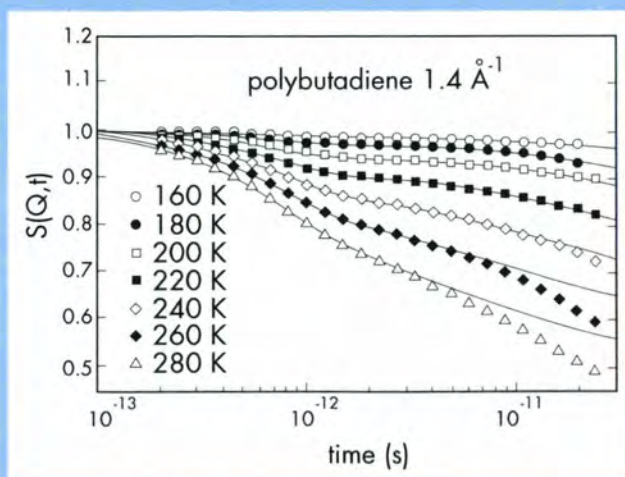


Fig. 2a: Intermediate scattering function of polybutadiene at $Q = 1.4 \text{ \AA}^{-1}$ for different temperatures. The solid line fit curves for the VR-model (parameters see Fig. 2b) show good agreement for the initial decay, due to vibrational excitations, and for a second decay ascribed to relaxations in double well potentials. The experimentally observed decay at longer times is due to the α relaxation which is not treated in the VR-model [19]. The data are Fourier transformed IN6 data.

The same data are compared with another empirical model (Fig. 2c), which was recently applied to polyvinylchloride (PVC) [20] and which describes the two step decay of the intermediate scattering function only by relaxation contributions: a Debye relaxation at short times and the initial part of the α -relaxation at longer times. In this model, the fast Debye relaxation

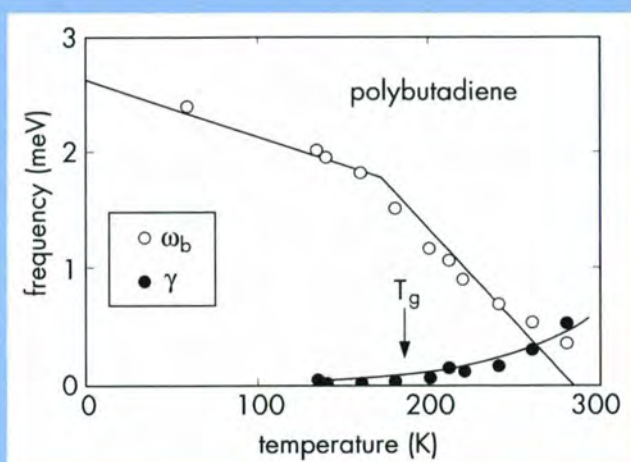


Fig. 2b: Parameters used to fit data in Fig. 2a: Boson peak frequency ω_B and damping γ [19]. The Boson peak shifts towards lower frequencies with increasing temperature and the slope becomes much steeper close to T_g .

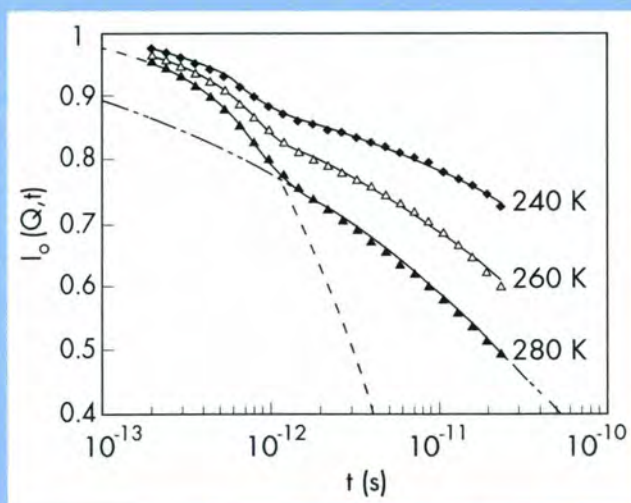


Fig. 2c: Intermediate scattering function of polybutadiene at $Q = 1.4 \text{ \AA}^{-1}$ for different temperatures [19]. The solid line fit curves for a phenomenological model by Ref. [20] (parameters see Fig. 2d) show good agreement over the time range accessed via Fourier transformed IN6 data (same data as in Fig. 2a). The first fast decay is ascribed to non-interacting exponential Debye decay and the second decay to more cooperative processes, the stretched exponential decay of the α -relaxation. Note that the crossover frequency is Q - and temperature-independent as for PVC [20].

process shows Arrhenius behaviour and the α -relaxation the known Vogel-Fulcher temperature dependence (Fig. 2d). Both models describe the experimental data well (note that the VR-model does not aim to describe the α -relaxation which is observed for long times) and from neutron scattering alone one can obviously not decide which is the correct model.

From the discussion above it can be seen that the question about the nature of the fast process is tightly related to the question about the **origin of the Boson peak**. The Boson peak is not included in the MC-theory. An explanation for it might be given, however, in the SP-model. It is also established that the low temperature anomalies of glasses are related to the existence of the Boson peak (for a discussion see e.g. [21]). Most data concerning the Boson peak are from Raman scattering and it is mostly assumed that it is due to some kind of localised vibrations. Employing neutron scattering one could exclude that the reason for the appearance of the Boson peak is a maximum in the frequency dependence of the light vibration coupling coefficient $C(\omega)$, as the Boson peak shows up in neutron spectra as well.

This brings us to another important role which neutron scattering will play in the near future. Via neutron scattering one can directly measure the vibrational density of states whereas the interpretation of light scattering data is complicated by an additional **light-vibration coupling coefficient** $C(\omega)$. Thus neutron scattering data on the same sample can be compared with light scattering data in order to get information about the frequency dependence of the light-vibration coupling coefficient $C(\omega)$. The proposed frequency dependence for $C(\omega)$ ranges from $C(\omega)$ being a constant [22,23], over

being proportional to ω [24,25,26], to being proportional to ω^2 [27]. However, the frequency dependence of $C(\omega)$ is apparently different in the frequency range of vibrations and relaxations. This is shown by an analysis of polystyrene data from neutron and Raman scattering [28]. In Fig. 3 the density of states is shown assuming in Fig. 3a $C(\omega) \sim \omega$ and in Fig. 3b $C(\omega) = \text{const.}$. The relative weight of vibration and relaxation contributions changes with temperature, which can give additional information. The data in Fig. 3 suggest that $C(\omega) \sim \omega$ is valid at frequencies where vibrations dominate and $C(\omega) = \text{const.}$ at frequencies where relaxations dominate. Therefore, in Fig.3a, assuming $C(\omega) \sim \omega$, neutron and Raman scattering data agree at low temperatures, where only vibrational excitations are present. At high temperature the agreement is only found for the high frequency part. In Fig. 3b an agreement is only observed at high temperature and at low frequencies, where relaxations are dominating.

More insight into the discussion about relaxation or vibration might be achieved applying **pressure** onto glass forming liquids and thus inducing an isothermal

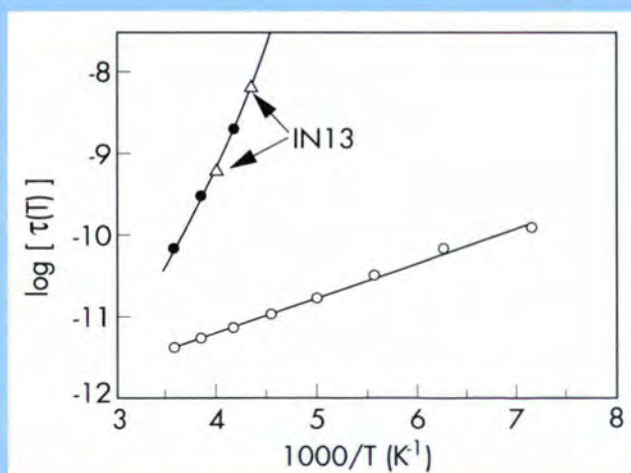


Fig. 2d: Relaxation times used to fit data in Fig. 2c: the α -relaxation times show Vogel-Fulcher temperature dependence (dots from IN6 data; triangles from IN13 data) and the fast Debye process (open circles; data from IN6) shows Arrhenius behaviour [19].

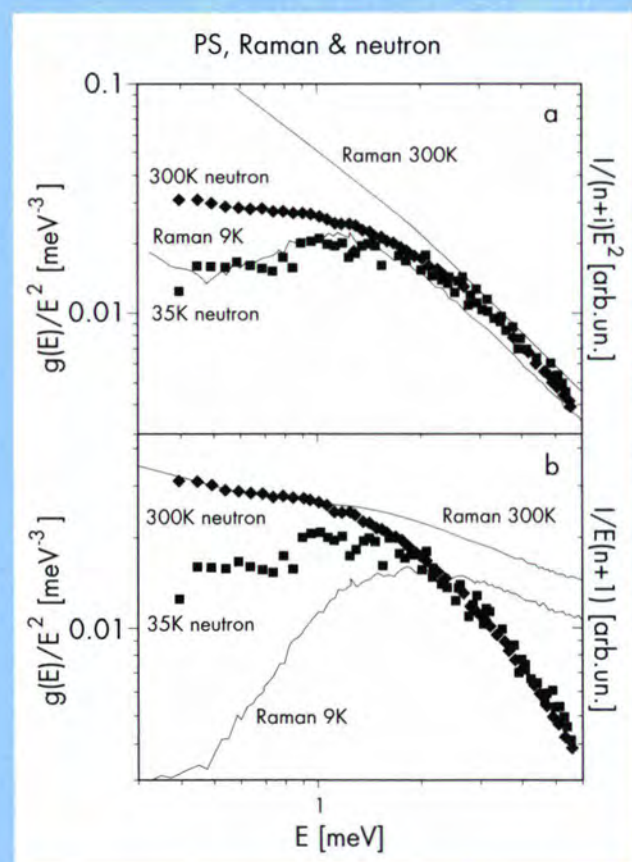


Fig. 3: Comparison of neutron and Raman scattering data of polystyrene [28] to determine the light-vibration coupling coefficient $C(\omega)$ assuming $C(\omega) \sim \omega$ (Fig. 3a) and $C(\omega) = \text{const.}$ (Fig. 3b).

instead of an isobaric glass transition [29]. The critical temperature of the MC-theory should be observable independently of the control parameter, i.e. pressure or temperature. Neutron scattering experiments to investigate the glass transition under pressure are just starting and several experiments will be carried out with this respect at the ILL in the near future.

Let me mention a last point where neutron scattering can make essential contributions. Since **Johari-Goldstein** [30] the existence of a β -relaxation accompanying the structural or α -relaxation is established. The microscopic origin of this Johari-Goldstein β -relaxation, however, is by no means understood. For some time it was claimed that the fast process predicted by the MC-theory can be identified with the Johari-Goldstein β -process. In the meantime it seems much more likely that we have to consider two different processes: the Johari-Goldstein slow β -relaxation and the fast β -relaxation of the MC-theory. This is evident from neutron spin echo data on polybutadiene Fig. 4. Besides the fast picosecond process with a very weak temperature dependence of the relaxation time ("fast β -process"), one observes a second, Arrhenius like "slow β -process". From dielectric and rheological experiments one deduces that this is the Johari-Goldstein β -relaxation, which splits off from the α -relaxation branch, and follows a Vogel-Fulcher temperature dependence. The fast relaxation is observed on the picosecond timescale by time-of-flight experiments. Thus neutron spin-echo experiments might help to learn more concerning the microscopic origin of the Johari-Goldstein β -relaxation. This closes the circle and brings us back to the proposition of the VR-model about vibrations and relaxations in double well potentials.

The examples described above show how open the research in this field still is (the reader may compare again the fits with different models in Fig. 1, Fig. 2a and Fig. 2c). Definitely we have to go on studying the glass transition. Necessarily we will need a wide dynamic range and thus the HR/TOF instruments at the ILL. We will have to compare different techniques (neutron, light, dielectric and NMR) and ultimately we will have to use control parameters other than temperature. The interest in the glass transition is by no means slowing down, it is still growing and neutron scattering in combination with other techniques is needed. We hope to learn more about "slowing down phenomena" near the glass transition.

Finally many thanks go to A. Arbe, U. Buchenau, J. Colmenero, D. Richter, A. Sokolov, J. Wuttke and R. Zorn for their help and permission to print their figures.

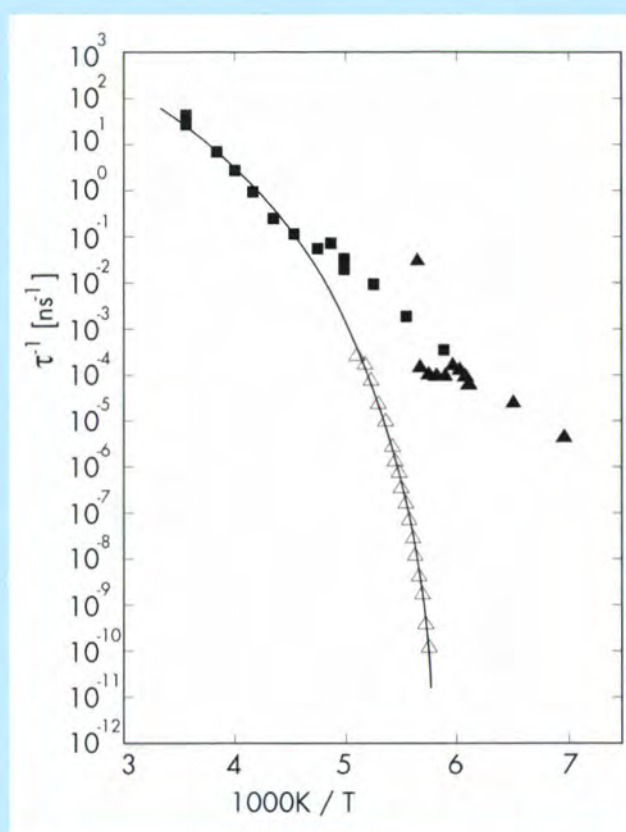


Fig. 4: Relaxation rates from neutron spin echo (■) [31], dielectric (▲) [32] and rheological (△) measurements [33] on polybutadiene, showing the Vogel-Fulcher temperature dependence of the α -relaxation and the Arrhenius temperature dependence of the "slow" β -relaxation. All rates are normalised by constant factors to scale the NSE data.

INFO-BOX I:

Mode-coupling theory (MC) - some formulae

The viscosity η at $T_c > T_g$ is predicted to follow a power law [3]:

$$\eta \approx \frac{1}{\varepsilon^\gamma} \text{ with } \gamma = \frac{1}{2a} + \frac{1}{2b} \quad (1)$$

where $\varepsilon = \frac{T - T_c}{T_c}$ or $\varepsilon = \frac{P - P_c}{P_c}$ is the control parameter or distance from the critical temperature T_c or pressure P_c ; a and b are exponent parameters which are related by

$$\frac{\Gamma(1-a)^2}{\Gamma(1-2a)} = \lambda = \frac{\Gamma(1+b)^2}{\Gamma(1+2b)} \quad (2)$$

Γ being the gamma function and $0.5 < \lambda \leq 1$, $0 < a < 0.5$ and $0 < b < 1$.

The same exponent parameters a and b appear in the dynamic scattering law as power law exponents for the α -relaxation and the predicted fast β -relaxation, respectively. Following the idealized MC-theory, the slower α -process splits off at T_c from the so called fast β -process, and only the β -process remains below T_c . The extended MC-theory includes hopping processes, with the consequence, that the α -process may still exist below T_c . This is more consistent with the experimental observation, because the shear viscosity is often well described by the Vogel-Fulcher law: $\eta = \eta_\infty \exp(\frac{c \text{const.}}{T - T_0})$, with the Vogel temperature T_0 located 40-50 K below the glass transition temperature T_g . Glass forming samples which show an extremely strong Vogel-Fulcher temperature dependence are called "fragile" (e. g. orthoterphenyl) or "strong" in the opposite case of an Arrhenius temperature dependence (e.g. vitreous SiO_2).

Close to T_c the spectral dependence of the α - and fast β -process can be described by two scaling regions, which are best seen via the rescaled susceptibility $\chi'' = (\omega/kT) S(Q, \omega)$. MC-theory predicts that the two asymptotic scaling regimes are separated by a minimum. Two scaling frequencies dominate the spectra: the frequency of the minimum $\omega_{\min} \sim |\varepsilon|^{1/2a}$, which separates the α - and β -scaling regime and $\omega_\alpha \sim |\varepsilon|^{1/2b}$, which governs the α -process. The scattering law in the region around ω_{\min} should have the following form:

$$S(Q, \omega) = f \delta(\omega) + \sqrt{\varepsilon} h_Q f(\hat{\omega}) / \omega_{\min} \quad (3)$$

with the rescaled frequency $\hat{\omega} = \frac{\omega}{\omega_{\min}}$ and the non-ergodicity parameter f (the system is ergodic for $T > T_c$, thus $f = 0$ and non-ergodic below T_c , even for infinite time, thus $f \neq 0$). Note that the second term in eq. (3) factorises into a Q dependent amplitude h_Q and a Q independent spectral function $f(\hat{\omega})$ [3]. The spectral

master function $f(\hat{\omega})$ shows asymptotic power laws for:

the fast β -relaxation

$$f(\hat{\omega}) = \frac{1}{\hat{\omega}^{1-a}} \quad 1 \ll \hat{\omega} \ll \frac{\Omega}{\omega_{\min}}$$

and the "van Schweidler law" (4)

$$f(\hat{\omega}) = \frac{1}{\hat{\omega}^{1+b}} \quad \frac{\omega_\alpha}{\omega_{\min}} \ll \hat{\omega} \ll 1$$

where the "van Schweidler law" presents the tail of the α -relaxation towards the minimum. In the time domain, the intermediate scattering function $S(Q, t)$ will therefore exhibit a two step decay, if phonons are not considered: an initial decay from the fast β -relaxation and a second decay due to the α -relaxation. The time decay of the α -relaxation is thus not simple exponential, but stretches longer in time ("stretched exponential") as is observed by many experimental techniques.

INFO-BOX II:

Vibration-relaxation (VR) model [15]

An empirical scattering law which accounts for the vibrational and relaxational contributions in a multilevel potential energy landscape and which describes experimental data well is given here. The scattering law has the correct low frequency (Debye) and high frequency (random matrix) limits:

$$S_{\text{vib}}(Q, \omega) = \frac{3k_B T Q^2}{2M\omega_0} \sqrt{\frac{A + \omega^2}{B + \omega^4}} \quad (5)$$

with

$$A = \frac{\omega_0^4 \omega_b^4}{\omega_D^6 - 2\omega_0^4 \omega_B^2}, \text{ and } B = \frac{\omega_D^6 \omega_b^4}{\omega_D^6 - 2\omega_0^4 \omega_B^2}$$

with the two free parameters: ω_B the Boson peak frequency and the cutoff frequency ω_0 ; the Debye frequency ω_D is calculated from Brillouin data. The relaxational part of the double well potentials or the quasielastic scattering is calculated assuming that the anharmonic interaction between different modes acts like a stochastic force on a given mode, giving rise to a Langevin equation with friction term γ . Where one assumes a jump rate $\gamma \frac{E_a}{k_B T} \cdot \exp(-\frac{E_a}{k_B T})$ and the activation energy E_a . Integrating over all double well potentials with barrier heights v exceeding $k_B T$ the following relaxation contribution is found:

$$S_{\text{rel}}(Q, \omega) = \frac{4k_B T Q^2}{M \omega_0} \int_1^{\infty} dv \frac{2v\gamma \exp(-v)t}{4v^2 \gamma^2 \exp(-2v) + \omega^2} \quad (6)$$

The friction coefficient γ is the 3rd free parameter of the VR-model. Within the VR-model most of the anomalous intensity increase (or the fast process) is attributed to a softening of the vibrations [15].

These scattering functions maybe considered in the time-domain, with the advantage, that the resulting intermediate scattering function then includes all multiphonon contributions, but the experimental data have to be Fourier-transformed, see Fig. 2a [19]. The intermediate scattering function shows then a two step decay, at short times due to vibrations and at longer times due to relaxation over potential barriers. The α -relaxation, which should be observed for even longer times, would lead to an additional decay and is not considered in the VR-model.

References

- [1] E. Leutheusser, Phys. Rev. A **29** (1984) 2765.
- [2] E. Bengtzelius, W. Götze, A. Sjölander, J. Phys. C **17** (1984) 5915.
- [3] W. Götze, Liquids, Freezing and the Glass Transition, J.P. Hansen D. Levesque, J. Zinn-Justin, Eds., (North-Holland, Amsterdam, 1991).
- [4] F. Mezei, W. Knaak, B. Farago, Phys. Rev. Lett. **58** (1987) 571.
- [5] F. Fujara, W. Petry, Europhys. Lett. **4** (1987) 921.
- [6] B. Frick, D. Richter, W. Petry, U. Buchenau, Z. Phys. B **70** (1988) 73.
- [7] D. Richter, A.J. Dianoux, W. Petry, J. Teixeira, Eds., Dynamics of Disordered Materials, vol. 37 (Springer Verlag, Berlin, Heidelberg, New York, 1989).
- [8] A.J. Dianoux, W. Petry, D. Richter, Dynamics of Disordered Materials II, (Physica A, Grenoble, 1993), vol. 201.
- [9] H.Z. Cummins, W.M. Du, M. Fuchs, W. Götze, A. Latz, G. Li, N.J. Tao, Physica A **201** (1993) 207-222.
- [10] D. Richter, B. Frick, B. Farago, Phys. Rev. Lett. **61** (1988) 2465.
- [11] J. Wuttke, M. Kiebel, E. Bartsch, F. Fujara, W. Petry, H. Sillescu, Z. Phys. B **91** (1993) 357.
- [12] R. Zorn, D. Richter, B. Frick, B. Farago, Physica A **201** (1993) 52-66.
- [13] B. Frick, D. Richter, R. Zorn, L.J. Fetters, J. Non-Crystalline Solids **172-174** (1994) 272-285.
- [14] B. Frick, D. Richter, Phys. Rev. B **47** (1993) 14795.
- [15] U. Buchenau, C. Schönfeld, D. Richter, T. Kanaya, K. Kaji, R. Wehrmann, Phys. Rev. Lett. **73** (1994) 2344.
- [16] B. Frick, U. Buchenau, D. Richter, Colloid & Polymer Science (1994).
- [17] V.G. Karpov, M.I. Klinger, F.N. Ignat'ev, Zh. Eksp. Teor. Fiz. **84** (1983) 760.
- [18] E.P. Wigner, Ann.Math. **67** (1958) 325.
- [19] R. Zorn, A. Arbe, J. Colmenero, B. Frick, D. Richter, U. Buchenau; 1994, unpublished.
- [20] J. Colmenero, A. Arbe, A. Alegria, Phys. Rev. Lett. **71** (1993) 2603.
- [21] U. Buchenau, Europhys. News **24** (1993) 77.
- [22] G. Li, W. M. Du, X.K. Chen, H.Z. Cummins, N.J. Tao, Phys. Rev. A **45** (1992) 3867.
- [23] V.L. Gurevich, Phys. Rev. B **48** (1993) 16318.
- [24] A. Fontana, F. Rocca, M.P. Fontana, A.J. Dianoux, Phys. Rev. B **41** (1990) 3778.
- [25] T. Achibat, A. Boukenter, E. Duval, B. Frick, N. Garcia, J. Serughetti, Physica A **201** (1993) 257-262.
- [26] A.P. Sokolov, A. Kisliuk, D. Quitmann, E. Duval, Phys. Rev. B **48** (1993) 7692.
- [27] A.J. Martin, W. Brenig, Phys. Status Solidi B **64** (1974) 163.
- [28] A.P. Sokolov, U. Buchenau, B. Frick, unpublished (1994).
- [29] C. Alba-Simonesco, J. Chem. Phys. **100** (1994) 2250.
- [30] G.P. Johari, M. Goldstein, J. Chem. Phys. **53** (1970) 2372.
- [31] D. Richter, R. Zorn, B. Farago, B. Frick, L.J. Fetters, Phys. Rev. Lett. **68** (1992) 71.
- [32] R. Zorn, F.I. Mopsik, 1994, unpublished.
- [33] R. Zorn, G.B. McKenna, L. Willner, D. Richter, Macromolecules 1994, in press.

Biological Structures and Dynamics

Members of the College at ILL

P. Chenavas	R.P. May
A.J. Dianoux	E. Pebay-Peyroula (IBS)
K. Ibel	P.A. Timmins
M.S. Lehmann	L. Vuillard
P. Lindner	G. Zaccai (IBS)
S.A. Mason	

External members

At IBS

J. Chrobczek	N. Louis
C. Cohen-Addad	D. Madern
A.M. Di Guilmi	M. Roth
C. Ebel	M. Van der Rest
B. Jacrot	

At EMBL

A. Åbergg	T. Kawashima
A. Barge	U. Kapp
F. Baudin	K. Klumpp
G. Beg	K. Larsen
H. Belrhali	R. Leberman
C. Berthet	S. Malbet-Monaco
L. Boqué	S. Price
F. Borel	B. Rasmussen
K. Brown	R. Ruigrok
S. Cusack	L. Seignoret
M.T. Dauvergne	C. Taupin
S. Doublé	A. Thompson
C. Elster	M. Toukalo
M.L. Ferri	C. Wilkinson
M. Härtlein	A. Yoremchuk

At ESRF

C. Brändén
A. Kvick
M. Saad

At Faculté de Pharmacie

M. Cussac

Scientific Trends and Highlights in 1994

Laue and quasi-Laue diffraction work

Instrument development for the Quasi-Laue diffractometer has continued and is described in some detail in the report of the activity within the large-scale structures group. As no neutrons were available at the ILL,

experimental tests have been done elsewhere, this year at the DR3 Reactor at Risø, Denmark, supported by the EEC Large Installation Program.

Measurements to test the detector were done at the TAS7 position using a monochromatic wavelength of 3.5 Å and to optimise access to the beam, the normal spectrometer was removed completely. Moreover, to reduce the background of γ -radiation to which the detector is very sensitive, a 5 cm thick lead wall was built in the region between the monochromator housing and the diffractometer. Even with this precaution the γ -background was high, but not high enough to prevent further experimentation.

Crystals of triclinic lysozyme (hen egg-white) were used for the recording of limited sets of diffraction data. 5 spectra were measured, each with a 5° oscillation of the crystal around the horizontal cylinder axis.

The final spectra, a 6° oscillation of a 2x2x2 mm² large crystal, shown in figure 1 page 141, contains about 100 Bragg-reflections. A simulation based on the indexed pattern gave 160 reflections, as expected, so with lower background most of the data will be observable.

Work on new methods for indexing Laue-patterns has also been started in collaboration with members of the EMBL both for the expected neutron patterns, but also for X-ray diffraction patterns recorded with synchrotron radiation [1].

In the X-ray case it should be possible to index multiple-crystal patterns, and thus partially combine powder and high-collimation Laue diffraction. First measurements at ESRF on BL3 using small crystals dispersed on adhesive tape showed that the method is feasible experimentally, and till now a number of simulated patterns have been indexed and used to define the further experimental requirements. X-ray Laue-measurements on polycrystalline material would, despite the obvious complexity, be of great interest both for small and large molecule crystallography because it allows recording of a complete set of data in just one exposure.

Purple Membrane

The purple membrane of *Halobacterium halobium* remains extremely interesting to study by neutron diffraction and inelastic scattering, despite the amount of work that has already been done on this system using these approaches during the last decade. The membrane contains one protein, bacteriorhodopsin, naturally arranged with lipid on a highly ordered two-dimensional lattice that makes it amenable to crystallographic methods. Bacteriorhodopsin was so named because, like rhodopsin in animal retinas, it binds one molecule of retinal. It functions as a light-driven proton pump, converting photon energy to pump protons against the chemical potential gradient, from inside the cell to the outside. One proton is pumped for one photon absorbed and a photocycle of colour changes for the retinal, related to

changes in its structure and protein environment, is associated with this process. The ultimate goal of work on bacteriorhodopsin is to gain an understanding of the principles underlining the structure of alpha helical membrane proteins as well as the molecular, atomic and electronic mechanisms of energy transduction.

Early neutron experiments focused on hydration and structural studies, making good use of H₂O/D₂O exchange and deuterium labelling, respectively. Current interest centres on structure-function and dynamic-function relationships. Functional mutants, which have been prepared and characterised by spectroscopic and other structural methods, will become the objects of neutron diffraction studies under different conditions. New deuterium labelling techniques are being developed to investigate the functional motions of different parts of bacteriorhodopsin by neutron scattering with energy resolution, in a conjunction with the diffraction experiments that located deuterium labels in the structural studies. The aim of these experiments is to refine the correlation already observed between the protein's ability to convert energy and pump protons and the anharmonicity of its thermal motions. It is interesting to point out, however, that because incoherent (and not coherent) scattering is analysed in these dynamics experiments, the signal is dominated by H labels in a fully deuterated structure, rather than D in an H structure as in the neutron diffraction work. This is similar to the situation in NMR work. Therefore neutron and NMR scientists have a common interest in the development of deuterium and hydrogen labelling. An EMBO workshop on the subject was organised jointly by the two communities, in 1994, near Grenoble, see report at the end of the College 8 contribution.

The bacteriorhodopsin neutron work is the object of various collaborations involving mainly the Institut de Biologie Structurale, in Grenoble, groups at the MPI in Martinsried near Munich, at the HMI in Berlin and in Jülich. Complementary visible light absorption, other spectroscopic experiments and structural studies by electron microscopy or synchrotron radiation are being performed in France, Germany, Italy, Japan, UK and USA.

Molecular modelling of Photosynthetic Reaction Centres

Photosynthetic reaction centres are transmembrane protein-pigment complexes that perform light-induced charge separation during the primary steps of photosynthesis.

The three-dimensional structures of the bacterial photosynthetic reaction centre from *Rhodospseudomonas (Rps.) viridis* and *Rhodobacter (Rb.) sphaeroides* have been solved to atomic resolution. This has provided impetus for theoretical and experimental work on the mechanism of primary charge separation in the photosynthetic reaction centres.

Site-directed mutagenesis has been most developed for a reaction centre for which the structure has not yet been solved: that of *Rhodobacter capsulatus*. A three-dimensional

structure for the *Rb. capsulatus* RC would thus be of particular interest as a first step towards an atomic-level interpretation of the biochemical and biophysical data available as well as to facilitate the rational design of new mutants. We thus use computational techniques to derive a model for the structure of the *Rb. capsulatus* RC.

It is now well documented that proteins closely related in sequence usually exhibit very similar folds. Indeed, *Rps. viridis* and *Rb. sphaeroides* reaction centres are structurally homologous with 54% of sequence identity on average for their L and M subunits. The root mean square deviation between the backbone atoms of proteins with > 50% sequence identity is commonly ~ 1.0Å. Furthermore it has been shown that, in highly homologous proteins, many dihedral angles are to be similar in topologically equivalent side-chains, whether or not the residues are identical.

In the modelling procedure the *Rps. viridis* backbone and identical side-chains coordinates were transferred to *Rb. capsulatus*. The non-identical side-chains and cofactors were positioned using molecular mechanics calculations (using the Charmm force field) suitable for deriving a structure when that of a highly homologous protein exists. In a last step, the local environment of each pigment was refined using simulated annealing combined to molecular dynamics with stochastic boundary conditions.

We focused the analysis of the final model structure on the pigment regions. The structure contains a number of differences from the *Rps. viridis* and *Rb. sphaeroides* RCs and detailed information has been derived from this new model [2]. This now provides a basis from which the rationalisation of the effect of mutagenesis can be envisaged.

Chaperones

Chaperones are proteins which act on the conformations of substrate proteins. In fact, environmental influences (e.g. heat, chemicals) may unfold proteins so that they are unable to exert their functions. Chaperones play an important role in these processes because they can stabilise (or recover) the active conformations of unfolded proteins by shifting the equilibrium towards the active state. Chaperones are multi-component complexes. The active protein is made of a main protein, GroEL consisting of 14 monomers of 57.3 kD and a helper protein, GroES, consisting of seven monomers of 10 kD. An X-ray crystallographic study of the GroEL ring was published this year. There is multiple evidence that the function of the Chaperones is a highly dynamic process requiring the association and dissociation of GroEL and GroES. Such processes cannot be investigated in a crystal. However, they are easily studied in solution by X-ray and neutron scattering. X-rays are suitable for investigating the association/dissociation kinetics, whereas neutrons allow one to study isotopic hybrid molecules, and thus the partial form factors of the single components. In an ILL/MPI Martinsried/Universität Zürich collaboration, first attempts

concerning the solution behaviour of Chaperones were made at the Small-Angle Scattering Instrument at the HMI, Berlin [3].

DNA-dependent RNA polymerase

DNA-dependent RNA polymerase is the enzyme which creates an RNA "blue print" of the genetic information contained in DNA. The messenger RNA so produced by the enzyme is used by the ribosome to synthesise proteins. RNA polymerase has been studied at the ILL for many years. This year, the movement of RNA polymerase along a specially constructed piece of DNA was studied during a small-angle scattering experiment at the HMI (ILL - MPI für Biochemie, University of Erlangen). The DNA also carried a Tet repressor as a marker molecule. The scattering curves of the complex consisting of DNA, Tet repressor and polymerase were measured in order to determine the distance between the polymerase and the Tet repressor at the initiation (binding to DNA) of polymerase and after a nucleotide-controlled shift of polymerase along the DNA [4].

New agents for protein purification

Last year a collaboration between the ILL biochemistry laboratory and a CEA -INSERM laboratory from Grenoble led to the discovery of **non-detergent sulfobetaines** (figure 2) as a new class of mild solubilising agents for proteins. These agents were originally intended to be used for purification by isoelectric focusing of protein specimens destined for crystallography. In 1994 new work has shown that non-detergent sulfobetaines not only solubilised but also stabilised proteins and could be applied widely in biochemistry.

Extraction of proteins: The increase in extraction yields of proteins in the presence of non-detergent sulfobetaines was observed in several protein systems such as freeze-dried blood platelets, cell nucleus and cell membranes [5]. This property of non-detergent sulfobetaines is now being applied at the Institut Pasteur in Paris for the purification of important membrane proteins from the malaria parasite.

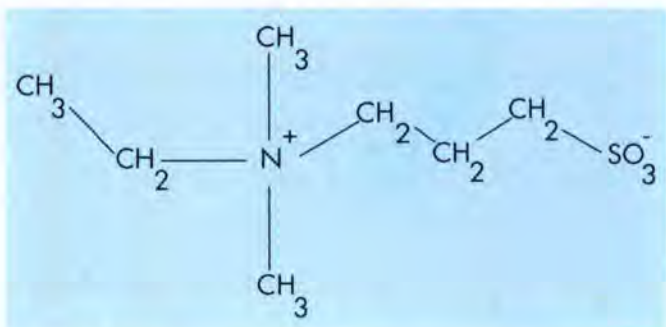


Fig. 2: SA195 a new mild protein solubilisation agent from the non-detergent sulfobetaine family.

Stabilisation of proteins: non-detergent sulfobetaines can stabilise proteins against denaturation as shown either by measurements of enzyme activity during heat denaturation or with conformation-sensitive immunological techniques.

Crystallisation of proteins: We have started to apply non-detergent sulfobetaines to protein crystallisation in a collaboration with several teams and particularly with the EMBL Grenoble outstation. We started with the classic test protein for crystallisation: hen egg white lysozyme. Lysozyme can crystallise under a large set of conditions but the use of ammonium sulphate as precipitant has always led to amorphous precipitation. In the presence of non-detergent sulfobetaines, we have been able to obtain diffracting crystals of Lysozyme using ammonium sulphate as a precipitant [6]. This work demonstrates that non-detergent sulfobetaines can be successfully applied to obtain protein crystals in unfavourable conditions.

Neutron scattering experiments should help to understand how non-detergent sulfobetaines affect proteins.

Secretary: Laurent Vuillard

References

- [1] M.S. Lehmann, C. Wilkinson, work in progress.
- [2] N. Foloppe, M. Ferrand, J. Breton & J. C. Smith, *submitted to Proteins* (1994).
- [3] N. Stegmann, H. Heumann, A. Plüclerthun, R. May, work in progress.
- [4] H. Heumann et al., work in progress.
- [5] L. Vuillard, C. Braun-Breton, T. Rabilloud, *Biochem. J.* (1995) 305 339-343.
- [6] L. Vuillard, T. Rabilloud, R. Leberman, C. Berthet, S. Cusack, *FEBS* (1994) 353 294-296.

EMBO Workshop on Deuteration of Biological Molecules for Neutron Scattering and for NMR

A workshop on the "Deuteration of Biological Molecules for Neutron Scattering and for NMR" was held at Autrans, September 26-October 1, 1994. The workshop, funded by EMBO, was organised by P.A. Timmins (ILL), R. Leberman (EMBL, Grenoble), D. Marion (IBS, Grenoble) and J. Parello (Montpellier).

The goal of the workshop was to establish a link between two communities of scientists in structural biology, those using neutron scattering methods on the one hand and those using multi-dimensional NMR methods on the other. Both have been using deuterium labelling approaches with the aim of determining the tertiary folding of biological macromolecules at atomic resolution, either in solution or in the crystalline state, and the tertiary organization of multicomponent assemblies, as well as characterizing their interactions with small molecules.

Whereas the instrumental and conceptual approaches differ totally in the two scientific communities, an obvious link exists between them in regard to the deuterium labelling strategies. Such strategies are dependent of the present state of the art of different biochemical and chemical methodologies. The selectivity of deuterium incorporation appears a crucial problem which needed to be addressed during the workshop as part of a future challenge in structural biology. The Workshop therefore included the participation of biochemists working in the field of stable isotope incorporation into a variety of biological molecules through biosynthetic procedures (deuteration of *E. Coli* biomass, *in vivo* deuteration of tRNAs, ...), as well as organic chemists opening new synthetic routes for preparing novel deuterium labelled compounds to be used in biosynthetic incorporations (membrane lipids, regio- and stereoselectively deuterated amino acids).

Deuterium labelling of biological macromolecules for neutron scattering studies in solution has emerged as a favorable and complementary approach to the contrast variation method (based on the use of $^1\text{H}_2\text{O}/\text{D}_2\text{O}$ mixtures). This approach essentially involves the use of perdeuterated molecules which in principle can be obtained through biosynthesis in the case of bacterial or algal proteins. Such an approach is well documented by the neutron scattering triangulation studies of multicomponent systems which can be reconstituted with one or several of its proteins selectively perdeuterated (ribosome, RNA polymerase-promoter complex).

A similar need for perdeuterated proteins appears in relation to crystallographic studies using neutron diffraction. Until now this approach, which allows the hydrogen atoms in the protein to be located directly, as well as to accurately characterize hydrogen bond networks in the hydration shell of the protein, has suffered from the lack of crystallized deuterated proteins. By reducing the contribution of incoherent scattering due to the occurrence of a large population of protons in the protein, neutron crystallographic studies of deuterated proteins and other biological macromolecules will offer a clear advantage in regard to signal-to-noise ratio in contrast to normally protonated proteins.

The expression in bacteria of exogenous proteins as perdeuterated molecules appears to be less straightforward than in the case of intrinsic proteins. Bacterial growth conditions in media not exceeding 90% D_2O appears to be

the rule for a successful expression, as demonstrated in the case of several proteins expressed in *E. Coli* (chloramphenicol acetyltransferase, Trp repressor, FMN-binding domain of cytochrome P450 reductase, dihydrofolate reductase). Such deuterated proteins can be favourably used for NMR studies at atomic resolution in regard to a variety of interactions with small ligands. Similarly the conformation of peptide antigens bound to deuterated antibodies through incorporation of deuterated amino acids can be determined by difference NOESY (Nuclear Overhauser enhancement spectroscopy) spectroscopy. Another example was the determination of the conformation of cyclosporin A (normally protonated) bound to perdeuterated cyclophilin. In all cases the reduction of spin diffusion allowed NOE's (Nuclear Overhauser effect) to be measured more accurately, thus offering a strong basis for the determination of the bound conformations.

The access to chemically synthetic proteins in the 75-residue range (HIV1 TAT protein) of suitable purity offers a unique perspective of selectively labelling small proteins (in the 100 residues range) site by site in contrast to the biosynthetic approach. Semi-synthetic procedures with larger proteins can also be envisaged with similar results.

Internal dynamics are actively investigated by inelastic neutron scattering on the picosecond time scale. Up to now the contribution of deuteration to the understanding of functional dynamics has remained restricted due to the large quantities of biological material required. However, it is anticipated that selective deuteration will provide a suitable approach for analyzing the contributions of different structural elements to protein dynamics.

The use of deuterated molecules appears of the highest interest for neutron scattering and NMR studies in structural biology. The production of such deuterated molecules in a highly controlled manner is a requirement which is only partly fulfilled. The workshop thus allowed scientists to confront their results on the scope and limitations of the use and production of deuterated molecules in neutron scattering and NMR studies of biological macromolecules. In this context, the final Round Table clearly raised the need for centralizing information concerning different deuteration procedures, as well as deuterated media and molecules. Prof. Paul Rösch (Bayreuth, Germany) will effectively centralise requests for and offers of material via e-mail.

P. Timmins

Molecular Spectroscopy, Surfaces and Mesophases

Members of the College at ILL

I. Anderson	H.J. Lauter
H. Büttner	A. Lied
S. Bramwell	K. Liss
A.J. Dianoux	A. Magerl
C. Doll	J. Pannetier
B. Farago	C. Ritter
A. Heidemann	P. Terech (CENG)
G. Kearley	

External members

J.P. Beaufiles (ENS Lyon)	I. Morfin (UJF)
M. Bée (UJF)	C. Poinignon (UJF)
M. Benmouna (UJF)	D. Quenard (CSTB)
E. Geissler (UJF)	F. Rieutord (CENG)
A. M. Hecht (UJF)	M. Rinaudo (UF)

Introduction

The reactor was still down for another full year. The scientific life, however, continued. Apart from getting the spectrometers ready for operation, further scientific results were obtained from visits to other centers as in the previous years.

Low-energy excitations, density of states experiments

Inelastic neutron scattering studies of poly (*p*-phenylene vinylene)

[University of Pennsylvania, NIST, Université Montpellier II, ILL, University of Wisconsin, University of Massachusetts]

Poly-(*p*-phenylene vinylene) (PPV) is a prototypical conjugated polymer with a non-degenerate ground state. The polymer chains are composed of alternating phenylene rings ($-C_6H_4-$) and vinylene segments ($-CH=CH-$). PPV exhibits interesting electronic and nonlinear optical properties, and the electrical conductivity of a highly stretched film of PPV after doping with concentrated sulfuric acid is reported to be as high as $1.12 \times 10^4 \text{ S cm}^{-1}$. PPV derivatives can be used to fabricate light-emitting diodes.

PPV films synthesized by thermal conversion and simultaneous uniaxial stretching of soluble precursors exhibit a high degree of crystallinity and relatively large coherence lengths. Several electron and X-ray diffraction measurements have been performed in order to determine the crystal structure, yielding similar results. The interchain packing is very regular, with the characteristic herringbone arrangement of two inequivalent chains per projected 2-dimensional rectangular unit cell.

Diffusion of dopant ions provokes substantial changes in the host structure, which can be generally described in terms of single chain rotations and translations. Furthermore, the intrachain vibrations (particularly those of the phenylene rings) and the concomitant changes in dihedral angle are believed to be closely related to the electronic properties of the polymer. Therefore, detailed knowledge of the dynamics are clearly needed. Intrachain vibrational data are available from infrared- and Raman-active mode above 400 cm^{-1} (50 meV), while very little is known about the inter- or intrachain dynamics at lower energies.

Mode polarization and energy spectra for the lattice modes of poly (*p*-phenylene vinylene) are obtained by inelastic incoherent neutron scattering methods [1]. Experiments were performed on stretch-oriented, highly crystalline films with time-of-flight and filter-analyser spectrometers. By measuring all-hydrogen and vinylene-deuterated samples, we show that almost all of the observed modes can be attributed to phenylene motions. The low energy features in the vibrational density of states consist of a longitudinal 2.5 meV mode assigned to a damped translational motion along the chain axis, a 7 meV phenyl ring in-phase librational mode (transverse with respect to the chain axis), and strong bands at 15 and 25 meV showing mixed polarization (Figures 1 and 2). Higher frequency modes are in excellent agreement with published IR and Raman studies.

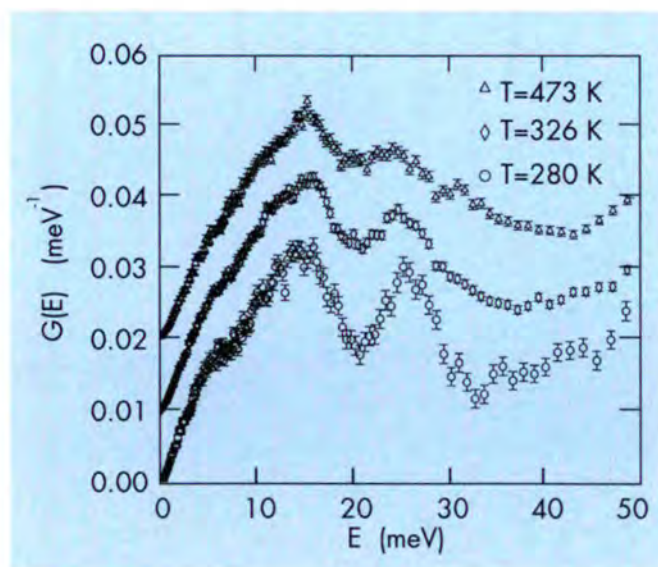


Fig. 1: The effect of temperature on the perpendicular component G_{\perp} of the density of states. The improvement of the signal-to-noise ratio was achieved in the C_{\perp} geometry by summing the response from all detectors in $7^{\circ} < 2\theta < 127^{\circ}$ range. The $G_{\perp}(E)$'s were normalized to unity in 0.50 meV and offset vertically by 0.01 meV^{-1} for clarity. The data have been obtained with the spectrometer MIBEMOL at the LLB (Saclay).

Furthermore, we have found that the strong band at 25 meV polarized mainly (but not exclusively) in the transverse direction with respect to the chain axis shows significant anharmonic character, shifting to lower frequency with increasing T (i.e. with increasing dihedral angle of the phenylene rings). To our knowledge this is the first time in the field of conducting polymers that a clear correlation between structural features and low-frequency vibrational dynamics has been established. Our vibrational analysis based on AM1 force constants suggests possible phenylene ring librations near 25 meV coupled with considerable chain torsions and "wobble" of the ring axis (figure 3).

Electronic interactions in small-molecule magnets

[University of East Anglia, ILL]

The group of Cannon and Jayasooria at the University of East Anglia exploited neutron scattering for the study of magnetic properties of ligand-bridged polynuclear metal complexes. Such complexes provide models for active sites in various metalloenzymes, and they are excellent materials for testing theories of electronic interactions between magnetic atoms. This is because molecules of the same structural type can be made with a wide range of metal atoms including mixed-metal combinations and mixed valencies, and with various bridging units effecting small systematic changes in the geometry. The trinuclear structure type shown in Figure 4 is particularly versatile.

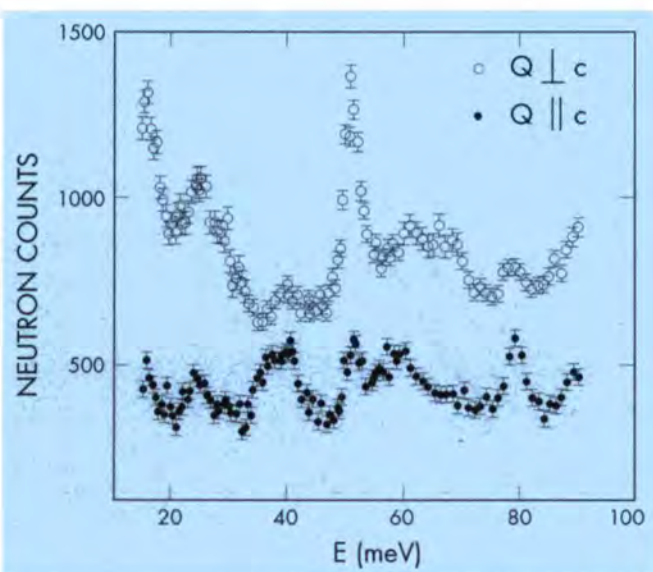


Fig. 2: The comparison of the D2-PPV spectra obtained in the parallel (filled circles) and perpendicular (open circles) configuration for samples temperature 150 K. Both spectra were measured for the same monitor count of the incident beam. The $Q \perp c$ spectrum is shifted upwards by 300 counts for clarity. The data have been obtained with the filter-analyser spectrometer at NIST (Gaithersburg).

The complex $[\text{Cr}_3\text{O}(\text{OOCCH}_3)_6(\text{H}_2\text{O})_3]\text{Cl} \cdot 5\text{H}_2\text{O}$, shows INS spectra consistent with predominantly antiferromagnetic coupling between pairs of chromium ions [2]. The complete spectrum of transitions between successive states with total spin $S = 1/2, 3/2, 5/2, 7/2$ and $9/2$ has been observed [3]. Splittings of the ground state $S = 1/2$ have been observed directly and attributed to lowering of symmetry of the triangular cluster. Recent data confirm that two sets of complex cations with different degrees of symmetry lowering are present in the crystal, at the low temperatures used (1.4 to 50K) and they show for the first time that at least one of these complexes has a scalene triangular structure. In other words the three values are all different and

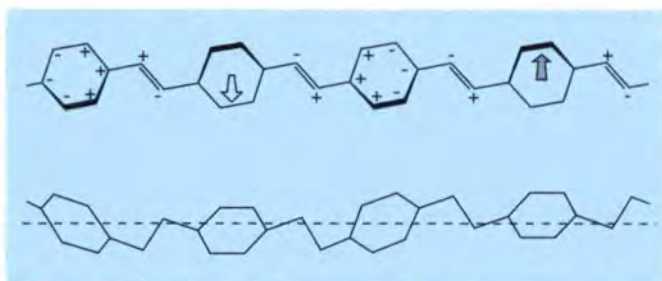


Fig. 3: Calculated vibrational mode at 25.2 meV in the 4-segment repeat unit AM1 calculation. Upper figure - side view of the chain; lower figure - top view (the dashed line denotes the equilibrium vinylene plane). The displacements are exaggerated for clarity.

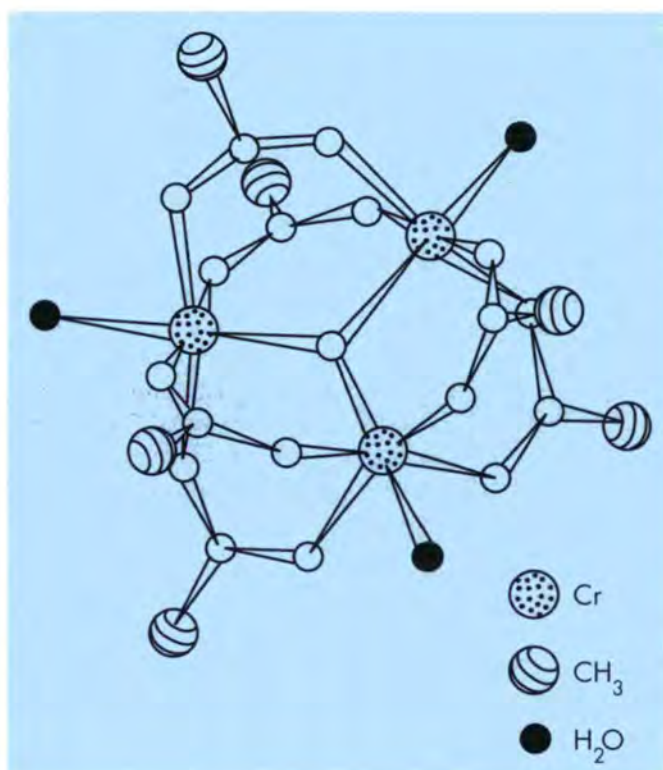


Fig. 4: Structural unit of the complex $[\text{Cr}_3\text{O}(\text{OOCCH}_3)_6(\text{OH}_2)]^{3+}$

almost equally separated 11.5 ± 0.2 , 10.5 ± 0.2 and 9.7 ± 0.2 cm^{-1} [3]. With these parameters, the Heisenberg spin-only coupling model accounts well for the observed energies and intensities of the magnetic transitions. The implied differences in metal-metal bond lengths are very small, and possibly below the limits of reliable measurement by X-ray diffraction. Similar small differences have been inferred in the related tetra-nuclear copper (II) complexes, $[\text{Cu}_4\text{OC}_6\text{L}_4]$, using FT-IR spectroscopy, and the first neutron scattering measurements on these materials have now also been reported. The question arises, whether the magnetic properties are simply the result of the geometric distortions, or whether the distortions are driven by the magnetic (i.e. electronic) interactions and further experiments have been designed to answer this.

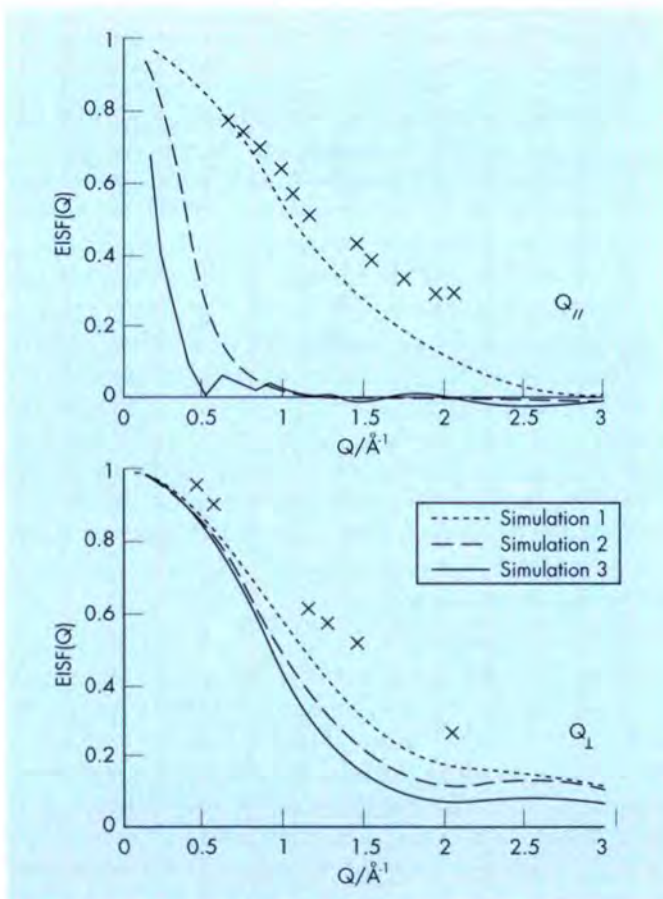


Fig. 5: Experimental (X) and simulation-derived (lines) EISFs at 180 K for the $\text{C}_{19}\text{H}_{40}/\text{urea-d}_4$ inclusion compounds in the Q_{\parallel} and Q_{\perp} geometries.

Simulation 1. Five nonadecane chains per channel with four channels in the primary box, the periodic repeat distance c_g of the guest molecules within one channel is 26.44 Å.

Simulation 2. The system was made of three nonadecane chains per channel with four channels in the primary box, so that the periodic repeat distance c_g : 29.38 Å.

Simulation 3. One nonadecane chain per channel with 4 channels in the primary box.

Quasielastic Scattering

Dynamics of N-nonadecane chains in urea inclusion compounds as seen by incoherent quasielastic neutron scattering and computer simulations

[C.E. Saclay, ILL, Université de Bordeaux I]

The aim of this study is to show the fundamental complementary of computer simulations and IQNS (Incoherent Quasielastic Neutron Scattering) techniques [4]. Such a complementary can be used not only to help in the interpretation of the experimental observations, but also for testing system and potential models. Differences between the calculated and experimental profiles must be analyzed in terms of the various approximations made in the simulation models and in the methods used to derive the profiles. However, much can be learned from such comparisons, particularly when dealing with complicated systems such as n -alkane/urea inclusion compounds.

One approximation made when building the model $\text{C}_{19}\text{H}_{40}/\text{urea-d}_4$ system was to consider a commensurate host/guest relationship. Indeed n -alkane/urea inclusion compounds belong to the class of incommensurate composite structures. Among the three different systems used in this work, only the one constructed with a realistic guest packing (simulation 1) gave results which were consistent with the IQNS experiments (see Figures 5,6). In particular, the dynamical behaviour of the guest molecules as deduced from the simulation-derived EISFs (Elastic Incoherent Structure Factor) is in fairly good agreement with that observed from the experimental ones. Further analysis of the simulation-derived spectra (not shown here) indicates that the simulation may be in somewhat better agreement with the experiment in the Q_{\perp} scattering geometry than in the Q_{\parallel} geometry. We are presently investigating in more detail the elastic and quasielastic scattering from the simulations with a view to pinpoint the sources of agreement and error. The improved simulation models obtained by this

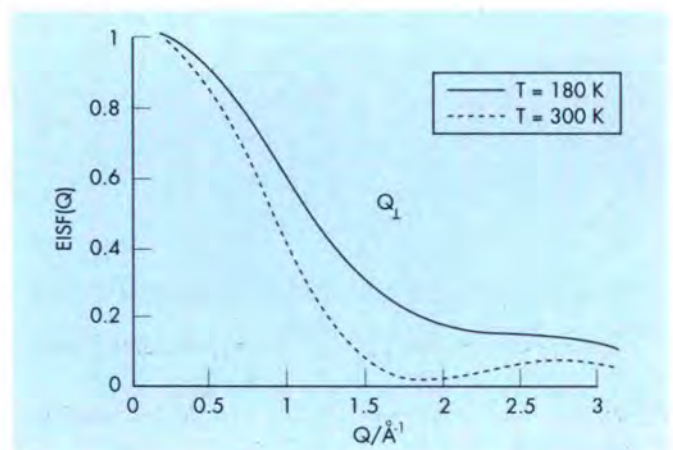


Fig. 6: Simulation-derived EISFs at 180 K and 300 K for the $\text{C}_{19}\text{H}_{40}/\text{urea-d}_4$ inclusion compounds in the Q_{\perp} geometry.

way will be used for a direct fitting of analytical description of the guest dynamics. Simulations can therefore be used to provide relatively safe stepping-stones from experiment to a simplified analytical picture of the dynamics of complex molecular systems.

Dynamical behaviour of methane in a clathrasil (dodecasil 3C) studied by quasi-elastic neutron scattering [Universität Kiel, ILL, Universität Bochum]

The dynamics of CH_4 molecules enclosed in the two types of cavity of different volume in dodecasil 3C have been studied by means of incoherent neutron scattering at temperatures $2\text{K} \leq T \leq 500\text{K}$ [5]. Clathrates, an example of host-guest compounds, are specified by a common feature: they consist of a stoichiometric host matrix, forming a net with cage-like voids, which may include guest atoms or molecules. The matrix of clathrasils, one class of clathrates, is built up by SiO_4 tetrahedra. Unlike zeolites, in clathrasils the guest molecules cannot leave their cages. Little is known about the location and motion of the guest molecules. Incoherent neutron scattering is well suited to the investigation of the dynamic behaviour, because the guest molecules usually contain hydrogen.

In Figure 7 a selection of measured spectra in the temperature range from $T = 2\text{K}$ to $T = 500\text{K}$ is presented. The spectrum at $T = 2\text{K}$ shows a broad distribution besides the elastic peak, extending to energy transfers $|\Delta E| \sim 1\text{meV}$, i.e. close to the energy of the first excited rotational state of a free CH_4 rotor at $\Delta E = 1.3\text{meV}$. The broad distribution of states indicates disorder, possibly caused by (a) empty cavities, (b) formation of micro-domains at the phase transition, or (c) transition into a state with frozen-in orientational disorder. We consider (c) as the most likely.

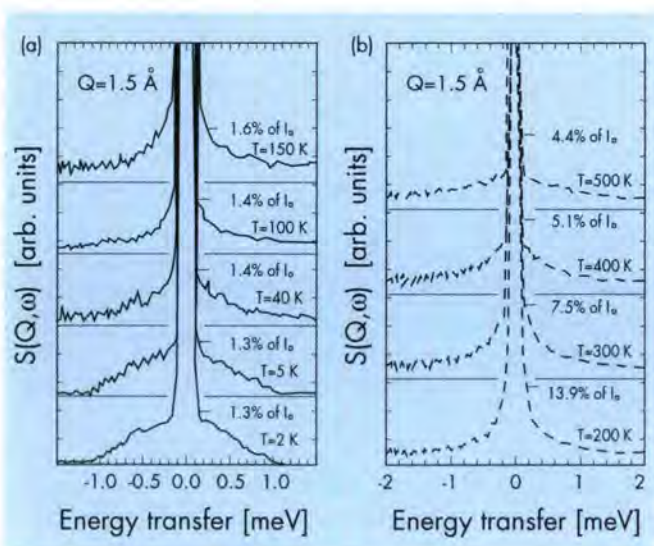


Fig. 7: Neutron scattering spectra of CH_4 on dodecasil 3C taken (a) at temperatures $2\text{K} \leq T \leq 150\text{K}$, and (b) at temperatures $200\text{K} \leq T \leq 500\text{K}$. The momentum transfer at the peak position is $Q = 1.5\text{Å}^{-1}$ and the incident neutron energy is 3.27meV ($\lambda = 5\text{Å}$). I_0 means the intensity of the elastic line.

Similar spectra were obtained with $\text{K}_x(\text{NH}_4)_{1-x}\text{I}$ samples [5] and also with solid CH_4 + rare gas mixtures, where the substitution of methane molecules by krypton atoms or by argon atoms leads to orientational disorder. Here, it may be caused by interactions of guest molecules in neighbouring cavities through the relatively large pores of the hexagons in conjunction with a statistical occupancy of cavities. We shall restrict the analysis and discussion to measurements at temperatures above $T = 180\text{K}$. A quantitative description of the measurements at lower temperatures has not yet been developed.

Because methane occurs in two different surroundings - the large and the small cavities- one may expect at least two different kinds of motion of the hydrogen atoms. With the premise of very different time scales for these motions they cannot be seen within a single experiment. The resolution must be adapted to the width of the respective scattering function. With too low a resolution, certain quasi-elastic features may appear as elastic; with too good a resolution, broad quasi-elastic scattering may not be separated from the background.

Besides the elastic line, the spectra contain quasi-elastic contributions, which are described as the superposition of two Lorentzians of different widths. The experimental data were interpreted in terms of a model based on the assumption that the overall motion of the CH_4 molecules in the larger cavities is a combination of free translation and rotation within a sphere of radius R . This assumption is clearly an over simplification. In reality one should introduce a potential of symmetry $m3$, e.g. an expansion into symmetry adapted rotor functions, whose coefficients are mainly determined by the CH_4/O_2 interaction. While this step still appears feasible, the solution of the rotational diffusion equation in such a potential looks extremely difficult. For this reason, we have restricted ourselves to this simple approach which, however, was able to explain most of the experimental findings.

We have shown that the quasi-elastic scattering can be explained by the dynamics of methane molecules in the large cavities. No quasi-elastic components ascribable to the guest molecules in the smaller cavities were observed. However, there is evidence of scattering from these molecules. This means that the motion in the smaller cavities must be slow on the time scale accessible to the experiment. A rough estimate for a lower boundary for the correlation time τ can be made as follows: even at $T = 500\text{K}$ the width Γ of a quasi-elastic distribution corresponding to the dynamics within the smaller cavities must be small compared with the energy resolution $\delta E = 0.109\text{meV}$, i.e.,

$$\tau \gg \frac{\hbar}{\delta E} \approx 6 \times 10^{-12}\text{s}$$

Hence, the CH_4 molecules in these cavities must experience a considerably stronger orientational potential than in the larger cavities, probably due to the smaller distance to the oxygen atoms. Additionally, it is likely that lattice vibrations, which cause increasing fluctuations of the

orientational potential with rising temperature and thus smear out the minima and maxima have only a minor effect compared with molecular crystals like, e.g., solid methane.

The broad Lorentzian corresponds to rotational diffusion of the CH_4 molecule about its COM (Center of Mass) and the narrow one to the translation of the COM within a restricted volume. Our model predicts the correct intensity of the two quasi-elastic contributions as well as that of the EISF as a function of momentum transfer Q . A description of the scattering arising from the methane molecules in the larger cavities for all Q values was possible by adjusting only three parameters (normalization constant and two widths Γ_{trans} , Γ_{rot} , which are Q independent, in agreement with the assumption of free diffusion). At temperatures $T > 250$ K, the value $R = 1.8 \text{ \AA}$ for the radius of the sphere available for the motion of the COM agrees very well with the value following from simple geometrical considerations.

At lower temperatures, a potential is more effective for the motion of the guest molecules, resulting in a reduction of the volume accessible for the COM. In all likelihood, the molecules initially get more localized to the walls of the cavities. Finally, at the lowest temperature ($T = 2$ K) within the regime of quantum rotation, a frozen-in disorder in the larger cavities occurs, which may result from the interaction of neighbouring guest molecules through the apertures of the hexagons and by empty cavities.

The limitations of the model become apparent when considering the temperature dependence of the line widths. An Arrhenius behaviour with activation temperatures of the order of $T_A = 1000$ K indicates the presence of a sizeable potential.

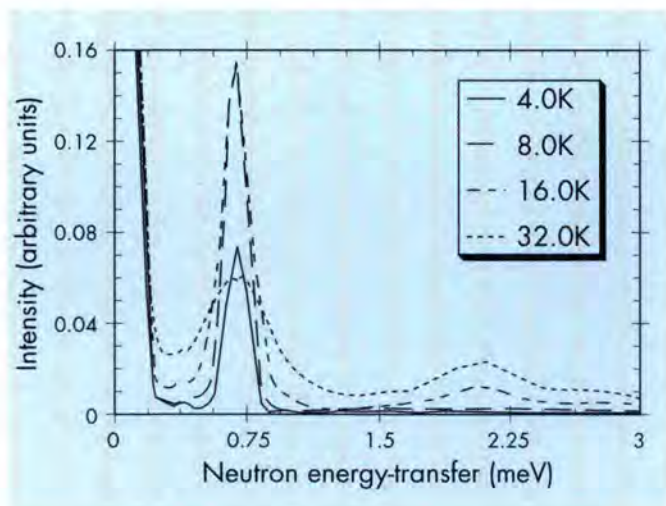


Fig. 8: Temperature dependence of the INS spectrum of the $J=0 \rightarrow J=1$ and $J=0 \rightarrow J=2$ transitions of the NH_3 rotor in $\text{Ni}(\text{NH}_3)_2(\text{CN})_4 \cdot 2\text{C}_6\text{D}_6$.

Future investigations need to consider a non-vanishing cage potential. A jump model based on the actual symmetry of the cages might be able to explain the measured EISF in analogy with the 2-dimensional case. It is shown in [6] that a jump model among N equivalent sites equally spaced on a circle leads for $N \geq 6$ to practically the same EISF for sufficiently small Q values as for continuous diffusion on a circle. Measurements in an extended Q range are also required. They have to be supplemented by structure investigations at temperatures below room temperature.

Quantum rotations

Coupling between phonons and quantum rotors

[ILL, LASIR-CNRS, KEK, Osaka University]

Although the theory for temperature dependence of rotational tunnelling is well developed [7], the temperature dependence of free rotors has yet to be studied in detail. So far we can identify two contrasting situations [8]: On the one hand the spectrum of NH_3 rotors in $\text{CO}(\text{NH}_3)_6(\text{PF}_6)_2$ is washed out by broadening above about 10K, whilst on the other, the spectrum of NH_3 rotors in $\text{Ni}(\text{NH}_3)_2(\text{CN})_4 \cdot 2\text{C}_6\text{D}_6$ is discernible up to at least 80K. We will examine the ability of a simple theory based on life-times to account for the observed broadening of the inelastic neutron scattering (INS) spectrum of $\text{Ni}(\text{NH}_3)_2(\text{CN})_4 \cdot 2\text{C}_6\text{D}_6$.

We assume that each rotational level, J , is broadened by the rate, γ_J , at which it decays into another plus a phonon of the corresponding energy difference. Considering only transitions involving the ground state, the width, Γ , is proportional to:

$$\Gamma \approx \sum_{j>0} \gamma_j \cdot n(E_j)$$

where $n(E_j)$ is the occupation factor for the J^{th} rotational level. Having shown that this relationship accounts for the observed spectra, we can use the observed temperature-dependence to determine distinct phonon energies which resonate with the NH_3 rotor.

The INS spectra of $\text{Ni}(\text{NH}_3)_2(\text{CN})_4 \cdot 2\text{C}_6\text{D}_6$ at different temperatures are illustrated in Figure 8. These spectra are easily fitted over the -1.0 to $+1.0$ meV range with a Lorentzian function for the $J=0 \leftrightarrow J=1$ peaks and for the quasielastic peak. All three functions were constrained to have the same intensity and width when corrected for the detailed balance. An example fit is illustrated in Figure 9. The upper limit ($4\mu\text{eV}$) for the peak width at 4K was obtained using the LAM80ET spectrometer at KEK, Tsukuba, and the upper limit at 80K (0.55 meV) using MIBEMOL at LLB, Saclay, with an incident wavelength of 3.0 \AA .

The very narrow peak-width at 4K constrains the $J=1$ term to be close to zero, and even at 80K the population factor for levels with $J>6$ is negligibly small. Consequently, the observed variation of peak-width with temperature was

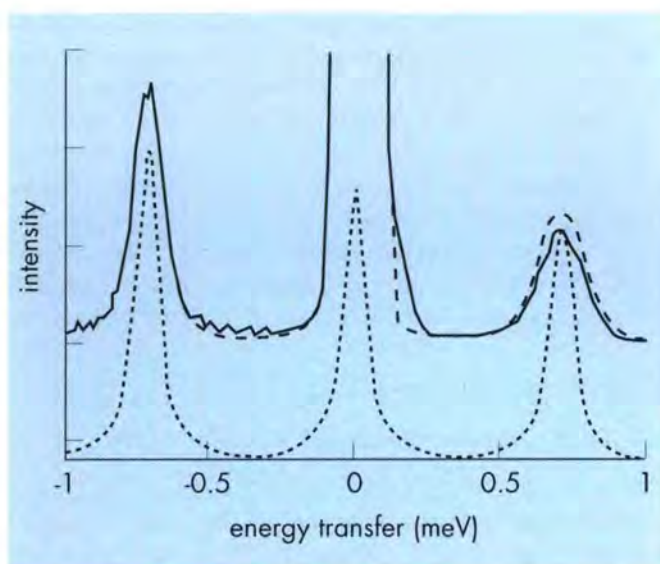


Fig. 9: An example fit of the $J=0 \rightarrow J=1$ and quasielastic peaks of the NH_3 rotor in $\text{Ni}(\text{NH}_3)_2(\text{CN})_4 \cdot 2\text{C}_6\text{D}_6$ at 16.0K. The solid line is the observed spectrum, the broken line is the fit, and the dotted lines represent the deconvoluted components.

fitted by adjusting γ_1 for $J=2$ to 6. Only γ_2 and γ_4 have significant values, 0.155 and 1.06 meV, respectively, which suggests that a distinct phonon resonates strongly with the rotational system and has an energy close to 11.36 meV. A possible candidate is a Raman-active mode at 13.65 meV in $\text{Ni}(\text{NH}_3)_2(\text{CN})_4 \cdot 2\text{C}_6\text{H}_6$ which shifts to 12.03 meV on deuteration of the benzene. This mode has not previously been assigned, but the observed shift on deuteration is consistent with a librational motion of the benzene molecule (frequency ratio: observed=0.885, calculated=0.897).

We have previously proposed that the crystalline 4-fold symmetry of the NH_3 groups arises from a precession of the centre of the H_3 triangle during the NH_3 rotation [9]. Given the juxtaposition of the benzene molecules with respect to the NH_3 rotors (figure 10), interaction between the rotors and the benzene librations is to be expected. Further experiments are planned to investigate this aspect of the rotational dynamics.

The rotational potential of NH_3 groups in metal hexammines

[ILL, LASIR-CNRS, ANSTO, CEA Saclay)

The sensitivity of rotational-tunnelling spectroscopy to changes in the local potential makes this an attractive technique for the determination of atom/atom potentials. These measured potentials are valuable for simulating classical motions of similar species. We have already made a study of the tunnelling spectrum of pure $\text{Ni}(\text{NH}_3)_6\text{I}_2$ at hydrostatic pressures up to 5 kbar, but this study was limited by different behaviour of tunnelling components and the absence of adequate crystallographic data. In the present

work [10] we manipulate interatomic distances by chemical substitution and evaluate this as an alternative method of deriving potentials. Our preliminary work [11] on $\text{Ni}(\text{NH}_3)_6\text{I}_{(2-x)}\text{Br}_x$, where $0 < x < 1$, shows the mixed crystals to be single-phase, and that the barrier for NH_3 rotation increases with x . In the present paper we extend this work to $0 < x < 2$ and make a more detailed analysis in which we estimate the relative contributions of chemical substitution and atomic separation to the rotational potential.

INS spectra were recorded using the IN5 spectrometer at the ILL and MIBEMOL at LLB. Neutron powder diffraction data were collected using HRPD at ANSTO Lucas Heights, Australia.

At room temperature nickel hexammine halides occupy the $\text{Fm}\bar{3}\text{m}$ space group. A low-temperature phase transition leads to a very small rhombohedral distortion, but for the purposes of the present work we will consider only the cubic structure. Although the exact crystal structure of the low-temperature phase of these hexammines is unknown the mixed crystals are known to be single-phase. Each NH_3 rotor has 8 nearest halide neighbours. As I^- is replaced by Br^- , two main effects occur. Firstly, the lattice contracts, although without structural rearrangement. Secondly, the distribution of rotors with between 0 and 8 Br^- neighbours changes - we denote these as $n\text{Br}$. Although we do not see separate tunnelling peaks for each of the eight chemically distinct NH_3 -rotor environments in the mixed crystals, their presence could be hidden by inhomogeneous broadening.

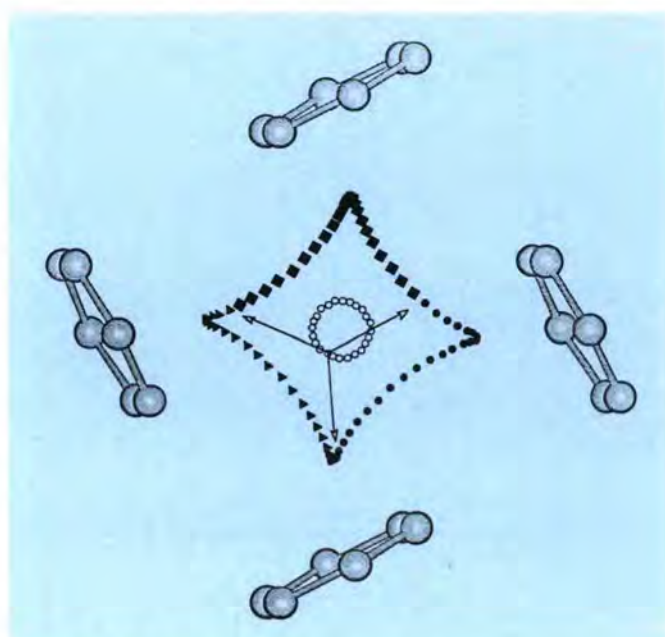


Fig. 10: Schematic illustration of the model used to fit the temperature dependence of the peak widths. The band-width of the $J=2$ and $J=4$ states is 0.155 and 1.06 meV, respectively.

In the present work we try to determine the rotational barriers $V_{(nBr),n=0,8}$, and their present individual Gaussian distributions $\Gamma_{(nBr)}$ to be equal for a given sample composition. Similarly, we require that the values of the potentials $V_{(nBr)}$ to be equally spaced: i.e. $V_{(nBr)} - V_{([n-1]Br)}$ is a constant, Δ . Finally, the ratio, R , of the non-elastic: elastic scattering was constrained to be constant over all samples.

The refinement was made using 3 parameters for each composition (V and Γ and Δ) and the overall R . Calculated spectra from this refinement, which include a detailed balance factor, are compared with measured spectra in Figure 11. Systematic errors which occur at the limits of the composition range may arise from clustering of like anions.

The barrier spacing parameter, Δ , represents the increase in the rotational barrier caused by substituting one I^- with a Br^- without changes of atomic positions. It transpired this value was always < 1.0 meV and in practice almost equally good refinements could be obtained with $\Delta=0$. Clearly, there is some correlation between the barrier-distribution, Γ , and barrier spacing, Δ , but they effect the spectral profile differently. It follows that substituting an I^- with Br^- changes the rotational barrier by less than 1.0 meV - probably much less.

Clearly, we cannot obtain a full description of the anisotropic rotational potential but we can obtain a good value for the effective exponent, m , in the expression:

$$V_{(r)} = V_{(r_0)} \cdot (r_0/r)^m$$

where r is the relevant interatomic distance and $V_{(\theta)} = 1/2 V \cos \theta$ (because $\Delta = 0$, $V_{(nBr)} = V_{(r)}$). Given the small chemical effect of substitution (above), it is reasonable

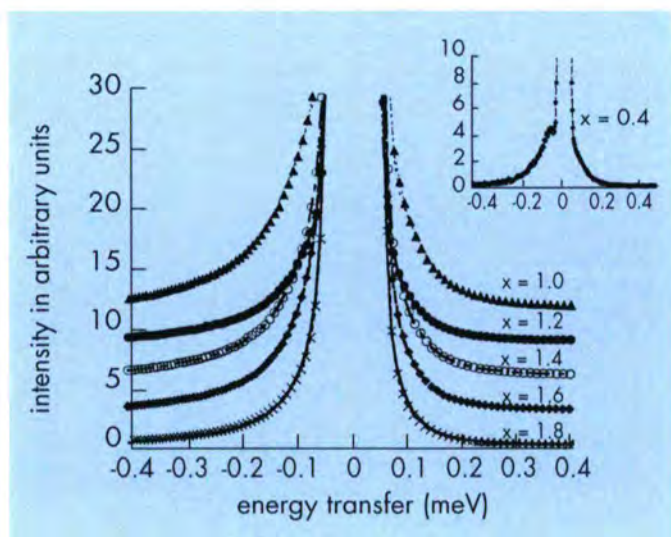


Fig. 11: Calculated and observed spectra of $Ni(NH_3)_6I_{(2-x)}Br_x$ collected at MIBEMOL, LLB Saclay, at 7.00 \AA at a sample temperature of 1.8 K . The inset shows one of the spectra with low Br^- concentration, collected earlier on IN5, see in ref. 2.

to treat the difference between the rotational barrier of the pure iodide (16.6 meV) and the pure bromide (31.5 meV), as arising from changes in r . It follows that the barrier arises from interaction between NH_3 groups, and since the NH_3 groups undergo quantum free rotation in the isostructural $Co(NH_3)_6(PF_6)_2$ this interaction must be between neighbouring hexammine ions. Therefore we take the effective r to be the distance between 3H planes on neighbouring cations and plot $\log V$ vs $\log r$ in order to obtain the effective exponent, m , from the gradient (Figure 12, Table1).

The measured value of $m = -5.9$ is in remarkably good agreement with the r^{-6} behaviour of dispersion energy between two molecular species. Our previous work found values of 5 and 8 for m , but these were based on an estimated compressibility and the pressure dependence of the two main tunnelling peaks. It is not surprising that

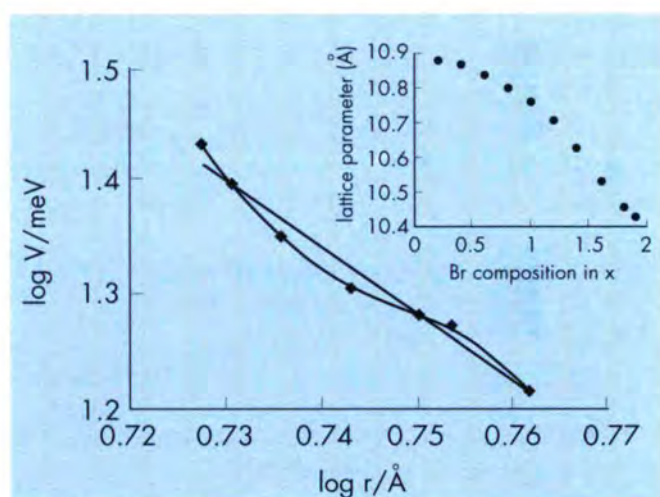


Fig. 12: Plot of logarithm of the rotational barrier, V , against logarithm of the interatomic distance, r , for the mixed $Ni(NH_3)_6I_{(2-x)}Br_x$ compounds. The gradient of the fitted line is $m = -5.9$. The inset shows the variation of the lattice parameter with composition of Br^- in values of x , see also Table 1. Diffraction experiments were made at 300 K .

$Br^- (x)$	V (meV)	Γ (meV)	r (Å)
$[Ni(NH_3)_6I_{(2-x)}Br_x]$			
1.0	19.15	4.958	5.6692
1.2	19.28	4.866	5.6156
1.4	20.18	4.913	5.5347
1.6	22.36	5.589	5.4409
1.8	25.28	6.285	5.3666

Table 1: Variation of barrier height, V , distribution width, Γ , and interatomic distance, r , with composition, x . For all fits Δ was zero and the ratio of the non-elastic:elastic scattering, R , was 3.9.

different components of the tunnelling multiplet give different values of m since there is clearly appreciable rotor-rotor coupling.

The technique of chemical substitution can be used to separate the importance of different atom-atom interactions, and determine the effective exponent of the major interaction. It would be interesting to extend the range of distances of this study using mixed crystals of $\text{Ni}(\text{NH}_3)_6\text{I}_2$ and $\text{Ni}(\text{NH}_3)_6\text{Cl}_2$. The most important question which remains is whether the NH_3 - NH_3 interaction is between coaxial or perpendicular Ni-NH_3 units (Figure 13).

Secretary: Hans J. Lauter

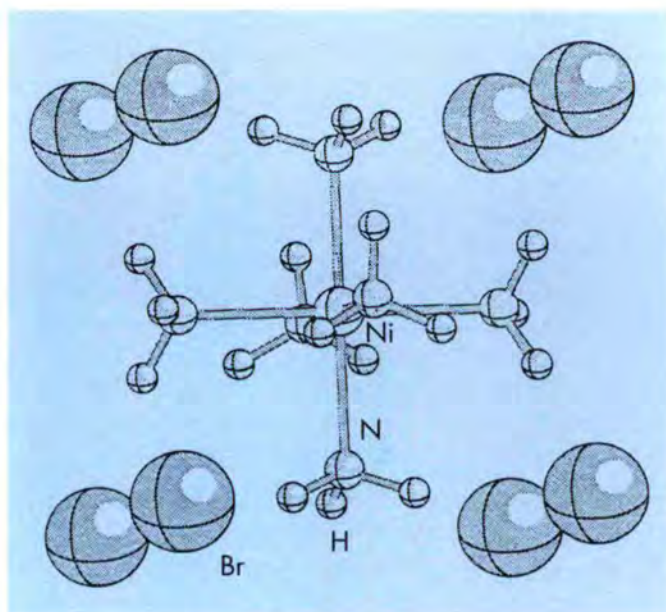


Fig. 13: Illustration of the relative atomic positions. Only one complete hexammine ion is illustrated for clarity.

References

- [1] P. Papanek, J.E. Fischer, J.L. Sauvajol, A.J. Dianoux, G. Mao, M.J. Winokur, F.A. Karasz, accepted Phys. Rev. B, June 1994.
- [2] R.D. Cannon and R.P. White, Progr. Inorg. Chem. **36**, 195 (1988).
- [3] U.A. Jayasooriya, R.D. Canon, R.P. White, J.A. Stride, R. Grinter and G.J. Kearley, J. Chem. Phys., **98**, 9303 (1993).
- [4] M. Souaille, J.C. Smith, A.J. Dianoux, F. Guillaume, Proceedings of the Enrico Fermi School of Physics, NATO-ASI, "Observation and phase transition in complex fluids", Varenne (Italy), July 26-August 5 1994.
- [5] A. Schröder-Heber, B. Asmussen, W. Press, H. Blank and H. Gies, Molecular Physics, **82**, 857-873 (1994).
- [6] M. Bée, 1989, Quasielastic Neutron Scattering (Bristol: Adam Hilger).
- [7] A. Würger and A. Heidemann, Z. Phys., **B80**, 113 (1990).
- [8] G.J. Kearley, H. Büttner, F. Fillaux, S. Ikeda, A. Inaba, to be published.
- [9] G.J. Kearley, G. Coddens, F. Fillaux, J. Tomkinson and W. Wegener, Chem. Phys., **176**, 279 (1993).
- [10] H.G. Büttner, G.J. Kearley, F. Fillaux, C.J. Howard and R. Kahn, to be published.
- [11] H. Blank and G.J. Kearley, J. de Physique IV, **1** (1991) C5-345.

Structure and Dynamics of Large Molecules, Colloids and Polymers

Members of the College at the ILL

E. Amalric-Bellet	C. Lartigue
P. Chieux	H. Lauter
B. Farago	P. Lindner
B. Frick	R. Oeser
K. Ibel	V. Rodri
A. Kollmar (KFA Jülich)	P. Timmins

External members

M. Alba (CENG)	C. Poinignon (INPG)
J.P. Beaufils (UJF)	D. Quenard (CSTB)
M. Bée (UJF)	C. Riekel (ESRF)
E. Geissler (UJF)	F. Rieutord (CENG)
A. Guillermo (UJF)	M. Rinaudo (UJF)
A. M. Hecht (UJF)	C. Rochas (UJF)
J.F. Legrand (ESRF)	P. Terech (CENG)
I. Morfin (UJF)	G. Vignaud (ESRF)

Introduction

The perspective for this year was the restart of the reactor and most of the ILL scientists went back on the instruments to put them into operation. In addition we have two new scientists: A. Kollmar seconded from KFA-Jülich, working on IN15, arrived in May 1994 and E. Amalric-Bellet, on D16, in July 1994.

B. Farago was still sharing his time between ILL and LLB where he could pursue his own research and at the same time introduce the new responsible for the LLB spin-echo spectrometer to this technique. Although C. Lartigue was back at the ILL in January 1994 she continued her collaboration with the RMN-Polymer group at the Laboratoire de Spectrométrie Physique - University J. Fourier-Grenoble. R. Oeser left ILL in September 1994 and took up a position at BENSCH-HMI-Berlin working on the reflectometer. K. Ibel retired from ILL in September 1994; he maintains his scientific activity by giving lectures at the University of Osnabrück.

Les "Journées des Polymères et Colloïdes" at ILL were organised by P. Lindner and E. Geissler (see below).

Shear induced orientation of nematic living polymers

SANS allows observation of the orientation of nematic solutions of equilibrium polymers or "living" polymers, which is one topic of scientific activity of the CNRS group in Montpellier working on complex fluids [1]. The elementary phases of these liquid crystalline phases are wormlike micelles, i.e. flexible cylindrical aggregates made

of amphiphilic molecules. An example for such an aqueous surfactant solution is Cetylpyridinium chloride and hexanol in 0.2 M NaCl-brine, which exhibits the classical structural sequence isotropic-nematic-hexagonal with increasing surfactant concentration ϕ . The nematic phase for $\phi = 34\% - 38\%$ consists of very long cylindrical micelles closely packed parallel to each other giving rise to long-range orientational order. Subjected to steady shear, the nematic phase of living polymers behaves very similarly to the conventional liquid crystalline polymers.

SANS measurements under shear have been performed in collaboration with colleagues from Montpellier at the Orphée Reactor at LLB. In Fig. 1a and 1b are displayed

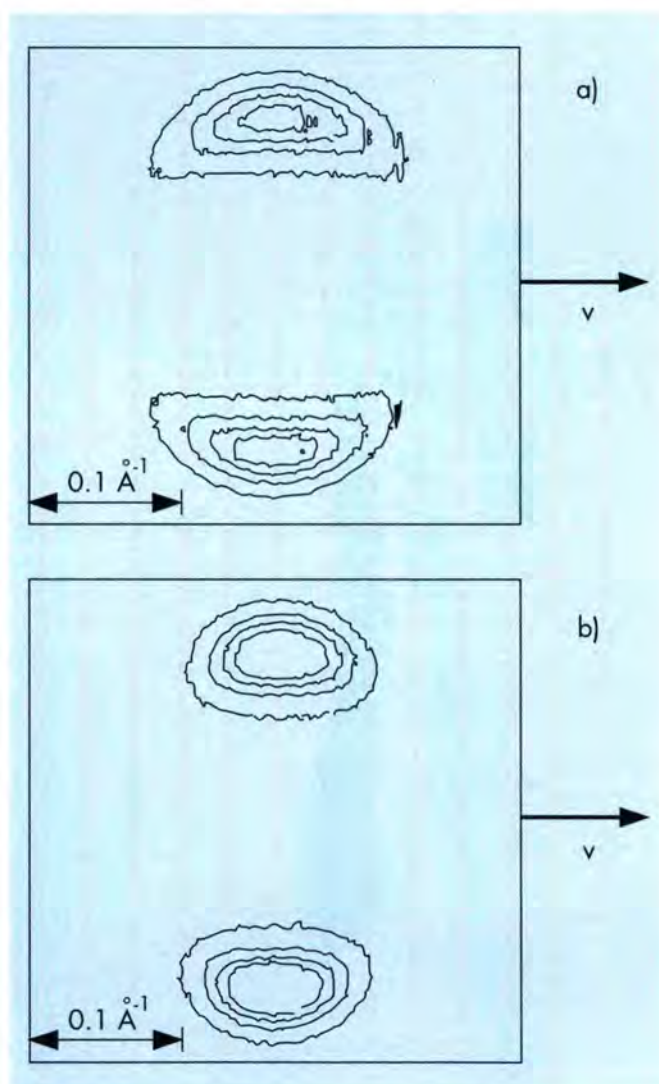


Fig. 1: Map of scattered neutron intensity obtained in SANS experiments for the nematic micellar solution of CPCI/Hex/D₂O ($\phi = 35.2\%$) under shear. a): $\dot{\gamma} = 0.75 \text{ s}^{-1}$ and b): $\dot{\gamma} = 250 \text{ s}^{-1}$. The arrow indicates the direction of flow. The SANS-data were obtained at a neutron wavelength $\lambda = 6.29 \text{ \AA}$ on a two dimensional detector (using 128x128 elements) and located at 2 m from the shearing device. The contour intensities are 600, 1200, 1800 and 2400 for both spectra (arbitrary units).

typical two-dimensional scattering patterns for a 35.2%-CPCI/Hex solution (in deuterated water) under shear. The flow direction is indicated by the arrow and the neutron beam is incoming parallel to the velocity gradient axis (i.e. perpendicular to the plane of the figures). Shear rates are 0.75 s^{-1} and 250 s^{-1} , respectively. The neutron intensities exhibit two crescent-like peaks in the direction perpendicular to the flow (shown by an arrow in Fig. 1a). Such an anisotropic scattering in the form of equatorial arcs is characteristic of nematic mesophases. It reflects the short-range translational order with respect to the centre-of-mass of the micellar aggregates and the longer range orientational order driven by the flow. The sharp maximum in the Q_{\perp} -direction appears at a momentum transfer $Q_m = 0.11 \text{ \AA}^{-1}$, corresponding to an average distance between polymer-chains of about $\sim 60 \text{ \AA}$. In addition, the width of the crescents in the Q_{\parallel} -direction is directly connected to the distribution function of the nematic director with respect to the flow, and hence to the orientational order parameter \bar{P}_2 .

When passing from 0.75 s^{-1} (Fig. 1a) to 250 s^{-1} (Fig. 1b), this width decreases noticeably. The effect is still better evidenced in Fig. 2 where for the two spectra reported above, the data are analysed in terms of the angular distribution of the scattered intensity. At constant azimuthal angle ψ , the neutron counts were integrated on momentum transfer around the maximum scattering (at Q_m) on a width $\Delta Q = \pm 0.02 \text{ \AA}^{-1}$ and plotted versus ψ . ΔQ was taken to correspond typically to the half width at half of the maximum scattering in \perp -direction.

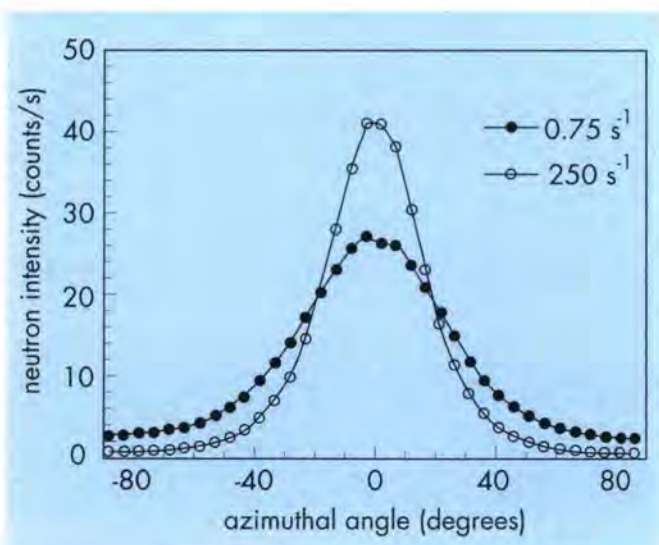


Fig. 2: Variation of the radially integrated neutron intensity as a function of the azimuthal angle ψ for the $\phi = 35.2\%$ CPCI/Hex solutions submitted to shear. Both intensities refer to the same 2D-spectra shown in Fig. 1. This neutron intensity $I(\psi)$ is then utilised to compute the spatially averaged order parameter \bar{P}_2 of the nematic phase under shear. The data shown here for $\dot{\gamma} = 0.75 \text{ s}^{-1}$ and $\dot{\gamma} = 250 \text{ s}^{-1}$ correspond to \bar{P}_2 -values of 0.47 and 0.71, respectively.

Dynamics of microemulsion lamellar phases

One of the best studied lamellar systems is the SDS (sodium dodecyl-sulphate)-pentanol-water-dodecane lyotropic phase. The lamellae are formed of a SDS - (water+pentanol) - SDS sandwich.

The stacking of these double layers was extensively studied by X-ray scattering and their dynamics by quasielastic light scattering. However, the layer thickness fluctuation is only accessible to neutrons. Applying the same trick as in the case of the droplet phase [2], we prepared dilute lamellar phases d-dodecane/h-SDS/h-pentanol, one sample with H_2O the other with D_2O . The first is seen by the neutrons as a thick full sheet, the second as a double sheet. Comparing $I(\mathbf{Q}, t)$ for the two, the sheet dynamics as a whole can be separated from the thickness fluctuations. We have already reported clear evidence for the existence of such fluctuations (ILL Annual Report 1988), but because of the shutdown of the ILL only very recently we could continue on the spin-echo spectrometer of the LLB - Saclay, this time on oriented samples. In fact the coupling between the scattering vector \mathbf{Q} and the wave vector \mathbf{k} of the planar eigenmodes is by far not as simple as in the case of droplets. A powder average with highly orientation-dependent form factors and the spontaneous formation of macroscopical domains makes the data evaluation very difficult.

We used a sample holder full of thin quartz plates separated by 0.3 mm. Most of the samples studied orient spontaneously under the shear flow while filling. Under the collimation conditions of a SANS instrument the mosaicity is hardly measurable (in the order of 5 degree). Fig. 3. shows the contour plots of a 60 % dodecane containing sample with double sheet contrast for two detector distances. From the small \mathbf{Q} region we can deduce a stacking distance of 153 \AA . The high \mathbf{Q} region shows a minimum followed by a bump which is a consequence of the double layer contrast and gives us a layer thickness of 22 \AA . NSE studies were made with \mathbf{Q} perpendicular to the layer for both contrasts and \mathbf{Q} parallel to the layer in the double sheet contrast. Fig. 4 presents the effective diffusion coefficient D_{eff} as a function of Q . There is a clear maximum in D_{eff} (Q perp) for the double sheet contrast in the Q region corresponding to the minimum of the static form factor, which is a signature of the presence of thickness fluctuations. A closer examination (Fig. 5) of the time dependence of $I(\mathbf{Q}, t)$ in this region shows that while the full sheet remains essentially single exponential, the double sheet consists of at least two well separated relaxation processes. The diffusive behaviour of the full sheet can be understood in the following simplistic way. In the absence of long range electrostatic interaction between the lamellae, the system is stabilised by the Helfrich mechanism, namely the sheets are undulating with all amplitudes allowed by the average interlayer distance. With Q perp we are probing the projection of the density on an axis perpendicular to the layers. As the layers feel each other effectively when they come into close contact, the interlayer space on time average is filled with the randomly undulating

sheet. In our case $1/Q$ = the interlayer distance, consequently on such a local scale we can expect a diffusive like behaviour. This is effectively observed for the full sheet, D_{eff} being nearly constant. A slight increase might come from the fact that we start to see the thickness fluctuation already for this contrast too. $I(Q,t)$ for the double sheet in the peak region can then be analysed with a functional form of $\exp(-t/\tau_1)((1-f_2) + f_2 \exp(-t/\tau_2))$ where $1/\tau_1 = D_{\text{eff}} Q^2$ and D_{eff} is fixed by the full sheet contrast measurement. Fig. 5 shows the results where we obtain a value of about $\tau_2 \approx 3$ ns in average over the 3 scans.

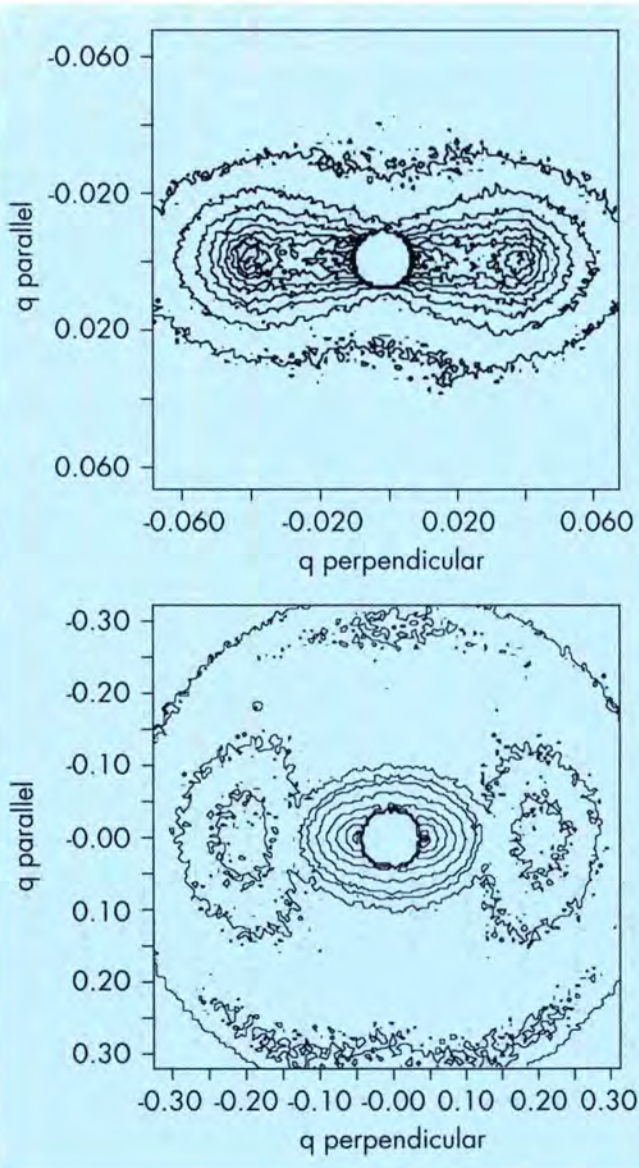


Fig. 3: SANS contour plots of the SDS-penthanol- D_2O -dodecane lamellar system for the low and high Q region in \AA^{-1} . The low Q contours show the periodicity and the good orientation of the sample, the other one shows the maxima due to the double sheet contrast.

With Q parallel to the layers, the density projection has to be taken on the parallel axis. The theoretical prediction in the high Q region of the NSE is $\tau = 4\eta/KQ^3$ with a single exponential decay. Fig. 4 (empty squares) shows that our data are compatible with this prediction and we did not observe significant deviation from a single exponential function. From the measured slope we deduce $K \approx 0.1$ kT which is a very low value. Here again the bulk viscosity value η of the solvent was used and as it was observed in the case of the droplet microemulsions this might be a wrong assumption up to factors of 4-6. Furthermore some precautions have to be taken, as in this direction the scattering is weak, mainly due to second order terms in the density projection, and the presence of defects. Domain boundaries might contribute significantly to the scattered intensity, thus to $I(Q,t)$. Further studies are needed to confirm this result.

This work was done by B. Farago in collaboration with A. Brulet (LLB Saclay), M. Monkenbusch, K.D. Goecking, D. Richter (KFA Jülich) and J.S. Huang (Exxon Annandale).

Chain dynamics in a compatible polymer blend: an NMR approach

Using NMR, we have investigated the temporary network structure in molten compatible binary polymer blends PEO/PMMA.

The transverse magnetic relaxation of protons attached to long polymer chains in a melt, observed well above the glass transition, behaves as in a permanent gel because of the existence of a temporary network structure. It exhibits a so-called pseudo-solid behaviour characterised by the formation of echoes. This behaviour arises from a non-zero time average of tensorial interactions of nuclear spins which

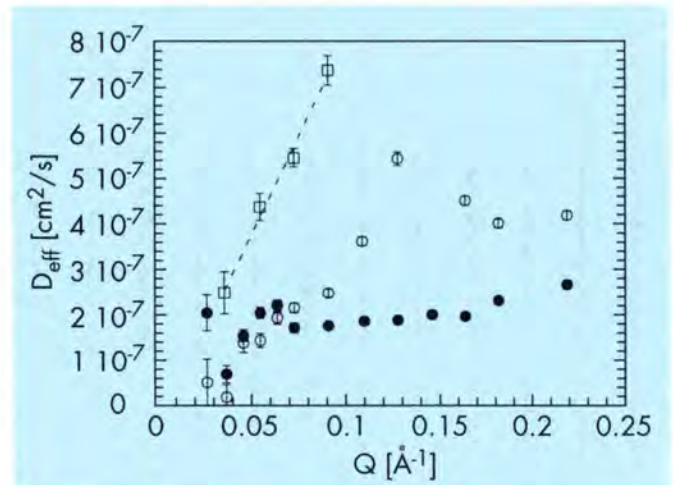


Fig. 4: D_{eff} versus Q for the SDS lamellar sample. Full circles are for the full contrast Q perpendicular to the layer, empty circles same orientation but double sheet contrast, empty squares double sheet contrast Q parallel to the layers.

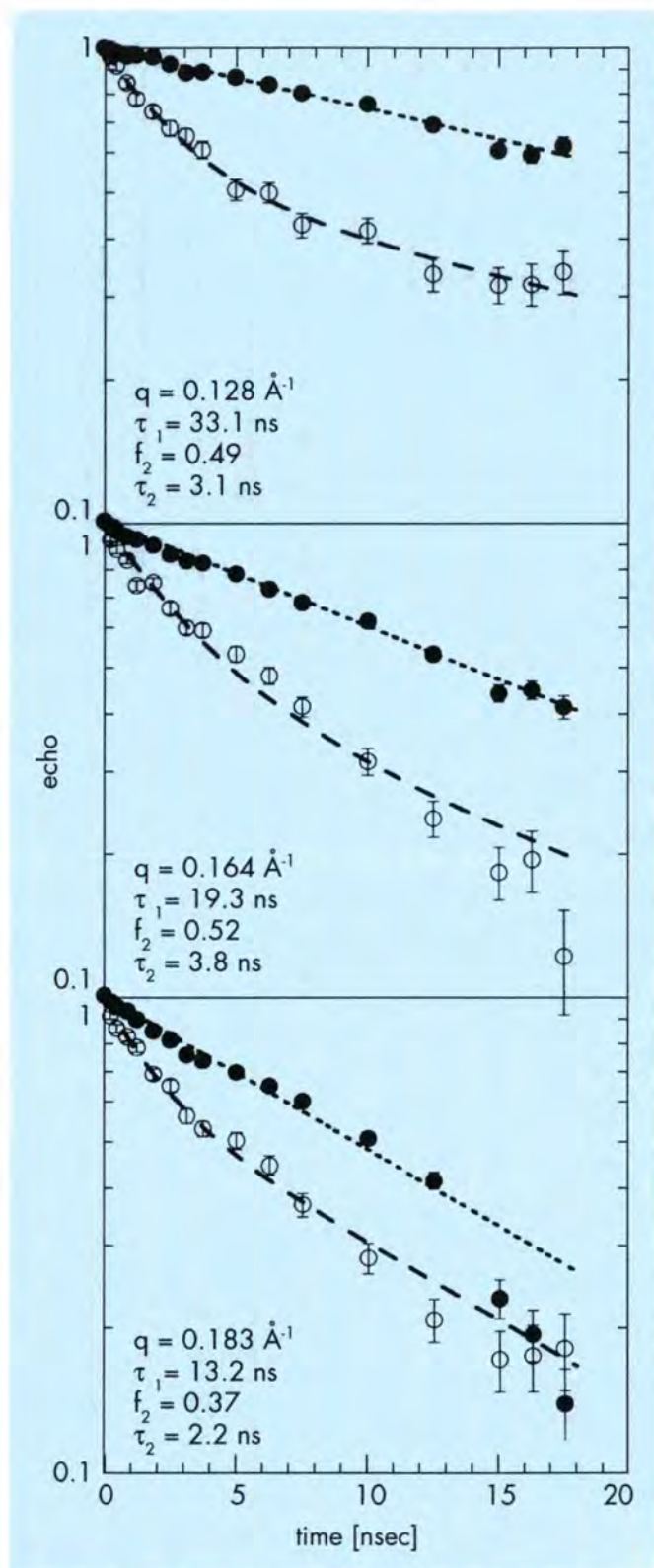


Fig. 5: $I(Q,t)$ for the SDS lamellar sample in the Q region of the peak of D_{eff} . Full symbols for full contrast, empty symbols for double sheet contrast. Dashed lines are the fits as described in the text.

result from non-isotropic rotations of skeletal bonds. Spin-spin interactions are considerably reduced by these rotations of monomeric units; the residual dipole-dipole interaction Δ which mainly governs the transverse relaxation process of nuclear spins is directly related to the mesh size of the network.

In a melt, this structural part is combined with a dynamic contribution representative of the chain fluctuations characterised with two sets of relaxation times: i) one associated to long range fluctuations and strongly dependent on molecular weight; ii) one associated to fluctuations within the mean segmental spacing between two consecutive entanglements and not dependent on molecular weight. Typically one considers 200 to 300 skeletal bonds per segment. As a result, this NMR approach probes chain properties on a scale of the order of 50 \AA (not monomeric units). As seen from the viscoelastic plateau, decoupling of the two sets of relaxation times can be observed on high molecular weight chains.

Typical relaxation curves observed for the pure PEO and for two molecular weights are shown in Figure 6, together with pseudo-solid echoes which give evidence of the presence of a residual spin-spin interaction. When decreasing the chain molecular weight, the relaxation time τ of the long range fluctuations becomes competitive with respect to the residual dipolar interaction ($\Delta\tau \approx 1 \text{ ms}$). As a result, the relaxation curve is lengthened while the echoes are flattened. The relaxation becomes molecular weight independent above $M_w = 760000$.

For the blends, at a given temperature, the PEO relaxation curves are shortened when decreasing the PEO concentration. However, it is known that the nuclear magnetic relaxation time depends upon the difference $(T - T_{eg})$: the closer to T_{eg} , the slower the motions, the shorter the relaxation times. For PMMA/PEO blends, the glass

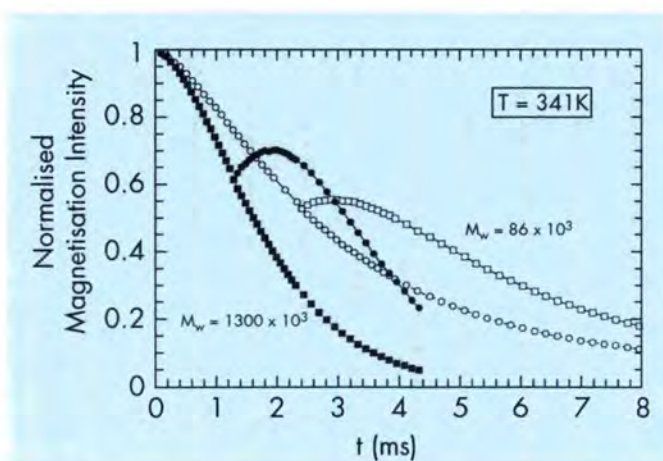


Fig. 6: Relaxation curves and pseudo-solid spin-echoes for PEO chains for two molecular weights.

transition is known to increase as the PEO content decreases following the Fox equation from $T_g(\text{PEO}) \approx 218\text{K}$ to $T_g(\text{PMMA}) \approx 378\text{K}$. This is in qualitative agreement with our observation.

Taking this into account, the evolution through the whole domain of temperature and concentration is reported as a function of $(T - T_g)$ on Figure 7. These variations are linear above $T - T_g \approx 50$. At fixed $(T - T_g)$, we observe that the PEO nmr relaxation time increases as the PEO concentration decreases. The question remains as to the origin of this increase. Keeping in mind that the values reported here contain both the effect of long range dynamics and of the temporary network, it could be attributed either to a diminution of the characteristic time of long range dynamics or to an increase in the mean spacing between entanglements in the temporary network.

Recently, we have proposed a new procedure to extract experimentally the residual spin spin interaction from the transverse magnetic relaxation even when long range fluctuations are involved in the relaxation process. It has been applied successfully to the pure PEO, leading to an invariant for all observed molecular weights [3].

Applying this technique to the PEO/PMMA blends could allow us to answer the above question.

This work was done in collaboration with A. Guillermo and J.P. Cohen-Addad during the reactor shutdown. C. Lartigue worked for two years in the group of "RMN des Polymères" at the Laboratoire de Spectrométrie Physique - University J.Fourier-Grenoble. The study of chain dynamics by NMR is one of the scientific topics of the group.

Secretary: Colette Lartigue

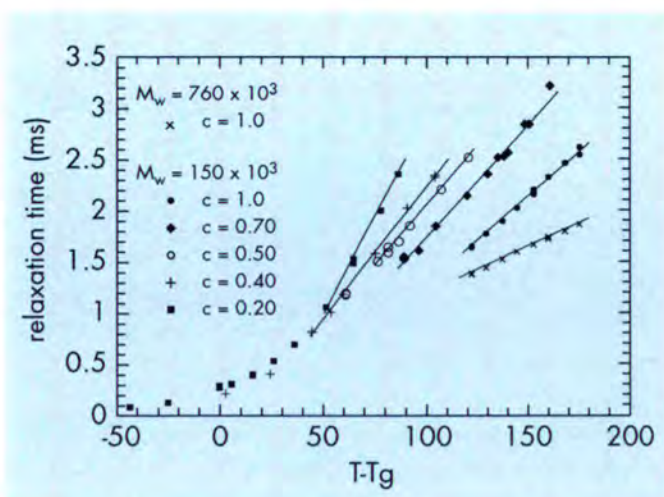


Fig. 7: Variations of the nmr PEO relaxation time as a function of $(T - T_g)$ for PEO/PMMA blends and pure PEO. c is the PEO weight concentration; it varies from 20% to 100% (w/w). The blends were prepared from hydrogenated PEO ($M_w = 150\,000$) and deuterated syndiotactic PMMA ($M_w = 262\,000$).

References

- [1] D. C. Roux, J.F. Berret, G. Porte, E. Peuvrel-Disdier, P. Lindner, *Macromolecules* (1994), accepted for publication.
- [2] J.S. Huang, S.T. Milner, B. Farago and D. Richter, *Phys. Rev. Lett.* 2600-2603, **59** (1987).
- [3] J.P. Cohen-Addad, A. Guillermo, C. Lartigue, *Phys. Rev. Lett.* accepted for publication.

Workshop "Journées des Polymères et Colloïdes"

Organisers: P. Lindner (ILL), E. Geissler and B. Berge (Laboratoire de Spectrométrie Physique)

On the 2nd and 3rd February 1994 the ILL hosted the "Journées des Polymères et des Colloïdes 1994". This two-day meeting, attended by almost a hundred members of the polymer community in the Rhône-Alpes region, was co-sponsored by the ILL, the Pole Européen Universitaire et Scientifique de Grenoble and the Groupe Français des Polymères. The twenty-one oral contributions from researchers working in different laboratories of the region covered a rich variety of research topics, involving investigations into Structures, Rheology, Polymer Materials, and Copolymers, Alloys and Networks. The lectures were complemented by a poster session which attracted some twenty posters of high quality.

The organisers acknowledge the invaluable help of Françoise Giraud.

Peter Lindner

DIRECTORATE SERVICE

Public Relations

The arrival of the new reflector tank on 24 February was not only a great relief for ILL staff, but it turned out to be a very important event for high-level people outside ILL.

R. DAUTRAY, Haut Commissaire du CEA/France, came to the ILL on 2 March to witness the reflector tank being lowered into its final position inside the swimming pool, see Fig. 6a page 152. He was accompanied by J.P. SCHWARZ, his Chef de Cabinet. This installation of the second reflector tank was particularly fascinating for Monsieur DAUTRAY, as he had been present when the first one was put in place in 1970, see Fig. 6b page 152. At that time he was Head of the High Flux Reactor project. He was delighted to see with his own eyes how effective the modular construction of the reactor has proven to be: it was possible to empty and clean the swimming pool to such a degree that the assembly of all the connections to the new reflector tank could be done without any protection.

On 13 April, J. GADBIN, Préfet du Département Isère, visited the ILL to look into the swimming pool (still without water). He could observe ILL engineers and technicians inside it, 12 m below, installing connecting sleeves and performing leak tests on the joints, see Fig. 7 page 152. He expressed his satisfaction that the refurbishment work was on schedule and that this Grenoble-based international institute would soon open its doors again to scientists eager to use the high neutron flux.

The Swiss delegation of G.M. SCHUWEY, Director of the Federal Office for Education and Science, P. ZINSLI, Vice-Director of this Federal Office, G. KOSTORZ, Professor at ETH Zürich, K. YVON, Professor at the University of Geneva and E. BLOCH, Responsible for Public Relations at the Federal Office, came on 20 April to attend the ceremony for the signing of the scientific membership agreement at the ILL. This agreement runs from 1 January 1994 until 31 December 1998 with the aim of an extension until 31 December 2003. This is the second agreement between Switzerland and the ILL after the first one from 1 January 1989 to 31 December 1992.

This signature, together with the ones with Spain (February 1994) and Austria (December 1994) reinforces the ILL's international scientific character. The delegation did not pass up the opportunity to see the new reflector tank and the activity around it.

On 7 September another Swiss delegation with H. URSPRUNG, Secretary of State, A. LOTTAZ, Deputy Secretary of State, M. K.EBERLE, Director of the Paul Scherrer Institut, R. ABELA, W. FISCHER, A. FURRER, W. HIRT, further members of the Paul Scherrer Institut and H. NEUKOMM, ETH-Board, was seeking information on the complementarity between experiments with neutrons and Synchrotron radiation. A. LEADBETTER, Assistant Director and Head of the Science Division, presented the ILL and outlined in particular the unique possibilities offered by polarised neutrons and by Hydrogen-Deuterium contrast variation with special emphasis on Biology and soft matter research.

Throughout the year articles in the local and international press reported on progress with the refurbishment of the reactor and the imminent start-up.

Bruno Dorner
Scientific Secretary

Safety, Medical and Health Physics Group

Health Physics (SPR)

Over the course of 1994, the SPR cooperated closely with the Reactor Division in cutting up the reactor vessel, conditioning and removing the radioactive waste materials produced.

As work progressed, beam tubes 2 and then 3 were gradually decontaminated, thus enabling staff responsible for reassembling the structures of the new reactor vessel to work without particular protection.

The machine tools used in the cutting operations were decontaminated after use, vinyl-wrapped and put in storage for possible re-utilisation.

The liquid waste recovery tanks were systematically cleaned.

As in the past, operations staff were issued with additional pocket dosimeters.

Test procedures for beam shutters and reception procedures for experimental devices were updated.

The SPR participated in the drafting of the instrument safety files.

Safety

Various measures have been taken :

- Follow-up of projects on the reactor, drafting of prevention plans;
- Safety training and training in the use of fire extinguishers for ILL staff;
- Participation in the drafting of the instrument safety files;
- Inspections of work stations to reduce industrial accidents.

Joint Works Medical Service

The Joint Works Medical Service (SMTC) is responsible for the medical surveillance of ILL, ESRF and EMBL staff, as required by the French labour law. The SMTC also checks that all staff members attend their annual medicals, analyses working conditions, provides information on occupational hazards, administers medical care in the event of illness or injury, and acts as health advisor to the three establishments.

Guy Germain

SCIENCE DIVISION (DS)

In May 1994 I came to ILL and took over as Head of Science Division from Reinhard Scherm, with the hope and expectation of seeing our first neutrons before the end of the summer. Unfortunately this did not happen because the administrative processes took longer than expected, but as I write this introduction at the beginning of 1995 we have indeed just restarted the reactor. The delay has, however, been used to the full and everything that could be done without neutrons to prepare for the restart has been done. The result is that we are able to reduce the commissioning period required for most instruments to less than the full cycle originally envisaged, so that the user programme is now planned to start on 27 February and will use the last 15 days of the first fuel element.

Essentially all the ILL staff who went to spend time at other institutions during the shutdown returned during the year but a number of staff have left on normal or early retirement. However, 14 new young scientists have taken up their posts during the year. This influx of very able and enthusiastic young people is of vital importance for the scientific health of the ILL and they are already making an impact on the life of the Institut.

Most of our efforts during the year have been devoted to preparations for restarting the scientific activity. This has involved the technical work of rebuilding the instruments in the reactor hall and the bringing to life again of all the instruments; preparation of the new instruments and projects such as IN15, IN16 and GAMS5 waiting for their first taste of neutrons, and very successful continuing development programmes on the He-3 polarising filter and the image plate neutron detector. These last programmes are now reaching the stage where they are ready for development into projects to produce working user facilities. In addition,

as staff time became available, we have returned to the coupled projects for straightening two guides (H17 & H18), building a reflectometer and improving D16 and IN5, and have almost completed the preliminary project definition and costing; more detailed work will follow. In relation to this and other potential projects, it has been a very important task during the year to begin, in conjunction with the Scientific Council, a re-examination of investment priorities in the new era of operation with a much reduced budget. This will be an ongoing activity which is clearly essential to ensure the best use of limited resources and to ensure that ILL maintains some level of high quality innovative development.

The returning user will notice some differences around the instruments with the appearance of barriers and safety interlocks limiting access to the experimental areas. This represents part of the results of a major review of our safety procedures aimed at ensuring safe operation consistent with an open user environment. This is a difficult line to tread but one that is of crucial importance to get right, especially with the restart of a major user programme with many new staff and users, around an essentially new reactor, after a very long shutdown.

The preparations are now done and all our thoughts and energies turn to the restart of the instruments, to the reappearance of users and to the resurgence of the scientific life of the Institut. We hope for an exciting and successful 1995.

Alan Leadbetter

Scientific Coordination Office

The Scientific Coordination Office helped with the organisation of several workshops held in 1994. The list is as follows:

Workshop	Organisers
Journées des Polymères et Colloïdes ILL/UJF/GFP Workshop Pôle Européen 2 - 3 February 94	P. Lindner, ILL E. Geissler/B. Berge, UJF
Nuclear Fission and Fission-Product Spectroscopy 2 - 4 May 94	H. Faust/ G. Fioni, ILL
Deuteration of Biological Molecules for Neutron Scattering and for NMR 26 Sept.- 1 Oct. 94	P. Timmins, ILL R. Leberman, EMBL D. Marion, IBS J. Parello, Montpellier
Séminaire France-Japon sur "L'utilisation des neutrons et du rayonnement synchrotron en biologie" 21 - 25 November 94	J. Zaccari, IBS & ILL
Meeting on Random Tiling & Quasi-Crystals 7 - 8 December 94	Ch. Janot, UJF & ILL M. De Boissieu, ENSEEG

World-Wide Web (WWW) at ILL

ILL's computer service installed a world-wide web server (WWW) for the ILL with the address: <http://www.ill.fr/>. There you will find information about the ILL in general, the "guide to neutron research facilities at the ILL", the "yellow book", with figures and photos, a library search utility (see also page 100) and a "what's new" page, which is updated as appropriate. This information service in electronic form is made available, so that it can be downloaded from outside the ILL. Hence instrumental characteristics, figures etc. can be accessed and copied to be used in publications or for other purposes. Proposal forms can also be retrieved as word files. From the ILL the experimental schedule can be examined with WWW. Other information on the database includes: phone directory, book catalogue.

Statistics of the Scientific Programme

In summer we had again a proposal round after a 3-year break. We received some 600 proposals, out of which about 400 proposals were allocated beam-time. Fig. 1 gives the beam-time requested and the availability of beam-time on the different instruments. 115 reactor days, i.e. two and a

half cycles, were available for beam-time distribution. In general about 80% of the beam-time was given to the subcommittees. In a few cases, D16, D17, D22 and IN20, less time was given due to extended instrument developments foreseen in the forthcoming round. D22 is the new small-angle scattering instrument. On average there was an overload factor of 2.3, but you can see in the histogram that in some cases the overload factor is almost 4. The CRG instruments were not yet available in this proposal round.

The distribution of beam-time amongst the colleges is shown in Fig. 2.

The basis for the statistical breakdown of beam-time allocation among the member countries is as follows:

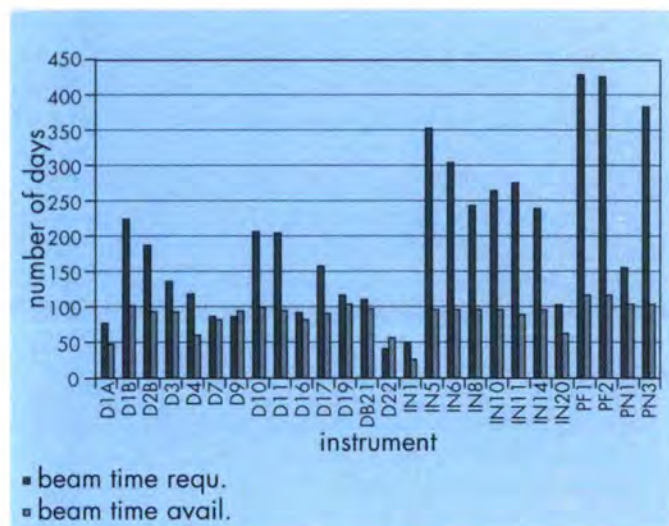


Fig. 1: Beam-time distribution - Scientific Council October.

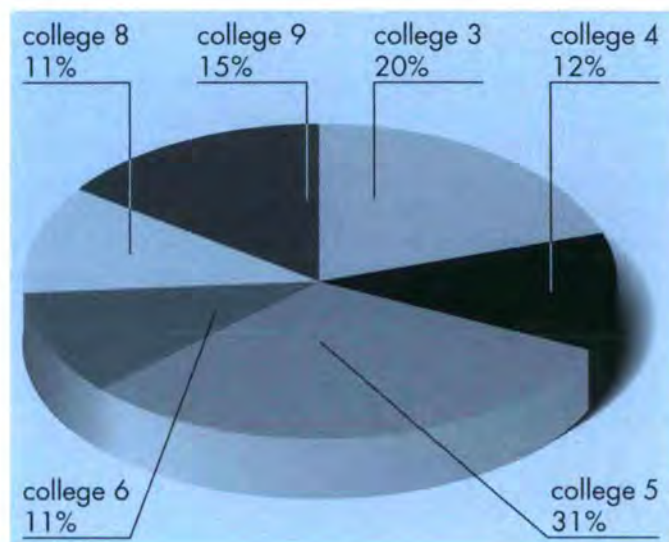


Fig. 2: Beam-time allocation amongst the colleges - Scientific Council October.

1. The member countries are France, Germany, UK, Switzerland, Spain and Austria. Italy also receives beam-time as a result of specific instrument contracts.

2. The attribution is based on the location of the laboratory of the proposers, not their individual nationality.

3. For a proposal involving laboratories from more than one member country, the total number of experiment days is divided equally among the collaborating countries.

4. When a proposal involves a collaboration with a non-member country, the allocated time is attributed entirely to the collaborating member country (or countries).

5. When ILL scientists are proposer or co-proposers, the allocated 'ILL' time is attributed among the member countries according to their financial contributions to ILL. Local contacts are not counted as proposers.

country	requested days	requested in %	allocated days	allocated in %
AUT	90,3	1,7%	62,1	2,8%
CH	299,7	5,6%	96,5	4,3%
D	1894,7	35,3%	816	36,6%
ESP	141,1	2,6%	30,5	1,4%
F	1335,9	24,9%	569,4	25,6%
GB	1524,9	28,4%	618,5	27,8%
ITA	75,5	1,2%	35	1,6%
total	5362,1	99,8%	2228,0	100,0%

Table 1: Requested and allocated beam-time among the ILL member countries for the scientific council October.

Table 1 shows the requested and allocated beam-time for ILL's member countries and the pie chart in Fig. 3 displays the beam-time allocation in percent.

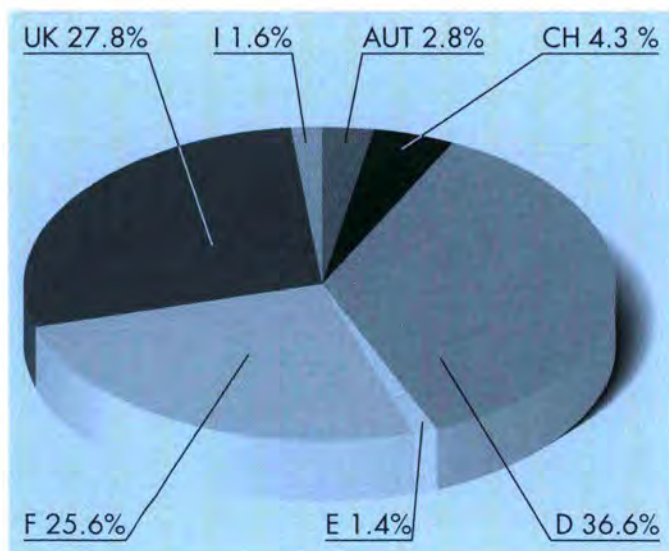


Fig. 3: Beam-time allocation - Scientific Council October.

Joint ILL-ESRF Library

1994 Scientific Literature Budget: 1 522,9 KFF, Excl. Taxes

ILL Share: 761,45 KFF, Excl. Taxes

Librarian: Christine Castets

According to the "Agreement on the Operation and Maintenance of a Joint ILL-ESRF Library" from 1994:

- The two Institutes participate equally in all costs of the joint ILL-ESRF Library, see Fig. 4.
- The literature acquisition budget will only increase according to inflation.

The very high increase (more than 12%) in the cost of journals led to a reduction in the number of books purchased and the number of volumes bound.

During the year

- 865 books were processed (1045 in 1993)
 - 275 for ESRF Departments or Divisions (396 in 1993)
 - 140 for ILL Departments or Divisions (100 in 1993)
 - 450 for the Joint Library (549 in 1993)
- 650 volumes were bound (900 in 1993).
- The cataloguing of books was completed (last 3000 new entries) on the Loris-Doris library management system and all books were equipped with bar code labels.
- The journal registration was computerised.
- Additional PCs were purchased.

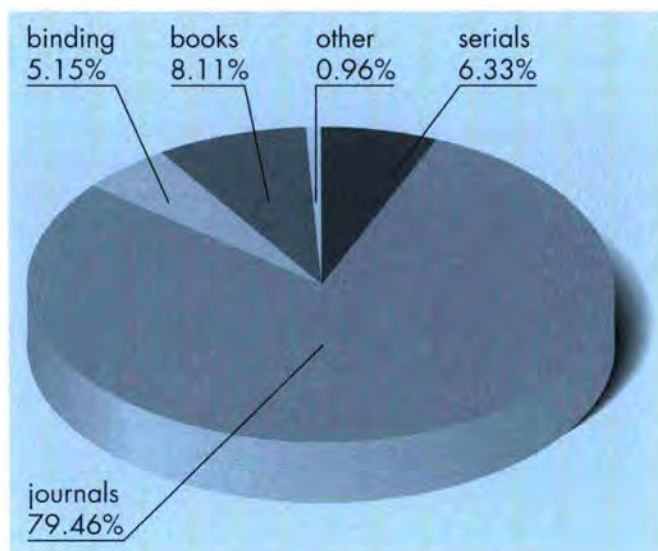


Fig. 4: Allocation of literature costs.

Library catalogue on the Internet

An exciting step for the library was the opportunity of transferring the computerized catalogue of books onto the Internet. This was initially the project of the "Commission Documentaire of the Pôle Européen" to gather all catalogues of the Grenoble Libraries and make them available on the Internet. Thanks to the ESRF expertise in the WWW and in particular to the work of W. Pulford, this was achieved efficiently and more rapidly than foreseen.

It was soon apparent that the installation of the library catalogue on WWW was not only a world wide system for dissemination of information but also an efficient tool for in-house information: Scientists from both institutes consult the information available from their respective institutes including the book catalogue.

At the moment, the WWW book catalogue is searchable by author, words of title, year of publication and publisher. It is currently being improved by ESRF Computer Services and W. Pulford in order to have a regular update and more criteria for searching (collection title, key-words...).

Access to the catalogue is possible through <http://www.esrf.fr/>, <http://www.ill.fr/>.

Databases on CD-ROM or Diskette

The CD-ROM station "libre service" is much appreciated and is now widely used. An extension is planned for 1995 with one additional consultation post equipped with 2 towers of 7 readers each.

Current Contents on Diskette with Abstracts (Physical, Chemical and Earth Sciences) installed on the network since 1992 remained a useful tool for current bibliographic searches.

Publications

The number of publications from ILL staff and users in journals, books, conference proceedings continued to decrease and will not exceed 250, see Fig. 5. This decrease in publications is a consequence of the non-operation of the reactor over the last 3 years and the reduced number of scientists in the last year of the shutdown and the reinstallation of the instruments, which left little time for experiments.

	1991	1992	1993	1994
Number of received publications	544	580	339	250

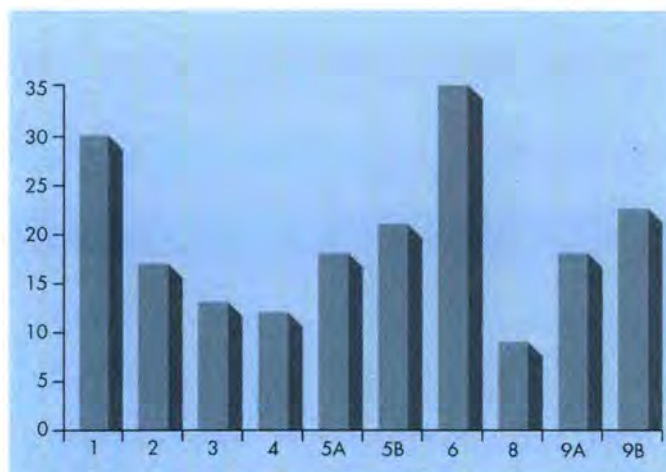


Fig. 5: Publications received by subject:

- 1 - Instruments and Methods
- 2 - Theory
- 3 - Fundamental and Nuclear Physics
- 4 - Excitations
- 5a- Crystallographic Structures
- 5b- Magnetism
- 6 - Liquids, Disordered Materials
- 8 - Biology
- 9a- Chemistry- Small molecules
- 9b- Chemistry- Colloids and Polymers

Scientific Computing

Members

Jane Brown (until 31/10/94)
Alain Filhol
Ron Ghosh
Don Kearley (since 1/11/94)
Christian Lacaille-Desse
Didier Richard

Introduction

The aim of the scientific computing group is to assist and advise ILL scientists and visitors with specific projects and day-to-day problems in scientific computing. Since its creation just over a year ago, the main tasks of the group have been associated with easing the transition from VMS to UNIX for scientists and future visitors. The group advises scientists for the purchase of computers and programs and does its best to federate the choice of software and hardware of general interest. Members of the group have been involved closely with the scientists and the DPT in selecting hardware (graphics printers, file-server, etc.) and in joint development of software for graphics and data storage. Members of the group have also collaborated with the ESRF, CNRS and Pechiney during the course of the year.

General Graphics

Whilst we have ensured that we have working libraries for graphics standards including GKS and PHIGS, some effort has been expended on implementing public-domain graphics software, avoiding high licence costs and offering easier exportability of working programs. These packages include stand-alone programs and a general purpose device-independent library for scientific graphics. An additional advantage offered is compatibility with OpenVMS, allowing identical usage on remaining VAX systems awaiting replacement. Individual scientists in each of the Instrument Groups have used and reported favourably on these facilities.

Tools for helping development of Graphical User Interfaces have been under constant review. MetaCard is one example of a hypertext based interface which has been used with some success in a number of projects within the Science Division.

Data Base

As part of the plan to make data available for UNIX systems in simple text form, part of the existing archive has been transcribed into the new format; much of the practical work was performed by our group. This has allowed joint development with the DPT of utilities for listing and cataloguing operational volumes of data. Inevitably, a number of unexpected problems has arisen, but which have now been successfully mastered.

Modernising and improving existing programs

The group has been able to offer general assistance with syntactic and conceptual differences between VMS and UNIX operating systems. One of the major projects was to rationalise the three-axis group programs: **Filing** (data file manipulation), **ResCal** (computation of the spectrometer resolution function), **Pkfit** (the main fitting program, see Fig. 1 on page 142), in collaboration with A. Bouvet. These programs are now readily portable and run on Vax, Macintosh or UNIX machines via a modern "point-and-click" graphical user interface, and much improved graphics. Several sets of data can be visualised together and it is now possible to deconvolute the multidimensional resolution function. A joint ILL-ESRF project has been to offer a Motif interface to **OrientExpress** (see Fig 2 on page 142), a program for the indexing and simulation of X ray or neutron Laue patterns. The improvement of programs **ABFfit** (profile fitting) and **ABCdata** (statistical analysis) has been pursued. The group also worked for the Reactor Division. An old, user-hostile VMS program for the computing of the Xenon poisoning effect was converted to **MacXenon**, a user-friendly Macintosh program.

New Applications

Current workstations are very powerful, and this fundamentally changes the way in which new user-programs are conceived. A new project was started with the aim of exploiting this power to provide a modern data manipulation/visualisation utility. This program, **LAMP** (Large Array Manipulation Program) is ideally suited to instruments collecting large arrays of data. It provides a simple interface through which the users can read most common types of data and apply a wide variety of functions to one or more data-sets. These operations can be: user-written macros, predefined, or one-line functions entered in a special window. Powerful integrated graphics allows the data to be visualised at any stage of the treatment. Intermediate and final data can be saved in many formats either for further analysis or for exporting to other applications. Then entire status of any session can be saved and then restarted at a latter time. LAMP (see Fig. 3 on page 142) not only has its own standard graphics (vectors, contours and surfaces) but it is linked directly to the application **SCAN** which allows the adventurous user a range of elaborate image manipulations.

Documentation

As projects progressed we have documented the working components, helping to get early feedback from users. The group collaborates with the preparation of the ILL general computing newsletters, as well as the ILL Micro News, an internal bulletin on use of personal computers.

Jane Brown and Don Kearley

UNIX-Seminars

The changeover from VMS to UNIX systems progressed at the ILL in 1993 as the first UNIX Workstations arrived in the Instrument Groups. As a continuation of a series of seminars (spring 93 to spring 94) on the most effective use of our Macintosh computers (see ILL Micro News 1, 7 (94)), a series of UNIX Workstation User Seminars (UWUS) was organised during spring and summer 1994 in order to simplify the access to this new system for everyone.

The aim of this project was to introduce beginners and future users of the UNIX Workstations to the systems chosen by the different Instrument Groups (HP or SGI) and to give advice for program conversion and tools available on these machines.

O. Tillier, C. de Polignac, G. Messoumian and M. Le Sourne tried to attract timid users for the new system in their general introduction. A similar approach was taken by A. Hewat (Diffraction Group) guiding the path from the familiar Macintosh terminal to the powerful Silicon Graphics system. He also demonstrated the power of the EXPLORER package on this machine and the use of MOTIF to convert command line programs into a "button" program interface. The fruits of a laborious adaptation of the PAW system (from CERN) for the Nuclear and Fundamental Physics Group and the use of X-terminals in connection with their HP workstations were presented by U. Mayerhofer. R. May explained the approach of the Large Scale Structure Group to their Silicon Graphics system and especially the traps into which one could fall when converting VAX-FORTRAN programs to UNIX workstations.

A rather detailed introduction into the use of MOTIF when modernising programs during conversion to UNIX systems was given by G. McIntyre and A. Hewat. Under the title "Requiescat Plot-10" R. Ghosh reviewed the history and present situation of plotting facilities and the graphics systems (PLOT-10, GKS, PHIGS, PGPLOT,...) at the ILL and tried to convince the audience to use the chance of the necessary program conversion to abandon antiquated and also service-intensive graphics systems in favour of simple free packages like PGPLOT which he had explored for the Scientific Computing Service. For the Time-of-Flight and High Resolution Group G. Kearley presented their Silicon Graphics system and especially different editors which could be used on UNIX machines avoiding the painful Vi-editor, the only real standard in UNIX. In the same seminar D. Richard and G. Kearley showed the progress made with the LAMP-system (Large Array Manipulation Program) to be used in connection with the large TOF data files in future in the group.

How to connect to the computer system of the US-president and how to fetch more useful information from everywhere in the world was demonstrated by J. Last in his seminar on "Internet Services and Resources", and finally H. Büttner praised the advantages of the World Wide Web (W3, developed by CERN again) using MOSAIC as an interface or browser (NCSA development), which she had come to estimate during her work at the ESRF.

These seminars were very well attended (especially also from outside the ILL) and all in all they were very useful, not only in making more transparent the different approaches towards the use of UNIX at the ILL, but also in lowering the activation barrier of not-yet-users of UNIX in the house, - and this was A. Heidemann's original intention when proposing the topic.

Jens-Boie Suck

Nuclear and Fundamental Physics (NFP) Group

- PN1 Fission product separator LOHENGRIN on beam tube H9 (H.R. Faust, G. Fioni, I. Gartshore)
- PN3 Curved and flat crystal spectrometers GAMS2/3, GAMS4, GAMS5 (project) on the through-tube H6-H7 (H. Börner, A. Williams, R. Oliver)
- PF1 Cold polarized neutron beam PARSIFAL at the end position of guide H53 (J. Last, U. Mayerhofer, A. Trouillon)
- PF2 Ultra-cold neutron source and distribution system on level D using the vertical guide from the cold source and neutron turbine (W. Drexel, P. Geltenbort, K. Eder (part-time), H. Just)

PN1 Fission product separator

The reinstallation of the instrument was the main activity during 1994 and required a considerable effort. The front-end of the spectrometer, consisting of the first analysing magnet and the source changing mechanism, was reinstalled and fully tested. The condenser was put back into operation with the reinstallation of the H.V. generators and the associated electronics which were partly modified. In the experimental area, the Reverse Energy Dispersion (RED) magnet, see Fig. 1 page 143, and all electronics, vacuum system and gas installations necessary for the different research programs, have been brought back into operation. The vacuum system has been partly modified and several components have been upgraded to improve experimental conditions.

A major investment was a new cooling system, which serves all magnets and power supply units of the spectrometer. It has been installed and connected to the instrument security system.

The development and implementation of an improved computer program for the operation of the spectrometer have been completed. The magnetic and electric field control, as well as the positioning of the two main diaphragms, is now performed by a PC connected to different units through an IEEE 448 bus.

PN3 Gamma ray spectrometers

The twin-curved spectrometer GAMS2/3 was reinstalled at its previous position at H6 on level C of the reactor, after a complete upgrade involving:

- The replacement of the old interferometers based on intensity comparisons, by new interferometers employing two frequency lasers which now permit γ -ray energy scans of arbitrarily small step width.

- Both electronics and data acquisition were completely replaced: The old system comprising essentially a microvac with a CAMAC-crate connected to its bus was replaced by a PC-controlled system making use of PC-cards as much as possible (i.e. MCA-cards for the multi-ROI energy spectra, logic control, an IEEE 488.2 controller card). The CAMAC-based interference-fringe counting, which provides the vital reference for the diffraction angle determination, i.e. the γ -ray energy measurement, was detached from the computer using a IEEE-interfaced CAMAC-controller, which guarantees its independence from the main instrument control and data transfer.

- The software was entirely rewritten and GAMS2/3 is now controlled by an MS-WINDOWS program written in BORLAND C++. The new program provides relatively easy use and also supplies the user with as much information as possible about the ongoing experiment. This program is designed to be the prototype for the software that will control GAMS4 and GAMS5 and was written with a maximum of standardisation between those three instruments in mind.

- A passive antivibration system was put in place for GAMS2/3. The first measurements of the effect of vibrations upon the interferometric angular resolution showed an improvement of a factor of 20 (better than 0.01 arsecs compared to about 0.16 arsec before). Now the only significant limit on the resolution of GAMS2/3 is imposed by the source geometry (finite target width).

GAMS4 was re-installed at its old position at H6. The electronics and the data acquisition systems were tested. The active anti-vibration system was upgraded introducing anti-tilt, anti-pitch and anti-roll as additional degrees of freedom and replacing the analogue control by PC-based digital electronics.

PROJECT GAMS5: The infrastructure of the new PN3 instrument GAMS5 has been installed. The ZERODUR®-base and the parts of the GAMS5-interferometer, see Fig. 2 page 143, were assembled off-line prior to installation at H7.

PF1 Cold polarized beam facility

During 1994 work on the new polarised beam facility for fundamental physics was completed. The concrete walls surrounding the experimental area and the casemate which houses the polariser were constructed during the first quarter of 1994. In June and July a high precision resin floor was installed allowing heavy experimental set-ups to be moved on air pads. The exterior preparation zone was leveled to the height of the experimental area.

In October followed the installation of the experimenters' cabin which features an air-conditioned section for experiment electronics and computers. Although the scientists may still have to put up with summerly heat waves, the air conditioner will certainly help to keep discriminator thresholds and amplifier gains more stable.

There is also an outlet for the stabilised, interruption-free power supply of the ILL (Réseau ARC). After the installation of the ILL-wide computer network an HP 71280 workstation will be available for data analysis.

All necessary safety installations are now in place. The PF1 beam shutter is made of ${}^6\text{LiF}$, a material that produces only a small amount of background when irradiated with neutrons. During normal operation with the full class 1 beam the experimental area will not be accessible. It is, however, possible to work with an attenuated beam inside this zone.

Work on the neutron focusing device has also progressed. During a test run at the EROS spectrometer in Saclay a bent stack of supermirror-coated silicon wafers was studied for its transmission characteristics. The results concur with the simulated behaviour of the device. As a next step it is planned to build a prototype bender with $3 \times 5 \text{ cm}^2$ usable cross-section.

PF2 The source of very cold and ultra cold neutrons

All efforts this year were directed towards improvements of the experimental equipment of PF2 and final endurance tests in view of the approaching reactor restart.

A nearly totally renewed curved part of the neutron guide TGV (Tube Guide Vertical) of PF2, has been assembled and installed. The four lower vacuum boxes were fabricated from bulk material thus avoiding any weld in the region of relatively high flux; there, too, new types of o-rings that have higher resistance to radiation have been used. All neutron mirrors within the TGV have been replaced; some of them were fabricated by diamond milling that gives a surface roughness very similar to that of the original pieces which were fabricated exclusively using a replica technique (3 nm and 2.5 nm, resp.). The know-how and help of H. Nagel and F. W. Schreiber from the TU Munich were highly appreciated.

A replacement neutron guide for the straight vertical part, the TGV (Tube Guide Vertical), has been assembled from the individual elements in a very satisfactory manner in collaboration with the Dupuy-company of Lyon. This reserve neutron guide is stored in a vacuum container on level D.

With permanent renewal and standardisation of equipment in mind, a new turbine motor drive based on the REFU frequency generators, which are widely used at the ILL, is being tested; a new positioning system for the UCN (Ultra Cold Neutron) beam changer at the exit side of the neutron turbine is under development.

Another trend, started this year, is towards the replacement of all oil-containing vacuum pumps by "dry" pumps, esp. on vacuum cans housing large quantities of high quality neutron mirrors. A first step in this direction is the change of turbopumps with oil-greased bearings to models

using ceramic bearings with low vapour pressure grease. Other dry pump systems are being tested. This is an important matter as most recipients are pumped over many years and oil traces - though tiny - had been found in the curved part of the TGV neutron guide (after 6 years of operation).

The lead shutter between the straight and the curved part of the TGV, which was operated manually before, has been automated. It received the standard ILL system onto which the necessary inhibitions imposed by safety rules could easily be connected.

A "VCN-bender" (Very Cold Neutrons) is under construction and should be available for the restart of the reactor. The available VCN-beam position is normally occupied by the neutron optical setup of the University of Innsbruck group. This setup uses only half of the available VCN-beam. The "VCN-bender" will allow the other half of the VCN-beam to be used with the optical setup remaining in place. It consists of a bunch of parallel glass lamellae of 0.2 mm thickness and reflecting mirror layers on both surfaces housed in grooves in the bottom and top holder plates. Its effective dimensions are 17 mm wide and 80 mm high; the outer radius of curvature is 335 mm and the deflection angle is 65 degrees. A total of 22 lamellae give 10 channels where the VCN are transported mainly by garland reflections. The transmitted wavelength band is centered around 60 Ångström. Proper neutron diaphragms will reduce the background radiation around the bender.

Computer simulations on the transportation of VCN in the vertical TGV/TGC guides and their transformation into UCN under the action of a neutron turbine have been continued with low priority. This work is essentially based on computer programs from a group at the Dept. of Physics at the University of Rhode Island (URI; M. C. Crow, A. Steyerl). This group has worked out a proposal for a VCN/UCN source for the American ANS project. In this context, the original FORTRAN programs developed at the TU Munich have been extended at URI to take into consideration the effects of centrifugal and Coriolis forces, that the neutrons experience when they are Doppler shifted within the neutron turbine. The calculations applied to our case are not yet finished, but possible consequences for the near future can be expected.

Besides normal maintenance work, long-term endurance tests have been performed in order to bring the installation back into a reliable state for the restart of the reactor.

Preparation of the next EDM experiment

The preparatory work for the next neutron electric dipole measurement has been devoted to three aspects of the equipment. These have been the development and installation of a new computer control and data acquisition system based on PCs, the development of the system for creating the high and automatically reversible electric field

in the volume occupied by stored ultracold neutrons, and the completion of the final design sensitivity for the ^{199}Hg magnetometer.

The high voltage control system based on one dedicated PC has been completed and tested. All the control and monitoring communication with the high voltage system is by fibre optic cables to reduce the chance of influencing other parts of the data acquisition system through shared currents. For the insulating wall of the UCN storage cell, to which the high voltage is applied, two precision-machined fused quartz annuli, 20 cm high and 40 and 50 cm diameter respectively, have been purchased through PNPI, Gatchina from manufacturers in St. Petersburg and brought into use at ILL in November. The performance in sustaining electric field is now at least 2.5 times better than the alumina cylinder used in the first trials. Following this step, the electric field strength has reached about half the design value, and is almost certainly limited by the prototype high voltage vacuum feed-through and aluminium electrodes which are due to be replaced by more highly-engineered items at the end of the year.

The data acquisition cycle of the main apparatus is now run by a second PC which can send data files to a Unix workstation, and which provides graphical results that are updated in real time and downloaded to a third PC in ILL1.

The ^{199}Hg magnetometer has reached its design specification with a self noise of $5 \cdot 10^{-10}$ Gauss RMS during the two-minute magnetic field measurements. Concerning the magnetic shield, a magnetic field shaking system at a frequency of about 100 Hz has been found to greatly improve the shielding action, reducing the penetration from the level D crane, for example, by about a factor of 25.

Hans Börner

Diffraction (DIF) Group

D1A:	High Resolution 2-Axis Diffractometer (1/2 CRG-A)	(A.W. Hewat, F. Fauth, P. Cross)
D1B:	High Efficiency PSD Diffractometer (CRG-A)	(B. Ouladdiaf, C. Ritter, K. Ben Saïdane)
D2B:	High Resolution Powder Diffractometer	(P. Radaelli, E. Suard, P. Cross)
D3:	Polarized neutron diffractometer	(F. Tasset, E. Lelièvre-Berna, K. Ben Saïdane)
CRYOPAD:	Cryogenic Polarization Analysis Device	(F. Tasset, S. Pujol)
D4:	Disordered Materials and Liquids Diffractometer	(H. Fischer, P. Palleau)
D9:	Four-Circle Diffractometer	(C. Ritter, M.-T. Fernandez-Diaz, J. Archer)
D10:	Four-Circle 3-Axis Diffractometer	(G. McIntyre, B. Ouladdiaf, G. Schmidt)
D15:	Two-Axis Diffractometer with Lifting Counter (CRG-B)	(E. Ressouche, J. Brown, G. Schmidt)
D19:	High-flux single crystal multidetector diffractometer	(S.A. Mason, P. Langan, J. Archer)
D20:	High-flux multidetector	(J. Pannetier, P. Convert, J. Torregrossa)

The second part of 1994 saw the re-installation and testing of all of the diffractometers. D1A returned from Saclay in the summer, and was set up on its old position on thermal guide H23. D1A and IN3 were the first ILL instruments for which CRG contracts were signed, with the PSI-Villingen/Switzerland. D1A will continue to be available as a scheduled instrument for 50% of the time, and some time is foreseen for neutron strain scanning experiments, for which a Ph.D. student (Jason Buckley) has been recruited together with an EU postdoctoral fellow.

D1B will continue to be used for most of 1995 as a scheduled instrument, before it too becomes a CRG with the completion of D20. The latter instrument has been further delayed by difficulties with the glass substrate used for the large position sensitive detector, but the mechanics on reactor beam tube H11 have been installed.

Problems were also encountered with the construction of the new larger PSD for D19, which is being manufactured by CERCA, and with the production of the new focussing monochromator for D2B. These will now not be available until mid-1995.

Diffraction Group Computing

Much progress was however made with the Unix plan for data treatment on the instruments. All diffractometers now have dedicated Silicon Graphics (SGI) Unix computers, the main data treatment programmes have been transferred to these machines, and user-friendly graphic interfaces have been added using Motif and MetaCard, with the pplot library for 1-D and 2-D graphics. Applications based on Iris Explorer and Inventor are available for 3-D visualisation of data from position-sensitive detectors, of nuclear and magnetic structures, and of charge/spin density and probability. We expect that the processing and graphics power now available, together with the ease of use of these machines, will transform the way scientists analyse their experiments.

Because they will be able to treat their data as fast as they can collect it, this should also mean that more efficient use is made of the limited beam time. Data is automatically transferred to the central SGI file server, whose disks can be mounted on the local workstations via the ethernet. When the experiment is finished and a new team arrives, the previous users can transfer to a similar workstation and continue data analysis with access to exactly the same disk areas and computer programmes. The price of these workstations has been decreasing rapidly, so that they now cost no more than an ordinary graphics computer terminal or Macintosh at the time of the reactor shutdown.

We were particularly fortunate to have enthusiastic summer students, Olivier Ernst, Pierre Morganti, Jacqui Cole, Marcus Hewat and Michael Knapp, who helped re-construct instruments and develop programmes and graphics interfaces e.g. for exploring the Laplacian of the charge density, for drawing crystal structures in 3-D, for powder-data visualisation etc. Of course, commercial products are not ignored; the crystal-modelling package Cerius from Molecular Simulations Inc. has proved invaluable for the understanding of subtle features in the ferroelectric transitions of several structures. A collage of these interfaces, graphics applications and graphical structural solutions can be found in colour Fig. 1 on page 143.

In 1995 we hope to make similar progress with instrument control under Unix. Again the advantage should be user friendly graphic interfaces, reducing the learning time for new users and making them more independent of the smaller numbers of ILL scientists.

D1A High Resolution Powder Diffractometer on thermal guide H23

The D1A technician, Peter Cross, returned from Saclay with the machine, which meant that the re-installation at ILL went very smoothly. In October, the new CRG scientist, François Fauth from PSI-ETH Zürich arrived and will be responsible for 50% of the operation of the instrument. Also in October, Jason Buckley arrived from the University of Loughborough to start his Ph.D. in strain scanning on

D1A. A new XYZ heavy duty goniometer together with laser alignment equipment and sets of fine slits have been purchased for this work.

Some modifications to the shielding were needed to meet the new safety regulations, but since the flux on the sample from this high resolution machine is (just) under 2.10^6 n.cm².sec⁻¹, no interlock system is needed to prevent access to the experimental area. The control computer is now a micro-Vax running the standard MAD package, and the data format has been changed slightly to make it identical to that of most other diffractometers.

Michael Knapp, a summer vacation student from the University of Darmstadt (Prof. H. Fuess) implemented new data retrieval and display programmes on the D1A workstation. The user can simply click on a button to obtain a summary of the experiments performed, on another button to retrieve and collate the data for a particular experiment, on another to display it etc.

The new 25-detector/collimator bank will be installed in 1995, since first priority this year was to get everything operational again as soon as possible.

D1B High Efficiency PSD Powder Diffractometer on thermal guide H23

After recuperation of various parts which had been on loan at other neutron centres, D1B has been restarted and thoroughly tested. The new data acquisition electronics, which had been changed in 1991, have been tested and tuned using an artificial neutron source. After polishing the supporting rail and readjusting the driving wheel, the multidetector is moving now without external help. The focussing graphite monochromator has been reassembled on a new monochromator holder and aligned with neutrons in Saclay. The secondary neutron path has also been aligned using a laser beam. Finally the cryostat has been equiped and tested with an automatic nitrogen and helium refill system.

The data reduction programs (retrieve, addition, subtraction,...) such as TEKD1B and FILD1B have been modified and are available on the instrument MicroVax workstation, as well as all programs needed for data treatment (Rietveld, graphical display, integrated intensities). As for other instruments in the Diffraction Group, an SGI workstation has been installed in the cabin of D1B with a direct ethernet connection to the control computer and network. Almost all programs for powder data treatment, including Rietveld refinement (FULLPROF) and graphic display are now also available on this workstation.

D2B High Resolution Powder Diffractometer on thermal beam H11

D2B has been reconstructed in the reactor, and tested thoroughly without neutrons. The reconstruction of the three instruments on the H11 beam was a big job, since literally everything had been removed. Tom Vogt is still on

detachment to Brookhaven, but Paulo Radaelli from Argonne was recruited in October to run the machine, together with Emmanuelle Suard, formally from Bernard Raveau's group in Caen, in December.

As we have already noted, the new Ge monochromator, which will improve the line shape in the high resolution geometry, is still under construction. The present monochromator, which gives high intensity (10^7 n.cm².sec⁻¹) at good resolution (1.5×10^{-3}), will continue to be used for the first experiments, but in the high resolution mode (design limit 5×10^{-4}) the peak shape is not sufficiently uniform. The new bent wafers that have been produced so far have been tested at Saclay, and have been shown to have a very uniform Gaussian mosaic distribution. The completion of this new monochromator is the highest priority for the ILL monochromator group.

The data retrieval programme of Michael Knapp is also available on the D2B workstation, and another vacation student, Marcus Hewat, implemented a 3D structure drawing programme using Silicon Graphics 'Inventor' language. Together with the standard Rietveld refinement programmes, the SGI 'Explorer' visualisation package, and the Molecular Simulations Cerius crystallographic package, we now have some powerful new tools.

D3 Polarized Diffractometer on hot beam H4

As soon as the beam tube had been reinserted in the new reactor vessel, the biological shield was re-installed and precisely aligned, the only change being a new magnetic guide field on the secondary beam (the old one had suffered from radiation damage at the tip close to the primary beam). The diffractometer was installed and carefully aligned on its air cushion base on a new marble floor. The sample table, which was having trouble supporting the heavy cryomagnets on the sample axis, has now been replaced by a strong coaxial system recovered after the decommissioning of similar instruments at Harwell. The 4.6 Tesla magnet and the cryoflipper were used on DN2 at Siloé during most of the reactor shutdown. They are now back at ILL, and the cryomagnet is being successfully equipped with a newer pneumatic cold-valve under development at DPT/Cryogenie. The various automatic shafts and beam systems have been tested on-line with the instrument computers and electronics, and the instrument is now ready for neutron tests and calibration. We thank all the ILL Services who collaborated very effectively in quickly rebuilding the instrument.

A new instrument co-responsible, Eddy LeLièvre-Berna, was recruited in October, and is in charge of the reorganization of the data reduction system on a newly acquired SGI Indigo work station. The idea is to merge the existing programs written by J. Brown with the Madmax (Maximum Entropy Fourier inversion) program developed recently by R. Papoular and E. Ressouche, in a D3-Explorer module based on the SGI-Explorer visualisation system. This should quickly provide us with good graphical interaction and very powerful 3-D visualization of the

magnetization density for a modest programming investment. In 1995, we plan a complete UNIX remodelling of the aging data acquisition system (RSX 11M) with the help of the DPT-data acquisition group.

CRYOPAD- Cryogenic Polarization Analysis Device for SNP on IN20

As it was foreseen in last year's report, the small toroidal superconducting coils for Cryopad-II were delivered early in 1994. They had been difficult to manufacture, and finally exhibited two electrical faults at room temperature. The coils were sent back to the supplier and the smaller coil rewound under warranty, but there was a long delay, mostly due to difficulties in getting the wire. The supplier finally had to slightly change the original mechanical design, since this was responsible for the faults.

In September the coils were reinserted in the cryostat and satisfactorily cooled for the first time. They could be tested at low temperature in the superconducting state.

The Mu-metal shield, which is used to shield the earth's magnetic field against cooling, had also been improved in the meantime.

The design for the nutators guide-fields had been delayed due to a heavy work load and the high priority given to the rebuilding of D3. We now have the good design as well as a good industrial supplier, and the order is being prepared.

We now need a neutron test, which is essential in qualifying our new design for the toroidal precession coils. Being different in Cryopad-II relative to Cryopad-I this new design is much more practical and does not require any moving coil in the cryostat. The test is essential because the magnetic field prediction results from a finite elements calculation, in which it was necessary to take into account the proximity of the two cylindrical superconducting magnetic screens surrounding the coils and acting like magnetic mirrors.

D4 Disordered Materials and Liquids Diffractometer on the hot beam H8

The departure of Pierre Chieux necessitated the appointment of a new instrument responsible for D4, Henry Fischer, who assumed his duties in August 94. During the 3-year reactor shut down several modifications were made to the D4 instrument, which shares its time with IN1. The replacement of the H8 doigt de gant involved moving the entire casemate (containing the monochromator), after which the Tanzboden marble surface was replaced and polished, followed by a laser alignment of the sample/monochromator axis.

The PDP11 computer has been replaced with a DEC α station (VMS) for piloting the experiment, and a faster Camac controller has been installed. The resulting increase in computer power and hard disk space has allowed an elaboration of the experimental control environment. New MAD commands have been added and a new ASCII numor

data file format has been implemented which will include the automatic recording of a considerable number of experimental parameters. Efforts are being made to make this data format compatible with that of the other Diffraction Group instruments. An SGI workstation has been ordered for D4's data reduction needs, but the data will also continue to be analysed on the VAX cluster. The user area at D4 has received new furniture (chairs and table space), geared towards the comfort and convenience of the instrument users.

The increased attention given to radiation security at ILL has resulted in several changes to D4: the installation of an interlock system for entering the experimental (i.e. Tanzboden) zone, the addition of thick boron-impregnated wood panelling for added shielding inside the casemate, an improved technique of handling the radioactive Iridium filter, and modifications to the secondary shutter to avoid accidental irradiation by gamma rays from the Cu monochromator.

At present, no significant modifications have been made to the sample chamber, the D4 oven, or the two 64-cell PSD detectors. However, there are plans to eventually increase the angular range of detection at D4, probably making use of microstrip detector technology.

D9 Four-Circle Diffractometer on the hot beam H3

With the departure of Mogens Lehmann to build an image plate detector in the Large Scale Structures group, and Manfred Reehuis to take up a post at HMI Berlin, Clemens Ritter became responsible for D9, together with Maria-Teresa Fernandez-Diaz, who was recruited in December from Saclay. We were fortunate in persuading John Archer to return from Berlin to work on both D9 and D19.

Reassembled in May/June 1994 the instrument is waiting for the restart of the reactor in order to be aligned with neutrons. The multidetector and the data acquisition electronics have been tested using an artificial neutron source. The displax cooler works well for temperatures down to 16 K, and a project for the adaptation of a helium flow cryostat on the D9 cradle has been started. It should allow routine measurements down to 1.6 K starting from 1996. The diaphragms which control the size of the primary beam have been motorised and can now be controlled from outside the casemate.

Data acquisition is still controlled by a micro Vax; the data treatment is performed online or using the central computer. Once the new responsables of D9 have gained experience, part of the data treatment programs will be transferred to the SGI workstation already reserved for D9.

D10 Four-Circle 3-Axis Diffractometer on thermal guide H24

Computer control of the new large-cryostat goniometer was implemented and tested in 1994. The algorithm allows two modes of operation, in the first the user chooses a particular reciprocal plane to be horizontal, in the second the tilt of the cryostat away from vertical is minimized, which

maximizes the volume of the accessible region of reciprocal space. We anticipate that this goniometer will become increasingly popular for diffraction experiments using the ILL pressure cells, to partly fill the gap left by D15.

In the cycles following the reactor restart, the emphasis will be on assuring the reliability of the new large-cryostat goniometer, of the new offset Eulerian cradle, and most importantly of the four-circle dilution cryostat, during the rigours of the user program. With that established attention will be directed to conversion of the instrument control program to Unix and to development of a graphical user interface. D10 has been proposed as the development instrument for this project because of its many configurations. As well as giving the new user more self-evident and understandable control of the instruments, such interfaces should ultimately extend the range of experiments possible on all instruments.

We also eagerly await the commissioning of D19's new larger position-sensitive detector, since only then can D19's present detector be installed on D10. Offered as an option in place of the present two-axis detector, this will improve the efficiency of structural data collection and measurement of diffuse scattering. In the meantime trials will be made with smaller position-sensitive detectors, in collaboration with the EMBL, both in two-axis and in three-axis mode.

D15 Two-Axis Diffractometer with Lifting Counter on inclined thermal beam IH4.

Several experiments were performed by ILL scientists on the four-circle diffractometer E5 at HMI using D15's position-sensitive detector, on loan during the shut-down. Significant improvements were made to the peak integration software, applicable also to D9 and D19, to allow unbiased integration of closely lying Bragg reflections, by limiting the integration to volumes similar to the first Brillouin zone (Fig.2 page 144). This allows larger unit cells to be studied at a given wavelength than normally possible with a conventional detector.

The instrument D15 itself will be sold and become a CRG-B instrument.

D19 High-Flux Single Crystal Multidetector Diffractometer on the thermal beam H11

A detailed account of D19's configuration at start-up was given in the 1993 Annual Report. Below we concentrate on the user interface. A new instrument co-responsible, Paul Langan, was recruited from the University of Keele in October. A former ILL user, Paul is interested in large structures.

A dedicated SGI workstation is now available for data processing and graphic displays of D19 data and results. Programs are being converted from VMS to the Unix environment as required. At present D19 is controlled by a dedicated Microvax, and in the past diffraction data were displayed and analysed on the D19 Vaxstation 3100. The Vaxstation will be kept for the moment, and users can

also use the ILL's DEC α 3000-500AXP running under Open VMS. However it is expected that the more demanding applications, such as crystallographic least-squares refinement, and real-time rotation and manipulation of 3d images, will be run on the SGI.

On-line documentation on operation of D19 will be made available on the SGI as it is written. This will supplement the on-line documentation already available on the Microvax for the MAD diffractometer control system.

The raw D19 data are transferred to the ILL central data bases for archiving, and can be accessed using the standard ILL programs, so that D19 data will no longer be a special case. A common ASCII data format will be used for almost all instruments in the Diffraction Group.

A brief description of D19 can be found on the World Wide Web under "Single Crystal Diffractometers" in the section "What facilities are available" on the ILL WWW server (at the time of writing <http://jade.ill.fr/>). This description follows that in the ILL Yellow Book, but it can be updated more frequently. Please e-mail suggested improvements to the D19 entry to mason@ill.fr or langan@ill.fr.

D20 High-Flux Multidetector on the thermal beam H11

During 1993 extensive tests of a microstrip prototype detector were carried out at the ILL with a neutron source, and at the LLB (Saclay) and at Siloe (Grenoble) with neutron beams. By the end of 1993, detection problems appeared as a distortion of the amplitude spectrum of the detector leading to a progressive decay of its performance. As the presence of impurities in the detection gas ($^3\text{He}+\text{CF}_4$) could rapidly be ruled out, it was suspected that a modification of the metal electrodes and/or of the glass substrate had taken place over the eight months of continuous use. Optical and electron microscope investigations of several detector plates revealed extensive modifications of the glass substrate under strong electric fields (about 4.10^4 V.cm^{-1}) between anode and cathode strips. These modifications result from the mobility of Na^+ cations present in the glass substrate. Their irreversible displacement under the action of the electric field leads to a depletion of charge carriers in the vicinity of the anodes, and to a deposit of sodium at the edges of the cathodes (see DPT report by A. Oed).

During 1994, several methods to overcome the ageing of the microstrip substrate have been considered and tested. Promising results have been obtained with a new glass with electronic conductivity, and further tests are being carried out before a full set of microstrip plates is ordered. Provided we have the money for the new electrodes, and no further unexpected problems linked to the use of the new glass are found, we expect to be able to complete the banana by the end of 1995. In the meantime, D1B will continue to operate as the ILL high flux powder diffractometer.

Alan Hewat

Large Scale Structures (LSS) Group

- D11 Small-angle scattering diffractometer on the cold guide H15 (P. Lindner, L. Vuillard, K. Ibel, A. Polsak)
- D16 Four-circle diffractometer on cold guide H16 (J. Zaccai (IBS), E. Bellet-Amalric, S. Wood)
- D17 High resolution small-angle scattering diffractometer and reflectometer on the cold guide H17 (H.-J. Lauter, P. Timmins, R. Cubitt, M. Bonnaud)
- DB21 Diffractometer for very large unit cells on cold guide H15 (E. Pebay-Peyroula (IBS), C. Wilkinson (EMBL), S. Wood)
- D22 New small-angle scattering diffractometer on cold guide H512 (R. May, R. Oeser, K. Ibel, R. Gay, P. George)
- EVA Evanescent wave diffractometer on cold guide (CRG-B) H53 (S. Odenbach, R. Günther, B. Cottin)
- Laue detector
Collaborative project with EMBL and Freie Universität, Berlin (M. Lehmann), see "Small Projects in DS"

The major part of 1994 was spent in restarting and testing the instruments of the group in preparation for the restart of the reactor. After much discussion it was decided that after the departure of K. Wotschak on early retirement it would no longer be possible to support the existing data acquisition system for the small angle scattering instruments. Consequently the Instruments and Networks Service undertook to modify and implement the standard ILL data acquisition program, MAD, on D11, D17 and D22. For data treatment the group acquired two Silicon Graphics Indy computers and will purchase a further two in 1995. It is envisaged that users will be able to treat data on DIVA/VEGA under VMS in the first months after the restart but the move to UNIX will be rather rapid.

Instrument projects within the group have moved forward rapidly. D22 is ready for commissioning and is expected to be available to users in the second user cycle of 1995. Discussions on the conversion of D17 to a dedicated reflectometer have made important progress. In collaboration with the Project Office plans have been drawn up for the resiting of D17 and D16 on straightened versions of the guides H18 and H17. Detailed design work on the reflectometer itself will begin soon once a definite choice between monochromator and TOF techniques has been made.

Safety devices (beam shutter control interlocked with the main and ancillary access doors) were installed on all instruments and tested according to the new security regulations at the ILL.

There have been a large number of staff changes in the group during the year. Two new instrument technicians were appointed, Michel Bonnaud (D17) and Simon Wood (D16,

DB21). Regis Gay left D22 to join the Electronics Service and was replaced by Pierre George from the same service. Three new scientists were appointed: Edith Bellet-Amalric (D16) arrived in July, Bob Cubitt (D17) in December and Stefan Egelhaf (D22) will arrive early in 1995. Finally there were two departures: Ralf Oeser to HMI Berlin and Konrad Ibel to early retirement. Konrad was known to all as the builder of D11 and leaves behind him an instrument which is as heavily demanded today as when it first saw neutrons 22 years ago. We wish him all the best in his pre-retirement.

D11 Small-Angle Scattering Diffractometer on the cold guide H15

The year 1994 has been used for a systematic testing and, where necessary, improvement of all the components of the instrument.

The major renovation has been the putting into operation of the new instrument control program MAD, together with the final implementation of the new VME electronics.

The various parameters such as selector speed, collimation distance, attenuator choice and positioning, detector positioning, beamstop change, positioning of the sample changer and data acquisition, are now completely under computer control.

A new alarm transmitter has been installed which allows the user or local contact to be notified by telephone in case of an alarm at the instrument (e.g. shutdown of the reactor).

The chopper has been overhauled and the suspension of the motor has been modified. The chopper is now powered by the former power supply (REFU 308) of the selector "Brunhilde".

The pumping system has been completely revised. The large pumps of the detector tube, which had been lent to the Reactor Division for leak tests of the new reactor tank, have been cleaned. An acoustic insulation has been mounted around the pumping groups at the instrument in order to reduce the noise level. After some modifications, the pumping control has been put back to "automatic" mode which facilitates operation of the system. Following leak tests and necessary replacement of all seals and modifications to the front plate of the diaphragm box, the vacuum in general has been significantly improved in the three sections (detector tube, sample zone, collimation). The detector now has a vacuum of $p \approx 0.01$ mbar and the sample zone $p \leq 0.02$ mbar.

New standard rack plates for common use at the sample changers of D11, D17 and D22 are now available. The heating block sample changer for temperatures up to 250 °C has been improved.

D16 Four-circle Diffractometer on cold guide H16

D16 was completely over-hauled in 1994, and, similarly to all the other ILL instruments, new beam and working area security systems were installed. Wherever possible and within budget limits, improvements were implemented without changing the basic specifications of the

diffractometer that allow a very good Q-resolution over a wide Q range for the study of crystalline or partially ordered systems with large unit cells. The monochromator carriage was improved for more efficient wavelength changes. The defining slits upstream of the sample were improved for more precise beam definition at small settings to permit better measurements at glancing angles. For small angle measurements, a beam stop with motor and encoder was mounted on the detector face. It will be programmed to stay with the beam centre as the detector is scanned. For data treatment, D16 was equipped with a Power Macintosh and colour printer. This computer can also be used as a terminal on the present Vax cluster or as an X terminal.

Future plans for D16 depend on whether or not it will be moved to a new position following the reorganisation of the D16-D17 experimental area of the guide hall. If the move takes place D16 will be put on a new guide with full beam height, i.e. three times its present guide height. A study is underway to equip the diffractometer, in its new position, with a focussing monochromator and variable monochromator-sample distance.

D17 High Resolution Small-Angle Scattering Diffractometer and Reflectometer on the cold guide H17

The small improvements mentioned in last years report are now installed: A new power supply for the velocity selector, laser alignment system and attenuators. The instrument will restart in the same configuration as it was at the reactor shutdown. Thus it will run as a small-angle spectrometer and as reflectometer for experiments appropriate to its long wavelength. In the medium term the instrument will be optimised and used predominantly for reflectometry. The first step in this direction is to make shorter wavelengths available, which are present in a narrow region of the neutron guide and are known as "garland reflections". If the wavelength band transmitted through the guide turns out to be broad enough, the spectrometer could run using TOF-technique, for which the electronics is already installed. In a later phase it is foreseen to straighten the H17 and H18 guides, which will have D16 and D17, respectively, on their end positions, in order to produce a greatly increased neutron flux in the range of 3 to 10 Å. Also the spectrometer itself will be redesigned. It will be very flexible in resolution in order to adapt to the requirements of the various kinds of samples and thus to give optimised signal intensities.

DB21 Diffractometer for very large unit cells on cold guide H15

During the last year a monochromator changer was installed (J.C. Castagna, EMBL) which allows to switch easily between two monochromators without opening the casemate. Different monochromators are available: graphite ($\lambda=4.5$ Å), mica ($\lambda=10$ Å) and a Potassium intercalated graphite ($\lambda=7.5$ Å). Tests using γ -rays showed a good mosaicity (less than 1°) for the mica but a large mosaicity

(2°) for the KC8. It is planned to start the instrument with the graphite and the mica monochromators and to continue working on the KC8.

The positioning of the collimator was improved. The absolute alignment of the instrument was checked (by theodolite) and the camera which controls the positioning of the collimator and the beam-stop relative to the sample has been installed.

The new detector is still under construction (A. Rambaud), with some leak problems having still to be solved. The experimental program will restart with the old detector in order to test the new one with the optimal neutron flux before replacement. Air pads were installed for the angular detector movement.

For data acquisition and instrument control DB21 will start with a Vax-station which was installed just after the reactor shut-down but which has never been tested under experimental conditions.

D22 New small-angle scattering Diffractometer on cold guide H512

D22 is now ready for commissioning tests. Many improvements were made in the course of 1994.

Regis Gay, the instrument technician, left at the end of September to join the Electronics Group, where he is in charge of the electronics of D22 and of other instruments as well as process controllers. He continued to develop the supervision of D22's process controller and the integration of further devices into it (selector control, detector security, attenuator control etc.) and included corresponding windows in the InTouch program running on a PC. He was replaced by Pierre George at the beginning of October.

The last mechanical items necessary to perform scattering experiments arrived in November (beamstops and beamstop supports) and were installed on the detector carriage. Three different rack plates are available for the automatic sample changer. The sample table was equipped with an electrical, incrementally encoded lifting device. The rest of the motors and encoders were cabled and connected to the electronic bays in the instrument cabin. A summer student, Nicolas Vacher, improved the VME interface program for encoded motor movements on the instrument's Macintosh and helped us optimizing the regulation parameters (PID).

It was decided early in the year to implement the MAD program used by other (diffraction) instruments at the ILL for data acquisition and instrument control. This conversion took some time and major efforts of Michel Roure, but we now have a control program which is able to perform the main functions of the instrument. A basic version of MAD was able to run a complete dummy experiment including change of collimation and detectors, attenuator control and counting on a series of samples. Several functions available in the previous control program are yet to be added to MAD (e.g. automatic adjustment of the sample changer positions in front of the entrance aperture, wavelength control).

Preparation of a manual for the use of D22 is under way. It is planned that this document will be available for reading on computers via the World-Wide Web.

EVA (CRG-B) Evanescent wave diffractometer on cold guide H53

In anticipation of the restart of activities at ILL, the EVA-team (now Bergische Universität Gesamthochschule Wuppertal, IMW, H. Dosch) took up its work at the beginning of May this year. The main activities carried out during the past months were focused on an upgrading of the instrument. This upgrading will enhance the practicability for external users with respect to the new CRG-B status as well as enabling the development of new experimental techniques.

To allow external users to do experiments at EVA conveniently, a general upgrading of the computer system which controls all procedures necessary for experiments is currently under way. The new system is based on a 486 PC running the SPEC software package which is now common at several beamlines at ESRF. In addition, often used parts like the beryllium filter have been automatised. Together with a renewed driving system for the diffractometer and the new software package easy programming of user defined scans will be possible in future.

Beside this enhancement of practicability which was specially carried out for future CRG-B users, we have undertaken several steps to increase the number of experimental possibilities at EVA. In this framework three main approaches should be mentioned:

First, the construction of a neutron polarizing system has been started. It will enable the user to undertake polarization dependent investigations with evanescent neutron waves. The system, composed of a polarizing mirror, a spin flipper and a magnetic guide field, is expected to be tested and working in the middle of next year.

In addition, the construction of a new magnetization stage that will allow the investigation of magnetized samples at EVA is under way. The magnetization system will be tested together with the polarization equipment. Together they will, for example, allow evanescent magnetic neutron Bragg scattering experiments.

The third important enhancement to be noted here is the implementation of a thermal gradient monochromator. This monochromator containing a CaF_2 -crystal subjected to a temperature gradient was installed in 1990 shortly before the stop of activities at ILL. It will increase the available intensity at EVA by a factor of two. The monochromator is under test now and is expected to be working soon.

Several technical changes became necessary due to the planned ADAM instrument which will be located next to EVA on the same neutron guide, as well as due to the new safety structure at ILL. These changes like e.g. some reconstruction of the cabin, a concrete sliding door at the top of the casemate and several new safety installations have been finished. A movable B_4C -wall between IN16 and EVA

will be established soon. Together with new lead shieldings at the neutron guide near IN16 as well as at EVA a further reduction of neutron- and gamma-background is expected.

Chemistry and Biochemistry Laboratories

Chemistry Laboratory

(P. Lindner, P. Chenavas, M. Romero)

Major investment for the ILL chemistry laboratory was the buying of a Rheometrics fluids spectrometer RFSII. This instrument allows the determination of the rheological properties of a wide variety of complex fluids under many test conditions. It is a dynamic mechanical test system for evaluating such viscoelastic properties as steady shear viscosity, complex viscosity, complex modulus, elastic modulus, loss modulus and damping of low viscosity materials of polymer solutions or surfactant systems. As basic equipment a Couette and a cone-and-plate test geometry are available. The instrument allows for normal force measurement. The RFSII (see photo, page 144) is installed in ILL20 room 209. Potential users are requested to contact P. Lindner for further information.

As in the previous years, the ILL has made available its chemistry laboratory to ESRF scientists and users. The needs for chemical preparation facilities and characterization techniques for users and in-house scientists of ILL and ESRF are very similar. The establishment of a joint chemistry laboratory would make available a wider range of equipment than either institute could provide on its own. Therefore, at the time of writing, ILL and ESRF are preparing an agreement to organize the existing chemical facilities of each institute as a joint service for both institutes. The aim of the joint chemistry laboratory is to provide visitors of the institutes and in-house scientists with facilities for chemical preparation and characterization techniques meeting their needs. ILL will of course maintain the chemistry facilities in ILL 20 and keep responsibility for them.

Biochemistry Laboratory

(L. Vuillard, P. Chenavas, M. Romero)

ILL possesses a biochemistry laboratory equipped with low pressure chromatography, FPLC, electrophoresis equipment, UV/visible spectrophotometer as well as standard biochemical apparatus and chemicals. This laboratory is used for in-house research as well as by ILL and ESRF visitors. The laboratory has also been used extensively in 1994 by members of EMBL whilst awaiting completion of the extension to their own laboratories. Centrifuges and other specialised equipment as well as additional bench space for visitors will be available in the enlarged EMBL outstation.

Major improvements in 1994 included the replacement of the old UV/Visible spectrophotometer, which was 10 years old, and the purchase of a new stereomicroscope.

Peter Timmins

Three-Axis Spectrometers (TAS) Group

IN1, IN1Be	3-axis and Be-filter spectrometers on the hot source beam tube H8 (B. Dorner, B. Roessli and P. Palleau)
IN3 (CRG-A)	3-axis spectrometer on the thermal guide H24 (M. Zolliker, P. Decarpentrie)
IN8	3-axis spectrometer on the thermal beam tube H10 (J. Bossy and D. Puschner)
IN12 (CRG-B)	3-axis spectrometer on the cold guide H142 (B. Fak, J. Previtali)
IN14	3-axis spectrometer on the cold guide H53 on the horizontal cold source (N. Pyka, R. Currat and A. Brochier)
IN20	3-axis spectrometer for neutron polarization analysis and spin-echo option (TASSE) on the thermal beam tube H13 (J. Kulda, T. Baumbach and P. Flores; C.M.E. Zeyen for the TASSE option)

The year 1994 was one of intense activity. In parallel with the work connected with the reassembly of the spectrometers in the reactor hall, a major upgrading and standardisation programme was carried out: new control electronics on 3 instruments, replacement of the PDP computers by μ -VAX's or DEC- α workstations, development and tests of a new MAD-based spectrometer control software, modernisation and extension of the PKFIT data analysis programme. Thanks to the motivation of the technical and scientific staff involved, all these tasks could be completed within the initial time and budget limits and all instruments will be ready for neutron tests by January 95.

IN1 and IN1Be: 3-axis and Be-filter spectrometers on the hot source beam tube H8

The 3-axis spectrometer IN1 shares the H8 hot-beam position with the Be-filter spectrometer IN1Be and the liquid diffractometer D4. The three instruments operate on a time-sharing basis with a common monochromator and primary protection. With the help of the 'tanzboden' technique the exchange time between two instrument configurations is less than one hour.

During the period from April to June 1994, following the H8 beam tube replacement, the primary protection and monochromator stage was reassembled. Thick boron-impregnated wood paneling and B₄C shieldings were added in order to improve biological protections and reduce radiation leaks. The 'tanzboden' floor was rectified and repolished in order to improve positioning accuracy.

In parallel, a major electronic upgrading programme was carried out on both IN1 and IN1Be. This included: the replacement of the existing shaft encoders by modern standard units and the development of a new VME-based control electronics. Following initial tests on IN1, this new electronic control system was later installed on IN8 and IN20, a major step towards electronic standardization within the group.

Other work on the instrument dealt with the replacement of the existing IN1 multiwire detector system by a standard 10-bar ³He counter with lower background, the complete overhaul of the IN1Be cooling system including replacement of the liquid N₂-cryostat. In July the instrument was connected to its dedicated DEC- α 300L workstation and was used thereon as a test-bench for the new MAD-based version of the TAS instrument control program. The instrument is also equipped with an X-window terminal and a Macintosh Quadra for measurement control and on-line data analysis.

Both IN1 and IN1Be have completed the required safety acceptance procedures and are ready for neutron tests and commissioning.

IN8: 3-axis spectrometer on the thermal beam tube H10

The IN8 primary protection was reassembled in July 1994, following the replacement of the H10 beam tube in April 1994. The reassembly work on IN8 is a more elaborate operation than on most other instruments in the reactor hall, due to the particular geometry of the casemate, its inaccessibility by crane and the presence of the D15 platform, immediately above, which was also reassembled. Work on the experimental zone included: the replacement of all electrical cables, the repolishing of the 'tanzboden' floor and a modification of the protections around the experimental area in order to comply with the new safety regulations. In addition, a 'quiet room', located next to the instrument, is currently under construction and will hopefully be available to users at the start of the first user cycle.

After recabling and replacement of the shaft encoders, the spectrometer itself was reinstalled and optically realigned. Major modifications to the instrument concern the data acquisition system (control electronics, new DEC- α workstation and control software) and the analyser stage (new horizontally-focusing PG analyser).

The new pyrolytic graphite analyser, presently under optical testing (see Fig. 1, page 144), has a fixed vertical curvature and a motorised, computer-controlled horizontal curvature. It will be used in conjunction with a cylindrical 5-bar ³He counter, mounted with its axis vertical. The total reflecting area of the 36-piece composite analyser is 225x100 mm² (lengthxheight), as compared to 150x62.5 mm² for the setup in use so far. This is the maximum size compatible with the present analyser housing. For experiments where momentum resolution is not crucial, e.g. for the measurement of flat optic branches, an intensity gain of over a factor 2 is expected, at same energy

resolution. The option to use the analyser in the conventional (i.e. flat) mode, in conjunction with Soller collimators, will be maintained.

The instrument has complied with the safety acceptance procedures and is ready for neutron tests and commissioning. The new focusing PG analyser will be installed shortly and should be available at the start of the first user cycle.

IN14: 3-axis spectrometer on the cold guide H53 on the horizontal cold source

A modification of the IN14 monochromatic beam geometry, aimed at reducing the monochromator-to-sample distance, has been satisfactorily implemented during the first half of the year. The secondary beam shutter and the Soller collimator (or polarizing bender) is now integrated into the primary protection. As a result, one expects an increase of the monochromatic neutron flux at the sample position by a factor 1.5 and a lower 'beam-off' γ -background in the experimental area.

Other modifications connected with instrument safety involved: the installation of a primary beam-shutter upstream from the IN14 monochromator position to minimize radiation leaks in case of an anomaly on the instrument's primary protection blocks; integration of new elements into the secondary beam-shutter's safety loop (up/down position of the beam-stop, position of the mobile biological protections on the periphery of the experimental area).

The instrument has been equipped with a new HYTEC CAMAC crate controller and is connected, via Ethernet, to a dedicated DEC- α 300L workstation. Work planned for the first reactor cycle include a complete recalibration of the instrument, neutron tests on a new polarising bender optimized for work in the 4-6 Å wavelength range, as well as tests on a variable-wavelength graphite filter.

IN20: 3-axis spectrometer for neutron polarization analysis on the thermal beam tube H13

Similarly to the other TAS instruments, IN20 was fully dismantled for the reactor reconstruction, most of its components remaining, however, stored at or near to its experimental zone. On the other hand its beam tube (H13) was used for reactor vessel vibration tests so that the main reinstallation work could start only in July. The period before has been used for careful optical alignment of the monochromator with respect to the incident beam axis and for slight mechanical modifications to permit a reproducible positioning of the monochromator holder inside the shielding drum.

A horizontally and vertically focusing assembly of elastically bent perfect Si(111) crystals, developed in collaboration with NPI Rez (Czech Republic), was installed into a free position of the monochromator changer and a similar silicon analyzer was acquired (see Fig. 2, page 145). The software needed to calculate and optimize the resolution

function of a 3-axis instrument equipped with curved crystals, has been obtained from M. Popovici (University of Missouri) and further developed through a collaboration with J. Saroun (NPI Rez). Experiments are to be carried out during the first reactor cycle to assess the performance of this new type of setup. Its advantages are expected to arise from the variable horizontal focusing, homogeneous reflectivity, sharply cut rocking curves with negligible tails and the discrimination against $\lambda/2$ neutrons.

The PDP11 instrument computer was finally replaced by a DEC- α 300LX workstation which provides the computing power required for on-line data treatment as well as for the magnetic field profile optimization in the spin-echo mode. At the time of reinstallation, a decision was taken to replace the microcomputer-controlled interface of the spectrometer motors by VME electronics. This change fully benefited from the current standardization effort within the group: using electronic modules initially bought to be used as spares on IN1 and IN8, it took only a couple of weeks to reproduce the configuration already available on IN1/IN8 and supplementary development work was only needed for the control of the power supplies for the polarized neutron part of the spectrometer. Despite the late start of its reinstallation, IN20 was ready for unpolarized neutron tests before the end of the year.

IN3: 3-axis spectrometer on the thermal guide H24

In December a CRG contract was signed between ILL and a Swiss group from PSI-Würenlingen (local representative: M. Zolliker). For the next 3 years, IN3 will operate as a CRG-A instrument, with 50% of the beam time allocated to the contracting CRG group and 50% to ILL users.

Prior to the signature of the contract, an extensive campaign of maintenance work was launched in order to deliver the instrument in a fully operational state. Mechanical work included the installation of an absolute shaft-encoder on the monochromator translation; maintenance and readjustments of the cams controlling the position of the casemate protection blocks; rectification and repolishing of the 'tanzboden' floor. A considerable amount of electronic maintenance work turned out to be required, notably in order to arrive at a proper positioning of the 'tanzboden' elements. This work was made particularly difficult due to the non-standard nature (and poor documentation) of the existing control electronics.

The PDP computer has been replaced by a μ VAX on which the new spectrometer control software (TAS-MAD) has been installed. The instrument has complied with the safety acceptance procedures and is ready for neutron tests and commissioning.

IN12: 3-axis spectrometer on the cold guide H142

At the reactor start-up IN12 will operate as a CRG-B instrument. The beam time will be divided between the contracting CRG group (KFA-Jülich) and ILL users on a 70%-30% basis.

Several improvements and safety modifications have been implemented during the reactor shut down. As on all other instruments, the experimental zone has been fenced off; the only access is through a gate that is interlocked with the secondary beam shutter. A new safety loop closes the primary beam shutter in the neutron guide in case of an anomaly of the automatic monochromator protection (block remaining in open position). For other anomalies (block not opening), the movement of the sample table (motor A2) is inhibited, thus reducing the risk for mechanical collisions. The secondary beam shutter has been moved inside the monochromator protection unit; this allows easier change of the collimator between monochromator and sample. The support for the optical bench in the incident beam has been replaced to decrease the monochromator-sample distance and to make the alignment of the supermirror polarizer easier. The support of the collimator before the analyzer has been redesigned and has now a permanent guide field that also leaves more space for the second monitor. The connections between power supplies and flippers/Helmholtz coils are recabled. The PDP computer has been replaced by a μ -VAX, which required some changes to the electronics. The new spectrometer control program MAD-TAS is presently being tested.

TASSE: Spin-echo option on the polarized beam three-axis spectrometer IN20 (C. Zeyen)

Before the reactor shutdown, a pair of super conducting OFS coils had been built at the ILL, but could not be used or even tested because of the reactor shutdown. OFS stands for optimal field shape spin-echo magnets and is the result of an optimisation calculation to yield the best possible magnets [1]. They have been designed to reach line integrals of 1.5 Tesla.meter with corresponding homogeneities. Their implantation on the thermal TAS IN20 is now completed and tests are planned for April 1995. Relative energy resolutions of the order of 10^{-6} are expected, which will allow thermal Three-Axis Spectrometry to reach the nanoeV domain. Such strong magnets could be used even for hot source neutron spectrometers.

Recently a relative energy resolution of 10^{-5} has been obtained by adding OFS precession coils to the PONTA polarised TAS [2] of the Institute for Solid State Physics (ISSP) of the University of Tokyo and located at the JAERI JRR-3M reactor in Tokai-mura. The OFS coils were fitted with new correction coils which are capable of removing both the residual radial inhomogeneity of the coils and the path length effects due to the significant ($\sim 2^\circ$) beam divergence which is needed on a TAS for reasons of luminosity.

The Japanese OFS coils are of a rather inexpensive and short (80 cm) design, using classical conductors and delivering a line integral of 0.06 Tesla.meter. They were built in the framework of a collaboration between ILL, the Tohoku University, Sendai, and the ISSP Tokyo. Fig. 3 shows the PONTA spin echo set-up, see page 145.

As a result of the Japanese collaboration during the ILL shutdown we were able to demonstrate the feasibility and excellent performance of the OFS technique, providing the Japanese neutron community with the first operational spin echo three-axis spectrometer. The picture shows PONTA during the first tests of the spin-echo option in April 1994. The red cylinders are the OFS precession coils.

The Japanese TASSE was set -up in a short week in May 1994. Figure 4 shows the effect of the spiral correction coils on the line integral homogeneity and hence the quality of the spin-echo polarisation which remains essentially flat across the entire Fourier time domain. Figure 5 shows the first test experiment results on the critical slowing-down of phenyl ring rotations in a parterphenyl crystal (see College 4 section for more experimental results with this spin-echo three-axis spectrometer).

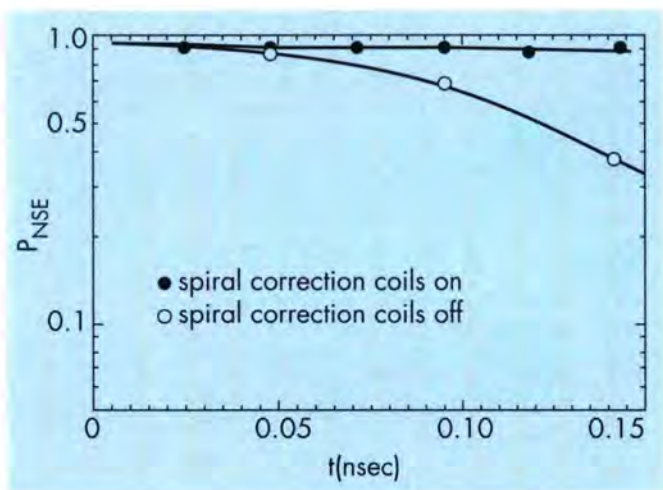


Fig. 4: The diagram shows a logarithmic scale of the spin-echo polarisation, the measured quantity in these experiments, as a function of the Fourier-time $t = \lambda^3 \int |B| dl$ for the OFS coil alone and corrected with spiral coils.

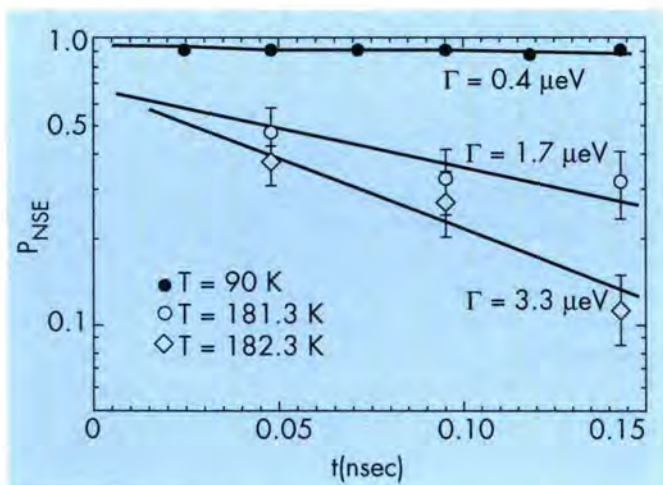


Fig. 5: CRITICAL SLOWING DOWN of phenyl molecular rotations near the order disorder phase transition at $T_c = 180K$.

The experience collected with this apparatus will considerably ease the implementation of the superconducting versions on IN20 since apart from the same OFS principle, identical homogeneity correction spiral coils, and the same type of power supplies and control software have been successfully used.

C. Zeyen would like to thank the numerous Japanese colleagues who have efficiently helped with this project and acknowledge financial assistance from the Yamada foundation and Grant-in-Aid for Scientific Research from the Ministry of Education, Science and Culture, Japan. Special thanks to Professors K. Kakurai and Y. Fujii, head of the ISSP neutron scattering laboratory and Professor Y. Endoh from Tohoku University for their permanent hospitality and help.

Data analysis programs (A. Bouvet, A. Filhol, J. Kulda)

The three most important programs for TAS experiment planning and for subsequent data treatment - RESCAL (TAS resolution calculation), FILING (data file manipulation) and PKFIT (profile fitting) - have been completely revised in collaboration with the scientific computing group. The main goals pursued were

- clean and platform independent code for the program kernels performing the main computing tasks
- up-to-date graphical user interfaces for the computer platforms presently supported in the group: Macintosh, Open VMS (DEC- α) and UNIX (HP, DEC- α)
- correct treatment of resolution effects via 4-dimensional convolution in Q, ω space

The TAS data format has been redefined so that the data files contain complete information on the spectrometer configuration in an easily readable and self explaining form which facilitates proper treatment of resolution effects in cases when non-ILL software is used for data evaluation. Both the RESCAL and PKFIT programs have been rewritten to take full advantage of this information and an extended facility is provided for visualization of the mutual orientation of the TAS resolution ellipsoid and of the dispersion surface in Q, ω space. A newly developed Monte-Carlo algorithm permits to evaluate very efficiently the 4-dimensional convolution of the spectrometer resolution function with the scattering function for general functional forms of the dispersion relation $\omega(q)$ in the case of constant Q scans. This feature opens new possibilities in direct interpretation of asymmetric peak shapes in addition to the conventional Gaussian and Lorentzian profiles. Both RESCAL and PKFIT offer a choice of several preprogrammed forms of $\omega(q)$ - linear, quadratic, sinusoidal - as well as a possibility to include a user supplied general function including a Q dependent structure factor.

At present the Macintosh and Open-VMS (using PGPLOT graphics) versions of all three programs have been extensively tested and are available to ILL users.

The development of a MOTIF version of the graphical user interface to be run on the UNIX workstations (HP, DEC- α) is underway in parallel to further evolution of the PKFIT kernel (4D treatment of quasielastic scattering, improved fitting procedure etc.).

Roland Currat

References

- [1] C.M.E. Zeyen et al, IEEE Transactions on Magnetics **24** no. 2 (1988).
- [2] C.M.E. Zeyen, M. Nishi, K. Nakajima, Y. Kawamura, S. Watanabe, K. Sasaki, T. Sakaguchi, K. Kakurai and Y. Endoh, Proceedings ICNS'94 to be published in Physica B.

High energy transfers at small momentum transfers on the three-axis spectrometer IN1

B. Roessli, R. Currat and B. Dorner

The three-axis spectrometer (TAS) IN1 is located at the hot source which produces a Maxwell distribution of neutron energies with a maximum at 200 meV. Due to the high incident energies, TAS IN1 is suited for inelastic measurements requiring important energy transfers. Inspection of the users' results in past years reveals that this spectrometer was often used to study magnetic excitations in itinerant magnets and high- T_c superconductors with energy transfers between $80 \text{ meV} \leq \hbar\omega \leq 200 \text{ meV}$. Among the difficulties encountered by the experimentalists, the high background level is often mentioned as limiting the quality of the data collected on TAS IN1. In the following article we shall show that the low signal-to-noise ratio partly originates from the constraints on the scattering geometry imposed by the kinematic conditions.

To characterise the experimental capabilities of TAS IN1, we consider amorphous ferromagnetic samples described by the Heisenberg model. In such systems, inelastic measurements are performed at very small

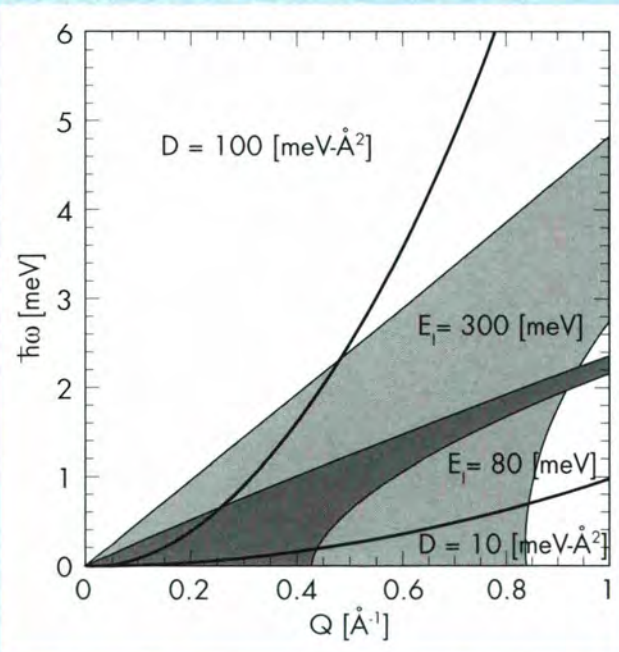


Fig. 1: Intersection of the neutron dispersion with a collective mode described by a quadratic dispersion $\hbar\omega = DQ^2$ (solid lines). The shaded areas correspond to incident neutron energies $E_I = 80 \text{ [meV]}$ and $E_I = 300 \text{ [meV]}$ and scattering angles $0 \text{ [deg]} \leq \phi \leq 4 \text{ [deg]}$.

values of momentum transfer \vec{Q} , as the magnetic excitation wave-vector \vec{q} is necessarily defined with respect to the forward beam direction, i.e.:

$$\vec{Q} = \vec{K}_I - \vec{K}_F = \vec{q} \quad (1)$$

The dispersion of the magnetic excitations is given by the relation $\omega(\mathbf{q}) = Dq^2$. The spin-wave stiffness D has typical values between $10 \text{ meV}\cdot\text{\AA}^2 \leq D \leq 100 \text{ meV}\cdot\text{\AA}^2$. For example, three-axis experiments performed in the amorphous transition-metal boron glasses $\text{Fe}_{20}\text{Ni}_{60}\text{B}_{19}\text{P}_1$ or $\text{Fe}_{83}\text{B}_{16.5}\text{Si}_{0.5}$ have yielded extremely stiff spin-wave dispersions, respectively $D = 80 \text{ meV}\cdot\text{\AA}^2$ and $D = 120 \text{ meV}\cdot\text{\AA}^2$ [1]. Fig. (1) shows the intersection of two dispersion curves ($D = 10 \text{ meV}\cdot\text{\AA}^2$ and $D = 100 \text{ meV}\cdot\text{\AA}^2$) with the loci of the allowed (Q, ω) -values for scattering angles $0 \text{ [deg]} \leq \phi \leq 4 \text{ [deg]}$ and fixed neutron incident energies $E_I = 80 \text{ [meV]}$ and $E_I = 300 \text{ [meV]}$. As evidenced by Fig. (1), the useful scattering geometries are restricted to small angles and the accessible Q -range becomes more and more limited as the stiffness of the spin-waves D increases. Going to higher neutron incident energies indeed increases the allowed energy transfer window, but deteriorates both the flux and the resolution. Moreover, the scattering angles do not increase significantly in the momentum transfer range of interest.

Momentum and energy conservation laws imply the following relationship between scattering angle ϕ , neutron incident energy E_I , energy transfer to sample $\hbar\omega$ (>0 for neutron energy-loss) and scattering vector \vec{Q} :

$$\cos(\phi) = \frac{2E_I - \hbar\omega - 2.0717Q^2}{2\sqrt{(E_I - \hbar\omega)E_I}} \quad (2)$$

Differentiation of Eq. (2) shows that the largest possible scattering angle to reach a point in (Q, ω) -space is obtained for the incident neutron energy

$$E_I = \frac{\hbar\omega}{2} \left(1 + \frac{\hbar\omega}{2.0717Q^2} \right) \quad (3)$$

In an attempt to optimise the spectrometer geometry we may, in a first step, consider that the best configuration corresponds to the largest achievable scattering angle ϕ_{max} satisfying the kinematic conditions (Fig. 2). Inserting Eq. (3) in Eq. (2) and using $\hbar\omega = DQ^2$, calculation yields that ϕ_{max} is Q independent:

$$\phi_{\text{max}} = \cos^{-1} \left(\sqrt{1 - \left(\frac{2.0717}{D} \right)^2} \right) \quad (4)$$

and decreases as D^{-1} for large values of D . These optimised geometries require neutron incident energies above the thermal range ($E_I \geq 80 \text{ meV}$) e.g. for

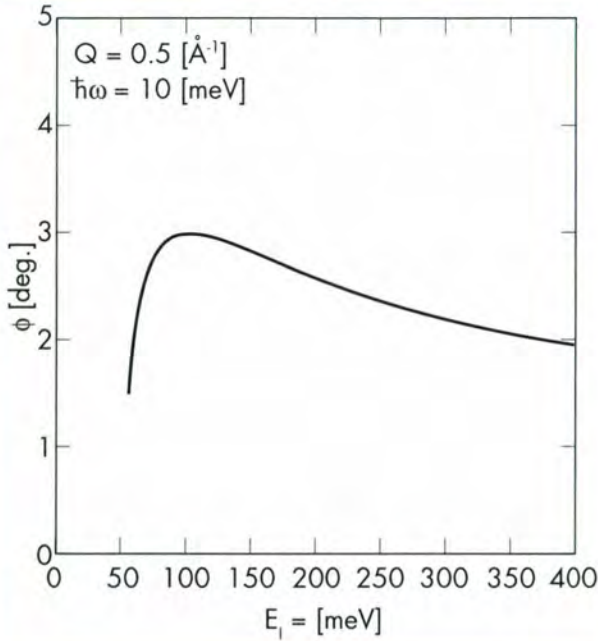


Fig. 2: Scattering angle ϕ as a function of the neutron incident energy E_1 for the point $Q = 0.5 \text{ \AA}^{-1}$ and energy transfer $\hbar\omega = 10 \text{ meV}$ in (Q, ω) -space.

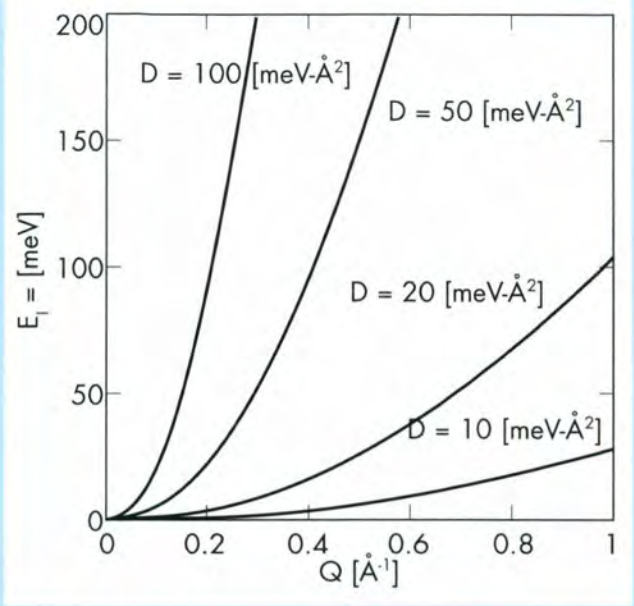


Fig. 3: Neutron incident energies needed to obtain the max. scattering angle ϕ_{\max} at sample plotted for a quadratic dispersion $\hbar\omega = DQ^2$ as a function of momentum transfer Q .

$Q \geq 0.9 \text{ \AA}^{-1}$ ($\hbar\omega \geq 16 \text{ meV}$) when $D = 20 \text{ meV-\AA}^2$ and already for $Q \geq 0.2 \text{ \AA}^{-1}$ ($\hbar\omega \geq 4 \text{ meV}$) when $D = 100 \text{ meV-\AA}^2$ (Fig. 3). However, not every optimised scattering configuration (in the sense defined above) is expected to give valuable experimental information, as resolution effects become important with increasing incident neutron energies.

To estimate the energy resolution achievable on TAS IN1, we consider the $30^\circ\text{-Cu}_{331}\text{-}30^\circ\text{-}30^\circ\text{-Cu}_{220}\text{-}30^\circ$ spectrometer configuration. The energy resolution ΔE is calculated with the Cooper and Nathans method. The incident energies drawn as dotted lines in Fig. 4 are chosen to maximise the scattering angle ϕ for every set (D, ω) . The thick line divides the regions with $\Delta E < \hbar\omega$ and $\Delta E > \hbar\omega$, respectively. Fig. 4 shows that resolution effects restrict the useful $(Q, \hbar\omega)$ range (taken as $\Delta E < \hbar\omega$) at large spin-wave stiffnesses D . For example, magnetic excitations corresponding to the spin-wave stiffness $D = 100 \text{ meV-\AA}^2$ can be observed up to only $Q \approx 0.25 \text{ \AA}^{-1}$ ($\hbar\omega = 6.5 \text{ meV}$) with $\phi_{\max} = 1.2 \text{ deg}$ when $E_1 = 154 \text{ meV}$. In materials with low D ($\leq 30 \text{ meV-\AA}^2$), the optimised incident energies lie in the thermal range ($E_1 \leq 80 \text{ meV}$) for small energy transfers ($\hbar\omega \leq 10 \text{ meV}$). For $10 \text{ meV} \leq \hbar\omega \leq 35 \text{ meV}$ TAS IN1 is then complementary to thermal spectrometers.

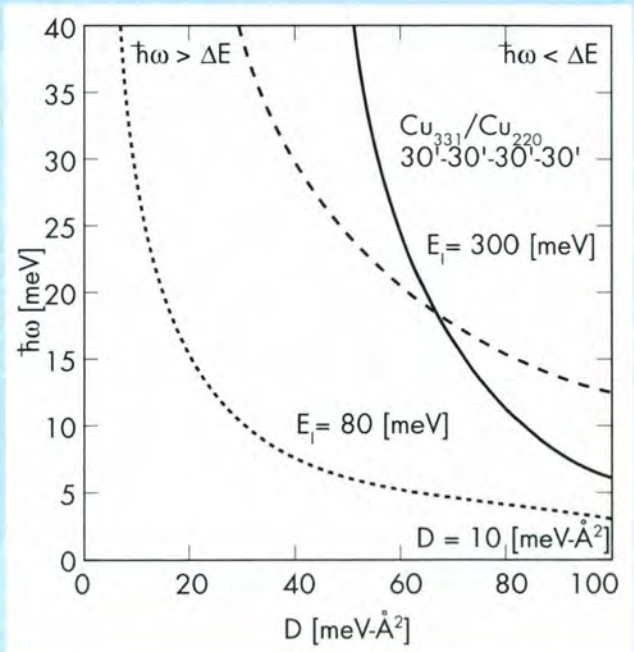


Fig. 4: Resolution effects still restrict the useful measurement range. The thick line separates the regions with $\Delta E < \hbar\omega$ and $\Delta E > \hbar\omega$. The dotted lines are the incident neutron energies which allow measurements at ϕ_{\max} .

To determine the useful ($Q, \hbar\omega$) range available on TAS IN1, we considered the special case of magnetic excitations in Heisenberg amorphous ferromagnets. Due to the small values of momentum Q , kinematic and resolution constraints drastically limit the observable energy transfer range. On the other hand, inelastic magnetic scattering in single crystals is less restrictive since \vec{q} is defined with respect to any Brillouin zone-centre. However, due to the influence of the magnetic form factor and of the phonon contribution, magnetic excitations are better defined at small values of momentum transfers. For example, spin-waves have been measured in antiferromagnetic La_2CuO_4 in the energy transfer range $30 \text{ meV} \leq \hbar\omega \leq 150 \text{ meV}$ [2] using TAS IN1. The measurements were performed at the optimum Q which satisfied the constraints cited above, and most of the scans required low scattering angle values in the range $4 \text{ [deg]} \leq \phi \leq 13 \text{ [deg]}$ [3]. Therefore, improving the environment toward low scattering angles ϕ is expected to increase the capabilities of TAS IN1 for every experiment on magnetic systems. To that end we intend to construct air-evacuated neutron paths to reduce the low-angle air-scattering. The technique of beam focusing on the detector is also considered as an option to increase the versatility of TAS IN1 toward low scattering angles. This implies designing converging collimators and/or doubly-bent monochromators and analysers. Finally, recent advances in the development of the ^3He spin-filter offer the opportunity of implementing polarised neutrons on TAS IN1, which is expected to help extract the magnetic cross-section, particularly in ferromagnetic samples.

References

- [1] J.J. Rhyne, J.W. Lynn, F.E. Luborsky and J.L. Walter, *J. Appl. Phys.* **50**, 1583-1585 (1979).
- [2] G. Aeppli, S.M. Hayden, H.A. Mook, Z. Fisk, S.-W. Cheong, D. Rytz, J.P. Remeika, G.P. Espinosa and A.S. Cooper, *Phys. Rev. Lett.* **62**, 2052 (1989);
G. Aeppli, S.M. Hayden and H.A. Mook, *I.L.L. Exp. Rep.*, 84 (1990).
- [3] The values of scattering angles were calculated from the data published in Ref. 2.

Time-of-Flight and High Resolution (TOF/HR) Group

- IN4C New TOF spectrometer on the thermal beam tube H12 (project) (H. Mutka, D. Weddle)
- IN5 Multichopper TOF spectrometer on the cold guide H16 (J. Cook, M. Ferrand, S. Jenkins)
- IN6 Focussing TOF spectrometer on the cold guide H15 (H. Schober, A. J. Dianoux, S. Jenkins)
- IN10 Backscattering spectrometer on the cold guide H15 (O. Randl, P. Joubert)
- IN11 Spin-Echo spectrometer on the cold guide H141 (B. Farago, S. Pouget, E. Thaveron)
- IN15 High resolution spin-echo spectrometer for long wavelengths on the cold guide H511 (project) (C. Lartigue, A. Kollmar (KFA))
- IN16 New backscattering spectrometer on the cold guide H53 (project) (B. Frick)
- D7 Diffuse scattering instrument with polarization analysis on cold guide H15 (I. Anderson, A. Murani, R. Rebesco)
- IID Brillouin setup on the thermal beam tube H12 (test instrument) (J.-B. Suck)
Group Engineer: J.F. Barthélemy

In order to be ready for the restart of the user's programme, four new scientists have been hired in our group. Following the date of arrival they are: Michel Ferrand, Stéphanie Pouget, Oliver Randl and Helmut Schober. We anticipate the arrival of two more scientists at the beginning of 1995. Two persons have left the group: Otto Schärpf went into a busy retirement and Gordon Kearley had to leave IN5 to become head of the Scientific Computing group. Following these departures, Jeremy Cook has taken over the position of First Instrument Responsible on IN5, Ian Anderson the one on D7 and Oliver Randl the one on IN10. Helmut Schober is now 1st Instrument Responsible on IN6. Besides the ameliorations done on the instruments which are detailed below, another important activity has been in the area of computing.

The implementation of distributed computing facilities has resulted in a reform of the data inspection on the instruments. SGI Indy stations are now available on IN5, IN6, IN10, D7, in addition to the other available processors (SGI Indigo Station and HP300 station).

The development of data inspection software adapted to the needs of TOF instruments has progressed in collaboration with the scientific computing group. Several procedures and functions have been included in the LAMP utility (Large Array Manipulation Program, see contribution of the Scientific Computing Group) aimed for rapid evaluation of experiments on line. For example, inspection spectrum-by-spectrum over a selected range, transformation

from time to energy with or without vanadium calibration and background subtraction, display of a Q - ω map can be quickly done either by simple single word commands or by graphical interfaces (see Fig. 1 on page 145). The remarkable ease of manipulating simultaneously the full TOF spectrum (all angles, all time channels) is surely going to be appreciated in the daily work on the instrument. The development of these tools was done by the student trainees B. Vettier and A. Dallmayer under the supervision of group scientists and Scientific Computing.

The installation of other useful routines with graphical interfaces has progressed in parallel. M. Bée, a long term visitor, has adapted in the UNIX environment of the group's HP station his suite of programs AGATHE, Application for General Analysis of TOF and High-Resolution Experiments, using the PGPLOT library for graphics. Another student, N. Haack, produced graphical interfaces for some simple fitting programs as well as for the Bayesian analysis routine of inelastic and quasielastic data originating from D. Sivia at ISIS.

At present part of the instrument data analysis is still on the VMS computers while the plan is to have UNIX stations on every instrument. The aim is to keep the software available also in the VMS environment until the transition period to the UNIX is over. A pool of X-terminals will be available for members of the TOF/HR group and their visitors. The data inspection (LAMP) and the evaluation (INX, AGATHE etc.) can be made using either the instrument UNIX stations or X-terminals, or the group UNIX stations.

The progress in the group's computing owes a lot to the former responsible G. Kearley. Since his departure M. Ferrand is in charge of the development part and H. Mutka of the general co-ordination.

IN4C New TOF spectrometer on the thermal beam tube H12

The project of reconstruction of the time-of-flight spectrometer on the thermal beam H12 is a cooperation with Italian neutron users (co-ordinator F. Sacchetti, Perugia) with part of the financing coming from the CNR-Italy, within a specific contract.

The site work, including the installation of the primary casemate has progressed in parallel with the remounting of the scheduled instruments. The elements of interior walls and supports as well as the framework for the ceiling have been completed and the mounting has started. During 1995 the primary spectrometer with choppers and monochromator is to be installed

In the organisation of the Institut this project is attached to the Department of Projects and Techniques (see there for further information).

IN5 Multichopper TOF spectrometer on the cold guide H16

The periphery of the chopper disks were originally coated with Gd_2O_3 powder in an epoxy resin. Attempts to repair this coating were unsuccessful, so in the early part of 1994 tests were made with a sputtered coating. It was feared that this technique would cause unacceptable distortions to the disk, but in practice the distortions were slight. The front and back faces of the disk were machined to be symmetric since finite element calculations by M. Thomas from DPT revealed that the original asymmetry lead to an out-of-plane distortion of the disk at high speeds. This symmetry was preserved by sputtering a coating of Gd_2O_3 on both sides of the disk.

The first disk with this coating was fitted with the new rigid axles and tested at the maximum operating speed of 20000 rpm. These tests were totally successful and all *damaged* choppers, and a spare chopper have now been recoated and modified.

IN5 has a very large number of detectors and each of these has been tested for noise and efficiency using a neutron source. The combined effect of the improved choppers, baffles in the secondary flight-path, and detector maintenance should reduce any residual background.

Following all of the chopper modifications it was possible to completely realign the guide system. Guides had been realigned many times in the past, usually following a permutation of choppers following a failure. Compensation for errors had accumulated and the opportunity was taken to realign not only the guides but also their supporting structure.

IN6 Focussing TOF spectrometer for long wavelengths on the cold guide H15

The instrument is now fully converted to VME electronics. The electronics as well as the instrument control software have been tested successfully. In order to still further improve the chopper stability an additional electronic damping mechanism is under development and will be operational by the end of the year. A UNIX workstation is installed at the instrument allowing fast graphical data assessment during and after the acquisition. Some minor mechanical modifications have been carried out to comply with new safety regulations.

On the sample environment side, the instrument has now another furnace reaching at least 1400°C with a useful sample diameter of 49 mm. For an automatic operation with the cryostat a new transfer system for liquid He has been installed; it works with a heating system inside the He vessel.

IN10 backscattering spectrometer on the cold guide H15

This year significant improvements have been made to IN10. These include the availability of an oxygen-doped Si(311) monochromator which will be used in conjunction with a new full set (12 large angle plates) of Si(311)

analysers. Neutron reflectivity measurements at relaxed resolution* indicate that the new monochromator will offer more than an order of magnitude increase in backscattered intensity with respect to a perfect Si(311) crystal. Because of the resolution limitations of the above measurements, it has not been possible to estimate its energy resolution as yet with certainty. The interest in Si(311) lies mainly in the fact that it gives access to a significantly increased upper elastic Q-range ($Q_{max} = 3.8 \text{ \AA}^{-1}$) with respect to other configurations of IN10 where wavelengths around 6 Å are used ($Q_{max} \sim 2 \text{ \AA}^{-1}$). The availability of a full set of Si(311) analysers will also open new possibilities for high Q measurements in IN10B configuration.

During the year, the new nitrogen-cooled IN10B cryofurnace (which incorporates a Nb heat exchanger) has been comprehensively tested and its performance has proved very satisfactory. The interior of the monochromator shielding is in the process of being entirely fitted out with the necessary nitrogen transfer and compressed air lines necessary for remote operation of the new cryofurnace. These are the first elements of an IN10B control/monitoring station (to be completed in 1995) which will be located outside the shielding at ground level in the area between IN10 and IN11. One spare sample stick has been assembled for the cryofurnace and five monochromator holders have been prepared with eight additional holders on order. These holders have been constructed in niobium metal and are designed to provide a good thermal contact and to reduce temperature gradients over the length of the monochromator crystals. For IN10B monochromator exchanges, a lead castle has been mounted inside the shielding to await recently irradiated monochromators. Particular attention has been paid to improvements of the γ shielding and additional lead has been placed on the interior of the biological shielding in the vicinity of the monochromator. The lead is protected from direct and scattered neutron beams by boron carbide to minimise additional prompt γ emission from the former. The height of the lead shielding that surrounds the IN10B cryofurnace tail has been increased as planned and a removable steel frame with lifting lugs allows this shielding to be rapidly installed or removed at IN10B/A changeovers.

Regarding the Doppler drive, a very accurately-machined guiding mechanism for the magnetic pickup has been constructed to eliminate parasite vibrations produced by friction in the previous system. The drive belt and pulleys have been renewed and the monochromator support has been redesigned to eliminate small amplitude vibrations due to a bending mode of the support at its point of coupling with the pickup.

A new digital frequency generator (an adaption of the unit purchased originally for IN6) replaces an ageing (and obsolete) analogue unit used to power the synchronous

* Measurements performed at LLB by A. Magerl and Y. Blanc.

motor of the background chopper. This unit offers comprehensive programmability (both locally and remotely) which significantly simplifies its configuration for maintaining the motor synchronous throughout acceleration/deceleration phases. A new VME rpm meter has been developed and will be installed shortly. A free port on the Xycom and a positive TTL pulse available from the chopper signal amplifier will permit easy monitoring of the chopper speed in a identical fashion to the Doppler speed analysis.

In the region of the deflector crystal, some neutron shielding has been added and improved end-switches have been installed on the deflector rotation giving reliable end-point positioning in the restricted range between the limits of the useful angular range and the limits of the encoder range.

New PROMs have been installed in each of the 4-axis VME motor control modules (Mizars). These PROMs overcome a fundamental problem of the previous version whereby hard-programmed binary encoder offsets were systematically erased when initialising the corresponding encoder angle at OS9 level. This development means that it is possible to eliminate software offsets and therefore the task of modifying instrument parameter data or recompiling affected programs if their values are changed (e.g. by mechanical offsets). For the binary-coded-decimal (BCD) encoders, software offsets are unavoidable for the moment. IN10 now possesses an expanded Macintosh II for exploitation of the new version of Quad Closed Loop necessary for programming of the new PROMs.

The development work on tuneable resolution monochromators by ultrasonically-induced strain fields has been boosted by the arrival of a diploma thesis student based at the University of Bochum in Germany. He will be working for one year on the project (financed jointly by the ILL and Bochum) with the goal carrying this work through to a new instrument option on IN10 towards the end of next year.

Concerning computing hardware, IN10 has recently acquired a SGI Indy workstation which is primarily reserved for data treatment and display at the instrument. A new HP 4L laser printer, connected locally to the workstation, is intended for instrument users' printing needs. The μ Vax 3000 serving as instrument control computer was exchanged for a μ Vax II running VMS v5.5 with DEC Windows. This machine has a slightly faster processor and two disks of increased capacity. A 6100/60 Power Macintosh was also purchased for IN10 this year.

On the software side, the instrument setup program has been entirely rewritten to incorporate the full features of IN10B options and the IN10B control program has undergone significant improvements. Also some bugs were found in the most recent version of the data treatment program SQW which have been corrected.

Other (miscellaneous) improvements to IN10 include a complete testing of the detectors (with and without neutron sources) with readjustment of the discriminator levels and improvements to noisy detectors. The supermirror guide has been accurately realigned on the deflector crystal axis and the sample axis has been re-centred. An angular scale for the analyser housing position is currently under construction. A Pirani and a cold-cathode (inverse magnetron) gauge have been ordered for monitoring of the IN10B cryofurnace vacuum for which the power supply/display units will be incorporated in the IN10B control station.

IN11 Spin-echo spectrometer on the cold guide H141

Let us borrow a recent advertisement of a car making company when changing the version of one of their model: "We changed everything but the name." As all advertisement of course this is not completely true, but close to. The most important changes are the following:

We have changed the main precession coils due to corrosion of the old ones and at the same time we tried to have better precision winding, changed to even number of layers (eliminating a net current flow from one end to the other), better current lead connectors to eliminate end-effects, two coils instead of three on each side to reduce alignment errors and installed a closed circuit cooling system to avoid corrosion.

The polariser has been changed from reflecting mirrors to a "cavity" type transmission polariser (with special thanks to F. Mezei and T. Krist HMI for producing the supermirrors). This should allow us to change quickly the wavelength without changing the instrument configuration, thus easy excursions back and forth in the resolution-intensity compromise. We hope also an intensity gain although numbers and polarisation ratios will be available only after the reactor restart. This improvement should be completed soon, hopefully after the first reactor cycle, with a prepolariser guide between the selector and the polariser thus extending the available wavelength band down to 4 Å and with a further intensity gain.

The electronics part of the instrument has been partly renovated, while keeping the CAMAC system. (16 bit DAC converters for the supply controls and more recent positioning system) The old PDP-11 has retired and the CAMAC is controlled by an GPIB/CAMAC controller and a Macintosh computer. The acquisition program is Igor-Pro (Wavemetrics) which was extended with a few special commands. This gives an extremely versatile solution with built in graphics and macro language. Any GPIB instrument can be added in practically no time for special measurements.

IN11C is completed to a level that the first neutron tests can be performed although the standard IN11A configuration has to be commissioned at highest priority. While we are still missing a lot of supermirrors to complete the analyser for the multiarray detectors, we should be able to give a first evaluation of the performance soon. All connection of the

current leads, water cooling, detector cabling has been modified such that the exchange of the IN11A and IN11C moving arms can be done in a short time.

IN15 High resolution spin-echo spectrometer for long wavelengths on the cold guide H511. (cooperation ILL-HMI-KFA)

With the reactor restart, the IN15 project will enter a 2 year period for testing and commissioning of the spectrometer including testing and understanding of its 2 options under real experimental conditions: the pulsed operation and the optical focusing of the incoming neutron beam, both to be run as options but always with spin-echo.

For the time-of-flight option the velocity selector is being replaced by a chopper which consists of three disks with 30 mm distance between them to control the resolution. A fourth chopper with larger diameter (880 mm) is installed to avoid frame overlap. Unfortunately the mechanical part does not yet operate reliably but the chopper control system (hardware/software) developed by KFA is performing well. Following its "damage", the fourth chopper has been repaired and modified. Recently but for the second time, a problem appeared on the set of 3 disks which may be due to an internal mode of vibration. The system is still being tested.

For the optical focusing option, a toroidal mirror, 4 m long (8 elements) and 17 cm high, has been ordered at Zeiss. Following X-ray and neutron measurements (end 1993), a zerodur substrate coated with a ^{65}Cu layer has been retained. In addition, the Cu layer will be protected from oxidation by a thin Aluminium layer. The mirror will be used for wavelengths above 15 Å and should allow to reach a momentum transfer of the order of 10^{-3} \AA^{-1} . The whole mechanics to hold and align the mirror is designed at KFA. It should be installed and aligned in late 1995.

IN16 New backscattering spectrometer on the cold guide H53

Much progress has been made on IN16 to get a set of 7 m² analyser single crystals ready for the start of the reactor. A complete but mixed angle set of analysers, consisting of 3 high energy resolution Si(111) analysers at large scattering angles and of modest energy resolution Si(111) analysers (3 analysers for large scattering angles, 4 half rings for $40^\circ < 2\theta < 15^\circ$ and 6 small angle analyser rings below $2\theta = 15^\circ$) are now glued (R. Rebesco) and ready for neutron tests. High energy resolution ($\sim 0.2 \mu\text{eV}$) is achieved by using perfect silicon single crystals which are flat and small, thus minimising the deviation from backscattering. Modest energy resolution is produced by increasing $\Delta d/d$ by deforming the single crystals; we aim to get about 1.2 μeV energy resolution. As described earlier new techniques for gluing the analyser crystals were developed for both analyser sets and have now to be tested on IN16 for energy resolution and flux with neutrons. For the modest energy resolution setup the Si(111) single

crystals were deformed onto the 2 m radius analyser sphere by a high precision mechanical device built specially for this purpose. Large hexagons with a side length of 55 mm and a thickness of 0.7 mm are used. The strain profile of the deformed IN16 and IN10 Si(111) crystals were measured in the beginning of the year at the T13 spectrometer in Saclay (Frick, Magerl). It was found that the strain is quite homogeneous in the centre but relaxes fast close to the border. In total we expect a more homogenous deformation for the large crystals compared to the small hexagons used on IN10.

The shielding of the primary spectrometer has been improved by building a 20 mm thick lead tunnel, covered on the inside with 4 mm B₄C, around the focusing neutron guide and the Be-filter. The copper block for cooling the Be-filter is now shielded with Lithium.

All electronic modules are tested, motors are calibrated and tested as well as the detectors. A set of detector holders was built in order to be able to use single detectors instead of the multidetector at large angles.

For raw data inspection the purchase of a working station is planned for next year. For the moment a Macintosh Quadra 600 was bought which serves both the electronics VME tests and the raw data inspection. The raw data inspection is based on the 'IGOR-PRO' software and was programmed to allow plotting and manipulation (adding, normalising, binning, fitting...) of IN16 raw data files (B. Frick). Data inspection can also be done from any ILL X-Window terminal using 'LAMP' (D. Kearley, M. Ferrand, D. Richard) or a 'METACARD' driven data fitting program 'FITTING' (N. Haack, stagiaire IN16) which handles the programs 'PROFIT' (D. Kearley) and 'QUASI-LINES' (D. Sivia, D. Kearley). Data correction can be done with 'SQW' which was modified for UNIX systems (O. Randl).

D7 Diffuse scattering instrument with polarisation analysis on cold guide H15

The operational state of D7 has been fully verified and the instrument is ready for testing with neutrons. A Silicon Graphics workstation has been acquired under the UNIX plan and is installed at the instrument for data treatment and analysis. Work has progressed within the Optics group of the development branch to produce improved polarisers by sputter deposition of thin films which will be fully tested when the reactor restarts.

The instrument technician has been occupied full time with the IN16 project.

IID Brillouin setup on the thermal beam tube H12 (test instrment)

In the ILL/University of Aquila-contract concerning the use of the Italian two-dimensional LETI detector at the HFR for Neutron Brillouin Scattering (NBS) experiments the partners agreed on the use of the detector on IN5 and IN4

(cold and thermal neutrons, respectively). While the installation of the detector on IN5 has essentially been finished since 1991, the decision to build the new IN4 rendered the installation of the detector on this instrument impossible. In view of the very small investment budget available an optimised installation of the detector on a thermal beam could not be envisaged. It was therefore decided to install the detector above the new IN4 on an independent beam obtained by a double monochromator on H12 using left-overs from previous instruments and help from our partners as far as possible. This Installation of the Italian Detector (IID) will be used as a test instrument for low angle inelastic scattering experiments (TOF) with incident energies between 5 and 40 meV, i.e. for the measurements of dispersions (e.g. liquids) with sound velocities between 500 and 2000 m/s.

This year the IID has made encouraging progress. The overall design work has largely been finished and drawings of the details are presently made for the interior of the detector tube (old evacuated detector tube from the n-n experiment) and the basis of the first monochromator in front of the first background chopper of IN4. The monochromator itself, for which the PG-crystals of the former IN4 will be used, still has to be constructed. The concrete-shielding of IN4, on which part of the IID is placed, is presently being mounted. The design of the mechanics, which will hold and replace the old background chopper of IN4 (beam cross-section 6 x 10 cm) above the first monochromator has nearly been finished and the 2nd double focusing monochromator is being built at the University of Perugia. It will be delivered in Spring 95. The detailed drawings of the beam stop in the monochromatic beam of IID are made and the beam stop will be installed as soon as the concrete shielding of the background chopper and of the second monochromator has been installed above the new IN4 choppers. The construction of the converging multibeam guide has been started, but we prefer to finish this after first test experiments have been performed. (probably by the end of 95 - depending on the budget available for finishing the test facility) using the vacuum tube alone in its place.

The old Fermichopper of IN4 will be reused - in spite of its unfavourable rectangular cross-section of 2.5 x 10 cm - in front of the sample environment, which is presently being designed (a simple vacuum container for standard furnaces and cryostats of the ILL). The cover of the entrance window of the detector (presently too thin to support the vacuum in the detector tube), and the cover of the electronics on the back of the detector (which cannot work in the vacuum of the detector tube) is presently build by the CNR in Florence. The platform for this 8 m detector tube, i.e. the prolongation of the "roof" of the new IN4, will be delivered before the end of 94, so that the detector with its vacuum shielding can be mounted after completion of the vacuum tube.

The chopper-electronics of the old IN4 will be reused. For the two-dimensional detector VME-electronics has been acquired, in order to be able to handle the information available (4096 pixels with 512 time channels each at the origin). Likewise the amplifiers for the coders are presently completed for IID and for the new IN4. The software for the data acquisition is essentially finished, as we shall use largely the same which had been developed after the changeover to the new VME-electronics on the "sister instrument", the two-dimensional detector on IN5.

Albert-José Dianoux

Optimum transmission for a ^3He neutron polariser

Francis Tasset

Following recent achievements in polarising gaseous ^3He targets by optical pumping at room temperature, polarised Helium-3 is now the most promising polariser for thermal and epithermal neutrons [1] and should soon compete favorably with existing Heusler polarising crystals. Because it is gaseous, a degree of freedom exists in such a filter: the pressure of the gas in the cell. This parameter allows, for a given length of the filters, a choice to be made in the design: for a given polarisation of ^3He , one is able either to increase the pressure in order to favour the neutron beam polarisation P or to stay at relatively low pressure to favour the filter transmission T .

With spin-density determination in mind, this point has been investigated [2] in the framework of a classical polarised-neutron experiment where the spin dependence of the cross-section is measured and leads to the ratio γ of the magnetic and nuclear amplitudes. It has been shown that the usual quality factor $Q = P\sqrt{T}$, is in fact only an approximation to the inverse estimated standard deviation (ESD) of γ . The exact expression is complicated, depending on γ itself, and has poles at $\gamma = \pm 1$.

In the regime of small γ , i.e. low magnetic amplitudes, which is where classical polarised-neutron diffraction experiments are the most powerful, the ESD formula reduces to the inverse of the usual quality factor, which is therefore the appropriate quantity to optimise. On the other hand when the magnetic amplitudes are strong, i.e. comparable with the nuclear amplitudes, the ESD diverges, calling for higher incident-beam polarisation in order to maintain good precision.

Between these two limiting cases, an extra parameter Σ , the width of a hypothetical Gaussian distribution for the γ 's, has been introduced in a heuristic attempt to conclude the discussion. A value of 0.4 for Σ , which corresponds to the domain over which the method is highly powerful, leads to a filter 20% thicker than with the classical $Q = P\sqrt{T}$ criterion.

References

- [1] F. Tasset, *Physica B*, (in press, Proceedings of ICNS'94)
- [2] F. Tasset and E. Ressouche, *Nucl. Instr. Methods, A* (in press)

Laue-detectors

M. Lehmann

Work has continued on the analysis of various detectors for protein crystallography. This work was spurred by a proposal for a diffractometer for the study of large unit cells, based on the use of a quasi-Laue methods with cold neutrons and a limited wavelength range. No instrument is being built, but it is obvious that no neutron diffraction instrument for macromolecular crystallography is of much use without a large position sensitive detector, and it is therefore natural to continue the search. Two approaches are studied. In one case the detector is a position sensitive photomultiplier while in the other case image plate technology is used.

For the photomultiplier a Li glass scintillator is placed in front of the 4.5 by 5.5 cm² detector area. The x and y anode signals are converted into two pulses for each axis using a resistor chain. These four voltages are then recorded into a PC using a fast ADC converter and the position is calculated.

First test at DN4 of the Siloë reactor in 1993 (M. Bonnet and C. Ruchon, CENG, J. Troska, Imperial College, London, J. Allibon and C. Wilkinson, EMBL, M.S. Lehmann, ILL) showed that the overall counting efficiency was 30 %, and that the neutron pulses were on the short side compared to the interval between samplings of the fast ADC. To improve the counting efficiency a signal stretcher was therefore constructed and included in the counting chain, and further tests at the Orphée reactor (J. Troska, Imperial College, London, J. Allibon and C. Wilkinson, EMBL, M.S. Lehmann, ILL and T. Roisnel, CEA) showed efficiencies near 100 %.

The other more ambitious project is the construction of an image plate for neutrons, presently being undertaken at the EMBL outstation in Grenoble (F. Cipriani, J.-C. Castagna and C. Wilkinson, EMBL and M.S. Lehmann, ILL) with support from the KFA, Jülich (G. Büldt).

Image plates are flexible sheets holding a photostimable phosphor. The material is most commonly BaFBr doped with Eu^{2+} ions. When irradiated, the electrons liberated by ionising Eu^{2+} to Eu^{3+} are trapped in states just below the conduction band which has been created by the substitution of Eu for Ba. For detection of neutrons Gd_2O_3 is added to the plates (made available to us by H. v. Seggern at Siemens).

The detector shown in figure 1 is a 40 cm long, 30 cm wide aluminium cylinder with the axis in the horizontal plane. The sample is placed in the middle of the cylinder and the diffracted neutrons pass through the aluminium to be detected by the image plate which is placed at the outside of the cylinder. After exposure this is read off much like a phonograph. The approximately 6 Mega pixels (0.25 by 0.25 mm²) can be read in about 5 min.

After first tests using X-rays, preliminary neutron tests were made at Risø and are reported under college VIII. The experiment showed successfully that the image plate detector can be used in diffraction studies, allowing one to two orders of magnitude increase in data collection rate due to the large detector surfaces.

During the year preparations have been made for the first test when neutrons are available again. Preliminary measurements are planned to take place at the H142 end position about 110 m from the reactor core using a cold white beam with highest flux in the range from 3 to 6 Å.

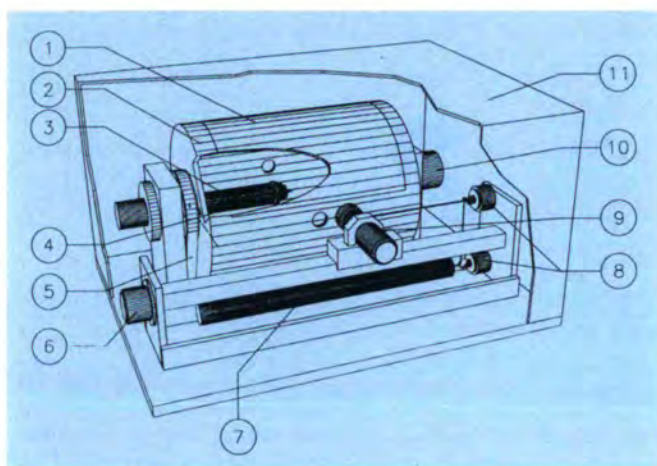


Fig. 1: The image plate diffractometer.

The neutron beam enters the detector surface through the small hole on the back and exits diametrically opposite to be trapped by a beam-stop not shown on the figure.

- 1: Image plate mounted on the outside of the drum.
- 2: Drum.
- 3: Sample holder.
- 4: Crystal.
- 5: Transmission belt to drive drum. Motor is under table.
- 6: Carrier for reading head with photomultiplier.
- 7: He-Ne laser.
- 8: Mirrors for bringing the laser light to the reader head.
- 9: Reader head with photomultiplier.
- 10: Encoder for drum rotation.
- 11: Cover.

PROJECTS AND TECHNIQUES DIVISION (DPT)

The Projects and Techniques Division (DPT) has had three directors over the course of this year. Peter Schofield created it and faced the stress of convincing everybody that changes and adaptation were necessary. Then, he prepared the reinstallation of the instruments, which was done under the direction of Reinhard Scherm. The personnel proved to be highly motivated and very efficient in this operation. At the end of the year, I arrived to begin work with DPT in its normal configuration, and as soon as the reactor restarted, to experience the day to day pressure of the running experiments. The newly created DPT has never worked under such conditions with reduced manpower and there will certainly be a need for a few modifications. The golden rule will be solidarity and adaptability.

In keeping with the spirit of the organisation at ILL, DPT has to work in close coordination with the Science Division (DS) in order to provide “ *engineering services and project management support for all experimental activities* “. The general rule for sharing responsibilities between DPT and DS is that matters of joint concern should be handled by DPT. In addition, DPT gains impetus and unity by managing large projects like D20 and IN4c.

While DPT may have its own technical tools and skilled personnel, it must be a bridge toward the outside industrial world. It must be remembered that every piece of apparatus which is offered on the general market by an industrial company, is subject to optimisation by much greater pressure than what could come from inside the ILL. Therefore, we will not attempt to fabricate something close to what industry offers already. However, in the realm of special fabrications or *ad hoc* services, external and internal costs must be carefully compared. Recent experiences have proven that in some cases, complex devices have been manufactured by industry in a very inefficient way. This should remind us that the art of sub-contracting is a difficult one and that we must constantly improve our skills.

On observing and listening to the personnel of DPT, I have been impressed by their strong dedication to the service of the ILL scientific activities. Following this line rigorously is, I believe, our honour, our pain and our pleasure. As a long-term benefit, ILL will *resume its role of creativity and development in neutron instrumentation*.

Philippe Leconte

Project Office (BP)

(W. Kaiser, M.C. Filhol)

In 1994 the investments on the instruments were 21.2 MF i.e. 8.0 % of the revised normal budget of 264.9 MF. 6.8 MF were shared between the instrument projects of the Science Division (GAMS5, He 3 Polarizer, Laue Detector) and the Projects & Techniques Division (Neutron Guides, D20 Detector, IN4C). The Project Office has provided up-to-date information on the spending and budget provision for the investments and the operating costs of the instruments for both Divisions.

Whereas the He 3 Polarizer and the Laue detector projects are proceeding very successfully, other projects are delayed either by manpower availability in the drawing office (IN4C), technical problems (D20 Detector), or by the delayed reactor restart (GAMS5, H25 neutron guide).

Neutron Guides

(W. Kaiser)

H1-H2 Neutron Guides

In the framework of the refurbishment of the neutron guides, the new in-pile part with 7 cold guides and 5 thermal guides was mounted in the new H1-H2 beam tube in March 1994. The 2 new cold guides NG12 and NG13 are included in this part. The refurbishment of the out-of-pile part in the swimming pool and the casemate in the reactor hall was finished at the end of May. (See Figs. 1-3 on page 146).

H17-H18 Guides

Looking ahead to the dedicated reflectometer project on the H18 guide, the old H18 guide was not mounted and the H17 guide for the present D17 instrument was mounted mostly with old glass elements with the old geometry in the out-of-pile part.

Design work in the drawing office was performed early in the year, allowing the call for tenders for the housings of the new H17-H18 guides in October. The quotations were available. But the budget situation did not allow the orders to be placed.

H25 Guide

The refurbished H25 guide is mounted as a super mirror guide in the 6 m long swimming-pool part. Another length of 5 m is delivered. The 21 m long part in the casemate is dismantled, pending a possible reactor shutdown period at the end of March 1995 for remounting with super mirror guides.

Design work for the part downstream of the S18 instrument was finished in October. This allowed the call for tenders to go ahead for the replacement of the remaining 25 m and the 10 m of a new guide for the CRG project with the CEA. The deadline for quotations was mid December.

H511 Guide

The order for the replacement of 16.5 m of the polarizing guide for the IN15 instrument was placed at the end of last year. The 9 m long Nickel-coated part has been delivered and the elements for the FeCo coating by HMI have been delivered in Berlin.

IN4C Thermal Time-of-Flight Project

(H Mutka) Collaboration with Istituto di Struttura della Materia, CNR, Italy.

Due to the reorganisation of the institute and the subsequent staff changes overall progress has been slower than expected. At present the situation has stabilised and satisfactory solutions have been found to ensure swift advance in the most critical part concerning the work on the secondary flight box and the sample environment.

Meanwhile, the construction of the mechanical components for the primary spectrometer has advanced. The Italian partner (coordinator Prof. F. Sacchetti) has delivered the curved monochromator assembly (see Fig. 4 on page 146). The precision of the mechanics is in time with expectations. The already purchased graphite crystals will be mounted for tests with neutrons at the beginning of 1995. Part of the Cu crystals has been produced at the ILL. All the goniometer elements for the monochromator will be delivered by the end of 1994.

Preparation of the site for receiving the new spectrometer is close to being finished and the final installation of the primary shielding elements has started. Material for the factory tests of the choppers, i.e. supports, vacuum equipment, drive power-unit and motors, was sent to the supplier but the delivery has been delayed due to technical problems with the Cd-coating of the rotors. The choppers are to be installed during the first half of 1995 after bench tests at the ILL. Other beam-line elements such as the secondary shutter and the primary diaphragm are also ready for mounting.

The Italian partner has completed work on the electronics for the detector tubes according to the layout provided by the ILL detector department. The testing of the circuit boards is in progress. The mechanical design of the central forward scattering detector is finished and the construction as well as the fabrication of the electronics has begun in Italy.

Beam Shutter Replacement and Personal Safety System

(W. Kaiser)

Together with teams from other services (DA/SAE, DPT/BD, DPT/BI/SDN, DRe/SEE) the work including beam shutters and their control, interlocks and key interlocks between shutter control (see Fig. 5 on page 146) and access gates was implemented in the reactor hall in parallel with the

reinstallation of the instruments. The acceptance procedure provides for verifications of the shutters with neutrons during the first reactor cycle.

Instrument safety

(W. Kaiser)

The acceptance procedure for the instruments has been formalized. Based on a specification for the instrument safety edited for each instrument and future CRG-instruments (Instrument Safety File), safety checks were issued on nearly all instruments. The authorisation for normal operation will be given after approval of the instrument safety and final checks with neutrons at 2 % and full reactor power.

Instrumentation Branch (BI)

(A. Heidemann)

Introduction

Three tasks put a heavy load on the staff of the instrumentation branch in 1994:

- The main action was to get the instruments operational again after the long reactor shutdown. This task was successfully accomplished thanks to the tremendous efforts of the technical staff of the ILL. All '25' ILL instruments and 4 CRG instruments (IN3, IN12, IN13, D15) were ready for tests in October 1994. Significant improvements have accompanied the reinstallation of the instruments in several cases, such as modernisation of the electronics of IN1, IN8 and IN20, where CAMAC was replaced by VME.

- The implementation of the main part of the UNIX plan in close collaboration with the ILL scientists occupied the computing Services. The essential part of the new computing infrastructure has been in place since the end of 1994.

- The drawing office of the mechanical engineering Service was busy with new instrument projects like the TOF spectrometer IN4C and the Gamma spectrometer GAMS5. Manpower shortages caused by the staff reductions were compensated by additional subcontracting.

Reinstallation of the instruments

(D. A. Wheeler (*left on early retirement*), A. Beynet)

The recommissioning of the instruments in the guide halls started in September 1993 with a vast cleaning action and finished in June 1994 with an official instrument check procedure. The new instruments D22, IN15, IN16, PF1 have been finished and are also ready for first tests with neutrons.

The instruments in the lower and upper reactor hall (Level C and Level D) had been dismantled completely in 1991/1992, except IN14, to enable the reactor team to extract the beam tubes.

The reinstallation of these instruments started at the end of March 1994, when the first beam tube, H11, was in place. The plan was to install as many instruments as possible by the middle of July 1994, the date foreseen for the reactor to be technically ready to produce neutrons. In order to achieve this goal, a careful scheduling of all the actions was necessary. Shift work of the technical staff was introduced in order to cope with the problem of having only one crane in the reactor hall. Progressively D19, D2B and D20 (see Fig. 6 on page 147) were put into place. The next instruments were IN1 and D4, then D3 and D9 (see Fig. 7 on page 147), later IN8 and IN20. The restart of the electronics and instrument control computers followed the mechanical installation. New neutron guides were installed on the front end to feed the old guide hall instruments with neutrons. This operation was finished in June 1994, followed by the reinstallation of the guide system for the new guide hall.

By the end of October 1994 all ILL reactor hall instruments were ready for tests with neutrons except three instruments: IN4C, the new thermal TOF spectrometer which is under construction, D20 where the new large multidetector based on the microstrip technique poses new and unforeseen technical problems, and the Gamma spectrometer GAMS5 of the Nuclear and Fundamental Physics Group. The prototype of GAMS5 was installed in December 1994.

The CRG diffractometer D15 has also been reinstalled. The former S- instruments SN5 (the ultracold neutron platform in the lower reactor hall) and the fission products spectrometer COSI FAN TUTTE SN8 as well as the very cold beam position on H18 have not been reinstalled. Therefore three inclined beam hole positions are now available, one for cold (IH1), one for thermal (IH3) and one for hot (IH2) neutrons. The future of H18 is linked to the ILL reflectometer which is in the design phase.

Neutron Distribution and Central Services:

(R. Mathieu)

The **Neutron Distribution Service** is in charge of neutron distribution and general organisation in the experimental halls. In 1994 the main activities were as follows:

Contribution to:

- The project for modernising the beam shutters, installation of the instrument control cabins, operating tests, etc.

- The introduction of quality assurance management procedures for the beam shutters.

- The drafting of operating procedures in conjunction with the Reactor Division.

Coordination of preparatory work:

- For the experimental facilities EVA, ADAM, PF1, GAMS 5, LADI.

- In all experimental areas (in line with the recommendations of the ILL Internal Safety Committee).

Production of poster boards for each experiment.

Preparation of the 1995 Transurania programme.

Follow-up of several nuclear physics experiments - ¹⁷⁷Lu on PN7, ¹⁹⁸Au - for the Internal Safety Committee.

Refurbishment of the experimental halls ILL7 and ILL22: electrical networks, fluids, painting, cleaning.

Reassembly of instruments on Level C (timetable follow-up and work coordination).

Vacuum laboratory

In-situ interventions on pump sets IN11 - D22 - IN15 - IN16 - DRE, etc.

Campaign for maintenance, repair and improvements to the pump sets, turbo-molecular pumps and He pumps during the long shutdown.

Contribution to the numerous leak detection tests performed on the reactor installations and instruments.

Maintenance and sundry services for He4 leak detectors.

Assistance to users: Calibration of measurement devices; glass-bead blasting; definition of equipment for new pumping installations; loan of equipment.

Mechanical Engineering Service

(M. Thomas)

The S.C.M. comprises 2 units:

- The Drawing Office (B.E.) and its calculation laboratory
- The Assembly Hall (H.E.) and its workshop

Assembly Hall and Workshop

The FNE early retirement scheme accounted for the departure of the head of the Assembly Hall, M. Mourrat, as well as three other employees (R. Chagas, A. Cumin and M. Piotti). The new head is P. Thomas.

The Assembly Hall's activities focussed on instrument reassembly in the reactor hall, the rebuilding of the beam shutters, safety loops and the reinstallation of the neutron guides.

In the first half of the year, the workshop machined major peripheral equipment for the reactor: thimble support flanges, beam tube thimbles, coupling sleeve flanges, and thimble alignment tools.

This work took place under very unusual conditions (with staggered working hours and with quality assurance system on contaminated materials).

The second half of the year was devoted to large-scale modifications to certain rotating machines:

- Disks and shafts for the choppers on IN5
- Shafts and bearings for the choppers on IN15
- Shafts and bearings for the velocity selector on D11.

Drawing Office

The drawing office's activities focussed on improving existing instruments, the construction of new ones and the preliminary layout studies for future instruments.

Due to the sheer volume of work requests, the drawing office has called on subcontractors.

The computers on which the Computer-Assisted Design programme runs (AutoCAD) have been changed. The result is a very considerable improvement in performance (processing speed x 6).

Improvements to existing instruments:

- D19: Modification of multidetector shielding
- D19 and D2B: Modification of monochromators
- IN11: End of studies for the instrument refurbishment
- D20: End of design work for shielding of the multidetector and its platform
- D22: End of design work for the sample area
- D3: Design of primary collimation
- IN15: Continued instrument improvement studies and modification of polarisation system by super mirrors.

New instruments:

- IN4C: Strengthening of the design team (2 ILL designers and 1 subcontracted designer)
 - end of design for primary spectrometer and continuation of design for secondary spectrometer.
- IID: Design work continues.
- GAMS 5: Minor additional design work.
- LADI: Design of bench to test the multidetector prototype built by EMBL.

Preliminary layout studies:

- Installation of PF1 and ADAM on neutron guide H53
- IN22 and DN23; CRG-instrument belonging to CENG (neutron guide H25).
 - Work on neutron guides H17/H18 and reinstallation of D16 and D17.
 - Numerous design studies have been carried out for the project to rebuild the beam shutters and attenuators

Calculation laboratory

General calculations have been performed on some projects:

- Device for lifting the new magnet on PN1.
- Analysis of the fracture mechanics of the choppers on IN4C.
- Analysis of the curvature mechanisms of the focussing monochromators of IN4C.

A number of finite element calculations have been carried out also.

- Possibility of cutting a window in the current chopper disks of IN5.
- High pressure furnace that allows plastic deformations of monocrystals.
- Modal analysis of the rotor on the 3-chopper system on IN15.
- Design calculations for the background chopper of IN15.
- Mechanical design of the multidetector on IN4C (see Figure 8 on page 148).

The IN4C small-angle multidetector filled with ^3He at a pressure of 7.3 bar has the shape of a truncated cone tangent to the sphere centred on the sample. Since the geometry of the electrode system creates zones where neutrons cannot be detected, radial ribs can be introduced at these precise points. The ribs serve to reinforce the front side of the detector and thus allow the thickness of the scattered neutron entry window to be minimised.

Numerical simulation of the vessel's mechanical behaviour under the ^3He gas pressure is done by the finite elements method using the ANSYS software. The conditions of symmetry created by the angular periodicity of the ribs allow the size of the model to be considerably reduced.

Electronics Service

(R. Klesse)

The activities in the past year have been dominated by the forthcoming reactor restart. The electronics of 'all' instruments was switched on, tested and repaired when necessary and was ready for operation at the end of 1994. 'All' means about 40, i.e. the officially scheduled ILL instruments, the ILL instruments before the commissioning phase D22, IN15, IN16, test and development instruments and the CRG instruments. This difficult operation was successful due to tremendous engagement of the staff of the Electronics Service. The operation was difficult because

- The reinstallation of the instruments was hindered by the priority for reactor refurbishment work;
- The Electronics Service was handicapped by a severe drain on its personnel (elimination of 5 posts);

- Old instrument responsables were replaced by new, younger less experienced ones;

- A number of instruments needed extensions or improvements to their electronics.

Most of the reactor hall instruments have been rewired entirely. Some subcontracting was necessary for this action. Six instruments, which ran under CAMAC until the reactor shutdown, have been converted to VME electronics: IN1, IN8, IN20, IN5 (see Fig. 9 on page 148), D11, D20.

Some instruments have been equipped with extended functions:

- IN5 was fitted with an additional multidetector with positionable beam-stop.
- For IN10 additional shafts were automated.
- IN4C and IID are under developpement.

Computing: Instruments and Network Infrastructure

(A. Barthélemy)

The Service's main aim in 1994 was to reinstall and restart the instrument computers, especially in the reactor hall. The highlights were as follows:

- Commissioning of the five Digital DEC Alpha 3000 workstations under OpenVMS on IN1, IN8, IN14, IN20 and D4;
- Start-up of the CAMAC HYTEC controllers on Ethernet (IN14 and D4);
- Conversion of three instruments (IN1, IN8 and IN20) to VME electronics.

The Service also pursued its aim of software standardisation: the "MAD" measurement, control and acquisition software, already installed on the diffractometers, was adapted for the three-axis and time-of-flight instruments; this software is operational on all the D and IN instruments except IN10, IN16, D7 and IN11. For the VME link, the link software was completely re-written to bring it into line with market standards (TCP/IP and RPC). Several developments were carried out on certain neutron guide instruments, in particular IN5, D22, D11, D17, IN15 and IN16, see Fig. 10 on page 148.

Several projects have continued: work has begun on a prototype user interface for MAD, based on OSF/Motif, while the study of Windows NT for PCs has not progressed, through lack of manpower and time.

At the end of the year, a study of the technical choices for the instruments under the Unix plan was performed; as soon as the instruments restart with neutrons, the Unix plan will be fully implemented for these instruments.

For the tests, an IEEE test bench based on a PC under Windows has been installed and is operational.

A call-back system has been developed in conjunction with ESRF to provide access to the ILL network, and hence the instruments, from terminals or personal computers installed in employees' homes.

As far as the Local Area Network (LAN) is concerned, due to the massive increase in traffic, a system of sensors monitoring each Ethernet segment, based on the Simple Management Network Protocol, has been purchased and installed at the end of 1994. A study has been launched to coordinate the means of testing and monitoring the LAN. Several cabling modifications have been undertaken to ensure higher traffic distribution efficiency and to facilitate trouble-shooting. The project to replace terminal servers supporting only the Digital LAT protocol with multi-protocol servers has been carried out, so that all types of workstation at ILL can be accessed from any terminal. However, the MICOM hub has been permanently shut down and dismantled.

The reactor hall has been entirely recabled to allow installation of instrument computers and processing equipment (workstations, X terminals, printers, personal computers).

The computer network plans (see Fig. 11 on page 149) have been saved on a personal computer.

Finally, 1994 saw the joint site's connection to the ARAMIS regional network, which gives access to the RENATER national network, itself connected to the worldwide computer networks, including Internet. This project, which began in 1992, was pursued in close collaboration with the other Institutes on the site (ESRF, EMBL).

The staff of the Instrument and Networks Computing Service achieved the objectives set for 1994, despite a dangerous reduction in staff numbers and a very worrying prospect for 1995.

Computing: Systems and Communications

(M. Le Sourne)

Introduction

1994 was an important year in the implementation of the UNIX plan, under which we were able to purchase workstations for the different groups of scientists and install several dedicated servers, and in particular the file server. The Nuclear Physics Group used this infrastructure to implement the new techniques for automating its instruments.

Furthermore, we maintained the VMS service by installing a DEC Alpha to replace the old VAX machines, which were too costly from the maintenance point of view.

Department personnel had a heavy workload setting up this equipment, developing and maintaining the different UNIX, VMS and Micro platforms, and finally providing user support in these various environments.

Our overall hardware infrastructure at the end of 1994 is shown in Figure 12 on page 149.

Systems and Communications Service

UNIX

Under the UNIX plan drawn up in 1992, a considerable investment budget was earmarked for general infrastructure in 1994. This led us to purchase workstations for all five instrument groups:

- 3 HP stations for the Nuclear and Fundamental Physics Group
- 1 HP station for the Three-Axis Group
- 7 SGI stations for the Diffraction Group
- 4 SGI stations for the Time-of-Flight and High Resolution Group
- 2 SGI stations for the Large-Scale Structures Group.

To this must be added other equipment associated with these workstations, such as X terminals (Tektronix, HP) or Macintoshes with X- emulation and printers.

The task of installing these workstations was particularly arduous and involved providing product installation kits on the network, compiling a Unix manager guide and writing scripts to access the networked printers.

On the software front, investments were also made to purchase IDL user licenses for some ten machines. The IDL programme is used mainly by two Groups (LSS, TOF/HR) for data manipulation and display.

One of this year's aims has been to install a file server. The model eventually chosen was "Challenge" from SGI, due to its good input/output performance. This server's function is to receive experiment data under an ASCII standard format, offer workstations additional storage capacity and place libraries and various general-interest tools at users' disposal.

In parallel, we aimed to organise a central back-up service. Having conducted a survey into the different back-up products available on the market, we selected the Epoch software, with the Exabyte stacker back-up equipment. Daily back-ups are currently being performed for some thirty workstations.

VMS

This year the Scientists have made tremendous efforts to transfer their applications to UNIX; even so, this work is still not finished and will be intensively pursued in the coming year. Given this state of affairs, it is essential to maintain a VMS service specially for a certain number of visitors conducting the initial experiments at the ILL after the reactor restarts.

To ensure this continuity, we have added to the cluster a DEC Alpha 3000-500 AXP computer and stopped maintaining the two old VAX machines which comprised the basic cluster. Although this new machine runs a VMS system, a lot of manpower was needed to create an environment as close as possible to that of the old VAX

machines, and some differences still remain. After one year of operation, this new machine satisfies most calculation requests in the VMS environment. Furthermore, it acts as the gateway for incoming E-mail; this function will soon be taken over by a UNIX server.

Another important activity this year has been the switch to a rewritable optical disk as the medium for the ILL and guest scientists' archives; this move has enabled us to cut down considerably on the use of magnetic tapes.

Micro-computers

This sector is developing continually, from both the hardware and software points of view, and requires further network integration. Activities have been as follows:

- Installation of a consistent "Windows for Workgroup" - based communication standard for the PC environment, analogous to the Macintosh network;
- Introduction of a system (ARA) for calling up ILL computers from one's own home; this service provides automatic call-back and enables Macs to use the TCP/IP functions on the IP network;
- Support and updating of the Mac server, the PC (Pathwork-VMS) server and all the micro-computers in the scientific and technical fields.

Data Base

In close collaboration with the computing group in the Science Division, this work included:

- Defining a new format for experiment data in ASCII so that all data can be easily accessed from our various system environments;
- Putting this data base into operation on a UNIX server parallel to the old VMS binary data base;
- Making a library written in Fortran available to users, allowing them to access data from their workstations;
- Recovering existing VMS data and archiving them in the new UNIX data standard, and in particular making the last reactor cycle of 1991 available on the file server.

Communications and E-mail

The key aspect of the past year has been the expansion of E-mail to include all ILL personnel, on both micro-computer and UNIX.

As far as communication with the outside is concerned, we will be moving the gateway function for the ill.fr domain onto a recently-acquired HP computer.

Furthermore, we have been working with the Scientific Support Service to install a WWW server for in-house and external distribution of documents and general information on the various services offered by the ILL.

Software libraries

The mathematical libraries NAG, Harwell, IMSL and Numerical Recipes have been installed on the new file server and are now accessible to both the HP and SGI environments. Other products, such as Mathematica, Matlab and associated tools have also been made available under UNIX.

As regards Fortran 90, we have acquired the NAG compiler, which has helped us get to know this new standard. However, we feel it is too early to ask the Scientists to use this new Fortran standard before the manufacturers have produced native compilers. For the PC world, on the other hand, we are using a Fortran 90 from Lahey, which is more efficient than Fortran 77.

Support for the NFP Group

(Ph. Ledebt)

The aims fixed in 1993 have practically been achieved. As shown in Figure 13, the network structure set up for the NFP group of the Science Division in 1994 to connect experiments PN1, PN3, PF1 and PF2 is well defined and operational; the experiment-workstation traffic is isolated from the rest of the ILL network by a bridge, thus avoiding overloads and ensuring the integrity of the particularly important data on certain instruments (List mode).

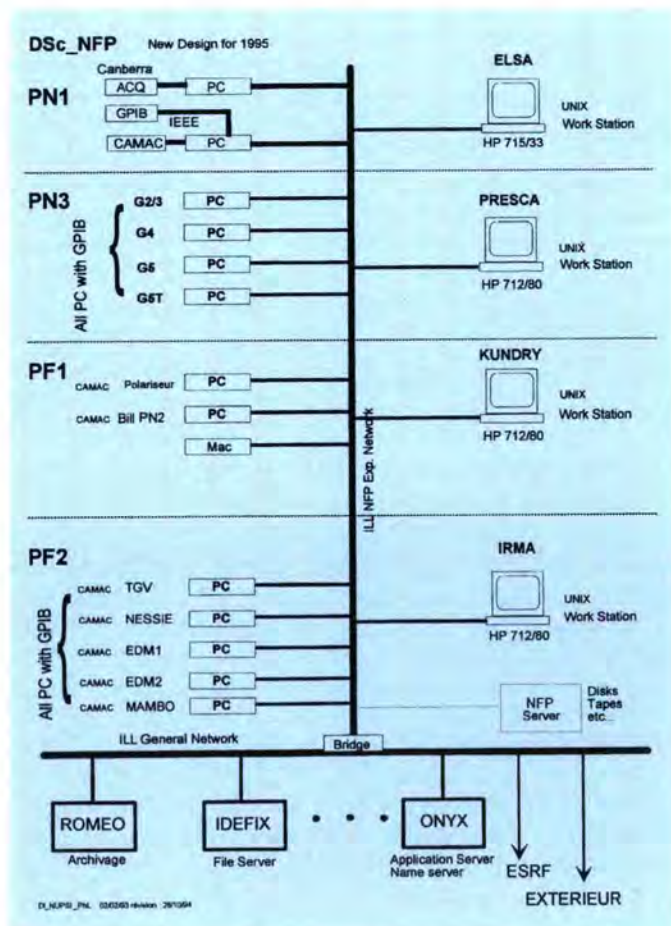


Fig. 13: Network structure of the NFP group computers

Each experiment consists of several entities (spectrometers, etc.), run by a PC that provides electronic control and data acquisition; data are sent directly to the corresponding workstation (NFS function) if the network is operational, otherwise the information is stored on hard disk inside the PC. This ensures local storage of the data, which can then be re-emitted onto the network once the connection has been re-established; in this way, the experiment is not interrupted for undetermined lengths of time. To make these exchanges, we used the MS-TCP/IP-32 programme and XFS-32 for the NFS part, EUDORA for the MAIL and WNQ for the TELNET and FTP functions.

As far as the experiments are concerned, the installation of the IEEE-GPIB bus posed no particular problem except for the choice of electronics, which must comply exactly with the 488.2 standard. The control and acquisition software is based on "Visual Basic V3.0" for everything related to screen management and graphics; calculations are performed in C++, which considerably increases the processing speed; users switch from one programme to another by means of the standard DLL mechanisms of "Windows for Workgroup 3.11".

We have also been testing the LINUX system on PC. This is a "UNIX-true" system with all the UNIX functions, command languages, networks, compilers, X11, etc. We are most impressed with the speed, simplicity and capabilities of this UNIX-PC system and will press ahead with further studies and tests on LINUX in 1995, focussing especially on the possibility of hooking it up to X-window terminals.

Development Branch (BD)

(C. Zeyen)

Introduction

This year several more departures under the FNE Convention have taken place. They include Yvon Blanc, engineer in the Monochromator Group, Dominique Brochier, head of the Cryogenics Group, Klaus Gobrecht, in charge of special projects such as the reorganisation of the Helium distribution at the ILL, and Danielle Arnaud, secretary of the Development Branch. Of the above, only the secretary has been replaced, by Françoise Giraud. Furthermore Pierre Flores from the Monochromator Group moved back to the Three-Axis Group.

Early December all activities concerned with cryogenics, temperature measurements and control, circuits and cryogenic fluids were merged with the high temperature and high pressure groups to form the Sample Environment Laboratory, headed by Serge Pujol.

New personnel: Peter Høghøj for the Multilayer/Optics Group.

Monochromator Laboratory

(A. Magerl)

The main emphasis in 1994 was on the fabrication of monochromators for ILL. The work of the group has therefore concentrated strongly on the Ge monochromator for D2B and on the Cu monochromator for IN4C.

Concerning Ge monochromators we have demonstrated that a high crystal quality can be produced with our equipment. In Fig. 14 we show a sequence of transmission spectra taken at our test station T13A at LLB, Saclay. The data demonstrate that well-shaped diffraction profiles and high reflectivity can be obtained when piling up a sufficient number of 1 mm thick Ge blades which have been plastically deformed. These results are further evaluated in Fig. 15. Fig. 15a shows the saturation of the peak intensity while building up the compound crystal, and fig. 15b demonstrates that the peak width remains constant for any crystal thickness.

Concerning IN4C about half the Cu crystals needed have been fabricated. Meanwhile the monochromator mechanics made by the Italian partners has been received for testing and mounting.

In spite of the strong focus on production, the fabrication of monochromator crystals has not advanced as rapidly as planned. This relates primarily to the changes in the group personnel. In particular, we regret the departure of Mr. Yvon Blanc within the early retirement programme of the ILL. This has weakened the group, and is felt even more strongly because this vacancy has not yet been filled.

In addition to the main tasks, mentioned above, the group has provided assistance for other instruments whenever possible. Detailed measurements have been performed for IN16 to determine the strain distribution in bent Si 111 crystals. This instrument has also been prepared to implement a set of Si 311 crystals, and the group became involved in both the definition of the crystal parameters and the preparation of the crystals. Further support was provided for IN10 for which a medium resolution Si 311 monochromator, made from oxygen precipitated Cz-material, has been prepared and aligned. Other involvements concerned e. g. characterisation of mica crystals and of some intercalated graphite specimens for DB21, assistance in repairing a Ge monochromator for D1A at LLB or the preparation of a mechanical mount and alignment of the graphite monochromator for D1B.

Development-oriented projects were reduced to a very low level during 1994. Although a PhD thesis and a diploma thesis concerning an investigation of the potential of gradient crystals as novel neutron optical elements have been finished successfully, it has not been possible so far to continue along this line. We are now making greater efforts to join research activities relating to monochromator developments at other institutes. In this context we should mention the problem of creating an appropriate

microstructure in Be crystals grown in an earlier programme including other neutron scattering centres. This question is now addressed at the Bergakademie Freiberg within the thesis work of C. May, a former colleague at the ILL.

In particular the potential of a plastic deformation of crystal blades with a progressively varying bending radius is being looked into. A diploma work has been started in collaboration with the Universities of Bochum and Würzburg to use the dynamical strain in ultrasonically excited crystals to tune the intensity for high resolution monochromators.

Relating to the shut down of the ILL reactor there has been a constant strong demand for the diffraction equipment maintained by the group. This concerns the two neutron diffractometers T13A and T13C, which had been transferred earlier to the reactors of the CENG, Grenoble, and of the LLB, Saclay, respectively. T13C has been brought back recently to the ILL and installed again at its former site. T13A is scheduled to return early 1995. These instruments have been very valuable for both the needs of the monochromator group and for other scientists either from the ILL or from external laboratories. In addition to experiments relating directly to monochromator development there have been studies concerned with e. g. detector technology, performance of focussing elements made from capillary fibres or with the quality of Heusler crystals grown with a seed crystal from a crucible-free melt in a reducing hydrogen atmosphere.

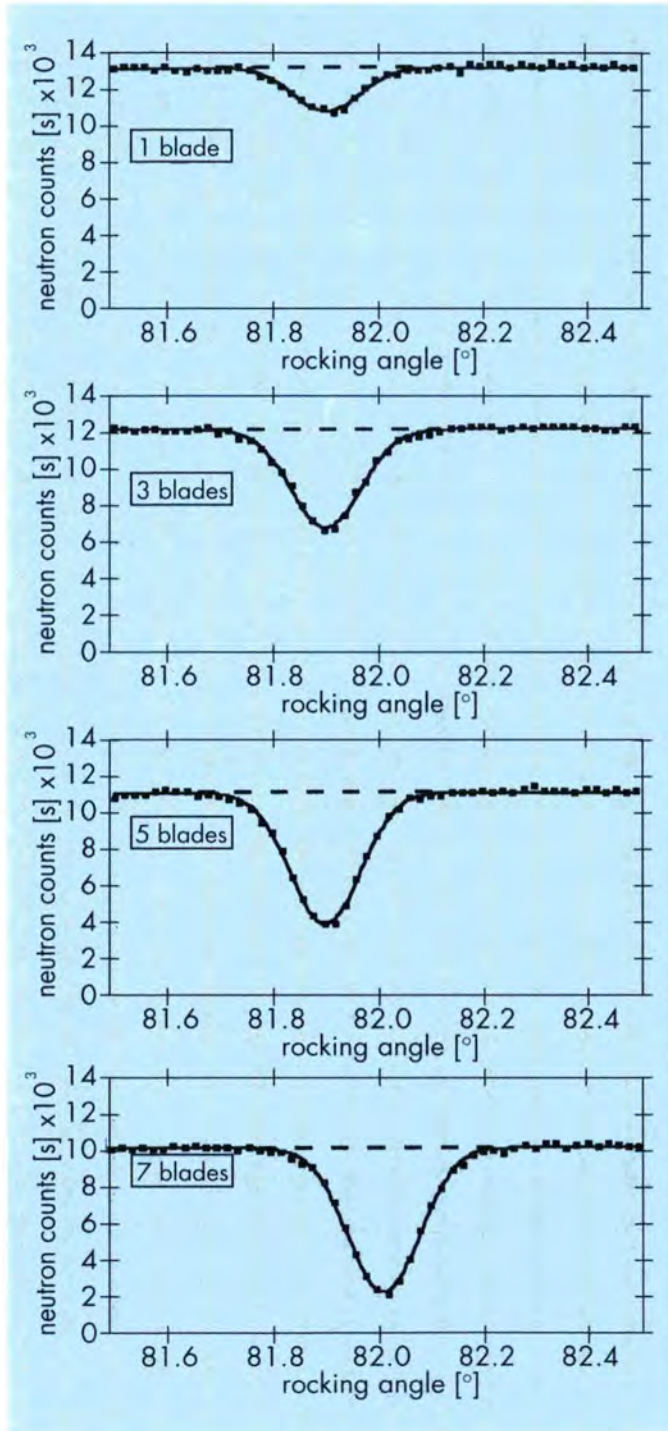


Fig. 14: Evolution of the reflection properties of a stack of Ge wafers with increasing number of wafers. Measurements were performed in transmission on the 311 reflection with a wavelength of 2.33 Å on T13A at LLB. The individual thickness of the wafer is 1.0 mm. The solid line represents a fit with a Gaussian profile.

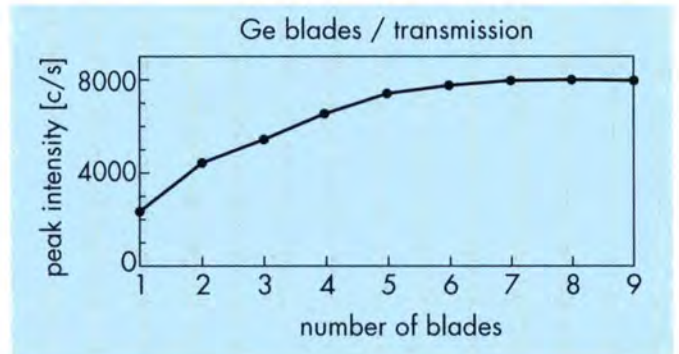


Fig. 15a: Peak intensity as a function of the number of Ge blades.

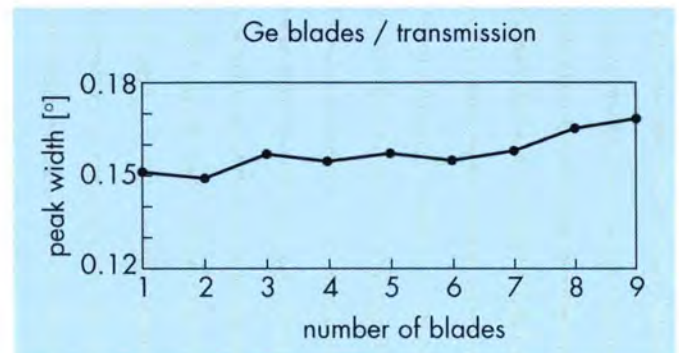


Fig. 15b: Peak width as a function of the number of Ge blades.

Similarly, the X-ray equipment and the γ -ray diffractometers of the group have been in heavy demand throughout the year. However this equipment has become old and fragile and an upgrade of the electronics and part of the mechanics seems overdue.

For the near future it seems necessary to invest in modernised diffraction equipment. Together with a commissioning of a new hot press in the very beginning of next year for a speedier production of monochromator crystals to finish e. g. D2B and IN4C are the objectives which we carry over into 1995. It also seems desirable in the future to balance production and research activities once more which implies strengthening the monochromator group by associating young scientific personnel.

Detector Laboratory

(A. Oed)

For the reactor start, experimental equipment had to be operational immediately. For this reason all the detectors of every instrument were put into operation and thoroughly checked in order to replace or repair any damaged module.

The instrument D20 receives an extremely high neutron flux (ca 10^8 n/cm² s) at the sample site. To take full advantage of this fact, it was decided, many years ago, to equip its curved position sensitive detector (banana type) with so-called micro-strip-plates (MS) which are designed to accept high intensities.

A prototype containing 3 plates, installed in exactly the same way as in the final detector, has been used to examine all the details of operating conditions. Measurements over 8 months in 1993 with a neutron source at the laboratory have shown, however, a change in the signal amplitude. Moreover the amplitudes became dependent on the count rates, a particularly serious defect. After a detailed examination of the substrate surface with an analytical scanning electron microscope (Laboratoire d'Investigations Structurales, Centre de Recherche de Péchiney, Voreppe) the reason for this alteration was discovered: under the influence of the high electric field between the strips, the composition of the glass substrate changed by ion migration. By means of a thermal treatment, we are now able to reproduce exactly these long-term alterations in the space of a few hours.

The 50 plates for the detector had already been fabricated. In order to save these 50 plates, it was attempted to coat the surface with thin electronically conducting layers. The performance of about 20 test MS-plates with different coatings made by "Schott, Mainz, Germany" and by the "Lab. Matériaux et Génie Physique, ENSPG - INPG, Grenoble" has been examined. These investigations are not yet finished. Meanwhile an absolutely stable glass substrate with only electronic and no ionic conductivity has been identified and tested with test MS-plates. The pulse height does not change even after long thermal ageing and with

extremely high count rates. The results are in accordance with those from other groups which are developing MS-plate detectors.

For the new prototype detector, three MS-plates on this substrate are assembled and the detector will be tested rigorously when the first neutron-beam becomes available. Despite some promising results with the surface coating, the safest way to build a reliable detector for the D20 instrument is to order and manufacture new MS-plates.

In the meantime the complete electronic and data storage system for D20 (see Fig. 16 on page 149) have also been finished and are ready for use.

For the construction of gas detectors and their further improvement, precise information on electric field distribution is absolutely necessary. A computer programme (ELFI), which has been developed by Siegen University and takes into account materials of different conductivity, has been successfully used to modify some details of the internal detector arrangement.

Moreover, a new amplifier and discriminator module have been developed for series production in order to replace, over the coming years, the amplifiers designed 20 years ago. These modules allow a coaxial cable length of more than 6 meters between counter tube and amplifier.

Multilayer/Optics Laboratory

(I. Anderson, O. Schärpf (*on retirement*))

The group continues to operate two evaporators and an RF sputtering facility together with the ancillary analysis equipment. We were pleased to welcome Peter Høghøj who joined the group in July after finishing his thesis studies on X-ray multilayers at the ESRF. We are also grateful for the untiring support of Otto Schärpf whose presence is a huge asset to the group.

The group had three major goals to fulfil during 1994:

- 1) The continuing production (by evaporation) of the standard "ILL" polarisers for IN11.
- 2) Development of a process on the sputtering facility for producing improved polarisers.
- 3) Development of multilayer monochromators with good wavelength selectivity.

The production of the Co/Ti polarisers has continued almost exclusively on the Electrotech evaporator which, unfortunately, after 10 years of operation is beginning to show its age as the control electronics become less reliable. Intermittent faults slowed down production considerably during the latter half of the year. The evaporator will be shut down at the end of the year for the control electronics to be replaced. During this time routine production will be taken over on the Riber machine.

Although the qualities of the "ILL polarisers" are well known and appreciated by the numerous users in various laboratories it is true that the production methods have not changed for many years. On the other hand there is a demand for polarisers with improved efficiency at short wavelength and for multilayer monochromators with small d spacing, which cannot be met using the present evaporation techniques. Hence the multilayer group has taken advantage of the period without neutrons to develop sputtering techniques for the production of small d-spacing polarisers and monochromators.

Significant progress has been made in this direction as can be seen from the X-ray reflection profile from a constant period Co/Ti multilayer shown in Fig. 17. The results demonstrate that well defined thin layers can be produced with interface roughness of the order of 7 Å, however without neutrons we have been unable to test the reflectivity and polarisation efficiency of the multilayers

We look forward to the new year when the progress made during the present year can be put to the test with neutrons.

Sample environment laboratory

(S. Pujol)

Cryogenics

(D. Brochier (*left on early retirement*), S. Pujol)

Standard Cryogenics

All storage vessels for liquid helium and liquid nitrogen have been inspected, tested, repaired when necessary, and are being put into service according to requirements.

The loaned standard cryostats have been taken back. A campaign of modernisation and tests of all the standard "orange" cryostats is being terminated. Some improvements, such as remote control to the cold valve, have been fully and

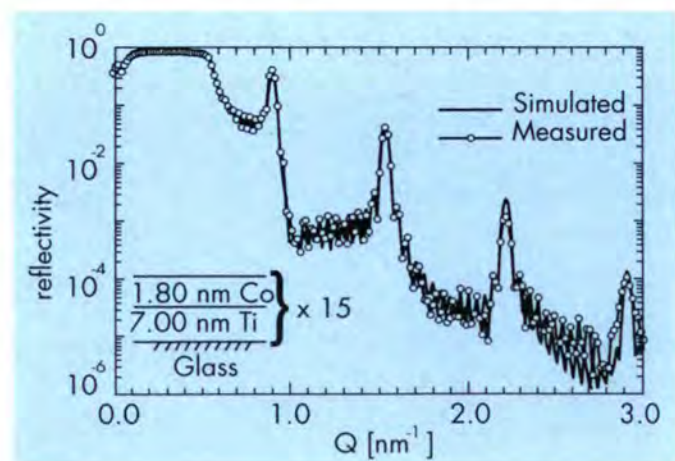


Fig. 17: Measured and fitted X-ray reflection profile from a Co/Ti multilayer.

successfully tested in laboratory, but are not yet installed on all cryostats. In fact the first 15 of them will be tested under real experimental conditions.

The servicing of all ILL's cryo-refrigerators has been carefully continued, with the clear purpose of saving liquid helium in the future.

The liquid helium servicing and the helium gas recovery management have been reorganised to improve efficiency and minimise losses.

A vacuum chamber adapted to a Leybold cold heart has been mounted for neutron experiments at the GEEL LINAC (GELINA) in Belgium in the framework of a collaboration project.

Very low temperatures

In cooperation with CRTBT a prototype of a spatial dilution refrigerator (not sensitive to gravity) has been mounted, for bolometric measurements at 100 mK, on the telescope in Testa-Grigia (Italy). The same technical principles are used to obtain very low temperatures on 4-circle diffractometers in ILL.

The work on these completely new dilution cryostats has been the subject of Serge Pujol's thesis.

The double stage dilution refrigerator (on loan to CENG) has been repaired. An improved version of this cryostat with better heat exchangers is being assembled. A significant gain in cooling time and ultimate temperatures is expected, as well as a more user-friendly operation.

The dilution refrigerator built in cooperation with H. Godfrin (CRTBT) has been tested. Temperatures of 5.2 mK have been obtained in the laboratory. Suitable thermometers have been calibrated, versus NBS fixed points and CMN salt. The cooling power has been measured.

Superconducting magnets

After a loan to LLB, the TAS magnet has revealed a serious default (quenches at about 4.3 T for a nominal field of 6 T). This cryostat was returned to the manufacturer for diagnosis and repair in March 1994. There is some hope to have it in operation for the reactor restart.

The horizontal magnet (5 T) and the vertical 7.3 magnet have been tested.

The Zeeman magnet (7 T, horizontal field, clear bore at room temperature) has been fully tested.

The spin echo IN20 precession OFS (Optimal Field Shape) magnets have been test-run for a long period of time (the system has its own refrigerators and needs no cryogenic liquids).

A small magnet (2.5 to 3 T) asymmetric for polarised neutrons, with a gap of 35 mm, and a clear bore of 58 mm) has been designed and ordered. It will be mounted in a standard orange cryostat, allowing the standard 49 mm diameter.

Thermometry and electronics

Most of the electronic equipment directly associated with sample environment has been tested and repaired as required. In particular 6 liquid nitrogen (LN₂) automatic refill controllers were repaired and 21 of the original ILL Precision Temperature controllers were checked, recalibrated and repaired as necessary.

The prototype of a new LN₂ capacitance level gauge has been built. It appears to give good results but will have to be tested further to establish its stability and reliability.

The helium reservoir level gauges have been re-examined after a number of years service. Some improvements to increase reliability and autonomy have been identified and will be implemented.

Five pre-production models of the new Sample Environment Controller (ILLSEC) have been purchased by the ILL and CENG. They are soon to be tested under real experimental conditions using an initial version of the software which will be improved and modified according to the initial results and users' comments. During the summer, work on a self-adapting control algorithm was carried out by a student from the Laboratoire d'Automatique de Grenoble. This work, which was awarded a prize by the SEEE, established a solid base on which to construct a truly self-adaptive algorithm to control the sample temperature of ILL cryostats.

Cryogenic fluids

The LN₂ supply at the different sites of the ILL has been put back into operation.

The reactor now has its own N₂ Gas supply, installed to avoid interference with the LN₂ supply for the experiments inside the reactor building.

The LHe distribution has been slightly modified. The content of the LHe vessels is now measured with a high precision scale. LHe can be ordered via ethernet.

LHe consumption has been low (< 10 000 litres) due to lack of experimental activity.

Gaseous He from ESRF cryostats will in future be recompressed at ILL and sent to the liquefier station. The corresponding plumbing, gas meter, and purity analysis are operational.

High Temperature - High Pressure

The activities of this group were slowed down due to the reactor refurbishment for which manpower had been drained from the group for most of the year.

Furnaces

10 new normalised power supplies for the standard furnaces have been built and successfully tested.

The 1200K furnace with its 3-ton uni-axial pressure rig for the ILL monochromator group has been built and will be slightly modified. Its power supply is ready for use.

The furnaces for IN10C, IN5 / IN6, IN11 and their power supplies are modified to comply with the new standards.

3 standard 2000K furnaces, 2 'A.Wright'-type furnaces, and their power supplies are ready for use.

After the move-out of the high pressure laboratory the furnace lab has been rearranged in a more efficient manner.

Future projects include a 3 000 K furnace which can be used for long experiments.

Two mirror furnaces have been completed for delivery to outside laboratories.

High Pressure Sample Environment

The technician in charge of the high pressure equipment was busy with the reactor repair for the first 7 months of the year.

High pressure equipment which had been let to the Labor für Neutronenstreuung ETH Zürich, in particular pressure cells, a 15 kbar pump, an orange cryostat, a high pressure He gas generator and electronics, has been recuperated.

The high pressure laboratory has moved into a new, larger area. The inventory has been completed, and most of the equipment is ready for the forthcoming high pressure experiments.

Further development in this field, in particular towards a diffraction cell for pressures above 5 kbar, will be carried out in collaboration with other institutions.

Instrumental Techniques

(B. Hamelin)

As the leader of this group was involved in the repair of the reactor (D₂O-H₂O components and mechanical strain studies in the 'Project Group'), it only really started its activities at the beginning of September 1994.

The group was set up recently within the Development Branch with the aim of providing technical support for the improvement of instruments or the development of new ones.

The idea governing its activity is to be particularly attentive to the needs and requests of the scientific community with regard to the neutron beams and instruments, and also to coordinate the different needs, if necessary.

It should not be considered as being in competition with the other groups and services but rather as a support group providing engineering and technical studies, construction of prototypes and test analyses.

A first field of activity has now got under way:

- Neutron beam optics:

a) Better knowledge of characteristics (mapping of neutron flux, mapping of energy spectrum distribution).

b) Testing and development of high-sensitivity thermal neutron cameras for high resolution (0.2 mm) imaging applications (neutron topography, real-time sample orientation with neutron Laue diagram, beam and sample control, etc.) to replace cumbersome photographic plates.

- Sample environment:

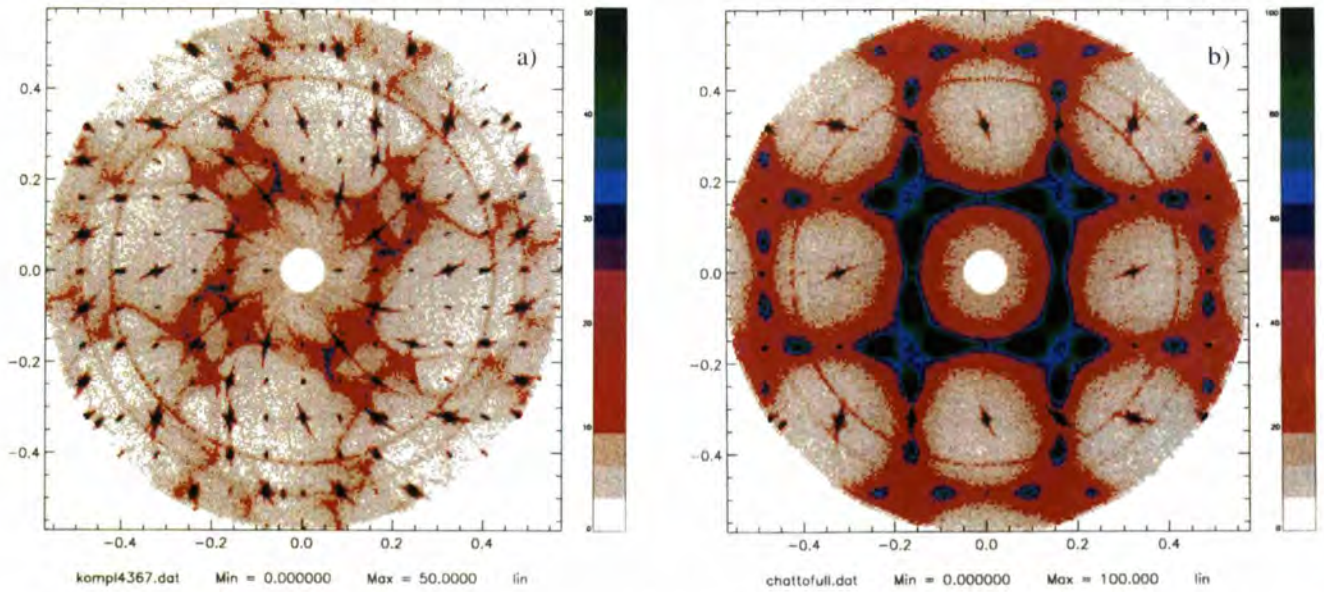
Development of small size mechanical devices for particular applications (sample orientation in cryostats, high-precision orientation devices for interferometry, special coils for Spin Echo, etc.).

- Hard X-ray laboratory: A fine-focus hard X-ray source, used in conjunction with high resolution two-dimensional X-ray detectors and cameras, has useful industrial applications, such as fast testing of single crystal turbine blades. The same techniques can be used for γ -ray like diffractometry. The implementation of such a Hard X-ray laboratory at ILL has been proposed.

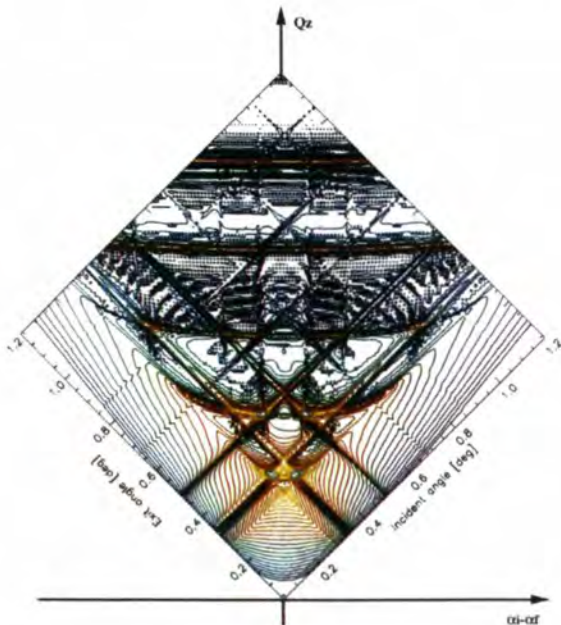
Technical support for 1994:

Thanks to the efficient work of the group's draughtsman, several studies were undertaken to improve the sample environment:

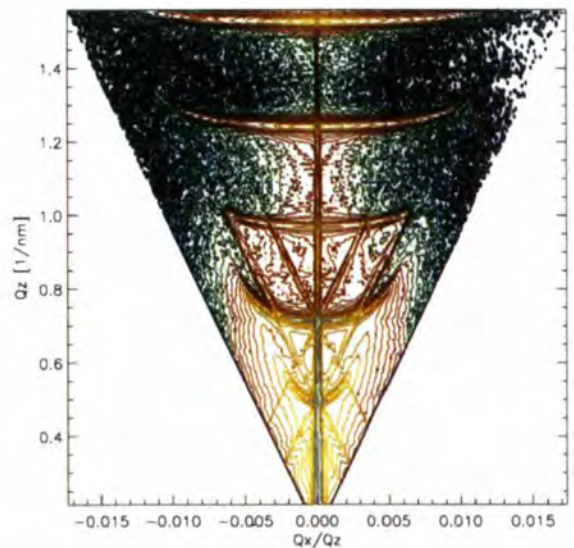
- D20: mechanical structure for the multidetector.
- Adaptation of the ILL cryostat to 4-circle devices.
- Study of a special hot press for the Monochromator Group.



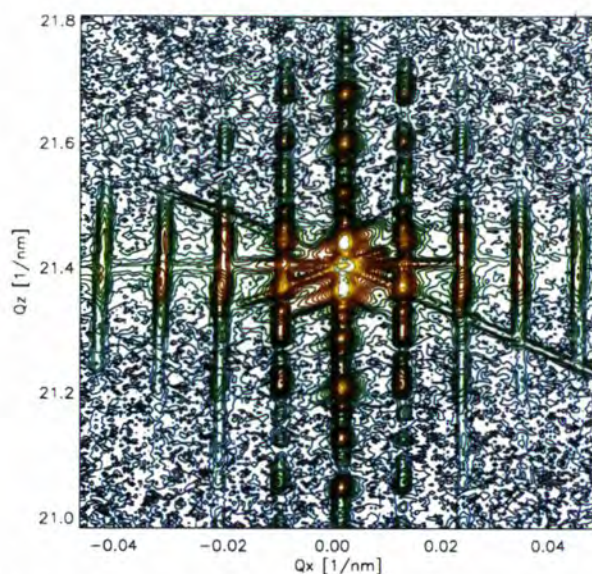
Coll. 5 - Fig. 3: Scans of the hkl reciprocal layer of MnS_2 at (a) $T=8.3$ K and (b) $T=51.9$ K. We have actually performed these scans covering only 200 degrees, the rest has been generated by symmetry. At $T = 51.9$ K which is above the ordering temperature, strong diffuse scattering due to magnetic correlations are observed. The diffuse scattering maxima are centered at incommensurate positions. At $T = 8.3$ K which is below the ordering temperature magnetic Bragg reflections are observed at strictly commensurate positions corresponding to the wave vector $k = (1, 1/2, 0)$. Weak diffuse scattering is also observed along with the Bragg scattering at this temperature. We have interpreted this diffuse scattering to be due to magnetic excitations in the ordered magnetic phase. See report p. 51.



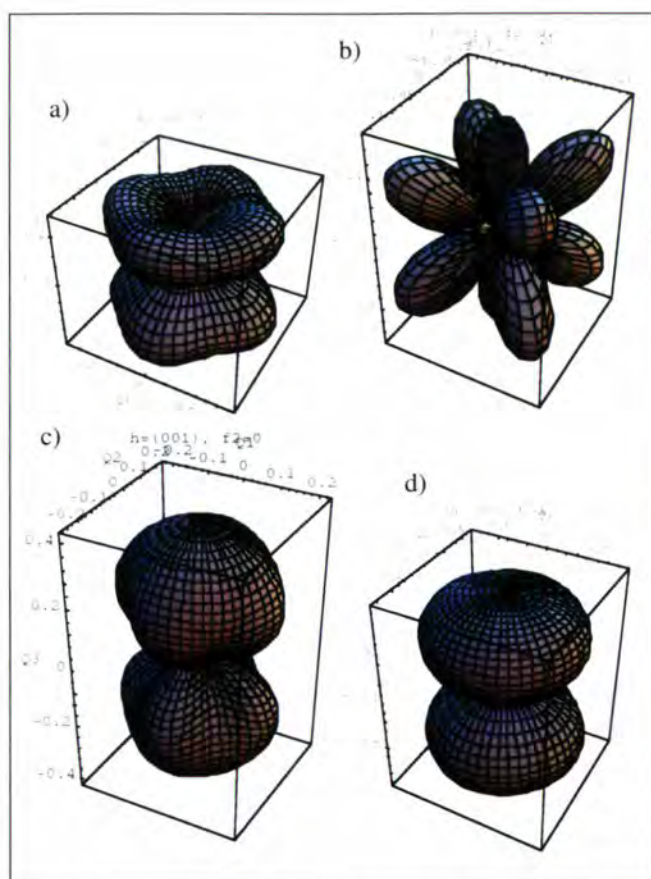
Coll. 6 - Fig. 4: Contour plot of a calculated $(Q_z, \alpha_i, \alpha_f)$ -mapping; (220) GID-intensity from a GaAs/AlAs-superlattice; α_i and α_f are the angles of incidence and exit. There are the bent transversal sheets of "true diffraction satellites" and the grid of Bragg-like peaks due to simultaneous interface reflection. See report p. 62.



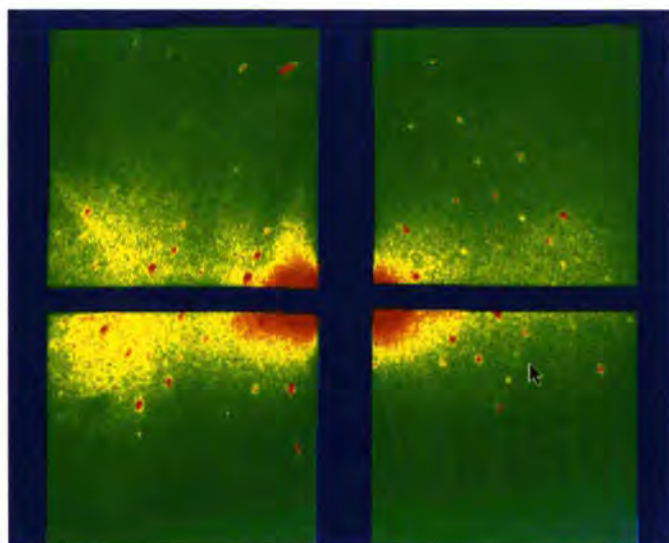
Coll. 6 - Fig. 5: Contour plot of a NSXR- $(Q_z, Q_x/Q_z)$ mapping from a GaAs/AlAs superlattice near 000. The transverse sheets of resonant diffuse scattering cross the 000 truncation rod in the superlattice satellites. See report p. 62.



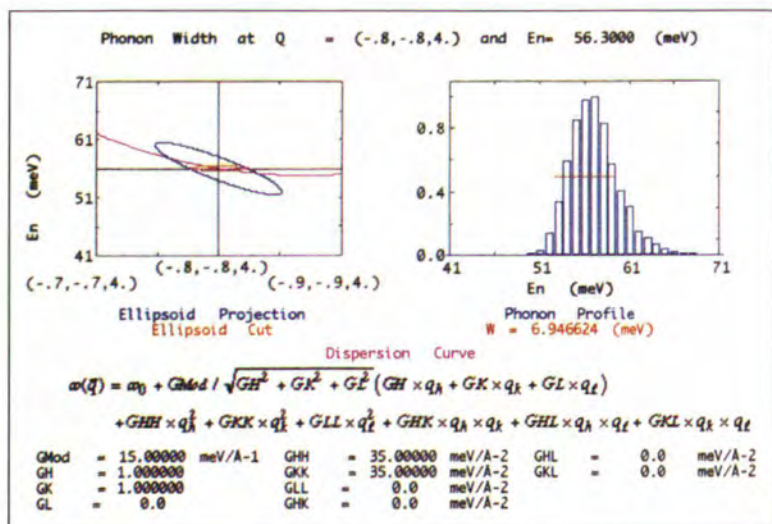
Coll. 6 - Fig. 6: Contour plot of a Q_z/Q_x -mapping from a (Galn)As/InP multilayered surface grating. The fine structure with the equidistant truncation rods is the evidence for the surface grating structure. See report p. 62.



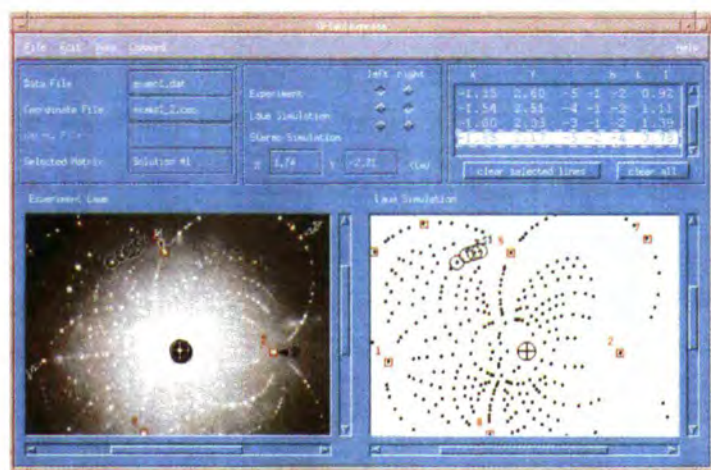
Coll. 6 - Fig. 11: Iso-intensity plots of the symmetric Huang diffuse scattering at the (001) reciprocal lattice point for deuterium occupying tetrahedral sites in yttrium. The calculations were made assuming a first Kanzaki force $f_1 = 1.0 \text{ eV \AA}^{-1}$ and a) $f_2 = -1.0 \text{ eV \AA}^{-1}$, b) $f_2 = -0.5 \text{ eV \AA}^{-1}$, c) $f_2 = 0 \text{ eV \AA}^{-1}$ (ie cubic) and d) $f_2 = 1.0 \text{ eV \AA}^{-1}$. See report p. 65.



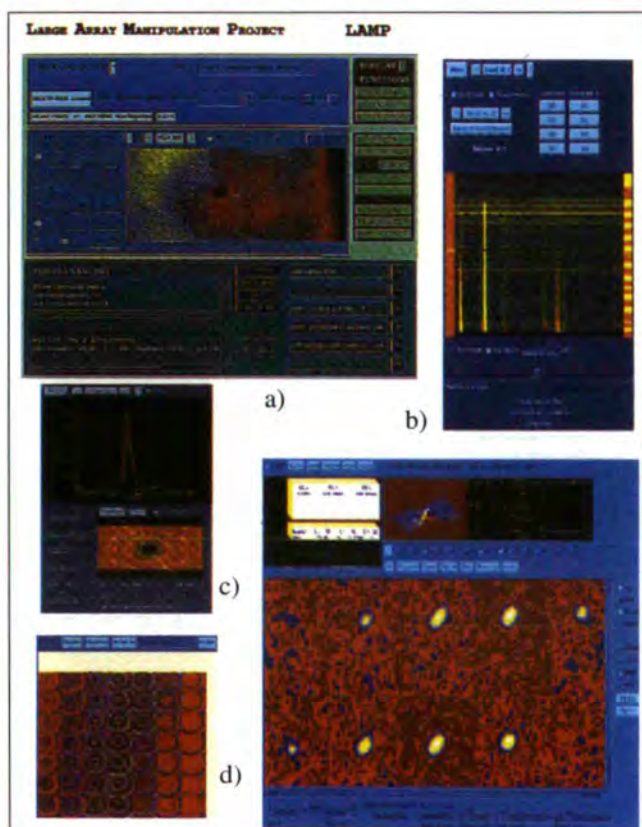
Coll. 8 - Fig. 1: Crystal of triclinic hen egg-white lysozyme oscillated 6° around the rotation axis of the EMBL cylinder image plate detector placed on TAS7 at Risø ($\lambda = 3.5 \text{ \AA}$). Measurement time: 5.5 hours. The diffraction pattern is seen on 4 individual image plates, taped onto the forward scattering part of the detector and covering $\pm 72^\circ$ from the horizontal plane. This corresponds to d -spacings of 3 \AA at the top and bottom edges. See report p. 77.



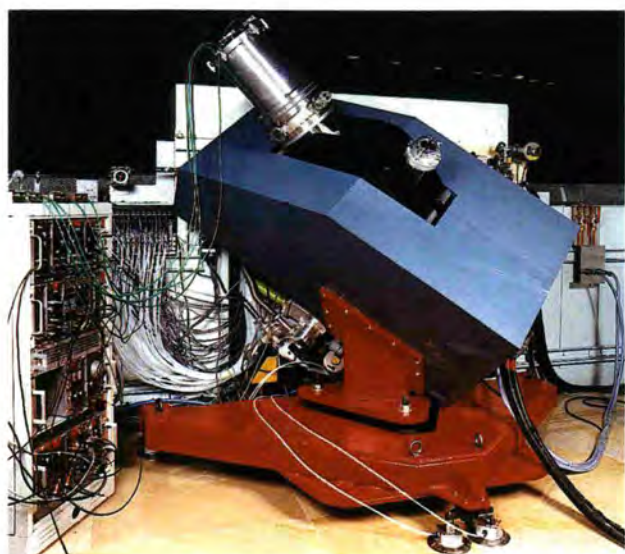
DS-Scientific Computing - Fig. 1: The display for calculation of the resolution function in **PKFIT**, showing the dispersion curve and resolution ellipsoid obtained from a Monte Carlo simulation. The result of folding a phonon with this resolution function is shown with the parameterised equation for the dispersion curve below. See report p. 101.



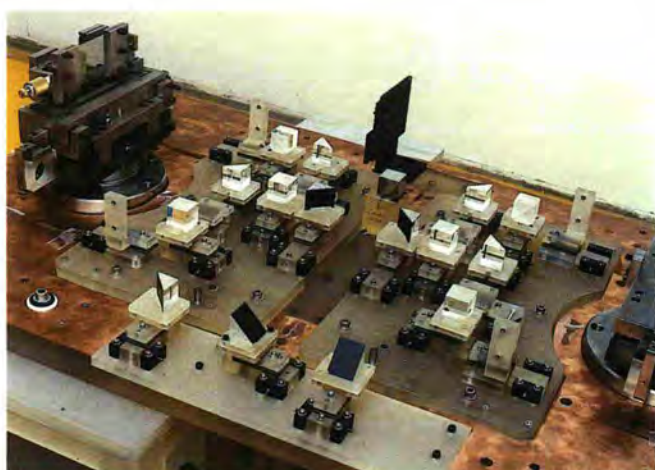
DS-Scientific Computing - Fig. 2: The top-level window of **OrientExpress**. See report p. 101.



DS-Scientific Computing - Fig. 3: The **LAMP** project. (a). The main user interface with a simple display of a data buffer. (b). A specialised interface for defining filters and groupings for time of flight data. (c). A specialised interface for radial integration and mask definition for small-angle scattering. (d). A full display of spin echo calibrations. (e). The **SCAN** interface for image manipulation showing D19 single crystal data. See report p. 101.



DS-NFP - Fig. 1: The RED-magnet installed at the Lohengrin exit slit. The support frame is mounted on an air-pad system to provide an easy positioning and to give the possibility of having access to the old focal plane. Attached to the exit flange of the vacuum chamber of the RED-magnet, there is the new E- ΔE ionisation chamber where the trajectory of the incoming fission fragment can also be determined. Part of the control unit of the new thirteen shutters diaphragm and of the modified vacuum system is also visible. See report p. 103.



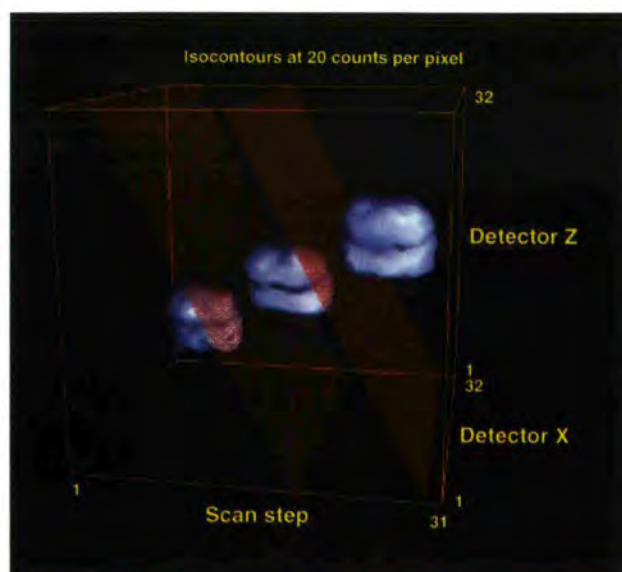
DS-NFP - Fig. 2: View of components of GAMS5 Twin Interferometers, with one of the bent crystals and its mounting visible on the left hand side. The optical components are mounted on supports made from ZERODUR ceramic, in order to reduce thermal effects. See report p. 103.

DS-DIF - Fig. 1: Graphical user interfaces and applications for the analysis of diffraction data. Clockwise from top left:

- *) DIB time resolved data visualized with SGI-Explorer (G.J. McIntyre).
- *) An SGI-Inventor application with MetaCard interface for plotting 3D crystal structures, showing.
- *) The structure of $AlPO_4-18$ (Marc Hewat).
- *) A MetaCard/pgplot interface for retrieving and displaying powder patterns (M. Knapp).
- *) A simple Motif program for listing scan parameters (G.J. McIntyre).
- *) A MetaCard interface to Lazy Pulverix for calculating powder patterns (A.W. Hewat).
- *) D19 single-crystal position-sensitive detector data with SGI-Explorer (G.J. McIntyre).
- *) The 3D structure of ferroelectric betaine phosphite visualized with Cerius 2. See report p. 106.

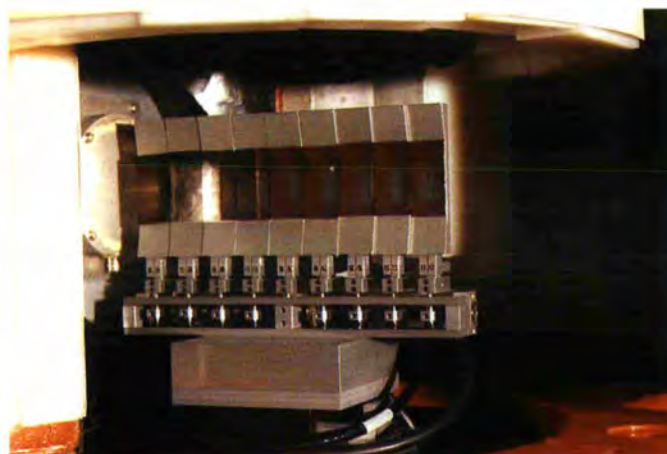


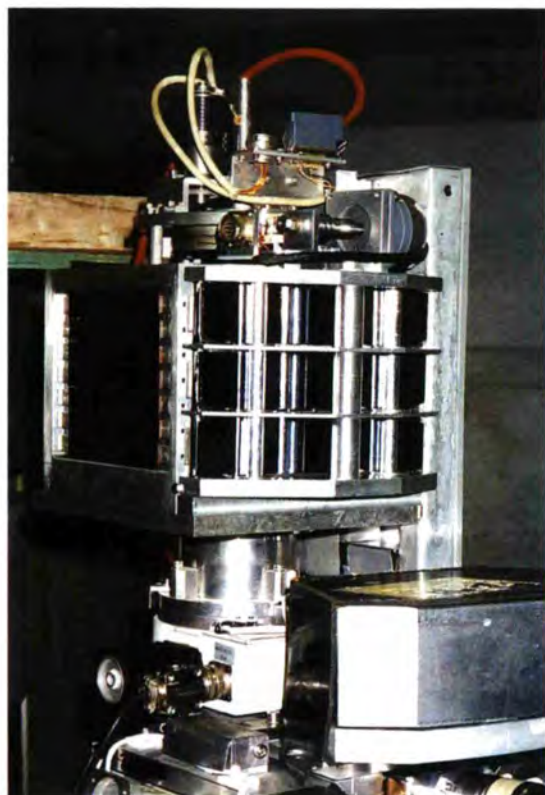
DS-DIF - Fig. 2: The reflections $[5\ 3\ l]$ with $l = 11$ to 13, from monoclinic $MgSO_4 \cdot 6H_2O$ observed on E5 at HMI with D15's position-sensitive detector. The c axis of the primitive cell is $24\ \text{\AA}$, and the wavelength is rather short $0.90\ \text{\AA}$, yet the detector allows the reflections to be integrated without bias from neighbouring reflections. The planes indicate the limits of the integration volume for the central reflection. See report p. 109.



DS-LSS - Fluids spectrometer RFS II rheometrics. See report p. 112.

DS-TAS - Fig. 1: General view of the new horizontally focusing analyser of IN8 mounted in the analyser housing. Mirrors have been mounted in the position of the pyrolytic graphite pieces for optical prealignment. See report page 113.

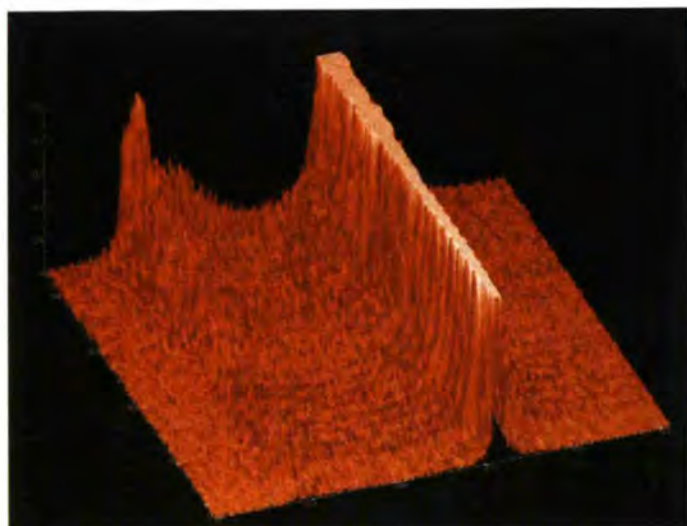




DS-TAS - Fig. 2: The new horizontally and vertically focusing Si (111) monochromator built into the IN20 carousel between the pyrolytic graphite (left) and Heusler (right) monochromators. Each of its three stages contains a sandwich of two elastically bent silicon plates of $200 \times 40 \times 4.5 \text{ mm}^3$. Horizontal curvature is controlled by the stepping motor and gear placed on the top of the holder. The front faces of the top and bottom pairs are inclined by 3.2° with respect to the (111) plane to provide fixed vertical focusing. See report page 114.



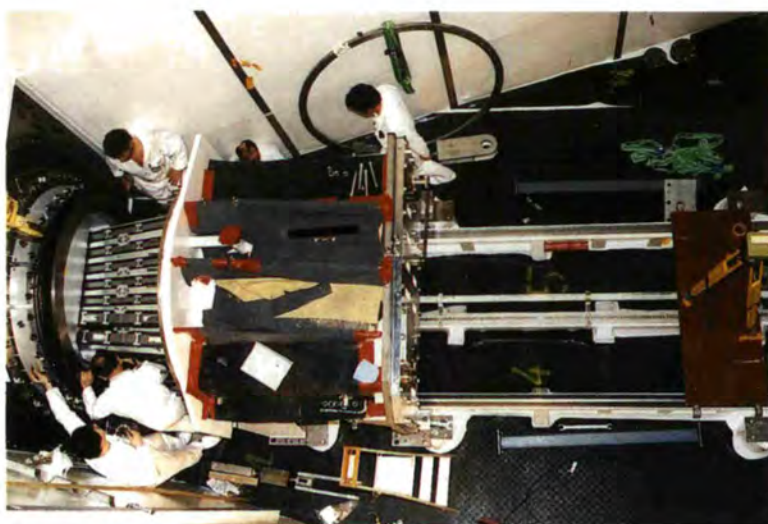
DS-TAS - Fig. 3: C. ZEYEN with S. WATANABE and Pr. KAWARAZAKE setting-up the spiral correction coils for the OFS precessions coils (red cylinders). See report page 115.



DS-TOF/HR - Fig. 1: Time-of-flight spectrum from lyophilized Bacteriorhodopsin ($h = 0.02 \text{ gD}_2\text{O/g protein}$) measured on IN6 at ILL. The incident wavelength was 5.12 \AA . Scattering angles are between 10° and 110° . The elastic peak (situated near channel 300, i.e. near $1200 \mu\text{s/m}$) has been truncated for clearer viewing. See report page 120.



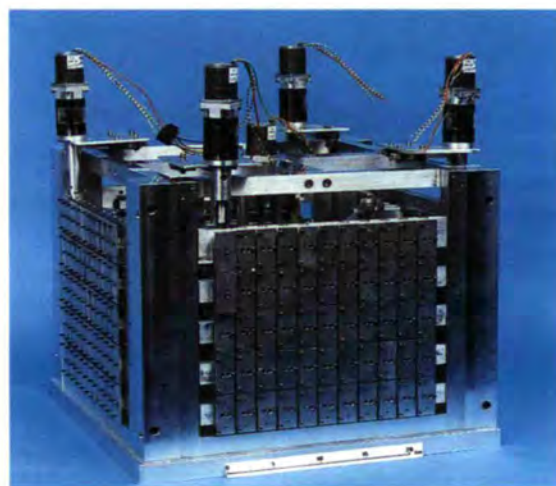
DPT - Fig. 1: The housing of the in-pile part of H1-H2 neutron guides under pressure test at the manufacturer. See report p. 128.



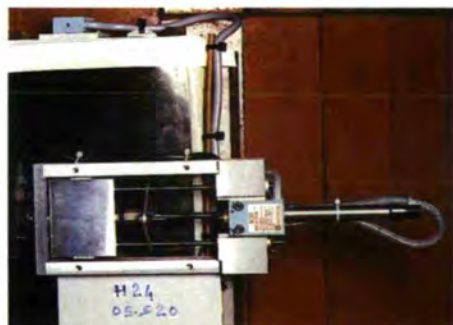
DPT - Fig. 2: The housing and the mechanical supports during the final mounting in the swimming-pool H1-H2 March 1994. See report p. 128.



DPT - Fig. 3: The housing of the mechanical support in place on the H1-H2 beam tube. See report p. 128. On the left hand the blanks for the NG12 and NG13 guides, on the right hand the blank of the H18 guide. These guides are not mounted in the out-of-pile part.



DPT - Fig. 4: The four-face monochromator exchanger for IN4C, constructed in Italy. Each face has 5 x 11 orientable elements for obtaining the double curvature. See report p. 128.



DPT - Fig. 5a: New beamshutter. See report p. 128.



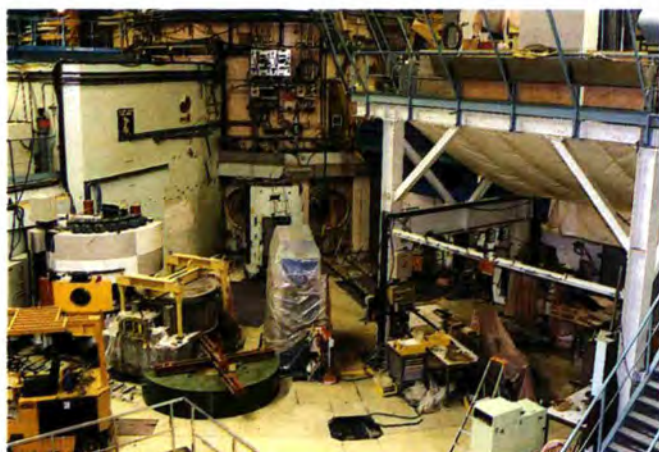
DPT - Fig. 5b: New beamshutter control box. See report p. 128.



DPT - Fig. 6a: Beam Holes H9, H10 and H11 before the reinstallation of the instruments. See report p. 129.



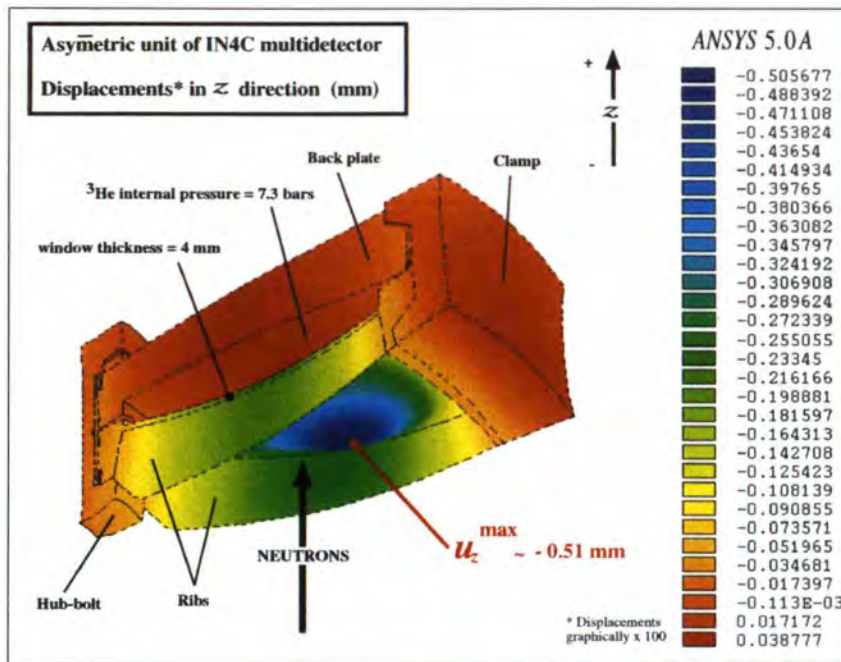
DPT - Fig. 6b: Beam Holes H9, H10 and H11 after the reinstallation of the instruments Lohengrin, IN8 and D20. See report p. 129.



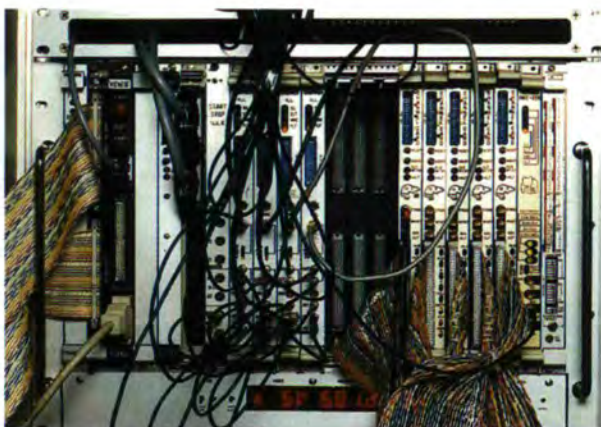
DPT - Fig. 7a: The instrument sites of D3 and D9 before the reinstallation. See report p. 129.



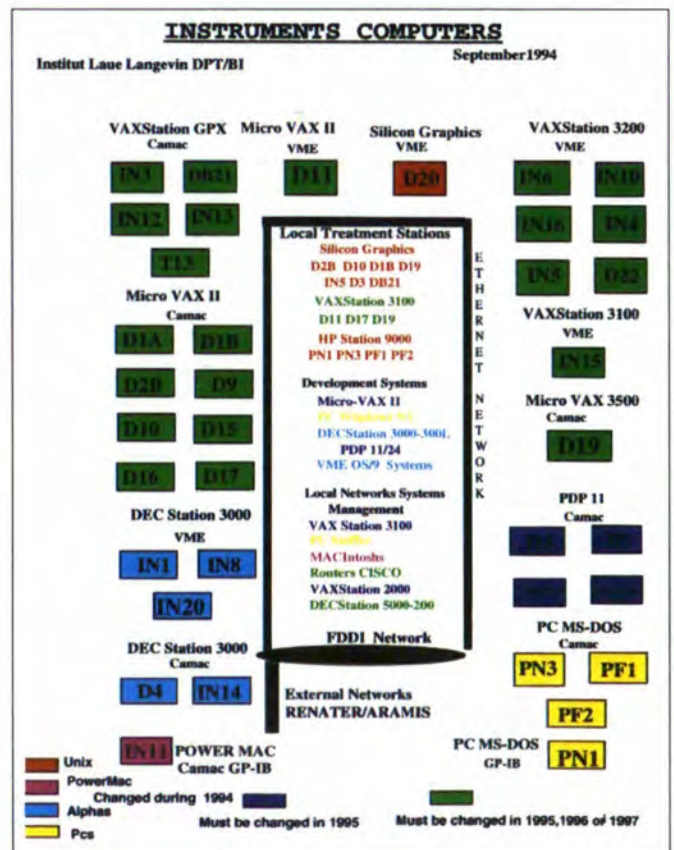
DPT - Fig. 7b: The instrument sites of D3 and D9 after the reinstallation. See report p. 129.



DPT - Fig. 8: Shows the calculated field of displacements of the asymmetric unit of the IN4C small-angle multidetector. See report p. 131.

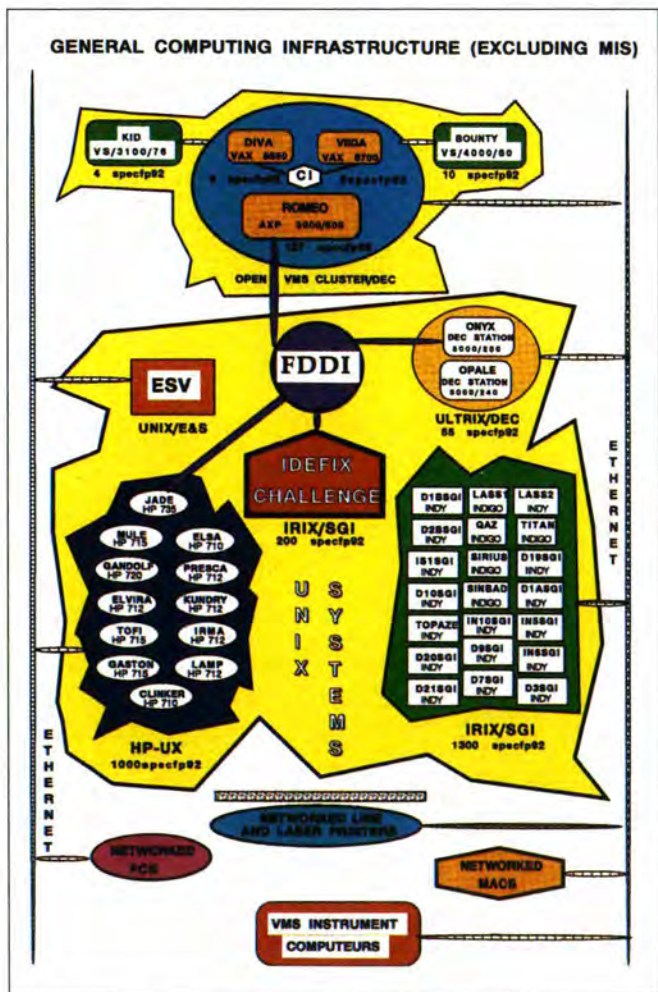
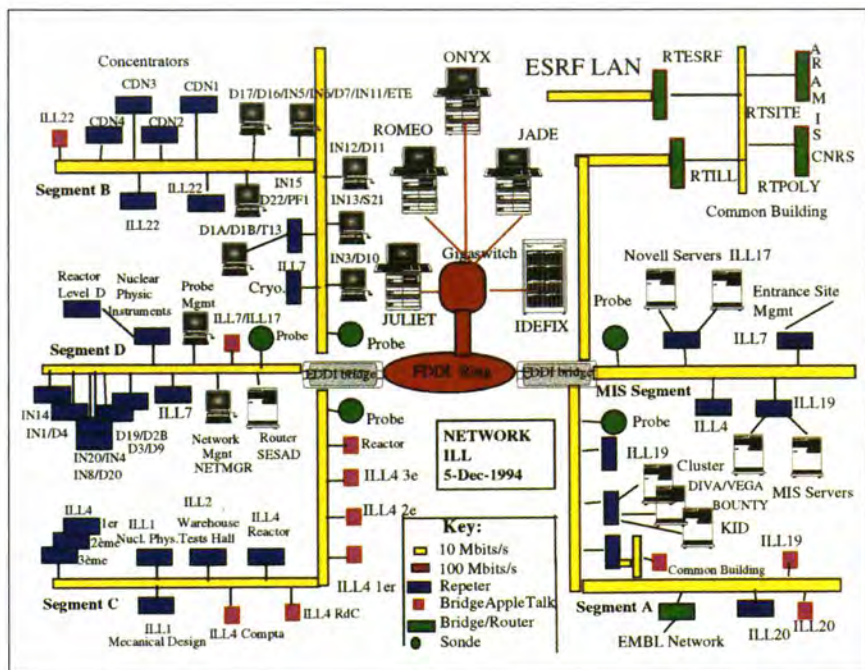


DPT - Fig. 9: VME electronics of IN5 See report p. 131.



DPT - Fig. 10: ILL instrument computers end of 1994. See report p. 131.

DPT - Fig. 11: ILL computing network. See report p. 132.



DPT - Fig. 12: The hardware Infrastructure end of 1994. See report p. 132.



DPT - Fig. 16: D20-PSD dedicated electronics and data acquisition system. See report p. 136.

- From top to bottom:
- André RAMBAUD, who is nursing these electronics
 - 50 boxes of 33 amplifiers and discriminators each
 - 5 racks containing the 50 units of the logic system and low voltage power supplies
 - 5 VME racks containing the 50 units of the data acquisition system.

REACTOR DIVISION (DR)



In 1994, the lion's share of the Reactor Division's work was devoted to completing the reactor refurbishment and the restart.

By the beginning of the year, all the major parts had been delivered, with the exception of the reactor vessel, the D₂O collectors and the coupling sleeves. The swimming pool was controlled, cleaned and made ready to receive the new structures. The cutting-up and disposal of the old structures was under completion.

The Reactor Division crews had been complemented by the Project Group and the Industrial Architect, but direct work on the reactor was essentially entrusted to ILL teams, working within the framework of the ILL Quality Assurance system.

The centrepiece of the reactor refurbishment work was the new vessel; the key operations were its installation in the swimming pool and the connection of auxiliary equipment.

The new vessel arrived by special convoy on the evening of 23 February 1994.

Figure 1 shows the transport vehicle and the case containing the vessel in front of the reactor building.



Figure 2 shows the vessel just after its introduction into the reactor building through the lorry gate. Rotating the vessel into its vertical



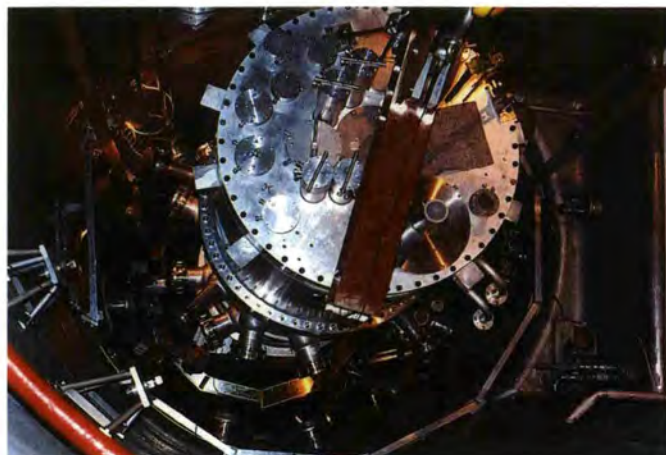
position was a particularly delicate operation, with the loads taken simultaneously by the main reactor crane and a mobile crane (Figure 3).



Figure 4 shows the assembled vessel stored on Level D of the reactor building before its final installation in the swimming pool.



Figure 5 shows the swimming pool prior to the installation of the vessel. Note the covered channels through the reactor pool - the coupling sleeves that will contain the beam tubes will be moved in through these channels and connected to the vessel.



In Figure 6a we can see the reactor vessel being lowered into the swimming pool. In this context, we came across a photo (Figure 6b) from 1970 in the ILL archives, showing the assembly of the first reactor vessel inside the swimming pool.

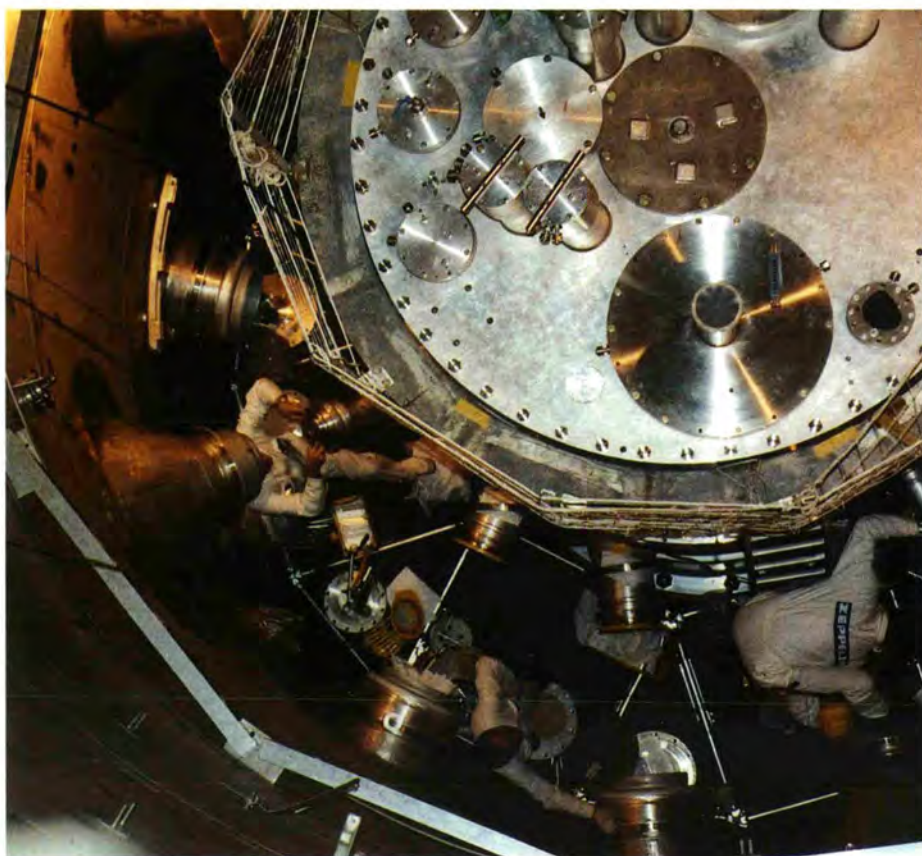


Figure 7: A first series of checks shows the perfect alignment of the vessel extrusion axes and the reactor containment channels.

The final weld connecting the vessel to the control rod sleeve was to be carried out in situ.



Figure 8 shows the bottom of the vessel placed on supports with a template used to adjust the sleeve with respect to the vessel axis. Figure 9 shows the same sleeve undergoing leak tests just after welding.



The front flange of each coupling tube had to be connected to the vessel extrusions using a coupling sleeve.

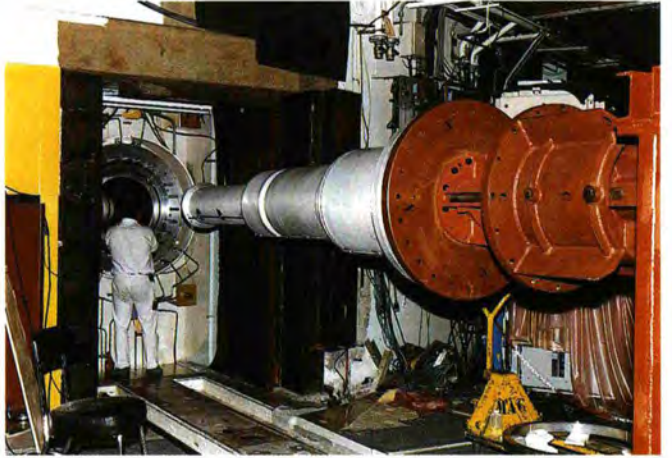
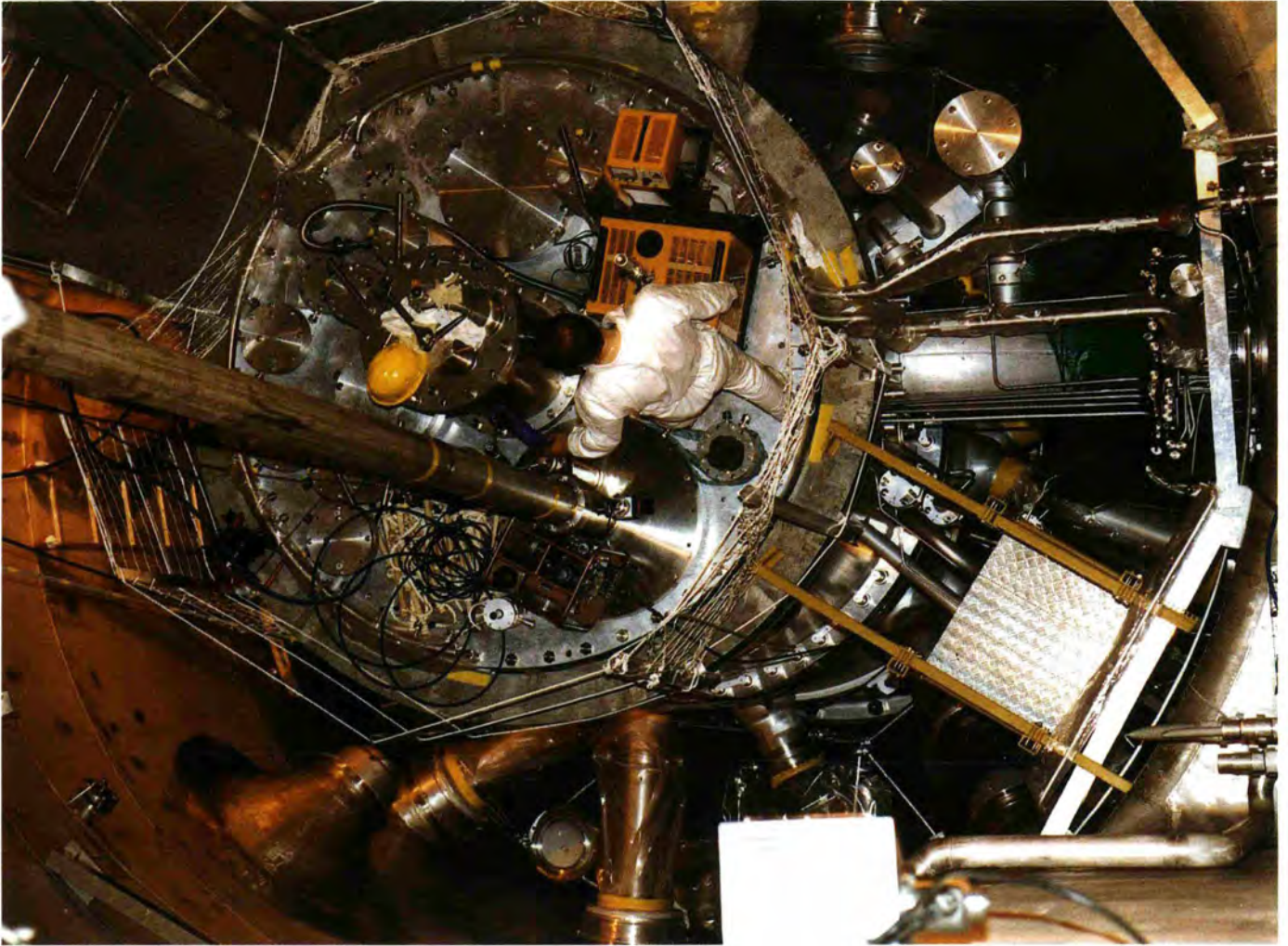


Figure 10 shows a coupling sleeve and tube ready to be fitted, mounted on the handling gear outside the swimming pool in the experiment hall.

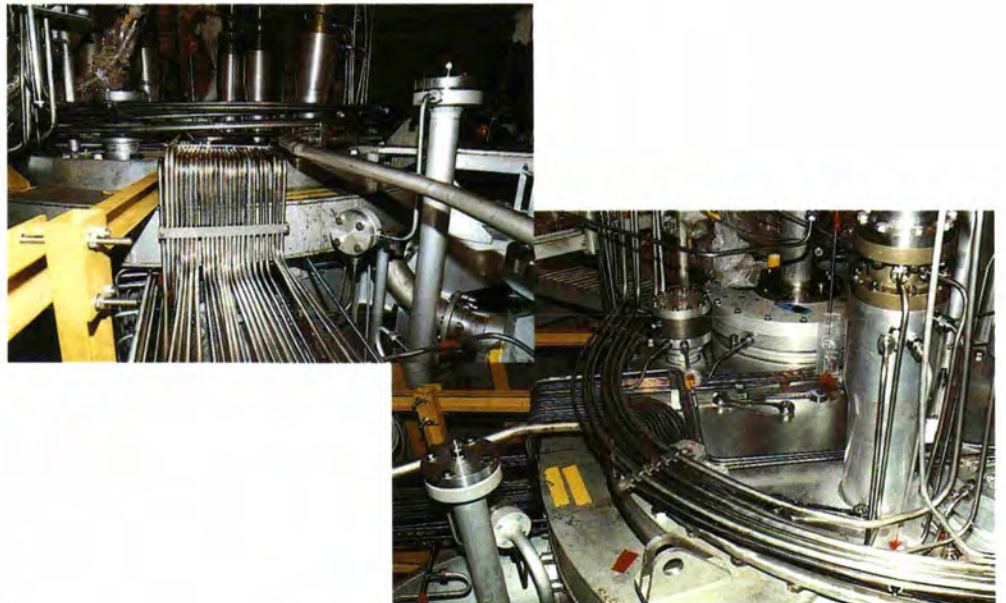


In Figure 11, the front section of the coupling sleeve is being moved towards the vessel extrusion, while an operator checks the alignment of the two parts. Leak tests were carried out after every such assembly operation.



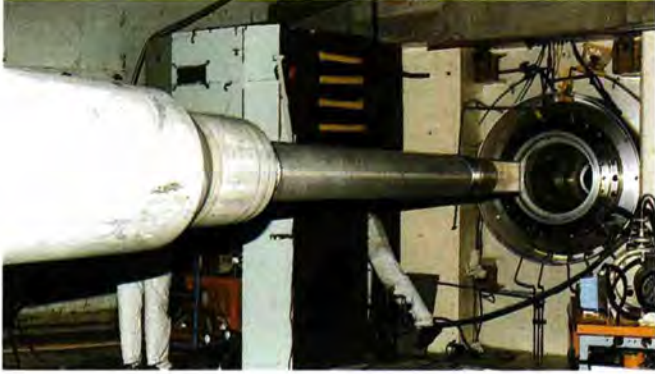
On Figure 12 can be seen the upper section of the vessel with control devices and several assembled coupling sleeves in the process of being checked.

The reinstallation of all the auxiliary equipment needed for the reactor to operate, as seen on Figures 13 and 14, was a major task.



Another important phase was the insertion of the beam tubes (thimbles), while the rear flange was being connected to the outer end of the corresponding reactor containment channel.

Figure 15 shows a rectangular beam tube ready to be inserted.



After completion of all these assembly and control operations, the assembled reactor was as shown in Figure 16.



The “new reactor” is identical to the “old” one, except for the anti-turbulence grid, which has been replaced by a smaller-dimension “turned-down” grid that can be removed without opening the vessel. The hydraulic performance levels of the new grid (Figure 17) are comparable to the old one’s, thanks to a system of holes and slits ensuring the smooth flow of water inside the vessel.

Most of the old parts were replaced, with the exception of the horizontal cold source, the vertical cold source with its zircaloy beam tube, and the hot source. Sub-assemblies such as the safety and control rod mechanisms were completely overhauled.

Operating tests showed that the hydraulic performance levels of the new reactor were similar to those of the old one. The water flow-rates, pressure drops and vibratory behaviour of the structures proved to be satisfactory, and the reactor was thus pronounced “technically ready” on 27 July.

In parallel to the technical work, steps were being taken to push ahead with the licensing procedure. This involved a public enquiry between 9 May and 10 June, which resulted in the Enquiry Commission giving its approval. The draft decree was examined and finalised by an Interministerial Commission on 13 September, and signed on 6 December. The authorisation to load the fuel element, to start up the reactor and to resume normal operation was issued on 30 December 1994, reaching ILL on 3 January 1995.

Finally, the reactor restarted without any difficulty on 6 January 1995 and nominal power was reached on 7 January.

ADMINISTRATION DIVISION (DA)

Providing maximum administrative support to the reactor refurbishment and the instrument reinstallation was seen by the Administration as its main task. Policy relating to personnel, purchasing and all other administrative services were singularly focused on meeting these priorities.

The reorganisation of the Institut that took effect on 1.7.1993 has now been successfully concluded in practically all the areas affected. Under this process, a number of technical services (Telecommunications, Management Information Systems, Building and Site Maintenance) were attached to the Administration Division so that it now comprises, in addition to personnel and finance, all technical support functions of a general nature. On the whole, these services' integration into a non-technical environment went ahead smoothly, and no particular difficulties are expected in the future.

The process of reorganisation entailed a large number of internal transfers, which had to be carefully prepared and followed through from an administrative angle. Such measures were the prerequisite for balancing out the Divisions on the basis of reduced staff numbers. At the same time, due to a high number of departures (including early retirements under the FNE programme), the opportunity was seized to conduct a limited campaign of staff renewal.

The Division provided the secretariat for the two meetings of the Steering Committee on 31 May/1 June 1994 in Karlsruhe and on 29/30 November 1994 in Grenoble. The

Subcommittee on Reactor Refurbishment had 4 meetings (17 March, 2 May, 27 July, 22 November). The final report of its Chairman concluded that the project had been completed on schedule and within the planned budget, and that the mandate received by the Subcommittee could be considered as fulfilled.

The Administration Division also runs an in-house Translation Bureau. ILL's very status as a trilingual organisation makes translation an operational necessity, and the service is therefore available to all staff members from all Divisions. Scientific, administrative, financial and legal documents are translated from German, French and English.

The Head of Administration continues to meet regularly with the Directors of Administration of ESRF and EMBL to settle questions of common interest. The Division provided the secretariat for the Management Committee on the extension of EMBL, whose constituent meeting took place on 21 September 1994 in Grenoble and ended with the resolution that France's separate contribution of 7 MF (currently held by ILL) for the extension of the ILL-EMBL building (ILL20) could, in principle, be released. The extension will provide employees and visitors of all three organisations (ILL, EMBL and ESRF) with additional research possibilities. Due to the great synergies offered by the joint use of the new facilities, the ILL Administration was vigorous in its support of the extension right from the outset.

Finance and Management Information Systems

Finance

Implementation of the 1994 Budget

The first priority of the 1994 Budget remained the successful completion of the reactor refurbishment and the expected restart in the second half of 1994. The Institut's other activities aimed at maintaining the existing scientific and instrument potential of the ILL, completing instrument projects and preparing for the restart, in particular as regards the reinstallation of instruments. Total expenditure was originally expected to amount to 316.3 MF, comprising a normal budget of 263.7 MF with one reactor operating cycle, and expenditure for the reactor refurbishment of 52.7 MF which alone represents 16.7 % of the total budget.

The following table shows the changes in expenditure between 1993 and 1994.

Expenditure - Comparison of 1993 and 1994 Budgets

Expenditure	Expenditure 1993		Estimated expenditure 1994		Change %
	kF	%	kF	%	
1. Staff costs	167 223	51.9	181 590	57.4	8.6
2. Fuel elements	6 292	2.0	6 400	2.0	1.7
Consumables	16 271	5.0	21 895	6.9	34.6
Long-term supplies and services	6 380	2.0	8 095	2.6	26.9
Short-term supplies and services	8 038	2.5	11 513	3.6	43.2
Travel	1 643	0.5	2 224	0.7	35.4
Miscellaneous adm. costs	2 483	0.8	3 767	1.2	51.7
Taxes and fees	1 506	0.5	1 680	0.5	11.6
3. Operation	36 321	11.3	49 174	15.5	35.4
Buildings	3	0.0	0	0.0	-100.0
Equipment	2 027	0.6	2 636	0.8	30.0
Instruments	10 617	3.3	12 085	3.8	13.8
Other investments	5 220	1.6	11 804	3.7	126.1
4. Total Investments	17 867	5.5	26 525	8.4	48.5
5. Normal Budget (1-4)	227 703	70.6	263 689	83.4	15.8
Reactor refurbishment:					
6. Setting-up of reserve	(94 600)	29.4	(0)		
7. Expenditure	63 275		52 672	16.7	-16.8
8. Balance of reserve at end of year	31 325		0		
9. Total expenditure (5 + 7 + 8 + 9)	322 303	100	316 361	100	-1.8

The normal budget increased by 15.8 % from 227.7 MF in 1993 to 263.7 MF in 1994.

Staff costs rose by 8.6 % compared to 1993, despite the reduction in staff numbers from 393 to 379 man/year as a consequence of the FNE early retirement programme and despite the reduction in the FNE cost. This increase is mainly due to the recruitment of scientists and excess costs as well as overtime and staggered working hours for the reactor refurbishment and reinstallation of instruments.

Fuel costs slightly increased in line with the budget; these costs included the interim storage of 18 irradiated fuel elements at Cadarache and the production of one fuel element.

The sharp 35.4 % rise in operating costs (13 MF) was caused by the preparatory activities for the reactor restart and by the expected operation of one reactor cycle in the second half of the year, including the preparation of the experimental environment for the restart.

The main increase in ILL's expenditure relates to investments (+ 48.5 %) and more specifically "other investments" (+ 126 % and + 6.6 MF), which correspond to the UNIX conversion programme in computing and the renewal of equipment for the Science and Projects and Techniques Divisions, such as temperature controllers, high-temperature furnaces, equipment for cryogenics, detectors, monochromators, viscometer for chemistry laboratory, etc. Scientific investments increased by 13.8 % to 12.1 MF. Main investment projects are PN2 (GAMS 5), polarised ³He filter, H1/H2 beam tube and H17/H18, detector D20 and IN4C.

The reactor refurbishment has been successfully completed and the Management expects overall external expenditure within the framework of the Project to be 163.1 MF, below the first estimate of 173.1 MF; this includes outstanding payments to be carried forward to 1995 (8.4 MF). This expenditure has been fully financed by the setting-up of a reactor reserve on the normal budgets in 1991, 1992 and 1993.

The Associates' contributions amounted to 252.8 MF which represents 80 % of the ILL's income. The scientific members, Austria, Spain and Switzerland, have signed new contracts after 1.1.1994, extending their scientific co-operation.

As regards other sources of income, the decreased collaboration with E.S.R.F. is linked to the desire for more balanced collaboration between the Institutes, while the ILL's own income decreased because there was less internal production of scientific equipment and less sale of services and technical equipment.

Despite the savings made due to the cancellation of one reactor cycle and the delayed restart, the Associates' contributions have not been revised and the available credits, estimated at 9.1 MF, will be carried forward to the 1995 budget.

Income - Comparison of 1993 and 1994 Budgets

Income	Income 1993 (actual)		Estimated Income 1994		Change %
	kF	%	kF	%	
Collaboration with ESRF	1 833	0.6	1 350	0.4	-26.4
ILL's own income	3 155	1.0	2 550	0.8	-19.2
Spanish contribution	4 859	1.5	4 240	1.3	-12.7
Swiss contribution	0	0.0	6 530	2.1	NC
Austrian contribution	1 620	0.5	5 310	1.7	227.8
Associates' contributions	304 062	94.3	252 839	79.9	-16.8
Carry forward 93/94	-1 979	-0.6	0	0.0	NC
Utilization of interest	3 936	1.2	0	0.0	NC
Carry forward 92/93	1 874	0.6	0	0.0	NC
Provision (utilisation)	2 943	0.9	0	0.0	NC
Carry forward 94/95			-9 130	-2.9	NC
Carry forward of reactor reserve			52 672	16.6	NC
Total	322 303	100.0	316 361	100.0	-1.8

Outlook

The year 1995 is characterised by the restart of the reactor for 5 cycles which will allow the resumption of a normal scientific programme on the basis of 25 scheduled instruments, including a major recruitment effort in the scientific sector. The 1995 budget was adopted by the Steering Committee on 30th November 1994, with a total of 318.2 MF, comprising 24.4 MF investments (10 % lower than in 1994), 18.1 MF investment as outstanding payment for the reactor refurbishment (8.4 MF) and as extra work due to the licensing procedure (9.7 MF), and 30.7 MF for the fuel elements including the purchase of uranium.

Overall survey: The ILL Budget 1995 - 2000

In current prices, the level of the Institut's budget will fall in 1996 and 1997 because there will be less purchasing of uranium, less manufacturing of fuel elements and no more payments for the reactor refurbishment; investments will remain stable at 26.5 MF, i.e. 8.3 % of the budget. After 1997, the slight increase in the budget to around 310 MF will mainly be the consequence of the storage of irradiated fuel and the production of new fuel elements, while other operating costs will remain roughly stable.

Management Information Systems

Joint ILL/ESRF applications

The joint server was upgraded to enhance operating security and to receive the two institutes' new scientific activity management application, which was implemented prior to ESRF's first round of experiment proposal examination. This server now handles site management, medical surveillance and scientific management. The corresponding databases are interactively used by some forty people. On-line consultation via WWW servers has been developed to provide general access to information.

New applications

Software development has allowed the implementation of new applications in the following fields: medical surveillance (ILL/ESRF/EMBL) in February, User Office (ESRF) prior to the first round of experiment proposal examination (21 and 22 April), dosimetry (ILL) in May, Scientific Coordination Office (ILL) for the first Scientific Council since the reactor shutdown (5 - 7 October), telephone directory (ILL/ESRF/EMBL), supplementary medical insurance (ILL) for January 1995.

Personal computers

The service supervises the operation of 90 personal computers (PC, MAC) with access to numerous printers and the data servers. An overall assessment of this stock led to the following measures being adopted: homogenisation of products used; rigorous monitoring of personal computers through the installation of a database; interconnection using a Novell server to facilitate exchanges, group work and resource pooling. A major priority is to enhance communication through the installation of new computer tools. Corresponding measures for user assistance and training are being studied.

New technologies

To keep pace with the rapid changes in the information systems market it is vital for us to monitor new technologies constantly. Without being slaves to fashion or giving in to the aggressive marketing of our hardware and software suppliers, we will press ahead with the controlled migration of our products and applications. All our databases have been migrated to the latest version of Oracle V7. New developments under Forms4 are very promising and we have been testing the migration of applications written with Forms3 to Forms4 and other equivalent products. However, the decision to undertake the massive task of migrating all Forms3 applications has not yet been taken. The use of CASE (computer-aided systems engineering) tools has been improved by the acquisition of a market product.

Purchasing

The Purchasing Service participated actively in all commercial aspects of the reactor refurbishment project and negotiated a number of other purchases in the scientific and technical sectors.

Reactor refurbishment

Purchasing continued to cooperate closely with the Project Group for the reactor refurbishment who have now completed their mission. As all the major purchase orders were placed in 1992 and 1993 no new orders of high value were placed in 1994 for the reactor refurbishment. However, important negotiations were carried out in order to reach final settlements with some of the suppliers. These negotiations resulted in amendments of considerable value, some positive, some negative, notably:

- ZEPPELIN (D) for the reactor block;
- NEYRPIEC FRAMATOME MECANIQUE (F) for the coupling sleeves;
- GRAVATOM (GB) for the cutting tools.

The final result is that the reactor refurbishment project has been completed on time and within the budget (173 MF).

All but six of the budget lines are complete at the time of writing, and by year end only two credit lines will remain open; one for studies required by the safety authorities, the other for re-stocking. In the latter case international calls for tenders were carried out and offers received for all spare parts which include H1-H2 beam tube housing and coupling sleeve, the through-going beam tube H6-H7, convection and anti-siphon valves and a fuel element holder.

Other purchases

Other major purchases for the reactor include compressors from BAUER (D) and ATLAS COPCO financed from the normal budget. Leak tightness tests on the reactor vessel were carried out by VERITAS (F). The electrical installations for lighting and small loads were supplied by MERLIN GERIN (F).

Considerable sums are being invested in replacing different sections of the neutron guides; both optical (glass) components and housings (mechanical parts). CILAS (F) received the highest value contract for the manufacture of 27 m neutron guide H 25 with super mirror coating. The contract is financed by the CENG as part of a *Collaborating Research Group* involving the transfer of two instruments from the CENG to ILL. An invitation to tender is in progress for the replacement of a further 25 m of the guide H25 and a 10 m extension. Offers have been received after an international call for tenders for the housing of the out-of-pile parts of the neutron guides H1-H2.

For the instruments, the highest value purchase was awarded to ZEISS (D) for the production of the toroidal focusing mirror for IN15. Other notable purchases in the scientific sector include:

- graphite monochromators for IN8 from ADVANCED CERAMICS (USA);

- viscometer for the Chemistry Laboratory from RHEOMETRIC SCIENTIFIC (D);

- compressor for Helium recuperation from COMPAIR LUCHARD (F) which will save money by reducing the losses of Helium.

In the computing area some important investments were made in the conversion to UNIX. Several SILICON GRAPHICS (CH) Indy workstations were purchased as well as a server for the Diffraction Group. Whereas HEWLETT PACKARD (USA) workstations were bought for the Nuclear Physics Group.

For the Health Physics Group a radioactivity detector for monitoring vehicles entering and leaving the site was ordered from NOVELEC (F) who also supplied a laundry monitor.

Distribution of purchases in the member states

Considerable savings were achieved by competitive tendering for major purchases as well as by negotiating discounts with regular suppliers. Offers were compared on an ex works basis so as not to disadvantage British and German firms compared with local suppliers.

The distribution of ILL purchases (orders exceeding 50 KF) in the first 10 months of 1994 is shown in the diagram. The figure includes purchases for which a free choice of suppliers was possible excluding therefore the fuel cycle, electricity and small purchases less than 50 KF.

Transport and customs

A new computerised system for customs declarations was installed in 1994. The system runs on a PC and simplifies and improves the monthly customs declarations for trade within the European Union.

Fig. Distribution of purchases (orders > 50 KF)

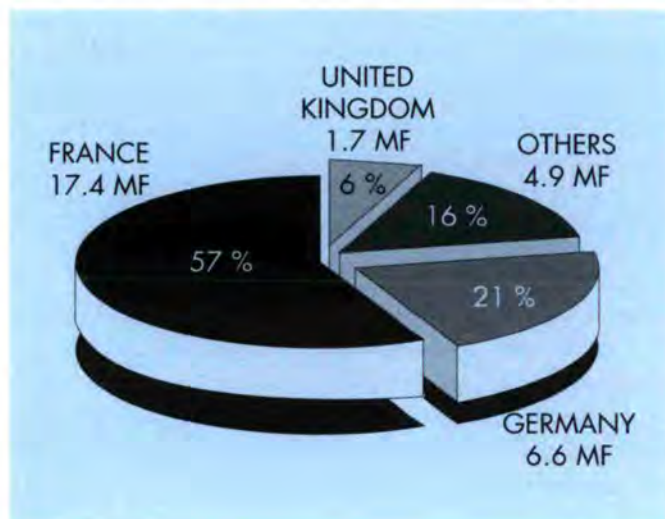


Table 2:

Staff nationalities

The overall breakdown by nationality is given in Table 1, above. The breakdown in the scientific sector (experimentalists) is as follows:

French	:	27.4%
German	:	33.3%
British	:	9.8%
Other	:	29.4%

Average age

The average age at ILL on 31.12.94 was 44. Table 2, below, shows the 93/94 comparison in the Institut's different sectors of activity.

Salaries

With respect to general salary increases, the Management and union organisations did not reach an agreement in 1994.

A unilaterally-decided increase of 0.6% was therefore implemented by the Management on 1 Juin 1994.

Training

Under French law, companies are obliged to devote 1.5% of their payroll to professional training. A percentage is paid directly to central government to help fund state-run sandwich courses for the young and special training leave ("congé individuel de formation"). The other percentage pays for training dispensed to ILL personnel. In 1994, 180 members of staff benefited from the linguistic, computing and technical training courses on offer.

French as a foreign language

To help staff of foreign nationality adapt quickly to life in France, the ILL organises French classes, which are also open to ESRF personnel. During the 1993/94 academic year, these classes were attended by some 90 people.

Student traineeships

The Institut opened its doors to 102 students from various schools and universities, one of whom received the prize for best project at the Ecole Nationale Supérieure des Ingénieurs Electriciens de Grenoble in 1993/1994, awarded by the Société des Electriciens et Electroniciens.

International schooling

Schooling for children continues to be a key factor in the integration of families. ILL, ESRF and other multinational organisations based in Grenoble have set up an organisation ("Association pour le Développement de l'Enseignement International en Région Grenobloise") that aims to improve the existing system. Thanks to the Association's work and its contacts at various levels, the local authorities have agreed to grant new premises to the "Cité Stendhal" (where the international school is located). The headmaster of the Lycée International Stendhal has been placed in charge of international schooling in Grenoble (from the primary schools through to the "Lycée") by the "Recteur d'Académie", and given a mandate to co-ordinate the restructuring of the "Cité Stendhal" site. On a broader level, the Association's partners, in particular ILL, are closely involved in the discussions currently under way for drawing up a charter for international schooling in Grenoble.

Telecommunications and General Services

The Joint Telephone Service continued to provide telephone lines for ESRF and ILL. This group also provides a number of general services to facilitate the work of all staff (mail, printing and photocopying, messenger services, audio-visual equipment, etc.).

Division	"Cadres"				Thesis Students				Non-"Cadres"				Total			
	Staff		Average Ages		Staff		Average Ages		Staff		Average Ages		Staff		Average Ages	
	1993	1994	1993	1994	1993	1994	1993	1994	1993	1994	1993	1994	1993	1994	1993	1994
Director's Services	4	3	51,2	47,2					13	13	42,4	43	17	16	44,5	43,8
Science	60	66	44,2	42,9	5	4,5	25,6	23,9	27,5	33,5	45,6	45	92,5	104	43,5	42,7
Projects and techniques	27	24	51,4	49,8		1		25,5	82	69	46,2	45,8	109	94	47,1	46,6
Reactor	8	9	49,4	46,7					90	91	43,8	43,6	98	100	44,3	43,9
Administration	12	12	47,1	44,9					53,5	51	42,4	42,1	65,5	63	43,2	42,6
Total	111	114	46,9	45	5	5,5	25,6	24,2	266	257,5	44,3	44	382	377	44,7	44,0

Table 2

Building and Site Maintenance Service

The essential activities of the service comprise maintenance, repairs, improvements, construction, renovation, modifications and equipment of the ILL site as well as buildings and technical installations (except the reactor) and experimental positions. It also provides the necessary technical assistance in its fields to the whole Institut.

Maintenance, repairs and improvement

The service is in charge of the ILL site (roads and car parks, fences, drainage system, open spaces, clearing of snow and waste removal), buildings (structure and fittings, waterproofing, cleaning) and technical installations (electricity, plumbing, heating, ventilation, air conditioning, handling), associated with buildings and experiments. Systematic maintenance is planned to prevent breakdowns and to minimise "down time" for repairs and improvements are made to increase reliability. The service carries out these interventions with its workshops and by placing of external contracts.

Construction, renovation and modifications

The service designs and follows up the construction, renovation and modification of buildings, offices, laboratories and technical installations. The principal work in 1994 included the partial renovation of waterproofing on the ILL7 roof, the modifications and transfers of offices due to the reorganisation and the supervision of the repainting of the reactor shell. The service was also closely involved in the refurbishment of the reactor through the reinstallation (shielding, electrical distribution, safety barriers) of instruments and the items made for the reactor by main sheet metal workshop.

To prepare the restart of the scientific programme, the service carried out the installation of shielding and equipment for IN4C, ADAM and PF1.

Technical assistance

The service is in charge of relations with other laboratories. It followed up the construction of the building extension for EMBL and was involved in matters concerning the joint ESRF/ILL site (canteen, road network).

COMMUNICATIONS

Workshops organized or sponsored by the ILL in 1994

Institut Laue Langevin Grenoble, France, February 2-3, 1994

Journées des polymères et des colloïdes
Organisers: GEISSLER E., LINDNER P.

Seyssins, France, May 2-4, 1994

Workshop on Nuclear Fission and Fission-Product Spectroscopy
Organisers: FAUST H.R., FIONI G.
(published as REPORT ILL94FA5T)

Autrans, France, September 26-October 1, 1994

Deuteration of biological macromolecules for neutron scattering and for NMR
EMBO Workshop
Organisers: TIMMINS P.A., LEBERMAN R., MARION D., PARELLO J.

St. Nizier, France, November 21-25, 1994

Séminaire France-Japon sur "L'utilisation des neutrons et du rayonnement synchrotron en biologie"
Organiser: ZACCAI G.

Institut Laue Langevin Grenoble, France, December 7-8, 1994

GDR 5- Réunion thématique - Pavage aléatoire et quasicristaux/ Random Tiling and Quasicrystals
Organisers: BOISSIEU M. DE, JANOT C., MOSSERI R.

Books Published

BARUCHEL J., HODEAU J.L., LEHMANN M.S., REGNARD J.R., SCHLENKER C. [Editors]
Neutron and Synchrotron Radiation for Condensed Matter Studies. Volume 2: Applications to Solid State Physics and Chemistry
Les Editions de Physique/ Springer Verlag, 1994
ISBN 2-86883-211-3

BARUCHEL J., HODEAU J.L., LEHMANN M.S., REGNARD J.R., SCHLENKER C. [Editors]
Neutron and Synchrotron Radiation for Condensed Matter Studies. Volume 3: Applications to Soft Condensed Matter and Biology
Les Editions de Physique/ Springer Verlag, 1994
ISBN 2-86883-212-1

JANOT C.
Quasicrystals. A primer
Second Edition.
Clarendon Press, Oxford 1994

Conferences Proceedings Published as Journal Issues

Proceedings of the Workshop on Focusing Bragg Optics, Braunschweig, Germany, May 10-11, 1993
MAGERL A., WAGNER V. [Editors]
Nuclear Instruments and Methods in Physics Research A **338**, 1-150 (1994)

Proceedings of the International Conference on Surface X-ray and Neutron Scattering. SXNS-3, Dubna, Russia, June 1993.
LAUTER H.J., PASYUK V.V. [Guest Editors]
Physica B **198**, 1-266 (1994)

Theses

AL USTA K.

Experimentelle Untersuchung zur Beugung von Neutronen unter streifendem Einfallswinkel und Ausfallswinkel.
Dissertation, Fakultät für Physik der Ludwig-Maximilians-Universität München, Februar 1993.

DESPLAT J.

Mesures et simulation par Monte-Carlo d'ordre local et de déplacements élastiques dans l'alliage Al-Zn.
Thèse de Doctorat, INPG Grenoble, Avril 1994.

GARCIA-MATRES E.

Estudio estructural y magnético de la familia de óxidos $R_2\text{BaNiO}_5$ ($R = \text{Nd, Gd, Tb, Dy, Y, Ho, Er, Tm, Yb}$).
Memoria para optar al grado de Doctora en Ciencias Físicas Universidad Autónoma de Madrid, Departamento de Física de la Materia Condensada, Febrero 1994.

ISNARD O.

Rôle des éléments interstitiels sur les alliages pour aimants permanents à base d'éléments de terre rare et de fer. Synthèse, étude structurale, analyse spectroscopique en relation avec les propriétés magnétiques.
Thèse de Doctorat, Université Joseph Fourier, Grenoble, Décembre 1993.

LELIEVRE-BERNA E.

Frustration et instabilité de l'antiferromagnétisme itinérant (composés TMn_2).
Thèse de Doctorat, Université Joseph Fourier, Grenoble, Février 1994.

LISS K.D.

Strukturelle Charakterisierung und Optimierung der Beugungseigenschaften von $\text{Si}_{1-x}\text{Ge}_x$ Gradientenkristallen, die aus der Gasphase gezogen wurden.
Dissertation, Mathematisch-Naturwissenschaftlichen Fakultät der Rheinisch-Westfälischen Technischen Hochschule Aachen, Oktober 1994.

MARSHALL W.G.

A neutron scattering study of anomalous f-electron metallic systems.
Ph. D. thesis, University of London, January 1994.

MEYER D.F.

Analysis of the structural changes that occur during the oxidation of human low density lipoproteins.
Ph. D. thesis, University of London, 1994.

NUNEZ V.

The determination of magnetic structures using zero-field neutron polarimetry.
University of London, 1992

POUGET S.

Contribution à l'étude de l'influence de la dilution sur les propriétés magnétiques de composés isolants frustrés.
Thèse de Doctorat, Institut National des Sciences Appliquées de Toulouse, Décembre 1993.

RANDL O.G.

Fast diffusion in the intermetallics Ni_3Sb and Fe_3Si : a neutron scattering study.
Dissertation, Universität Wien, Februar 1994.

VOIT J.

Physical properties, stability and instability of Luttinger liquids.
Habilitationsschrift, Bayreuther Institut für Makromolekülforschung (BIMF) and Theoretische Physik 1, Universität Bayreuth, November 1993.

Seminars

College 2

Theory

“Heavy-quasiparticles in electron-doped cuprates”.
P. FULDE, MPI, Stuttgart, Germany.

“Frottement solide à basse vitesse”: fluage et “stick-slip”.
C. CAROLI, Physique Solides, Univ. Paris VII, France.

“Pompage asymétrique de particules”.
J. PROST, Ecole Physique et Chimie, Paris, France.

“Finite size and bulk properties of interacting electrons coupled to low energy bosons in one dimension”.
T. MARTIN, CNLS, Los Alamos Nat. Lab. New Mexico, U.S.A.

“Anisotropic heavy fermion superconductors: correlations, QP-interactions and the symmetry of the gap function”.
B. WELSLAU, Inst. f. Festkörperphysik, Darmstadt, Germany.

“Strongly correlated spin phonon systems and new scenario for heavy fermions”.
A. IOSELEVICH, T.H. Aachen, Germany et Institut Landau, Moscow, Russia.

“Quantum Monte Carlo treatment of a rotator impurity in a crystal”.
W. HELBING, University of Mainz, Germany.

“Spinons and holons - fact or fiction?”.
S. BARNES, Univ. de Genève, Suisse.

“Physique extensive vs physique non extensive: mécanique statistique et thermodynamique généralisées”.
C. TSALLIS, CBPF Rio de Janeiro, Brésil et Univ. Joseph Fourier, France.

“Magnetic impurities on the surface”.
V.S. STEPANUK, KFA Jülich, Germany.

“Vésicules de haute topologie: diffusion conforme et fluctuations géantes”.
X. MICHALET, Ecole Normale Supérieure, Paris, France.

“Anomalous spin dynamics and relaxation in Fermi liquids”.
A.E. MEYEROVICH, Univ. of Rhode Island, USA.

“Tunneling between two 2-dimensional electron systems in a strong magnetic field”.
P. JOHANSSON, Nordita, Copenhagen, Denmark.

“Superconductivity with local electron pairing: BCS vs Bose condensation”.
R. MICNAS, Univ. Adama Mickiewicza, Poznan, Poland.

“Properties of odd-gap superconductors”.
A. BALATSKY, Los Alamos Nat. Lab. New Mexico, USA.

“The microscopic theory of high T_c superconductivity”.
P.W. ANDERSON, Univ. of Princeton, USA, & Oxford, UK.

“Spontaneous structure formation in driven systems with two species”.
I. VILFAN, Josef Stefan Institute, Ljubljana, Yugoslavia.

“Local properties of 1-D metals”.
A. GOGOLIN, ILL, Grenoble, France.

“Collective excitations in strongly correlated systems”.
R. RAIMONDI CEN-Grenoble, France.

“Quasiclassical theory for layered superconductors”.
N. SCHOPOHL, CRTBT-CNRS, Grenoble, France.

“Mode coupling theory for the dissipative dynamics of tunneling defects in dielectrics”.
A. WÜRGER, Heidelberg, Germany.

“Resonant Raman scattering in the fractional quantum Hall regime”.
P. PLATZMANN, Bell Laboratories, USA.

“Hyperfine interaction in the quantum Hall effect”.
I. WAGNER, MPI-SNCI-CNRS, Grenoble, France.

“Une formule analytique pour la dispersion des magnons dans un antiferromagnétique de Heisenberg”.
P. SCHUCK, ISN, Grenoble, France.

“Quantum transport in random magnetic fields”.
P. WÖLFLE, Univ. Karlsruhe, Germany.

“Beyond the Fermi liquid: strange metals, high T_c and the $(\nu-1/2)$ Hall effect”.
P. STAMP, Univ. of British Columbia, USA.

“The quantum 2-D XXZ ferromagnet”.
V. TOGNETTI, Univ. of Florence - E. Fermi Dept. of Physics, Italy.

“Excitations and the condensate in superfluid ^4He ”.
H.R. GLYDE, The University of Delaware, Canada.

“Heavy particle in a Fermi liquid: ions in normal and superfluid ^3He ”.
N. PROKOF'EV, University of British Columbia, USA.

“Exactly soluble models for non adiabatic processes in local centers”.
K. VELICKY, University Charles, Prague, Czechoslovakia.

“Gaz quantiques dégénérés”.
F. LALOË, Laboratoire Kastler-Brossel, E.N.S., Paris.

“Time parity violation and magneto-optics”.
I.E. DZIALOSHINSKI, Univ. of California, Irvine, USA.

“Phenomenological theory of the Wohlleben-effect”.
C.A. BALSEIRO, Centro Atómico Bariloche, Argentina.

“Quantum liquid drops”.
E. KROTSCHECK, Texas A&M Univ. College Station, Texas, USA.

"Molecular dynamics for rare events: the case of vacancy diffusion".

G. CICCOTI, CECAM Lyon, France
et Université de Rome, Italie.

"Brownian motion and disorder".

S. SCHEIDL, ILL, Grenoble, France.

"High resolution X-ray resonance scattering".

P. CARRA, ESRF, Grenoble, France.

"Randomly frustrated quantum magnets in 2-D".

J. RODRIGUEZ, Los Alamos Nat. Lab. New Mexico, USA.

"A crystal field model of the magnetic properties of URu_2Si_2 ".

P. SANTINI, Université de Lausanne, Suisse.

"Elasticité et croissance cristalline".

C. DUPORT, CEN-Grenoble, France.

"Le modèle Kondo à 2 impuretés et 2 canaux".

A. GEORGES, Ecole Normale Supérieure, Paris.

"Frustration and the magnetic non-magnetic transition".

M. DOLORES NÚÑEZ-REGUEIRO, ESRF,
Grenoble, France.

"Différents effets de différents types de désordre gelé sur le modèle XY classique".

A. VALLAT, CEN-Grenoble, France.

"Size-effect in point-contact spectroscopy of magnetic impurities in metals".

I.K. YANSON, Physicotechnical Inst. Kharkov,
Ukraine & SNCI-CNRS, Grenoble, France.

"Orbital realization of the two channel Kondo problem in amorphous systems".

A. ZAWADOWSKI, Technical University,
Budapest, Hungary.

"Raman scattering on superconductors. Are the high T_c materials d-wave?".

A. ZAWADOWSKI, Technical University,
Budapest, Hungary.

"Etats nouveaux cohérents excités dans ^3He superfluide B".

Yu. BUNKOV, CRTBT-CNRS, Grenoble, France.

"Spin dynamics in high T_c cuprates: theory and analysis of inelastic neutron scattering experiments".

F. ONUFRIEVA, Laboratoire Léon Brillouin,
CEN-Saclay, France.

"Electro-capillarité et mouillage de films isolants par l'eau".

Bruno BERGE, Laboratoire de Spectrométrie Physique, UJF
Saint Martin d'Hères, France.

"Magnetic response of localized states in solids and molecules".

Y. IMRY, Weizmann Institute, Rehovoth, Israel.

"Disordered Hubbard model".

D. LOGAN, Physical Chemistry Laboratory, Oxford, UK.

College 3

Fundamental and nuclear physics

"New possibility to search for P,T-violation".

A. SEREBROV, St. Petersburg Nucl. Phys. Inst. Russia.

"Atomic parity and time reversal experiments at the University of Washington".

D. LAMOREAUX, University of Washington,
Seattle, USA.

"Optimization of the MSGC structure and operation conditions (substrata, pattern geometry, gas mixture, ageing properties)".

Lev. SHEKHTMAN, CERN, Geneva, Suisse.

"Mass measurement of far from stability nuclei with a Smith type mass spectrometer".

M. de St. SIMON, CNRS, Orsay, France.

"Electromagnetic decay properties and nuclear structure on neutron deficient Mo and Tc isotopes".

D. RUDOLPH, Universität Göttingen, Germany.

"Positrons on heavy atoms: new window on the (e^+e^-) puzzle".

James J. GRIFFIN, University of Maryland, USA.

"Radiative corrections to neutron decay distributions".

F. GLÜCK, CERN, Geneva, Switzerland.

"Competing structures in nuclei near closed shells".

S. ROBINSON, Tennessee Technical University,
Cookville, TN, USA.

"The GRID method with monocrystalline samples - New possibilities due to fine structure in γ -line shape".

K.-H. HEINIG, Forschungszentrum Rossendorf, Germany.

"Parity violation in fission".

F. GÖNNENWEIN, Universität Tübingen, Germany.

"Complete multiparticle yrast lines and seniority inversion in $N = 84$ nuclei".

P. KLEINHEINZ, KFA, Jülich, Germany.

"Nuclear astrophysics and the origin of the heavy elements by neutron captures".

R. GALLINO, Université de Turin, Italie.

"A proposed new technique for measuring the neutron beta decay lifetime".

S. LAMOREAUX, University of Washington, Seattle, USA.

"New symmetries in nuclear structure near semi-closed shells".

J. JOLIE, University of Fribourg, Switzerland.

"Application of molecular dynamics method to study diffusion and to simulate complex experiments".

V. KONOPLEV, Institut für Ionenstrahlphysik und Mater.,
FZ-Rossendorf, Germany.

"The shift of conversion lines due to atom ionization in radioactive decay and in (n, γ) -reaction of thermal neutrons".

V. KUPRYASHKIN, Institut für Nuclear Research, Kiev,
Ukraine.

"New measurement of the A_0 coefficient in the beta decay of polarized neutrons".
K. SCHRECKENBACH, Technische Universität München, Germany.

College 4

Structural and magnetic excitations

"The formation of cooperative phenomena and their relation to superconductivity investigated by EPR".
Yu. V. YABLOKOV, Phys. Technical Inst. Kazan, Tatarstan, Russia.

"Progress in neutron monochromators using elastically bent perfect crystals".
P. MIKULA, Nucl. Phys. Inst., Rez near Prague, Czech Republic.

"Point defects in insulators: a modern calculational approach".
E. KOTOMIN, Univ. of Latvia, Riga, Russia and MPI für Metallforschung, Stuttgart, Germany.

"Interpretation of neutron scattering data on excitations in superfluid ^4He ".
H.R. GLYDE, Dept. of Phys. & Astronomy, Univ. of Delaware, Newark, USA.

"Optimal field shape (OFS) for neutron spin echo spectrometers: theory and experiment".
C. ZEYEN, ILL, Grenoble, France.

"Structural disorder in high T_c superconductors as seen by EPR and NMR on Re^{3+} ions".
M.A. TEPLOV, Dept. of Quantum Electronics and Radiospectroscopy, Kazan State Univ. Russia.

"Magnetic polaron lattice in the low carrier density system CeP ".
M. KOHGI, Tohoku Univ. Sendai, Japan.

"The magnetic state and spin dynamics of magnetodielectric oxides CuGeO_3 and Bi_2CuO_4 ".
G. PETRAKOVSKII, Inst. of Physics ASR, Krasnoyarsk, Russia.

"Coupled rotational tunnelling systems in the harmonic substitute model".
V. EYRING, Inst. f. Theor. Physik I., Univ. of Erlangen, Germany.

"Critical dynamics on EuO above and below the Curie point".
S. SCHORR, Hahn Meitner Institut, Berlin, Germany.

"Non-Fermi liquid scaling of the magnetic response of $\text{UCu}_{5-x}\text{Pd}_x$ ".
R. OSBORN, Argonne Nat. Lab., U.S.A.

"Quantum effects in finite linear chain antiferromagnets".
K. KATSUMATA, The Inst. of Phys. and Chem. Res. (RIKEN) Wako, Saitama, Japan.

"Paramagnetic dynamics and inelastic neutron scattering in spin-1 systems with strong anisotropy".
B.P. TOPERVERG, Petersburg Nucl. Phys. Inst., Gatchina, St. Petersburg, Russia.

College 5

Crystallographic and magnetic structures

"Phase transition and related structures in rare earth oxides".
E. SCHWEDA, Tübingen, Germany.

"Magnetic symmetry and linear magneto-electric effect in high- T_c superconductor compounds of R_2CuO_4 type".
I.M. VITEBSKY, Institute for Single Crystals, Kharkov, Ukraine, Russia.

"Novel structural studies using time-of-flight Laue diffraction".
C.C. WILSON, Rutherford Appleton Lab., Oxford, UK.

"Structural and superconducting properties of mercury-based cuprate superconductors: single and double HgO_8 layers".
P. RADAELLI, CNRS, Grenoble, France.

"News from the front - the latest results from poor man's crystallography".
T. VOGT, Dept. of Physics, Brookhaven Nat. Lab., USA.

"Metastable magnetic behaviour of some uranium compounds with ThCr_2Si_2 structure".
S.B. ROY, Imperial College, London, and CAT, Indore, India.

"Master of nothing and Jack of it all - current activities in neutron diffraction at Lucas Heights".
S.J. KENNEDY, Australian Nucl. Sci. and Tech. Organisation, Lucas Heights, New South Wales, Australia.

"The Australian powder diffractometer at the photon factory, Japan".
T.M. SABINE, Australian Nucl. Sci. and Tech. Organization, Lucas Heights, New South Wales, Australia.

"Magnetism studied with circularly polarized X-rays".
G. SCHÜTZ, Experimentalphysik II, Augsburg Univ. Germany.

"Antiferromagnetic structures and giant magnetoresistance (GMR) in UTX compounds".
V. SECHOVSKY, Charles University, Prague, Czechoslovakia.

"Pressure-induced phase transitions in copper and silver halides".
S. HULL, ISIS, Rutherford Appleton Facility, UK.

"Copper ordering in the lamellar CuMP_2S_6 ($M = \text{Cr, In}$): Transitions to antiferroelectric and ferroelectric phases".
V.B. CAJIPE, Institut des Matériaux, Nantes, France.

"Neutron strain measurement - A unique materials science tool".
P.J. WITHERS, Dept. of Mat. Sci. & Metallurgy, Cambridge, UK.

College 6**Liquids, disordered materials
& Metal Physics**

"Relaxations and vibrations in amorphous polymers".
U. BUCHENAU, IFF, KFA, Jülich, Germany.

"Phonons in quasicrystals: propagating
and confined modes".
J. HAFNER, Vienna, Austria.

"Dynamical and kinematical diffraction in randomly
disturbed crystals".
Václav HOLY, Masaryk Univ. Brno, Dept. of Solid State
Physics, Czech Republic.

"RF-flippers in n-scattering".
R. GÄHLER, Technische Univ. München,
Garching, Germany.

"Magnetic and metal-semiconductor transitions
in rare earth hydrides, β -RH_{2+x}".
P. VAJDA, Ecole Polytechnique, Palaiseau, France.

"Observation of non-stationary quantum mechanical
effects by means of very cold neutrons".
J. FELBER, Technische Univ. München,
Garching, Germany.

"Scanning tunneling microscopy at low and high
temperatures: Observation of surface phase transitions".
H. NEDDERMEYER, Fakultät für Physik und Astronomie
Ruhr-Universität Bochum, Germany.

"The rotational dynamics and orientational potential
of C₆₀ and its compounds".
D.A. NEUMANN, N.I.S.T., Gaithersburg, Maryland, U.S.A.

"Cold neutron focusing using capillary optics".
H. CHEN, N.I.S.T. Gaithersburg, Maryland, USA.

"The mystery of fast diffusion in some intermetallics".
O. RANDL, ILL, Grenoble, France.

"Non-specular polarised neutron scattering
from rough interfaces".
B.P. TOPERVERG, Petersburg Nucl. Phys. Inst., Gatchina,
St. Petersburg, Russia.

College 8**Biological Structures & Dynamics**

"cAMP-dependent protein kinase: structural insights into
the protein kinase family".
S. TAYLOR, Dept. of Chemistry, San Diego, Cal., USA.

"Mac programs for protein data bank analysis".
J.C. JESIOR, Université Joseph Fourier,
Saint Martin d'Hères, France.

"Comment détecter des neutrons
avec un photomultiplicateur...".
J. TROSKA, Imperial College London, UK.

"Comparison of molecular dynamics and neutron
diffraction structures: experimental evaluation
of force-field potentials".
A. A. KOSSIAKOF, Genentech., San Francisco, USA.

"The dynamics of water in oriented dipalmitoyl-glycero-
phosphocholine multilayers: a combined study by incoherent
quasi-elastic neutron scattering and ²H-NMR".
S. KÖNIG, Centre de Recherche Paul-Pascal CNRS,
Pessac (Bordeaux), France.

College 9**Chemistry**

"Neutron detectors using slow scan CCD cameras".
B. SCHILLINGER, C. RAUSCH, TÜ München,
Garching, Germany.

"The role of backbonding in the coordination
of molecular hydrogen in a metal complex".
J. ECKERT, Los Alamos Nat. Lab., New Mexico, USA.

"Small-angle X-ray analysis of the morphology
and interaction in polymeric latex systems".
M. BALLAUFF, Polymer-Institut der Univ.
Karlsruhe, Germany.

"X-ray investigations of the structure and of structural
transformations of organic multilayers".
U. PIETSCH, Universität Potsdam, Germany.

"Neutron scattering at Argonne National Laboratory:
structure and motion of adsorbates".
F. TROUW, IPNS, Argonne Nat. Lab. USA.

"Chain conformation of thermotropic main chain
polyesters".
A. BRULET, Laboratoire Léon Brillouin,
CEN-Saclay, France.

"Structural investigations on microemulsions.
Relation to the elastic properties of the amphiphilic film".
M. GRADZIELSKI, ENS, Laboratoire de Physique
Statistique, Paris, France.

"Feasibility of polarized neutron scattering from low
field flux quanta in high T_c superconducting ceramics based
Josephson media".
B.P. TOPERVERG, Petersburg Nucl. Phys. Inst., Gatchina,
St. Petersburg, Russia.

Thursday colloquium

"Relations structure-fonction des glycoprotéines".
J. MONTREUIL, Laboratoire de Chimie Biologique,
Université de Lille, France.

"Molecular motion at the glass transition studied by
NMR, forced Rayleigh scattering and neutron scattering".
H. SILLESCU, University of Mainz, Germany.

Conference Contributions

- "Heavy fermions: a critical review".
H. CAPELLMANN, Technische Hochschule - Aachen, Germany.
- "Phase transitions at quantum surfaces".
P. LEIDERER, Univ. Konstanz, Germany.
- "Magnetic relaxation and mesoscopic quantum tunneling of the magnetization".
B. BARBARA, Laboratoire Louis-Néel, CNRS, Grenoble, France.
- "Neutrons and synchrotron radiation in the study of magnetism". (Joint Colloquium ILL-ESRF).
D. M. BLUME, Brookhaven Nat. Lab. USA.
- "Quantum coherence in semiconductors probed by transient non linear spectroscopy".
P. THOMAS, Philipps-University of Marburg, Germany.
- "Dynamic fluctuation effects in membranes".
E.I. KATS, Landau Inst. for Theoretical Phys., Moscow, Russia, & Univ. Joseph Fourier, Saint Martin d'Hères, France.
- "Modulated and other novel magnetic phases".
T. CHATTOPADHYAY, ILL, Grenoble, France and MPI für Festkörperforschung, Stuttgart, Germany.
- "Interatomic interactions in dense fluid metals".
F. HENSEL, Philipps-University of Marburg, Germany.
- "Can the neutron EDM be detected by Coulomb fields in crystals?".
C. ZEYEN, ILL, Grenoble, France.
- "Vortex-antivortex excitations in two-dimensional ^4He and thin ^4He films".
M. SAARELA, University of Oulu, Finland.
- "Two-dimensional nuclear magnets".
H. GODFRIN, CRTBT-CNRS, Grenoble, France.
- "Structural aspects of solid halogens under high pressure - metallization, molecular dissociation, and phase transitions".
Y. FUJII, Inst. for Solid State Physics, Univ. of Tokyo, Japan.
- "Correlated electrons in solids: Beyond the standard model?".
J.W. ALLEN, Dept. of Physics, Univ. of Michigan, Ann Arbor, MI, USA.

ABERDEEN, UK: British Electrophoresis Society - 1994/09/14-15

VUILLARD L., RABILLOUD T. Sulfobetaines, a new class of mild protein solubilising agents with applications to electrophoretic processes.

ANN ARBOR, USA: Symposium on Radiation Measurements and Applications - 1994/05/16-19

GELTENBORT P. Review on microstrip gas chambers. (Invited talk)

ANNECY, France: XIIIe Colloque Annuel de la Société Française de Biophysique - 1994/09/08-12

JESIOR J.C., FILHOL A., TRANQUI D. 'FoldIt (light)': un programme interactif d'analyse des structures de protéines sur Macintosh. (Poster)

ATLANTA, USA: ASNT Fall Conference. NDT-The Olympics for Quality Competitiveness - 1994/09/19-23

GUAZZONE J.P., HAMELIN B., BASTIE P. Radiocrystallographic diagnosis methods for single crystal components. (Contributed paper)

AUTRANS, France: EMBO Workshop "Deuteration of Biological Molecules for Neutron Scattering and for NMR" - 1994/09/26-10/01

FERRAND M., RÉAT V., ZACCAI G. Global dynamics of bacteriorhodopsin studied by neutron scattering. Contribution of deuteration to understand functional dynamics. (Invited talk)

FORSYTH T., LANGAN P., MAHENDRASINGAM A., FULLER W., MASON S.A., WILSON C.C. Deuteration in fibre diffraction studies of DNA hydration.

LEHMANN M. Deuteration is important in neutron protein crystallography. (Talk)

MAY R. How deuterium labelling and small angle neutron scattering allow us to study the structures of complex biological macromolecules.

ZACCAI G. Specific deuteration of bacteriorhodopsin.

ZACCAI G. Heavy water effects on protein stability.

BAD HERRENALB, Germany: European Research Conference "EuChem Conference on Molten Salts" - 1994/08/21-26

SUCK J.-B. Collective atomic dynamics in liquid metal-molten salt solutions. (Invited talk)

BERKELEY, USA: Conference on Physics from Large Gamma-Ray Arrays - 1994/08/02-06

LISTER C.J., AHMAD I., AUSTIN S.M., BACK B.B., BAZIN D., BETTS R.R., CALAPRICE F.P., CHAN K.C., CHISHTI A., CHOWDHURY P., DUNFORD R.W., FOX J.D., FREEDMAN S.J., FREERG M., GREENBERG J.S., HALLIN A.L., HAPP T., LAST J.,

KALOSKAMIS N., KASHY E., KUTSCHERA W., LIU M., MAIER M.R., MERCER D., PERERA A., RHEIN M.D., ROA D.E., SCHIFFER J.P., TRAINOR T., WILT P., WINFIELD J.S., WOLANSKI M., WOLFS F.L.H., WUOSMAA A.H., XU G., YOUNG A., YURKON J.E. Recent results from APEX. (Contributed paper)

BOULDER, USA: 14th International Conference on Atomic Physics - 1994/07/31-08/05

CHIBANE Y., HECKEL B.R., GREEN K., IAYDJIEV P., IVANOV S.N., KILVINGTON I., LAMOREAUX S.K., PENDLEBURY J.M., RAMSEY N.F., SMITH K.F. Precision mercury magnetometry for large volumes. (Poster)

BREST, France: Sagamore XI Charge, Spin and Momentum Densities - 1994/08/07-12

WILSON C. Experimental charge density study of a dyotropic isomer: $C_{16}H_9C_{19}$ at 123K. (Poster)

BUDAPEST, Hungary: Workshop on the International Use of Centres of Excellence and Joint Projects on Materials Science - 1994/04/26-27

HEIDEMANN A. The ILL, an international research institute. (Poster)

BUDAPEST, Hungary: International Liquid Crystal Conference - 1994/07/04-08

CHARVOLIN J. Films of amphiphiles and their cubic structures. (Invited talk)

CHEMNITZ, Germany: WE-Heraeus-Ferienkurs für Physik, Physikalische Effekte auf der Nanometerskala, - Physik zwischen Nah- und Fernordnung - 1994/09/05-16

SUCK J.-B. Kollektive ionische Anregungen in Flüssigkeiten und Gläsern. (Invited talk)

SUCK J.-B. Dynamik in Quasikristallen. (Invited talk)

COMO, Italy: International Conference on Advanced Technology and Particle Physics - 1994/10/03-07

GELTENBORT P. MicroStrip gas chamber and MicroGap chamber development - an overview.

FUJI-YOSHIDA, Japan: International Symposium on Metal-Hydrogen Systems- Fundamentals & Applications - 1994/11/06-11

GYGAX F.N., AMATO A., FEYERHERM R., SCHENCK A., ANDERSON I.S., UDOVIC T.J., SOLT G. Dynamics of μ^+ in Sc and ScH_x .

HUANG Q., UDOVIC T.J., RUSH J.J., SCHEFER J., ANDERSON I.S. Characterization of the structure of $TbD_{2.26}$ at 70 K by neutron powder diffraction.

UDOVIC T.J., RUSH J.J., ANDERSON I.S. Neutron spectroscopic comparison of β -phase rare-earth hydrides.

GRENOBLE, France: Journées des Polymères et Colloïdes - 1994/02/02-03

LARTIGUE C., GUILLERMO A., COHEN-ADDAD J.P. Propriétés dynamiques et structurales d'un alliage de polymères compatibles. (Talk)

GRENOBLE, France: International Symposium on Metastable, Mechanically Alloyed and Nanocrystalline Materials, European Meeting on Disordering and Amorphization - 1994/06/27-07/01

SUCK J.-B. Mode softening in rapidly quenched AlSi solutions. (Contributed paper)

GRENOBLE, France: IVth International Conference on Materials and Mechanisms of Superconductivity and High-Temperature Superconductors, M2S-HTSC-IV - 1994/07/04-09

CHATTOPADHYAY T., SIEMENSMEYER K. Observation of hyperfine-induced nuclear polarization in N_2CuO_4 . (Poster)

PYKA N., IVANOV A.S., BRADEN M., REICHARDT W., RUMIANTSEV A.Y., MITROFANOV N.L. Lattice dynamics of Pr_2CuO_4 studied by inelastic neutron scattering. (Poster)

SCHOBER H., RENKER B., GOMPF F., ADELMANN P. Neutron scattering study of low-frequency excitations in Rb_3C_{60} and Rb_6C_{60} . (Poster)

SCHOBER H., RENKER B., ADELMANN P., GOMPF F. Inelastic neutron scattering study of new mercury based superconductors. (Poster)

IL CIOCCO, near Lucca, Italy: European Research Conferences "Dynamical properties of Solids: Phonon in Solids and at Surfaces" - 1994/09/17-21

DORNER B. Magnetic excitations in quasi 1-D systems in an external magnetic field parallel and perpendicular to the chain direction. (Talk)

SCHERM R. Neutron scattering facilities at the Institut Laue-Langevin. (Invited talk)

KEELE, U.K.: Complementary Neutron and X-ray Scattering in the Study of Biological Systems - 1994/04/14-15

LANGAN P., FORSYTH V.T., MAHENDRASINGAM A., ALEXEEV D., MASON S.A., FULLER W. Neutron and X-ray fibre diffraction studies of nucleic acids. (Invited talk)

LINDLEY P.F., BOUQUIERE J., SAVAGE H., LEHMANN M.S., TIMMINS P.A., FINNEY J.L. High resolution X-ray and neutron refinement of vitamin B12 coenzyme.

KONSTANZ, Germany: ESF Conference on Quantum Fluids and Solids: Surface and Interfaces - 1994/08/25-31

CLEMENTS B. Phase transitions in Bose quantum films. (Invited talk)

LE CAP D'AGDE, France: Troisièmes Journées de la Diffusion Neutronique - 1994/05/18-20

DIANOUX A.J., SAUVAJOL J.L., KNELLER G.R., SMITH J.C. Dynamique du polyacétyle dopé au sodium. (Contributed paper)

DIANOUX A.J., SAUVAJOL J.L., PAPANEK P., FISCHER J.E., MAO G., WINOKUR M.J., KARASZ F.A. Etude par diffusion incohérente neutronique de la dynamique des modes de vibration de basse-fréquence du poly(p-phénylène vinylène).

FERRAND M., RÉAT V., DIANOUX A.J., SMITH J., ZACCAI G. Etude de mouvements internes de la bacteriorhodopsine par diffusion inélastique de neutrons et simulation de dynamique moléculaire. (Invited talk)

GIRARD P., GUILLAUME F., DIANOUX A.J., CODDENS G. Dynamique réorientationnelle et translationnelle de l'acide nonanoïque inclus dans de l'urée.

MUTKA H. Temps de vol thermique IN4C - état actuel. (Poster)

TASSET F. Le polariseur ^3He , rêve ou réalité ? (Invited talk)

LES DIABLERETS, Switzerland: International Conference on Aperiodic Crystals - 1994/09/18-22

JANOT C., DE BOISSIEU M., BOUDARD M. Structure determination of the icosahedral quasicrystals: state of the art and prospect. (Contributed paper)

LES HOUCHES, France: Winter School - 1994/02/21-26

CHARVOLIN J. Prolamellar bodies in etioplasts. (Invited talk)

LES HOUCHES, France: Workshop on "Polarised Beams and Targets: Sensitive Tools for the Study of Solids, Nuclei and Particles" - 1994/06/07-10

TASSET F. Polarized ^3He targets as neutron spin filters. (Invited talk)

MADRID, Spain: 14th General Conference of the Condensed Matter Division - 1994/03/28-31

PYKA N.M., REICHARDT W., PINTSCHOVIVUS L., CHAPLOT S.L., SCHWEISS P., ERB A., MÜLLER-VOGT G. Neutron scattering study of chain-oxygen vibrations in $\text{YBa}_2\text{Cu}_3\text{O}_7$. (Poster)

MÜNCHEN, Germany: Spring Meeting of the German Physical Society, Section Hadrons and Nuclei - 1994/03/21-25

GELTENBORT P. Neueste Ergebnisse mit MikrostreifenProportionalZählern.

MÜNSTER, Germany: Frühjahrstagung des Arbeitskreises Festkörperphysik der DPG - 1994/03/21-25

FRICK B., RICHTER D. Einfluß der molekularen Beweglichkeit der Schmelze auf die Vibrationseigenschaften im Glas. (Talk)

SUCK J.-B., CHIEUX P., DUPUY-PHILON J., JAL J.-F., MORKEL C.

Temperaturabhängigkeit der kollektiven atomaren Dynamik in flüssigen Rubidium. (Talk)

SUCK J.-B. Dynamischer Strukturfaktor der ikosaedrischen Legierung $\text{Al}_{71}\text{Pd}_{19}\text{Mn}_{10}$. (Contributed paper)

NEWCASTLE-UPON-TYNE, UK: British Crystallographic Association Spring Meeting - 1994/03/28-31

LANGAN P., FORSYTH V.T., SIMPSON L., FULLER W. New structure for chemically modified DNA. (Invited talk)

WILSON C. Structure-reactivity study of a series of dyotropic isomers. (Poster)

BERGURGL, Austria: Journées des Actinides - 1994/04/15-19

EBEL T., JEITSCHKO W., REEHUIS M., SONNTAG R., STÜBER N. Magnetic properties of the ternary uranium-nickel-phosphide $\text{U}_3\text{Ni}_{3.34}\text{P}_6$. (Poster)

PARIS, France: Colloquium "To the Memory of Laird Schearer" - 1994/06/01-02

TASSET F. ^3He targets as neutron spin filters. (Invited talk)

PRAHA, Czech Republic: 6th International Conference on the Structure of Non-Crystalline Materials - 1994/08/29-09/02

SUCK J.-B. Dynamic structure factor of icosahedral $\text{Al}_{17}\text{Pd}_{19}\text{Mn}_{10}$. (Talk)

RENNES, France: 4èmes Journées de la Matière Condensée - 1994/08/31-09/02

BELLET-AMALRIC E., LEGRAND J.F. Structure cristalline des polymères ferroélectriques P(VDF-TrFe): effets de la composition.

DIANOUX A.J., SAUVAJOL J.L., KNELLER G.R., SMITH J.C. Dynamique du polyacétyle dopé au sodium.

SAUVAJOL J.L., PAPANEK P., DIANOUX A.J., FISCHER J.E., MAO G., WINOKUR M.J., KARATZ F.A. Etude par diffusion incohérente neutronique de la dynamique des modes de vibration de basse-fréquence du poly(p-phénylène vinylène).

TASSET F. CRYOPAD et le polariseur- He^3 : Deux outils neutroniques nouveaux pour le magnétisme microscopique. (Talk)

RENVYLE, Republic of Ireland: European Foam Conference - 1994/03/27-30

CHARVOLIN J. Cubic micellar structures in liquid crystals. (Invited talk)

SANTA FE, USA: Neutrons in Biology - 1994/10/24-28

FORSYTH V.T., LANGAN P., MAHENDRASINGAM A., HUGHES D.J., FULLER W., WILSON C.C., MASON S.A., GIESEN U., DAUVERGNE M.T.

Time-of-flight Laue fibre diffraction studies of DNA. (Contributed paper)

FULLER W., FORSYTH V.T., MAHENDRASINGAM A., LANGAN P., PIGRAM W.J., MASON S.A., WILSON C.C. DNA hydration studied by neutron fibre diffraction. (Talk & Contributed paper)

MASON S.A. Neutron instrumentation for biology.

TIMMINS P.A., PEBAY-PEYROULA, WELTE W. Protein - Detergent interactions in single crystals of membrane proteins studied by neutron crystallography. (Invited talk)

SENDAI, Japan: International Conference on Neutron Scattering - 1994/10/11-14

BÜTTNER H.G., KEARLEY G.J., HOWARD C.J., KAHN R. The rotational potential of NH₃ groups in metal hexammines. (Poster & Contributed paper)

FILLAUX F., BARON M.H., LEYGUE N., TOMKINSON J., KEARLEY G.J.

Inelastic neutron scattering study of proton transfer dynamics in polyglycine. (Contributed paper)

FILLAUX F., CARLILE C.J., COOK J., HEIDEMANN A., KEARLEY G.J., IKEDA S., INABA A. Relaxation kinetics of the sine-Gordon breather mode in the 4-methyl-pyridine crystal at low temperature. (Poster)

FRICK B., TREVIÑO S., WILLIAMS J.H. Difference in the vibrational behaviour of amorphous and crystalline ethylbenzene. (Poster)

FRICK B., WILLIAMS J., TREVIÑO S., ERWIN R. Vibrational behaviour of amorphous and crystalline ethylbenzene. (Contributed paper)

KEARLEY G.J., BUTTNER H., FILLAUX F., IDEDA S., INABA A. Coupling between phonons and quantum rotors. (Contributed paper)

KULDA J. Towards ideal focusing monochromators. (Contributed paper)

KULDA J., ISHII Y., KATANO S. Dynamical structure analysis applied to Si and Ge. (Contributed paper)

LANGAN P., FORSYTH V.T., MAHENDRASINGAM A., MASON S.A., WILSON C.C., FULLER W. Neutron fibre diffraction studies of DNA hydration. (Poster & Contributed paper)

LEHMANN M.S. A large image plate detector for neutrons. (Poster)

McINTYRE G.J., VISSER D., BARTELS K., CARLING S.G. The membrane diffractometer V1 at BENS: Applications to materials science. (Poster)

McINTYRE G.J., VISSER D. Phases and phase transitions in the hexagonal perovskite RbMnBr₃. (Poster)

McINTYRE G.J., VISSER D. Structural phase transitions in the hexagonal perovskite TlFeCl₃. (Poster)

McINTYRE G.J., VISSER D., KEEN D.A., CHERNENKO V.A., KOKORIN V.V. Phase transitions in the memory alloy Ni₂MnGa. (Poster)

McINTYRE G.J., VISSER D., SHEARMUR T.E., KEEN D.A. Determination of S(Q) in the Ising-like triangular antiferromagnet CsMnI₃. (Poster)

MUTKA H., PAYEN C., MOLINIÉ P., ECCLESTON R.S. Quasi-1D antiferromagnets with S=1 and S=3/2. The isostructural compounds AgVP₂S₆ and AgCrP₂S₆. (Poster & Contributed paper)

OULADDIAF B., DEPORTES J., RODRIGUEZ-CARVAJAL J. Magnetic structure of Er₆Mn₂₃ and Dy₆Mn₂₃. (Contributed paper)

REEHUIS M., RODRIGUEZ-CARVAJAL J., DANEBROCK M., JEITSCHKO W. Magnetic structure of Tb₂ReC₂, Ho₂ReC₂ and Er₂ReC₂. (Poster)

TASSET F. Towards helium-3 neutron polarizers. (Invited talk & Contributed paper)

TIMMINS P.A. Structural molecular biology. Recent results from neutron diffraction.

SITGES, Spain: Les Phénomènes non linéaires - 1994/06

VILLAIN J., DUPORT C., NOZIERES P. Elastic instabilities in crystal growth. (Contributed paper)

ST. NIZIER, France: Séminaire France-Japon. L'utilisation des Neutrons et du Rayonnement Synchrotron en Biologie: Diffusion Centrale,

Diffusion Diffuse et Diffusion Inélastique - 1994/11/21-25

FERRAND M., RÉAT V., SMITH J., ZACCAI G. Global dynamics of bacteriorhodopsin: an approach combining neutron scattering experiments and molecular dynamics simulation. (Invited talk)

LEHMANN M.S. Neutron scattering studies of protein interactions with small solutes.

MAY R. Biological structures and dynamics at the ILL.

MAY R. SANS at ILL: large protein-nucleic acid complexes.

TIMMINS P.A. Protein - Detergent interactions in single crystals of membrane proteins studied by neutron crystallography. (Invited talk)

STRASBOURG, France: Journées Polymères Conducteurs - 1994/09/20-23

SAUVAJOL J.L., PAPANÉK, P., FISCHER J.E., DIANOUX A.J., MAO G., WINOKUR M.J., KARASZ F.E. Densités d'états vibrationnelles du poly(p-phénylène vinylène). Une étude par diffusion incohérente des neutrons. (Contributed paper)

STYRIA, Austria: Eighth International Conference on Recent Progress in Many-Body Theories - 1994/08/22-27

CLEMENTS B. Multiphonon excitations in Bose films. (Invited talk)

VALENCIA, Spain: The XVIII International Conference on Condensed Matter Theories - 1994/06/06-10

CLEMENTS B. Bose quantum films at finite temperatures. (Invited talk)

VARENNA, Italy: International School of Physics "Enrico Fermi", NATO-ASI, "Observation and Prediction of Phase Transitions in Complex Fluids" - 1994/07/26-08/05

SOUAILLE M., SMITH J.C., DIANOUX A.J., GUILLAUME F. Dynamics of N-nonadecane chains in urea inclusion compounds as seen by incoherent quasielastic neutron scattering and computer simulations. (Contributed paper)

WARSAW, Poland: International Conference on Magnetism '94 - 1994/08/22-26

CHATTOPADHYAY T., BRÜCKEL T., HOHLWEIN D., SONNTAG R. Magnetic diffuse scattering from the frustrated antiferromagnet MnS_2 . (Contributed paper & Talk)

CHATTOPADHYAY T., SCOTT C.A., LÖHNEYSEN H.V. μ SR investigation of the magnetic ordering in $CeCu_{5.5}Au_{0.5}$. (Contributed paper & Talk)

KESSLER M., DEPORTES J., OULADDIAF B., SAYETAT F. Magnetic properties of $Sc_xTi_{1-x}Fe_2$. (Contributed paper)

LOEWENHAUPT M., FABI P., SOSNOWSKA I., FRICK B., ECCLESTON R. Temperature dependence of the magnetic excitation spectrum of $Dy_2Fe_{14}B$. (Contributed paper)

McINTYRE G.J., VISSER D., GRAF H., IRWIN I.P., PLUMER M.L., WEISS L., ZEISKE T. Electric field induced changes in the magnetic ordering of the stacked triangular antiferromagnet $CsMnBr_3$. (Poster)

PAYEN C., MUTKA H., MOLINIÉ P. Finite segments in quasi-1D Heisenberg antiferromagnets: comparison of the isostructural systems $AgVP_2S_6$ ($S=1$) and $AgCrP_2S_6$ ($S=3/2$). (Poster & Contributed paper)

POUGET S., ALBA M., NOGUES M. Influence of disorder on the static critical behaviour in the frustrated ferromagnetic system $CdCr_{2(1-x)}In_{2x}S_4$. (Contributed paper)

RITTER C., MARQUINA C., IBARRA M.R. Field induced magnetic transitions in $Dy_xY_{1-x}Mn_3$ intermetallics. (Poster)

ROSOV N., LYNN J.W., KÄSTNER J., WASSERMANN E.F., CHATTOPADHYAY T., BACH H. Polarization analysis of the magnetic excitations in $Fe_{72}Pt_{28}$ alloys. (Talk)

WASHINGTON, USA: ACS Symposium "Flow Induced Structure in Polymers" - 1994/08/21-26

BOUE F., LINDNER P. SANS from semidilute solutions under shear: Butterflies. (Contributed paper)

WURZBURG, Germany: International Euroconference on Magnetic Correlations, Metal-Insulator Transitions, and Superconductivity in Novel Materials - 1994/09/26-30

FABRIZIO M., GOGOLIN A.O., SCHEIDL S. Impurity scattering in quantum wires with Coulomb interaction. (Contributed paper)

GEBHARD F., BARES P.A. Asymptotic Bethe-Ansatz results for a Hubbard chain with $1/\sin H$ -hopping.

ZUOZ, Switzerland: Second Summer School on Neutron Scattering "Neutron Scattering from Hydrogen in Materials" - 1994/08/14-20

ANDERSON I.S. The dynamics of hydrogen in metals studied by inelastic neutron scattering. (Contributed paper)

DORNER B. Introduction to neutron scattering. (Contributed paper)

Publications – ILL-Reports 1994

This list groups publications received during 1994 resulting from the research at the ILL.

ILL-Reports are listed first. They are followed by the list of publications in journals, conference proceedings, books with ILL authors and co-authors and by publications related to experimental work performed by visiting scientists at the ILL but without ILL co-authors.

ILL-Reports

(Code number 1 to 30)

94FA1

FAUST H.R. Exotic isotope production from nuclear fission. ILL-Report.

94FA2

FAUST H.R., THE PIAFE COLLABORATION. Proposal for an exotic beam facility at the ILL. ILL-Report.

94GI3

GIVELET N., LEDEBT P., FIONI G. Interface multiplexeur afficheur pour codeurs à contacts 24 Bits B.C.D. ILL-Report.

94FA5

FAUST H.R., FIONI G. Nuclear fission and fission-product spectroscopy. Proceedings of the workshop on "Nuclear Fission and Fission-Product Spectroscopy". Seyssins, France, May 2-4 1994. ILL-Report.

94VA6

VACHER N. Notice d'utilisation du programme QCL. ILL-Report.

94SC7

SCHMID S. Users guide for EXPLORER 2.0. Bericht über das Praktikum. ILL-Report.

94IB8

IBEL K. 1994 World directory of SANS instruments available for outside users. ILL-Report.

94GO9

GOBERT G. Les appareils de recherche glissent sur film d'air. ILL-Report.

94VU10

VUILLARD L., RABILLOUD T. Agents de solubilisation de biomolécules constitués par des zwitterions non détergents et leurs utilisations.

Demande de brevet français n° 94 00241 du 12 Janvier 1994. ILL-Report.

94BE11

BERRUYER G., BLANC T., FILHOL A., LAUGIER J. User's manual for OrientExpress. ILL-Report.

94FI12

FILHOL A. Manuel de MacXenon. Xe RHF poisoning. ILL-Report.

94KO13

KOESTER U. Beamline calculations for PIAFE - Phase 1. Implantation of the high resolution BILL magnet. ILL-Report.

94MI14

MIKULA P., WAGNER V., SCHERM R. On the focusing in neutron diffraction by elastically bent perfect crystals. PTB-Bericht-PTB-N-17 ILL-Report.

94IB15

IBEL K. Roentgenmikroskopie. Universitaet Osnabrueck ILL-Report.

94NO16

NOZIERES P. Variables d'état, fluctuations, irréversibilité: réflexions sur la thermodynamique près et loin de l'équilibre. (Cours au Collège de France 1993-1994). ILL-Report.

94TH17

THOMAS M. Comportement mécanique des choppers d'IN5. ILL-Report.

94TH18

THOMAS M., BILLINGTON A. Dimensionnement mécanique du multidétecteur d'IN4C. ILL-Report.

94MA19

MALBERT P. IN15 - 3 Choppers - Calcul de la vitesse critique du rotor. (DPT/BI - 94 394 PhM). ILL-Report.

94MA20

MALBERT P. Monochromateurs - Presse à chaud pour monocristaux - Calcul mécanique de la déformation sous charge. (DPT/BI - 94 401 PhM).
ILL-Report.

94MA21

MALBERT P. Calcul de l'outillage de levage de l'aimant PN1. (DPT/BI - 94 345 PhM).
ILL-Report.

94MA22

MALBERT P. IN4C choppers test procedures. (DPT/BI - 94 185 PhM).
ILL-Report.

94MA23

MALBERT P. Analyse de la rupture du chopper IN15 survenue le 20 avril 1994. Correctif à la note de calcul DPT/BI - 94 202 PhM du 22/04/94. (DPT/BI - 94 217 PhM).
ILL-Report.

94MA24

MALBERT P. Calcul de la fenêtre du multidétecteur IN10. (DPT/BI - 94 507 PhM)
ILL-Report.

94MA25

MALBERT P. IN4C - Monochromateur - Etude du mécanisme de courbure. (DPT/BI - 94 113 PhM)
ILL-Report.

94MA26

MALBERT P. Réacteur à haut flux - Guides de neutrons H1-H2 - Partie en pile - Mécanique - Calcul des plaques de fermeture des guides NG12-NG13 et H18. (DPT/BI - 93 176 - PM)
ILL-Report.

94MA27

MALBERT P. IN4C - Chopper de Fermi - Calcul de la première fréquence propre. (DPT/BI - 93 212 - PM - A)
ILL-Report.

94FI28

FIONI G., BELMONT J.L., CONTO J.M. DE, FAUST H.R., THE PIAFE COLLABORATION. An electrostatic beam line for low energy ions.
ILL-Report.

94GE29

GEISSLER R., LINDNER P. Journées des Polymères et des Colloïdes. Livret des résumés
ILL-Report

94BO30

BOISSIEU M. DE, JANOT C., MOSSERI R. GDR 5. Résumés pour la Réunion Thématique "Pavage Aléatoire et Quasicristaux", ILL, Grenoble, 7-8 Décembre 1994
ILL-Report

Papers published in Scientific Periodicals, Books and Conference Proceedings:

**1. With ILL authors & co-authors
(Code number 101 to 329)**

94MA101

MAGERL A., LISS K.D., DOLL C., MADAR R., STEICHELE E. Will gradient crystals become available for neutron diffraction ?
Nuclear Instruments and Methods in Physics Research A **338**, 83-89 (1994).

94LI102

LISS K.D., MAGERL A. Can a gradient crystal compete with a mosaic crystal as a monochromator in neutron- or x-ray diffraction ?
Nuclear Instruments and Methods in Physics Research A **338**, 90-98 (1994).

94JU103

JUNGCLAUS A., BOERNER H.G. High resolution gamma spectroscopy with ideal crystals.
Nuclear Instruments and Methods in Physics Research A **338**, 120-124 (1994).

94MU104

MUTKA H. Coupled time and space focusing for time-of-flight inelastic scattering.
Nuclear Instruments and Methods in Physics Research A **338**, 144-150 (1994).

94MI105

MISBAH C., VALANCE A. Secondary instabilities in the stabilized Kuramoto-Sivashinsky equation.
Physical Review E **49**, 166-183 (1994).

94GO106

GOENNENWEIN F., BELOZEROV A.V., BEDA A.G., BUROV S.I., DANILYAN G.V., MARTEM'YANOV A.N., PAVLOV V.S., SHCHENEV V.A., BONDARENKO L.N., MOSTOVOI Y.A., GELTENBORT P., LAST J., SCHRECKENBACH K. Parity violation in ternary fission.
Nuclear Physics A **567**, 303-316 (1994).

94SE107

SEPIOL B., RANDL O.G., KARNER C., HEIMING A.,
VOGL G. Ni diffusion in the high-temperature intermetallics
Ni₃Sb studied by quasielastic neutron scattering.
Journal of Physics: Condensed Matter **6**, L43-L46 (1994).

94BE108

BELLET-AMALRIC E., LEGRAND J.F.,
STOCK-SCHWEYER M., MEURER B.
Ferroelectric transition under hydrostatic pressure
in poly(vinylidene fluoride-trifluoroethylene) copolymers.
Polymer **35**, 34-46 (1994).

94PR109

PREVEL B., DUPUY-PHILON J., JAL J.F.,
LEGRAND J.F., CHIEUX P. Structural relaxation
in supercooled glass-forming solutions: a neutron
spin-echo study of LiCl, 6D₂O.
Journal of Physics: Condensed Matter **6**, 1279-1290 (1994).

94RA110

RAMZI A., MENDES E., ZIELINSKI F., ROUF C.,
HAKIKI A., HERZ J., OESER R., BOUE F., BASTIDE J.
Strain induced fluctuations in polymer networks,
melts and gels (butterfly patterns).
Journal de Physique IV, Colloque **3**, C8-91-C8-98 (1993).

94DO111

DORNER B. Comparison of gradient and mosaic crystals
by means of *k*-distributions in reciprocal space.
Nuclear Instruments and Methods in Physics Research
A **338**, 33-37 (1994).

94BE112

BERMEJO F.J., CRIADO A., GARCIA-HERNANDEZ M.,
ALONSO J., PRIETO C., MARTINEZ J.L.
Collective low-frequency excitations in a molecular glass.
Journal of Physics: Condensed Matter **6**, 405-420 (1994).

94GU113

GUENET J.M., MENELLE A., SCHAFFHAUSER V.,
TERECH P., THIERRY A. Isotactic polystyrene/cis-
decaline mixtures: phase diagram and molecular structures.
Colloid and Polymer Science **272**, 36-47 (1994).

94BO114

BOUE F., LINDNER P. Semi-dilute polymer solutions
under shear.
Europhysics Letters **25**, 421-427 (1994).

94VU115

VUILLARD L., HULMES D.J.S., PURDOM I.F.,
MILLER A. Heparin binding to monodisperse plasma
fibronectin induces aggregation without large-scale changes
in conformation in solution.
International Journal of Biological Macromolecules **16**,
21-26 (1994).

94MI116

MICHALET X., BENSIMON D., FOURCADE B.
Fluctuating vesicles of nonspherical topology.
Physical Review Letters **72**, 168-171 (1994).

94CH117

CHEVRIER J., SUCK J.B., LASJAUNIAS J.C.,
PERROUX M., CAPPONI J.J. Nonequilibrium state
and lattice instability in supersaturated aluminum silicon
solid solutions.
Physical Review B **49**, 961-968 (1994).

94VA118

VAN DER MAAREL J.R.C., GROOT L.C.A.,
HOLLANDER J.G., JESSE W., KUIL M.E., LEYTE J.C.,
LEYTE-ZUIDERWEG L.H., MANDEL M., COTTON J.P.,
JANNINK G., LAPP A., FARAGO B. On the charge
distribution in aqueous poly(styrenesulfonic acid) solutions.
A small angle neutron scattering study.
Macromolecules **26**, 7295-7299 (1993).

94HA119

DENSCHLAG H.O., ALHASSANIEH O., WEIS M.,
FAUBEL W., FAUST H.R. On the absolute γ -ray line
intensities in the decay of ⁹⁹Nb and the branching ratio
in the decay of ⁹⁹Zr to ^{99m}Nb and ^{99g}Nb.
Radiochimica Acta **62**, 177-179 (1993).

94HA120

HAGENMAYER R.M., ZEYEN C.M.E.,
LAMPARTER P., STEEB S. Ultra small angle neutron
scattering from amorphous Ni-Pd-P-alloys.
Zeitschrift fuer Naturforschung A **49**, 1203-1206 (1994).

94BE121

BEE M., GIROUD-GODQUIN A.M., MALDIVI P.,
WILLIAMS J. Incoherent quasi-elastic neutron scattering
study of highly oriented fibres of copper laurate in the
columnar mesophase.
Molecular Physics **81**, 57-68 (1994).

94MC122

MCDERMOTT D.C., MCCARNEY J., THOMAS R.K.,
RENNIE A.R. Study of an adsorbed layer
of hexadecyltrimethylammonium bromide using
the technique of neutron reflection.
Journal of Colloid and Interface Science **162**,
304-310 (1994).

94RA123

RAMSAY J.D.F., LINDNER P. Small-angle neutron
scattering investigations of the structure of thixotropic
dispersions of smectite clay colloids.
Journal of the Chemical Society. Faraday Transactions **89**,
4207-4214 (1993).

94PO124

POUSSIGUE G., BENOIT C., BOISSIEU M. DE, CURRAT R. Inelastic neutron scattering by quasi-crystals: a model for icosahedral Al-Mn; for Al-Mn-Pd comparison with the experimental results. *Journal of Physics: Condensed Matter* **6**, 659-678 (1994).

94SC125

SCHERM R., KRUEGER E. Bragg optics - focusing in real and k -space. *Nuclear Instruments and Methods in Physics Research A* **338**, 1-8 (1994).

94WA126

WAGNER V., MAGERL A. Workshop on focusing Bragg optics. *Neutron News* **4**, 10-11 (1993).

94UD127

UDOVIC T.J., RUSH J.J., BERK N.F., ANDERSON I.S., DAOU J.N., VAJDA P., BLASCHKO O. Neutron spectroscopic comparison of rare-earth/hydrogen α -phase systems. *Zeitschrift fuer Physikalische Chemie* **179**, 349-357 (1993).

94AN128

ANDERSEN K.H., STIRLING W.G., SCHERM R., STUNAU A., FÅK B., GODFRIN H., DIANOUX A.J. Collective excitations in liquid ^4He : I. Experiment and presentation of data. *Journal of Physics: Condensed Matter* **6**, 821-834 (1994).

94FR129

FRICK B., RICHTER D., TREVINO S.F. Inelastic fast relaxation in a weakly fragile polymer glass near T_g . *Physica A* **201**, 88-94 (1993).

94NA130

NAVARRO J.M., FUERTES A., GOMEZ-ROMERO P., RODRIGUEZ CARVAJAL J. Crystal structure of $\text{La}_{1.85}\text{Ba}_{0.15}\text{CaCu}_2\text{O}_{6+y}$ determined by neutron powder diffraction. *Solid State Communications* **81**, 677-681 (1992).

94BO131

BOOTH J.G., COSTA M.M.R., RODRIGUEZ CARVAJAL J., PAIXAO J.A. Magnetic phase diagram of the dilute Cr-Ge system. *Journal of Magnetism and Magnetic Materials* **104-107**, 735-736 (1992).

94FI132

FISCHER P., LUDI A., PATTERSON H.H., HEWAT A.W. Anomalous temperature dependence of the structure of $\text{TlAu}(\text{CN})_2$ investigated by high-resolution neutron powder diffraction. *Inorganic Chemistry* **33**, 62-66 (1994).

94PE133

PENDLEBURY J.M., RICHARDSON D.J. Effects of gravity on the storage of ultracold neutrons. *Nuclear Instruments and Methods in Physics Research A* **337**, 504-511 (1994).

94TA134

TASSET F. Magnetic structures and neutron polarimetry. *Journal of Magnetism and Magnetic Materials* **129**, 47-52 (1994).

94RA135

RAISON P., LANDER G.H., DELAPALME A., WILLIAMS J.H., KAHN R., CARLILE C.J., KANELLAKOPOULOS B. Studies of $\text{U}(\text{C}_5\text{H}_5)_3\text{Cl}$: reorientational motions of cyclopentadienyl rings. *Molecular Physics* **81**, 369-383 (1994).

94HI136

HILFRICH K., KOELKER W., PETRY W., SCHAERPF O., NEMBACH E. The states of order and the phase diagram of $\text{Fe}_{1-x}\text{Si}_x$, $0.06 \leq x \leq 0.20$, investigated by neutron scattering. *Acta Metallurgica & Materiala* **42**, 743-748 (1994).

94HI137

HILFRICH K., PETRY W., SCHAERPF O., NEMBACH E. Phase diagram, superlattices and antiphase domains of Fe_3Al_x , $0.75 \leq x \leq 1.3$, investigated by neutron scattering. *Acta Metallurgica & Materiala* **42**, 731-741 (1994).

94OU138

OULADDIAF B., NEUMANN K.U., CRANGLE J., ZAYER N.K., ZIEBECK K.R.A., RESSOUCHE E. A neutron diffraction study of the phase transition in Pd_2TiIn . *Journal of Physics: Condensed Matter* **6**, 1563-1570 (1994).

94BE140

BERRET J.F., ROUX D.C., PORTE G., LINDNER P. Shear-induced isotropic-to-nematic phase transition in equilibrium polymers. *Europhysics Letters* **25**, 521-526 (1994).

94FR141

FRICK B., FETTERS L.J. Methyl group dynamics in glassy polyisoprene: a neutron backscattering investigation. *Macromolecules* **27**, 974-980 (1994).

94BO142

BONHOMME F., STETSON N.T., YVON K., FISCHER P., HEWAT A.W. Orthorhombic Mg_4IrD_5 with disordered deuterium distribution. *Journal of Alloys and Compounds* **200**, 65-68 (1993).

94UW143

UWAHA M., SAITO Y., SEKI S. Aggregation in a diffusion field-velocity selection via fractal dimension of DLA and a flow-induced first order transition. In "Dynamical Phenomena at Interfaces, Surfaces and Membranes", BEYSENS D., BOCCARA N., FORGACS G. Eds. (Nova Science Publishers, 1992) pp. 177-189.

94VO144

VOGT T., FITCH A.N., COCKCROFT J.K. Crystal and molecular structures of rhenium heptafluoride. *Science* **263**, 1265-1267 (1994).

94GU145

GUILLAUME F., SMART S.P., HARRIS K.D.M., DIANOUX A.J. Neutron scattering investigations of guest molecular dynamics in α , ω -dibromoalkane-urea inclusion compounds. *Journal of Physics: Condensed Matter* **6**, 2169-2184 (1994).

94RA146

RABILLOUD T., VUILLARD L., GILLY C., LAWRENCE J.J. Silver-staining of proteins in polyacrylamide gels: a general overview. *Cellular and Molecular Biology* **40**, 57-75 (1994).

94JU147

JUNGCLAUS A., CASTEN R.F., GILL R.L., BOERNER H.G. Levels in ^{168}Er above 2 MeV and the onset of chaos. *Physical Review C: Nuclear Physics* **49**, 88-102 (1994).

94ME148

MEDARDE M., RODRIGUEZ CARVAJAL J., VALLET-REGI M., GONZALEZ-CALBET J.M., ALONSO J. Crystal structure and microstructure of $\text{Nd}_{1.8}\text{Sr}_{0.2}\text{NiO}_{3.72}$: a K_2NiF_4 -type nickelate with monoclinic symmetry and ordered oxygen vacancies. *Physical Review B* **49**, 8591-8599 (1994).

94ME149

MEDARDE M., RODRIGUEZ CARVAJAL J., MARTINEZ B., BATLLE X., OBRADORS X. Magnetic ordering and spin reorientations in $\text{Nd}_{1.8}\text{Sr}_{0.2}\text{NiO}_{3.72}$. *Physical Review B* **49**, 9138-9149 (1994).

94CH150

CHATTOPADHYAY T., LYNN J.W., ROISOV N., GRIGEREIT T.E., BARILO S.N., ZHIGUNOV D.I. Magnetic ordering in Eu_2CuO_4 . *Physical Review B* **49**, 9944-9948 (1994).

94AL151

ALONSO J.A., RASINES I., RODRIGUEZ CARVAJAL J., TORRANCE J.B. Hole and electron doping of $R_2\text{BaNiO}_5$ (R =Rare Earths). *Journal of Solid State Chemistry* **109**, 231-240 (1994).

94KU152

KULDA J., WAGNER V., MIKULA P., SAROUN J. Comparative tests of neutron monochromators using elastically bent silicon and mosaic crystals. *Nuclear Instruments and Methods in Physics Research A* **338**, 60-64 (1994).

94BE153

BENOIT A., CAUSSIGNAC M., PUJOL S. New types of dilution refrigerator and space applications. *Physica B* **197**, 48-53 (1994).

94FA154

FÅK B., SCHERM R. Neutron scattering studies of liquid ^3He and ^3He - ^4He mixtures. *Physica B* **197**, 206-214 (1994).

94VI155

VITEBSKY I.M., STEPANOV A.A., CHATTOPADHYAY T., BROWN P.J. The nature of the unusual magnetic properties of Gd_2CuO_4 . *Low-Temperature Physics* **20**, 18-27 (1994).

94CH156

CHATTOPADHYAY T. Modulated magnetic phases in rare earth metallic systems. *Science* **264**, 226-231 (1994).

94AE157

AEBERSOLD M.A., GUEDEL H.U., FURRER A., BLANK H. Inelastic neutron scattering and optical spectroscopy of Dy^{3+} single ions and dimers in $\text{Cs}_3\text{Y}_2\text{Br}_9:10\% \text{Dy}^{3+}$ and $\text{Cs}_3\text{Dy}_2\text{Br}_9$. *Inorganic Chemistry* **33**, 1133-1138 (1994).

94AL158

ALCOBE X., ESTOP E., ALIEV A.E., HARRIS K.D.M., RODRIGUEZ CARVAJAL J., RIUS J. Temperature-dependent structural properties of *p*-diiodobenzene: neutron diffraction and high-resolution solid state ^{13}C NMR investigations. *Journal of Solid State Chemistry* **110**, 20-27 (1994).

94JA159

JANOT C., BOISSIEU M. DE. Quasicrystals as a hierarchy of clusters. *Physical Review Letters* **72**, 1674-1677 (1994).

94EV160

EVEN J., BERTAULT M., TOUDIC B., CAILLEAU H., FAVE J.L., CURRAT R., MOUSSA F. Dynamics of the phase transition of the fully polymerized and deuterated diacetylene 2,4-hexadiynylene bis(*p*-toluenesulfonate). *Physical Review B* **49**, 11602-11612 (1994).

94BO161

BONNET M., BOUCHERLE J.X., GIVORD F., LAPIERRE F., LEJAY P., ODIN J., MURANI A.P., SCHWEIZER J., STUNAUULT A. Anomalous magnetic behavior of cerium in Ce_2Sn_5 and Ce_3Sn_7 , two superstructures of $CeSn_3$.
Journal of Magnetism and Magnetic Materials **132**, 289-302 (1994).

94BO162

BOISSIEU M. DE, STEPHENS P., BOUDARD M., JANOT C., CHAPMAN D., AUDIER M. Disorder and complexity in the atomic structure of the perfect icosahedral alloy Al-Pd-Mn.
Physical Review Letters **72**, 3538-3541 (1994).

94IS163

ISNARD O., FRUCHART D. Magnetism in Fe-Based intermetallics: relationships between local environments and local magnetic moments.
Journal of Alloys and Compounds **205**, 1-15 (1994).

94ST164

STUHR U., WIPF H., KREMER R.K., MATTAUSCH H.J., SIMON A., COOK J.C. A neutron-spectroscopy study of two-dimensional hydrogen diffusion in the hydride halide $YBrH_{0.78}$.
Journal of Physics: Condensed Matter **6**, 147-158 (1994).

94RO165

ROYER A., BASTIE P., BELLET D., ZEYEN C.M.E. Relation entre les propriétés structurales et la morphologie des précipités γ' du superalliage monocristallin à base de nickel AM1.
Journal de Physique IV **4**, Colloque 3, C3-105-C3-110 (1994).

94HA166

HANLEY H.J.M., STRATY G.C., LINDNER P. Partial scattered intensities from a binary suspension of polystyrene and silica.
Langmuir **10**, 72-79 (1994).

94GU167

GUILLAUME M., FISCHER P., ROESSLI B., PODLESNYAK A., SCHEFER J., FURRER A. Magnetic order of Pr ions in related perovskite-type Pr 123 compounds.
Journal of Applied Physics **75**, 6331-6333 (1994).

94MU168

MUENCH C., HOFFMANN H., IBEL K., KALUS J., NEUBAUER G., SCHMELZER U., SELBACH J. Transient small-angle neutron scattering experiments on micellar solutions with a shear-induced structural transition.
Journal of Physical Chemistry **97**, 4514-4522 (1993).

94BR169

BRAMWELL S.T., HOLDSWORTH P.C.W. Can the universal jump be observed in two-dimensional XY magnets.
Journal of Applied Physics **75**, 5955-5957 (1994).

94AR170

ARONS R.R., COCKCROFT J.K., RESSOUCHE E. Structural and magnetic ordering in the cerium hydride (abstract).
Journal of Applied Physics **75**, 7050 (1994).

94KE171

KEARLEY G.J., FILLAUX F., BARON M.H., BENNINGTON S., TOMKINSON J. A new look at proton transfer dynamics along the hydrogen bonds in amides and peptides.
Science **264**, 1285-1289 (1994).

94CH172

CHATTOPADHYAY T., BROWN P.J., ROESSLI B. Disappearance of three-dimensional magnetic ordering in Gd_2CuO_4 .
Journal of Applied Physics **75**, 6816-6818 (1994).

94RO173

ROSOV N., LYNN J.W., KAESTNER J., WASSERMANN E.F., CHATTOPADHYAY T., BACH H. Temperature dependence of the magnetic excitations in ordered and disordered $Fe_{72}Pt_{28}$.
Journal of Applied Physics **75**, 6072-6074 (1994).

94CH174

CHATTOPADHYAY T., BURLET P., ROSSAT-MIGNOD J.M., BARTHOLIN H., VETTIER C., VOGT O. High-pressure neutron and magnetization investigations of the magnetic ordering in CeSb.
Physical Review B **49**, 15096-15103 (1994).

94HE175

HENTZSCHEL R., FAUST H.R., DENSCHLAG H.O., WILKINS B.D., GINDLER J. Mass, charge and energy distributions in the very asymmetric fission of ^{249}Cf induced by thermal neutrons.
Nuclear Physics A **571**, 427-446 (1994).

94KR176

KREMER R.K., COCKCROFT J.K., MATTAUSCH H.J., SIMON A., KEARLEY G.J. Optical vibrations of hydrogen in some rare-earth monohalide hydrides.
Journal of Physics: Condensed Matter **6**, 4053-4066 (1994).

94MA177

MAY R.P. Geometrical optimization of neutron small-angle scattering instruments.
Journal of Applied Crystallography **27**, 298-301 (1994).

94FA178

FARAGO B. Dynamics and diffusion in macromolecules, colloids and microemulsions
In "Neutron and Synchrotron Radiation for Condensed Matter Studies: Hercules (course)" Vol. 3, BARUCHEL J., HODEAU J.L., LEHMANN M.S., REGNARD J.R., SCHLENKER C. Eds. (Les Editions de Physique/Springer Verlag, 1994) pp. 93-108

94BA179

BAUMBACH G.T., HOLY V., PIETSCH U., GAILHANOU M. The influence of specular interface reflection on grazing incidence x-ray diffraction and diffuse scattering from superlattices.
Physica B **198**, 249-252 (1994).

94SC180

SCHAERPF O., ANDERSON I.S. The role of surfaces and interfaces in the behaviour of non-polarizing and polarizing supermirrors.
Physica B **198**, 203-212 (1994).

94LI181

LIED A., DOSCH H., BILGRAM J.H. Glancing angle x-ray scattering from single crystal ice surfaces.
Physica B **198**, 92-96 (1994).

94CO182

COPLEY J.R.D., COOK J.C. An analysis of the effectiveness of oscillating radial collimators in neutron scattering applications.
Nuclear Instruments and Methods in Physics Research A **345**, 313-323 (1994).

94CH183

CHARVOLIN J. Systèmes d'amphiphiles: films et structures cloisonnées.
Images de la Recherche **2**, 1-4 (1994).

94HE184

HEWAT A.W. Neutron powder diffraction on the ILL high flux reactor and high Tc superconductors.
In "NATO ASI Series - Vol. 263 - Materials and Crystallographic Aspects of HTc-Superconductivity", KALDIS E. Ed. (Kluwer Academic Publishers, 1994) pp. 17-44.

94CO185

COCKCROFT J.K., FITCH A.N.
Structure of solid trichlorofluoromethane, CFC1₃, by powder neutron diffraction.
Zeitschrift fuer Kristallographie **209**, 488-490 (1994).

94KA186

KASSNER K., MISBAH C., MUELLER-KRUMBHAAR H., VALANCE A. Directional solidification at high speed. I. Secondary instabilities.
Physical Review E **49**, 5477-5494 (1994).

94SC187

SCHMID B., DORNER B., PETITGRAND D., REGNAULT L.P., STEINER M. Magnetic excitations of CsFeCl₃ in an external magnetic field parallel to the hexagonal plane.
Zeitschrift fuer Physik B **95**, 13-21 (1994).

94MU188

MURANI A.P. Comment on "Temperature dependence of Kondo resonance in YbAl₃".
Physical Review Letters **72**, 4153 (1994).

94KA189

KASSNER K., MISBAH C., MUELLER-KRUMBHAAR H., VALANCE A. Directional solidification at high speed. II. Transition to chaos.
Physical Review E **49**, 5495-5515 (1994).

94DR190

DRUYTS S., WAGEMANS C., GELTENBORT P. Determination of the ³⁵Cl(n,p)³⁵S reaction cross section and its astrophysical implications.
Nuclear Physics A **573**, 291-305 (1994).

94DI191

DIANOUX A.J., KNELLER G.R., SAUVAJOL J.L., SMITH J.C. Dynamics of sodium-doped polyacetylene.
Journal of Chemical Physics **101**, 634-644 (1994).

94BA192

BAUSENWEIN T., BERTAGNOLLI H., DAVID A., GOLLER K., ZWEIER H., TOEDHEIDE K., CHIEUX P. Structure and intermolecular interactions in fluid ammonia: an investigation by neutron diffraction at high pressure, statistical-mechanical calculations and computer simulations.
Journal of Chemical Physics **101**, 672-682 (1994).

94ST193

STRAUSS G., ZWEIER H., BERTAGNOLLI H., BAUSENWEIN T., TOEDHEIDE K., CHIEUX P. High-pressure neutron diffraction on liquid sulphur hexafluoride and interpretation by statistical-mechanical theories and computer simulations.
Journal of Chemical Physics **101**, 662-671 (1994).

94CH194

CHATTOPADHYAY T., SIEMENSMEYER K. Observation of hyperfine-induced nuclear polarization in Nd₂CuO₄.
Physica C **235-240**, 1563-1564 (1994).

94IS195

ISNARD O., MIRAGLIA S., GUILLOT M., FRUCHART D. High field magnetization measurements of Sm₂Fe₁₇, Sm₂Fe₁₇N₃, Sm₂Fe₁₇D₅, and Pr₂Fe₁₇, Pr₂Fe₁₇N₃ (invited).
Journal of Applied Physics **75**, 5988-5993 (1994).

94BR196

BRAMWELL S.T., GINGRAS M.J.P., REIMERS J.N.
Order by disorder in an anisotropic pyrochlore lattice
antiferromagnet.
Journal of Applied Physics **75**, 5523-5525 (1994).

94SC197

SCHOENFELD C., HEMPELMANN R., RICHTER D.,
SPRINGER T., DIANOUX A.J., RUSH J.J., UDOVIC T.J.,
BENNINGTON S.M. Dynamics of hydrogen in α -LaNi₅
hydride investigated by neutron scattering.
Physical Review B **50**, 853-865 (1994).

94WA198

WAGEMANS C., DRUYTS S., GELTENBORT P.
Characteristics of the $^{50}\text{V}(n_{\text{th}},p)^{50}\text{Ti}$ reaction.
Physical Review C **50**, 487-489 (1994).

94GA199

GARCIA-MUNOZ J.L., RODRIGUEZ CARVAJAL J.,
LACORRE P. Neutron-diffraction study of the magnetic
ordering in the insulating regime of the perovskites RNiO₃
(R=Pr and Nd).
Physical Review B **50**, 978-992 (1994).

94RO200

ROBINSON S.J., JOLIE J., BOERNER H.G.,
SCHILLEBEECKX P., ULBIG S., LIEB K.P.
E₂ and E₃ transitions from quadrupole-octupole coupled
states in ^{144}Nd .
Physical Review Letters **73**, 412-415 (1994).

94AN201

ANTONOV V.E., BOKHENKOV E.L., LATYNIN A.I.,
RASHUPKIN V.I., DORNER B., BAIER M.,
WAGNER F.E. Crystal structure and superconductivity
of high pressure hydrides and deuterides of HfRu
and ZrRu compounds.
Journal of Alloys and Compounds **209**, 291-297 (1994).

94ST202

STAUB U., MESOT J., GUILLAUME M.,
ALLENSPACH P., FURRER A., MUTKA H.,
BOWDEN Z., TAYLOR A. Neutron spectroscopic
studies of the crystal field in HoBa₂Cu₃O_x (6≤x≤7).
Physical Review B **50**, 4068-4074 (1994).

94NU203

NUTLEY M.P., BOOTHROYD A.T., STADDON C.R.,
PAUL D.McK., PENFOLD J. Magnetic-induction profile in
a type-I superconductor by polarized-neutron reflectometry.
Physical Review B **49**, 15789-15798 (1994).

94IS204

ISNARD O., MIRAGLIA S., FRUCHART D.,
GIORGETTI C., PIZZINI S., DARTYGE E., KRILL G.,
KAPPLER J.P. Magnetic study of the Ce₂Fe₁₇H_x
compounds: magnetic circular x-ray dichroism,
x-ray absorption near-edge structure, magnetization,
and diffraction results.
Physical Review B **49**, 15692-15701 (1994).

94SC205

SCHROEDER-HEBER A., ASMUSSEN B., PRESS W.,
BLANK H., GIES H. Dynamical behaviour of methane
in a clathrasil (dodecasil 3C) studied by quasi-elastic
neutron scattering.
Molecular Physics **82**, 857-873 (1994).

94SC206

SCHOBER H., DORNER B. Lattice dynamics of berlinite
(AlPO₄): a comparative study with quartz (SiO₂).
Journal of Physics: Condensed Matter **6**, 5351-5372 (1994).

94NO207

NOZIERES P. The effect of recoil on edge singularities.
Journal de Physique I **4**, 1275-1280 (1994).

94DU208

DUPORT C., NOZIERES P., VILLAIN J.
Elasticity-driven instability in molecular beam epitaxy.
Acta Physica Slovaca **44**, 261-268 (1994).

94AL209

ALLENSPACH P., MESOT J., STAUB U.,
GUILLAUME M., FURRER A., YOO S.I., KRAMER M.J.,
MCCALLUM R.W., MALETTA H., BLANK H.,
MUTKA H., OSBORN R., ARAI M., BOWDEN Z.,
TAYLOR A.D. Magnetic properties of Nd³⁺
in Nd-Ba-Cu-O-compounds.
Zeitschrift fuer Physik B **95**, 301-310 (1994).

94LO210

LOPEZ-CABARCOS E., GEYER A. DE,
GALERA GOMEZ P. Study of the aggregation of
undecylammonium chloride in presence of sodium chloride
using small angle neutron scattering.
Journal de Physique IV **3**, Colloque 8, C8- 205-C8-210 (1993).

94RA211

RAISON P., REBIZANT J., APOSTOLIDIS C.,
LANDER G.H., DELAPALME A., KIAT J.M.,
SCHWEISS P., KANELAKOPULOS B.,
GONTHIER-VASSAL A., BROWN P.J.
Studies of U(C₅H₅)₃Cl: I - Evidence for structural phase
transitions below room temperature.
Zeitschrift fuer Kristallographie **209**, 720-726 (1994).

94CL212

CLEMENTS B.E., FORBERT H., KROTSHECK E.,
LAUTER H.J., SAARELA M., TYMCZAK C.J.
Dynamics of boson quantum films.
Physical Review B **50**, 6958-6981 (1994).

94BR213

BRAZOVSKII S., MATVEENKO S., NOZIERES P.
Spin excitations carry charge currents: one-dimensional
Hubbard model.
Journal de Physique I **4**, 571-578 (1994).

94SC214

SCHWAB W., CLERC H.G., MUTTERER M., THEOBALD J.P., FAUST H.R. Cold fission of $^{233}\text{U}(\text{n}_{\text{th}},\text{f})$. Nuclear Physics A **577**, 674-690 (1994).

94FI215

FILHOL A. Organic conductors: the crystallographic approach. In "Organic Conductors Fundamentals and Applications", FARGES J.P. Ed. (Marcel Dekker, 1994) Chap. 5, pp. 147-228.

94BA216

BALIBAR S., NOZIERES P. Helium crystals as a probe in materials science. Solid State Communications **92**, 19-29 (1994).

94FR217

FRICK B., RICHTER D., ZORN R., FETTERS L.J. The fast relaxation process near the glass transition in amorphous polymers with different microstructure. Journal of Non-Crystalline Solids **172-174**, 272-285 (1994).

94DI218

DIANOUX A.J., SAUVAJOL J.L., KNELLER G.R., SMITH J.C. Dynamics of pristine and doped polyacetylene: a combined inelastic neutron scattering and computer simulation analysis. Journal of Non-Crystalline Solids **172-174**, 472-480 (1994).

94SC219

SCHAEFER D.W., OLIVIER B.J., ASHLEY C., BEAUCAGE G., RICHTER D., FARAGO B., FRICK B., FISCHER A.D. Structure and topology of silica aerogels during densification. Journal of Non-Crystalline Solids **172-174**, 647-655 (1994).

94CH220

CHARVOLIN J., SADO C. Geometrical foundation of mesomorphic polymorphism. In "Micelles, Membranes, Microemulsions, and Monolayers", GELBART W.M., BEN-SHAUL A., ROUX D. Eds. (Springer Verlag, 1994) Chap. 4, pp. 219-249.

94SC221

SCHAUB T.M., BUERGLER D.E., GUENTHERODT H.J., SUCK J.B. Quasicrystalline structure of icosahedral $\text{Al}_{68}\text{Pd}_{23}\text{Mn}_9$ resolved by scanning tunneling microscopy. Physical Review Letters **73**, 1255-1258 (1994).

94CH222

CHIEUX P., DUPUY-PHILON J., JAL J.F., MORKEL C., SUCK J.B. Collective atomic dynamics in mixtures of liquid alkali metals and molten alkali halides. Journal of Physics: Condensed Matter **6**, A235-A240 (1994).

94UD223

UDOVIC T.J., RUSH J.J., ANDERSON I.S. Neutron spectroscopic evidence of concentration-dependent hydrogen ordering in the octahedral sublattice of $\beta\text{-TbH}_{2+x}$. Physical Review B **50**, 7144-7146 (1994).

94MU224

MURANI A.P. Paramagnetic scattering from the valence-fluctuation compound YbAl_3 . Physical Review B **50**, 9882-9893 (1994).

94CH225

CHARVOLIN J. Membrane in chloroplasts. A topological approach to grana and frets. Biophysical Chemistry **49**, 23-26 (1994).

94RE226

REEHUIS M., ZEPPEFELD K., JEITSCHKO W., RESSOUCHE E. Magnetic structure of $\text{Dy}_2\text{Cr}_2\text{C}_3$. Journal of Alloys and Compounds **209**, 217-220 (1994).

94RI227

RITTER C., CYWINSKI R., KILCOYNE S.H., MONDAL S., RAINFORD B.D. Intrinsic and induced Mn moments in $\text{Dy}_{1-x}\text{Y}_x\text{Mn}_2$. Physical Review B **50**, 9894-9905 (1994).

94RU228

RUBIN J., BARTOLOME J., ANNE M., KEARLEY G.J., MAGERL A. The dynamics of NH_4^+ in the NH_4MF_3 perovskites: I. A quasielastic neutron scattering study. Journal of Physics: Condensed Matter **6**, 8449-8468 (1994).

94RE229

REEHUIS M., VOMHOF T., JEITSCHKO W. The magnetic structure of UCo_2P_2 . Journal of Physics and Chemistry of Solids **55**, 625-630 (1994).

94IS230

ISNARD O., MIRAGLIA S., FRUCHART D., DEPORTES J., L'HERITIER P. Magnetic properties of fully nitrogenated $\text{R}_2\text{Fe}_{17}\text{N}_3$ ($\text{R} = \text{Ce}, \text{Nd}, \text{Pr}$). Journal of Magnetism and Magnetic Materials **131**, 76-82 (1994).

94JA231

JANOT C. Hierarchical phase transitions and vibrational modes localisation in quasicrystals. International Journal of Modern Physics B **8**, 2245-2281 (1994).

94HE232

HENNION M., BELLOUARD C., MIREBEAU I., BLANK H., DORMANN J.L., DJEGA-MARIADASSOU C. Static and dynamic study of fine particles by neutron scattering. In "Studies of Magnetic Properties of Fine Particles and their Relevance to Materials Science", DORMANN J.L., FIORANI D. Eds. (Elsevier Science Publishers, 1992) pp. 27-32.

94CH233

CHARVOLIN J. Soft condensed matter.
In "Neutron and Synchrotron Radiation for Condensed Matter Studies: Hercules (course)" Vol. 3, BARUCHEL J., HODEAU J.L., LEHMANN M.S., REGNARD J.R., SCHLENKER C. Eds. (Les Editions de Physique/Springer Verlag, 1994) pp. 3-6.

94DO234

DORNER B. A comparison of time-of-flight (TOF) and three axis spectrometer (TAS) techniques for the study of excitations in single crystals.
Journal of Neutron Research **2**, 115-127 (1994).

94SC235

SCHILLEBEECKX P., WAGEMANS C., GELTENBORT P., GOENNENWEIN F., OED A.
Investigation of mass, charge and energy of $^{241}\text{Pu}(n_{\text{th}},f)$ fragments with the Cosi-Fan-Tutte spectrometer.
Nuclear Physics A **580**, 15-32 (1994).

94AS236

ASMUSSEN B., BALSZUNAT D., PRESS W., PRAGER M., CARLILE C.J., BUETTNER H.
Quantum rotation of methane in argon: the isotope effect.
Physica B **202**, 224-228 (1994).

94FI237

FILLAUX F., CARLILE C.J., KEARLEY G.J., PRAGER M. Inelastic neutron-scattering study of methyl tunnelling and the quantum sine-Gordon breather mode in isotopic mixtures of 2,6-dimethyl-pyridine at low temperature.
Physica B **202**, 302-310 (1994).

94HE238

HEIDEMANN A. New methods in high resolution neutron spectroscopy.
Physica B **202**, 207-214 (1994).

94VE239

VERSMOLD H., LINDNER P. Reinterpretation of small-angle neutron-scattering studies on ordered colloid dispersions.
Langmuir **10**, 3043-3045 (1994).

94VU240

VUILLARD L., RABILLOUD T., LEBERMAN R., BERTHET-COLOMINAS C., CUSACK S.
A new additive for protein crystallization.
FEBS Letters **353**, 294-296 (1994).

94QU241

QUEMERAIS P. Model of growth for long-range chemically ordered compounds: application to quasicrystals.
Journal de Physique I **4**, 1669-1697 (1994).

94TH242

THOLE B.T., VAN DER LAAN G., FABRIZIO M.
Magnetic ground-state properties and spectral distributions. I. X-ray-absorption spectra.
Physical Review B **50**, 11466-11473 (1994).

94SU243

SUMARLIN I.W., LYNN J.W., CHATTOPADHYAY T., BARILO S.N., ZHIGUNOV D.I. Dispersion of the magnetic excitations of the Pr ions in Pr_2CuO_4 .
Physica C **219**, 195-199 (1994).

94BU244

BUETTNER H., KEARLEY G.J., HOWARD C.J., FILLAUX F. Structure of the Hofmann clathrates $\text{Ni}(\text{NH}_3)_2\text{Ni}(\text{CN})_4 \cdot 2\text{C}_6\text{D}_6$ and $\text{Zn}(\text{NH}_3)_2\text{Ni}(\text{CN})_4 \cdot 2\text{C}_6\text{H}_6$.
Acta Crystallographica B **50**, 431-435 (1994).

94DE245

DEUTSCHER G., NOZIERES P.
Cancellation of quasiparticle mass enhancement in the conductance of point contacts.
Physical Review B **50**, 13557-13562 (1994).

94WI246

WINKELMANN M., GRAF H.A., WAGNER B., HEWAT A.W. Substitutional disorder in the system $\text{Mg}_{1-x}\text{Cu}_{2+x}\text{O}_3$: Cu^{2+} in a compressed octahedral environment.
Zeitschrift fuer Kristallographie **209**, 870-873 (1994).

94LO247

LOPEZ-CABARCOS E., BATALLAN F., FRICK B., EZQUERRA T.A., BALTA CALLEJA F.J.
Molecular dynamics of ferroelectric polymeric systems as studied by incoherent quasielastic neutron scattering.
Physical Review B **50**, 13214-13224 (1994).

94SC248

SCHERM R., FÄK B. Neutrons.
In "Neutron and Synchrotron Radiation for Condensed Matter Studies: Hercules (course)" Vol. 1, BARUCHEL J., HODEAU J.L., LEHMANN M.S., REGNARD J.R., SCHLENKER C. Eds. (Les Editions de Physique/Springer Verlag, 1994) pp. 113-143.

94AL249

ALTORFER F., BUEHRER W., ANDERSON I., SCHAERPF O., BILL H., CARRON P.L.
Fast ionic diffusion in Li_2S investigated by quasielastic neutron scattering.
Journal of Physics: Condensed Matter **6**, 9937-9947 (1994).

94RE250

REEHUIS M., RITTER C., BALLOU R., JEITSCHKO W.
Ferromagnetism in the ThCr_2Si_2 type phosphide LaCo_2P_2 .
Journal of Magnetism and Magnetic Materials **138**, 85-93 (1994).

94TE251

TENNANT D.A., MCMORROW D.F., NAGLER S.E., COWLEY R.A., FÄK B. Spin waves in the spin-flop phase of RbMnF₃.
Journal of Physics: Condensed Matter **6**, 10341-10355 (1994).

94BA252

BALDO CEOLIN M., BENETTI P., BITTER T., BOBISUT F., CALLIGARICH E., DOLFINI R., DUBBERS D., EL-MUZEINI P., GENONI M., GIBIN D., GIGLI BERZOLARI A., GOBRECHT K., GUGLIELMI A., LAST J., LAVEDER M., LIPPERT W., MATTIOLI F., MAURI F., MEZZOTO M., MONTANARI C., PIAZZOLI A., PUGLIERIN G., RAPPOLDI A., RASELLI G.L., SCANNICCHIO D., SCONZA A., VASCON M., VISENTIN L. A new experimental limit on neutron-antineutron oscillations.
Zeitschrift fuer Physik C **63**, 409-416 (1994).

94GO253

GOMPF F., RENKER B., SCHOBER H., ADELMANN P., HEID R. Inelastic neutron scattering results on pure and doped fullerenes.
Journal of Superconductivity **7**, 643-645 (1994).

94RE254

RENKER B., GOMPF F., SCHOBER H., ADELMANN P., HEID R. Intermolecular vibrations in pure and doped C₆₀: an inelastic neutron scattering study.
Journal of Superconductivity **7**, 647-649 (1994).

94RO255

ROESSLI B., FISCHER P., SCHEFER J., BUEHRER W., FURRER A., VOGT T., PETRAVOVSKII G., SABLINA K. Elastic and inelastic neutron study of CuGeO₃.
Journal of Physics: Condensed Matter **6**, 8469-8477 (1994).

94BE256

BELRHALI H., YAREMCHUK A., TUKALO M., LARSEN K., BERTHET-COLOMINAS C., LEBERMAN R., BEIJER B., SPROAT B., ALS-NIELSEN J., GRUEBEL G., LEGRAND J.F., LEHMANN M., CUSACK S. Crystal structures at 2.5 Angstrom resolution of seryl-tRNA synthetase complexed with two analogs of seryl adenylate.
Science **263**, 1432-1436 (1994).

94ST257

STUHRMANN H.B., LEHMANN M.S. Anomalous dispersion of x-ray scattering from low-z elements. In "Resonant Anomalous X-Ray Scattering, Theory and applications", MATERLIK G., SPARKS C.J., FISCHER K. Eds. (Elsevier Science Publishers, 1994) pp. 175-194.

94LE258

LEHMANN M.S. Neutron crystallography of biological molecules. In "Neutron and Synchrotron Radiation for Condensed Matter Studies: Hercules (course)" Vol. 3, BARUCHEL J., HODEAU J.L., LEHMANN M.S., REGNARD J.R., SCHLENKER C. Eds. (Les Editions de Physique/Springer Verlag, 1994) pp. 221-237.

94DO259

DORNER B., MAY R. Physik-Nobelpreis 1994 Strukturuntersuchung mit Neutronen. Physik in Unserer Zeit **6**, 278-279 (1994).

94UD260

UDOVIC T.J., RUSH J.J., ANDERSON I.S. Local-mode dynamics in YH₂ and YD₂ by isotope-dilution neutron spectroscopy.
Physical Review B **50**, 15739-15743 (1994).

94PA261

PAPANEK P., FISCHER J.E., SAUVAJOL J.L., DIANOUX A.J., MAO G., WINOKUR M.J., KARASZ F.E. Inelastic-neutron-scattering studies of poly(*p*-phenylene vinylene).
Physical Review B **50**, 15668-15677 (1994).

94PI262

PINTSCHOVIVUS L., PYKA N., KUSSMAUL R., MUNZ D., EIGENMANN B., SCHOLTES B. Experimental and theoretical investigation of the residual stress distribution in brazed ceramic-steel components.
Materials Science and Engineering A **177**, 55-61 (1994).

94HO263

HOSER A., MARTIN M., SCHWEIKA W., CARLSSON A.E., CAUDRON R., PYKA N. Diffuse neutron scattering of iron-doped nickel oxide.
Solid State Ionics **72**, 72-75 (1994).

94BR264

BRADEN M., SCHNELLE W., SCHWARZ W., PYKA N., HEGER G., FISK Z., GAMAYUNOV K., TANAKA I., KOJIMA H. Elastic and inelastic neutron scattering studies on the tetragonal to orthorhombic phase transition of La_{2-x}Sr_xCuO_{4+δ}.
Zeitschrift fuer Physik B **94**, 29-37 (1994).

94JE265

JESIOR J.C., FILHOL A., TRANQUI D. *FOLDIT(LIGHT)* - An interactive program for Macintosh computers to analyze and display Protein Data Bank coordinates files.
Journal of Applied Crystallography **27**, 1075 (1994).

94VO266

VOGL G., PETRY W. Wie springen die Atome in Metallen ? Bestimmung des Elementarsprungs der Diffusion mit interferierender Strahlung. *Physikalische Blätter* **50**, 925-928 (1994).

94WH267

WHITE R.P., STRIDE J.A., BOLLEN S.K., CHAI SA-ARD N., KEARLEY G.J., JAYASOORIYA U.A., CANNON R.D. Electronic interactions in mixed-valence and mixed-metal ion clusters: inelastic neutron scattering spectra of the complexes $[\text{Fe}^{\text{III}}_2\text{M}^{\text{II}}\text{O}(\text{OOCMe})_6(\text{py})_3](\text{py})$, where M = Mn, Ni. *Journal of the American Chemical Society* **115**, 7778-7782 (1993).

94HY268

KOLESNIKOV A.I., BASHKIN I.O., PONYATOVSKY E.G., HEMPELMANN R., RICHTER D., DIANOX A.J. Hydrogen diffusion in BCC $\text{Ti}_{0.84}\text{V}_{0.16}\text{H}_{0.61}$ hydride. In "Proceedings of the Quasielastic Neutron Scattering Workshop QENS'93", COLMENERO J., ALEGRIA A., BERMEJO F.J. Eds. (World Scientific, 1994) pp. 184-193.

94EL269

EL BAGHDADI A., GUILLAUME F., BOYSEN H., DIANOX A.J., CODDENS G. Translational and rotational motions of n-alkane molecules within the channels of urea inclusion compounds. In "Proceedings of the Quasielastic Neutron Scattering Workshop QENS'93", COLMENERO J., ALEGRIA A., BERMEJO F.J. Eds. (World Scientific, 1994) pp. 131-140.

94BA270

BARUCHEL J., EPELBOIN Y., GASTALDI J., HAERTWIG J., KULDA J., REJMANKOVA P., SCHLENKER M., ZONTONE F. First topographic results at the European Synchrotron Radiation Facility. *Physica Status Solidi (a)* **141**, 59-69 (1994).

94KU271

KULDA J., STRAUCH D., PAVONE P., ISHII Y. Inelastic-neutron-scattering study of phonon eigenvectors and frequencies in Si. *Physical Review B* **50**, 13347-13354 (1994).

94VR272

VRANA M., LUKAS P., MIKULA P., KULDA J. Bragg diffraction optics in high resolution strain measurements. *Nuclear Instruments and Methods in Physics Research A* **338**, 125-131 (1994).

94HO273

HOCK R., KULDA J. Monte Carlo simulations of neutron backscattering from vibrating silicon crystals. *Nuclear Instruments and Methods in Physics Research A* **338**, 38-43 (1994).

94MI274

MIKULA P., KULDA J., LUKAS P., VRANA M., WAGNER V. Bent perfect crystals in asymmetric diffraction geometry in neutron scattering experiments. *Nuclear Instruments and Methods in Physics Research A* **338**, 18-26 (1994).

94LE275

LEADBETTER A.J. The role of large facilities in understanding silicate glasses. *Journal of Non-Crystalline Solids* **179**, 116-124 (1994).

94SU276

SUCK J.B., SCHERM R. Spaete Ehrung fuer zwei Pioniere der Neutronenstreuung. *Physikalische Blätter* **50**, 137-139 (1994).

94LE277

LE BAS G., MASON S.A. Neutron diffraction structure of α -cyclodextrin cyclopentanone hydrate at 20 K: host-guest interactive disorder. *Acta Crystallographica B* **50**, 717-724 (1994).

94RO278

ROESSLI B., FISCHER P., STAUB U., ZOLLIKER M., FURRER A. Combined electronic-nuclear magnetic ordering of the Ho^{3+} ions and magnetic stacking faults in $\text{HoBa}_2\text{Cu}_3\text{O}_x$ ($x = 7.0, 6.8, 6.3$). *Journal of Applied Physics* **75**, 6337-6339 (1994).

94BO279

BOISSIEU M. DE, STEPHENS P., BOUDARD M., JANOT C. Is the Al-Pd-Mn icosahedral phase centrosymmetrical ? *Journal of Physics: Condensed Matter* **6**, 363-373 (1994).

94JE280

JEANTEUR D., PATTUS F., TIMMINS P.A. Membrane-bound form of the pore-forming domain of colicin A - A neutron scattering study. *Journal of Molecular Biology* **235**, 898-907 (1994).

94TI281

TIMMINS P.A. Neutron scattering in biology. In "Neutron Scattering - Lecture Notes of the First Summer School on Neutron Scattering", FURRER A. Ed. (1993) pp. 157-176, PSI Proceedings 1993 - 01.

94TI282

TIMMINS P.A. The structure and assembly of viruses: contributions from x-ray synchrotron and neutron radiation. In "Neutron and Synchrotron Radiation for Condensed Matter Studies: Hercules (course)" Vol. 3, BARUCHEL J., HODEAU J.L., LEHMANN M.S., REGNARD J.R., SCHLENKER C. Eds. (Les Editions de Physique/Springer Verlag, 1994) pp. 239-256.

94DE283

DEWEY M.S., KESSLER E.G., GREENE G.L., DESLATTES R.D., SACCHETTI F., PETRILLO C., FREUND A.K., BOERNER H.G., ROBINSON S.J., SCHILLEBEECKX P. Structure factors in germanium at 0.342 and 1.382 MeV. *Physical Review B* **50**, 2800-2808 (1994).

94DO284

DORNER B. Structural excitations. In "Neutron Scattering - Lecture Notes of the First Summer School on Neutron Scattering", FURRER A. Ed. (1993) pp. 111-127, PSI Proceedings 1993 - 01.

94QU285

QUIVY A., LEFEBVRE S., SOUBEYROUX J.L., FILHOL A., BELLISSENT R., IBBERSON R.M. High-resolution time-of-flight measurements of the lattice parameter and thermal expansion of the icosahedral phase $Al_{62}Cu_{25.5}Fe_{12.5}$. *Journal of Applied Crystallography* **27**, 1010-1014 (1994).

94WI286

WILLIAMS C.E., MAY R.P., GUINIER A. Small-angle scattering of x-rays and neutrons. *Materials Science and Technology* **2B**, 611-656 (1994).

94IB287

IBARRA M.R., MARQUINA C., ALGARABEL P.A., TERESA J.M. DE, RITTER C., DEL MORAL A. High magnetostrictive materials RMn_2 . In "Proceedings of the 13th International Workshop on RE Magnets & their Applications", MANWANING C.A.F., JONES D.G.R., WILLIAMS A.J., HARRIS I.R. Eds. (1994) pp. 127-136.

94GE288

GERTEL-KLOOS H., BROKMEIER H.G., RITTER C. The effect of various processing conditions on the texture development in extruded Al-Cu composites. *Zeitschrift fuer Metallkunde* **85**, 603-608 (1994).

94GE289

GERTEL-KLOOS H., BROKMEIER H.G., BUNGE H.J., RITTER C. High temperature *in situ* texture measurements at the neutron powder diffractometer D1B. *Journal of Materials Science Letters* **13**, 547-550 (1994).

94KU290

KULDA J. Neutronova difrakce. Summer School of Czech Crystallographic Society, Ostrava, Czech Republic, June 6-10, 1994.

94LE291

LELIEVRE-BERNA E., ROUCHY J., BALLOU R. Field induced first order magnetic transition and associated volume effect in $TbMn_2$. *Journal of Magnetism and Magnetic Materials* **137**, L6-L10 (1994).

94RA292

RANDL O.G., SEPIOL B., VOGL G., FELDWISCH R., SCHROEDER K. Quasielastic Moessbauer spectroscopy and quasielastic neutron scattering from non-Bravais lattices with differently occupied sublattices. *Physical Review B* **49**, 8768-8773 (1994).

94TE293

TERECH P., RODRIGUEZ V., BARNES J.D., MCKENNA G.B. Organogels and aerogels of racemic and chiral 12-hydroxyoctadecanoic acid. *Langmuir* **10**, 3406-3418 (1994).

94TE294

TERECH P., MALDIVI P., DAMMER C. "Living polymers" in organic solvents: stress relaxation in bicopper tetracarboxylate/tert-butyl cyclohexane solutions. *Journal de Physique II* **4**, 1799-1811 (1994).

94TE295

TERECH P. Agrégation de surfactants en milieu organique: gels physiques et "polymères vivants". *Images de la Recherche*, 209-212 (1994).

94FE296

FEREY G., PANNETIER J. The pyrochlore \rightarrow H.T.B. \rightarrow ReO_3 successive phase transitions of FeF_3 . *European Journal of Solid State & Inorganic Chemistry* **31**, 697-704 (1994).

94BO297

BOISSIEU M. DE, STEPHENS P., BOUDARD M., JANOT C., CHAPMAN D., AUDIER M. Anomalous x-ray diffraction study of the $AlPdMn$ icosahedral phase. *Journal of Physics: Condensed Matter* **6**, 10725-10745 (1994).

94RI298

RICHTER D., WILLNER L., ZIRKEL A., FARAGO B., FETTERS L.J., HUANG J.S. Polymer motion at the crossover from Rouse to reptation dynamics. *Macromolecules* **27**, 7437-7446 (1994).

94SC299

SCHAUB T.M., BUERGLER D.E., GUENTHERODT H.J., SUCK J.B. Investigation of the icosahedral quasicrystal $\text{Al}_{68}\text{Pd}_{23}\text{Mn}_9$ by LEED and STM. *Zeitschrift fuer Physik B* **96**, 93-96 (1994).

94HE300

HEIDEMANN A. Directions in instrumentation for quasielastic neutron scattering. In "Proceedings of the Quasielastic Neutron Scattering Workshop QENS'93", COLMENERO J., ALEGRIA A., BERMEJO F.J. Eds. (World Scientific, 1994) pp. 15-27.

94MU301

MUTKA H. Energy-resolved small-angle thermal neutron scattering: a challenge for instrumentation. In "Proceedings of the Quasielastic Neutron Scattering Workshop QENS'93", COLMENERO J., ALEGRIA A., BERMEJO F.J. Eds. (World Scientific, 1994) pp. 29-37.

94GY302

GYGAX F.N., AMATO A., SCHENCK A., ANDERSON I.S., RUSH J.J., SOLT G. μ^+ Localization and tunnelling in Sc. *Hyperfine Interactions* **85**, 73-78 (1994).

94GR303

GRIMMER H., BOENI P., ELSENHANS O., FRIEDLI H.P., LEIFER K., BUFFAT P., ANDERSON I.S. Characterization of multilayers for neutron optics. *Materials Science Forum* **166-169**, 279-284 (1994).

94EL304

ELSENHANS O., BOENI P., FRIEDLI H.P., GRIMMER H., BUFFAT P., LEIFER K., SOECHTIG J., ANDERSON I.S. Development of Ni/Ni multilayers supermirrors for neutron optics. *Thin Solid Films* **246**, 110-119 (1994).

94UD305

UDOVIC T.J., RUSH J.J., ANDERSON I.S., DAOU J.N., VAJDA P., BLASCHKO O. Vibrations of hydrogen and deuterium in solid solution with lutetium. *Physical Review B* **50**, 3696-3701 (1994).

94RO306

ROJAS R.M., HERRERO P., GARCIA CHAIN P.J., RODRIGUEZ CARVAJAL J. Structural study of the rhombohedral fluorite-related R_{III} phase $\text{U}_{1-y}\text{La}_y\text{O}_{2\pm x}$, $0.56 \leq y \leq 0.67$. *Journal of Solid State Chemistry* **112**, 322-328 (1994).

94PA307

PALACIN M.R., BASSAS J., RODRIGUEZ CARVAJAL J., FUERTES A., CASAN-PASTOR N., GOMEZ-ROMERO P. Studies of the formation and reduction of a mixed three-dimensional perovskite of copper and titanium. *Materials Research Bulletin* **29**, 973-980 (1994).

94IS308

ISNARD O., VULLIET P., BLAISE A., SANCHEZ J.P., MIRAGLIA S., FRUCHART D. ^{155}Gd Moessbauer spectroscopy study of the $\text{Gd}_2\text{Fe}_{17}\text{H}_x$ system. *Journal of Magnetism and Magnetic Materials* **131**, 83-89 (1994).

94IS309

ISNARD O., MIRAGLIA S., SOUBEYROUX J.L., FRUCHART D., L'HERITIER P. A structural analysis and some magnetic properties of the $\text{R}_2\text{Fe}_{17}\text{H}_x$ series. *Journal of Magnetism and Magnetic Materials* **137**, 151-156 (1994).

94JO310

JOBIC H., BEE M., KEARLEY G.J. Mobility of methane in zeolite NaY between 100K and 250K: a quasielastic neutron scattering study. *Journal of Physical Chemistry* **98**, 4660-4665 (1994).

94GA311

GABRYS B., SCHAERPF O., PEIFFER D.G. Polymers studied with spin polarized neutrons. *Macromolecular Reports* **A31**, 1069-1076 (1994).

94GU312

GUILLAUME M., ALLENSPACH P., HENGGELER W., MESOT J., ROESSLI B., STAUB U., FISCHER P., FURRER A., TROUNOV V. A systematic low-temperature neutron diffraction study of the $\text{RBa}_2\text{Cu}_3\text{O}_x$ (R = yttrium and rare earths; x = 6 and 7) compounds. *Journal of Physics: Condensed Matter* **6**, 7963-7976 (1994).

94RO313

ROESSLI B., FISCHER P., GUILLAUME M., MESOT J., STAUB U., ZOLLIKER M., FURRER A., KALDIS E., KARPINSKI J., JILEK E. Antiferromagnetic ordering and crystal-field splittings of the Ho^{3+} ions in $\text{HoBa}_2\text{Cu}_4\text{O}_8$. *Journal of Physics: Condensed Matter* **6**, 4147-4152 (1994).

94DO314

DOENNI A., FISCHER P., ROESSLI B., KITAZAWA H. Neutron diffraction study of crystal structure and antiferromagnetic ordering in the heavy fermion compound CePd_2Al_3 . *Zeitschrift fuer Physik B* **93**, 449-454 (1994).

94CI315

CIPRIANI F., DAUVERGNE F., GABRIEL A., WILKINSON C., LEHMANN M.S. Image plate detectors for macromolecular neutron diffractometry. *Biophysical Chemistry* **53**, 5-14 (1994).

94GA316

GARCIA-MATRES E., GARCIA-MUNOZ J.L., MARTINEZ J.L., RODRIGUEZ CARVAJAL J. Magnetic properties of R_2BaNiO_5 oxides. *Physica B* **194-196**, 193-194 (1994).

94GA317

GARCIA-MUNOZ J.L., OBRADORS X., RODRIGUEZ CARVAJAL J. Competition between copper and rare earth magnetic sublattices in $\text{Ho}_2\text{Cu}_2\text{O}_5$ and $\text{Yb}_2\text{Cu}_2\text{O}_5$. *Physica B* **194-196**, 277-278 (1994).

94FA318

FAUST H., FIONI G. Estimates for far asymmetric fission yields from Lohengrin data. In "Proceedings of the Workshop on Nuclear Fission and Fission-Product Spectroscopy", FAUST H., FIONI G. Eds. (1994) (ILL Report 94FA5) pp. 91-96.

94CL319

CLEMENTS B.E., KROTSCHKEK E., SAARELA M. Analytic structure of long-wavelength excitations in ^4He surfaces. *Zeitschrift fuer Physik B* **94**, 115-122 (1994).

94CL320

CLEMENTS B.E., FORBERT H., KROTSCHKEK E., SAARELA M. ^4He on weakly attractive substrates: structure, stability, and wetting behavior. *Journal of Low-Temperature Physics* **95**, 849-881 (1994).

94CL321

CLEMENTS B.E., KROTSCHKEK E., LAUTER H.J., SAARELA M. Recent progress in the theory of Bose liquid films. In "Condensed Matter Theories" Vol. 9, CLARK J.W., SADIQ A., SOHAIB K.A. Eds. (Science Publishers, 1994).

94CL322

CLEMENTS B.E., FORBERT H., KROTSCHKEK E., LAUTER H.J., TYMCZAK C.J. Dynamics of quantum films. *Physica B* **194-196**, 659-660 (1994).

94CL323

CLEMENTS B.E., KROTSCHKEK E., LAUTER H.J., SAARELA M. Temperature dependence of third sound in helium monolayers. *Physica B* **194-196**, 657-658 (1994).

94CL324

CLEMENTS B.E., KROTSCHKEK E., LAUTER H.J., SAARELA M. Structure and growth of quantum films. *Physica B* **194-196**, 655-656 (1994).

94TI325

TIMMINS P., PEBAY-PEYROULA E., WELTE W. Detergent organisation in solutions and in crystals of membrane proteins. *Biophysical Chemistry* **53**, 27-36 (1994).

94TI326

TIMMINS P.A., WILD D., WITZ J. The three-dimensional distribution of RNA and protein in the interior of tomato bushy stunt virus: a neutron low-resolution single-crystal diffraction study. *Structure* **2**, 1191-1201 (1994).

94CO327

CONDER K., ZECH D., KRUEGER C., KALDIS E., KELLER H., HEWAT A.W., JILEK E. Indications for a phase separation in $\text{YBa}_2\text{Cu}_3\text{O}_{7-x}$ ($x < 0.1$). *Physica C* **235-240**, 425-426 (1994).

94RO328

ROISNEL T., RODRIGUEZ CARVAJAL J., PINOT M., ANDRE G., BOUREE F. Neutron powder diffraction facilities at the Laboratoire Léon Brillouin. *Materials Science Forum* **166-169**, 245-250 (1994).

94BE329

BENOIT A., BRADSHAW T., ORLOWSKA A., JEWELL C., MACIASZEK T., PUJOL S. A long life refrigerator for 0.1K cooling in space. In "24th International Conference on Environmental Systems and 5th European Symposium on Space Environmental Control Systems". SAE Technical Paper Series 94 276, pp. 1-10 (1994).

**2. Without ILL authors and co-authors
(Code number 1001 to 1026)**

94HO1001

HORKAY F., HECHT A.M., STANLEY H.B., GEISSLER E. Scattering in polymer solutions: determination of osmotic properties in the concentrated regime. *European Polymer Journal* **30**, 215-219 (1994).

94GE1002

GEISSLER E., HORKAY F., HECHT A.M. Scattering from network polydispersity in polymer gels. *Physical Review Letters* **71**, 645-648 (1993).

94HO1003

HORKAY F., BURCHARD W., HECHT A.M., GEISSLER E. Scattering properties of poly(vinyl acetate) gels in different solvents. *Macromolecules* **26**, 4203-4207 (1993).

94HO1004

HORKAY F., BURCHARD W., GEISSLER E., HECHT A.M. Thermodynamic properties of poly(vinyl alcohol) and poly(vinyl alcohol-vinyl acetate) hydrogels. *Macromolecules* **26**, 1296-1303 (1993).

94CO1005

COLMENERO J., ARBE A., ALEGRIA A. Crossover from Debye to non-Debye dynamical behavior of the α -relaxation observed by quasielastic neutron scattering in a glass-forming polymer. *Physical Review Letters* **71**, 2603-2606 (1993).

94LA1006

LAPPAS A., PRASSIDES K. Oxygen-defect geometry in oxygen-rich $\text{La}_2\text{Co}_x\text{Cu}_{1-x}\text{O}_{4+\delta}$ layered oxides. *Journal of Solid State Chemistry* **108**, 59-67 (1994).

94LA1007

LAPPAS A., PRASSIDES K., ARMSTRONG A.R., EDWARDS P.P. $\text{Sr}_{2-x}\text{Ba}_x\text{CuO}_2(\text{CO}_3)$: a series of antiferromagnetic layered oxide carbonates. *Inorganic Chemistry* **32**, 383-385 (1993).

94MO1008

MOMBRU A.W., CHRISTIDES C., LAPPAS A., PRASSIDES K., PISSAS M., MITROS C., NIARCHOS D. Magnetic structure of the oxygen-deficient perovskite $\text{YBaCuFeO}_{5+\delta}$. *Inorganic Chemistry* **33**, 1255-1258 (1994).

94KA1009

KALUS J., SCHMELZER U. Small angle neutron (SANS) and x-ray (SAXS) scattering on micellar systems. *Physica Scripta* **T49**, 629-635 (1993).

94HE1010

HERBST L., KALUS J., SCHMELZER U. The internal structure of a rodlike micelle. *Journal of Physical Chemistry* **97**, 7774-7778 (1993).

94KA1011

KALUS J., SCHMELZER U. Static and transient small angle neutron and x-ray scattering measurements on micellar systems. *Trends in Physical Chemistry* **3**, 299-325 (1992).

94BE1012

BEE M., DEROLLEZ P., DESCAMPS M. Relaxations near the glass transition of a molecular crystal. *Journal of Non-Crystalline Solids* **172-174**, 520-530 (1994).

94PR1013

PRAGER M., ZACHWIEJA U., CARLILE C.J. Tunnelling of coupled methyl groups in $\text{Sn}_2(\text{CH}_3)_6$. *Physica B* **202**, 360-363 (1994).

94KR1014

KRUEGER J.K., SCHREIBER J., JIMENEZ R., BOHN K-P., SMUTNY F., KUBAT M., PETZELT J., HRABOVSKA-BRADSHAW J., KAMBA S., LEGRAND J.F. Unconventional orientational glass transitions in symmetrical difluorotetrachloroethane. *Journal of Physics: Condensed Matter* **6**, 6947-6964 (1994).

94RE1015

REGNAULT L.P., ZALIZNYAK I., RENARD J.P., VETTER C. Inelastic-neutron-scattering study of the spin dynamics in the Haldane-gap system $\text{Ni}(\text{C}_2\text{H}_8\text{N}_2)_2\text{NO}_2\text{ClO}_4$. *Physical Review B* **50**, 9174-9187 (1994).

94BE1016

BEE M. Large-amplitude motions in molecular crystals and polymers. In "Neutron and Synchrotron Radiation for Condensed Matter Studies: Hercules (course)". Vol. 3, BARUCHEL J., HODEAU J.L., LEHMANN M.S., REGNARD J.R., SCHLENKER C. Eds. (Les Editions de Physique/Springer Verlag, 1994) pp. 82-92.

94RI1017

RICHTER D. Slow dynamics in complex materials. In "Proceedings of the Quasielastic Neutron Scattering Workshop QENS'93", COLMENERO J., ALEGRIA A., BERMEJO F.J. Eds. (World Scientific, 1994) pp. 92-106.

94DE1018

DESCAMPS M., BEE M., DEROLLEZ P., WILLART J.F., CARPENTIER L. Dynamics and kinetics in glassy crystal cyanoadamantane. In "Proceedings of the Quasielastic Neutron Scattering Workshop QENS'93", COLMENERO J., ALEGRIA A., BERMEJO F.J. Eds. (World Scientific, 1994) pp. 107-127.

94BL1019

BLANCO J.A., SANDONIS J., RODRIGUEZ FERNANDEZ J., GOMEZ SAL J.C., PLAZAOLA F., BARANDIARAN J.M. Inelastic and quasielastic neutron scattering in $\text{CeNi}_x\text{Pt}_{1-x}$ and its dilute compounds. In "Proceedings of the Quasielastic Neutron Scattering Workshop QENS'93", COLMENERO J., ALEGRIA A., BERMEJO F.J. Eds. (World Scientific, 1994) pp. 211-219.

94CH1020

CHAHID A., ALEGRIA A., COLMENERO J. Distribution of the activation energy for the methyl side group rotation in poly(vinyl methyl ether). In "Proceedings of the Quasielastic Neutron Scattering Workshop QENS'93", COLMENERO J., ALEGRIA A., BERMEJO F.J. Eds. (World Scientific, 1994) pp. 227-235.

94RU1021

RUBIN J., BARTOLOME J. Single-particle motions of NH_4^+ in the NH_4MF_3 perovskites series. In "Proceedings of the Quasielastic Neutron Scattering Workshop QENS'93", COLMENERO J., ALEGRIA A., BERMEJO F.J. Eds. (World Scientific, 1994) pp. 236-251.

94AR1022

ARBE A., COLMENERO J., ALEGRIA A. Comparative study of the α and β relaxations of poly(vinyl chloride) by means of quasielastic neutron scattering and dielectric spectroscopy. In "Proceedings of the Quasielastic Neutron Scattering Workshop QENS'93", COLMENERO J., ALEGRIA A., BERMEJO F.J. Eds. (World Scientific, 1994) pp. 296-305.

94GE1023

GEBHARD F., GIRNDT A. Comparison of variational approaches for the exactly solvable $1/r$ -Hubbard chain. Zeitschrift fuer Physik B **93**, 455-463 (1994).

94GE1024

GEBHARD F., GIRNDT A., RUCKENSTEIN A.E. Charge- and spin-gap formation in exactly solvable Hubbard chains with long-range hopping. Physical Review B **49**, 10926-10946 (1994).

94PL1025

PLUMIER R., SOUGI M. Magnetic structure of $\text{Cu}_4\text{Mn}_2\text{Te}_4$. Materials Science Forum **166-169**, 687-692 (1994).

94BA1026

BACMANN M., SOUBEYROUX J.L., BARRETT R., FRUCHART D., ZACH R., NIZIOL S., FRUCHART R. Magnetoelastic transition and antiferro-ferromagnetic ordering in the system $\text{MnFeP}_{1-y}\text{As}_y$. Journal of Magnetism and Magnetic Materials **134**, 59-67 (1994).

AUTHOR INDEX

Author Index

Publications
and ILL-Reports 1994

ADELMANN P.	94GO253	BARRETT R.	94BA1026	BOENI P.	94EL304
	94RE254	BARTHOLIN H.	94CH174		94GR303
AEBERSOLD M.A.	94AE157	BARTOLOME J.	94AR1022	BOERNER H.G.	94DE283
ALCOBE X.	94AL158		94RU1021		94JU103
ALEGRIA A.	94CO1005	BARUCHEL J.	94RU228		94JU147
ALGARABEL P.A.	94IB287	BASHKIN I.O.	94BA270	BOHN K-P.	94RO200
ALHASSANIEH O.	94HA119	BASSAS J.	94HY268	BOISSIEU M. DE	94KR1014
ALIEV A.E.	94AL158	BASTIDE J.	94PA307		94BO162
ALLENSPACH P.	94AL209	BASTIE P.	94RA110		94BO279
	94GU312	BATALLAN F.	94RO165		94BO297
	94ST202	BATLLE X.	94LO247		94BO30
ALONSO J.	94BE112	BAUMBACH G.T.	94ME149		94JA159
	94ME148	BAUSENWEIN T.	94BA179		94PO124
ALONSO J.A.	94AL151		94BA192	BOKHENKOV E.L.	94AN201
ALS-NIELSEN J.	94BE256	BEAUCAGE G.	94ST193	BOLLEN S.K.	94WH267
ALTORFER F.	94AL249	BEDA A.G.	94SC219	BONDARENKO L.N.	94GO106
AMATO A.	94GY302	BEE M.	94GO106	BONHOMME F.	94BO142
ANDERSEN K.H.	94AN128		94BE1012	BONNET M.	94BO161
ANDERSON I.S.	94AL249		94BE1016	BOOTH J.G.	94BO131
	94EL304	BEIJER B.	94BE121	BOOTHROYD A.T.	94NU203
	94GR303	BELLET D.	94DE1018	BOUCHERLE J.X.	94BO161
	94GY302	BELLET-AMALRIC E.	94JO310	BOUDARD M.	94BO162
	94SC180	BELLISSANT R.	94BE256		94BO279
	94UD127	BELLOUARD C.	94RO165		94BO297
	94UD223	BELMONT J.-L.	94BE108	BOUE F.	94BO114
	94UD260	BELOZEROV A.V.	94QU285		94BO114
	94UD305	BELRHALI H.	94HE232	BOUREE F.	94RO328
ANDRE G.	94RO328	BENETTI P.	94FI28	BOWDEN Z.	94AL209
ANNE M.	94RU228	BENNINGTON S.	94GO106		94ST202
ANTONOV V.E.	94AN201		94BE256	BOYSEN H.	94EL269
APOSTOLIDIS C.	94RA211	BENOIT A.	94BA252	BRADEN M.	94BR264
ARAI M.	94AL209		94KE171	BRADSHAW T.	94BE329
ARBE A.	94CO1005	BENOIT C.	94SC197	BRAMWELL S.T.	94BR169
ARMSTRONG A.R.	94LA1007	BENSIMON D.	94PO124		94BR196
ARONS R.R.	94AR170	BERK N.F.	94MI116	BRAZOVSKII S.	94BR213
ASHLEY C.	94SC219	BERMEJO F.J.	94UD127	BROKMEIER H.G.	94GE288
ASMUSSEN B.	94AS236	BERRRET J.F.	94BE112		94GE289
	94SC205	BERTAGNOLLI H.	94BE140	BROWN P.J.	94CH172
AUDIER M.	94BO162		94BE11		94RA211
	94BO297	BERTAULT M.	94BA192		94VI155
BACH H.	94RO173	BERTHET-COLOMINAS C.	94ST193	BUEHRER W.	94AL249
BACMANN M.	94BA1026		94EV160		94RO255
BAIER M.	94AN201	BILGRAM J.H.	94BE256	BUERGLER D.E.	94SC221
BALDO CEOLIN M.	94BA252	BILL H.	94VU240		94SC299
BALIBAR S.	94BA216	BILLINGTON A.	94LI181	BUETTNER H.	94AS236
BALLOU R.	94LE291	BITTER T.	94AL249		94BU244
	94RE250	BLAISE A.	94TH18	BUFFAT P.	94EL304
BALSZUNAT D.	94AS236	BLANC T.	94BA252		94GR303
BALTA CALLEJA F.J.	94LO247	BLANCO J.A.	94IS308	BUNGE H.J.	94GE289
BARANDIARAN J.M.	94BL1019	BLANK H.	94BE11	BURCHARD W.	94HO1003
BARILO S.N.	94CH150		94BL1019		94HO1004
	94SU243	BLASCHKO O.	94AE157	BURLET P.	94CH174
BARNES J.D.	94TE293		94AL209	BUROV S.I.	94GO106
BARON M.H.	94KE171	BOBISUT F.	94HE232	CAILLEAU H.	94EV160
			94SC205	CALLIGARICH E.	94BA252
			94UD127	CANNON R.D.	94WH267
			94UD305	CAPPONI J.J.	94CH117
			94BA252		

AUTHOR INDEX

CARLILE C.J.	94AS236 94FI237 94PR1013 94RA135	CUSACK S.	94BE256 94VU240 94RI227 94TE294	FÅK B.	94AN128 94FA154 94SC248 94TE251
CARLSSON A.E.	94HO263	CYWINSKI R.	94GO106	FARAGO B.	94FA178 94RI298 94SC219 94VA118
CARPENTIER L.	94DE1018	DAMMER C.	94UD127	FAUBEL W.	94HA119
CARRON P.L.	94AL249	DANILYAN G.V.	94RA395	FAUST H.R.	94FA1 94FA2 94FA318 94FA5 94FI28 94HA119 94HE175 94HE175 94SC214 94EV160
CASAN-PASTOR N.	94PA307	DAOU J.N.	94IS204	FAVE J.L.	94RA292
CASTEN R.F.	94JU147	DARTYGE E.	94CI315	FELDWISCH R.	94FE296
CAUDRON R.	94HO263	DAUVERGNE F.	94BA192	FEREY G.	94FR141 94FR217 94RI298
CAUSSIGNAC M.	94BE153	DAVID A.	94IB287	FETTERS L.J.	
CHAHID A.	94CH1020	DEL MORAL A.	94RA135	FILHOL A.	94BE11 94FI12 94FI215 94JE265 94QU285
CHAI SA-ARD N.	94WH267	DELAPALME A.	94RA211	FILLAUX F.	94BU244 94FI237 94KE171 94FA318 94FA5 94FI28 94GI3 94SC219 94PA261 94BO142 94DO314 94FI132 94GU167 94GU312 94RO255 94RO278 94RO313 94BR264 94CO185 94VO144 94CL212 94CL320 94CL322 94CL322 94CL323 94CL324
CHAPMAN D.	94BO162 94BO297 94CH183 94CH220 94CH225 94CH233 94CH150 94CH156 94CH172 94CH174 94CH194 94RO173 94SU243 94VI155	DENSCHLAG H.O.	94HA119 94HE175 94HE175 94IS230	FIONI G.	
CHARVOLIN J.	94CH183 94CH220 94CH225 94CH233	DEPORTES J.	94IS230	FISCHER A.D.	
CHATTOPADHYAY T.	94CH150 94CH156 94CH172 94CH174 94CH194 94RO173 94SU243 94VI155	DEROLLEZ P.	94BE1012 94DE1018 94BE1012 94DE1018	FISCHER J.E.	
CHEVRIER J.	94CH117	DESCAMPS M.	94DE283 94DE245 94DE283	FISCHER P.	
CHIEUX P.	94BA192 94CH222 94PR109 94ST193	DESLATTES R.D.	94AN128 94DI191 94DI218 94EL269 94GU145 94HY268 94PA261 94SC197	FOURCADE B.	
CHRISTIDES C.	94MO1008	DEUTSCHER G.	94HE232 94DO314 94BA252 94MA101 94AN201 94DO111 94DO234 94DO259 94DO284 94SC187 94SC206	FREUND A.K.	
CIPRIANI F.	94CI315	DEWEY M.S.	94DI191 94DI218 94EL269 94GU145 94HY268 94PA261 94SC197	FRICK B.	
CLEMENTS B.E.	94CL212 94CL319 94CL320 94CL321 94CL322 94CL323 94CL324	DIANOUX A.J.	94AN128 94DI191 94DI218 94EL269 94GU145 94HY268 94PA261 94SC197	FRIEDLI H.P.	
CLERC H.G.	94SC214	DJEGA-MARIADASSOU C.	94AN128 94DI191 94DI218 94EL269 94GU145 94HY268 94PA261 94SC197		
COCKCROFT J.K.	94AR170 94CO185 94KR176 94VO144	DOENNI A.	94HE232 94DO314 94BA252 94MA101 94AN201 94DO111 94DO234 94DO259 94DO284 94SC187 94SC206		
CODDENS G.	94EL269	DOLFINI R.	94LI181 94DR190 94WA198 94BA252 94DU208 94CH222 94PR109		
COLMENERO J.	94CO1005	DOLL C.	94LI181 94DR190 94WA198 94BA252 94DU208 94CH222 94PR109		
CONDER K.	94CO327	DORNER B.	94LI181 94DR190 94WA198 94BA252 94DU208 94CH222 94PR109		
CONTO DE J.-M.	94FI28	DUBBERS D.	94LI181 94DR190 94WA198 94BA252 94DU208 94CH222 94PR109		
COOK J.C.	94CO182 94ST164	DUPORT C.	94LI181 94DR190 94WA198 94BA252 94DU208 94CH222 94PR109		
COPLEY J.R.D.	94CO182	DUPUY-PHILON J.	94LI181 94DR190 94WA198 94BA252 94DU208 94CH222 94PR109		
COSTA M.M.R.	94BO131	EDWARDS P.P.	94LI181 94DR190 94WA198 94BA252 94DU208 94CH222 94PR109		
COTTON J.P.	94VA118	EIGENMANN B.	94LI181 94DR190 94WA198 94BA252 94DU208 94CH222 94PR109		
COWLEY R.A.	94TE251	EL BAGHDADI A.	94LI181 94DR190 94WA198 94BA252 94DU208 94CH222 94PR109		
CRANGLE J.	94OU138	EL-MUZEINI P.	94LI181 94DR190 94WA198 94BA252 94DU208 94CH222 94PR109		
CRiado A.	94BE112	ELSENHANS O.	94LI181 94DR190 94WA198 94BA252 94DU208 94CH222 94PR109		
CURRAT R.	94EV160 94PO124	EPELBOIN Y.	94LI181 94DR190 94WA198 94BA252 94DU208 94CH222 94PR109		
		ESTOP E.	94LI181 94DR190 94WA198 94BA252 94DU208 94CH222 94PR109		
		EVEN J.	94LI181 94DR190 94WA198 94BA252 94DU208 94CH222 94PR109		
		EZQUERRA T.A.	94LI181 94DR190 94WA198 94BA252 94DU208 94CH222 94PR109		
		FABRIZIO M.	94LI181 94DR190 94WA198 94BA252 94DU208 94CH222 94PR109		

AUTHOR INDEX

FRUCHART D.	94BA1026	GOBERT G.	94GO9	HEWAT A.W.	94BO142
	94IS163	GOBRECHT K.	94BA252		94CO327
	94IS195	GODFRIN H.	94AN128		94FI132
	94IS204	GOENNENWEIN F.	94GO106		94HE184
	94IS230		94SC235		94WI246
	94IS308	GOLLER K.	94BA192	HILFRICH K.	94HI136
	94IS309	GOMEZ SAL J.C.	94BL1019		94HI137
FRUCHART R.	94BA1026	GOMEZ-ROMERO P.	94NA130	HOCK R.	94HO273
FUERTES A.	94NA130		94PA307	HOFFMANN H.	94MU168
	94PA307	GOMPFF F.	94GO253	HOLDSWORTH P.C.W.	94BR169
FURRER A.	94AE157		94RE254	HOLLANDER J.G.	94VA118
	94AL209	GONTHIER-VASSAL A.	94RA211	HOLY V.	94BA179
	94DO284	GONZALEZ-CALBET J.M.	94ME148	HORKAY F.	94GE1002
	94GU167	GRAF H.A.	94WI246		94HO1001
	94GU312	GREENE G.L.	94DE283		94HO1003
	94RO255	GRIGEREIT T.E.	94CH150		94HO1004
	94RO278	GRIMMER H.	94EL304	HOSER A.	94HO263
	94RO313		94GR303	HOWARD C.J.	94BU244
	94ST202	GROOT L.C.A.	94VA118	HRABOVSKA-BRADSHAW J.	94KR1014
	94TI281	GRUEBEL G.	94BE256	HUANG J.S.	94RI298
GABRIEL A.	94CI315	GUEDEL H.U.	94AE157	HULMES D.J.S.	94VU115
GABRYS B.	94GA311	GUENET J.M.	94GU113	IBARRA M.R.	94IB287
GAILHANOU M.	94BA179	GUENTHERODT H.J.	94SC221	IBBERSON R.M.	94QU285
GALERA GOMEZ P.	94LO210		94SC299	IBEL K.	94IB15
GAMAYUNOV K.	94BR264	GUGLIELMI A.	94BA252		94IB8
GARCIA CHAIN P.J.	94RO306	GUILLAUME F.	94EL269		94MU168
GARCIA-HERNANDEZ M.	94BE112		94GU145	ISHII Y.	94KU271
GARCIA-MATRES E.	94GA316	GUILLAUME M.	94AL209	ISNARD O.	94IS163
GARCIA-MUNOZ J.L.	94GA199		94GU167		94IS195
	94GA316		94GU312		94IS204
	94GA317		94RO313		94IS230
GASTALDI J.	94BA270		94ST202		94IS308
GEBHARD F.	94GE1023	GUILLOT M.	94IS195		94IS309
	94GE1024	GUINIER A.	94WI286	JAL J.F.	94CH222
GEISLER E.	94GE1002	GYGAX F.N.	94GY302		94PR109
	94GE29	HAERTWIG J.	94BA270	JANNINK G.	94VA118
	94HO1001	HAGENMAYER R.M.	94HA120	JANOT C.	94BO162
	94HO1003	HAKIKI A.	94RA110		94BO279
	94HO1004	HANLEY H.J.M.	94HA166		94BO297
GELTENBORT P.	94DR190	HARRIS K.D.M.	94AL158		94BO30
	94GO106		94GU145		94JA159
	94SC235	HECHT A.M.	94GE1002		94JA231
	94WA198		94HO1001	JAYASOORIYA U.A.	94WH267
GENONI M.	94BA252		94HO1003	JEANTEUR D.	94JE280
GERTEL-KLOOS H.	94GE288	HEGER G.	94HO1004	JEITSCHKO W.	94RE226
	94GE289	HEID R.	94BR264		94RE229
GEYER A. DE	94LO210		94GO253		94RE250
GIBIN D.	94BA252	HEIDEMANN A.	94RE254	JESIOR J.C.	94JE265
GIES H.	94SC205		94HE238	JESSE W.	94VA118
GIGLI BERZOLARI A.	94BA252	HEIMING A.	94HE300	JEWELL C.	94BE329
GILL R.L.	94JU147	HEMPELMANN R.	94SE107	JILEK E.	94CO327
GILLY C.	94RA146		94HY268		94RO313
GINDLER J.	94HE175	HENGGELER W.	94SC197	JIMENEZ R.	94KR1014
GINGRAS M.J.P.	94BR196		94GU312	JOBIC H.	94JO310
GIORGETTI C.	94IS204	HENNION M.	94HE232	JOLIE J.	94RO200
GIRNDT A.	94GE1023	HENTZSCHEL R.	94HE175	JUNGCLAUS A.	94JU103
	94GE1024	HERBST L.	94HE1010		94JU147
GIROUD-GODQUIN A.M.	94BE121	HERRERO P.	94RO306	KAESTNER J.	94RO173
GIVELET N.	94GI3	HERZ J.	94RA110		
GIVORD F.	94BO161				

AUTHOR INDEX

KAHN R.	94RA135	LACORRE P.	94GA199	LYNN J.W.	94CH150
KALDIS E.	94CO327	LAMPARTER P.	94HA120		94RO173
	94RO313	LANDER G.H.	94RA135		94SU243
KALUS J.	94HE1010		94RA211	MCCALLUM R.W.	94AL209
	94KA1009	LAPIERRE F.	94BO161	MCCARNEY J.	94MC122
	94KA1011	LAPP A.	94VA118	MCDERMOTT D.C.	94MC122
	94MU168	LAPPAS A.	94LA1006	MCKENNA G.B.	94TE293
KAMBA S.	94KR1014		94LA1007	MCMORROW D.F.	94TE251
KANELLAKOPOULOS B.	94RA135		94MO1008	MACIASZEK T.	94BE329
	94RA211	LARSEN K.	94BE256	MADAR R.	94MA101
KAPPLER J.P.	94IS204	LASJAUNIAS J.C.	94CH117	MAGERL A.	94LI102
KARASZ F.E.	94PA261	LAST J.	94BA252		94MA101
KARNER C.	94SE107		94GO106		94RU228
KARPINSKI J.	94RO313	LATYNIN A.I.	94AN201		94WA126
KASSNER K.	94KA186	LAUGIER J.	94BE11	MALBERT P.	94MA19
	94KA189	LAUTER H.J.	94CL212		94MA20
KEARLEY G.J.	94BU244		94CL321		94MA21
	94FI237		94CL322		94MA22
	94JO310		94CL323		94MA23
	94KE171		94CL324		94MA24
	94KR176	LAVEDER M.	94BA252		94MA25
	94RU228	LAWRENCE J.J.	94RA146		94MA26
	94WH267	LE BAS G.	94LE277		94MA27
KELLER H.	94CO327	LEADBETTER A.J.	94LE275	MALDIVI P.	94BE121
KESSLER E.G.	94DE283	LEBERMAN R.	94BE256		94TE294
KIAT J.M.	94RA211		94VU240	MALETTA H.	94AL209
KILCOYNE S.H.	94RI227	LEDEBT P.	94GI3	MANDEL M.	94VA118
KITAZAWA H.	94DO314	LEFEBVRE S.	94QU285	MAO G.	94PA261
KNELLER G.R.	94DI191	LEGRAND J.F.	94BE108	MARQUINA C.	94IB287
	94DI218		94BE256	MARTEM'YANOV A.N.	94GO106
KOELKER W.	94HI136		94KR1014	MARTIN M.	94HO263
KOESTER U.	94KO13		94PR109	MARTINEZ B.	94ME149
KOJIMA H.	94BR264	LEHMANN M.S.	94BE256	MARTINEZ J.L.	94BE112
KOLESNIKOV A.I.	94HY268		94CI315		94GA316
KRAMER M.J.	94AL209		94LE258	MASON S.A.	94LE277
KREMER R.K.	94KR176		94ST257	MATTAUSCH H.J.	94KR176
	94ST164	LEIFER K.	94EL304		94ST164
KRILL G.	94IS204		94GR303	MATTIOLI F.	94BA252
KROTSCHECK E.	94CL212	LEJAY P.	94BO161	MATVEENKO S.	94BR213
	94CL319	LELIEVRE-BERNA E.	94LE291	MAURI F.	94BA252
	94CL320	LEYTE J.C.	94VA118	MAY R.P.	94DO259
	94CL321	LEYTE-ZUIDERWEG L.H.	94VA118		94MA177
	94CL322	LIEB K.P.	94RO200		94WI286
	94CL323	LIED A.	94LI181	MEDARDE M.	94ME148
	94CL324	LINDNER P.	94BE140		94ME149
KRUEGER C.	94CO327		94BO114	MENDES E.	94RA110
KRUEGER E.	94SC125		94GE29	MENELLE A.	94GU113
KRUEGER J.K.	94KR1014		94HA166	MESOT J.	94AL209
KUBAT M.	94KR1014	LIPPERT W.	94RA123		94GU312
KUIL M.E.	94VA118	LISS K.D.	94VE239		94RO313
KULDA J.	94BA270		94BA252		94ST202
	94HO273	LOPEZ-CABARCOS E.	94LI102	MEURER B.	94BE108
	94KU152		94MA101	MEZZETTO M.	94BA252
	94KU271	LUDI A.	94LO210	MICHALET X.	94MI116
	94KU290	LUKAS P.	94LO247	MIKULA P.	94KU152
	94MI274		94FI132		94MI14
	94VR272		94MI274		94MI274
KUSSMAUL R.	94PI262		94VR272		94VR272
L'HERITIER P.	94IS230				
	94IS309				

AUTHOR INDEX

MILLER A.	94VU115	PAUL D. McK.	94NU203	REBIZANT J.	94RA211
MIRAGLIA S.	94IS195	PAVLOV V.S.	94GO106	REEHUIS M.	94RE226
	94IS204	PAVONE P.	94KU271		94RE229
	94IS230	PEBAY-PEYROULA E.	94TI325		94RE250
	94IS308	PEIFFER D.G.	94GA311	REGNAULT L.P.	94RE1015
	94IS309	PENDLEBURY J.M.	94PE133		94SC187
MIREBEAU I.	94HE232	PENFOLD J.	94NU203	REIMERS J.N.	94BR196
MISBAH C.	94KA186	PERROUX M.	94CH117	REJMANKOVA P.	94BA270
	94KA189	PETITGRAND D.	94SC187	RENARD J.P.	94RE1015
	94MI105	PETRAVOVSKII G.	94RO255	RENKER B.	94GO253
MITROS C.	94MO1008	PETRILLO C.	94DE283		94RE254
MOMBRU A.W.	94MO1008	PETRY W.	94HI136	RENNIE A.R.	94MC122
MONDAL S.	94RI227		94HI137	RESSOUCHE E.	94AR170
MONTANARI C.	94BA252		94VO266		94OU138
MORKEL C.	94CH222	PETZELT J.	94KR1014		94RE226
MOSSERI R.	94BO30	PIAZZOLI A.	94BA252	RICHARDSON D.J.	94PE133
MOSTOVOI Y.A.	94GO106	PIETSCH U.	94BA179	RICHTER D.	94FR129
MOUSSA F.	94EV160	PINOT M.	94RO328		94FR217
MUELLER-KRUMBHAAR H.	94KA186	PINTSCHOVIVS L.	94PI262		94HY268
	94KA189	PISSAS M.	94MO1008		94RI1017
MUENCH C.	94MU168	PIZZINI S.	94IS204		94RI298
MUNZ D.	94PI262	PLAZAOLA F.	94BL1019		94SC197
MURANI A.P.	94BO161	PLUMIER R.	94PL1025		94SC219
	94MU188	PODLESNYAK A.	94GU167	RITTER C.	94GE288
	94MU224	PONYATOVSKY E.G.	94HY268		94GE289
MUTKA H.	94AL209	PORTE G.	94BE140		94IB287
	94MU104	POUSSIGUE G.	94PO124		94RE250
	94MU301	PRAGER M.	94AS236		94RI227
	94ST202		94FI237	RIUS J.	94AL158
MUTTERER M.	94SC214		94PR1013	ROBINSON S.J.	94DE283
NAGLER S.E.	94TE251	PRASSIDES K.	94LA1006		94RO200
NAVARRO J.M.	94NA130		94LA1007	RODRIGUEZ CARVAJAL J.	94AL151
NEMBACH E.	94HI136		94MO1008		94AL158
	94HI137	PRESS W.	94AS236		94BO131
NEUBAUER G.	94MU168		94SC205		94GA199
NEUMANN K.U.	94OU138	PREVEL B.	94PR109		94GA316
NIARCHOS D.	94MO1008	PRIETO C.	94BE112		94GA317
NIZIOL S.	94BA1026	PUGLIERIN G.	94BA252		94ME148
NOZIERES P.	94BA216	PUJOL S.	94BE153		94ME149
	94BR213		94BE329		94NA130
	94DE245	PURDOM I.F.	94VU115		94PA307
	94DU208	PYKA N.	94BR264		94RO306
	94NO16		94HO263		94RO328
	94NO207	QUEMERAIS P.	94PI262	RODRIGUEZ FERNANDEZ J.	94BL1019
NUTLEY M.P.	94NU203	QUIVY A.	94QU241	RODRIGUEZ V.	94TE293
OBRADORS X.	94GA317	RABILLOUD T.	94QU285	ROESSLI B.	94CH172
	94ME149		94RA146		94DO314
ODIN J.	94BO161		94VU10		94GU167
OED A.	94SC235	RAINFORD B.D.	94VU240		94GU312
OESER R.	94RA110	RAISON P.	94RI227		94RO255
OLIVIER B.J.	94SC219		94RA135		94RO278
ORLOWSKA A.	94BE329	RAMSAY J.D.F.	94RA211		94RO313
OSBORN R.	94AL209	RAMZI A.	94RA123	ROISNEL T.	94RO328
OULADDIAF B.	94OU138	RANDL O.G.	94RA110	ROJAS R.M.	94RO306
PAIXAO J.A.	94BO131		94RA292	ROSOV N.	94CH150
PALACIN M.R.	94PA307	RAPPOLDI A.	94SE107		94RO173
PANNETIER J.	94FE296	RASELLI G.L.	94BA252	ROSSAT-MIGNOD J.M.	94CH174
PAPANEK P.	94PA261	RASHUPKIN V.I.	94BA252	ROUCHY J.	94LE291
PATTERSON H.H.	94FI132	RASINES I.	94AN201	ROUF C.	94RA110
PATTUS F.	94JE280		94AL151	ROUX D.C.	94BE140

AUTHOR INDEX

ROYER A.	94RO165	SCHOENFELD C.	94SC197	SUCK J.B.	94CH117
RUBIN J.	94AR1022	SCHOLTES B.	94PI262		94CH222
	94RU1021	SCHRECKENBACH K.	94GO106		94SC221
	94RU228	SCHREIBER J.	94KR1014		94SC299
RUCKENSTEIN A.E.	94GE1024	SCHROEDER K.	94RA292		94SU276
RUSH J.J.	94GY302	SCHROEDER-HEBER A.	94SC205	SUMARLIN I.W.	94SU243
	94SC197	SCHWAB W.	94SC214	TANAKA I.	94BR264
	94UD127	SCHWARZ W.	94BR264	TASSET F.	94TA134
	94UD223	SCHWEIKA W.	94HO263	TAYLOR A.	94ST202
	94UD260	SCHWEISS P.	94RA211	TAYLOR A.D.	94AL209
	94UD305	SCHWEIZER J.	94BO161	TENNANT D.A.	94TE251
SAARELA M.	94CL212	SCONZA A.	94BA252	TERECH P.	94GU113
	94CL319	SEKI S.	94UW143		94TE293
	94CL320	SELBACH J.	94MU168		94TE294
	94CL321	SEPIOL B.	94RA292		94TE295
	94CL323		94SE107	TERESA J.M. DE	94IB287
	94CL324		94GO106	THE PIAFE COLLABORATION	94FA2
SABLINA K.	94RO255	SHCHENEV V.A.	94CH194		94FI28
SACCHETTI F.	94DE283	SIEMENSMEYER K.	94KR176	THEOBALD J.P.	94SC214
SADOC J. F.	94CH220	SIMON A.	94ST164	THIERRY A.	94GU113
SAITO Y.	94UW143		94GU145	THOLE B.T.	94TH242
SANCHEZ J.P.	94IS308	SMART S.P.	94DI191	THOMAS M.	94TH17
SANDONIS J.	94BL1019	SMITH J.C.	94DI218		94TH18
SAROUN J.	94KU152		94KR1014	THOMAS R.K.	94MC122
SAUVAJOL J.L.	94DI191	SMUTNY F.	94EL304	TIMMINS P.A.	94JE280
	94DI218	SOECHTIG J.	94GY302		94TI281
	94PA261	SOLT G.	94BA1026		94TI282
SCANNICCHIO D.	94BA252	SOUBEYROUX J.L.	94IS309		94TI325
SCHAEFER D.W.	94SC219		94QU285		94TI326
SCHAERPF O.	94AL249		94PL1025	TOEDHEIDE K.	94BA192
	94GA311	SOUGI M.	94SC197		94ST193
	94HI136	SPRINGER T.	94BE256	TOMKINSON J.	94KE171
	94HI137	SPROAT B.	94NU203	TORRANCE J.B.	94AL151
	94SC180	STADDON C.R.	94HO1001	TOUDIC B.	94EV160
SCHAFFHAUSER V.	94GU113	STANLEY H.B.	94AL209	TRANQUI D.	94JE265
SCHAUB T.M.	94SC221	STAUB U.	94GU312	TREVINO S.F.	94FR129
	94SC299		94RO278	TROUNOV V.	94GU312
SCHEFER J.	94GU167		94RO313	TUKALO M.	94BE256
	94RO255		94ST202	TYMCZAK C.J.	94CL212
SCHENCK A.	94GY302		94HA120		94CL322
SCHERM R.	94AN128	STEEB S.	94MA101	UDOVIC T.J.	94SC197
	94FA154	STEICHELE E.	94SC187		94UD127
	94MI14	STEINER M.	94VI155		94UD223
	94SC125	STEPANOV A.A.	94BO162		94UD260
	94SC248	STEPHENS P.	94BO279		94UD305
	94SU276		94BO297	ULBIG S.	94RO200
SCHILLEBEECKX P.	94DE283	STETSON N.T.	94BO142	UWAHA M.	94UW143
	94RO200	STIRLING W.G.	94AN128	VACHER N.	94VA6
	94SC235	STOCK-SCHWEYER M.	94BE108	VAJDA P.	94UD127
	94BA270	STRATY G.C.	94HA166		94UD305
SCHLENKER M.	94HE1010	STRAUCH D.	94KU271	VALANCE A.	94KA186
SCHMELZER U.	94KA1009	STRAUSS G.	94ST193		94KA189
	94KA1011	STRIDE J.A.	94WH267	VALLET-REGI M.	94MI105
	94MU168	STUHR U.	94ST164	VAN DER LAAN G.	94ME148
SCHMID B.	94SC187	STUHRMANN H.B.	94ST257	VAN DER MAAREL J.R.C.	94TH242
SCHMID S.	94SC7	STUNAUULT A.	94AN128	VASCON M.	94VA118
SCHNELLE W.	94BR264		94BO161	VASCON M.	94BA252
SCHOBER H.	94GO253			VERSMOLD H.	94VE239
	94RE254			VETTIER C.	94CH174
	94SC206				94RE1015

AUTHOR INDEX

VILLAIN J.	94DU208	ZOLLIKER M.	94RO278
VISENTIN L.	94BA252		94RO313
VITEBSKY I.M.	94VI155	ZONTONE F.	94BA270
VOGL G.	94RA292	ZORN R.	94FR217
	94SE107	ZWEIER H.	94BA192
	94VO266		94ST193
VOGT O.	94CH174		
VOGT T.	94RO255		
	94VO144		
VOMHOF T.	94RE229		
VRANA M.	94MI274		
	94VR272		
VUILLARD L.	94RA146		
	94VU10		
	94VU115		
	94VU240		
VULLIET P.	94IS308		
WAGEMANS C.	94DR190		
	94SC235		
	94WA198		
WAGNER B.	94WI246		
WAGNER F.E.	94AN201		
WAGNER V.	94KU152		
	94MI14		
	94MI274		
	94WA126		
WASSERMANN E.F.	94RO173		
WEIS M.	94HA119		
WELTE W.	94TI325		
WHITE R.P.	94WH267		
WILD D.	94TI326		
WILKINS B.D.	94HE175		
WILKINSON C.	94CI315		
WILLART J.F.F.	94DE1018		
WILLIAMS C.E.	94WI286		
WILLIAMS J.	94BE121		
WILLIAMS J.H.	94RA135		
WILLNER L.	94RI298		
WINKELMANN M.	94WI246		
WINOKUR M.J.	94PA261		
WIPF H.	94ST164		
WITZ J.	94TI326		
YAREMCHUK A.	94BE256		
YOO S.I.	94AL209		
YVON K.	94BO142		
ZACH R.	94BA1026		
ZACHWIEJA U.	94PR1013		
ZALIZNYAK I.	94RE1015		
ZAYER N.K.	94OU138		
ZECH D.	94CO327		
ZEPPENFELD K.	94RE226		
ZEYEN C.M.E.	94HA120		
	94RO165		
ZHIGUNOV D.I.	94CH150		
	94SU243		
ZIEBECK K.R.A.	94OU138		
ZIELINSKI F.	94RA110		
ZIRKEL A.	94RI298		

Papers accepted for Publication

1. Neutron Instruments and Methods

ALTORFER F.B., COOK J.C., COPLEY J.R.D.

The multiple disk chopper neutron time-of-flight spectrometer at NIST. Materials Research Society Symposium Proceedings series Vol. 376 (94AL5087).

BÖNI P., ANDERSON I.S., BUFFAT P., ELSSENHANS O., FRIEDLI H.P., GRIMMER H., HAUERT R., LEIFER K., MENELLE A., PENFOLD J., SOCHTIG J.

Recent progress in supermirrors at PSI. Proceedings of the Twelfth Meeting of the International Collaboration on Advanced Neutron Sources ICANS-XII, Rutherford Appleton Laboratory Report Number 94-025, Volume 1, 1-347 (1994) (94BO5104).

CIPRIANI F., CASTAGNA J.C., LEHMANN M.S., WILKINSON C.

A large image-plate detector for neutrons. Physica B (94CI5107).

DORNER B.

Introduction to neutron scattering. PSI-Proceedings, Lecture Notes of the Second Summer School on "Neutron Scattering from Hydrogen in Materials", Zuoz, Switzerland, August 14-20, 1994 (94DO5065).

GRIMMER H., BÖNI P., ELSSENHANS O., FRIEDLI H.P., LEIFER K., BUFFAT P., ANDERSON I.S.

Growth and structural characterization of Ni/Ti supermirrors for neutrons. In "Physics of X-ray Multilayer Structures", 1994 Technical Digest Series, Volume 6, Optical Society of America, Washington DC (1994) (94GR5103).

GUAZZONNE J.P., HAMELIN B., BASTIE P.

Radiocrystallographic diagnosis methods for single crystal components. Proceedings of the ASNT Fall Conference, Atlanta, USA, September 19-23, 1994 (94GU5040).

KULDA J.

Towards ideal focusing monochromators. Physica B (Proceedings of the International Conference on "Neutron Scattering", Sendai, Japan, October 11-14, 1994) (94KU5054).

LANGAN P., FORSYTH V.T., MAHENDRASINGAM A.,

Attenuation corrections for X-ray and neutron fibre diffraction studies. Journal of Applied Crystallography (94LA5094).

TASSET F.

Towards helium-3 neutron polarizers. Physica B (Proceedings of the International Conference on "Neutron Scattering", Sendai, Japan, October 11-14, 1994) (94TA5042).

TASSET F., RESSOUCHE E.

Optimum transmission for an ^3He neutron polarizer. Nuclear Instruments and Methods A (94TA5050).

2. Theory

BARES P.A., GEBHARD F.

Asymptotic Bethe-Ansatz results for a Hubbard chain with $1/\sinh$ -hopping. Journal of Low Temperature Physics (94BA5092).

CLEMENTS B., KROTSCHKE E., SAARELA M., CAMPBELL C.E.
Bose quantum films at finite temperature.
Condensed Matter Theories - Vol. 10 (94CL5037).

FABRIZIO M., GOGOLIN A.O., SCHEIDL S.

Coulomb effects in transport properties of quantum wires. Physical Review Letters (94FA5009).

FABRIZIO M., GOGOLIN A.O., SCHEIDL S.

Impurity scattering in quantum wires with Coulomb interaction. Journal of Low Temperature Physics (Proceedings of the International Euroconference on "Magnetic Correlations, Metal Insulator Transitions, and Superconductivity in Novel Materials", Würzburg, Germany, September 26-30, 1994) (94FA5051).

FOURCADE B., MICHALET X., BENSIMON D.

Vesicles of complex topology. CRC Press (1994-1995) ed. D. Lasic (94FO5036).

VILLAIN J., DUPORT C., NOZIERES P.

Elastic instabilities in crystal growth. Conférence sur les phénomènes non linéaires, Sitgès, Espagne, Juin 1994 (94VI5044).

3. Fundamental and Nuclear Physics

BISHAI M.R., GERNDT E.K.E., SHIPSEY I.P.J., WANG P.N.,

BAGULYA A.C., GRISHIN V.M., NEGODAEV M.A., GELTENBORT P.
Performance of microstrip gas chambers passivated by thin semiconducting glass and plastic films. Proceedings of the 27th International Conference on High Energy Physics, Glasgow, U.K., July 20-27, 1994 (94BI5039).

FIONI G.

The PIAFE project and its possible implications in r-process studies. American Institute of Physics (94FI5029).

4. Structural and Magnetic excitations

BOUDARD M., BOISSIEU M. DE, GOLDMAN A.I., HENNION B., BELLISSENT R., QUILICHINI M., CURRAT R., JANOT C.

Dynamics of the AlPdMn icosahedral phase. Physica Scripta (Proceedings of Euroconference 94 on Neutron in Disordered Materials, Stockholm, Sweden, June 1994) (94BO5058).

DORNER B.

Introduction to neutron scattering. PSI-Proceedings, Lecture Notes of the Second Summer School on "Neutron Scattering from Hydrogen in Materials", Zuoz, Switzerland, August 14-20, 1994 (94DO5065).

KULDA J., ISHII Y., KATANO S.

Dynamical structure analysis applied to Si and Ge. Physica B (Proceedings of the International Conference on "Neutron Scattering", Sendai, Japan, October 11-14, 1994) (94KU5055).

LOEWENHAUPT M., FABI P., SOSNOWSKA I., FRICK B., ECCLESTON R.

Temperature dependence of the magnetic excitation spectrum of $\text{Dy}_2\text{Fe}_{14}\text{B}$. Journal of Magnetism and Magnetic Materials (Proceedings of the International Conference on Magnetism 1994, Warsaw, Poland, August 22-26, 1994) (94LO5084).

MURANI A.P., PIERRE J.

Low temperature paramagnetic scattering from YbInAu_2 and YbAl_3 .
Physica B (94MU5085).

MUTKA H., PAYEN C., MOLINIE P.

Finite segments in quasi-1D Heisenberg antiferromagnets: comparison of the isostructural systems AgVP_2S_6 ($S=1$) and AgCrP_2S_6 ($S=3/2$).
Journal of Magnetism and Magnetic Materials (Proceedings of the International Conference on Magnetism 1994, Warsaw, Poland, August 22-26, 1994) (94MU5023).

MUTKA H., PAYEN C., MOLINIE P., ECCLESTON R.S.

Quasi-1D antiferromagnets with $S=1$ and $S=3/2$. The isostructural compounds AgVP_2S_6 and AgCrP_2S_6 .
Physica B (Proceedings of the International Conference on "Neutron Scattering", Sendai, Japan, October 11-14, 1994) (94MU5056).

POUGET S., ALBA M., NOGUES M.

Influence of disorder on the static critical behaviour in the frustrated ferromagnetic system $\text{CdCr}_{2(1-x)}\text{In}_{2x}\text{S}_4$.
Journal of Magnetism and Magnetic Materials (Proceedings of the International Conference on Magnetism 1994, Warsaw, Poland, August 22-26, 1994) (94PO5019).

ROSOV N., LYNN J.W., KÄSTNER J., WASSERMANN E.F., CHATTOPADHYAY T., BACH H.

Polarization analysis of the magnetic excitations in $\text{Fe}_{72}\text{Pt}_{28}$.
Journal of Magnetism and Magnetic Materials (94RO5030).

SUMARLIN L.W., LYNN J.W., CHATTOPADHYAY T., BARILO S.N., ZHIGUNOV D.I., PENG J.L.

Magnetic structure and spin dynamics of the Pr and Cu in Pr_2CuO_4 .
Physical Review B (94SU5053).

5. Crystal and Magnetic Structures

5a - Crystallography of Non-Magnetic Systems

JANOT C.

Structure determination of the icosahedral quasicrystals: state of the art and prospect.
World Scientific Publishers Co. (International Conference on Aperiodic Crystals, Les Diablerets, Switzerland, September 18-22, 1994) (94JA5048).

UDOVIC T.J., HUANG Q., RUSH J.J., SCHEFER J., ANDERSON I.S.

Neutron-powder-diffraction study of the long-range order in the octahedral sublattice of $\text{LaD}_{2.25}$.
Physical Review B (94UD5093).

5b - Crystallography of magnetic Systems

CHATTOPADHYAY T., BRÜCKEL Th., HOHLWEIN D., SONNTAG R.

Magnetic diffuse scattering from the frustrated antiferromagnet MnS_2 .
Journal of Magnetism and Magnetic Materials (Proceedings of the International Conference on Magnetism 1994, Warsaw, Poland, August 22-26, 1994) (94CH5018).

CHATTOPADHYAY T., SCOTT C.A., LÖHNEYSSEN H.V.

μSR investigation of the magnetic ordering in $\text{CeCu}_{5.5}\text{Au}_{0.5}$.
Journal of Magnetism and Magnetic Materials (Proceedings of the International Conference on Magnetism 1994, Warsaw, Poland, August 22-26, 1994) (94CH5025).

KESSLER M., DEPORTES J., OULADDIAF B., SAYETAT F.

Magnetic properties of $\text{Sc}_x\text{Ti}_{1-x}\text{Fe}_2$.
Journal of Magnetism and Magnetic Materials (Proceedings of the International Conference on Magnetism 1994, Warsaw, Poland, August 22-26, 1994) (94KE5090).

OULADDIAF B., BALLOU R., DEPORTES J., LELIEVRE-BERNA E.

Magnetic frustration and instability in $\text{Dy}_{1-x}\text{La}_x\text{Mn}_2$.
Journal of Magnetism and Magnetic Materials (Proceedings of the International Conference on Magnetism 1994, Warsaw, Poland, August 22-26, 1994) (94OU5024).

OULADDIAF B., DEPORTES J., RODRIGUEZ-CARVAJAL J.

Magnetic structure of $\text{Er}_6\text{Mn}_{23}$ and $\text{Dy}_6\text{Mn}_{23}$.
Physica B (Proceedings of the International Conference on "Neutron Scattering", Sendai, Japan, October 11-14, 1994) (94OU5034).

RITTER C., CYWINSKI R., KILCOYNE S.H.

The nature of the Mn moment in Laves phase compounds: evolution of the magnetic order in $\text{Ho}_{1-x}\text{Y}_x\text{Mn}_2$.
Zeitschrift für Naturforschung a (94RI5088).

SUMARLIN L.W., LYNN J.W., CHATTOPADHYAY T., BARILO S.N., ZHIGUNOV D.I., PENG J.L.

Magnetic structure and spin dynamics of the Pr and Cu in Pr_2CuO_4 .
Physical Review B (94SU5053).

6. Liquids, Disordered Materials and Metal Physics

ANDERSON I.

The dynamics of hydrogen in metals studied by inelastic neutron scattering. Proceedings of the Summer School on Neutron Scattering from Hydrogen in Metals, Zuoz, Switzerland, August 14-10, 1994 (94AN5089).

DUNEAU M., JANOT C.

Matières à paradoxes.
in "Géométrie et Matériaux", Editions Odile Jacob, Paris (94DU5102).

FRICK B., WILLIAMS J., TREVIÑO S., ERWIN R.

Vibrational behaviour of amorphous and crystalline ethylbenzene.
Physica B (Proceedings of the International Conference on "Neutron Scattering", Sendai, Japan, October 11-14, 1994) (94FR5064).

FRICK B., BUCHENAU U., RICHTER D.

Boson peak and fast relaxation process near the glass transition in polystyrene.
Colloid & Polymer Science (94FR5069).

FRICK B., RICHTER D.

The microscopic basis for macroscopic properties changes of polymers - an investigation of the glass transition.
Science Magazine (94FR5083).

STROTHMANN H., SCHAERPF O.

Determination of Bloch wall thickness in $\text{Fe}(4 \text{ at } \% \text{ Si})$ single crystals by means of neutron refraction close to the Curie point.
Journal of Magnetism and Magnetic Materials (94ST5101).

SUCK J.-B.

Mode softening in rapidly quenched supersaturated $\text{Al}_{96.5}\text{Si}_{3.5}$.
In "Materials Science Forum", ed. Yavari R. (Proceedings of the International Symposium on "Metastable, Mechanically Alloyed and Nanocrystalline Materials" ISMANAM-94, Grenoble, France, June 27-July 1, 1994) (94SU5057).

8. Biological Structure and Dynamics

CHARVOLIN J.

Prolamellar bodies in etioplasts: membrane curvature and five-fold symmetry.

"Interplay of Genetic and Physical Processes in the Development of Biological Forms". Les Houches Winter Schools. Les Editions de Physique and Springer Verlag (94CH5067).

FULLER W., FORSYTH V.T., MAHENDRASINGAM A., LANGAN P., PIGRAM W.J., MASON S.A., WILSON C.C.

DNA hydration studied by neutron fibre diffraction.

Proceedings of "Neutrons in Biology", Santa Fé, USA, October 24-28, 1994 (94FU5105).

LANGAN P., FORSYTH V.T., MAHENDRASINGAM A., GIESEN U., DAUVERGNE M.T., MASON S.A., WILSON C.C., FULLER W.

Neutron fibre diffraction studies of DNA hydration.

Physica B (Proceedings of the International Conference on "Neutron Scattering", Sendai, Japan, October 11-14, 1994) (94LA5106).

TIMMINS P.A.

Low Resolution Neutron Crystallography of Large Macromolecular Assemblies.

Neutron News (94TI5017).

TIMMINS P.A.

Structural molecular biology: Recent results from neutron diffraction.

Physica B (94TI5052).

VUILLARD L., BRAUN-BRETON C., RABILLOUD T.

Non-detergent sulphobetaines: a new class of mild solubilization agents for protein purification.

Biochemical Journal (94VU5076).

VUILLARD L., MARRET N., RABILLOUD T.

Enhancing protein solubilization with non detergent sulfobetaines.

Electrophoresis (94VU5078).

9. Chemistry

9a - Molecular Spectroscopy, Surfaces and Mesophases

BÜTTNER H.G., KEARLEY G.J., FILLAUX F.,

HOWARD C.J., KAHN R.

The rotational potential of NH₃ groups in metal hexammines.

Physica B (94BU5071).

FILLAUX F., BARON M.H., LEYGUE N., TOMKINSON J.,

KEARLEY G.J.

Inelastic neutron-scattering study of the proton transfer dynamics in polyglycine.

Biophysical Chemistry (94FI5096).

FILLAUX F., FONTAINE J.P., BARON M.H., LEYGUE N.,

KEARLEY G.J., TOMKINSON J.

Inelastic neutron-scattering study of the proton transfer dynamics in polyglycine I at 20 K.

Physica B (94FI5098).

KEARLEY G.J., BÜTTNER H.G., FILLAUX F., IKEDA S., INABA A.

Coupling between phonons and quantum rotors.

Physica B (94KE5072).

KEARLEY G.J.

A review of the analysis of molecular vibrations using INS. Nuclear Instruments and Methods A (94KE5095).

SAUVAJOL J.L., PAPANEK P., FISCHER J.E., DIANOUX A.J.,

MAO G., WINOKUR M.J., KARASZ F.E.

Densités d'états vibrationnelles du poly(p-phénylène vinylène). Une étude par diffusion incohérente des neutrons.

Journal de Chimie Physique (Proceedings "Journées Polymères Conducteurs", Strasbourg, France, September 20-23, 1994) (94SA5059).

SOUAILLE M., SMITH J.C., DIANOUX A.J., GUILLAUME F.

Dynamics of N-nonadecane chains in urea inclusion compounds as seen by incoherent quasielastic neutron scattering and computer simulations.

Proceedings of the International School of Physics "Enrico Fermi" NATO-ASI, Varenna, Italy, July 26-August 5, 1994 (94SO5060).

TOMKINSON J., KEARLEY G.J.

The calculation of phonon wing intensities: anisotropic effects.

Nuclear Instruments and Methods A (94TO5097).

9b - Colloids and Polymer

BOUE F., LINDNER P.

SANS from semidilute solutions under shear: Butterflies.

Proceedings of the ACS Symposium "Flow Induced Structure in Polymers", Washington, USA, August 21-26, 1994 (94BO5035).

CHARVOLIN J.

Prolamellar bodies in etioplasts: membrane curvature and five-fold symmetry.

"Interplay of Genetic and Physical Processes in the Development of Biological Forms". Les Houches Winter Schools.

Les Editions de Physique and Springer Verlag (94CH5067).

GABRYS B., SCHÄRPF O., PEIFFER D.G.

Model ionomers studied with spin-polarized neutrons using spin-polarization analysis.

In "Physical Chemistry of Ionomers". Ed. S. Schlick, CRC Press, Chapter 4 (94GA5086).

LINDNER P.

Polymers in solution - flow techniques.

Modern Aspects of Small Angle Scattering, NATO ASI Series.

(Proceedings of the Conference held in Como, Italy, May 12-22, 1993) (94LI5005).

MILAS M., RINAUDO M., DUPLESSIX R., BORSALI R., LINDNER P.

Small angle neutron scattering from polyelectrolyte solutions: from disordered state to withdrawal of xanthan chain.

Macromolecules (94MI5013).

ROUX D., BERRET J.F., PORTE G., PEUVREL-DISDIER E.,

LINDNER P.

Shear-induced orientations and textures of nematic living polymers.

Macromolecules (94RO5043).

Acknowledgement

The Scientific Secretary, Bruno Dorner, editor of this report, wishes to thank all those who have contributed.

Layout and typesetting by Idra

Cover layout and printing by Technic Color

Photography by

J.L. Baudet (ILL), S. Claisse (ILL), J. Italia (ILL).

Other publications available

- Guide to Neutron Research Facilities, Edition 1994
- General Information and Regulations, Edition 1990.

The Scientific Secretary
Institut Max von Laue - Paul Langevin
BP 156
38042 Grenoble Cedex 9
France
Telephone: 76 20 72 93 – Telefax: 76 48 39 06 – Telex: 320621



**Institut Max von Laue
Paul Langevin
Grenoble - France**